

ANALYSIS OF WATER AND WASTEWATER

~~5886~~ 1099
72 IAWPR (vol. 3)

THE APPLICATION OF INFORMATION ABOUT CONDUCTIVITY IN THE COMPUTING OF ION CONCENTRATIONS, ILLUSTRATED BY CERTAIN SURFACE WATERS SITUATED IN LOWER SAXONY

W. Walther,* M. Gorsler,** J. Poltz** and D. Bock*

**Institut für Städtebauwesen, Technische Universität, Postfach 3329,
3300 Braunschweig, F.R.G.*

***Niedersächsisches Wasseruntersuchungsamt, Langelinienwall 27,
3200 Hildesheim, F.R.G.*

ABSTRACT

The electrical conductivity and pH value are, amongst other parameters, continuously recorded in monitoring stations at important surface waters in Lower Saxony. The data are directly transmitted to the surveillance centre in Hildesheim. This paper deals with the estimates of concentrations of the most important ions in water by using mathematical models. The basis for the calculations are the conductivity and, in case of a eutrophic lake, the pH value as well. The methods are demonstrated by using data from the river Weser and from the shallow lake Dümmer. The Weser is one of the main rivers in Lower Saxony. It is heavily polluted by potash mine wastes.

KEYWORDS

Conductivity; ion concentration; model; surface water; Lower Saxony

INTRODUCTION

Conductivity and pH value are two of the few properties of water which can be continuously recorded by electrodes. So for the surveillance of waters only a few parameters are directly available. Furthermore they give only unspecific information about the water quality at a certain control point. In Lower Saxony monitoring stations have been installed at the most important surface waters. The data of conductivity and pH value are, besides other parameters, transmitted online to the surveillance centre in Hildesheim. Once a month additional samples are taken on these stations and analysed. The aim of this investigation is to estimate the most important ions by means of actual conductivity values on the basis of the theory of conductivity and/or simple regression models. According to earlier hydrogeological researches (e.g. Davis and de Wiest, 1966) and earlier investigations on small surface waters (Korn and Walther, 1980) this seemed to be promising. Recent investigations in this field were made by the authors on the river Weser and on the shallow lake Dümmer. Some results of this research and data from the monitoring station Hemeln/Weser and from the control point Dümmer-runoff will be presented.

THE CHARACTERISTICS OF THE STUDIED WATERS

The Weser has a catchment area of 46.200 km², where about 8 million people live. From the geographical point of view it is a very diverse area having wide agricultural regions and woodlands as well as municipal and industrial centres. The water quality is affected by waste water effluents which cause oxygen consumption and eutrophication. But the ecology of the river and the utilization facilities are limited mainly by a very high and fluctuating salinity. More than 90% of the salt pollution is caused by potash mine wastes from Thuringia (GDR).

The conductivity of surface waters (adjusted for 20 °C) is usually within the range of about 200 to 1000 µS/cm. At the station Hemeln on the upper Weser, however, the values vary from 2700 to 13200 µS/cm. The long-term mean value is 6200 µS/cm. Even 330 km downstream above the tidal limits the average conductivity in the Weser is still about 2500 µS/cm. For the purposes of water pollution control, water management and regional planning a continual surveillance of the salt pollution is required. For the periods between monthly samplings the salt concentrations can now be estimated using a computing model in the surveillance centre in Hildesheim.

The lake Dümmer has a size of 12.5 km² and a mean depth of 1.1 m. It is situated on the southern edge of the North German Plain. The catchment area is 410 km² with a mainly agricultural use. So the lake constantly receives a surplus of plant nutrients. Consequently the lake is polytrophic and highly productive having extreme and long lasting mass developments of planktonic algae. Additionally during the second half of the vegetation period internal cycles become important for the nutrient supply of phytoplankton. Consequences of this high productivity are (1) extreme oscillations of oxygen concentrations and pH values as well as (2) a biogenic lime precipitation: In spring calcium concentrations decrease from about 80 - 90 mg/l down to about 50 - 60 mg/l. Correspondingly the conductivity of the lake water varies between about 600 µS/cm during the winter and 400 µS/cm in summer. The pH values range between 7.4 and 11.1.

The dynamics of short-term production and mineralization processes cannot be recognized by individual samplings as performed for many years. Therefore an automatic monitoring station has been installed on lake Dümmer. There is known to be a causal relationship between calcium concentration and pH value. Because of the above mentioned annual oscillations of calcium and conductivity we tried to calculate the actual calcium concentrations from the continuously measured pH value and conductivity. Our aim is to obtain more information on the dynamics of the biogenic lime precipitation and redissolving which are important processes in connection with sediment formation in this lake.

THE THEORY OF CONDUCTIVITY AND ITS APPLICATION

The conductivity of a water sample depends on the concentration, the valence and the mobility of the ions. The conductivity of a binary salt like NaCl or that of a solution which contains several kinds of ions can be described as follows:

$$\kappa(t) = \sum_i c_i(t) \cdot z_i \cdot u_i(t) \quad (1)$$

$\kappa(t)$ = conductivity in µS · cm⁻¹

$c_i(t)$ = concentration in mol · l⁻¹

z_i = valence of an ion

$u_i(t)$ = mobility in $\text{cm}^2 \cdot \Omega^{-1} \cdot \text{mol}^{-1}$

i = kind of ion

t = time when the sample was taken

According to equation (1) a linear relationship between conductivity on the one hand and the product of concentration, valence and mobility of the substance components on the other hand can be inferred. However, we know that the conductivity increases more slowly than the concentration. Deviance from the linear relationship can be caused by incomplete dissociation and by interaction of the ions. Due to this the mobility $u_i(t)$ becomes an environment dependent constant, Kortüm (1966). Because of these interactions the mobility of the single ions decreases as can be seen in the case of the station Hemeln, table 1. A mathematical approach taking ion interaction into account was described by Onsager and Fuoss (1932).

$$u(t) = u_{i\infty} - \left(\frac{2.004 \cdot 10^6}{(D_o T)^{3/2}} u_{i\infty} z'_i \sum_{n=0}^{\infty} C_n r_i^{(n)} + \frac{29.5}{\eta_o (D_o T)^{1/2}} \right) I_i^{1/2} \quad (2)$$

$u_{i\infty}$ = mobility of the ion i in an infinite dilution

D_o = dielectric constant = 78.57 (water, 25 °C)

T = temperature in Kelvin

z'_i = valence with sign

η_o = viscosity of water at 25 °C = 0.000895 Pa s

$I_i = (\rho_i(t) \cdot z_i^2)$

$I = \sum_i I_i$

$\rho_i(t)$ = concentration in $\text{mg} \cdot \text{l}^{-1}$

$C_n = -\frac{1}{2} \sqrt{2} \frac{1/2}{n}$ for $n \geq 1$ (binomial series)

$r_i^{(n)}$ = vector

The mobility values $u_i(t)$ can be computed using the matrix theory. This approach considers the relaxation effect (first term in the brackets) and the electro-phoretic effect (second term in the brackets). Further explanation of this approach can be found in Onsager and Fuoss (1932) and also, in briefer form, in Korn and Walther (1980).

In the Weser the conductivity is dependent on the ions calcium, magnesium, potassium, sodium, hydrogencarbonate, sulphate and chloride. In lake Dümmer the ions carbonate and nitrate are also of interest. Other ions may be neglected because of their low concentrations (< 1 mg/l). Equation (1), applied to the important ions of the solution in Hemeln/Weser, gives the environment dependent mobility value $u_i(t)$ (table 1, 2nd line). Line 1 shows the ideal values for mobility, in an infinite dilution, without ion interaction. Line 4 gives in percent the difference $\Delta u_i(t)$ between both values. Further tests with data from

Table 1 Hemeln/Weser_i conductivity information

| Variable | Ca ²⁺ | Mg ²⁺ | Na ⁺ | K ⁺ | HCO ₃ ⁻ | SO ₄ ²⁻ | Cl ⁻ |
|---|------------------------|------------------------|-----------------------|------------------------|-------------------------------|-------------------------------|-----------------------|
| u _{i∞} (cm ² ·Ω ⁻¹ ·mol ⁻¹) | 59.6 | 53.1 | 50.1 | 73.5 | 44.5 | 80.0 | 76.4 |
| ū _i (cm ² ·Ω ⁻¹ ·mol ⁻¹) | 31.5 | 27.6 | 37.5 | 61.2 | 35.1 | 41.9 | 70.9 |
| v _i (%) | 21.7 | 23.0 | 8.9 | 5.0 | 6.8 | 23.1 | 2.0 |
| Δu _i (%) | 47.2 | 48.0 | 25.2 | 16.7 | 21.1 | 47.6 | 7.2 |
| κ _i (μS·cm ⁻¹) | 145.2 | 313.9 | 1793.3 | 122.3 | 87.5 | 206.7 | 4205.7 |
| pk̄ _i (%) | 2.6 | 4.9 | 25.5 | 1.8 | 1.5 | 3.5 | 59.9 |
| sk̄ _i (μS·cm ⁻¹ ·mg ⁻¹) | 1.6 | 2.3 | 1.6 | 1.6 | 0.6 | 0.9 | 2.0 |
| k̄ _i (mg ⁻¹ ·cm ⁻¹ ·μS ⁻¹) | 0.157·10 ⁻⁷ | 0.218·10 ⁻¹ | 0.158·10 ⁰ | 0.114·10 ⁻¹ | 0.258·10 ⁻¹ | 0.387·10 ⁻¹ | 0.300·10 ⁰ |
| v _i (%) | 43.9 | 15.0 | 18.5 | 10.1 | 41.4 | 19.3 | 8.1 |

v: relative standard deviation (%) of the mean value of the time-series); arithmetic mean values of parameters are indicated by ()

other stations on the Weser and on lake Dümmer show that the deviation $\Delta u_i(t)$ and the influence of ion interaction respectively decrease with decreasing salt content.

Simple changes in equation (1) give us those data which are important for the interpretation of conductivity. If the computed mobility $u_i(t)$ is inserted we get the conductivity value $\kappa_i(t)$ which is related to the respective concentration of the ions (cf line 5). The sum of the individual conductivity values is the theoretical conductivity value of the whole solution. The proportional conductivity $P\kappa_i(t)$ of an individual ion type can now be deduced by calculating the individual conductivity as a percentage of the theoretical conductivity of the whole solution (cf line 6). Furthermore we can deduce from the quotient of mobility and relative equivalent weight an environment dependent conductivity value Sk_i (cf line 7). The mobility $u_i(t)$ varies slightly with time. The relative standard deviations of the mobility time-series of all the ions reach a maximum of 23% for sulphate and magnesium at the station Hemeln. The variation of $u_i(t)$ decreases with decreasing concentration. This can be seen on the Weser, which becomes progressively diluted by tributaries. In the Dümmer-runoff these variations are less than 2% of the mean mobility values. Consequently the computed mobility is specific for the respective control points. Using these values we can now construct equation systems which enable us to compute the concentration of the different kinds of ions. The equation for the dependence of specific electrical conductivity on concentration is as follows:

$$\rho_i(t) = k_i(t) \cdot \kappa_{25}(t) + e_i \quad (3)$$

$$\begin{aligned} \kappa_{25}(t) &= \text{recorded conductivity, adjusted for } 25^\circ\text{C} \\ &= 1.116 \cdot \kappa_{20}(t) \end{aligned}$$

$$\kappa_{20}(t) = \text{recorded conductivity, adjusted for } 20^\circ\text{C}$$

$$e_i = \text{residuals}$$

The parameter $k_i(t)$ can be constructed as follows:

$$k_i(t) = P\kappa_i(t) \cdot Sk_i(t) \quad (4)$$

The mean value \bar{k} of the parameter $k_i(t)$ is shown in line 8 of table 1. The respective standard deviation varies according to the characteristics of the water, the kinds of ions, and their concentrations (cf line 9 and fig. 1). If this relationship is taken into account in an adjustment equation we can calculate an ion time-series from the conductivity values. Equation (5) and (6) show the calculation of the ions chloride and potassium in the station Hemeln/Weser.

$$Cl^-(t) = (0.0656 \cdot \kappa_{20}^{0.175}(t)) \cdot 1.116 \cdot \kappa_{20}(t) + e_i \quad (5)$$

$$n = 19; s_{y.x} = \pm 185.4 \text{ mg} \cdot l^{-1}$$

n = number of samples included in computation

$s_{y.x}$ = standard deviation of the residuals

$Cl^-(t)$ and $K^+(t)$ = concentration in $\text{mg} \cdot l^{-1}$

$$\kappa^+(t) = (0.0043 + 0.0019 \cdot \log \kappa_{20}(t)) \cdot 1.116 \cdot \kappa_{20} + e_i \quad (6)$$

$n = 19; s_{y,x} = \pm 10.0 \text{ mg} \cdot l^{-1}$

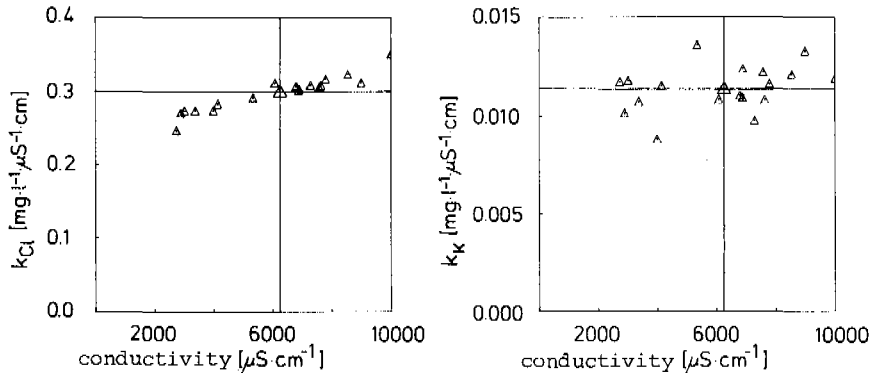


Fig. 1. Hemeln/Weser, relationship between $\kappa_{Cl}^+(t)$ and conductivity and κ_K^+ and conductivity

The reliability of this adjustment can be seen in fig. 2. The same was done for other ions. To show the validity of these equations we compare in table 2 the mean values ρ 'measured' \sim ρ 'computed' and the relative standard deviation v 'measured' \sim v 'computed'. The mean values and the variances agree satisfactorily except the variance in the case of calcium. Further tests with data from other stations on the Weser showed that it is possible to construct the same system of equations for these stations. However, the results for Dümmer are not yet quite satisfactory.

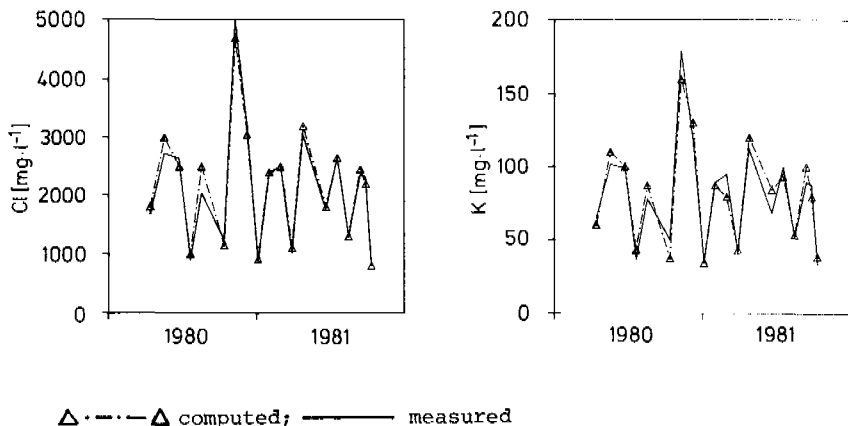


Fig. 2. Hemeln/Weser, measured and computed chloride and potassium time series (theory of Onsager and Fuoss)

Table 2 Hemeln/Weser, results of computation with equations based on the theory of Onsager and Fuoss

| | $\bar{\rho}$ (mg·l ⁻¹) measured | $\bar{\rho}$ (mg·l ⁻¹) computed | $\Delta\rho$ (%) | v (%) measured | v (%) computed |
|-------------------------------|--|--|------------------|-------------------|-------------------|
| Ca ²⁺ | 94.9 | 94.3 | 0.7 | 25.2 | 13.0 |
| Mg ²⁺ | 156.6 | 154.7 | 1.2 | 47.3 | 49.5 |
| Na ⁺ | 1193.7 | 1177.4 | 1.4 | 46.5 | 51.4 |
| HCO ₃ ⁻ | 153.3 | 151.4 | 1.3 | 13.6 | 10.7 |
| CO ₃ ²⁻ | 0.30 | 0.31 | -3.3 | 56.5 | 42.7 |
| SO ₄ ²⁻ | 254.2 | 253.9 | 0.1 | 28.6 | 30.6 |

$\bar{\rho}$ = arithmetic mean value; $\Delta\rho$ = difference of $\bar{\rho}$ 'measured' and $\bar{\rho}$ 'computed' in % of $\bar{\rho}$ 'measured'

v = standard deviation in % of the mean value of the time-series;
basis of computation are 19 samples

THE APPLICATION OF REGRESSION MODELS

The validity of the equation coefficients has to be checked from time to time using data from water analyses. Because of the matrix manipulation the solving of equation (2) is more complicated than estimating regression coefficients. These regression coefficients can easily be determined with a small computer. Therefore we investigated whether it is possible to compute the most important ions with regression models. For the station Hemeln/Weser the concentrations of magnesium, sodium, potassium, sulphate and chloride can be calculated according to equations (7) and (8), carbonate according to equation (9). Fig. 3 and table 3 show the results for the station Hemeln. The mean values and the variances can be estimated with sufficient reliability.

$$Cl^-(t) = -226.261 + 0.375 \cdot K_{20}(t) \pm e_i \quad (7)$$

$$n = 20; s_{y.x} = \pm 161.0 \text{ mg} \cdot l^{-1}$$

$$K^+(t) = -2.354 + 0.013 \cdot K_{20}(t) \pm e_i \quad (8)$$

$$n = 20; s_{y.x} = \pm 9.3 \text{ mg} \cdot l^{-1}$$

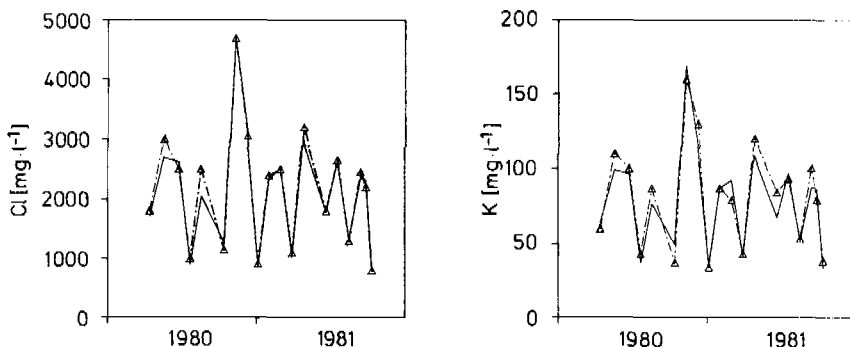


Fig. 3. Hemeln/Weser, recorded and computed chloride and potassium time-series (regression model)

Table 3 Hemeln/Weser, results of computation with regression models

| | $\Delta\rho$ (%) | v (%) | |
|-------------------------------|------------------|----------|----------|
| | | measured | computed |
| Mg ²⁺ | 3.4 | 47.3 | 48.3 |
| Na ⁺ | 4.0 | 46.5 | 49.1 |
| CO ₃ ²⁻ | 9.7 | 56.5 | 50.9 |
| SO ₄ ²⁻ | 2.0 | 28.6 | 27.7 |

For the shallow lake Dümmer it is, for the reasons shown above, of great interest to obtain calcium concentration values as frequently as possible. They can be deduced from conductivity and pH values using equation (9). As shown in Fig. 4 the concentrations of other ions can be calculated similarly.

$$\text{Ca}^{2+}(t) = 57.594 + 0.144 \cdot \kappa_{20}(t) - 6.376 \cdot \text{pH}(t) \pm e_i \quad (9)$$

$$n = 46; s_{y,x} \approx \pm 6.9 \text{ mg} \cdot l^{-1}$$

$$\text{HCO}_3^-(t) = 493.547 + 0.093 \cdot \kappa_{20}(t) - 47.829 \cdot \text{pH}(t) \pm e_i \quad (10)$$

$$n = 62; s_{y,x} \approx \pm 17.6 \text{ mg} \cdot l^{-1}$$

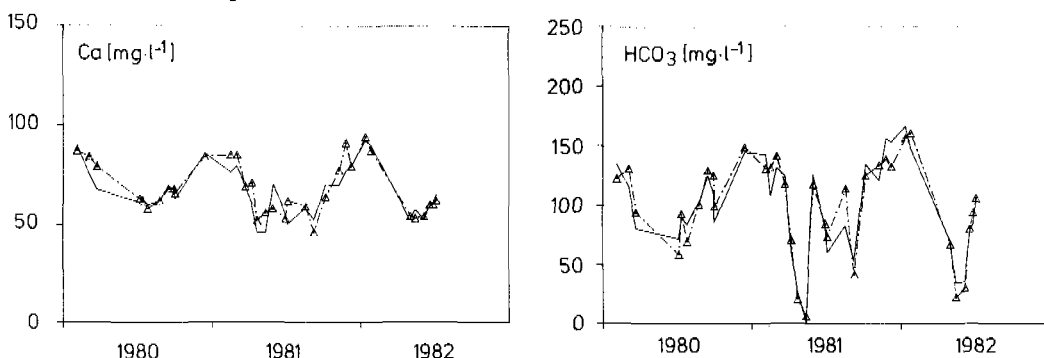


Fig. 4. Dümmer-runoff, recorded and computed calcium and hydrogencarbonate time-series (regression model)

CONCLUSIONS

The investigations show that it is possible to compute the concentrations of the most important solution constituents of surface waters from conductivity and pH value. The equations for these estimates are part of a computing programme in the surveillance centre in Hildesheim. They enable us, via electrodes values, to record continuously the concentrations of the important ions and their fluctuations. The characteristics and the quality of a body of water are the result of manifold processes in the catchment area as well as in the water. The equations for calculating the ion concentrations are specific for each water system and even for each part of it. The computing approaches shown above remain valid as long as the infrastructure of the respective catchment areas is not changed. Therefore these equations have to be checked from time to time against actual analyses. It is to be considered that the equations derive from data from chemical analyses. So their accuracy is qualified not only by the limitations of

the mathematical models presented, but also by the reliability of the analyses. As far as we know this is the first case in which the theory of Onsager and Fuoss has been applied to and tested with data from large inland waters.

REFERENCES

- Davis, S.N., De Wiest, R.J.M. (1966). Hydrogeology. John Wiley, New York, London, Sidney.
- Onsager, L., Fuoss, R.M. (1932). Irreversible process in electrolytes. Diffusion, conductance, and viscous flow in arbitrary mixtures of strong electrolytes. J. Phys. Chem., 36, 2689-2778.
- Korn, K., Walther, W. (1980). Information content and use of the electrical conductance to calculate concentrations of ions in flowing waters. Vom Wasser, 55, 77-94.
- Kortüm, G. (1970). Lehrbuch der Elektrochemie. Verlag Chemie, Weinheim, 4. Auflage.

HAZARDOUS SUBSTANCES IN WASTE WATER

A. B. van Luij and W. van Starkenburg

*Governmental Institute for Sewage and Waste Water Treatment (RIZA),
P.O. Box 17, 8200 Lelystad, The Netherlands*

ABSTRACT

The Governmental Institute for Sewage and Waste Water Treatment has studied the presence of a number of hazardous substances, selected by the EEC-Commission, in sewage and industrial waste water. The influent, effluent and sludge of six municipal waste water treatment plants and the waste water of 59 industries were sampled and analysed.

Volatile chlorinated hydrocarbons in sewage originate mainly from industrial discharges. Chlorophenols, γ -hexachlorocyclohexane, polychlorinated biphenyls (PCB) and polycyclic aromatic hydrocarbons (PAH) appear to be present at a low and constant background in municipal sewage and in many industrial waste waters. The removal in the municipal treatment plants amounts to:

- volatile chlorinated hydrocarbons 50-90%
- hexachlorobenzene 95%
- hexachlorocyclohexanes 40-65%
- chlorophenols 20-40%
- PCB about 90%
- PAH 85-95%

This study has given a survey of emissions of these hazardous substances. The total emission of the examined substances in the Netherlands has remained out of the scope of this investigation.

KEYWORDS

Hazardous substances, sewage, industrial waste water, black list.

INTRODUCTION

The Commission of the European Communities and the International Rhine Commission have drawn up directives to diminish the pollution of the aquatic environment (EEC, 1976; IRC, 1976).

They distinguish two groups of polluting substances:

- the most hazardous pollutants, mentioned in the black list (list I);
- the less hazardous pollutants, mentioned in the grey list (list II).

On the black list no separate substances -with exception of mercury and cadmium- but only groups of substances are mentioned. The final selection of

black-list-substances is based mainly on toxicity, persistence and bioaccumulation. Meanwhile 129 substances have been proposed for selection (EEC, 1982)+

The aim of this study is to collect data about the level of pollution of the Dutch surface waters by a number of those 129 substances. For this purpose a number of samples of sewage and industrial waste water was analysed for the presence of these pollutants. The study extended from April 1980 until December 1983.

THE SET-UP OF THE STUDY

The study has been designed with two aspects in mind. On one hand the presence of hazardous substances in sewage and the behaviour of these substance in biological treatment plants has been taken into consideration. On the other hand industrial waste water discharges were analysed to identify sources of the pollutants.

For this study those substances have been selected, which have been proposed for further examination by the EEC-Commission.

The Commission has these examinations carried out before deciding on including substances in the black list.

Six waste water treatment plants (table 1) were selected so that a variation was obtained concerning the next points:

- type of installation (oxidation ditch, activated sludge or trickling filter);
- size of the installation;
- nature of the treated sewage;
- type of industries connected to the (municipal) treatment plant.

Table 1: municipal waste water treatment plants

| plant A | type | i.e.(mun.) | i.e.(ind.) | kind of industries dyes,electroplating, abattoir,laundry, flavouring | flow(m ³ /d) ¹ |
|---------|------|------------|------------|---|--------------------------------------|
| | | 104.000 | 44.000 | | |
| B | TF | 10.500 | - | | 1.700 |
| C | AS | 75.750 | 1.250 | silver,electroplating | 23.900 |
| D | AS | 100.000 | 46.000 | dairy,chemicals, abattoir | 44.800 |
| E | OX | 85.000 | 88.000 | meat,pharmaceuticals, dairy,textile,tanker- cleaning,printing,tin- plating | 35.500 |
| F | OX | 18.000 | 20.300 | dairy,zinc-plating | 5.890 |

1)= mean year value

i.e. (inhabitant equivalent) = 54 g BOD/day; i.e.(mun.)= municipal; i.e.(ind.)= industrial

OX= oxidation ditch, AS= activated sludge, TF= trickling filter

The influent, effluent and sludge of each treatment plant was sampled seven times. The presence of hazardous substances in industrial waste water has been studied at 59 industries. The selection of potential discharges took place on the ground of information from literature and know-how about production processes (Van Luin & Van Starkenburg, 1983). The selected industries were more or less representative of the branch of industry they belong to, except the chemical industries which are not comparable with each other.

The study was carried out in two phases.

Phase 1 In the first phase the waste water of 22 industries from eight branches of industry was sampled (table 2). The object of this phase was to get some idea of the quantity of discharges by the industries. At the same time a link could be made with comparable industries. The drawing-up of a total balance of discharges in Dutch surface waters was outside the scope of this study.

Phase 2 The waste water of 37 industries of 22 branches of industry (table 2) was sampled two to four times. The aim of the study was to collect quantitative data on the presence of the selected substances in the waste water streams of a large number of industries. The sampling of the influents, effluents and industrial waste waters was principally volume-proportional.

Table 2: branches of industry and number of plants

| branch of industry | phase 1 | phase 2 | branch of industry | phase 1 | phase 2 |
|------------------------|---------|---------|-------------------------|---------|---------|
| chemicals | 9 | | soft drinks | | 1 |
| pharmaceuticals | 2 | | brewery | | 1 |
| dyes | 2 | 3 | wood impregnation | | 2 |
| textile | 2 | 2 | printing | | 1 |
| rubber | 2 | 2 | painting | | 2 |
| leather | 1 | 2 | soap and clean. prep. | | 1 |
| paper | 2 | 2 | electroplating | | 4 |
| formulating pesticides | 2 | | photographic lab. | | 1 |
| slaughter | | 2 | laundry | | 1 |
| dairy products | | 3 | motor-overhaul | | 1 |
| fruit and vegetables | | 1 | hospital | | 1 |
| margarine and fats | | 2 | incineration of re-fuse | | 1 |
| sugar | | 1 | | | |

The substances analysed are listed in table 3. Sludge was not analysed for volatile chlorinated hydrocarbons. The reason is that the concentrations in the influent could vary very much. The frequency of this investigation would have been intensified to obtain reliable figures. The substances were analysed with the usual methods (PAH with HPLC/UVF, PCB with CGC/ECD, VCH and NVCH with CGC/ECD).

RESULTS

Waste water treatment plants. The results of the analyses of influents, effluents and sewage sludges are given in tables 4 to 9. The mean concentration is mentioned, except for the VCH. The figures for the VCH varied widely. In this case the median concentration is given.

The PCB-concentrations has been averaged over the six plants and are presented in table 7. No figures of single plants are given because of the low frequency of detection.

Industrial waste water. The results of the first phase of the study are summarized in table 10. The results of the second phase are given in table 11.

Table 3: list of substances

Volatile chlorinated hydrocarbons

- dichloromethane
- trichloromethane
- tetrachloromethane
- 1,2-dichloroethane
- 1,1,1-trichloroethane
- trichloroethylene
- tetrachloroethylene
- 1,2-dichlorobenzene
- 1,4-dichlorobenzene

Non-volatile chlorinated hydrocarbons

- hexachlorobenzene (HCB)
- α -hexachlorocyclohexane (α -HCH)
- β -hexachlorocyclohexane (β -HCH)
- γ -hexachlorocyclohexane (γ -HCH)

Chlorinated phenols

- 2,4,5-trichlorophenol (2,4,5-TCP)
- 2,4,6-trichlorophenol (2,4,6-TCP)
- 2,3,4,5-tetrachlorophenol (2,3,4,5-TCP)
- 2,3,4,6-tetrachlorophenol (2,3,4,6-TCP)
- pentachlorophenol (PCP)

Polychlorinated biphenyls

- 17 isomers: PCB 8,18,28,33,44,49,52,66,70,72,100,101,136,138,149,153
and 180 (IUPAC-nomenclature) (Ballschmitter and Zell, 1980)

Polycyclic aromatic hydrocarbons

- fluoranthene
- benzo(b)fluoranthene
- benzo(k)fluoranthene
- benzo(a)pyrene
- benzo(g,h,i)perylene
- indeno(1,2,3-c,d)pyrene

Table 4: median concentrations of volatile chlorinated hydrocarbons in influent and effluent of six municipal waste water treatment plants (in ug/l)

| | A | B | C | D | E | F |
|-----------------------|-------------|-------------|-------------|-------------|-------------|-------------|
| | infl./effl. | infl./effl. | infl./effl. | infl./effl. | infl./effl. | infl./effl. |
| dichloromethane | 175 | 21 | 13 | 12 | 55 | 20 |
| trichloromethane | <1 | <1 | <1 | <1 | <1 | <1 |
| tetrachloromethane | <1 | <1 | <1 | <1 | <1 | <1 |
| 1,2-dichloroethane | 130 | 45 | <2 | <2 | <2 | <2 |
| 1,1,1-trichloroethane | <1 | <1 | 2 | <1 | 13 | <1 |
| trichloroethylene | <2,5 | <2,5 | <2,5 | <2,5 | <2,5 | <2,5 |
| tetrachloroethylene | <1 | <1 | <1 | <1 | <1 | <1 |
| 1,2-dichlorobenzene | <5 | <5 | <5 | <5 | <5 | <5 |
| 1,4-dichlorobenzene | <5 | <5 | <5 | <5 | <5 | <5 |

Table 5: mean concentrations of non-volatile chlorinated hydrocarbons in influent and effluent of six municipal waste water treatment plants (in ug/l)

| | A | B | C | D | E | F |
|---------------|-------------|-------------|-------------|-------------|-------------|-------------|
| | infl./effl. | infl./effl. | infl./effl. | infl./effl. | infl./effl. | infl./effl. |
| HCB | <0,05 | <0,01 | <0,05 | <0,01 | 0,18 | <0,01 |
| α -HCH | <0,05 | <0,01 | <0,05 | <0,01 | 0,06 | 0,02 |
| β -HCH | <0,05 | <0,01 | <0,05 | <0,01 | 0,07 | 0,02 |
| γ -HCH | 0,07 | 0,06 | 0,26 | 0,11 | 0,18 | 0,11 |

Table 6: mean concentrations of chlorophenols in influent and effluent of six municipal waste water treatment plants (in ug/l)

| | A | B | C | D | E | F |
|---------------------------|-------------|-------------|-------------|-------------|-------------|-------------|
| | infl./effl. | infl./effl. | infl./effl. | infl./effl. | infl./effl. | infl./effl. |
| 2,4,5-trichlorophenol | <0,1 | <0,04 | <0,1 | <0,04 | <0,1 | <0,04 |
| 2,4,6-trichlorophenol | <0,1 | 0,05 | <0,1 | 0,05 | <0,1 | 0,06 |
| 2,3,4,5-tetrachlorophenol | <0,05 | <0,02 | 0,06 | 0,07 | <0,05 | <0,02 |
| 2,3,4,6-tetrachlorophenol | 0,11 | 0,06 | 0,14 | 0,10 | 0,13 | 0,11 |
| pentachlorophenol | 0,46 | 0,43 | 0,75 | 0,50 | 0,76 | 0,65 |
| | | | | | 0,73 | 0,62 |
| | | | | | 0,67 | 0,41 |
| | | | | | 0,67 | 0,51 |
| | | | | | 0,67 | 0,19 |

Table 7: mean concentrations of PCB in influent and effluent of six municipal waste water treatment plants (in ug/l)

| | influent | effluent | numbers of samples measured above detection limits |
|-------|----------|----------|--|
| PCB 8 | 0,14 | 0,012 | 3 |
| 18 | 0,10 | 0,012 | 3 |
| 28 | 0,10 | <0,010 | 3 |
| 52 | 0,13 | 0,012 | 12 |

No other PCB are measured above detection limits:

influent: 0,1 ug/l; effluent: 0,01 ug/l

Table 8: mean concentrations of polycyclic aromatic hydrocarbons in influent and effluent of six municipal waste water treatment plants (in ug/l)

| | A | B | C | D | E | F |
|-------------------------|-------------|-------------|-------------|-------------|-------------|-------------|
| | infl./effl. | infl./effl. | infl./effl. | infl./effl. | infl./effl. | infl./effl. |
| fluoranthene | 1,01 | 0,029 | 1,18 | 0,044 | 0,72 | 0,048 |
| benzo(b)fluoranthene | 0,25 | 0,017 | 0,32 | 0,033 | 0,20 | 0,023 |
| benzo(k)fluoranthene | 0,14 | 0,014 | 0,16 | 0,015 | 0,12 | 0,013 |
| benzo(a)pyrene | 0,25 | 0,016 | 0,33 | 0,035 | 0,23 | 0,028 |
| benzo(g,h,i)perylene | 0,19 | 0,016 | 0,22 | 0,028 | 0,15 | 0,022 |
| indeno(1,2,3-c,d)pyrene | 0,16 | 0,012 | 0,18 | 0,019 | 0,11 | 0,015 |
| | | | | | 0,11 | 0,017 |
| | | | | | 0,37 | 0,011 |
| | | | | | 0,37 | 0,18 |
| | | | | | 0,37 | 0,013 |

Table 9: mean (and maximum)¹ concentrations of hazardous substances in sewage sludge of six municipal waste water treatment plants (in mg/kg dry weight)

| | A | B | C | D | E | F |
|----------------------------|-------------|-------------|-------------|-------------|-------------|-------------|
| | infl./effl. | infl./effl. | infl./effl. | infl./effl. | infl./effl. | infl./effl. |
| HCH | <0,05 | 0,06 (0,08) | <0,05 | 0,65 (1,0) | <0,05 | <0,05 |
| α -HCH | <0,05 | <0,05 | <0,05 | <0,05 | 0,08 (0,11) | <0,05 |
| 2,4,5-TrCP | <0,1 | <0,1 | <0,1 | 0,11 (0,13) | <0,1 | <0,1 |
| 2,3,4,5-TCP | <0,05 | <0,05 | <0,05 | <0,05 | 0,28 (0,41) | 0,09 (0,12) |
| 2,3,4,6-TCP | <0,05 | <0,05 | <0,05 | <0,05 | 0,06 (0,10) | <0,05 |
| PCP | <0,05 | <0,05 | <0,05 | <0,05 | 0,22 (0,36) | 0,30 (0,44) |
| PCB 6 isomers ² | 0,49 (0,59) | 0,66 (0,75) | 0,66 (0,76) | 0,68 (0,78) | 0,31 (0,43) | 0,21 (0,42) |
| 17 isomers | 0,88 (1,23) | 1,48 (1,62) | 1,07 (1,40) | 1,04 (1,43) | 0,41 (1,05) | 0,39 (0,99) |
| fluoranthene | 10,4 (14,3) | 4,4 (6,1) | 3,8 (5,7) | 2,6 (4,3) | 4,3 (11,6) | <1 |
| benzo(b)fluoranthene | 1,3 (2,0) | 1,2 (2,5) | <1 | <1 | 1,1 (1,5) | <1 |

 α -HCH and β -HCH are not measured in concentrations above 0,05 mg/kg dry weight;

2,4,6-trichlorophenol is not measured in concentrations above 0,1 mg/kg dry weight;

benzo(k)fluoranthene, benzo(g,h,i)perylene, benzo(a)pyrene and indeno(1,2,3-c,d)pyrene are not measured in concentrations above 1 mg/kg dry weight.

1) the maximum concentration has not been mentioned between brackets, when this concentration is equal to the median concentration

2) PCB 28,52,101,138,153 and 180 (Ballschmiter and Zell, 1980)

DISCUSSION

Volatile chlorinated hydrocarbons (VCH). The concentrations of the VCH in the influent and effluent fluctuate very strongly, especially for dichloromethane and 1,2-dichloroethane (figure 1). In this figure the minimum, maximum and mean concentration in the influent and effluent are set out against the median concentration. If concentrations were normally distributed, the mean concentrations would approximate the median concentration.

The difference between median and mean concentrations can be explained from incidental peak discharges by industries.

No correlation between the peak discharges and the quantity of the flow was found. A part of the VCH has originated from the traffic and wet and dry deposition. This is a conclusion from the results of installation B. Higher flows sometimes cause higher loads. The effect of washing out of sewer sludge after a dry period, a possible cause of higher influent concentrations, is not likely here, in view of the solubility of these substances in water. For most of the installations the share from deposition to total contribution appears to be small comparing industrial sources. There are however always local deviations from this general view.

VCH turn out to be present in most industrial waste water streams.

It appears that

- dichloromethane may be discharged by dyes, pharmaceutical and textile industries;
- trichloromethane by pharmaceutical and flavouring industries;
- dichloroethane by pharmaceutical industries and
- trichloroethane by textile industries.

With these results the occurrence of peak discharges, mentioned before, could be partly explained.

In table 12 the removal percentages of the VCH are mentioned. The average removal is 50-90%, which is in good agreement with the results of an American study (Patterson, 1981).

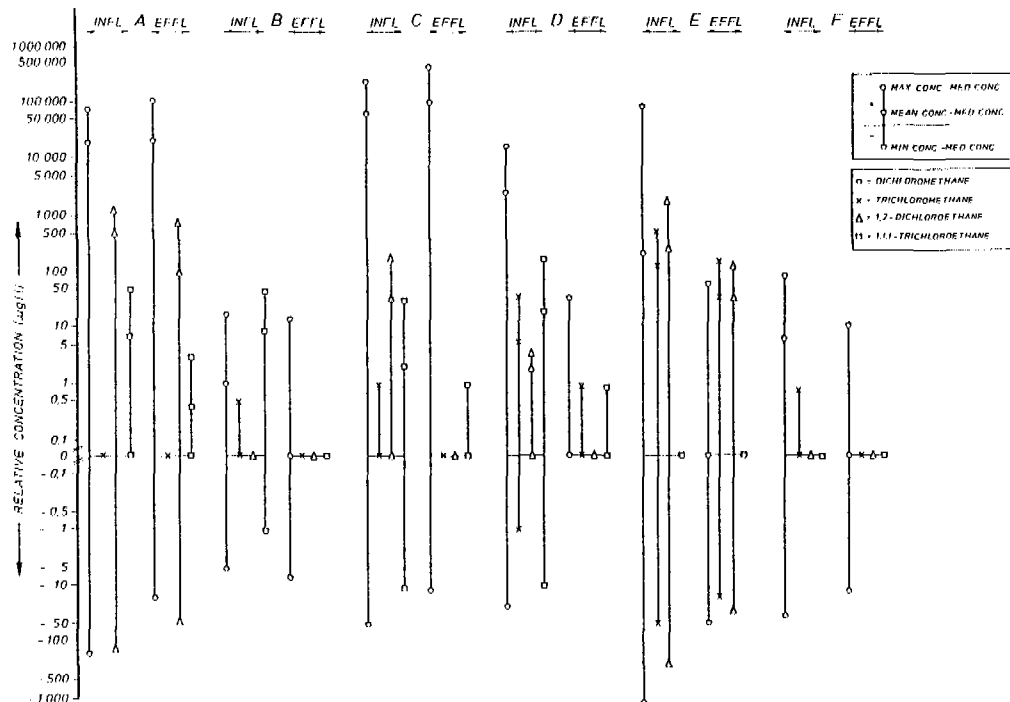


Figure 1: relative concentrations (in ug/l) of volatile chlorinated hydrocarbons in influent and effluent of six municipal waste water treatment plants (median concentration = o)

Table 10: total mean (median) loads of hazardous substances for different branches of industries
(in kg/year)

| substances | dichloromethane | trichloromethane | tetrachloromethane | 1,2-dichloroethane | 1,1,1-trichloroethane | trichloroethylene | tetrachloroethylene |
|---|-----------------|------------------|--------------------|--------------------|-----------------------|-------------------|---------------------|
| branche of industry (number of plants measured) | | | | | | | |
| chemical industry(9) | 650(135) | 380(200) | 260(210) | 9000(4000) | 1000(0) | 20(0) | 1000(150) |
| pharmaceutical industry(2) | 4300(1500) | 16(8) | 2(0,6) | 0 | 2(2) | 2(0,1) | 0,4(0) |
| dye industry(2) | 500(0) | 0,2(0) | 1(0,5) | 0 | 30(0) | 0,1(0) | 0 |
| textile industry(2) | 50(0) | 0 | 4(4) | 0 | 0 | 2000(2000) | 15(15) |
| rubber industry(2) | 1,5(1) | 0 | 0,1(0,1) | 0 | 0 | 0,03(0) | 0,03(0) |
| leather industry(1) | 20(15) | 0,03(0) | 1(0,6) | 0 | 0,1(0) | 0 | 0 |
| paper industry(2) | - | - | - | - | - | - | - |
| formulating industry(2) | - | - | - | - | - | - | - |

| | 1,2-dichlorobenzene | 1,4-dichlorobenzene | hexachlorobenzene | χ -hexachlorocyclohexane | Pentachlorophenol | polychlorinated biphenyls | polycyclic aromatic hydrocarbons |
|-------------------------------|---------------------|---------------------|-------------------|-------------------------------|-------------------|---------------------------|----------------------------------|
| chemical industry(9) | 0 0 | 300(300) | - | - | - | 1700(1500) | - |
| pharmaceutical industry(2) | 0 0 | - | - | - | - | - | - |
| dye industry(2) | 0 1(1) | 15(0,2) | - | - | - | - | - |
| textile industry(2) | 0 0 | - | - | 80(80) | 0 | - | - |
| rubber industry(2) | 0 0 | - | - | - | - | - | - |
| leather industry(1) | 0 0 | - | - | - | - | - | - |
| paper industry(2) | - - | - | - | 50(50) | 0 | - | - |
| formulating industry(2) | - - | - | 2(1) | - | - | - | - |

Non-volatile chlorinated hydrocarbons (NVCH) and chlorinated phenols. χ -HCH, 2,4,5,6-tetrachlorophenol and pentachlorophenol (PCP) are very commonly found in sewage. The supply of these substances is uniform as appears from calculations. These substances have also been found in comparable quantities at waste water treatment plants, where hardly any industrial waste water is treated. The conclusion could be that, for these substances in sewage, industries and households provide proportional contributions. The contribution from diffuse sources as traffic and deposition seems small in view of the small correlation with the influent flow.

The study of industrial waste water streams had shown that PCP and to a less extent 2,4,6-trichlorophenol, is ubiquitous.

The removal of chlorophenol in the treatment plants is moderate (20-40%). HCH's are removed for 40-65%. The removal of HCB is about 95%. These results can explain, as expected, the presence/absence of these substances in sewage sludge (table 9).

Table 11: survey of the presence of hazardous substances in industrial waste water from different industries.

| substance | trichloromethane | tetrachloromethane | 2,4,6-trichlorophenol | pentachlorophenol | hexachlorobenzene | polychlorinated biphenyls 1) |
|---|------------------|--------------------|-----------------------|-------------------|-------------------|------------------------------|
| branch of industry (number of plants measured) | | | | | | |
| slaughter(2) | + | + | + | + | + | - |
| dairy products(3) | + | + | + | + | + | - |
| fruits and vegetables(1) | + | + | + | + | - | - |
| margarine and fats(2) | 0 | + | 0 | + | + | + |
| sugar(1) | 0 | + | 0 | 0 | - | - |
| soft drinks and carbonated waters(1) | + | + | + | + | - | - |
| brewery(1) | 0 | + | + | + | - | - |
| textile(2) | + | + | + | + | + | + |
| leather(2) | 0 | + | + | + | - | - |
| paper, pulp and paperboard(2) | + | + | + | + | - | 0 |
| wood-impregnation (2) | 0 | + | 0 | + | 0 | 0 |
| printing(1) | 0 | 0 | 0 | + | 0 | 0 |
| painting(2) | 0 | + | + | + | + | - |
| soap and cleaning preparations(1) | + | + | 0 | + | 0 | + |
| rubber(2) | + | + | 0 | + | + | + |
| dye(3) | + | + | + | + | + | + |
| electroplating(4) | 0 | + | + | + | + | - |
| photographic laboratory(1) | - | + | 0 | + | - | - |
| laundry(1) | + | + | + | + | + | - |
| motor-overhaul(1) | 0 | + | 0 | + | 0 | + |
| hospital(1) | + | + | + | + | + | - |
| incineration of refuse(1) | 0 | + | 0 | + | 0 | 0 |

+= present in waste water

-= not detected in waste water

0= research has not been finished, no positive result until so far

1) (probably) one or more of the isomers: PCB 28,52,101,138,153 and 180
(Ballschmitter and Zell, 1980)

Table 12: percent removal of organic compounds in six municipal waste water treatment plants

| | mean | min. | max. | number of samples (max. 42) |
|--|------|------|------|--------------------------------|
| Volatile chlorinated hydrocarbons | | | | |
| . dichloromethane | 51 | 0 | 99,9 | 32 |
| . trichloromethane | > 70 | > 33 | > 97 | 14 |
| . 1,2-dichloroethane | 70 | 0 | 98 | 16 |
| . 1,1,1-trichloroethane | > 83 | > 50 | > 99 | 18 |
| . trichloroethylene | > 65 | > 55 | > 98 | 9 |
| . tetrachloroethylene | > 60 | > 50 | > 67 | 6 |
| . 1,2-dichlorobenzene | > 87 | > 67 | > 97 | 10 |
| . 1,4-dichlorobenzene | > 72 | | | 1 |
| Non-volatile chlorinated hydrocarbons | | | | |
| . hexachlorobenzene | 94 | > 90 | > 97 | 6 |
| . α -hexachlorocyclohexane | 63 | 45 | 78 | 7 |
| . β -hexachlorocyclohexane | 55 | 58 | 76 | 6 |
| . γ -hexachlorocyclohexane | 41 | 0 | 98 | 42 |
| Chlorinated phenols | | | | |
| . 2,4,6-trichlorophenol | 36 | 0 | 74 | 31 |
| . 2,3,4,5-tetrachlorophenol | 17 | 0 | 44 | 5 |
| . 2,3,4,6-tetrachlorophenol | 28 | 0 | 79 | 42 |
| . pentachlorophenol | 28 | 0 | 79 | 42 |
| Polychlorinated biphenyls | | | | |
| . PCB 8 | 90 | < 84 | > 95 | 3 |
| . PCB 18 | 88 | < 84 | < 90 | 3 |
| . PCB 28 | > 90 | > 90 | > 90 | 3 |
| . PCB 52 | 91 | 82 | 95 | 12 |
| Polycyclic aromatic hydrocarbons | | | | |
| . fluoranthene | 95 | 80 | > 99 | 37 |
| . benzo(b)fluoranthene | 90 | 75 | 99 | 35 |
| . benzo(k)fluoranthene | 90 | 73 | 99 | 26 |
| . benzo(a)pyrene | 88 | 68 | 99 | 35 |
| . benzo(g,h,i)perylene | 86 | 72 | 99 | 32 |
| . indeno(1,2,3-c,d)pyrene | 89 | 69 | 99 | 29 |

Polychlorinated biphenyls (PCB). PCB were incidentally detected in influent and effluent of waste water treatment plants. An exception is PCB-52, which is almost always present in the influent of installation D. PCB are nevertheless always present in sewage sludge (table 9). The apparent absence of PCB in influents is due to the high detection limits.

The concentrations of PCB in sewage sludge show hardly any difference per installation. PCB are probably ubiquitous in municipal as well as in industrial waste water.

The removal of the different PCB in the treatment plants was about 90%.

Sludge contains more PCB than sediment of the river Rhine and Lake IJssel on a dry weight basis. The PCB-concentration in Rhine and Lake IJssel-sediment is respectively 0,25 and 0,06 mg PCB/kg dry weight (Bruggeman, 1984). In this context with PCB the sum of the six isomers 28, 52, 101, 138, 153 and 180 is meant. The PCB-content of river sediments however is strongly dependent on the organic carbon content. Sediment contains about 2-9% organic carbon, sewage sludge about 40%.

Rhine-sediment and Lake IJssel-sediment contain respectively 5 and 1,25 mg PCB/kg org C (Bruggeman, 1984). Sewage sludge containing 1,25 mg PCB/kg org C is in this way comparable with Lake IJssel-sediment. This sediment is one of the less polluted sediments in the Netherlands.

Polycyclic aromatic hydrocarbons (PAH). PAH are commonly present in sewage. No peak discharges were found. The figures show that there is a certain correlation between the six examined PAH (table 8). In view of the above-mentioned one could assume that PAH are present in sewage at a background level.

A possible correlation between the load and the influent flow was observed. This relation is stronger than for the NVCH and chlorophenols.

The higher load at higher flow can be explained by the contribution of diffuse sources such as traffic and deposition and/or the washing out of sewer sludge.

The removal percentage in the plants is 85-95%. The most important mechanisms of removal are adsorption and evaporation (Van Starkenburg, 1981).

FURTHER RESEARCH

The accuracy of this kind of study should be increased, as one can see from this study.

It was not possible to make balances of the individual substances for the different treatment plants. For this an installation should be sampled at several points very frequently during a longer period, minimal the sludge-age.

A better insight needs be obtained into the composition of sewer-sludge. The influence of diffuse sources could then be estimated at its true value. The study of industrial waste water should be further intensified.

The source of industrial emissions is not always clear. A source could be the pollution of raw materials. Hazardous substances may also be formed as unwanted by-products during industrial processes. This item shall take a central place in the next years emission-studies of the Governmental Institute for Sewage and Waste Water Treatment. At the end of 1983 a rather extensive study into the formation of PCB during industrial chemical processes was started.

CONCLUSIONS

1. The study has given figures about the amount of hazardous components present in sewage and industrial waste water.
2. Volatile chlorinated hydrocarbons in sewage seem to originate mostly from industrial emissions. The amount of the emissions can fluctuate very strongly especially for dichloromethane and 1,2-dichloroethane.
3. Chlorofenols, γ -hexachlorocyclohexane, polychlorinated biphenyls (PCB) and polycyclic aromatic hydrocarbons are on a low basic level always present in municipal waste water and in many industrial waste water streams.
4. In addition to point sources there are also diffuse sources like deposition from the air and road traffic which are responsible for the extra pollution of sewage. In this study this is demonstrated especially for polycyclic aromatic hydrocarbons.
The research has to be continued to quantify this pollution.

5. In sewage sludge PCB and fluoranthene are always detected. Incidentally also hexachlorobenzene, 2,4,5-trichlorophenol, 2,3,4,6 tetrachlorophenol, pentachlorophenol and benzo(b)fluoranthene were present.
In this study it was not possible to make a complete balance of the fate of these substances in a treatment plant. For this purpose a more intensive research will be started.
6. The overall removal in the municipal treatment plants amounts to:
- | | |
|-------------------------------------|-----------|
| - volatile chlorinated hydrocarbons | 50-90% |
| - hexachlorobenzene | 95% |
| - hexachlorocyclohexanes | 40-65% |
| - chlorophenols | 20-40% |
| - PCB | about 90% |
| - polycyclic aromatic hydrocarbons | 85-95% |

REFERENCES

- Council directive of 4 May 1976 on pollution caused by certain dangerous substances discharged into the aquatic environment of the Community (76/464/EEC), Official Journal of the European Communities, No. L 129, 18.5.76.
- International convention concerning the protection of the Rhine against chemical pollution, International Rhine Commission, 3 December 1976.
- Commission communication to the Council on dangerous substances which might be included in List I of Council Directive 76/464/EEC, Official Journal of the European Communities, No. C 176, 14.7.82.
- Luin, A.B. van and Starkenburg, W. van (1983). Black List substances in industrial waste water (in Dutch).
H₂O, 16, 131-137.
- Patterson, J.W. and Kodukala, P.S. (1981). Biodegradation of Hazardous Organic Pollutants, CEP, April, 48-55.
- Ballschnitter, K. and Zell, M. (1980). Analysis of Polychlorinated Biphenyls (PCB) by Glass Capillary Gas Chromatography. Fresenius, Z. Anal. Chem. 302, 20-31.
- Bruggeman, W.A. (1984). PCB in Dutch surface waters and sediment (in Dutch)
RIZA (to be published).
- Starkenburg, W. van (1981). Polycyclic Aromatic Hydrocarbons: how to remove these PAH from waste water (in Dutch).
H₂O, 14, 537-540.

CONTINUOUS, AUTOMATIC DETECTION OF ORGANOPHOSPHATES AND CARBAMATES IN WATER UTILIZING ENZYME MICROCALORIMETRY

W. S. G. Morgan,* P. C. Kühn** and P. P. van Niekerk*

**National Institute for Water Research, Council for Scientific and Industrial Research, P.O. Box 395, Pretoria 0001, South Africa*

***National Electrical Engineering Research Institute, Council for Scientific and Industrial Research, P.O. Box 395, Pretoria 0001, South Africa*

ABSTRACT

An enzyme calorimetric method, employing immobilized cholinesterase to detect harmful levels of organophosphorus and carbamate insecticides in water, is described.

Immobilized cholinesterase activity was assessed automatically in a microcalorimeter by analyzing its catalytic efficiency in hydrolyzing a substrate solution which was passed over the enzyme at regular time intervals. A microcomputer was used to automate the procedure and for data acquisition.

The inhibitory effects of three organophosphorus and two carbamate pesticides upon cholinesterase were studied in order to evaluate the efficacy of the technique.

KEYWORDS

Water quality; water pollution; monitoring; enzyme microcalorimetry; cholinesterase; enzyme inhibition; organophosphates; carbamates; automatic pesticide detection.

INTRODUCTION

Industrial expansion, with the concomitant proliferation of chemicals, brings with it the danger that toxic substances will be released to surface waters in ever increasing quantities.

Such hazardous situations must be detected in time to avoid deleterious effects upon the aquatic environment and public health. For many water pollutants there is no automatic monitoring equipment available. This has led aquatic toxicologists to investigate techniques whereby the overall impact of pollution upon living organisms may be assessed. In recent years equipment has been developed for the continuous, automatic monitoring of the response of sensor fish to a wide variety of toxic influences (Morgan, 1977; Morgan, 1979; Cairns and Gruber, 1980; Cairns and van der Schalie, 1980). These systems have been successfully employed to monitor and control industrial effluent discharges to rivers and streams (Westlake and van der Schalie, 1976; Morgan *et al.*, 1982). However, living

organisms have an inherent capability of adapting to very low levels of stress, and therefore do not, in all cases, respond to toxic concentrations deemed harmful to human health over the long term. A non-living toxic hazard monitoring system could have many advantages in this respect.

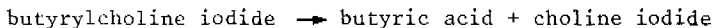
One of the most important mechanisms of toxic action is thought to be the poisoning of enzyme systems. Research was therefore initiated to develop a continuous monitoring system based on the automatic detection of toxic substances which inhibit enzymes.

This paper describes the use of a calorimetric technique to assess the inhibitory effects of organophosphorus and carbamate pesticides upon the enzyme cholinesterase, and discusses its application to environmental quality control.

THE DETECTION PRINCIPLE

Enzyme activity was determined by the use of flow microcalorimetry (Danielsson *et al.*, 1979), where the heat generated by a reacting substrate solution flowing through a calorimeter containing an immobilized enzyme preparation was measured. It has been shown experimentally (Monk and Wadsö, 1969) that the heat output rate for an enzyme reaction that is zero-order in substrate will give a recorded signal deflection proportional to enzyme activity. Enzyme inhibition may, therefore, be determined by a reduction in heat output rate.

The chemical reaction used to determine the activity of the immobilized enzyme was -



The enzyme (horse serum cholinesterase) hydrolyzed butyrylcholine three times as fast as acetylcholine, hence the use of the former as substrate (20 mM, prepared in phosphate buffer). Beezer and Stubbs (1973) stated that butyric acid reacts with a buffer solution in such a way that the enzyme/substrate reaction enthalpy is supplemented by the enthalpy of neutralization. Therefore, the heat output rate may have been enhanced through secondary reactions.

THE DETECTION DEVICE

The monitoring system comprised two main elements; an immobilized enzyme sensor unit and a data acquisition module incorporating control functions for the cyclic injection of test solutions (Fig. 1).

The Enzyme Sensor

The microcalorimeter employed (Fig. 2) was similar to that described by Danielsson *et al.* (1976), consisting of a glass column of 2 ml bed volume containing the immobilized enzyme preparation. The column was placed in a perspex barrel, leaving a small airspace between the column and the barrel for thermal insulation, an arrangement which also simplified the interchange of columns. Cotton wool was used as a bed support as well as being packed into the top of the column around the thermistor to hold the bed in position. A Negative Temperature Coefficient thermistor probe (Phillips No. 2322-627-1142, 4 700 Ω) was mounted in a removable perspex holder which fitted into the barrel in such a way that the probe was situated well into the packed column bed, so as to give an even temperature signal. All joints were O-ring sealed. A heat exchanger, constructed from

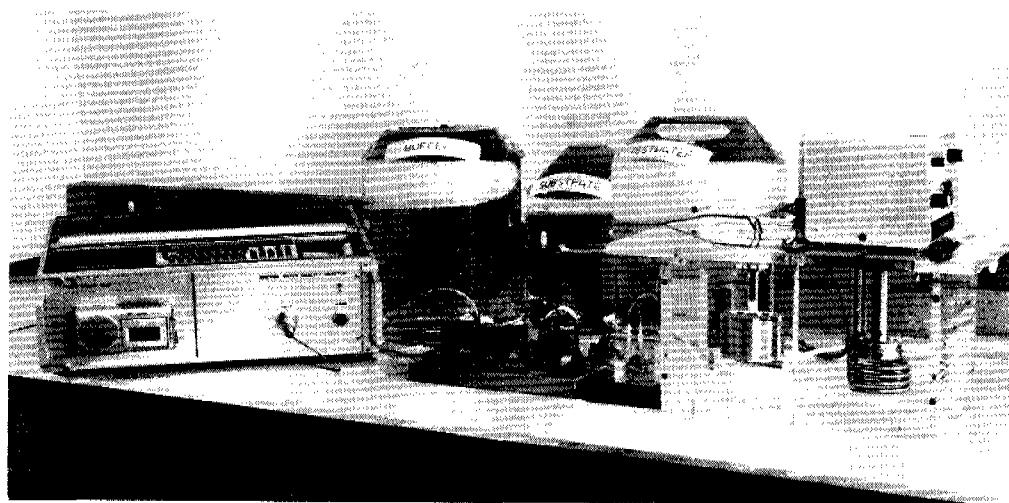


Fig. 1. Equipment set-up showing (from L to R) electronic data acquisition and control module, test solutions (behind) and solenoid valve array (front), and enzyme microcalorimeter in temperature controlled water bath

stainless steel capillary tubing (internal diameter 0.75 mm; length 250 mm) was placed immediately before the column in order to thermally equilibrate solutions before entry into the column. The unit stood on a stainless steel cylinder which enclosed the thermal equilibration coil, providing added thermal stabilization. The apparatus was almost totally immersed in a water bath maintained at a temperature of 27 ± 0.02 °C by an immersion circulator (Model P, Julabo Labor-technik, Seelbach, FDR). Buffer, substrate and test solutions were pumped through an automatically controlled solenoid valve array at a flow rate of approximately 2 ml/min. The temperature of a freshly prepared column stabilized within 30 min when buffer was allowed to flow continuously through the enzyme preparation.

The enzyme preparation was immobilized onto controlled pore glass (CPG), a support which is well characterized, has a high enzyme-binding capacity, is stable under pressure and is not attacked by micro-organisms. Glutaraldehyde and γ -aminopropyltriethoxysilane were used to activate the CPG-10 beads (120/200 mesh, 631 Å diameter). The preparation of the alkylamine glass and its subsequent derivatization were carried out according to the procedure of Weetall and Filbert (1974), using 2.5% glutaraldehyde in phosphate buffer (0.1 M, pH 7). Approximately 5.0 mg of enzyme (horse serum cholinesterase, 218 U/mg) were added to 2 g of the activated glass in phosphate buffer and coupling was allowed to continue for 2.5 h at 4 °C.

Data Acquisition and Control

The heat reaction in the microcalorimeter, when the substrate is passed through the enzyme preparation, causes temperature peaks in the range 0.01 to 1.0 °C. The sensor is a thermistor with a nominal value of 4.7 kΩ at 25 °C. This device exhibits a temperature coefficient at 125 Ω/°C for small excursions in temperature. This means that a temperature change of 0.1 °C results in a resistance change of 12.5 Ω/°C.

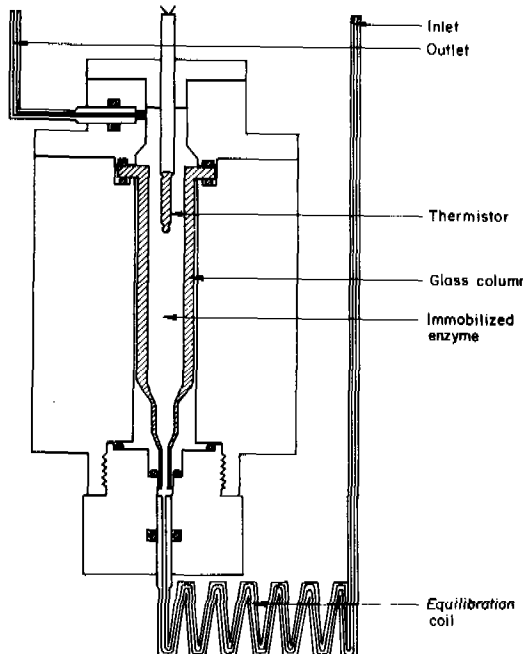


Fig. 2. Enzyme microcalorimeter

The resistance change is measured by passing a current with a stability of better than 100 parts in 10 through the thermistor and measuring the voltage drop across it. This is carried out by a precision current source (Fig. 3). The change in voltage across the sensor is amplified by a differential chopper stabilized amplifier stage with a temperature stability of better than 40 parts in 10^6 per $^{\circ}\text{C}$. This provides an output voltage change of 100 mV per $^{\circ}\text{C}$. It was found that fluctuations due to noise amounted to the equivalent of 0.003 $^{\circ}\text{C}$. Because of the high sensitivities involved, the circuitry exhibits baseline drift due to small fluctuations in the operating temperature. This is overcome by means of an automatic baseline correction scheme whereby a microcomputer controls a 12-bit digital-to-analogue converter (DAC), whose output provides a compensating signal to control the zero offset of the amplifier. The computer, by sending instructions to the DAC, can thus achieve automatic baseline correction (Kühn and Morgan, 1983).

Accordingly, the data acquisition and control functions fall into five general categories:

- Analogue-to-digital conversion of the processed thermistor signal.
- Digital-to-analogue conversion of the auto-zero signal.
- Timed control of the three solenoid valves.
- Keyboard entry of certain test parameters.
- Manipulation of measured data and printout of results.

These functions were all realized by using a programmable data acquisition and control unit recently developed at our laboratories for general-purpose use in a research environment. The unit consists of an eight-bit analogue-to-digital converter, a microcomputer with keyboard and liquid crystal display (programm-

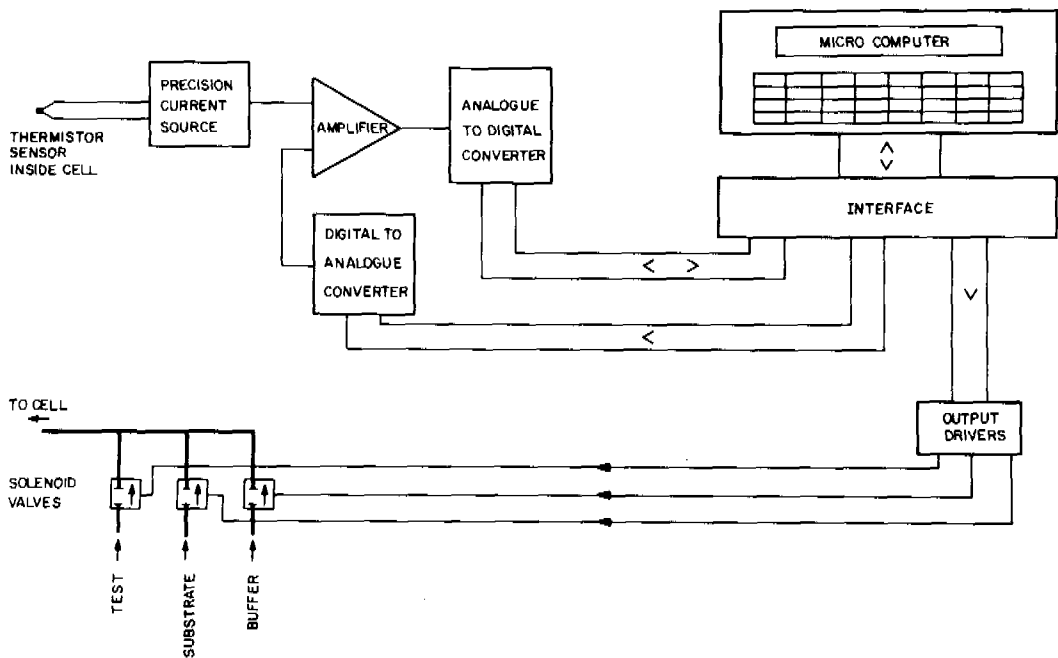


Fig. 3. Functional diagram

able in BASIC), a four-colour graphics printer/plotter and a cassette tape recorder for program and data storage.

The unit was customized by mounting the analogue and DAC circuitry, together with their power supplies, inside the unit and configuring three 230 V output driver modules to actuate the three solenoid valves, and one 12 V dc module to activate an external alarm.

The output signal from the analogue circuitry is applied to an eight-bit analogue-to-digital converter (ADC). This gives a basic resolution of 0.4% of full scale. The input sensitivity of the ADC can be set as desired - it is at present configured for 250 mV full scale. The amplitude of the analogue signal can thus be measured by the computer at any time via the interface and A/D converter, the smallest detectable temperature change being 0.01 °C with the present settings.

A 12-bit DAC is also connected to the computer via the interface and its analogue output is used to provide the automatic baseline correction (auto-zero).

Three ac solid-state relay modules provide for control of the three solenoid valves under computer control, and a fourth dc output module allows for activating the external alarm. A cassette tape recorder is incorporated in the instrument for program and data storage.

When the program is started, a menu appears on the display panel giving the user a choice of functions. These include 'NML', which executes a normal program; 'TIM', which allows for changing the solenoid valve timing parameters; 'CHT', which executes the normal program, and in addition plots a chart of the temperature peak while it is being monitored; and 'TAPE', which allows for data storage on cassette tape.

If the 'TIM' function is selected, the user is prompted through the process of determining the existing timing parameters and changing them, if required. Should either 'NML' or 'CHT' be selected, the user is prompted to enter certain parameters on the keyboard. These include date; type of toxicant and its concentration; and any general remarks about the specific test batch, as well as the required scaling factor.

The microcomputer initiates a test series as soon as the requisite parameters have been entered, and performs the automatic baseline correction routine whilst the test solution is passing through the cell. When the substrate solution passes through the cell, the computer begins to take a series of 100 samples at 2 s intervals of the peak amplitude in millivolts, which it stores in memory. If the 'CHT' function has been selected, then each value will also be plotted on a calibrated X-Y axis to form a chart recording of the temperature peak.

When the sampling period is over, the computer again measures the baseline value. If this has drifted from the initial residual value after auto-zero, the slope of the drift is automatically computed. The 100 sampled values are used to calculate the peak area which is corrected for residual baseline error and drift by the computer. The corrected peak area is then printed out, together with the number of the test. The area is printed in millivolt-second units.

At the end of each measurement cycle, the program returns to a point indicated on the flow diagram (Fig. 4) in order to continue with the next in a series of tests.

Throughout the above operations, messages are flashed onto the display panel to inform the user of the program status as well as the values of the measurements being taken.

DETECTION PROCEDURE AND SYSTEM EVALUATION

The test solution was allowed to flow through the enzyme column for a period of 5 min, followed immediately by the substrate, a 30 s pulse of butyrylcholine iodide (20 mM). Phosphate buffer was then used to flush the column until the temperature response, due to the heat of reaction, as measured by the signal output, had dissipated. This was indicated by the re-establishment of a stable baseline, a procedure which was accomplished in 3.5 min, providing a full cycle of 9 min. The cycle was repeated continuously, peak heights and areas being measured and graphically plotted against exposure time. An alarm status was initiated at a 50% decrease in original heat response. The inhibitory effects of Metasystox R [0-O dimethyl S-2-(ethylsulphinyl) ethyl phosphorothioate] DDVP [2,2-dichloro-vinyl dimethyl phosphate]; Lebaycid [50% Fenthion-0,0-dimethyl 0-([4-methyl-thio]-m-toly1) phosphorothioate]; Carbaryl [1-naphthyl methyl carbamate] and Carbofuran [2,3-dihydro-2,2 dimethyl-benzofuran-7-yl methyl carbamate], on cholinesterase, were studied. The pesticides were used as pure formulations (Polyscience Corp., Niles, Ill., USA) dissolved in hexane, a solvent which had no inhibitory effects upon cholinesterase under control conditions.

Subsequent to thermal equilibration of the enzyme preparation, an assay scheme such as that depicted in Fig. 5 was used to assess the inhibitory effects of the various nominal pesticide concentrations employed. A series of approximately ten cycles were carried out to establish a 100% activity value for the enzyme preparation, exposed to solvent only. Thereafter a nominal pesticide concentration was established in the test solution and cyclic injection of test, substrate and buffer continued until enzyme activity had decreased to 50% of its original value.

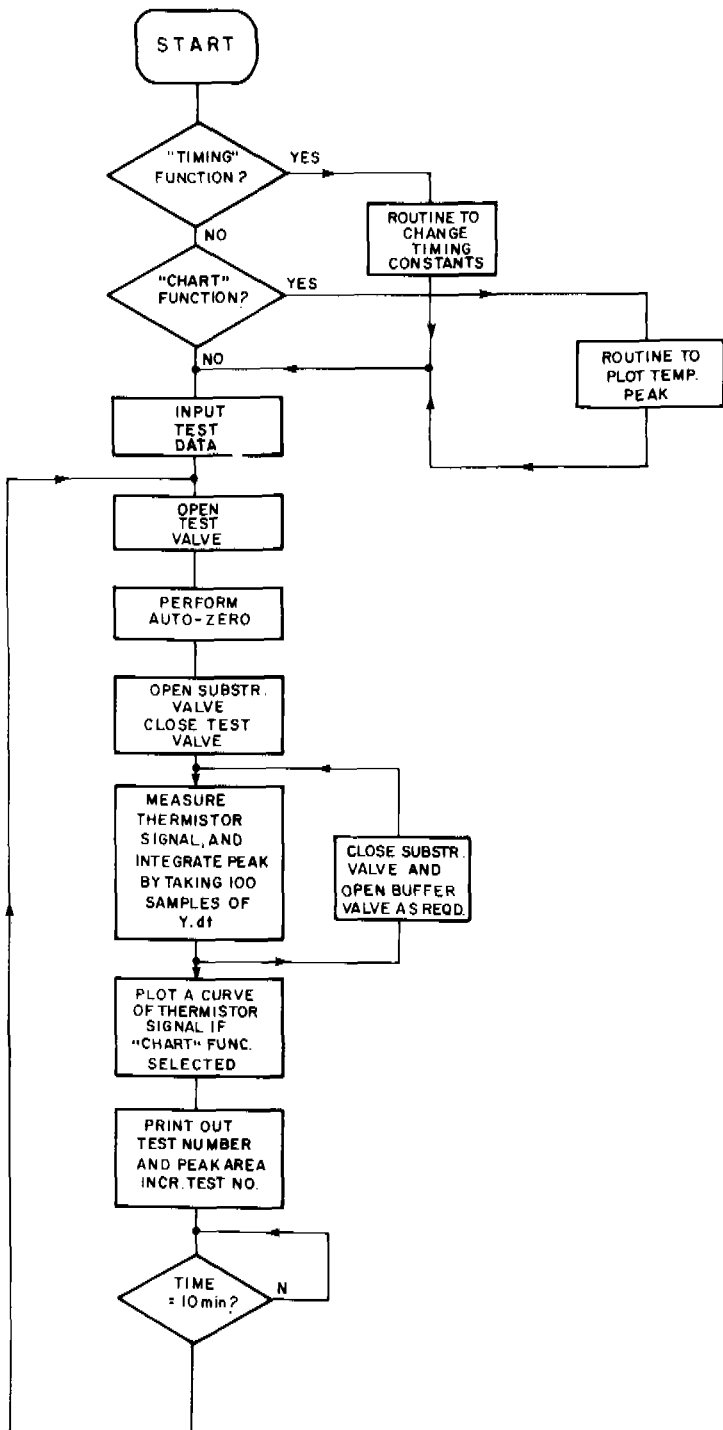


Fig. 4. Flow diagram

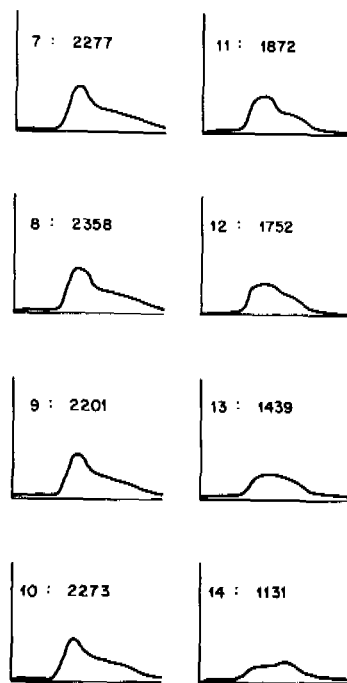


Fig. 5. Calorimetric records before (7 to 10) and after (11 to 14) exposure of cholinesterase to 10 mg DDVP/l

Inhibition of the cholinesterase was reflected by a lower response to the substrate pulse following administration of the test sample. Enzymatic degradation could be assessed by a visual observation of peak height. However, it was found that integration of the temperature peaks provided a better linear relation to substrate concentration and supplied more accurate data than peak height.

Fig. 6 depicts the inhibitory effects of various pesticide concentrations on cholinesterase activity. All pesticides inhibited enzyme activity to a greater or lesser extent with respect to exposure time, depending upon the concentration employed. The fact that higher concentrations inhibited enzyme activity in a shorter period of time would be of advantage when continuously assessing water quality. It would be possible, in an operative monitoring situation, to program the microcomputer to assess the slope of an inhibition curve to provide an estimate of hazard.

The large number of cycles required for detection, at 50% enzyme inhibition, of very low concentrations of pesticides (Table) may be considered as providing too great a time-lag for effective monitoring. Although the alarm status may be set at any arbitrary degree of enzyme inhibition, the degree of sensitivity established by producing an automatic alarm at the 50% enzyme inhibition level would, in our opinion, be adequate for the protection of individuals using water supplies. For example, the LD₅₀ of DDVP for man has been assumed to be 6 mg/kg (Heath, 1961). A man weighing 70 kg would need to consume 4 200 l of water containing 0.1 mg/l of DDVP to receive the LD₅₀ dose in the time taken to detect that quantity (approximately 24 h).

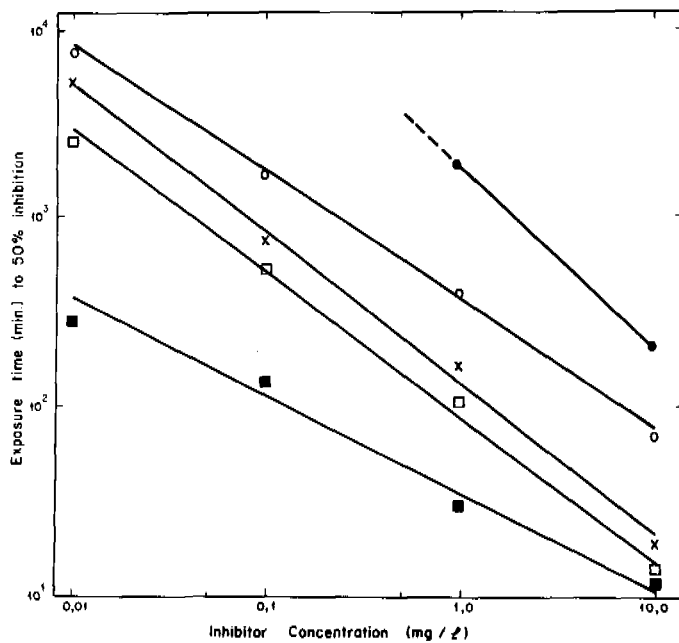


Fig. 6. Inhibition of cholinesterase by Metasystox R ($\square - \square$), DDVP ($x - x$), Lebaycid ($o - o$), Carbaryl ($\bullet - \bullet$) and Carbofuran ($\blacksquare - \blacksquare$). Log exposure time to a 50% decrease in enzyme activity is plotted versus log inhibitor concentration

TABLE Relationship between Exposure Time to 50 % Enzyme Inhibition (ET_{50}) and Pesticide Concentration

| Pesticide | Chemical type | Conc. (mg/l) | ET_{50} | No. of cycles |
|--------------|-----------------|--------------|-----------|---------------|
| Metasystox R | Organophosphate | 10.0 | 13.8 | 3 |
| | | 1.0 | 104.7 | 21 |
| | | 0.1 | 512.8 | 103 |
| | | 0.01 | 2 511.9 | 502 |
| DDVP | Organophosphate | 10.0 | 18.7 | 4 |
| | | 1.0 | 161.0 | 33 |
| | | 0.1 | 714.0 | 143 |
| | | 0.01 | 5 248.0 | 1 050 |
| Lebaycid | Organophosphate | 10.0 | 71.0 | 15 |
| | | 1.0 | 385.0 | 77 |
| | | 0.1 | 1 666.0 | 333 |
| | | 0.01 | 7 716.0 | 1 543 |
| Carbaryl | Carbamate | 10.0 | 200.0 | 40 |
| | | 1.0 | 1 842.0 | 369 |
| Carbofuran | Carbamate | 10.0 | 12.2 | 2 |
| | | 1.0 | 30.5 | 6 |
| | | 0.1 | 132.0 | 27 |
| | | 0.01 | 277.0 | 55 |

CONCLUSIONS

The preliminary investigation has demonstrated the feasibility of developing a monitoring system which will automatically detect many hazardous substances present in the environment. Initial experimentation has suggested that specific enzymes may be utilized to detect heavy metals (urease, invertase), phenolic compounds (tyrosinase), cyanide (rhodenase) and carcinogenic aromatic amines (horseradish peroxidase). A search for enzymes inhibited by specific toxicants is a logical step in the future development of the monitoring system. The enzymes selected could be immobilized and incorporated into a multi-enzyme detection system which may afford greater analytical specificity than can be achieved using biological sensors. In this context it should be pointed out that after the detection of a changed temperature signal the nature of the inhibiting material could be determined by conventional analytical procedures, such as atomic absorption spectroscopy, as it will remain bound to the enzyme column material.

Utilization of a microcomputer has made the instrumentation sufficiently flexible to cope with the changing demands of such a research program. It is quite possible to totally reconfigure the machine by changing the software. This can be done directly from the keyboard on the instrument by anyone with a knowledge of BASIC and the parameters of the system. It is also possible to add software to perform data analyses, for example to compare multiple sets of data, which should prove most useful once a database has been compiled.

ACKNOWLEDGEMENTS

We wish to acknowledge the contributions made by A.G.E. Webb and C.G. Hulme (National Electrical Engineering Research Institute (NEERI)) in the development of the data acquisition and control module, A.J. Hassett (National Institute for Water Research (NIWR)) for valuable advice on pesticide formulations and C.J. van Niekerk (NIWR) for assistance with the analyses. The paper is published with the approval of the Chief Directors of the NEERI and NIWR, whom we thank for their encouragement and support.

REFERENCES

- Beezer, A.E. and Stubbs, C.D. (1973). Application of flow microcalorimetry to analytical problems. I. Determination of organophosphorus pesticides by inhibition of cholinesterase. *Talanta*, 20, 27-31.
- Cairns, J. Jr and Gruber, D. (1980). A comparison of methods and instrumentation of biological early warning systems. *Wat. Resour. Bull.*, 16, 261-266.
- Cairns, J. Jr and van der Schalie, W.H. (1980). Biological monitoring. Part 1. Early warning systems. *Wat. Res.*, 14, 1179-1196.
- Danielsson, B., Gadd, K., Mattiasson, B. and Mosbach, K. (1976). Determination of serum urea with an enzyme thermistor using immobilized urease. *Analytical Letters*, 9, 987-1001.
- Danielsson, B., Mattiasson, B. and Mosbach, K. (1979). Enzyme thermistor analysis in clinical chemistry and biotechnology. *Pure and Appl. Chem.*, 51, 1443-1457.
- Heath, D.F. (1961). *Organophosphorus Poisons*. Pergamon Press, New York.
- Kuhn, P.C. and Morgan, W.S.G. (1983). Monitoring water quality by the electronic detection of enzyme inhibition. In: *Power and Control in Water Management*, D. Gilbert and M. Crabtree (Eds). Vector/Pulse, South Africa.
- Monk, P. and Wadsö, I. (1969). Flow microcalorimetry as an analytical tool in biochemistry and related areas. *Acta. Chem. Scand.*, 23, 29-36.

- Morgan, W.S.G. (1977). An electronic system to monitor the effects of changes in water quality on fish opercular rhythms. In: *Biological Monitoring of Water and Effluent Quality*, John Cairns Jr., K.L. Dickson and G.F. Westlake (Eds). ASTM STP 607, American Society for Testing and Materials. pp. 38-55.
- Morgan, W.S.G., Kühn, P.C., Allais, B. and Wallis, G. (1982). An appraisal of the performance of a continuous fish biomonitoring system at an industrial site. *Wat. Sci. & Tech.*, 114, 151-161.
- Weetall, H.H. and Filbert, A.M. (1974). Porous glass for affinity chromatography applications. In: *Methods in Enzymology*. 34, S.P. Colowick and W.O. Kaplan (Eds). Academic Press, New York. pp. 59-72.
- Westlake, G.F. and van der Schalie, W.H. (1976). Evaluation of an automated biological monitoring system at an industrial site. In: *Biological Monitoring of Water and Effluent Quality*, John Cairns Jr., K.L. Dickson and G.F. Westlake (Eds). ASTM STP 607, American Society for Testing and Materials. pp. 30-37.

BIOLOGICAL WATER QUALITY ASSESSMENT

BIOLOGICAL ASSESSMENT OF WATER QUALITY IN RUNNING WATER USING MACROINVERTEBRATES: A CASE STUDY FOR LIMBURG, THE NETHERLANDS

Harry H. Tolkamp

*Limburg Water Pollution Control Authority (LWPCA), Dept.
Hydrobiology, P.O. Box 314, 6040 AH Roermond, The Netherlands*

ABSTRACT

To obtain suitable biological methods for evaluating water quality several methods were applied to the macroinvertebrate composition of streams in the southern region of the province of Limburg (the Netherlands). After evaluation of the results through comparison followed by elimination of unsuitable methods (e.g. Trent Biotic Index, Indice Biotique, Indice de Qualité Biologique Globale) four methods remained promising: the Saprobiic-index, the Quality-index, the BMWP-aspt and the Chandler-aspt. A further selection of methods must be carried out in combination with a typological classification of the streams concerned, including a description of the achievable range for each method. To this end more research in the field of stream typology is needed, especially for the province of Limburg with its high diversity of streams.

KEYWORDS

Biological assessment; Saprobiic-index; Biotic-index; Macroinvertebrates; Stream typology; Water quality.

INTRODUCTION

The biological investigation of the aquatic environment, especially that of running water, by the Limburg Water Pollution Control Authority started in 1980 with two main objectives. First, to obtain an assessment of the water quality on a biological basis using macroinvertebrates in relation to water pollution by organic wastes and the measures taken by the authority to reduce these by an active and passive water pollution control policy. Secondly, to collect data on all running waters present in the area administered as a basis for a typology of running waters, i.e. to obtain reference macroinvertebrate communities characteristic for the various types of waters present, such as springs, spring-streams, brooks, streams and rivers. Such reference communities or biocenotic entities are necessary for the assessment of the scientific value of running waters in relation to nature conservation, measures planned by the riverboard responsible for the management of hydrological aspects, etc., as well as for the definition of the 'best' achievable macroinvertebrate community in a certain type of running water (an objective water quality standard).

In the Netherlands only one method of biological assessment was developed for lowland streams (Moller Pillot, 1971), a method expanded by a quantitative index by Gardeniers and Tolkamp (1976). Many methods of biological assessment developed elsewhere are available for use in running water, however. Most of these methods were developed in a restricted geographical area or a certain type of stream. These are therefore not suitable in other areas or other stream types, without local or typological modifications and adaptations, which can only be made on the basis of an extended research. Thus a third objective emerged, that is testing various potentially suitable methods for biological assessment in relation to the various types of running water. In combination with the construction of a typology of running waters on the basis of the macroinvertebrate community for unpolluted waters and the description of the best achievable community for each type of stream under a certain type of disturbance (such as organic pollution, channelization, etc.), it should be possible to select a suitable method of assessment for each type of running water. Or, at those situations where this is impossible, an indication should be given of the kind of research necessary to reach such a choice or to enable a modification of existing methods or the creation of a new method of assessment.

This means that the first objective of the ecological research by the LWPCA is that of the assessment of the water quality of the running waters on an ecological basis. This can only be of a preliminary nature until a stream-typology is available, including a description of the best achievable macroinvertebrate community at different levels of disturbance upon which specific assessment methods are chosen and/or developed.

STUDY AREA AND METHODS

During research in the province of Limburg since 1980 about 850 macroinvertebrate samples were taken in nearly every running water. Not all samples have been fully processed yet. This paper is based on the data collected for the streams in the southern part of the province (88 samples) and the borderstreams between Limburg and Germany (128 samples). The latter were sampled in spring and autumn of 1980 until 1983 at 16 stations. The river Geul was sampled at four stations during 10 months in 1980 and at 10 sites in a longitudinal series on one occasion in September 1980. All other streams were sampled once in spring at at least two stations, with an average of 2-3 km between sites, in 1980, 1981 and 1982.

Macroinvertebrate samples were taken with the standard handnet (30 cm wide with 0,5 mm mesh openings) which was used in upstream direction for kick-sampling (5 areas of 0,5 m length) or push-sampling through the top layer of softer bottoms (a total of 5 m length). When necessary a combination of both methods was used. In areas where both methods failed, hand-collecting substratum and hand-picking animals from larger objects was used, e.g. in some springs.

Macroinvertebrates were collected quantitatively except for very numerous taxa, of which a considerable portion (preferably one hundred specimens) was collected to ensure that all possible species were included, while the remaining numbers were counted or estimated.

All animals were stored in 80% ethanol except for flatworms which were identified alive. Identification was carried out to the highest taxonomical level possible with the available keys (mostly species level).

ASSESSMENT METHODS

Methods of biological assessment can be classified as one of the three principal approaches of the condition of the aquatic ecosystem. The saprobic-approach uses the total aquatic community as an indicator for the degree of organic pollution and is probably the best known through the saprobic system with the saprobic-in-

dex. The diversity-approach uses the species-richness as a measure for a difference with the natural situation (diversity-index). The biotic-approach uses diversity on the basis of certain taxonomical groups in combination with the pollution indication of individual species or higher taxa or groups. This concerns systems using a biotic-index, a combination of a saprobic-index and a diversity-index.

In this paper only methods using the saprobic-system or the biotic-system are tested. The use of diversity as a single instrument to measure differences in water quality is considered to be of limited value. Of the numerous methods available for biological assessment of water quality on the basis of macroinvertebrates, those potentially suitable for use in the Limburgian streams are listed in Table 1. This does not mean that all other methods are considered to be unfit. It means that it is expected that this selected collection includes sufficient differences within representatives of available methods using structural characteristics of the macroinvertebrate community.

TABLE 1. Methods of biological assessment applied to the Limburgian streams and considered in this paper

| System/Method | Symbol | References |
|--|---------------------------------|--|
| SAPROBIC SYSTEMS | | |
| Saprobic-index *1 using abundance (n) | S _h | Sládecěk (1973); LWA-NW (1982) |
| using numbers (n) | S _n | |
| Quality-index *1 | K ₁₃₅ | Gardeniers and Tolkamp (1976); Tolkamp and Gardeniers (1977) based on Moller Pillot (1971) |
| BIOTIC SYSTEMS | | |
| Trent Biotic Index | TBI | Woodiwiss (1964) |
| Expanded Biotic Index | EBI | Woodiwiss (1978) |
| Indice Biotique *2 | IB/IB-1 IB+1 | Tuffery and Verneaux(1967) |
| Indice de Qualité *2 Biologique Globale | IQBG/IQBG-1 IQBG+1 | Verneaux and Faessel (1976) |
| Chandler-score | Chandler-score Chandler-aspt | Chandler (1970) Jones (1973) |
| Biological Monitoring Working Party-score | BMW-score BMW-aspt | ISO-BMWP (1979; modified: 1980) Armitage et al. (1983) |

*1: using own expanded indicator spp. lists d.d. 30-3-1983 (LWPCA, unpubl.).

*2: excluding (-1) and including (+1) spp. with only one specimen.

RESULTS AND DISCUSSION

For the selection of methods suitable for the province of Limburg a choice will be made by using a system of elimination. The application of all methods listed in Table 1 to the data collected in the drainage area of the river Geul (Fig. 1) revealed that it is better to avoid the use of such a large number of methods (Tolkamp, 1984). Main reason is the fact that some methods were modified or changed and that these were true improvements, making the original obsolete. This concerns the TBI, the original BMW-score and BMW-aspt (based on values ranging from 1 - 100 in contrast to 1 - 10 in recent modifications). In fact it also con-

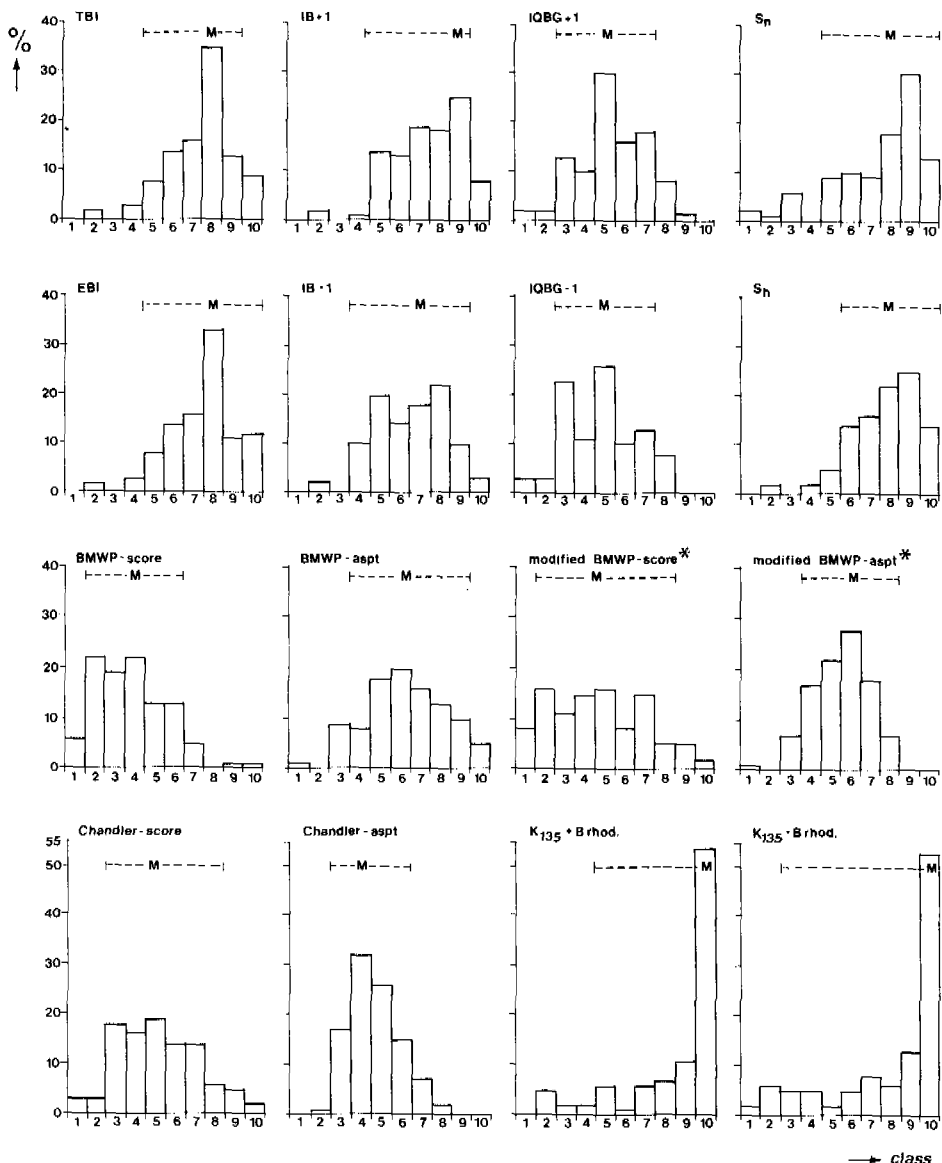


Fig. 1. Frequency distribution over 10 classes of 16 biological assessment indices in 88 samples from the drainage area of the river Geul. M indicates the median class and the horizontal line indicates the range for 80 % of the samples (from Tolkamp, 1984). *: In this paper the modified BMWP-score/aspt is referred to as the BMWP-score/aspt since the original score has been abandoned by the ISO.

cerns the scores of Chandler and BMWP because the aspt (average score per taxon) is better suited for biological assessment because the maximum is not unending but limited to 10.

A further aid in this selection process was obtained by the application of these methods to the data of 14 stations sampled September 8, 9 and 10, 1980 in the Geul from spring-stream to lower course. These results are presented in Fig. 2, not

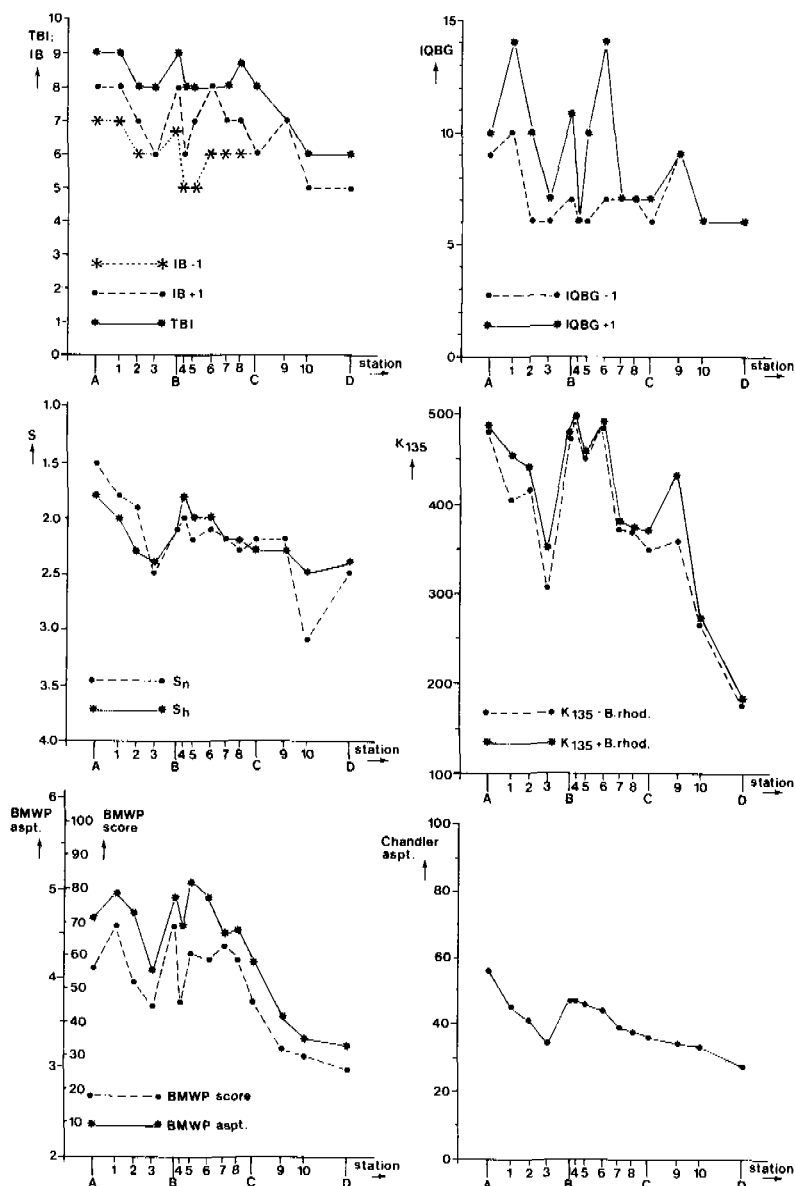


Fig. 2. Application of several biological assessment methods to the river Geul for a series of 14 samples taken in September 1980. A = km 7.5; B = km 21; C = km 34; D = km 50.

including the EBI because it hardly differed from the TBI (only 2 out of 50). An extra differentiation of the K_{135} -index, introduced in an earlier research (Tolkamp, 1984) (excluding *Baetis rhodani* as an indicator species) was also applied to these data but this did not lead to important differences.

All indices included in Fig. 2 show a similar trend from stations A to D. The water quality deteriorates between stations A and 3km, improves hereafter to almost the original level at station B, after which it gradually deteriorates further and further to station D. This general trend can also be seen in the chemical data on the water quality which show e.g. an increase of the average ammonia-N content of 0.3 mg/l at station B to 0.9 mg/l at station D in 1981, as well as an increase of total-phosphorus-P from 0.4 to 0.8 mg/l. Average BOD did not increase significantly between these stations (from 4 to 5 mg/l) nor did the oxygen saturation decrease very much (from 92 to 84 %).

Comparing the variations of the indices at the sampling stations relative to each other, some interesting differences in the trends are shown. Differences that could be important considering the goal: finding methods which can serve as a tool for the discrimination of different levels of water quality.

Comparison of the three biotic-indices TBI, IB-1 and IB+1 shows that the TBI does not vary more than one class from stations A to C, while IB+1 and IB-1, both vary strongly on this stretch, although IB-1 shows less variations. The latter is caused by the very fact that species occurring singly are excluded, levelling down the potential variations. There is a plausible explanation of this event, a matter already discussed by Bloesch (1980) as the so-called 'insect-effect' of biotic-indices of this kind. These methods rely heavily on the presence/absence of a few insect orders in the higher quality classes (i.e. Plecoptera, Ephemeroptera, Trichoptera) without accounting for the differences of the individual species (or more generally: taxa) within these orders. In fact the same explanation fits the large variation of the IQBG+1 from station A to station 7 and the almost constant values downstream of station 2 (except station 9) for IQBG-1.

Knowing pollutional state of the river Geul from source to confluence, i.e. by having knowledge of sources of pollution as effluent, tributaries, storm-water discharges of sewer-systems, confirmed by the monthly measurements of many chemical water quality parameters, it can be concluded that the biotic-indices (TBI, IB-1, IB+1, IQBG-1, IQBG+1) tested for this small river are not suitable for the description of the water quality, not even in a relative sense. Although not yet defined in an objective way the other four methods produce a trend that agrees with the expectations.

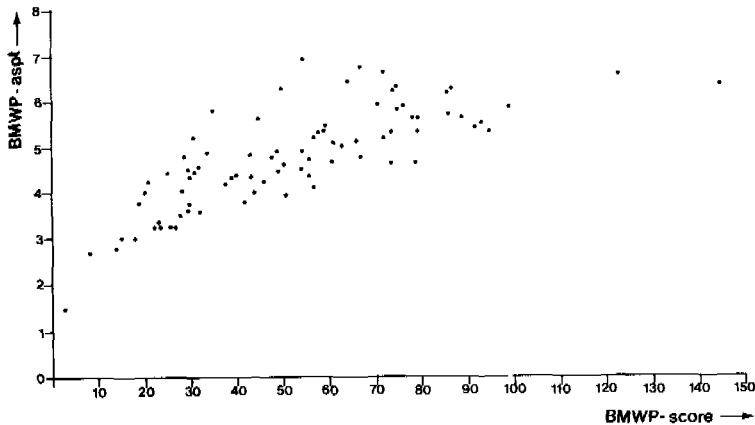


Fig. 3. The relationship between the BMWP-score and the BMWP-aspt for the tributaries of the river Geul.

At the same time it can be seen that the use of an abundance-scale in stead of real numbers of specimens (S_h as opposed to S) does temper down the differences caused by the abundant species in unpolluted waters and polluted waters, while it is of no great importance in the middle range.

There is practically no difference between the BMWP-score and the BMWP-aspt, which contrasts with the conclusions of Armitage et al. (1983) as well as the observations in the tributaries of the Geul (Fig. 3). However, since there are no differences for the Geul data and since the aspt should be preferred because then the height of the index is 'independent' of the number of taxa included, the BMWP-score can be omitted as a suitable index. Similar reasons can be put forward con-

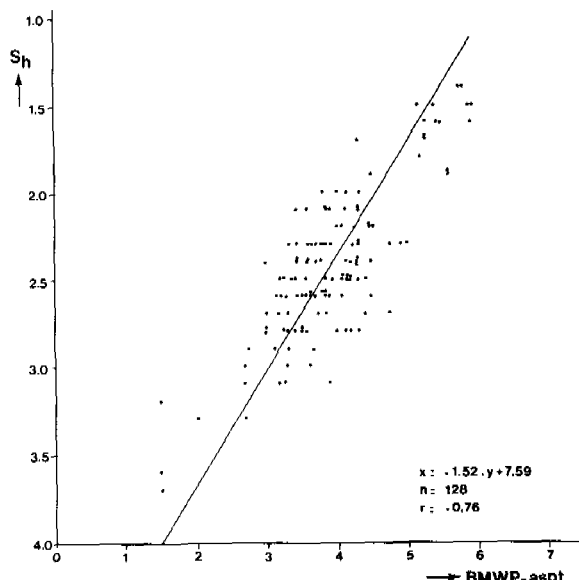


Fig. 4. The relationship between the Saprobič index (S_h) and the BMWP-aspt for 128 samples in the borderstreams of the Federal Republic of Germany and the province of Limburg.

cerning the Chandler-score, for which an aspt should be preferred as well. This leaves us with four methods, the Saprobič-index, the Quality-index, the BMWP-aspt and the Chandler-aspt as potentially suitable for the assessment of the water quality of the Geul. A conclusion confirmed by the results of the application of these methods on the tributaries of this small river (Fig. 1).

On theoretical grounds the Chandler-aspt should be preferred to the BMWP-aspt because the relative abundances of the indicators are taken into account and because the method uses species and genera as indicators, while the BMWP uses families only, which may be an unacceptable indiscrimination of species' indicator values. However, the BMWP-method has yet to be proven wrong because many comparisons have not yet shown that the method leads to conclusions that are less reliable than those based on e.g. the Saprobič-index, which also is a relatively unsensitive method because only a selection of the community is included as indicator species. As demonstrated in Fig. 4, where the BMWP-aspt and the S_h are compared for 128 samples in the borderstreams, there is a significant linear relationship between the two methods, although the deviation from the line is quite high in the most interesting quality range, the middle ranges (for S_h between 2 and 3 and for

BMWP-aspt between 3 and 4.5). Because of this large variation in the middle ranges it is not permitted to translate these two indices into each other, in spite of the statistically significant relationship.

The comparison of the Saprobiic-index (S_h) with the Quality-index (K_{135}) is more promising considering Fig. 5. Here it is clear that the K_{135} -index differentiates strongly in the middle range of the quality scale while the Saprobiic-index leads

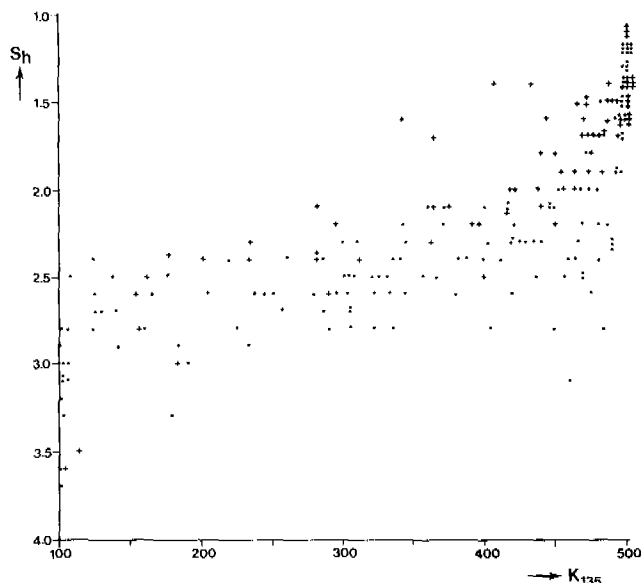


Fig. 5. The relationship between the Saprobiic-index (S_h) and the Quality-index (K_{135}) in the borderstreams of the FRG and Limburg (solid dots) and in the tributaries of the Geul (crosses).

to an unrevealing quality level in between 2 and 3. This confirms the previous statement that the S_h -index is not very sensitive to smaller changes in water quality in the middle range of the pollutional scale. Fig. 5 shows concentrations of dots and crosses in such positions that it is easy to see an S-curve as the relationship between the two indices, leading to an overestimation of the value for the S_h -index in the polluted range of the scale and to an underestimation in the unpolluted range, or vice versa with the K_{135} -index.

The use of the saprobiic-value per taxon in the Saprobiic-index automatically leads to a limitation of the achievable maximum (and to a lesser degree also the minimum) index-value. This is caused by the ecological phenomenon that a community never exists exclusively of species with a saprobiic-value of 1.0. This implies that the Saprobiic-index value for unpolluted waters lies in the order of magnitude of 1.4 - 2.0. Schmitz (pers.comm. 1983) even reported values for the Saprobiic-index in unpolluted upland streams varying from 1.6 - 2.2.

At the time this very problem was the reason to introduce the K_{135} -index (considering the Eristalis- and Chironomus-groups together, the Hirudinea-group separately and the Gammarus- and Calopteryx-groups together) instead of the K_{12345} -index (where each group was considered individually) because the maximal achievable score would be in the order of magnitude of 420 and not the theoretical 500. This narrowed the actual range of the index so much (in practice to 200 - 400) that

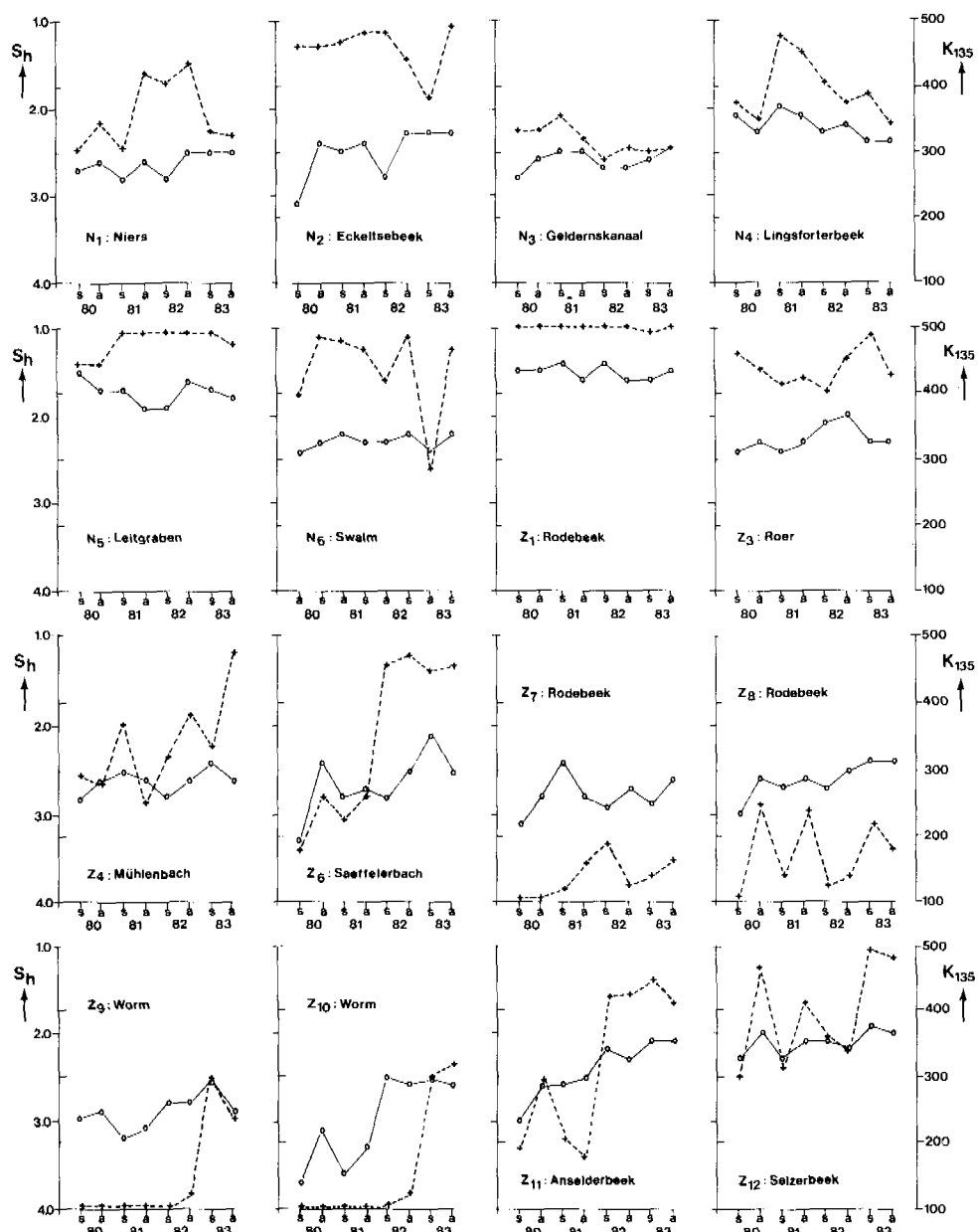


Fig. 6. Comparison of the Saprobiic-index (S_h) (solid line) and the Quality-index (K_{135}) (broken line) at the 16 sampling stations in the borderstreams of the FRG and Limburg in spring (s) and autumn (a) 1980-1983.

this middle range needed stretching.

Another way to compare the border streams (solid dots in Fig. 5) is presented in Fig. 6 where both the S_h -index and K_{135} -index are plotted for each station and every sample. Again the relatively constant Saprobiic-index contrasts with the relatively fluctuating K_{135} -index.

Especially for those stations (Z6, Z9, Z10, Z11) where a considerable improvement of the water quality was found in 1982/1983 from examining the chemical data, the K_{135} -index demonstrated a rather spectacular rise while the S_h -index rose only lightly for Z6 and Z11, hardly for Z9 and strongly for Z10.

Comparison of both indices in Fig. 6 also confirms the earlier statement that the Saprobiic-index does not reach its theoretical minimum and maximum. The station with the 'best' macroinvertebrate community and a good water quality throughout the years (Z1) still has a S_h -index of about 1.5, while the K_{135} -index shows a continuous 498 which approaches the maximum value of 500.

The most polluted stations in the borderstreams (Z9 and Z10) have a minimal K_{135} -index of about 102 in 1980 and 1981, when the S_h -index varied around 3.0 at Z9 and between 3.1 and 3.7 at Z10. Theoretically the minimum of 4.0 can be reached when species with a saprobiic-value of 4.0 are found exclusively (e.g. *Eristalis* spp.). Mostly Tubificidae (s-value 3.8) or *Chironomus* spp. (s-value 3.6) are present, narrowing the practical range of the index. Again the need for methods that can discriminate in the middle ranges of pollution is felt. The extremes are clear enough in most of the existing methods.

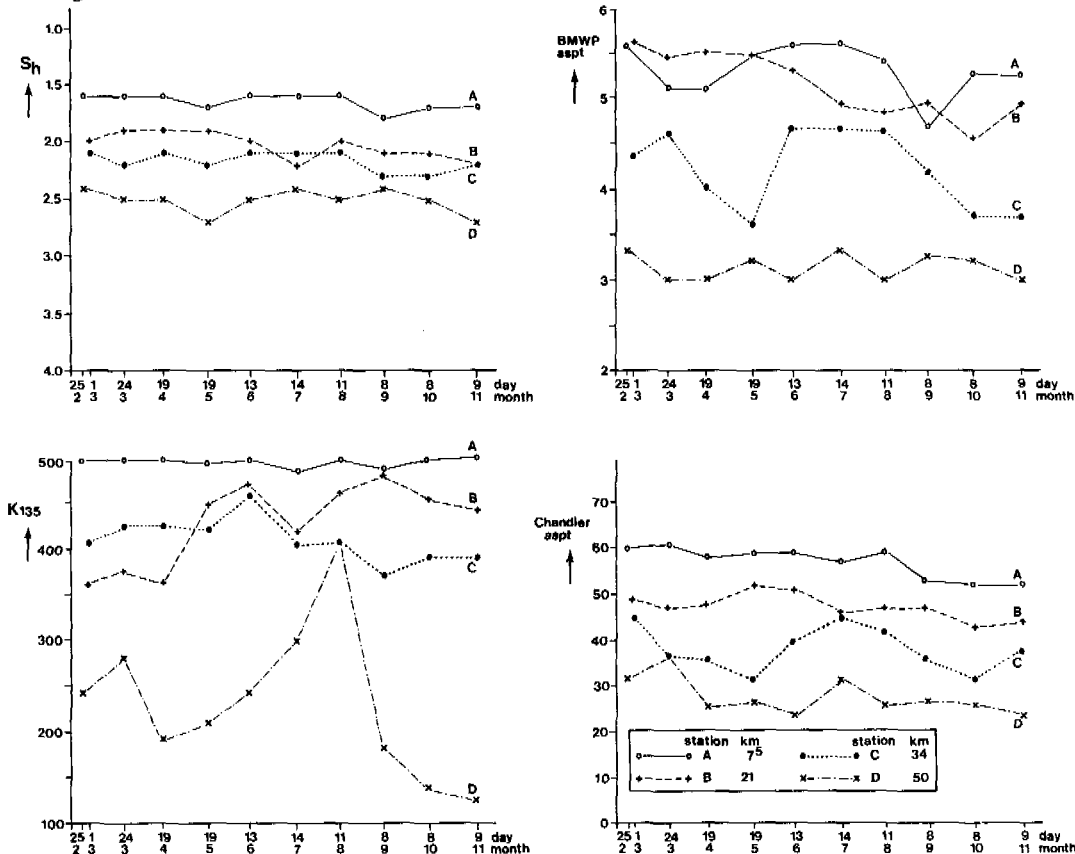


Fig. 7. Application of four biological assessment methods to a time series of samples from the river Geul in 1980.

For many of the stations presented in Fig. 6 the question remains to be answered whether the relative constancy of the S_h -index as compared with the K_{135} -index is a reflection of a relatively constant water quality or merely an illustration of the insensitivity of the Saprobiic-index for short term variations in the water quality, which may be detected by other methods.

Part of the answer can be found in Fig. 7 where the temporal changes of four indices for four stations in the river Geul are presented. Compared to the more varying level of the K_{135} -index, the BMWP-aspt and the Chandler-aspt in Fig. 7, the constant level of the S_h -index suggests that certain changes in the macroinvertebrate community are not detected. Of course this difference may have been caused by oversensitivity of the other methods as opposed to the insensitivity of the Saprobiic-index as well.

The temporal differences seen in Fig. 7 are a good illustration of the basic principle inherent to the application of biological assessment methods, i.e. the purpose of the assessment should determine the method applied. A relatively insensitive method should be preferred when the main goal is the rough assessment of the average water quality over a longer period (in the order of magnitude of 6 - 12 months), although conclusions in this respect should be drawn with care or not at all when just a single assessment (based on a single sample) is available.

Where the relative constancy of an index may be an advantage for assessing the situation of a longer previous period, a strong disadvantage is the lack of 'dissolving-power' in the middle ranges of the pollutional scale. These indices are therefore not very suited to be applied to a study of changes in water quality in the course of a river or to detect temporal changes in water quality. Nor can they be used to compare large numbers of sampling stations in a larger area, because all assessments lead to the same 'grey' quality class.

When the research is aimed at detecting short term changes in the water quality a more sensitive method should be used, and more frequent sampling is needed as well.

The higher sensitivity for changes in water quality as reflected by changes in the community structure also implies a higher sensitivity for variations in the numbers of specimens and the species composition not related to changes in the organic water quality. These methods go beyond the saprobic-indication of the community. They also give an indication of physical, chemical, geological and many other environmental variables, so much that it would be better to use the term environmental-index. It is therefore necessary to re-select some of the indicator species in various assessment methods; re-select in such a way that misinterpretation of a species' presence or absence in connection with organic water quality can be prevented.

CONCLUSION

The fact that all indices presented in this paper were calculated by using the same species lists for each station resulting in a strongly varying outcome of some indices for the same stations confirms the original assumption that biological assessment methods should be applied with care and always be accompanied by a definition of the achievable maximum, or the total index-range, applicable to the stream type concerned. To this end it is necessary to know the reference community for each stream type.

Concerning the four indices that have proved to give workable results in a selection of streams, a further selection cannot be made on the basis of collective data when more stream types are included. For each of the borderstreams a further selection will be made in the near future in combination with data for similar stream types. For the streams in the drainage area of the river Geul as well as for the Geul itself, the application of the K_{135} -index seems promising together with the BMWP-aspt. The various biotic-indices are considered unfit for use in their present form. Both the Saprobiic-index and the Chandler-aspt may prove useful after adaptation of the indicator-species list and the definition of the practical

limits of the indices especially in combination with the various stream types present in the province of Limburg.

It must be kept in mind that an optimal biological assessment can be achieved only through regional adaptations of methods, reflecting both biogeographical and biotopological differences between streams.

ACKNOWLEDGEMENTS

The author is indebted to the executive board of the LWPCA for offering the opportunity to write this paper and to permit the use of many unpublished data. The valuable comments of Ir. P.F.M. Verdonschot are gratefully acknowledged. Mr. H.J.G. Pex identified the majority of the macroinvertebrates and calculated many of the indices. The effort of Mrs. W.E.M. Wevers in typing the manuscript and Mr. C.H.H. Thijssen for drawing the figures is highly appreciated.

REFERENCES

- Armitage, P.D., D. Moss, J.F. Wright and M.T. Furse (1983). The performance of a new biological water quality score system based on macroinvertebrates over a wide range of unpolluted running water sites. *Water Research* 17 (3): 333-347.
- Bloesch, J. (1980). Bodenfaunistische Untersuchungen in Aare und Rhein, Teil II; Eine kritische Überprüfung der Probenahmetechnik und verschiedener Auswertungsmethoden. *Schweiz. Z. Hydrol.*, 42(2): 285-308.
- Chandler, J.R. (1970). A biological approach to water quality management. *Wat. Pollut. Control* 4: 415-422.
- Gardeniers, J.J.P. and H.H. Tolkamp (1976). Hydrobiologische kartering, waardering en schade aan de beekfauna in Achterhoekse beken. In: Th. v.d. Nes (ed.). Modelonderzoek '71-'74. Comm. Best. Waterhuish. Gld.: 26-29, 106-114, 294-296.
- ISO-BMWP (1979). Assessment of the biological quality of rivers by a macroinvertebrate score. Internat. Stand. Org. ISO/TC147/ SC5/WG6/N5, pp. 18.
- ISO-BMWP (1980). Assessment of the biological quality of rivers by a macroinvertebrate score. Internat. Stand. Org. ISO/TC147/SC5/WG6/N14, pp. 10.
- Jones, F. (1973). Quantitative changes in the benthic macroinvertebrate communities of the River Taf and the relationship between plant detritus and invertebrate numbers. M.Sc. Project Report, Univ. Aston in Birmingham; as cited by Hawkes, H.A., 1979. Chapter 2 in 'Biological indicators of water quality' (A. James and L. Evison, eds.) Wiley, pp. 45.
- LWA-NW (1982). Wasserwirtschaft Nordrhein-Westfalen-Fliessgewässer. Richtlinie für die Ermittlung der Gewässergüteklaasse. Landesamt für Wasser und Abfall-NW, pp. 6 + app.
- Moller Pillot, H.K.M. (1971). Faunistische beoordeling van de verontreiniging in laaglandbekken. Proefschrift, Pillot standaardboekhandel, Tilburg, pp. 286.
- Sládecek, V. (1973). System of water quality from the biological point of view. *Arch. Hydrobiol.*, Beih. Erg. Limnol. 7: 1-218.
- Tolkamp, H.H. (1984). Using Several indices for biological assessment of water quality in running water. *Verh. Internat. Ver. Limnol.* 22, (accepted).
- Tolkamp, H.H. and J.J.P. Gardeniers (1977). Hydrobiological survey of lowland streams in the Achterhoek (The Netherlands) by means of a system for the assessment of water quality and stream character based on macroinvertebrates. *Mitt. Inst. Wasserwirtschaft, Hydrologie u. Landwirtschaft. Wasserbau*, T.U. Hannover, H. 41: 215-235.
- Tuffery, G. and J. Verneaux (1967). Méthode de détermination de la qualité biologique des eaux courantes. Exploitation codifiée des inventaires de la faune de fond. *Trav. Sect. P. et P.*, Cerafer, Paris, pp. 23.
- Verneaux, J. and B. Faessel (1976). Note préliminaire à la proposition de nouvelles méthodes de détermination de la qualité des eaux courantes. Ronéo, 8 p.
- Woodiwiss, F.S. (1964). The biological system of stream classification used by the Trent River Board. *Chem. Ind.*, 443-447.
- Woodiwiss, F.S. (1978). The Trent Index. Macroinvertebrates in biological surveillance. In: J.W.G. Lund and G.G. Vinberg (eds.). "Elaboration of the scientific basis for monitoring the quality of surface water by hydrobiological indicator". Report of the first U.K./USSR Seminar at Valdai, USSR, 12-14 July 1976, p. 58-81.

AQUATIC HABITAT ANALYSIS AS AN ELEMENT OF WATER RESOURCES PLANNING AND MANAGEMENT

Edwin E. Herricks

Department of Civil Engineering, University of Illinois at Urbana-Champaign, 208 N. Romine, Urbana, Illinois 61801, U.S.A.

ABSTRACT

With increased emphasis on environmental quality objectives in water resources planning and management, past practices of simply considering water quality as the only environmental quality objective are inappropriate. Expanded environmental quality objectives include maintenance of high quality aquatic habitat. Water resource systems must provide both physical and chemical conditions appropriate for the propagation and maintenance of healthy diverse aquatic communities. Managing water resources to provide high quality habitat involves planning to meet both water quality and water quantity objectives. Existing technology based water quality controls and stream based water quality criteria can now be supplemented by aquatic habitat management. An approach to aquatic habitat management is illustrated by use of the Incremental Methodology developed by the U. S. Fish and Wildlife Service. The Incremental Methodology uses measures of aquatic habitat to assess instream flows required for by aquatic life. Thus the range of environmental quality objectives in resources planning and management is expanded by application of these methods to include aquatic habitat as well as water quality management. Methods used to determine instream flow needs for rivers in Illinois are reviewed, and the use of this information in developing regulations limiting water extraction for off stream use are described. Aquatic habitat based management is shown to provide workable methods to meet expanded environmental quality objectives in water resources planning and management.

KEYWORDS

Water resources, instream flow needs, aquatic habitat, river management, water resources management, hydraulic simulation, habitat frequency analysis.

INTRODUCTION

The management of water resources systems has taken on new dimensions as environmental quality (EQ) issues have grown in importance. In the past, water resources planning and management was narrowly directed to providing suitable quantities of water with acceptable quality for domestic and industrial needs. If EQ issues were included in the planning and management process, the primary focus was maintenance of stream water quality. Water quality management was often limited to providing dilution flows from reservoir storage. Even though the United States and most other countries have abandoned simple dilution as a solution to

water quality problems, the integration of water quality and water quantity planning still occurs through dilution calculations. Dilution factors, often determined from some statistically defined return flow such as the seven day ten year low flow (7-0-10), are the basis concentration limits in effluent permits. Water quality management is based on a set of criteria which define the acceptable concentration of pollutants which allow the maintenance of a specified stream use. In most river basin management, the primary mechanism of water quality control is implementation of wastewater treatment technology. When insufficient dilution flows are available, effluent limitations are often based on some minimum assumed dilution flow, such as the 7-0-10, which is a design flow for calculation of effluent concentration limits. Final permit limits are developed to assure that stream water quality criteria are not exceeded at or above the design dilution flow.

This emphasis on water quality in water resource systems often overshadows the need for more realistic EQ considerations in water resources management. An assumption is often made that maintenance of water quality will meet all EQ requirements, supporting healthy diverse aquatic communities. A closer examination of the relationship between flow quantity and water quality reveals a number of EQ issues which are aquatic habitat dependent. Aquatic habitats are time varying constructs of physical and chemical conditions which meet the requirements for the maintenance and propagation of aquatic organisms. Aquatic habitat can be narrowly defined in relation to single species "niche" requirements or generally described in terms of physical and chemical conditions which maintain healthy diverse aquatic communities. Karr and his co-workers (Gorman and Karr, 1978; Karr and Dudley, 1981, and Karr and Schlosser, 1981) have identified that physical habitat conditions may be the primary determinant of fisheries diversity, even under poor water quality conditions.

Quantifying aquatic habitat in stream and river bioassessments can often provide insight into conditions which produce field data which runs counter to common wisdom. For example, often biological assessments of rivers report good water quality but fisheries and aquatic insect communities have low diversity or population size is low. In other assessments, unusually high diversity is found when water quality would predict low diversity, degraded aquatic communities. The resolution to these unexpected findings is often found in the characteristics of the physical habitat. Where physical habitat conditions are good, the aquatic communities will often be diverse and healthy even when water quality is degraded. If suitable physical habitat is not provided, aquatic organisms will have low diversity even when water quality is good. Placed in the context of water resources management, simply maintaining good water quality may not support acceptable aquatic organism communities. Unless high quality physical habitat is maintained, EQ objectives may not be met.

The acquisition and utilization of aquatic habitat information in water quality management has been the subject of several recent meetings in the United States (Orsborn and Alleman, 1976 and Armantrout, 1981). Among the methods proposed, the U. S. Fish and Wildlife Service has devoted major resources to the development of the Incremental Methodology for the assessment of instream flow needs (IFN) (Stallnaker and Arnette, 1976; Bovee, 1981). IFN are directly related to minimum flow requirements, but in addition to dilution flows, IFN recognize that recreation, navigation, and aquatic life require maintenance of minimum instream flows. Instream flow, particularly flows which support healthy, productive aquatic communities can now be stated as a quantitative EQ objective in multi-objective planning and management of water resource systems (Fraser, 1972, Ward and Stanford, 1979; Sale, et al., 1982). The development of IFN for fish and aquatic life is dependent on the quantification of aquatic habitat as habitat conditions change with flow. The Incremental Methodology provides a quantitative

method of habitat assessment and is a powerful tool, assisting water resource managers to meet broadly defined EO objectives for river or stream systems.

This paper is presented to provide a review of the application of the Incremental Methodology in aquatic habitat assessment. Basin wide application of IFN analysis is demonstrated as a management tool which integrates EO objectives in water resource regulation. IFN analysis provides essential information for the establishment of regulatory flows and provides technical support for permit systems which limit extraction of water for off stream uses.

HABITAT ANALYSIS PROCEDURES

The Incremental Methodology is described by Bovee (1981) and Milhous, et al. (1981), and is implemented in a computer based analysis system termed PHABSIM (PHysical HABitat SIMulation). PHABSIM consists of two major elements. The first is a hydraulic simulation routine which requires the collection of field data, depth and velocity information for two or more cross sections of a representative reach. The field data is used to calibrate a hydraulic simulation model which provides depth and velocity data at various flows for the representative reach. Habitat is assessed for individual species and for various life stages of each species through the use of suitability curves for specific habitat parameters. Example suitability curves are illustrated in Figure 1. Suitability curves are

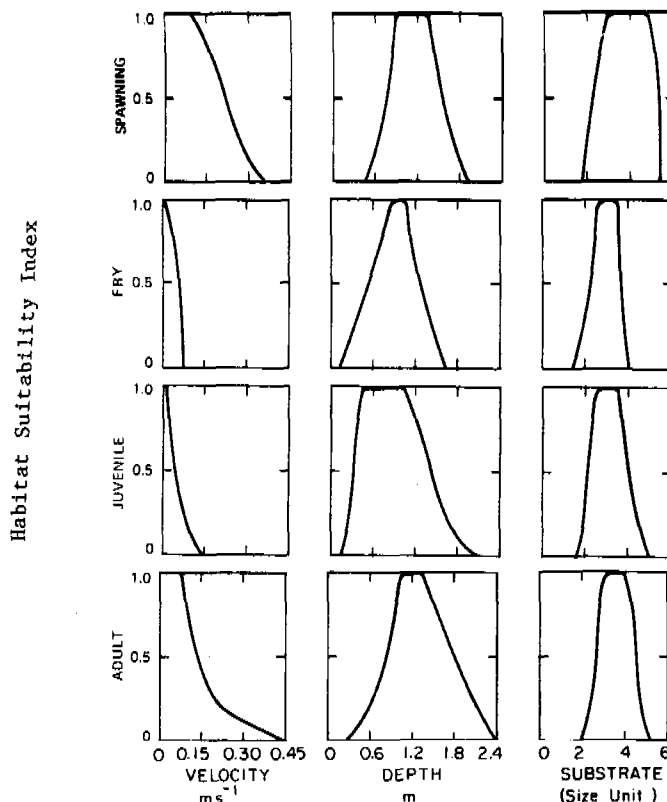


Fig. 1. Habitat suitability curves for four life stages of the bluegill Lepomis macrochirus for velocity, water depth, and substrate.

provided as a part of PHABSIM but can be generated by the user if required (Bovee and Cochraner, 1977). The primary output of PHABSIM is species and life stage specific habitat data, a weighted usable area (WUA) for a specified discharge value. The WUA is an index of habitat quality calculated from the suitability curves for depth, velocity, and substrate:

$$WUA = \sum_{i=1}^n S_d(d_i) \cdot S_v(v_i) \cdot S_s(s_i) \cdot A_i$$

where:

S_d , S_v , and S_s are suitability functions
 d_i , v_i , and s_i are the predicted physical conditions in the
 ith incremental area of the stream reach
 which has been modeled
 A_i is the area of the ith cell

It is possible to generate a habitat response curve by determining WUAs for a range of discharge values, Figure 2. The habitat response curves for each species and life stage will have different characteristics.

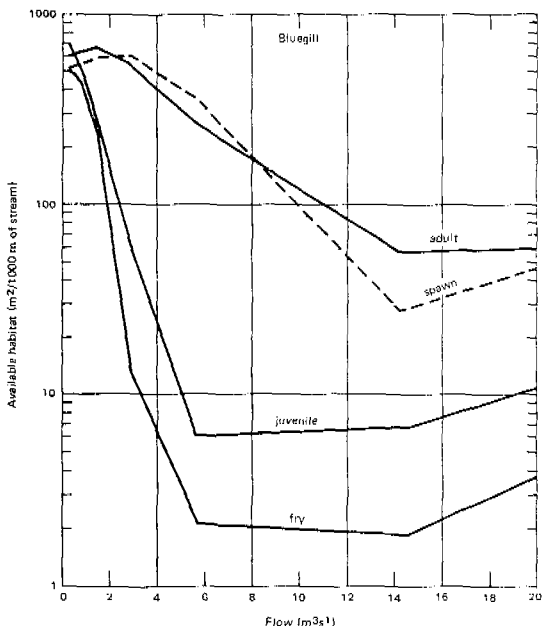


Fig. 2. Habitat response curve of the bluegill from the Clay City Reach of the Little Wabash River, Illinois.

Flow is highly variable in natural streams. Figure 3 illustrates the expected monthly variation in flow volumes which produce seasonal trends in habitat availability, Figure 4. Flow will also vary from year to year. From the historical flow records at a gaging station, it is possible to develop a probabilistic estimate of how often a given discharge occurs in a stream. This estimate is illustrated in Figure 3 as an expected exceedence frequency, the expected percentage of flows which will equal or exceed a specified discharge. In developing management strategies based on aquatic habitat, the natural variability in habitat conditions must be recognized. A review of the example habitat response curves reveals that more than one flow may produce the same WUA value.

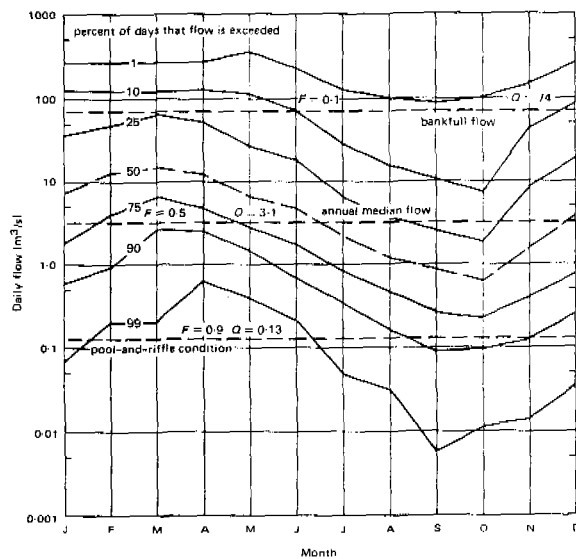


Fig. 3. Seasonal flow variability for the Little Wabash River near Clay City.

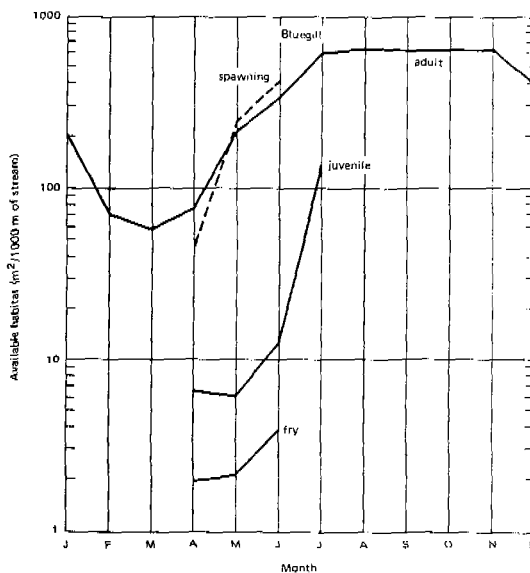


Fig. 4. Seasonal variability in habitat for the bluegill in the Clay City Reach of the Little Wabash River. Habitat values indicated only for months of expected presence in the reach.

Both high and low flows are important in aquatic habitat management. To account for expected flow variability, habitat response curve characteristics, and the effect of both high and low flow conditions, my co-workers and I have developed a method of habitat frequency analysis (Sale, et al., 1981). The calculation procedures is similar to flow duration analysis. Historical flows, in this case

daily flow values which are averaged weekly, and the habitat response curve are used to calculate a historical habitat record. The WUA values from this record are used to develop a probabilistic estimate of how often a particular WUA occurs and an exceedence table is constructed. The habitat exceedence frequency is similar to flow duration and provides similar information to a manager. For example, a habitat (WUA) which is equaled or exceeded with a frequency of 50% ($f = 0.5$) could be determined for each time period in the analysis (we have found monthly summaries the most convenient), Table 1. The habitat frequency information can be used in several ways. First, comparing the $f = 0.1$ with the $f = 0.9$ WUA provides an estimate of the range of habitat which might be expected to occur naturally. Comparison of these values between species provides an indication of the general suitability of the reach for species which might be subject to intensive management. The range of WUA values also provides insight into the general requirements of a species/life stage on a monthly basis, as well as how well the historical stream flow met these requirements.

Table 1.

Example habitat frequency data and minimum discharges required for species/life stage protection.

Species: Bluegill; Life Stage: Adult; Period of Record: 1916-1976

| | Jan | Feb | Mar | Apr | May | Jun | Jul | Aug | Sep | Oct | Nov | Dec | |
|-------|----------------------------|-------|------|------|-------|-------|-------|-------|-------|-------|-------|-------|--|
| $f =$ | Discharge (Q) in m^3/sec | | | | | | | | | | | | |
| 0.1 | 61.24 | 46.24 | 7.61 | 7.61 | 31.72 | 57.87 | 71.74 | 81.14 | 76.10 | 76.10 | 73.64 | 70.72 | |
| 0.3 | 8.18 | 8.18 | 8.18 | 8.18 | 8.18 | 8.18 | 36.31 | 50.03 | 45.36 | 53.71 | 35.80 | 22.39 | |
| 0.5 | 8.18 | 8.18 | 8.18 | 8.18 | 7.02 | 7.36 | 8.18 | 22.39 | 24.39 | 31.33 | 8.18 | 8.18 | |
| 0.7 | 2.21 | 4.25 | 2.41 | 2.24 | 2.07 | 2.01 | 2.38 | 4.36 | 7.64 | 8.94 | 3.28 | 2.41 | |
| 0.9 | 1.10 | 1.10 | 1.13 | 1.10 | 1.16 | 1.08 | 1.16 | 1.30 | 1.19 | 1.87 | 1.10 | 1.16 | |

Minimum discharge for the protection of a habitat frequency $f = 0.5$

| | Discharge (Q) in m^3/sec | | | | | | | | | | | |
|-------|----------------------------|------|------|------|------|------|------|------|------|------|------|------|
| adult | 0.31 | 0.31 | 0.31 | 0.31 | 0.34 | 0.31 | 0.57 | 0.57 | 0.45 | 0.37 | 0.31 | 0.31 |
| spawn | 0.45 | 0.42 | 0.42 | 0.42 | 0.51 | 0.51 | 0.82 | 0.65 | 0.51 | 0.45 | 0.45 | 0.48 |
| fry | 0.02 | 0.06 | 0.06 | 0.06 | 0.06 | 0.06 | 0.06 | 0.14 | 0.20 | 0.06 | 0.06 | 0.06 |

A second set of tables is also produced in the habitat frequency analysis. These tables identify for each species the minimum discharge required for the protection of a specified habitat frequency. The nomograph, Figure 5, constructed by plotting the habitat response and habitat frequency curves is used to illustrate the method of minimum flow selection. First the habitat exceedence is selected (ex. 0.8 or 80%). A line is drawn intersecting the habitat frequency. A horizontal line is then drawn to intersect the habitat response curve and a discharge determined which is the minimum discharge necessary to maintain a WUA value which is equaled or exceeded 80% of the time (Q_{min}). The utility of habitat frequency analysis in river basin management is found in the incorporation of historical flow conditions in the IFN analysis. Baseline conditions may be better defined, and historical habitat analysis may identify natural limitations to species considered for intensive management.

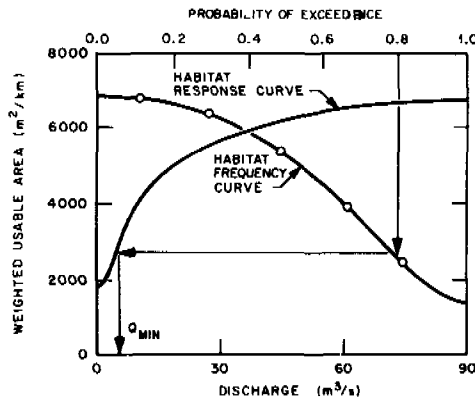


Fig. 5. Nomograph for calculating minimum flow using habitat response and habitat frequency data. (from Sale, et al., 1982)

BASIN HABITAT ANALYSIS

Using the habitat analysis methods reviewed in the previous section, supplemented by additional analysis of basin hydraulic geometry, it is possible to perform a basin habitat analysis. The Incremental Methodology is designed for use on a limited reach of stream. By careful selection of the reaches analyzed the data produced may be considered representative of a much larger reach of stream. This representative reach analysis can be applied to other streams of similar stream order or with similar watershed areas to support basin wide habitat analysis. A critical feature of basin habitat analysis, then, is selection of representative reaches and validation of the extrapolation of representative reach analysis results to the entire basin.

A fundamental assumption made in the representative reach selection is that even though streams or rivers change significantly from headwaters to higher order rivers, these changes occur gradually and long reaches of the stream will be quite similar. Thus if a representative reach is carefully selected, it will represent, or be similar to, all streams in the basin with that character. This approach recognizes the fundamental difficulty of designing a sampling program which characterizes each change in habitat throughout the stream continuum. It is assumed that if analysis is made on a reach where all major habitats are analyzed that this analysis can be used to generally assess other reaches where similar habitats occur. The limitations to a representative reach analysis should be apparent. In general, the analysis of a representative reach can only be applied to additional reaches along the same stream or to other reaches on similar streams in the same basin which have demonstrated similarities.

The demonstration of reach similarities begins with reach selection. The selection of the representative reach requires a detailed analysis of basin geology, land use, discharge, and hydraulic geometry. It is essential for habitat frequency analysis to have actual or synthetic historical flow records near the representative reach. We have found that reach selection is facilitated by aerial reconnaissance and development of a detailed photographic record of stream habitat characteristics. The validation of reach extrapolation is dependent on hydraulic geometry analysis (Stall and Herricks, 1982). Basin hydraulic geometry relationships are developed from a Horton-Strahler drainage network analysis

(Stall and Fok, 1968). Data on the number of streams, length, and slope of a given order are plotted, Figure 6. When consistent relationships between stream order for these parameters are demonstrated, it is possible to evaluate the "representativeness" of the representative reach in terms of hydraulic geometry and provide a justification for extrapolation of representative reach results.

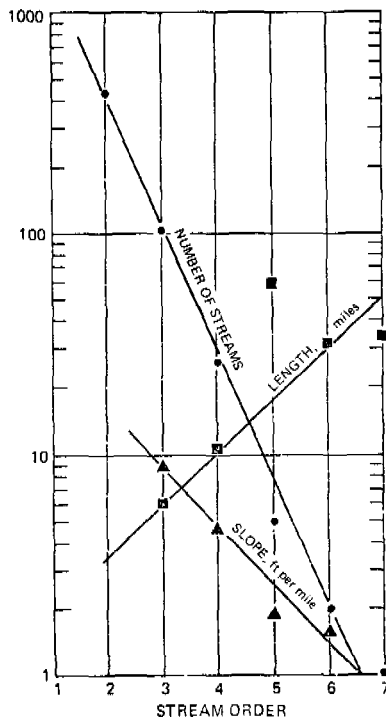


Fig. 6. Horton-Strahler relationships used in evaluation of extrapolation validity.

Following representative reach selection, hydraulic data is collected for each representative reach (Herrick, et al., 1980). A series of cross-sections are designated and surveyed in the reach. Cross-sections are placed to identify hydraulic controls, important habitat components, and general stream channel characteristics. Depth and velocity data is collected across each cross-section and substrate characteristics of the cross-section determined. The depth and velocity data is used to calibrate the hydraulic model component of PHABSIM and species suitability curves are selected from those available in the PHABSIM library or those developed as part of the basin study. PHABSIM output is in the form of habitat response curves which are further analyzed in habitat frequency analysis. The example habitat frequency analysis results, provided in Table 1, illustrate the form of data which can now be used in river basin planning and management.

The argument made in the introduction to this paper emphasized that planning and management of water resource systems could not rely entirely on water quality management to meet environmental quality objectives. Aquatic habitat was recommended as a useful measure of environmental quality. The use of the Incremental Methodology, in particular PHABSIM, provides a connection between physical and biological components of water resource systems. As instream uses are quantified, the management opportunities for water resources are expanded. An example of the utility of aquatic habitat quantification in water resources planning is provided in Sale, et al. (1982). An approach to optimizing reservoir operation was reviewed which combined linear decision rule modeling with an objective function representing the value of reservoir releases to downstream fisheries. In this optimization, ecological or environmental quality objectives can be considered together with flood control, water supply, and other considerations usually analyzed in an engineering analysis of reservoir operation.

Habitat analysis, in particular, habitat frequency analysis was also used to assist in the development of flow regulation policy in Illinois. Although the midwestern United States receives ample rainfall and is provided with major groundwater resources, the prospects of conflicting uses of surface water resources exist. For example, Eheart and Libby (1980) have identified a scenario where demand for irrigation water from surface sources may adversely affect meeting instream flow needs. In addition, extraction for both domestic and industrial water use may make additional demands on surface water resources. Construction of reservoir projects also modify flow regimes and may adversely affect instream uses. To deal with conflicting use of surface water resources, the State of Illinois has developed a basis for flow regulation in the form of an interim low flow standard. This low flow standard was evaluated using habitat analysis procedures.

The proposed standard was developed from a detailed analysis of historical flow records which identified an inflection in the range of the 75% duration flow (a flow equaled or exceeded 75% of the time). The interim standard was structured to account for the design dilution flow used in effluent permit preparation, while supporting a concept of shared resource utilization (e.g. between instream and off stream water use). The proposed interim standard is stated as: The flow available in a stream for offstream use (either storage or withdrawal) is the maximum value of either the streamflow minus the 75% duration flow or the difference of the streamflow minus the 7 day-ten year low flow divided by two. The effect of application of the interim standard would be to allow reduction of streamflow throughout the year to the average annual Q75. If flow dropped below the average annual Q75 only 50% of the difference between a 7-0-10 flow and the Q75 could be withdrawn.

Based on previous comments concerning the appropriateness of developing flow regulation on an annual flow value when seasonal and annual variability is recognized, the Illinois interim standard was evaluated using historical habitat frequency data. The Rock River basin was selected for analysis because representative reach characteristics were varied and corresponded to reaches analyzed in several other river basins in Illinois. Since the flow/habitat relationships are complicated by habitat response curve shape, two analyses were performed using both habitat frequency data and habitat response curves. For each species and life stage, the median habitat (WUA) for any month was determined and the corresponding WUA value was determined for the Q75. A percent change in habitat was calculated. A second analysis used the Q75 WUA to determine a frequency for the interpolated habitat value. The results of these analyses for an example representative reach are contained in Tables 2 and 3.

Table 2. Results of interim standard effects on aquatic habitat in the Kishwaukee River, a river characterized by shallow pool and riffle conditions.

| Species | month(s) of maximum habitat reduction | percent reduction | range of % reduction in other months |
|-----------------|---------------------------------------|-------------------|--------------------------------------|
| Black crappie | Mar-Jun | 25 | 2-5 |
| Bluegill | | | |
| fry | Mar-Jun | 60 | 9-16 |
| juvenile | increase | | |
| adult | Mar-Apr | 4 | increase |
| spawn | May | 10 | 2-3 |
| Carp | Mar-Jun | 60 | 14-20 |
| Channel catfish | | | |
| fry | Mar-Jun | 15 | 5-10 |
| juvenile | Mar-Jun | 80-90 | 38-50 |
| adult | Mar-Jun | 63 | 18-25 |
| spawn | Mar-Apr | 37 | 7-10 |
| Gizzard shad | Mar-Apr | 61 | 24-30 |
| Smallmouth bass | | | |
| fry | May-Jun | 9 | 2-8 |
| juvenile | increase | | |
| adult | Apr-May | 57 | 25-38 |
| spawn | Aug | 13 | increase |
| Largemouth bass | Mar-Apr | 24 | 8-10 |
| White sucker | Jun-Jul | 6 | 4 to increase |

Table 3. Results of interim standard effects on aquatic habitat in the Pecatonica River, a river characterized by deep riffles and large pools.

| Species | month(s) of maximum habitat reduction | percent reduction | range of % reduction in other months |
|-----------------|---------------------------------------|-------------------|--------------------------------------|
| Black crappie | | increase to 80% | |
| Bluegill | | | |
| fry | Feb-Mar | 9 | 1-5 |
| juvenile | Jan | 3 | increase |
| adult | | increase to 260% | |
| spawn | | increase to 200% | |
| Carp | Jan | 3 | increase |
| Channel catfish | | general increase | |
| fry | | | |
| juvenile | Mar-Apr | 48 | 18-30 |
| adult | Apr | 16 | 6-10 |
| spawn | | increase to 100% | |
| Smallmouth bass | | | |
| fry | | increase to 87% | |
| juvenile | | increase to 200% | |
| adult | | increase to 180% | |
| White sucker | | variable 1-2% | |

Based on habitat analysis, the most significant impact of the recommended interim standard would occur in March through June. For the species evaluated, a reduction of up to 90% of the species/life stage WUA would occur. In other than March through June, habitat reduction was in the 10 to 20% range. Of particular importance is the increase in available habitat for several species. The impact of the proposed interim standard was different on different rivers. Those rivers characterized by shallow riffle and pool conditions indicated a consistent reduction in habitat caused by adoption of the interim standard. Larger rivers, and rivers which had few riffles and large pools showed a consistent increase in habitat with fewer months with reduced habitat conditions.

In developing an interim flow standard for Illinois, habitat analysis contributed significantly to environmental quality evaluations. It was possible using habitat analysis to generalize the impacts which might be caused by the adoption of a standard and develop an understanding of differential impacts in some river basins. Of particular importance was the finding that habitat might actually be increased by somewhat reduced flows.

CONCLUSION

This paper has been intended as a demonstration of the contribution aquatic habitat analysis can make to water resources planning and management. Techniques such as the Incremental Methodology and computer based analysis systems such as PHABSIM and habitat frequency analysis can significantly improve environmental quality considerations in water resource systems planning.

ACKNOWLEDGEMENTS

The research supporting development of this paper was supported by the Illinois Department of Transportation, Division of Water Resources. Field data collection and analysis for the Little Wabash River basin was supported by the Ohio River Basin Commission through a grant to the Illinois Department of Transportation.

REFERENCES

- Armantrot, N. B. (1981). Acquisition and utilization of aquatic habitat inventory information. Symposium Proceedings. American Fisheries Soc. Western Division, Washington, D. C. 376 pp.
- Bovee, K. D. (1981). User's guide to the instream flow incremental methodology, Instream Flow Inf. Pap. 12, FWS/OBS-80-52, U. S. Fish and Wildlife Service, Ft. Collins, Colorado.
- Bovee, K. D. and Cochnauer, T. (1977). Development and evaluation of weighted criteria, probability-of-use curves for instream flow assessments: fisheries, Instream Flow Inf. Pap. 3, FWS/OBS-77/63, U. S. Fish and Wildlife Service, Ft. Collins, Colorado.
- Eheart, J. W. and Libby, A. E. (1980). Response of irrigation water use to the price of a key grain, viz. corn (*Zea Mays L.*). Civil Engineering Studies, Environmental Engineering Series #59, UILU-ENG-80-2024, University of Illinois, Urbana, IL.
- Fraser, J. C. (1972). Regulated stream discharge for fish and other aquatic resources: An annotated bibliography. FAO Fisheries Tech. Pap. 112, Food and Agric. Organ. of the U. N., Rome.
- Gorman, O. T. and Karr, J. R. (1978). Habitat structure and stream fish communities. Ecology 59:507-515.

- Herrick, E. E., Stall, J. B., Eheart, J. W., Libby, A. E., Railsback, S. F., and Sale, M. J. (1980). Instream flow needs analysis of the Little Wabash River basin. Civil Engineering Studies, Environmental Engineering Series No. 61, UILU-ENG-80-2026.
- Karr, J. R. and Dudley, D. R. (1981). Ecological perspective on water quality goals. Environ. Manage. 5(1):55-68.
- Karr, J. R. and Schlosser, I. J. (1978). Water resources and the land water interface. Science 201:229-234.
- Milhous, R. T., Wegner, D. L., and Waddle, T. (1981). User's guide to the physical habitat simulation system. Instream Flow Inf. Pap. 11, U. S. Fish and Wildlife Service, Ft. Collins, Colorado.
- Sale, M. J., Railsback, S. F., and Herricks, E. E. (1981). Frequency analysis of aquatic habitat: A procedure for determining instream flow needs. In Acquisition and Utilization of Aquatic Habitat Inventory Information. Am Fish. Soc. Washington D. C. p340-346.
- Sale, M. J., Brill, E. D., and Herricks, E. E. (1982). An approach to optimizing reservoir operation for downstream aquatic resources. Water Res. Research, 18(4):705-712.
- Stall, J. B. and Fok, Y. S. (1968) Hydraulic geometry of Illinois streams. Illinois State Water Survey Contract Report 92, Urbana, Ill.
- Stall, J. B. and Herricks, E. E. (1982). Evaluating aquatic habitat using stream network structure and streamflow predictions. in Applied Geomorphology, George Allen and Unwin, London and Boston. p240-253.
- Stallnaker, C. B., and Arnette, J. L. (1976). Methodologies for the determination of stream resource flow requirements: An assessment. FWS/OBS-76/03, U. S. Fish and Wildlife Service, Washington, D. C.
- Ward, J. V., and Stanford, J. A. (1979). The Ecology of Regulated Streams. Plenum, New York.

RESUSPENSION AND SEDIMENTATION

EROSIONAL PROCESS OF COHESIVE SEDIMENTS

T. Kusuda,* T. Umita,** K. Koga,* T. Futawatari* and Y. Awaya*

*Dept. of Civil Eng. Hydraulics, Faculty of Eng., Kyushu Univ., Fukuoka, 812, Japan

**Dept. of Civil Eng., Faculty of Eng., Iwate Univ., Morioka, 020, Japan

ABSTRACT

Tests on erosion of the cohesive sediments in the Chikugo estuary in Japan were conducted. The results indicate that the decrease in the rate of erosion at constant shear stresses is caused rapidly 20 to 30 minutes after the start of tests and that the decrease is caused by the increase in the solid fraction and the yield value of the sediment remaining uneroded due to shear stress. In order to simulate the erosion process of sediments, a model in which the increase in the yield value of sediment is assumed to be proportional to the integration value of the absolute value of the sediment velocity gradient with respect to time was developed. The simulation based on this model is shown to be available to estimate the amount of sediments eroded in the erosional process of cohesive sediments.

KEYWORDS

Erosion; sediment; critical shear stress; suspended solids; concentration; estuary.

INTRODUCTION

The problem of the erosion of cohesive sediments as well as the problem of deposition is of importance from the engineering standpoints, such as the estimation of the release rate of nutrients from beds and the maintenance of minimum depths in tidal rivers, estuaries, and water ways. Studies on the erosional process of hard mud-beds have been done previously (Partheniades, 1965; Mignot, 1968; Sawai, 1977), little knowledge, however, is known as yet on the erosional process of soft mud-beds. To control water pollution, it is necessary to develop a method for the estimation of the rate of erosion of soft mud-beds.

The purposes of this study are to clarify the erosional process of soft mud-beds which are found as most Japanese estuarine and bay sediments, to obtain a model to estimate the rate of erosion at constant and varied shear stresses in time, and to simulate the erosional process of sediments.

TEST MATERIAL

The test material in this study is taken at the mouth of the river Chikugo, flowing into Ariake bay in western Japan. This river is very famous for showing both a high tidal range, up to 6 m, and high concentration of suspended solids, up to 3 kg/m^3 . The particle size distribution is shown in Fig. 1. The particle density is 2610 kg/m^3 .

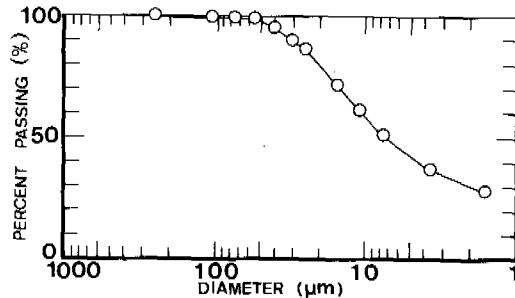


Fig. 1. Particle size distribution.

APPARATUS

An annular flume used in this study is depicted in Fig. 2. It consists of a

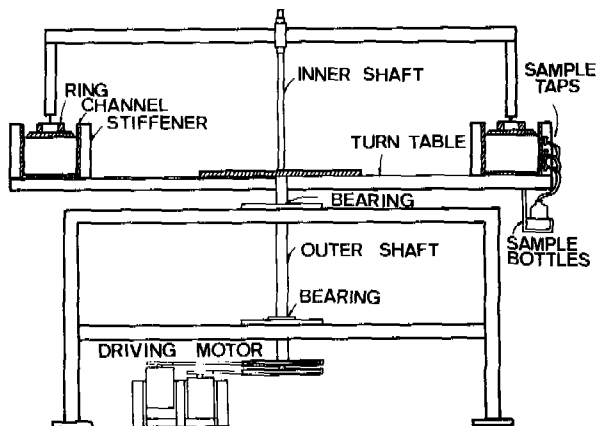


Fig. 2. Annular flume.

rotating annular ring and an annular channel which rotates in a direction opposite to that of the ring. In order to minimize the secondary current effect in the channel, especially immediately above the bed surface, the ring and the channel are required to be rotated not independently but at related speeds to each other with regard to different shear stress. As a result, this flume works as an infinitely long flume on the erosion process. The channel is 20 cm deep, 100 cm in mean radius, and 20 cm wide. The shear stress τ at the bed surface in the channel is calculated from the equation $\tau = \tau_r \cdot A_r / (A_b + A_w)$, where A_r , A_b , and A_w are the area of the ring, of the bed surface on the bottom of channel, and of

the wall of the channel, respectively, and τ_r is the shear stress of the ring which was directly measured. The calculated shear stress τ is in good agreement with the shear stress calculated from the velocity profile close to the channel bottom.

A sampling device for bed materials consists of a plexiglass cylinder which is 5 cm in inner diameter and 5 cm high and an injection needle with a flexible tube connected with a vacuum pump. After each run, the sediment remaining uneroded was sampled layer by layer by use of the sampling device at a slightly negative pressure. One layer is 0.5 to 1 mm thick. The whole experimental work was conducted at $20 \pm 1^\circ\text{C}$ and 15 cm in water depth. Every initial bed was 2 cm thick.

EXPERIMENTAL RESULTS

A series of erosion tests were conducted at constant shear stresses and water contents to examine the basic erosional properties of sediments. Several results of the erosion tests are shown in Fig. 3. These results indicate that the rate of erosion decreases rapidly after 20 to 30 minutes from the start of each test and becomes nearly naught after 1 hour and that each concentration of suspended solids after 1 hour reaches a steady state. The concentration in a steady state becomes larger as applied shear stress and the water content of sediment increase except the test of 0.4 N/m^2 and 365 % of water content. The appearance of peaks in concentration at 0.4 N/m^2 of shear stress is due not to surface erosion but slightly massive erosion (Yeh, 1979).

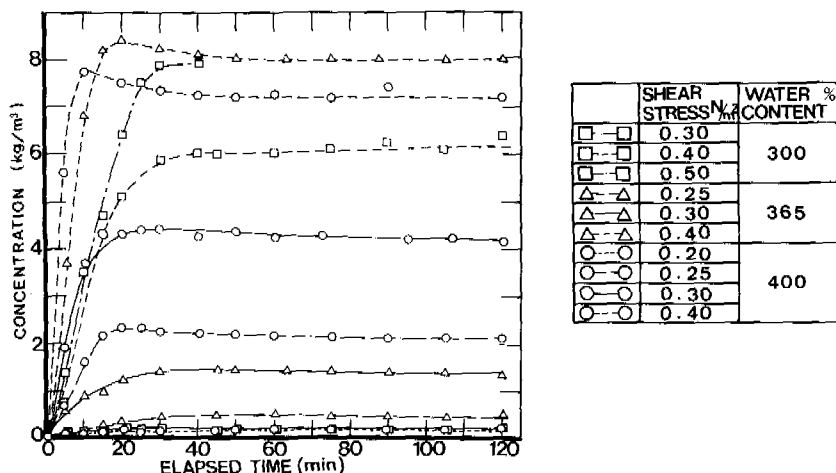


Fig. 3. Concentration of sediments eroded at various shear stresses and water contents.

As shown in Fig. 4, the critical shear stress, τ_c , above which the erosion of sediment is caused, decreases as the water content of sediment increases. This relationship is expressed as follows.

$$\tau_c = 6.5 (1-\epsilon)^{1.6} \quad (\text{N/m}^2) \quad (1)$$

where $1-\epsilon$ is solid fraction. Water content is equal to $\rho_w \epsilon / \rho_s (1-\epsilon)$, where ρ_w and ρ_s are the density of water and of sediment, respectively.

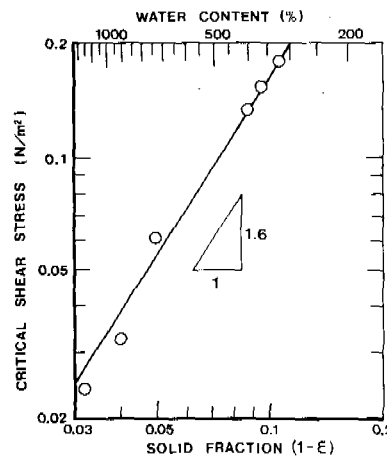


Fig. 4. Relationship of critical shear stress and solid fraction.

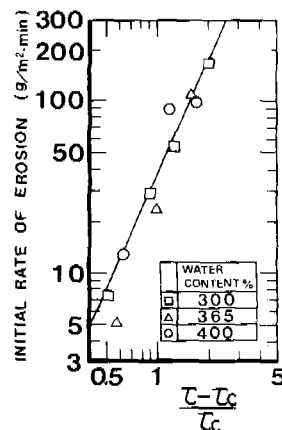


Fig. 5. Initial rate of erosion.

The initial rate of erosion, $E_{t=0}$, is a function of the non-dimensional shear stress, $(\tau - \tau_c) / \tau_c$, as shown in Fig. 5 and is written as

$$E_{t=0} = 0.036 (\tau / \tau_c - 1)^{2.2} \text{ (kg/m}^2 \cdot \text{min}) \quad \text{for } \tau \geq \tau_c \quad (2)$$

$$E_{t=0} = 0 \quad \text{for } \tau < \tau_c \quad (3)$$

where τ is applied shear stress. In each run, the time from the start of each test to the interception of a tangent of the concentration curve in the steady state and another one in the initial stage in which the sediment is eroded rapidly is related to the non-dimensional shear stress as shown in Fig. 6. The relationship of the critical shear stress, τ_c , and the plastic viscosity of

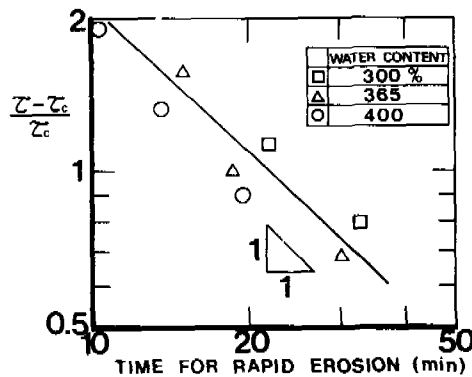


Fig. 6. Relationship of the time for rapid erosion and non-dimensional shear stress

sediment, μ_p , is given with respect to sediments in Japan as $\tau_c / \mu_p = 1$ (s^{-1}) (Ohtsubo, 1983). The relationship in Fig. 6 is given as

$$\frac{\tau - \tau_c}{\mu_p} T = 1400 \quad (4)$$

where T is the elapsed time from the start of each test until the interception. This indicates that the time for which sediments are eroded rapidly depends on the properties of sediments and the applied shear stress. It takes longer time for a hard bed to reach a steady state than for a soft bed at the same applied shear stress.

In order to clarify the reason why the rate of erosion decreases rapidly 10 to 30 minutes after the start of each run, several tests on the solid fraction and the size distribution of sediments were conducted concurrently. Some examples of the vertical distributions of solid fraction of sediments 2 hours after the start are shown in Fig. 7. The solid fraction of each sediment decreases from the surface toward the bottom. After taking the minimum value, the solid fraction increases gradually except the case of $0.4 N/m^2$. The solid fractions at both the surface and the bottom of sediments become larger as the applied shear stress increases. The increase in solid fraction at the surfaces of sediments is apparently caused by the applied shear stress since the solid fractions at the surfaces of sediments are related to the applied shear stress as shown in Fig. 8. Minimum solid fractions are also related to the applied shear stress. It is experimentally confirmed that the increase in solid fraction leads to the hardening of sediments. The gradual increase in solid fraction under the level of the minimum value depends on the gravitational thickening of sediment. Similar results also have been obtained with respect to other runs. An example of the size distributions of suspended solids is shown in Fig. 9. This is for $0.3 N/m^2$ of shear stress and 400% of water content. The size distribution does scarcely change as time elapses. The size distribution of each layer of the sediment in this case is given in Fig. 10. Coarse particles become relatively more at the first layer than at other layers. The size distributions in the layers lower than the second one agree with the original one shown in Fig. 1. The reason why the size distribution in the first layer shifts toward the coarse size side in comparison with those in other ones is due to selective erosion at the surface of the sediment. In case of $0.4 N/m^2$ of shear stress, no shift on the size distribution at the

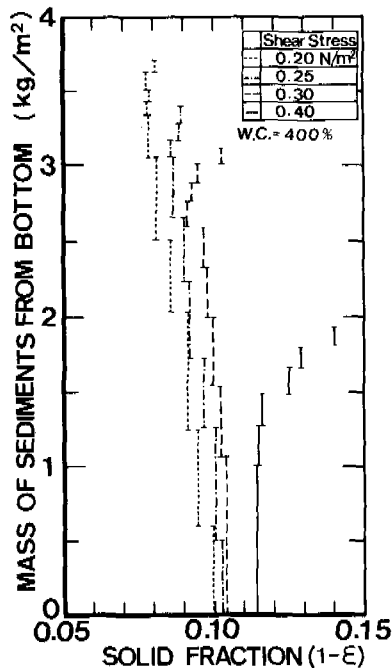


Fig. 7. Vertical distributions of solid fraction of sediments.

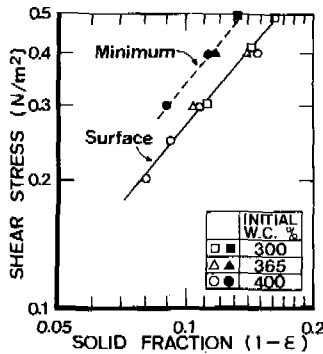


Fig. 8. Solid fraction at the bed surface and in the minimum.

surface of each sediment was observed. This indicates that selective erosion does not exist in case of 0.4 N/m^2 of shear stress. Figure 7 indicates that the hardening of sediments at surfaces can be caused without selective erosion. Depending on the Shields diagram, even the largest particle in sediments is placed in the region of scouring. Therefore the hardening of sediments at the surface is more effective and predominant on the rapid decrease in the erosion rate than selective erosion.

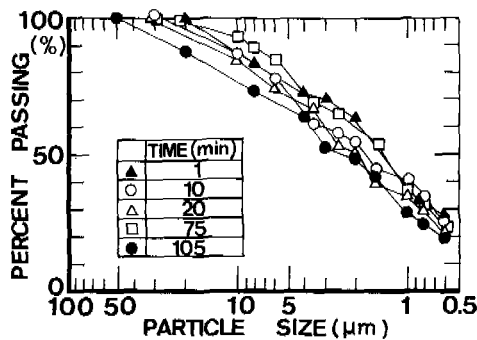


Fig. 9. Temporal variation of size distribution of suspended solids (0.3N/m^2 , W.C.=400%).

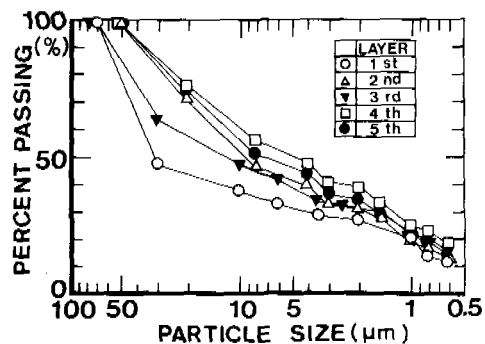


Fig. 10. Spatial variation of size distribution of sediment (0.3N/m^2 , W.C.=400%).

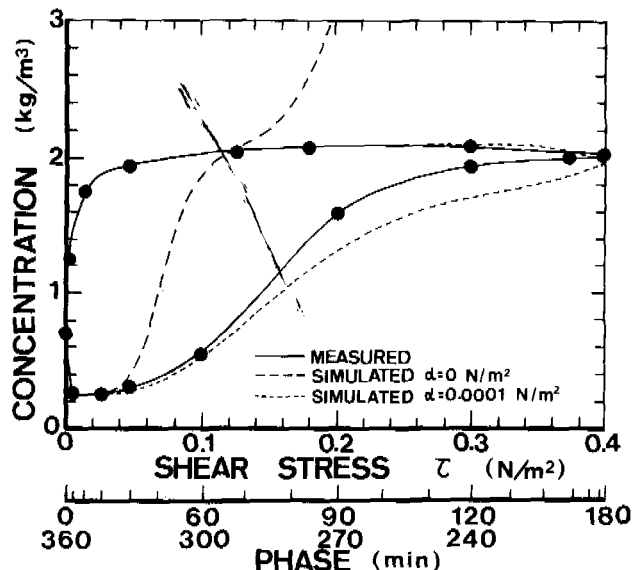


Fig. 11. Variation in concentration in a periodically steady state at sinusoidally varied shear stress

Several experiments were conducted at periodically changed shear stresses. The example shown in Fig. 11 was operated with a sinusoidally changed shear stress whose period was 6 hours and maximum shear stress was 0.4 N/m^2 . The result is one which attained to a periodically steady state. The concentration changes counterclockwise. After taking the minimum value, the concentration increases as far as the shear stress reaches 0.23 N/m^2 through 0.4 N/m^2 , the maximum stress. After that, the concentration decreases gradually and settling with flocculation causes the rapid decrease in concentration immediately before the shear stress turns to naught.

SIMULATION

To make it possible to simulate and to estimate the amount of sediments eroded, a model was developed on the basis of the following assumptions:

1. The physical behavior of sediments is expressible as a Bingham fluid;
 2. The increase in the yield value of sediment is proportional to the integration value of the absolute value of the sediment velocity gradient with respect to time;
 3. The yield value is equal to the critical shear stress;
 4. The half-value width of the spatial distribution of shear stress at the bed surface is more than an order of magnitude larger than the thickness of sediments.

The model developed here is as follows:

$$\rho \frac{\partial u}{\partial t} = - \frac{\partial \tau}{\partial x} \quad (5)$$

$$\left. \begin{aligned} \tau &= \tau_y - \mu_p \frac{\partial u}{\partial x} & , \quad \tau + \tau_y > 0 & \text{for } |\tau| \geq |\tau_y| \\ \tau &= 0 & & \text{for } |\tau| < |\tau_y| \end{aligned} \right\} \quad (6)$$

$$\mu_p = \tau_y / \beta \quad (7)$$

$$\tau_y = \alpha \int_0^t \left| \frac{\partial u}{\partial x} \right| dt + \tau_{c_0} \quad (8)$$

where ρ is the sediment density, τ is the shear stress at the bed surface, τ_y is the yield value of sediment, μ_p is the plastic viscosity of sediment, τ_{c_0} is the initial yield value of sediment, β is a coefficient (s^{-1}), and α is the coefficient which indicates the hardening of sediment and is equal to the increment of yield value of sediment per unit strain of sediment (N/m^2).

The computational grid is shown in Fig. 12. The computation points for the velocity component and the stress components are here separated to allow for a better approximation of derivatives by finite differences. In every computation, velocity was set naught for all velocity points as the initial condition and the velocity at the bottom velocity point was also set naught as a boundary condition. Another boundary condition was given as the shear stress at the bed surface. Because Blinco and Simons (1974) experimentally obtained that the

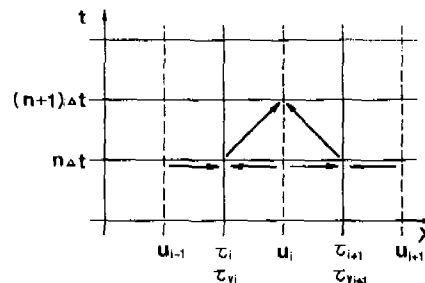


Fig. 12. Computational grid.

standard deviation of the bottom shear stress varies from 25 % to 45 % of the averaged shear stress depending on Reynolds number and that the micro time scale of the bottom shear stress is approximately 0.1 sec, 30 % of the averaged shear stress and 0.1 sec were adopted here for the standard deviation and the period for the shear stress at the bed surface respectively. Under these conditions, a sinusoidal curve of the shear stress at the bed surface was given for erosion at constant averaged shear stresses as follows:

$$\tau = \tau_{ave} (1 + 0.3 \sin 20\pi t) \quad (9)$$

where τ is shear stress and τ_{ave} is averaged shear stress. Several computational examples are shown in Fig. 13 in which 0.3 N/m^2 is averaged shear stress, 365% is initial water content which is equal to 1.5 N/m^2 as initial yield value, and several values as the coefficient, α , were used. Eqs.(2) and (3) were employed to estimate the rate of erosion. The value of the coefficient, β , is given as $1 (\text{sec}^{-1})$ as described before. When the hardening of sediment is ignored, that is,

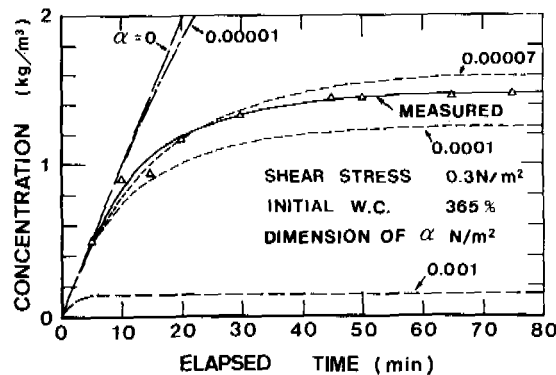


Fig. 13. Simulation of erosion at a constant shear stress.

$\alpha = 0 \text{ N/m}^2$, the concentration of suspended solids is completely different from the measured value. The value of α appropriate for the simulation was clarified to be of the order 0.0001 N/m^2 . The increase in the critical shear stress at $\alpha = 0.00007 \text{ N/m}^2$ is shown in Fig. 14. The value of the critical shear stress 60 minutes after the start is 0.275 N/m^2 which corresponds to 0.138 of solid fraction and it reaches 0.284 N/m^2 or 0.143 of solid fraction after 120 minutes from the start. The measured solid fraction of the first layer after 120 minutes from the start of the test with the same conditions as those in the simulated one is 0.105. The difference between the measured and the simulated solid fraction is probably attributed to the measured solid fraction being the averaged value for one layer. The solid fraction at the top surface might be larger than the averaged value for one layer. The vertical distribution of the simulated solid fraction is almost uniform from the surface to the bottom of sediment. This results from sediments flowing like viscous fluid under shear flow. This trend was observed in every result of simulation including the simulations in different periods and standard deviations. The reason why the solid fractions in middle layers do not increase much more in experiments may be the arch action against the shear stress in sediments. Results of simulations in which the averaged shear stress is varied sinusoidally with 6 hours in each period are shown in Fig. 11. In this case,

$$\tau = 4 \sin \left(\frac{\pi t}{10800} \right) (1 + 0.3 \sin 20\pi t) \quad (\text{N/m}^2) \quad (10)$$

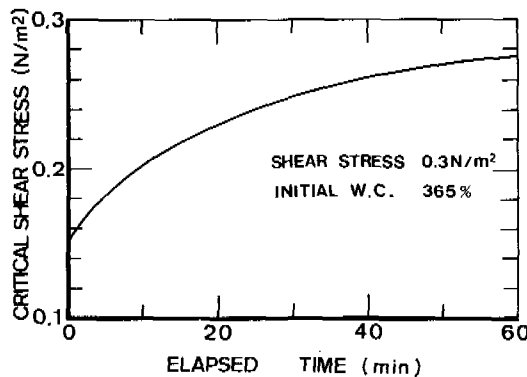


Fig. 14. Increase in critical shear stress in erosion.

where t is expressed in seconds. The dash line is for $\alpha=0 \text{ N/m}^2$ and the dotted line is for $\alpha=0.0001 \text{ N/m}^2$. The result of the simulation with $\alpha=0.0001 \text{ N/m}^2$ is in good agreement with the measured concentration in comparison with the result in which the hardening of sediment is ignored, that is, $\alpha=0 \text{ N/m}^2$. It is clear that the consideration of the increase in the yield value of sediment makes it possible to simulate the rate of erosion.

CONCLUSIONS

The erosional process of cohesive sediments was clarified experimentally. The rapid decrease in the rate of erosion after 10 to 30 minutes from the test start is caused mainly by the hardening of sediment due to shear stress. Selective erosion in silty-clay sediments does scarcely lead to the decrease in the rate of erosion. Based on the yield value of sediment increasing in proportion to the integration value of the absolute value of the sediment velocity gradient, a model to estimate the amount of sediments eroded was developed here. The model was shown to be available to estimate the amount of sediments eroded at both constant shear stresses and shear stresses varied in time. The coefficient to calculate the increase in the yield value from the integration value of the absolute value of the sediment velocity gradient with respect to time is of the order 0.0001 N/m^2 .

ACKNOWLEDGEMENT

This study was financially supported by grants from the Ministry of Education, Japan.

REFERENCES

- Blinco, P.H., and D.B. Simons (1974). Characteristics of turbulent boundary shear stress. *J. Engrg. Mech. Div.*, Em2, 100, 203-220.
- Migniot, P.C. (1968). Etude des propriétés physiques de différents sédiments très fins et de leur comportement sous des actions hydrodynamiques. *La Houille Blanche*, 23, 591-620.
- Ohtsubo, K. (1983). Experimental studies on the physical properties of mud and the characteristics of mud transportation. *Research Rep. from National*

- Institute for Environmental Studies, Japan, 42, 88-103.
Partheniades, E(1965). Erosion and deposition of cohesive solids.
J. Hydraulics Div., HY1, 91, 105-139.
Sawai, K.(1977). Erosion and cross section on the cohesive stream bed. Proc. Japan Soc. Civil Engr., 266, 73-86.
Yeh, H.Y.(1979). Resuspension properties of flow deposited cohesive sediment beds.
University of Florida Coastal Eng. Lab. Report, 79/018, 57-84.

QUANTIFICATION OF WIND INDUCED RESUSPENSION IN A SHALLOW LAKE

R. H. Aalderink,* L. Lijklema,* J. Breukelman,**
W. van Raaphorst** and A. G. Brinkman**

*Dept. of Water Pollution Control, Agricultural University, De Dreijen 12,
6703 BC Wageningen, The Netherlands

**Twente University of Technology, P.O. Box 217, 7500 AE Enschede,
The Netherlands

ABSTRACT

The mass balance of suspended solids in a shallow lake was modelled as the net result of resuspension and settling. Four different formulations for the flux of resuspension were used. Two equations were based on the conception of wave induced resuspension, the other two used the flow field induced shear stress as the driving force for resuspension. Parameter estimations based on experimental time series of wind velocity and SS concentration produced lower least square values with the models based on flow induced resuspension. The model parameter representing settling was in reasonable accordance with the settling velocity obtained from sediment traps. The spread in results can be explained by a lack of homogeneity and horizontal transport.

KEYWORDS

Resuspension, sedimentation, suspended solids, wind, shallow lake, parameter estimation.

INTRODUCTION

When considering control measures for eutrophication, the contribution of phosphates released by the sediments is often a key factor to the cycling of this nutrient. The mechanisms of this internal loading are diffusion through the water-sediment interface of phosphates dissolved in the pore water, and resuspension of sediment particles followed by desorption of phosphate from the particles into the overlying water. The latter process will be of special importance in shallow lakes exposed to relatively strong winds. Prediction of the phosphate flux associated with resuspension requires a description of both the adsorption and desorption characteristics of the resuspended material, and a quantification of the rate of resuspension. The research reported here deals with modelling resuspension and was part of an overall eutrophication study in a shallow Dutch lake.

Several methodologies can be envisaged for the assessment of resuspension as a function of wind. More generally, when studying a process controlled by stochastic external forces, three categories of approach can be considered:

- a deterministic description based on physical relations derived from theory and/or from experimental observations
- statistical relations based on field observations; for instance the comparison of frequency distributions of wind data and of concentrations of suspended material. Simple correlations also fall into this class.
- time series analysis, in which the parameters in a supposed relation between cause and effect are estimated from field data

Very often, a mixture of these approaches is applied. In the field of resuspension the work of Lick *c.s.* (1982) is an example of the first approach. Using an experimental device, they measured the relation between bottom shear stress and rate of resuspension. The shear stress was calculated in a hydrodynamic model. This paper discusses an analysis of time series using partly theoretical, and partly empirical relationships for the flux of resuspension.

MODELS

When neglecting horizontal gradients and transports, the depth-averaged suspended solids concentration \bar{c} is described by the differential equation:

$$\frac{d\bar{c}}{dt} = \frac{1}{D} (\Phi_E - \Phi_D) \quad (1)$$

in which D = water depth (m)

Φ_E = flux of resuspension ($\text{Kg m}^{-2} \text{ hr}^{-1}$)

Φ_D = flux of deposition at the bottom ($\text{Kg m}^{-2} \text{ hr}^{-1}$)

As a first approximation the sedimentation flux can be assumed to be proportional to the concentration of suspended solids. Near the water/sediment interface the transport will be controlled by turbulent and molecular diffusion and by sedimentation. For larger particles sedimentation predominates, small particles are subject to diffusion as well (Lick, 1982). The mathematical expression used is

$$\Phi_D = K_D \bar{c} \quad (2)$$

in which K_D = apparent settling velocity (m hr^{-1})

Two mechanisms can be held responsible for resuspension. One is through wind-induced circulation patterns in the lake, which cause shear stresses at the bottom by which sediment particles are entrained. The other mechanism is that wind-induced waves cause oscillating water movements which are attenuated with increasing depth. In shallow lakes especially, this harmonic movement may bring about shear stresses resulting in resuspension. For both mechanisms partly empirical and partly theoretical relationships between the rate of resuspension and wind velocity can be formulated.

RELATIONSHIPS BETWEEN WIND AND RATE OF RESUSPENSION

Empirical relationship according to Lam and Jacquet. Lam and Jacquet (1976) proposed a linear relationship between the surplus velocity with respect to a critical water velocity and the resuspension rate, based on the assumption that waves are responsible for the entrainment:

$$\Phi_E = K \rho_w \left(\frac{\rho_s}{\rho_s - \rho_w} \right) \left(\frac{U_{D,max} - U_{D,cr}}{U_{D,cr}} \right) \quad (3)$$

in which ρ_w , ρ_s are densities of water and sediment (Kg m^{-3})

K = proportionality constant (m s^{-1})

$U_{D,\max}$ = maximal horizontal water velocity at sediment-water interface due to waves (m s^{-1})

$U_{D,\text{cr}}$ = critical water velocity (m s^{-1})

When $U_{D,\max} \leq U_{D,\text{cr}}$ no resuspension occurs.

$U_{D,\max}$ is a function of water depth and of the height, length and frequency of the waves, which in turn depend upon wind velocity and effective fetch. Appendix I summarizes this relationship. Figure 1 presents the relationship between $U_{D,\max}$, water depth and wind velocity for a fixed fetch of 1000 m.

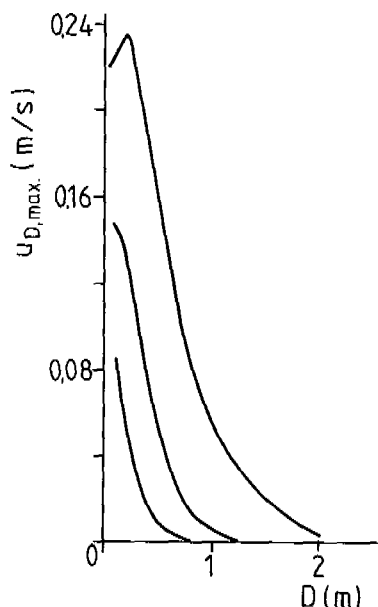


Figure 1. Relationship between $U_{D,\max}$ and water depth for a fixed fetch of 1000 m and a wind velocity of respectively 2.5, 5.0 and 10.0 m s^{-1} .

Theoretical relationship for wave induced resuspension. This relationship is based on an energy balance. The potential energy created by a resuspension flux Φ_E is:

$$N_D = \Phi_E \frac{\rho_s - \rho_w}{\rho_s} g \quad (4)$$

in which N_D = potential energy created per unit of time and per unit area of the water column ($\text{N m}^{-2} \text{s}^{-1}$)

g = acceleration of gravity (m s^{-2})

If the dissipation of turbulent energy into heat is neglected, the dissipation of energy at the bottom

$$\epsilon_D = \tau_D \left| \frac{\delta u}{\delta z} \right|_D \quad (5)$$

will be equal to N_D . In equation (5) τ_D is the bottom shear stress (N m^{-2})

$|\frac{\delta u}{\delta z}|_D$ is the velocity gradient at the bottom (s^{-1})

Appendix II shows how substitution of expressions for τ_D and $|\frac{\delta u}{\delta z}|_D$ results in the relationship:

$$\Phi_E = k \cdot n^{1.125} \cdot U_{D,\max}^{1.875} \quad (6)$$

in which n is the wave frequency (s^{-1})
and k is a constant.

Theoretical relationship for flow induced resuspension.

The same equations (4) and (5) are used but expressions for τ_D and $|\frac{\delta u}{\delta z}|_D$ are now obtained from expressions for the wind induced flow field, see Appendix III.
The resulting relationships for Φ_E are:

$$\Phi_E = k_1 W^{2.75} \text{ for } W \leq 5.67 \text{ m/s} \quad (7)$$

$$\Phi_E = k_2 W^{3.5} \text{ for } W > 5.67 \text{ m/s}$$

in which W = the Wind velocity

Empirical relationship according to Somlyödy.

Somlyödy (1981) in a study on Lake Balaton used Lam and Jacquet's relationship to yield:

$$\Phi_E = k \frac{\rho_w}{\rho_s} \frac{\rho_s w_e}{\rho_w w_e} \quad (8)$$

in which w_e = entrainment velocity ($m s^{-1}$)

According to this author

$$w_e = k_1 U_*^3 \text{ for stable sediments} \quad (9)$$

$$w_e = k_2 U_* \text{ for other sediments}$$

The shear stress velocity U_* is equal to

$$U_* = \sqrt{\tau_s / \rho_w} \quad (10)$$

and the shear stress τ_s at the surface is related to wind velocity W by

$$\tau_s = \rho_a C_f W^2 \quad (11)$$

in which ρ_a = density of air ($kg m^{-3}$)

C_f = friction coefficient

Hence

$$\Phi_E = k W^m \quad (12)$$

with $1 < m < 3$

Equation (1) was used for parameter estimation with field data from Lake Veluwe in the Netherlands and based on equation (2) for settling, and each of the four equations (3), (6), (7) and (12) for resuspension.

DATA, METHODS

Suspended solids concentrations were measured in grab samples during the fall of 1981 and the spring of 1982. The sampling interval was one hour; the period of sampling was at least two weeks. No gradients in the vertical were observed during the sampling periods in this shallow lake (average depth 1m). Due to the length (10 km) and width (varying between 1 and 3 km) horizontal gradients may occur. Next to ss concentration (mg l^{-1}) the loss on ignition was also measured in order to discern between organic and inorganic matter. Also a correction for the contribution of non-settling (blue-green) algae to ss could be made because algal counts were also available. Wind velocity and wind direction were measured continuously.

In order to obtain independent information on settling sediment traps were placed at 0.5 m depth during 3 - 7 days. From these traps the accumulated dry weight was estimated.

The parameter estimation technique of Marquard has been used. This is a mixture of a linearization method and the gradient technique and is based on the least squares criterium. (Draper and Smith, 1966). This method is appropriate for parameter estimation in non-linear models.

RESULTS

Table 1 summarizes the results of parameter estimations with the four models, based on 180 data points.

TABLE 1 Results of Parameter Estimation

| Model | Sum of Squares | Parameters | k_D (m.hr^{-1}) | C_B (mg.l^{-1}) |
|--|----------------|--|---------------------------------|---------------------------------|
| Somlyödy $D\frac{dC}{dt} = k_1 w^{k_2} - k_D(C - C_B)$ | 2382 | $k_1 = 1,63$ $k_2 = 0,40$ | 0,15 | 13,3 |
| Lam & Jacquet $D\frac{dC}{dt} = k_1 \left[\frac{U_{D,\max} - U_{D,cr}}{U_{D,cr}} \right] - k_D(C - C_B)$ | 3407 | $k_1 = 0,19$ $U_{D,cr} = 0,01 \text{ cm/s}$ | 0,10 | 28,7 |
| (wave induced resuspension) $D\frac{dC}{dt} = k_1 \cdot n^{k_2} \cdot U_{D,\max}^{k_3} - k_D(C - C_B)$ | 2888 | $k_1 = 0,05$ $k_2 = 3,91$ $k_3 = 0,94$ | 0,22 | 26,8 |
| (Flow induced resuspension) $D\frac{dC}{dt} = k_1 w^{k_2} - k_D(C - C_B)$ $w \leq 5,67 \text{ m/s}$ $D\frac{dC}{dt} = k_3 w^{k_4} - k_D(C - C_B)$ $w > 5,67 \text{ m/s}$ | 2382 | $k_1 = 1,63$ $k_2 = 0,40$ $k_3 = 1,63$ $k_4 = 0,40$ | 0,15 | 13,3 |

Figure 2 compares measured data and the simulated curve with Somlyödy's model, which had the lowest sum of squares.

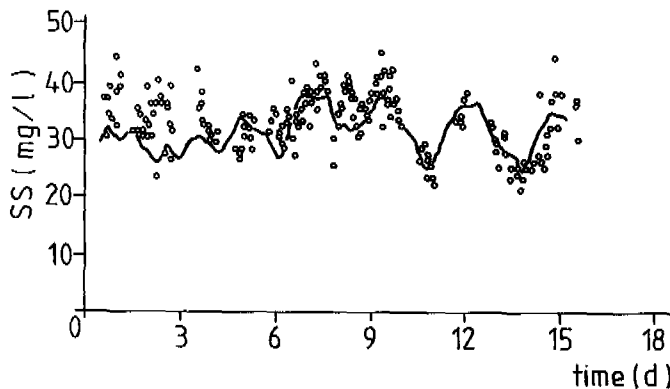


Figure 2. Comparison of simulated and measured SS-concentrations

The results in table 2 also include an estimate of C_B , the background concentration of suspended matter not subject to settling, which is supposed to represent blue-green algae.

The average difference between simulated and observed SS-concentration (figure 2) is fairly large: 3.6 mg l^{-1} , but a reasonable fit is obtained.

Although the theoretical model for flow induced resuspension in comparison with Somlyödy's model allows a discrimination between high and low wind velocities, this is not apparent in the results; both models have exactly the same parameter values and sum of squares and the additional factor of two wind regimes does not improve the results.

The relationships used for wave induced resuspension take the fetch into account through its influence upon $U_{D,\max}$. This does not lead to a better fit. Yet there is some effect of fetch upon SS. During one sampling period, samples were taken at more than one location; table 2 shows a comparison of the averaged results obtained in this period.

TABLE 2 Effect of fetch on observed SS-concentration

| Sampling station | Averaged effective Fetch (m) | Averaged conc. SS (mg l^{-1}) | Averaged Range (mg l^{-1}) |
|------------------|------------------------------|--|---------------------------------------|
| | | | |
| 1 | 1100 | 23.2 | 15 - 35 |
| 2 | 1430 | 30.2 | 21 - 41 |
| 3 | 1890 | 33.1 | 22 - 45 |

These results are an indication that horizontal gradients and transport are important phenomena affecting the SS balance. Probably the poor results of the wave-based models are due to the empirical relationship between wind and $U_{D,\max}$ which was imposed upon the system.

Somlyödy (1981) found a value of $k_2 = 1.0$ for Lake Balaton; the value from this study is much lower and outside the range of equation (12). However, figure 3 shows that the value of this power has been estimated reasonably well within the 95% confidence limits. Nevertheless, a fairly wide range of parameter values within these confidence limits are feasible and clearly there is a strong correlation between individual values.

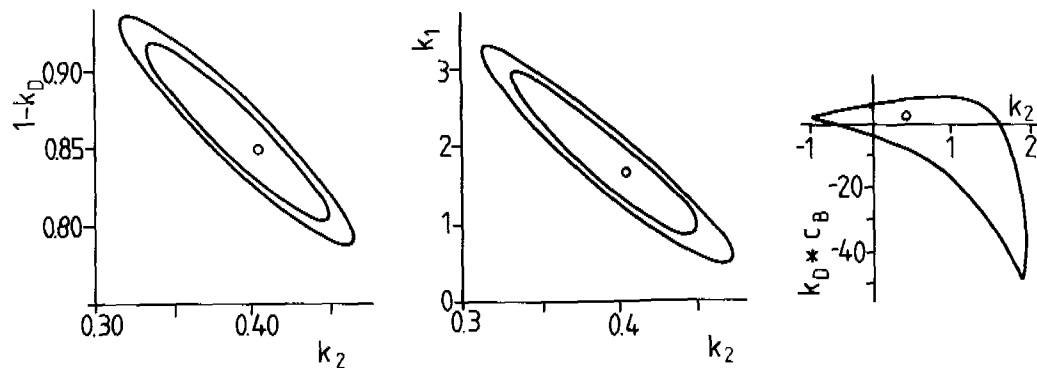


Figure 3. 90 and 95% confidence regions for some parameters

A further test of the results was the application of the optimal parameter set from Somlyödy's model in the simulation of independent time series. An example is presented in figure 4.

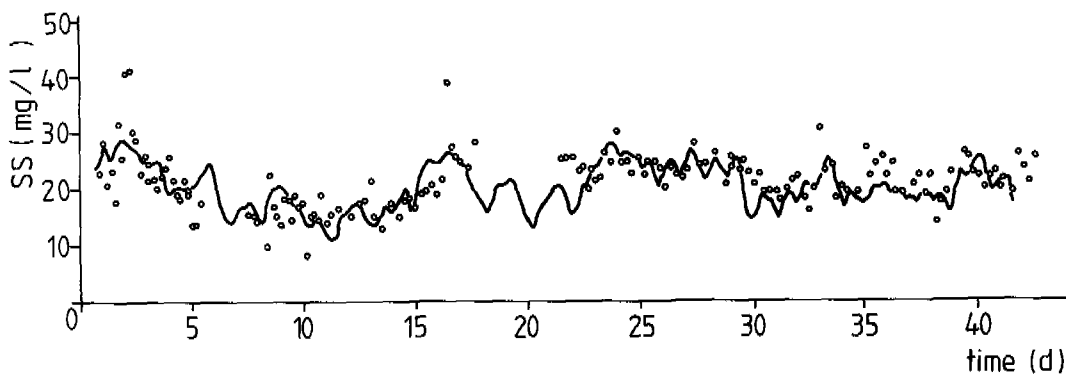


Figure 4. Comparison of the simulation of an independent time series and measured SS-concentration

The background concentration C_B in this series was varied and found to yield 2 mg l^{-1} as the optimum. This is in accordance with the low algal concentration in early spring when this series was measured. The average difference between observed and simulated SS-concentration was 3.8 mg l^{-1} , little more than in the set which was used for the parameter estimation.

A comparison of the fitted apparent settling velocity in the model ($k_D = 0.15 \text{ m hr}^{-1}$) with the data from the sediment traps was obtained by applying equation (2) to the field data: see figure 5.

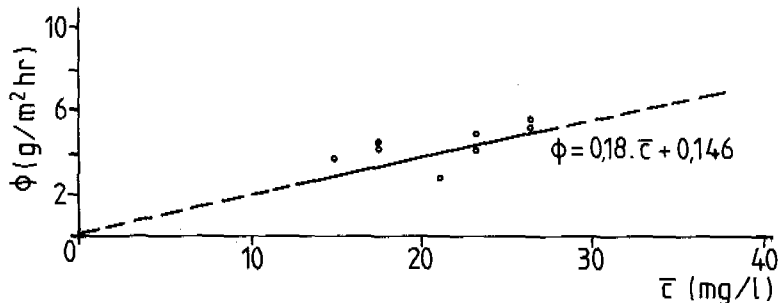


Figure 5. Regression line for measured SS flux and SS-concentration

The slope of the regression line is 0.18 m hr^{-1} , which compares favorably with the model. In the opinion of the authors there is a difference in the mechanisms involved in sedimentation within the trap and in the sediment - water boundary layer. In the latter sedimentation, molecular diffusion and turbulent diffusion contribute to the transport. In the sediment trap turbulence will dissipate completely near the bottom of the cylinder if the ratio length: diameter is sufficiently large (> 20). However, because the majority of the particles is in the range of $7\text{-}10 \mu\text{m}$, settling will be the predominant mechanism.

DISCUSSIONS AND CONCLUSIONS

Lake Veluwe is not homogeneous with regard to water depth, sediment composition and exposure to wind due to its morphology. There is also a dike bordering one side of the lake. Hence winds from varying directions will tend to have different effects upon the resuspension and sedimentation fluxes at different locations. At certain times a location may be subject to erosion and at other times it may be a net sedimentation area. Hence, internal horizontal transport will be an important phenomenon. Wind-induced water velocities are not very high, yet the average residence time for the suspended particles is about 7 hrs (calculated from depth divided by settling velocity). This is the reason why observed SS-concentrations at one location are the net result of some weighted function to which distances of over 7 hrs water flow will contribute. With wind velocities in the order of 10 m sec^{-1} this means that distances of at least several hundred meters may be involved. Particularly in the lateral direction, the lake sediment characteristics exhibit clear gradients on this scale. The three sampling locations indicated in table 2 were at distances of about 300-2000 m. It therefore can be inferred that there is no uniform and unique relationship between wind and suspended solids which is applicable to all times and at all locations. It should be noted that the parameter estimation did not take into account wind direction except for its effect upon fetch. Considering these aspects and also the complications resulting from the contribution of algae, the conclusion can be drawn that a reasonable estimate of SS-concentration can be made using Somlyödy's model. This model is more or less empirical but the sedimentation term is in accordance with independent physical evidence.

REFERENCES

- Banks, R.B. (1975). Some features of wind action on shallow lakes. J. of the Environmental Engineering division, 813-827.
- Bird, R.B., Stewart, W.E. and Lightfoot, E.N. (1960). Transport Phenomena. John Wiley & Sons, New York, 160.
- Draper, N.R. and Smith, H. (1966). Applied regression analysis. John Wiley & Sons, New York, 267-283.
- Groen, P. and Dorresteyn, R. (1976). Zeegolven. In: Opstellen op oceanografisch en maritiem gebied, vol. 11, K.N.M.I., Staatsdrukkerij, Den Haag, 1-124.
- Kamphuis, J.W. (1975). Friction factor under oscillatory waves. Journ. Waterways, Harbours. Coastel Eng. Div. ASCE, 101. 135-144.
- Lam, D.C.L. and Jaquet, M. (1976). Computations of physical transport and regeneration of phosphorus in Lake Erie. Journ. of the fisheries research board of Canada, 33, 550-563.
- Lick, W. (1982). Entrainment, deposition and transport of fine-grained sediments in lakes. Hydrobiologia, 91, 31-40.
- Phillips, O.M. (1966). The dynamics of the upper ocean. Cambridge University Press, Cambridge, 33-98.
- Schoemaker, H.J. (1979). Dynamica van morfologische processen. Collegedictaat TH Delft, Delft 1979.
- Somlyödy, L. (1981). Modeling a complex environmental system: The Lake Balaton Study. Working Paper WP-81-108, International Institute for Applied System Analysis. Laxenburg, Austria, 14-19.

Appendix I. Wave-induced water velocity

The maximum water velocity at the bottom $U_{D,\max}$ is controlled by wave height H , frequency $1/T$, wave length L and water depth D . The wave characteristics in turn depend upon wind velocity W and fetch F . According to Phillips (1966) and others:

$$U_{D,\max} = \frac{\pi H}{T \sinh(2\pi D/L_D)} \quad \text{I-1}$$

with L_D , the wave length at depth D :

$$L_D = L \tanh\left(\frac{2\pi D}{L_D}\right) \quad \text{I-2}$$

with L , the wave length in deep water ($D \geq 0.5L$):

$$L = \frac{g T^2}{2\pi}$$

Groen and Dorresteyn (1976) provided empirical relations for H and T in dimensionless form:

$$\hat{H} = \frac{gH}{W^2} = 0.24 \tanh\left[0.71 \hat{D}^{0.762}\right] \tanh\left[\frac{0.015 \hat{F}^{0.45}}{\tanh[0.71 \hat{D}^{0.762}]}\right] \quad \text{I-3}$$

$$\hat{T} = \frac{gT}{W} = 6.28 \tanh\left[0.855 \hat{D}^{0.365}\right] \tanh\left[\frac{0.0345 \hat{F}^{0.37}}{\tanh[0.855 \hat{D}^{0.365}]}\right] \quad \text{I-4}$$

$$\text{and } \hat{F} = \frac{gF}{W^2} \quad \text{I-5}$$

$$\hat{D} = \frac{gD}{W^2}$$

Figure 1 shows some values of $U_{D,\max}$ as a function of water depth for three wind velocities and a fetch of 1000m.

Appendix II. Wave-induced resuspension

Expressions for τ_D and $(\frac{\delta u}{\delta z})_D$ can be found using

Prandtl's relation:

$$\tau_D = \rho_w L_0^2 \left(\frac{\delta u}{\delta z}\right)_D^2 \quad \text{II-1}$$

in which L_0 is the mixing length (m). Further

$$\tau_D = \rho_w C_{f,b} U_D^2 \quad \text{II-2}$$

with $C_{f,b}$ the friction coefficient at the bottom.

Substitution of II-1 and II-2 in the energy dissipation

$$\epsilon_D = \tau_D \left(\frac{\delta u}{\delta z}\right)_D \quad (5)$$

yields:

$$\epsilon_D = \rho_w C_{f,b}^{1.5} U_D^3 / L_0 \quad \text{II-3}$$

The bottom velocity U_D can be obtained from $U_{D,\max}$ by averaging over the wave period:

$$\epsilon_B = \frac{4}{3} \rho_w C_{f,b}^{1.5} U_{D,\max}^3 / L_0 \cdot \pi \quad \text{II-4}$$

For L_0 Schoemaker (1979) proposed the approximation:

$$L_0 = -0.76 \frac{v}{U_*} + 0.014 K_n \quad \text{II-5}$$

in which v = kinematic viscosity ($\text{m}^2 \text{s}^{-1}$)
and K_n = Nikurads roughness height 0.1 m for sediment

According to Kamphuis (1975):

$$C_{f,b} = 0.2 \left(\frac{K_n}{A_D} \right)^{\frac{1}{3}} \quad \text{II-6}$$

with A_D the amplitude of the waves near the bottom, which can be approximated by
 $A_D = U_{D,\max}/n$ II-7

in which n is the wave frequency.

Neglecting the viscosity in II-5 and substitution of the expressions II-5, 6 and 7 in II-4 and equating ϵ_B to the rate of potential energy production by resuspension:

$$N_D = \Phi_E \frac{\rho_s - \rho_w}{\rho_s} g \quad (4)$$

results in

$$\Phi_E = K n^{1.125} U_{D,\max}^{1.875} \quad (6)$$

The constant K contains several other constants such as g , ρ_s , ρ_w and K_n .

Appendix III. Flow induced resuspension

The stationary linearised flow equation

$$\nabla \bar{p} - \rho_w g + \nabla \bar{\tau}(t) + \nabla \bar{\tau}(l) = 0 \quad \text{III-1}$$

in which \bar{p} = average hydrostatic pressure

$\bar{\tau}(t,l)$ = turbulent, laminar contribution the shear stress

can be solved using Boussineq's approximation for turbulent flow (Bird, Stewart, Lightfoot, 1960):

$$\tau_{zx}(l) = -v_l \rho_w \frac{\delta u_x}{\delta z} \text{ and} \quad \text{III-2a}$$

$$\tau_{zx}(t) = -v_t \rho_w \frac{\delta u_x}{\delta z} \quad \text{III-2b}$$

which yields:

$$u_x = \frac{\tau_0 D}{\rho_w v} \left[\frac{m-1}{2} \left(\left(\frac{z}{D} \right)^2 - 1 \right) - \left(\frac{z}{D} + 1 \right) \right] \quad \text{III-3}$$

in which v is the "total" viscosity $v_t + v_l$ and
 $m = \tau_D/\tau_0 = 0.5$

From III-3 it follows that

$$\left(\frac{\delta u_x}{\delta z}\right)_D = \frac{\tau_0}{\rho_w Y} \left[(m-1) \frac{z}{D} - 1 \right] \quad III-4$$

and also

$$\tau_{xz} = \tau_0 \left[(m-1) \frac{z}{D} - 1 \right] \quad III-5$$

Banks (1975) derived an empirical relation for τ_0 :

$$\tau_0 = \rho_a C_{f,a} W^2 \quad III-6$$

with ρ_a = density of air (Kg.m^{-3})

$C_{f,a}$ = friction coefficient air-water

W = wind velocity at 10 m height (m.s^{-1})

$C_{f,a}$ is a function of wind velocity due to increasing roughness of the water surface at higher velocity:

$$C_{f,a} = 9.0 \cdot 10^{-3} W^{-0.5} \quad \text{when } W \leq 5.67 \text{ m.s}^{-1}$$

$$C_{f,a} = 6.67 \cdot 10^{-4} W \quad \text{when } W > 5.67 \text{ m.s}^{-1}$$

III-7

Substitution of the expressions for τ and $\frac{\delta u}{\delta z}$ in equations (4) and (5) results in equation (7).

THE BEHAVIOUR OF SUSPENDED SEDIMENTS AND MUDS IN AN ESTUARY

T. Umita,* T. Kusuda,** Y. Awaya,** M. Onuma* and T. Futawatari**

**Department of Civil Engineering, Iwate University 4-3-5 Ueda, Morioka, Japan*

***Department of Civil Engineering, Kyushu University 6-10-1 Hakozaki, Fukuoka, Japan*

ABSTRACT

The fundamental behaviour of suspended sediments and muds was investigated using an annular flume with the condition of cyclically changed shear stress. The results from two series of experiments showed that particle sizes which participate in the variation of suspended sediments were restricted to smaller sizes of the material. It was also found that the cyclically steady state was finally attained with respect to the suspended sediments as the tidal cycle repeated. In that state the suspended sediments were subject to three phenomena: erosion; deposition with dispersed state; and deposition with flocculation. A simple model on the suspended sediments in an estuary was developed and its behaviour in a model estuary was simulated by using the fluxes of erosion and deposition in the experiment. That model well described the variation of the suspended sediments and muds.

KEYWORDS

Estuary; muds; suspended sediments; erosion; deposition.

NOMENCLATURE

| | | |
|------------|--|-------------|
| C | Concentration of the suspended sediments | M/L^3 |
| c_f | Chezy coefficient | $L^{1/2}/T$ |
| D | Dispersion coefficient | L^2/T |
| $D_{50,p}$ | Median particle diameter and median floc diameter in suspension | L |
| F_e, F_d | Erosion flux and deposition flux | $M/L^2 T$ |
| g | Gravity acceleration | L^2/T |
| H | Water depth | L |
| M | Amount of mud | M/L^2 |
| S | Bed slope | - |
| u, v | Vertically averaged velocity in a direction of the flow and that in a direction normal to the flow | L/T |

| | | |
|------------------------|--|----------|
| x, y | Direction of the flow (positive to upstream) and that normal to the flow | L |
| ρ | Water density | M/L^3 |
| τ | Bottom shear stress | M/LT^2 |
| τ_{ce}, τ_{cd} | Critical shear stress of erosion and deposition | M/LT^2 |

INTRODUCTION

The hydraulic behaviour in an estuary is mainly dependent on the geography, the tide, and the river flow. In an estuary suspended sediments are eroded and deposited according to the variation of the hydraulic condition. Suspended sediments play a significant role in the estuarine water quality because they have a large specific surface and consequently they absorb many kinds of heavy metals, nutrients, and organic matter. Suspended sediments cause, furthermore, shoaling and a decrease in the hatching rate. Although much information with respect to erosion and deposition under constant shear stress is available (Etter et al., 1968; Partheniades and Passwell, 1968; Partheniades, 1970; Raudkivi, 1974), less information under cyclically changed shear stress is obtained. Therefore, it is necessary to elucidate the behaviour of suspended sediments.

The purpose of this study is to investigate the fundamental mechanism on the variation of suspended sediments and muds under the condition of cyclically changed shear stress and to simulate the behaviour of them in the model estuary. The results obtained in this study will present useful fundamental information on water quality management and water pollution protection in an estuary.

TEST MATERIAL

The test material used in this study was taken at the mouth of the River Chikugo in Kyushu. Its particle size distribution is shown in Fig. 1, and certain other properties of this material are listed in Table 1. Of the material, 25% is in the clay range and the rest is in the medium- and fine-silt range. This material represents the typical properties of Japanese estuarine muds.

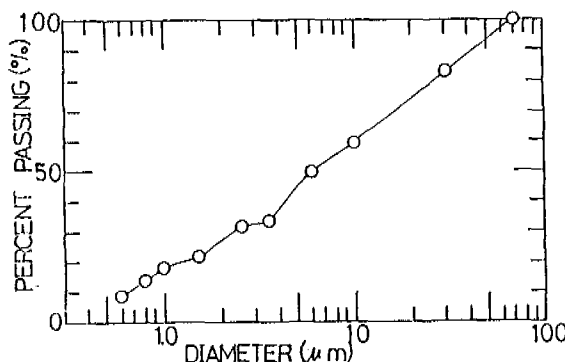


Fig. 1. Particle size distribution

TABLE 1 Material Properties Used in This Test

| Specific Gravity (-) | Liquid Limit (%) | Plastic Limit (%) | Ignition Loss (%) |
|-------------------------|---------------------|----------------------|----------------------|
| 2.51 | 99 | 41 | 12 |

EXPERIMENTAL APPARATUS AND PROCEDURES

The experimental apparatus used in this study is depicted in Fig. 2. It consists of an annular channel (20 cm deep, 100 cm in medium radius, and 20 cm wide) which rotates clockwise and an annular ring which rotates counterclockwise. The revolution number of the annular ring is 2.18 times as fast as that of the channel to minimize the radial secondary current effect at the interface between water and muds. This is the same as that used by Kusuda *et al.* (1982a). In this study salt water of specific gravity 1.025 was used and water temperature was kept at 20±1 °C during the experiment. The bed shear stress τ was changed with a period of 6 hours as shown in Fig. 3.

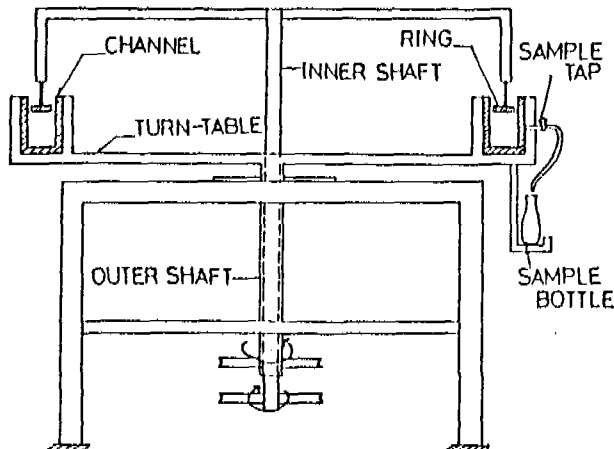


Fig. 2. Annular flume

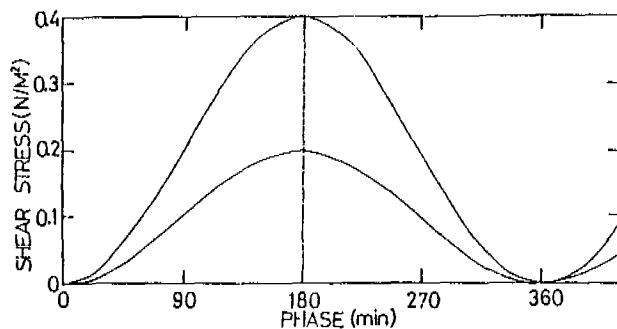


Fig. 3. Bed shear stress

The experiments were composed of two series. One was carried out at zero shear stress and the other at maximum shear stress. The former was performed on the condition of 5 hours vigorous premixing of a 15 kg/m³ suspension and 24 hours deposition in order to make a mud bed in advance, and the latter on the condition of 5 hours premixing in order to prevent the formation of a mud bed.

For the measurement of suspended sediment, concentration samples were drawn from a drain cock 8 cm high above the mud surface. Each sample was filtered through a filter 0.1 μm in pore size and its dry weight measured. Floc size distribution in suspension was measured by the photomicrographs of x100 magnification. Particle size distribution in suspension was measured by a Centrifugal Particle Size Analyzer after sodium hexametaphosphate (4%) was added to the sample diluted with salt water and dispersed by the homogenizer.

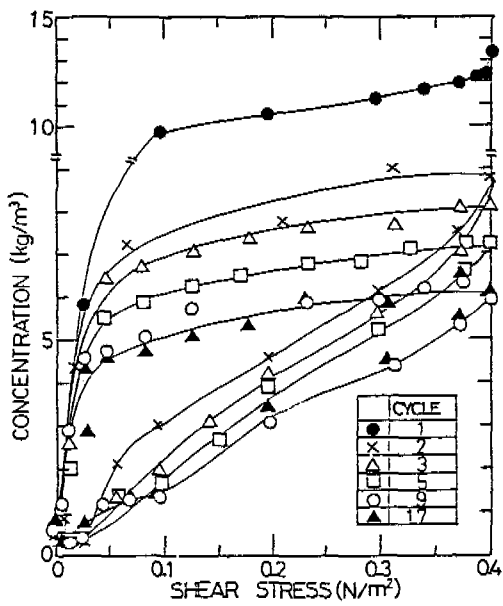


Fig. 4. Variation of suspended sediment concentration

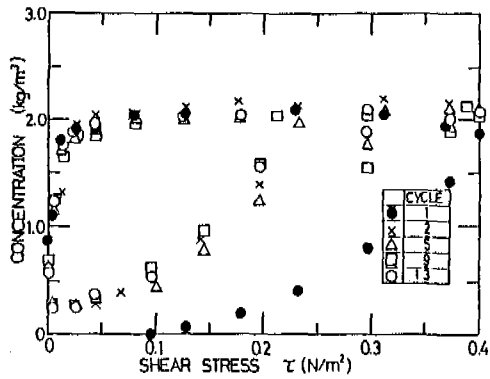


Fig. 5. Variation of suspended sediment concentration

EXPERIMENTAL RESULTS AND DISCUSSIONS

Figures 4 and 5 show the typical relationship between suspended sediment concentration and shear stress. In Fig. 4 the experiment is started at the maximum shear stress τ_{\max} and in Fig. 5 at zero shear stress. The suspended sediment concentration is plotted counterclockwise in each tidal cycle as the tide proceeds. The suspended sediment concentration begins to increase as the shear stress exceeds a certain value and continues to increase up to τ_{\max} or the slightly smaller shear stress than τ_{\max} after the shear stress reaches τ_{\max} . After that it decreases gradually, and rapidly below a certain shear stress. The minimum suspended sediment concentration is about 0.2 kg/m³ in each tidal cycle, so the eroded sediments on the

previous tidal cycle are almost deposited before the next tidal cycle begins. In a tidal cycle one shear stress has two different suspended sediment concentrations. This is a remarkable feature compared with that of non-cohesive materials such as sands.

The relationship between the number of tidal cycles and the maximum suspended sediment concentration C_{max} in each tidal cycle is shown in Fig. 6. In the experiment which begins at τ_{max} , C_{max} decreases with increasing the number of tidal cycles and finally reaches a constant value in each experiment. Furthermore, the behaviour of suspended sediment is almost the same in cases where the tidal number is over 9. On the other hand, in the experiment of zero shear stress, C_{max} increases gradually and reaches a constant value in each experiment. In order to make clear the variation of C_{max} , particle size distribution for C_{max} in each tidal cycle is measured. Figure 7 shows the relationship between the number of tidal cycles and the median particle diameter $D_{50,p}$. $D_{50,p}$ is small compared with that of the result shown in Fig. 1, so it is considered that selective erosion (Kusuda et al., 1982b) that is, erosion in which only small particles in muds are eroded, occurs in the erosion process. $D_{50,p}$ approaches a constant value in each experiment and the variation of D_{max} corresponds well to that of $C_{50,p}$ so the particle size distribution contributes to the variation of C_{max} . In each case suspended sediments reach "a cyclically steady state" as the tidal cycle progresses. It is satisfactory that the muds which form the bed at τ_{max} in the cyclically steady state do not contribute to the variation of the suspended sediment concentration. Therefore, the following discussions are restricted to the cyclically steady state.

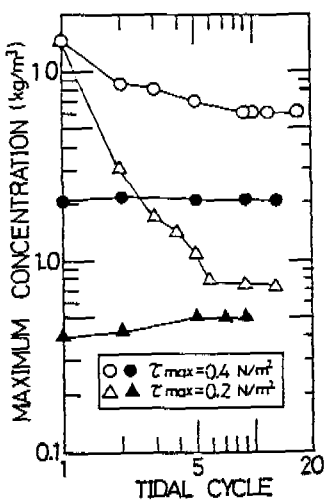


Fig. 6. Relationship between the number of tidal cycles and C_{max}

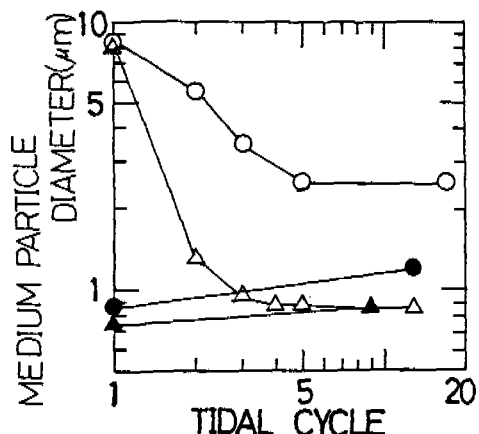


Fig. 7. Relationship between the number of tidal cycles and the median particle diameter

Figure 8 shows the variation of the median floc diameter $D_{50,f}$ and the median particle diameter $D_{50,p}$ in suspension. The variation of $D_{50,p}$ corresponds to that of the shear stress and, particularly in the case of $\tau_{max} = 0.4 \text{ N/m}^2$, the relatively large particles eroded near τ_{max} . On the other hand, the variation of $D_{50,f}$ shows the opposite

tendency to that of $D_{50,p}$. $D_{50,f}$ takes a minimum value at the high shear stress. This means that the flocs in suspension are destroyed to some extent by the shear stress; therefore, the floc size of this mud is controlled by the shear stress. From 240 to 300 minutes in a tide, suspended sediment concentration decreases slowly and $D_{50,f}$ scarcely changes. Therefore, it should be considered that relatively large size particles in suspension deposit with dispersed state during this time. Furthermore, it is a remarkable result that $D_{50,f}$ has a peak value at 340 minutes. After that suspended sediment decreases rapidly. This demonstrates that significant deposition with flocculation is occurring after 340 minutes. The shear stress at which deposition with flocculation predominates is about 0.025 N/m^2 , which corresponds to the critical shear stress of deposition τ_{cd} , reported by Kusuda *et al.* (1982b).

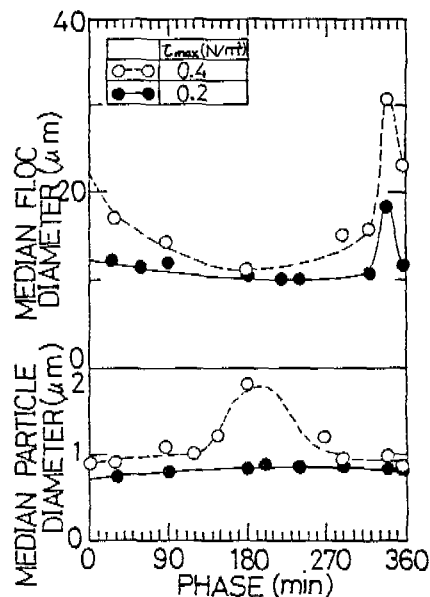


Fig. 8. Variation of the median floc diameter and the median particle diameter

MODEL ON THE BEHAVIOUR OF SUSPENDED SEDIMENTS IN AN ESTUARY

In this study all experiments are performed using the annular channel, which is considered as an endless channel. Therefore, it is considered that the experimental results in this study correspond to those performed under the condition of shear stress with no convection. Based on the above results, the behaviour of suspended sediments under the condition of cyclically changed shear stress can be expressed by three processes (1), (2) and (3) as shown in Fig. 9. In this figure (1), (2) and (3) show the erosion, the deposition with dispersed state, and the deposition with flocculation, respectively.

τ_{ce} and τ_{cd} represent the critical shear stresses of erosion and deposition, respectively. The suspended sediment concentration begins to increase when the shear stress becomes larger than τ_{ce} , increases up to τ_{max} , decreases gradually up to τ_{cd} , and decreases rapidly.

The behaviour of particle and floc size in suspension can be explained as shown in Table 2.

TABLE 2 Behaviour of Particle and Floc Size

| Shear stress | Particle size | Floc size |
|-----------------------------|---|---|
| $\tau_{ce} \sim \tau_{max}$ | increase because of the erosion of large particles | decrease because of the destruction by the shear stress |
| $\tau_{max} \sim \tau_{cd}$ | decrease because of the deposition with dispersed state | decrease because of the destruction by the shear stress |
| $\tau_{cd} \sim \tau_{ce}$ | decrease because of the deposition with flocculation | large because of the flocculation |

For practical purposes, the deposition with dispersed state ((2) in Fig. 9) can be neglected because the suspended sediment concentration scarcely decreases. It may be considered that the concentration of suspended sediment in erosion processes increases linearly as time passes.

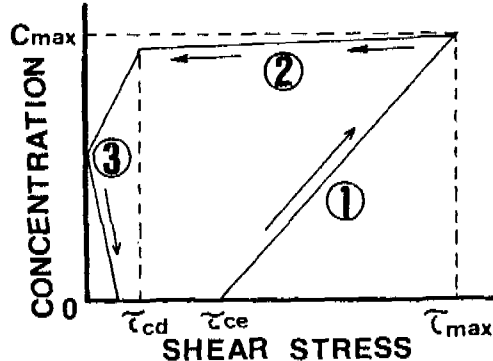


Fig. 9. Model of the behaviour of suspended sediments in an estuary

Based on the above model, the fluxes of deposition and erosion are calculated from the experimental results. The flux of erosion F_e can be expressed as a function of τ_{max} as shown in Fig. 10 and the flux of deposition F_d as that of the suspended sediment concentration as shown in Fig. 11. F_d is usually expressed as follows (Krone, 1962): $F_d = P w C$; where P , w and C are the probability that flocs stick to the bed, the settling velocity of floc, and the concentration of floc, respectively. w , however, is a function of floc size and floc density, and they are also a function of shear stress and floc concentration. Therefore, it is difficult to estimate the value of w under the condition of cyclically changed shear stress. The properties of muds are complicated because the vertical particle distribution and solid fraction of muds in an erosional process are

changing from hour to hour (Kusuda *et al.*, 1982b), so the theoretical or empirical erosion flux F_e is not obtained at the present time. Therefore, these simple relationships (Figs 10 and 11) are useful from the practical viewpoint.

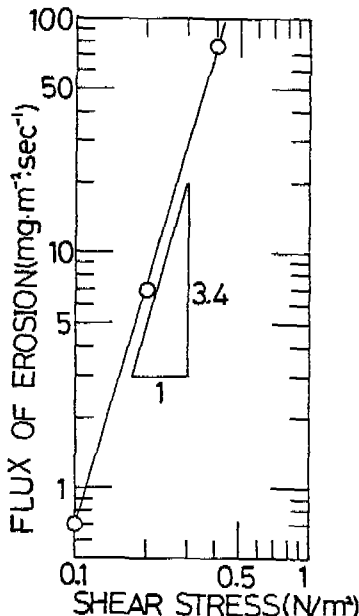


Fig. 10. Erosion flux as a function of the maximum shear stress

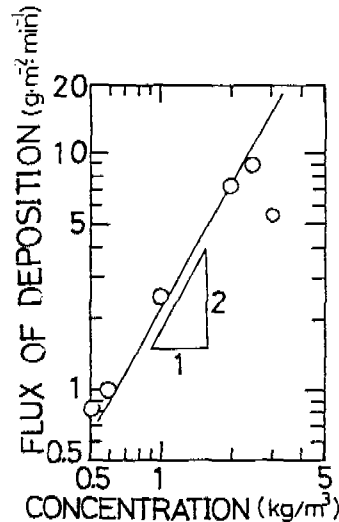


Fig. 11. Deposition flux as a function of the suspended sediment concentration

SIMULATION OF THE BEHAVIOUR OF SUSPENDED SEDIMENTS AND MUDS IN A MODEL ESTUARY

The model estuary for simulation of the behaviour of suspended sediments and muds is shown in Fig. 12. Its width, length, and bed slope S are 750 m, 12 km, and 2.85/12000, respectively. It is assumed that water depth changes cyclically at the downstream end and it has a constant value upstream. The governing equations, that is, the equation of continuity, the equations of motion, and the equation of mass transport, can be described as follows:

$$\frac{\partial H}{\partial t} + \frac{\partial}{\partial x}(uH) + \frac{\partial}{\partial y}(vH) = 0 \quad (1)$$

$$\frac{\partial u}{\partial t} + u \frac{\partial u}{\partial x} + v \frac{\partial u}{\partial y} + g \frac{\partial H}{\partial x} + gS + \frac{Tbx}{\rho H} = 0 \quad (2)$$

$$\frac{\partial v}{\partial t} + u \frac{\partial v}{\partial x} + v \frac{\partial v}{\partial y} + g \frac{\partial H}{\partial y} + \frac{Tby}{\rho H} = 0 \quad (3)$$

$$H \left(\frac{\partial C}{\partial t} + u \frac{\partial C}{\partial x} + v \frac{\partial C}{\partial y} \right) - \frac{\partial}{\partial x} (HD_x \frac{\partial C}{\partial x}) - \frac{\partial}{\partial y} (HD_y \frac{\partial C}{\partial y}) - F_{ed} = 0 \quad (4)$$

where x, y represent a direction of the flow (positive to upstream) and a direction normal to the flow, respectively. D , H , and g are the dispersion coefficient, water depth, and gravity acceleration,

respectively. u and v are vertically averaged velocities in the direction of flow and normal to the flow, respectively. The bottom frictions are assumed by the Chezy formula as:

$$\tau_{bx} = \rho g \sqrt{u^2 + v^2} u/c_f^2 \quad (5) \quad \tau_{by} = \rho g \sqrt{u^2 + v^2} v/c_f^2 \quad (6)$$

where c_f and ρ are the Chezy coefficient and density of water, respectively. D_x , D_y , and c_f are specified as $100 \text{ m}^2/\text{s}$, $15 \text{ m}^2/\text{s}$ and $40.4 \text{ m}^2/\text{s}$ respectively. The value of c_f corresponds to that of $u/u_* = 1.3$. In order to solve the above equations the standard Galarkin finite element method was employed for the spatial discretization and the explicit scheme for the numerical integration of the time derivative. The finite element idealization is shown in Fig. 13. The total number of nodal points and elements are 125 and 192, respectively. For the interpolation functions, standard linear shape functions based on the three node triangular finite element are used.

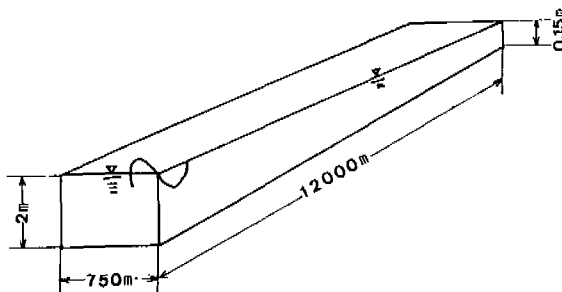


Fig. 12. Model estuary

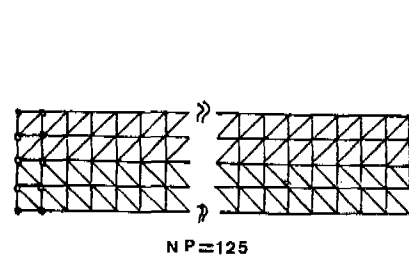


Fig. 13. Finite element idealization

The boundary conditions downstream and upstream are specified as:

$$H(\text{m}) = 1.0 \cos(2\pi t/12x60x60) + 2.0 \quad \frac{\partial C}{\partial x} = 0 \quad (7)$$

and

$$H(\text{m}) = 0.15 \quad \frac{\partial C}{\partial x} = 0 \quad (8)$$

On both sides of the estuary the no-slip boundary condition and the no-flux condition across the boundary are used.

The initial condition on all nodal points for velocity and suspended sediment is specified as zero, respectively, and for water depth it is $H(x) = 3.0 - 2.85x/12000(\text{m})$. The amount of mud on all nodal points is 1 kg/m^2 .

The time step interval for the numerical integration is 30 seconds, and the slit-time method is used for the numerical integration of water depth and velocities. τ_{ce} and τ_{cd} on all nodal points are 0.05 and 0.025 N/m^2 , respectively. The value of τ_{ce} corresponds to the critical shear stress for the muds with the surface solid fraction 0.04 . The fluxes of erosion and deposition are expressed by the following equations (see Figs 10 and 11).

$$F_e = 1713 \times 10^{-6} \tau_{max}^{3.4} \quad [\text{kg/m}^2\text{s}] \quad (9)$$

$$F_d = 1.33 \times 10^{-2} C^2/H \quad [\text{kg/m}^2\text{s}] \quad (10)$$

RESULTS AND DISCUSSIONS OF SIMULATION

The simulation was conducted for 26 hours. Figures 14 and 15 show the computed current velocity u and the water level at each station from the river mouth, respectively. These variations at the ebb are flatter than at the flood. The period influenced by the tide at the upstream end is shorter than downstream. The maximum current velocity at each station is obtained at the ebb. At 11 km the maximum current velocity to upstream is obtained about 4 hours later than at 1 km. At low tide zero current velocity is obtained within about 1 hour after the water level reaches a minimum value. On the other hand, at high tide it is obtained before the water level reaches it. From these results it is recognized that this model of an estuary well describes the cyclic flow pattern.

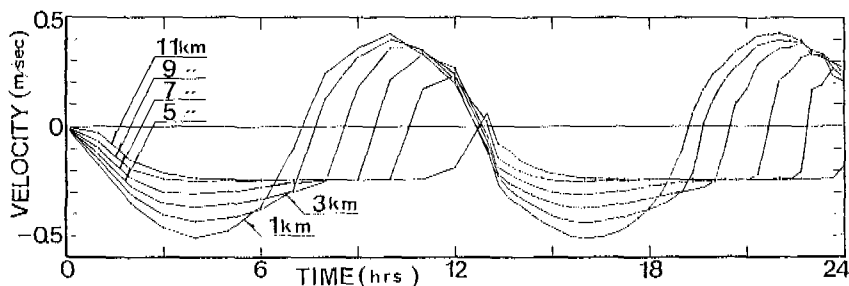


Fig. 14. Computed current velocity in a model estuary

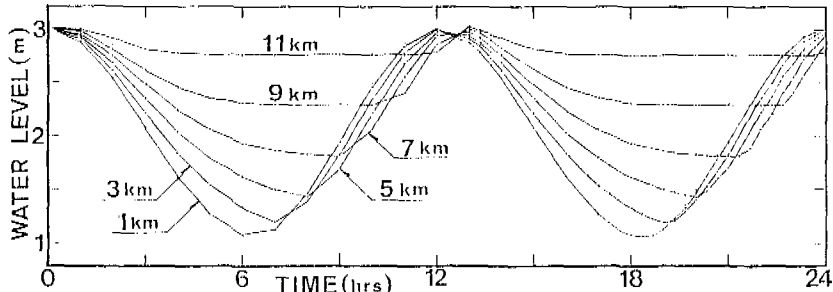


Fig. 15. Computed water level in a model estuary

Figures 16 and 17 show the computed amounts of suspended sediments and muds at each station, respectively. It is recognized that they are, as a whole, changing with a period of 12 hours according to the variation of the hydraulic condition. At the flood the erosion begins downstream about 6 hours sooner than at the upstream end because of the lag time of tidal travel along the estuary, while at the ebb it begins at almost the same time in the whole estuary, because of no lag time. For the same reason, in the latter half of the ebb the deposition begins downstream faster than upstream, while in the latter half of the flood it begins at the same time in the whole estuary. Downstream the amount of mud decreases rapidly and finally muds are removed from the bed within a short period because the shear stress downstream is larger than upstream, while upstream muds continue to be eroded gradually for a long time. It is also recognized that muds are accumulated upstream as the tidal cycle proceeds. It is considered that because (1) F_e upstream is smaller than that downstream, so the amount of mud which is eroded in a cycle is small upstream, (2) the critical shear stresses of erosion and deposition,

τ_{ce} and τ_{cd} , are introduced in this simulation, and (3) the suspended sediments are discharged even at the ebb from upstream in this simulation. These results support the conceptual idea with respect to the behaviour of suspended sediments and muds in an estuary proposed by Postma (1967).

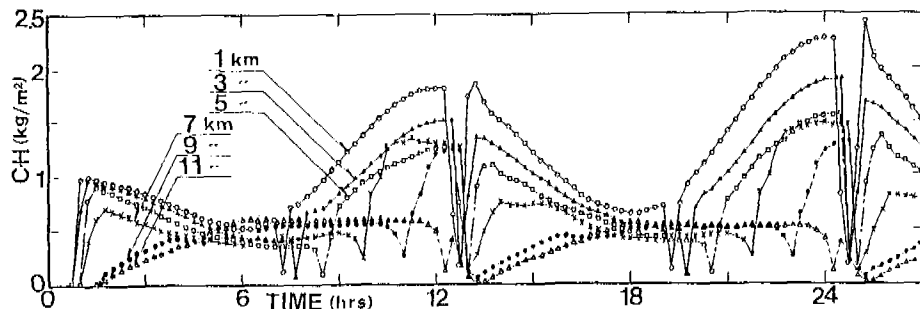


Fig. 16. Computed amount of suspended sediment in a model estuary

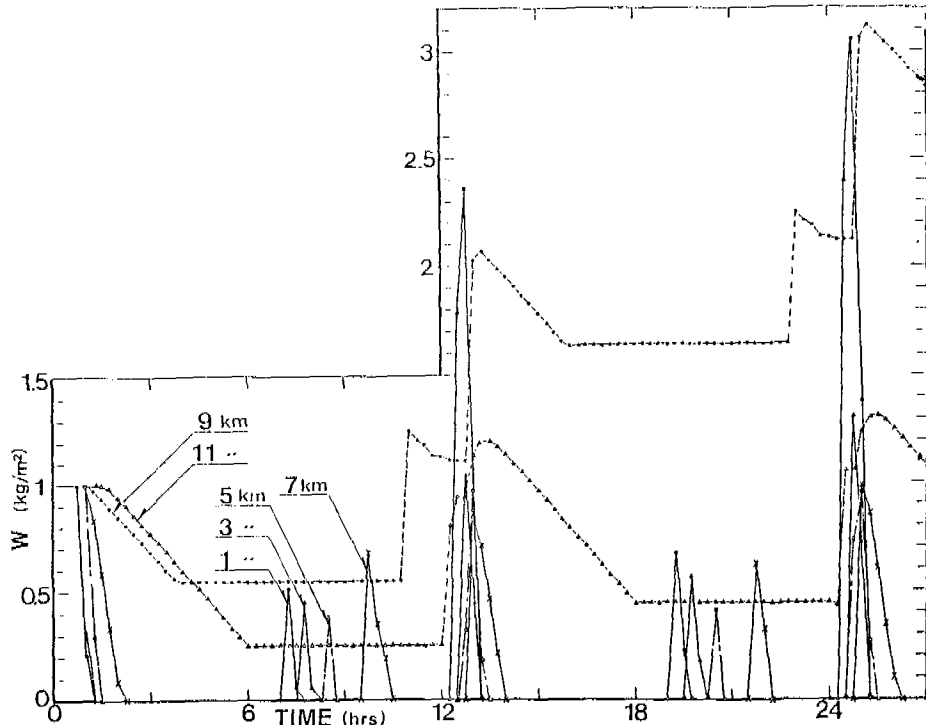


Fig. 17. Computed amount of muds in a model estuary

Figures 18 and 19 show the relationship between the current velocity and the suspended sediment concentration in one cycle. Figure 18 was obtained in this simulation. Figure 19 indicates the results of the field data investigated by the Ministry of Construction in the River Chikugo on October 5, 1967 (Umita et al., 1982). In these figures (s) represents the high tide, and the plot or curve starts at (s). The hydraulic conditions are apparently different from each other and the boundary conditions of the suspended sediments up- and downstream

in this simulation are a little different from the conditions observed. However, they qualitatively well describe the variation of the suspended sediments as the current velocity changes.

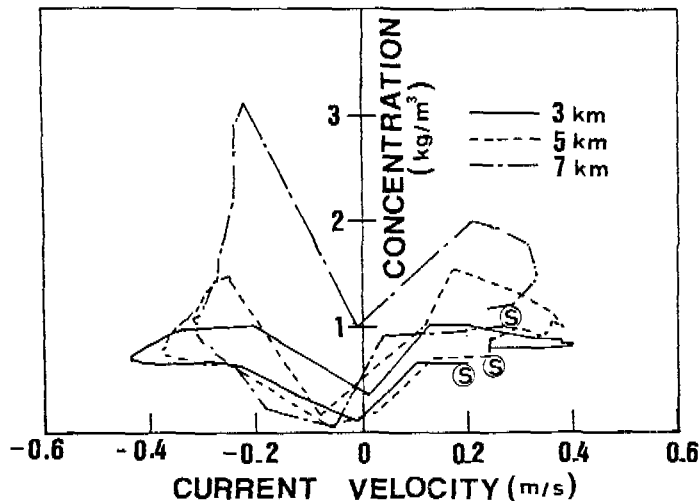


Fig. 18. Relationship between current velocity and suspended sediment concentration in a model estuary

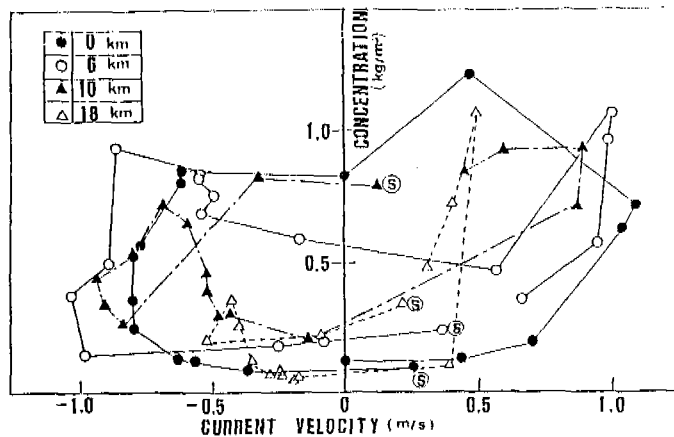


Fig. 19. Relationship between current velocity and suspended sediment concentration in the River Chikugo

CONCLUSION

The fundamental mechanisms of the variation of suspended sediments and muds under cyclically changed shear stress were investigated experimentally by use of an annular flume. The behaviour of suspended sediments and muds was simulated in the model estuary. Conclusions obtained in this study were as follows:

- 1) Under the condition of cyclically changed shear stress, deposition and erosion rose alternately and the concentration of suspended sediment fell into "a cyclically steady state" as the tidal cycle proceeded.
- 2) In a cyclically steady state the behaviour of suspended sediment was subject to three mechanisms: erosion, deposition with dispersed state, and deposition with flocculation.
- 3) The variations of floc and particle size in suspension were explained based on the above mechanisms.
- 4) The simple simulation model developed in this study well described the variations of velocity, water level, and transport phenomena of suspended sediments and muds in an estuary.

REFERENCES

- Umita, T., Kusuda, T. and Awaya, Y. (1982). The behaviour of suspended solids in an estuary. Pro. of the 37th Annual Conference of the JSCE, No.2, 139-140.
- Etter, R.J., Hoyer, R.P., Partheniades, E. and Kennedy, J. F. (1968). Depositional behaviour of kaolinite in turbulent flow. J. of the Hydraulic Division, ASCE, Vol. 94, No. HY6, November, 1439-1452.
- Krone, R.B. (1962). Flume studies of the transport of sediment in estuarine shoaling process. Technical report, Hydraulics Engineering Laboratory, University of California, Berkeley, California.
- Kusuda, T., Umita, T. and Awaya, Y. (1982a). Depositional process of fine sediments. Wat. Sci. Tech., Vol. 14, 175-184.
- Kusuda, T., Umita, T. and Awaya, Y. (1982b). Erosional process of fine cohesive sediments. Memoirs of the Faculty of Eng. Kyushu University, Vol. 42, No.4, December, 317-333.
- Partheniades, E. (1965). Erosion and deposition of cohesive soils. J. of the Hydraulics Division, ASCE, Vol. 91, HY1, January, 105-139.
- Partheniades, E. and Passwell, R.E. (1970). Erodibility of channels with cohesive boundaries. J. of the Hydraulics Division, ASCE, Vol. 96, No. HY3, March, 755-769.
- Postma, H. (1967). Sediment transport in the estuarine environment. In: Estuary, G. H. Lauff (Ed.). American Association for the Advancement of Science. pp. 158-179.
- Raudkivi, A.J. and Hutchison, D.L. (1965). Erosion of kaolinite clay by flowing water. Pro. R. Soc. Lond., A, 337, 537-554.

BENTHAL DEPOSITS

STABILIZATION OF ORGANIC CARBON AND NITROGEN IN CONSOLIDATING BENTHAL DEPOSITS

C. W. Bryant, Jr.* and L. G. Rich**

**Department of Civil Engineering and Engineering Mechanics, 310B CE Building, The University of Arizona, Tucson, Arizona, 85721, U.S.A.*

***Environmental Systems Engineering Department, 401 Rhodes Research Center, Clemson University, Clemson, South Carolina, 29631, U.S.A.*

ABSTRACT

The objective of this research was to develop and validate a predictive model of the benthal stabilization of organic carbon and nitrogen in deposits of waste activated sludge solids formed at the bottom of an aerated water column, under conditions of continual deposition. A benthal model was developed from a one-dimensional, generalized transport equation and a set of first-order biological reactions. For model verification, depth profiles of the major interstitial carbon and nitrogen components were measured from a set of deposits formed in the laboratory at 20°C and a controlled loading rate.

The observed sequence of volatile acid utilization in each benthal deposit was that which would be predicted by the Gibbs free energies of the individual degradation reactions and would be controlled by the reduction in interstitial hydrogen partial pressure with time. Biodegradable solids were solubilized rapidly during the first three weeks of benthal retention, but subsequent solubilization occurred much more slowly.

The benthal simulation effectively predicted the dynamics of consolidating, organic deposits. Simulation of organic loading rates up to 250 g BVSS/(m² day) indicated that the stabilization capacity of benthal deposits was far above the range of organic loading rates currently used in lagoon design.

KEYWORDS

Benthal stabilization, benthal modeling, deposit profiles, organic loading rates.

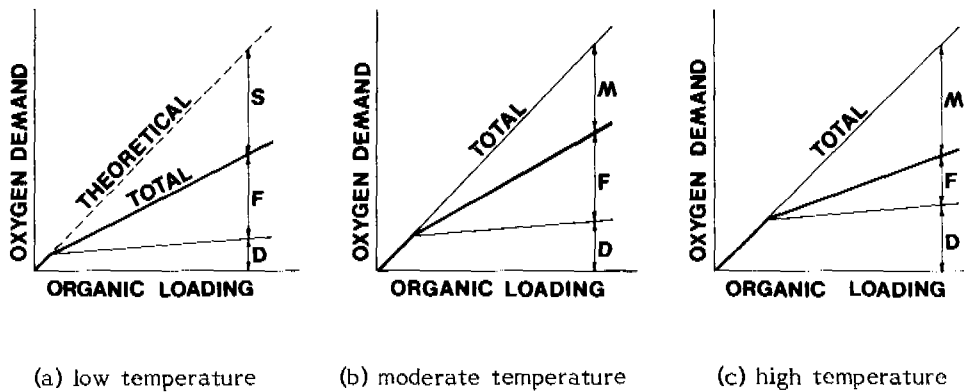
INTRODUCTION

Benthal stabilization of organic carbon and nitrogen in consolidating deposits is a phenomenon exerting major influence upon the water quality of aerated lagoons, oxidation ponds, receiving streams, and estuaries. Yet, to date, no effective description of this complex set of processes has been included in models predicting the overall performance of such systems.

Benthal stabilization can be defined as a vertically integrated, aerobic/anaerobic process (Fair et al., 1941) which results in the conversion of organic carbon and nitrogen to inorganic compounds and methane. If dissolved oxygen is maintained in the water column

above the deposit at concentrations greater than 2 mg/L, an aerobic layer only a few millimeters thick will exist at the top of the deposit (Mortimer, 1971; Fillos and Molof, 1972). In that layer, degradation mechanisms are supported by a direct uptake of dissolved oxygen transported from the overlying water. Below the aerobic layer, anaerobic conditions prevail in which methane gas is evolved, as well as other products of anaerobic degradation. Ammonia and some of the less-reduced products from the anaerobic layers, such as organic acids, are transported upward to the aerobic layer by means of diffusion and advection induced by consolidation of the deposit. These products are either oxidized in the deposit or escape into the overlying water where they contribute to the soluble biochemical oxygen demand (Fair *et al.*, 1941). The total oxygen demand of the benthal organic solids is met by direct oxygen uptake and soluble feedback, or averted by methane production.

The relative importance of temperature on the three mechanisms of stabilization (oxidation in the aerobic layer, BOD feedback to the water column, and methane production) is illustrated in Figure 1. At low temperatures methanogenesis is suppressed and storage of biodegradable organics occurs. At higher temperatures methane production becomes increasingly significant.



- S = storage of biodegradable organics
- M = methane formation
- F = feedback of soluble oxygen-demanding species
- D = direct oxygen uptake in the aerobic benthal layer

Fig. 1. Conceptual model of the influence of temperature and organic loading on oxygen demand components

A quantitative description of the influence of the benthal mechanisms on overlying water columns in streams, estuaries and lagoons would enhance the capability of existing models in the prediction of total oxygen demand. For example, recent work on the design of lagoon systems has emphasized the need to reduce the hydraulic retention time in order to reduce algal production (White and Rich, 1976; Rich, 1982). The effects of benthal feedback and sludge build-up on the quality of the overlying water are magnified in such a system, and a proper description of these benthal effects is essential. To address these needs, research was undertaken to develop and validate a quantitative model of the

benthal stabilization of organic carbon and nitrogen in deposits formed at the bottom of an aerated water column, under conditions approximating continual deposition.

EXPERIMENTAL APPROACH

To achieve the stated objective, a one-dimensional, generalized transport equation was used to model the benthal environment. For model verification, depth profiles of the major interstitial carbon and nitrogen components were measured from a set of deposits formed in the laboratory through the semi-continuous deposition of waste activated sludge solids. To insure that all major benthal mechanisms were addressed, mass balances were made for all measured sources and sinks of carbon and nitrogen in the system under study.

Laboratory data from the deposit experiment were collected primarily for model verification and mass balance calculations. Deposits were formed by weekly addition of waste activated sludge solids to eleven continuous-flow reactors, each measuring 0.34m by 0.34m by 1.3m high. Preliminary 30-day aeration tests and weekly analyses of volatile suspended solids (VSS) were used to control the loading rate near 50 grams of biodegradable VSS per square meter per day. The selected loading rate was feasible for the type of solids to be collected and was within the assimilative capacity of the deposit (Connor, 1981). To eliminate temperature as a variable, the ambient air and overlying water were maintained at 20°C.

Interstitial samples were taken weekly from four reactors and tested for volatile acids, soluble total and organic carbon (TC, TOC), ammonia, pH, and soluble chemical oxygen demand (COD). For deposit analysis, a pair of reactor deposits was sacrificed at three-week intervals over a 15-week period. A siphon device was used to separate each deposit into several representatives of varying deposit depths. The samples were analyzed for depth profiles of porosity, volatile suspended solids (VSS), biodegradable VSS (BVSS), total COD, total Kjeldahl nitrogen (TKN), and dewaterability. The porosity data was used to calibrate the proposed computer model, whereas the other measurements were used in model verification.

Additional measurements were required to close the mass balances of carbon and nitrogen. Each week the filtered effluents from four reactors were analyzed for ammonia, nitrate, TKN, dissolved nitrogen, TC and TOC. The volatile fraction of the filtered effluent solids was also determined. During the 15-week deposit experiment, recovery of both carbon and nitrogen exceeded 90 percent.

DEPOSIT MODEL

The model accounted for the effects of: (1) biological reactions such as solubilization, oxidation, nitrification, denitrification, acid formation, and methanogenesis; (2) the physical processes of consolidation, diffusion, and gas production; and (3) the equilibrium distribution of dissociated chemical species. Key equations which formed the benthal model were a general transport equation, a first-order dynamic consolidation equation, and an exponential steady-state porosity relationship:

$$\begin{aligned} C_A(\partial\phi/\partial t) + (\partial C_A/\partial t) + \phi v(\partial C_A/\partial x) \\ + C_A[\partial(\phi v)/\partial x] = \phi r_A + \partial[\phi D(\partial C_A/\partial x)]/\partial x \end{aligned} \quad (1)$$

$$(\partial\phi/\partial t)_x = \tau(\phi_{ss} - \phi)_x \quad (2)$$

$$(\phi_{ss})_x = \alpha + \beta e^{-\gamma x} \quad (3)$$

where

- C_A = fluid concentration of A, mg/cm^3
- r_A = production of A, $\text{mg}/(\text{cm}^3 \text{ sec})$
- ϕ = porosity, $\text{cm}^3 \text{ water}/\text{cm}^3 \text{ deposit}$
- x = deposit depth below the interface, cm
- t = time, sec
- D = bulk diffusion coefficient, cm^2/sec
- v = pore water velocity relative to interface, cm/sec
- ϕ_{ss} = steady state porosity at x
- τ = first-order time constant, days^{-1}
- α, β, γ = experimentally determined coefficients

The model also included thirteen first-order equations for biological reactions and seven equations for chemical equilibrium. The major chemical and biological effects of sulfur components were ignored because the system under study was dominated by carbon and nitrogen components. Numerical solution of Equations (1) through (3) was obtained by use of the State Variable analog (McCracken et al., 1970), which was unique in that it accepted any ratio of dispersion to advection effects (Melsheimer and Adler, 1975). By solving Equation (1), a prediction of the depth profile for each interstitial component was obtained.

Transport by diffusion was modeled with a single, constant diffusion coefficient of $10^{-8} \text{ cm}^2/\text{sec}$ for all soluble species in the interstices (Lerman, 1971). However, in rapidly consolidating deposits the effects of dispersion were usually more significant than those of diffusion. The dispersion effects were incorporated in the value of the diffusion coefficient and, based upon previous research (Klotz, 1975), the magnitude of the modified coefficient was determined as a function of the pore water velocity at any given deposit depth. Detailed description of all model equations is provided elsewhere (Bryant, 1983).

LABORATORY RESULTS

Volatile Acids

Concentrations of acetate, butyrate, isobutyrate, valerate, and isovalerate first increased and then decreased during the 15-week deposit experiment, whereas the concentrations of propionic acid and 2-methyl-butyric acid only increased. Similar prolonged build-up of propionic acid concentration has been observed in anaerobic digestor start-up (Hobson and Shaw, 1973) in batch studies of recovering digester conditions (Pohland and Ghosh, 1971), in digesters with available supplies of other volatile acids (Tzeng et al., 1975; Scharer and Moo-Young, 1979; van Velzen, 1979), and in *in vitro* rumen methanogenesis research (Nelson, 1958).

The overall sequence of volatile acid utilization listed in Table 1 was consistent with predictions based on the change in standard Gibbs free energies for identified degradation reactions (McInerney et al., 1979). Degradation of propionic acid required the lowest hydrogen partial pressure to become thermodynamically favorable under conditions that occur during effective methanogenesis. Thus, a decrease in the dissolved hydrogen concentration over time would produce the observed order of volatile acid utilization.

Table 1. Volatile Acid Utilization Near Deposit Bottom

| Volatile Acid | Time of Major Conc. Decline (weeks) | ΔG° |
|---------------|---|------------------|
| Acetic | 7 - 8 | -31.0 kJ/mole |
| Butyric | 8 - 9 | +48.1 |
| Isobutyric | 9 - 10 | |
| Valeric | 11 - 12 | +48.1 |
| Isovaleric | 12 - 13 | |
| 2-m-Butyric | 17 - 21* | |
| Propionic | 17 - 21* | +76.1 |

*Weekly addition of solids was terminated after 15 weeks

Biodegradable Solids

Analysis of deposit solids during the 15-week experiment indicated a two-phase solubilization of biodegradable material. As shown in Table 2, only a three-week period was required for the solubilization of nearly two-thirds of the biodegradable volatile suspended solids (BVSS) added to the deposits. No further appreciable net solubilization of BVSS was measured during the next twelve weeks. Previous research on similar deposits has shown that further solubilization of BVSS does occur, but at a very slow rate (Bryant, 1979; Tarnowski, 1979; Connor, 1981).

Table 2. Deposit Solids Stabilization

| Source | Detention (days) | Added BVSS* (g) | Final BVSS* (g) | Percent Stabilization |
|------------------|---------------------|--------------------|--------------------|--------------------------|
| This Study | 23 | 94.9 | 30.5 | 67.8 |
| This Study | 44 | 171.9 | 69.2 | 59.7 |
| This Study | 65 | 294.3 | 134.5 | 54.3 |
| This Study | 86 | 348.3 | 112.6 | 67.7 |
| This Study | 107 | 458.4 | 178.4 | 61.1 |
| Bryant (1979) | 179 | 337.3 | 54.9 | 83.7 |
| Connor (1982) | 293 | 454.3 | 77.4 | 86.2 |
| Tarnowski (1979) | 301 | 562.7 | 30.4 | 93.3 |

*Based on 30-day aeration tests

Gas Production

Production of off-gas was first observed and measured on Day 28 of the deposit experiment. On that day, the pH profiles of four reactors were measured, and spot samples were taken from four others. In all cases, the pH values were near 5.5, a value substantially below the range of 6.5 to 7.7 cited as suitable for methanogenesis in mixed reactors (Grady and Lim, 1980).

The composition of off-gas from the benthal deposits averaged 75-percent methane, 12-percent carbon dioxide, and 7-percent nitrogen. The off-gas was similar to that measured by other researchers (Fair et al., 1941; Bryant, 1979; Tarnowski, 1979; Connor, 1981) with regard to methane content, but differed in nitrogen and carbon dioxide content.

Data for total gas production in this and similar benthal studies is shown in Figure 2. Data was taken from other work only for the portions of study during which the temperature remained at 20°C. Since previous studies have modeled benthal gas production by an exponential expression (Fair et al., 1941; Marais, 1970), a least-squares analysis was performed to obtain parameter estimates for the expression

$$G = \alpha \{ 1 - \text{EXP}[-\gamma(t - 27)]\} \quad (4)$$

where

α, γ = parameter estimates

G = gas production rate, $\text{L}/(\text{m}^2 \text{ day})$

t = time, days

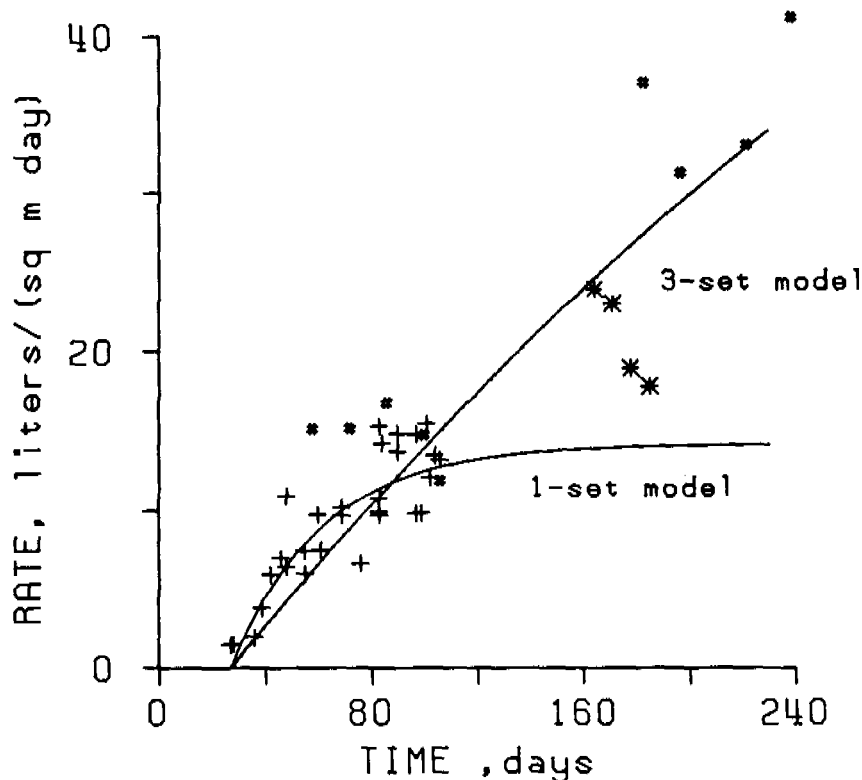


Fig. 2. Gas production in several benthal experiments: (+) this study, (*) Tarnowski (1979), and (#) Connor (1981)

As indicated by the models shown in Figure 2, the parameter estimates based upon data from this study alone were quite different from the estimates based upon data from all three studies. The parameter estimates included a maximum methane production rate of $14.5 \text{ L}/(\text{m}^2 \text{ day})$, which was obviously inconsistent with data collected beyond the 15-week timespan in the other experiments. Measured gas production rates in the latter studies were approximately twice the maximum value estimated for Equation (4). Apparently the discrepancy occurred because gas production had not reached a steady-state level during the 15-week deposit experiment.

MODEL RESULTS

Profile Comparison

Simulated and measured profiles of two major soluble species are presented in Figures 3 and 4 for key time periods during deposit build-up. Over several weeks the simulated acetic acid concentrations did not decrease as rapidly as observed values, but the shape of the profile was consistent with the laboratory data. For propionic acid, the discrepancy between measured and simulated profiles was more evident. The benthal model incorporated the effects of inhibition by unionized propionic acid suggested by Andrews and Graef (1971) rather than any direct pH effect. The form of the equation to describe the inhibition effect was

$$k = k_3 [1 + HPr/k_i] \quad (5)$$

where

k = effective rate for propionate degradation, days⁻¹

k_3 = baseline rate constant, days⁻¹

HPr = unionized propionic acid concentration, mmol/L

k_i = propionic acid inhibition constant, 0.67 mmol/L used initially to 0.08 mmol/L used in the final simulation shown herein.

Despite the use of a relatively low value for the inhibition constant, the simulated rate of propionic acid degradation exceeded the measured rate in lower portions of the deposits. Further research is needed to define the form and extent of inhibition for propionic acid degradation in anaerobic environments.

The predicted ammonia profile matched measured data in the early weeks of deposit development, but varied from the data after the eighth week. The variation, hypothesized to be due to deaminase inhibition or adsorption by organic solids, has been discussed in separate publications (Bryant, 1983; Bryant and Rich, 1983). Simulated methane production, presented in Table 3, exceeded observed values but closely approached the rates measured in previous studies (Bryant, 1979; Tarnowski, 1979; Connor, 1981). A similar discrepancy was seen for carbon dioxide production. Both simulation results were affected by the problem with propionic acid simulation discussed above.

Table 3 Predicted Gas Production Rates

| Time (days) | Methane | |
|----------------|----------|-----------|
| | Measured | Simulated |
| 26.50 | 0.0 | 2.9 |
| 33.25 | 1.3 | 5.4 |
| 40.00 | 2.6 | 10.2 |
| 46.75 | 3.8 | 10.7 |
| 53.50 | 4.8 | 10.4 |
| 87.25 | 7.6 | 12.3 |

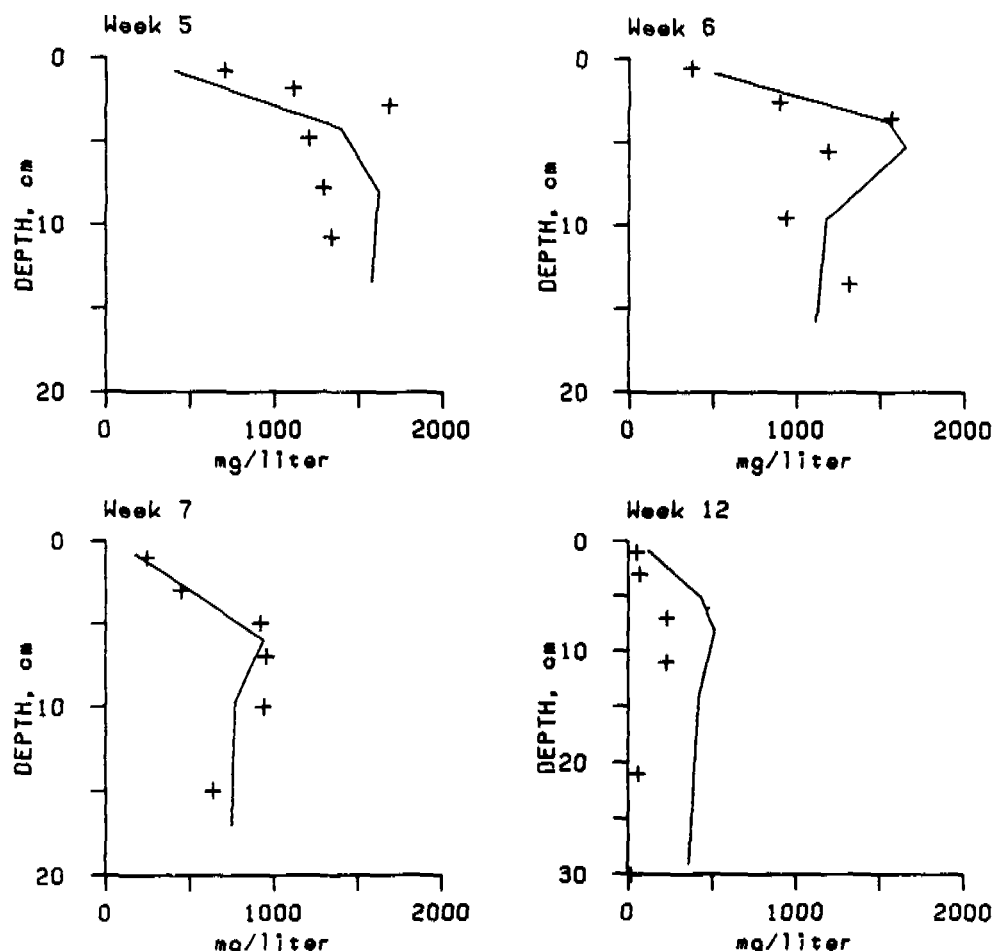
Note: All rates have units of liters/(m² day)

Predicted Loading Effects

A comparison of simulated deposit parameters for three organic loading rates is shown in Table 4. Simulated methane production at three loading rates is presented in Figure 5.

Table 4 Loading Effects on Deposit Performance After 53 Days

| Parameter | Loading Rate, g BVSS/(m ² day) | | |
|---|---|--------|--------|
| | 100 | 150 | 250 |
| Total depth, cm | 31.6 | 42.1 | 68.6 |
| Stabilization at bottom, % | 46.5 | 46.2 | 46.2 |
| BOD feedback g/m ² | 246.8 | 420.6 | 693.3 |
| BODN feedback, g/m ² | 50.2 | 57.1 | 84.7 |
| Direct oxygen uptake, g/m ² | 3.5 | 5.4 | 9.6 |
| Feedback and uptake, g/m ² | 318.5 | 483.1 | 787.6 |
| Methane oxygen equivalent, g/m ² | 1794.0 | 2752.0 | 4800.0 |

Fig. 3. Deposit acetic acid predictions, weeks 5, 6, 7, 12:
 (+) measured value, (-) simulated profile

For the range of values simulated, deposit oxygen demand and methane production were approximately proportional to loading rate. The results are consistent with the conceptual model of benthal oxygen demand shown in Figure 1(b), but the model requires improvement to reflect the ratio of direct uptake to soluble feedback that has been measured in previous work (Bryant, 1979; Tarnowski, 1979; Connor, 1981). No limitation of the stabilization capacity of the consolidating deposit was indicated. Since deposit depth tripled while methane production increased five-fold, higher volumetric stabilization efficiency was achieved for increased loading rates. Effective benthal stabilization of organic solids was simulated at loading rates significantly above the range of 2.8 - 20.0 g $BOD_5/(m^2 \text{ day})$ for facultative or mechanically aerated, partially suspended lagoons (Schroeder, 1977; Metcalf and Eddy, 1979; Reynolds, 1982).

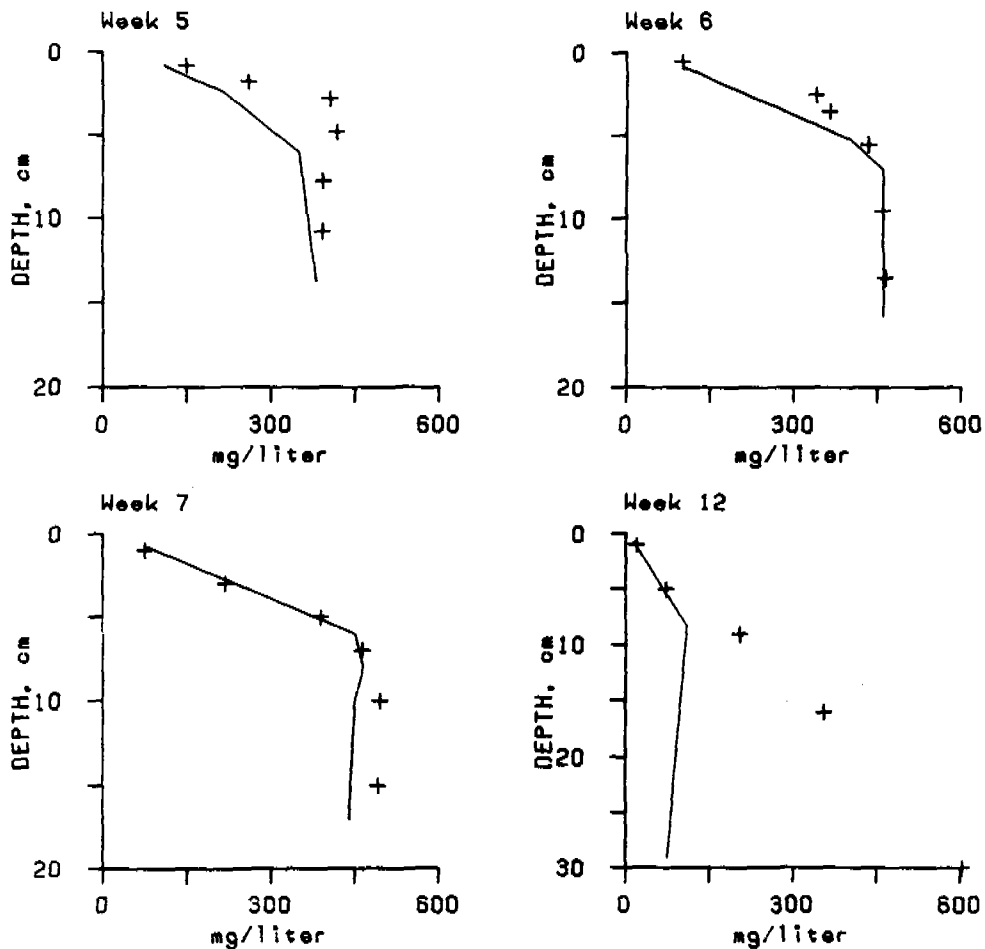


Fig. 4. Deposit propionic acid predictions, weeks 5, 6, 7, 12:
 (+) measured value, (-) simulated profile

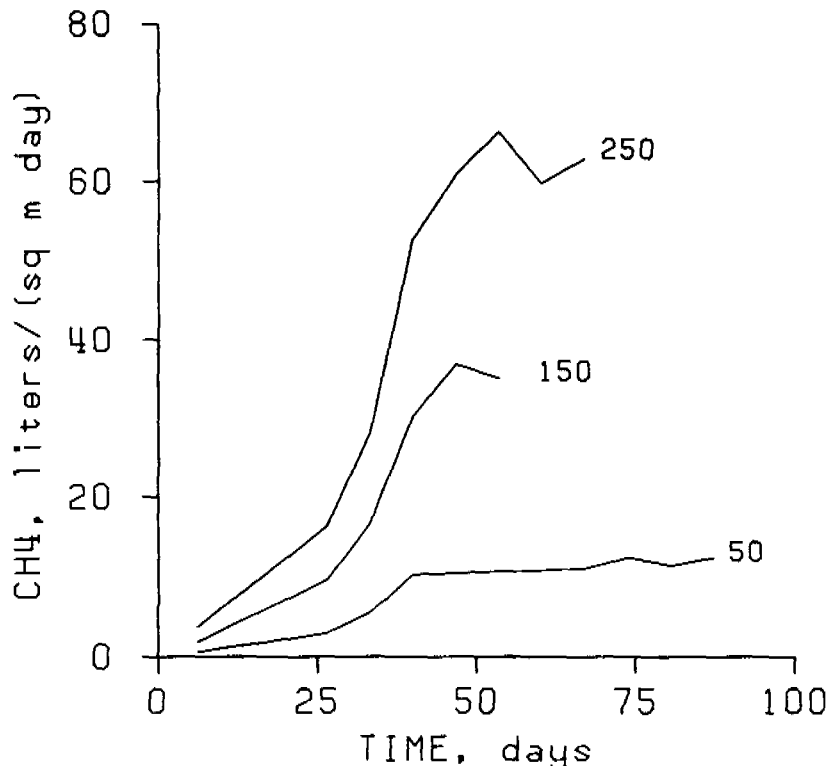


Fig. 5. Methane production for loading rates of 50, 150, and 250 g BVSS/ $(\text{m}^2 \text{ day})$

CONCLUSIONS

The benthal model, which was based on a general consolidation equation and a set of first-order biological reactions, effectively predicted the dynamics of consolidating, organic deposits at 20°C. However, development of the model is not complete, and several aspects of the program require further laboratory verification. For example, temperature sensitivities must be added to the benthal model for prediction of field performance.

Benthal simulations for a range of loading rates up to 250 g BVSS/ $(\text{m}^2 \text{ day})$ indicated that the stabilization capacity of benthal deposits is far above the range of loading rates currently recommended for design purposes.

Based upon simulation results, an increase in benthal loading rate should result in proportional increases in direct oxygen uptake, soluble feedback, and methane production. The relative importance of each component in the total oxygen demand of the deposit did not change significantly in simulations of loading rates from 100 to 250 g BVSS/ $(\text{m}^2 \text{ day})$.

The observed sequence of volatile acid utilization in the anaerobic portion of the benthal deposit can be explained by the thermodynamic effect of a gradual reduction of the hydrogen partial pressure over time.

REFERENCES

- Andrews, J. and Graef, S. (1971). Dynamics modeling and simulation of the anaerobic digestion process. Advances in Chemistry Series, 105:126.
- Bryant, C. (1979). Benthal stabilization of aerated lagoon solids. Master's Report, Clemson University.
- Bryant, C. (1983). Benthal stabilization of organic carbon and nitrogen. Dissertation, Clemson University.
- Bryant, C. and Rich, L. (1983). Benthal stabilization of organic carbon and nitrogen: the development of interstitial profiles. 56th Annual Conference on Water Pollution Control, Atlanta, Georgia.
- Connor, B. (1981). Benthal stabilization of activated sludge solids. Clemson University.
- Fair, G., Moore, E., and Thomas, H. (1941). The natural purification of river muds and pollutant sediments. Sewage Works Journal, 13:270, 756 and 1209.
- Fillos, J. and Molof, A. (1972). Effect of benthal deposits on oxygen and nutrient economy of flowing waters. Journal Water Poll. Control Fed., 44:644.
- Grady, C. and Lim, H. (1980). Biological Wastewater Treatment, Marcel Dekker, Inc., 849.
- Hobson, P. and Shaw, B. (1973). The anaerobic digestion of waste from an intensive pig unit, Water Resources, 7:437.
- Klotz, D. (1975). Physical fundamentals of the mixing of solutions of pollutants and sewage in porous media. Water Resources, 9:783.
- Lerman, A. (1971). Nonequilibrium systems in natural water chemistry. Advances in Chemistry Series, 106.
- Marias, G. (1970). Dynamic behavior of oxidation ponds. 2nd Intl. Symp. for Waste Treatment Lagoons, Kansas City, Mo.
- McCracken, E., Leefe, G., and Weaver, R. (1970). Transient numerical solutions for two-phase fluid-bed models. C.E.P. Symposium Series No. 101, 66:37.
- McInerney, J., Bryant, M., and Pfennig, N. (1979). Anaerobic bacterium that degrades fatty acids in syntrophic association with methanogens. Arch. Microbiol., 122:129.
- Melsheimer, S. and Adler, R. (1975). The characteristic averaging technique for dispersion-convection equations. In Advances in Computer Methods for Partial Differential Equations, Ed. R. Vichnevetsky.
- Metcalf and Eddy, Inc. (1979). Wastewater Engineering: Treatment Disposal, Reuse, G. Tchobanoglous (Ed.), 2nd ed. McGraw-Hill, Inc., New York, 553.
- Mortimer, C. (1971). Chemical exchanges between sediments and water in the Great Lakes - speculations on probable regulatory mechanisms. Limn. and Oceanography, 16:387.
- Nelson, W., Oppermann, R., and Brown, R. (1958). In Vitro studies on methanogenic rumen bacteria. II. Fermentation of butyric and valeric acids. Journal of Dairy Science, 41:545.
- Pohland, F. and Ghosh, S. (1971). Developments in anaerobic treatment processes. Bio-tech. and Bioengr., 2:85.
- Reynolds, T. (1982). Unit Operations and Processes in Environmental Engineering, Wadsworth, Inc., Belmont, California, 391.
- Rich, L. (1982). Design approach to dual-power aerated lagoons. Journai Environmental Engineering Division Proc. ASCE, 108:532.
- Scharer, J. and Moo-Young, M. (1979). Methane generation by anaerobic digestion of cellulose-containing wastes. Adv. Biochem. Engr., 11:85.
- Schroeder, E. (1977). Water and Wastewater Treatment, McGraw-Hill, Inc., New York, p. 278.

- Tarnowski, D. (1979). Benthal decomposition of continuously deposited aerated lagoon solids. Clemson University.
- Tzeng, S., Wolfe, R., and Bryant, M. (1975). Factor 420-dependent pyridine nucleotide-linked hydrogenase system of Methanobacterium rumanantium. Journal of Bacteriology, 121:184.
- van Velzen, A. (1979). Adaptation of methanogenic sludge to high ammonia-nitrogen concentrations. Water Resources, 13:995.
- White, S. and Rich, L. (1976). How to design aerated lagoon systems to meet 1977 effluent standards - BOD removal from aerated lagoon systems. Water and Sewage Works, 48:90.

THE CALCULATION OF TRANSPORT COEFFICIENTS OF PHOSPHATE AND CALCIUM FLUXES ACROSS THE SEDIMENT-WATER INTERFACE, FROM EXPERIMENTS WITH UNDISTURBED SEDIMENT CORES

W. van Raaphorst and A. G. Brinkman

Twente University of Technology, Dept. of Chemical Technology, P.O. Box 217, 7500 AE Enschede, The Netherlands

ABSTRACT

Fluxes of phosphate and calcium across the sediment-water interface of six undisturbed cores are investigated. Attention is paid to the accuracy of porewater extraction and the influence of this sampling upon the experiments. From this, it is concluded that sampling time should at least be one day. Continuous and batch experiments resulted in a rapid release of phosphorus and calcium from the sediment. The influence of induced seepage could not be shown. On a theoretical base, it is concluded that the benthic fluxes are fed by desorption at or just below the interface, rather than by diffusion from deeper layers. Hence, data of interstitial water could not directly be used for calculating the driving forces of these fluxes. Instead, endconcentrations in the overlaying water of the batch experiments are used, which resulted in values of transportcoefficients of $3\text{--}10 \cdot 10^{-7} \text{ m.s}^{-1}$, being in good agreement with theoretical as well as field data.

KEYWORDS

Sediment, benthic fluxes, interstitial water, sampling, transport coefficients

INTRODUCTION

Transport of dissolved materials across the sediment-water interface is an important factor, affecting the chemical characteristics of lakes. For calculating benthic fluxes, concentration gradients and transportcoefficients have to be known. Other factors important in modelling these processes are for example chemical interactions and biochemical degradation.

In this contribution laboratory experiments are described which are used to assess the transport coefficients of phosphates and calcium across the sediment-water interface. Study area is a shallow lake (Lake Veluwe) in the Netherlands, with an average depth of about 1.2 m. Mass budget studies showed a net phosphorus release from the sediment during summer, whereas in winter the sediment acts as a sink.

Many papers can be found in which the measurement of benthic fluxes during laboratory experiments are described (Fillos & Molof, 1972; Kamp-Nielsen, 1974; Rip-

pey, 1977; Holdren & Armstrong, 1980; Hieltjes, 1980; Van Liere & Mur, 1982; Van Liere et al., 1982). All these deal with experiments on undisturbed sediment cores, set up in a batch or continuous flow system. Only a few authors tried to relate measured fluxes to concentration gradients (Holdren & Armstrong, 1980; Van Liere & Mur, 1982; Van Liere et al., 1982). It should be stressed, however, that without this relation only limited information can be gained.

Sampling of interstitial water may disturb existing gradients because of infiltration of water from other sediment layers during recovery. It is therefore necessary to pay attention to the induced flow in the sediment and to analyse possible effects. Another reason for this is that analysis of the infiltration can give information about the origin of the sampled pore water. These phenomena will be dealt with before describing experimental results.

MATERIALS AND METHODS

Experimental Procedures

Undisturbed cores were taken with a 5.0 cm inner diameter sampler, see figure 1. The corer can be used in soft as well as in rather hard sediments. The perspex inner tube contains senta, allowing sampling of interstitial water and can be placed into the experimental set-up immediately. Time between sampling and the start of the experiments was about one day.

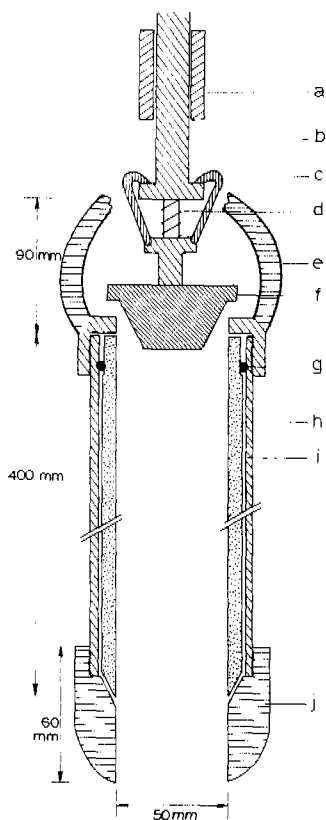


Fig. 1: Sediment corer

- a: messenger.
- b: pushing/recovery bar. Length 1-7 m.
With socket to hold c and for fixation of e.
- c: claws. Keep rubber stopper f in opened position. Removed from socket by messenger a in order to close f.
- d: spring for reliable closure of tube by f.
- e: fixation of outside tube cap to pushing bar b.
- f: rubber stopper. In opened position free outlet of water.
- g: O-ring seal.
- h: perspex inner tube for sample storage. After each sample a new tube may be used.
- i: stainless steel outertube.
- j: tempered steel tube head.

For extracting pore water a thread of cotton was brought into a polyethylene duct ($\emptyset = 2.5$ mm). The lower part ended in a glass bottle, volume 10 ml, via a rubber stopper. The other side was put into the core via one of the septa in the tube wall. By opening the valve on the bottle underpressure could be set to the sampling system. With this technique samples of about 5 ml were obtained within 2 or 3 days, depending on the sediment constitution. Phosphate desorption from, or adsorption on the cotton thread was shown to be negligible.

For the flux experiments two different set-ups, a batch and a continuous flow system, were used. In both, the heart consisted of the undisturbed core. The upperside of this core was covered by a lid, in which conduits for in- and outflow of water, as well as an escape for air were constructed. Under this lid a little platform, on which a magnetic stirring rod was situated. Agitation was effected by a magnetic stirrer. Mixing of the waterlayer was ideal, without any disturbance of the sediment layers. Seepage of groundwater was simulated by inflow of oxygen-free water via a sintered glass diffusor at the lower end of the tube.

In the batch type reactor (BR) water was recirculated to a store bottle, where flushing with air, nitrogen, etc. and sampling of water could take place. Values of pH and oxygenconcentration were recorded in the effluent of the core.

In the continuous stirred tank reactor (CSTR) the effluent was discharged. Samples for chemical analysis were taken from the in- as well as the effluent. Values of pH and oxygenconcentration were recorded just before and after the core. Mean retention time of the bulkwater above the sediment was about 1 day.

Water used as influent was either originating from Lake Veluwé or distilled water to which NaCl was added for adjustment of the ionic strength up to that of lake water. After filtration (0.45 μm Millipore-filter), the lake water was made phosphate free, using an ion exchange column (Biorad, AgIX₄ on chloride base). The value of the pH was increased by flushing with CO₂-free air, or in case anaerobic situations had to be simulated, with nitrogen only.

After the experiments the sediment cores were cut into slices and frozen at -30°C. Analysis of this material took place after freeze-drying.

Fluxes of ions across the sediment-water interface, in the continuous experiment, were calculated from a simple mass-balance for a well mixed reactor:

$$\frac{d(C)}{dt} = \tau^{-1} \cdot (C_0 - C) + h^{-1} \cdot F \quad [1]$$

where C and C₀ are the concentrations in the reactor and the influent (g.m^{-3}), τ is the retention time (hr), h is height of the reactor above the sediment layer (m) and F is the flux across the interface ($\text{g.m}^{-2}.\text{hr}^{-1}$). The value of the derivative in eq. [1] was approximated by a central discretization:

$$\left[\frac{d(C)}{dt} \right]_n \approx \frac{[C]_{(n+1)} - [C]_{(n-1)}}{t_{(n+1)} - t_{(n-1)}} \quad [2]$$

where the subscript n denotes the time t_n. In the BR experiments fluxes could simply be calculated from the change in concentrations in the overlaying water with time.

Analytical procedures

The phosphate concentration in watersamples was analysed according to the method of Murphy & Riley (1962), while Ca and Fe were analysed by atomic absorption spectrometry.

Loss on ignition (LOI) of sediment samples was obtained after heating at 400°C during one hour. Porosity was calculated from the difference in weight before and after freeze-drying. Destruction of bottommaterial, with HNO₃ and H₂SO₄ for P-analysis and with HNO₃, HF and HClO₄ for Ca and Fe, was followed by the same analytical procedures as the water samples.

All materials used were carefully cleaned by steaming and rinsing with distilled water.

SAMPLING OF INTERSTITIAL WATER

A review of existing techniques is given by Brinkman et al. (1982). In case pore water has to be sampled more than once during the experiments, only flow inducing procedures seem to be possible.

Assuming an isotropic medium, this flow can be described by Darcy's Law:

$$\dot{q} = -K \nabla h \quad [3]$$

where \dot{q} is the specific discharge in (m.s⁻¹), K the hydraulic conductivity in (m.s⁻¹), and h the hydraulic head in (m). Defining a potential function as $\phi = K.h$, and setting up a mass balance it follows that:

$$\nabla^2 \phi = 0 \quad [4.a]$$

or in cylindrical coordinates (r, z, ζ):

$$r^{-1} \cdot \frac{\partial}{\partial r} (r \cdot \frac{\partial \phi}{\partial r}) + r^{-2} \cdot \frac{\partial^2 \phi}{\partial \zeta^2} + \frac{\partial^2 \phi}{\partial z^2} = 0 \quad [4.b]$$

In case of axial symmetry (extraction in r = z = 0), the second term in [4.b] disappears, and a streamfunction ψ can be defined as (Batchelor, 1967):

$$q_z = r^{-1} \cdot \frac{\partial \psi}{\partial r}; q_r = -r^{-1} \cdot \frac{\partial \psi}{\partial z} \quad [5]$$

Important property of this function is that the discharge perpendicular to the ($\psi = \text{constant}$)-surfaces is zero.

An approximation for the solution of [4.b] in case water is extracted from a point z = r = 0 is given by Morse & Feshbach (1953). Assuming a cylinder of infinite length:

$$\phi = -\frac{Q}{\pi \cdot a^2} \cdot |z| \cdot \sum_{n=1}^{\infty} \left\{ \frac{Q}{\pi \cdot a \cdot \alpha_{0,n}} \cdot (J_0(\alpha_{0,n}))^{-2} \cdot J_0(\alpha_{0,n} \cdot \frac{r}{a}) \cdot \exp(-\alpha_{0,n} \cdot \frac{|z|}{a}) \right\} \quad [6]$$

Where Q is the total discharge due to sampling (m³.s⁻¹), in one point, a is the radius of the core (m), J₀ is a Besselfunction of zero order, and $\alpha_{0,n}$ is defined as the n-th root of the equation:

$$\frac{d}{da} (J_0(a)) = 0 \quad [7]$$

Using eq. [3], [5] and [6] a similar approximation can be given for the streamfunction:

$$\psi = -\beta \cdot Q - \gamma \cdot Q \cdot \frac{r^2}{a^2} - \gamma \cdot \sum_{n=1}^{\infty} \left\{ \frac{2 \cdot Q}{a \cdot \alpha_{0,n}} \cdot r \cdot (J_0(\alpha_{0,n}))^{-2} \cdot J_1(\alpha_{0,n} \cdot \frac{r}{a}) \cdot \exp(-\alpha_{0,n} \cdot \frac{|z|}{a}) \right\} \quad [8]$$

where for z > 0, $\beta = 0$ and $\gamma = 1$; for z = 0, $\beta = 0.5$ and $\gamma = 0$; and for z < 0, $\beta = 1$ and $\gamma = -1$. J₁ is a Besselfunction of order one. The value of Q can easily be obtained by:

$$Q = V/T \quad [9]$$

where V is the sample volume in (m³) and T is the sampling time in (s).

The influence of the sediment-water interface, where the radial flow has to be zero, is taken into account by superposition of the solution for a negative mirror-extraction in $z = 2D$, where D is the distance of the sampling point to the interface. In the same way superposition of solutions for different sampling depths, gives values for the potential and streamfunction in case of simultaneous sampling at several points in the core. An example of the results of such calculations is given in fig. 2 (righthand side).

The streamdivides for the different extractions can be obtained by stating that the flux of fluid volume across the surface formed by rotating an arbitrary curve between two points in an axial plane, about the axis of symmetry, is 2π times the difference between the values of the streamfunction in these points (Batchelor, 1967). This means that the value of ψ in the divides can be formulated as:

$$\psi_{\text{divide}} = \frac{0}{2\pi} \cdot i \quad [10]$$

where i is an integer.

The travelling distance ($s_2 - s_1$) of the pore water due to sampling can be calculated by integration (of eq. [11] from s_1 to s_2) along a streamline:

$$T = \epsilon^{-1} \cdot \int_{s_1}^{s_2} \frac{1}{q_s} ds \quad [11]$$

where ϵ is the volumetric porosity, and s dedicates the coordinate along the streamline. Solving eq. [11] for different streamfunctions, the drainage-area of the sampling points, and the depth to which bulk water infiltrates into the sediment can be calculated. An example is given in fig. 2 (lefthand side).

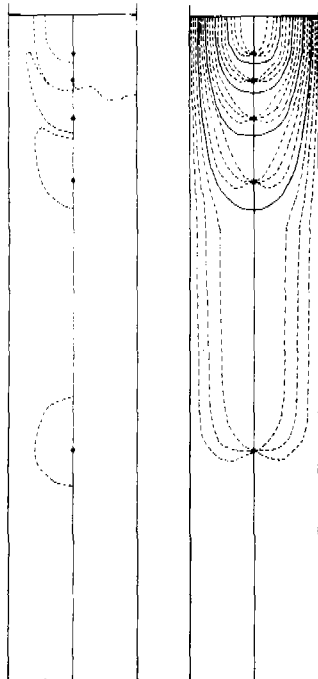


Fig. 2, lefthand side:
Drainage-areas (left-half) and infiltration depth (right-half) due to simultaneous sampling in 5 points.

Fig. 2, righthand side:
Streamlines due to simultaneous sampling in 5 points. Solid streamlines denote the streamdivides.

Corelength : 260 mm
Sampling time : 50 hr.
Sample volumes : 5 ml
Porosity : 0.31
Sampling depths: 15, 25, 40, 65, 175 mm

From this example it is obvious that the sample is not originating from one depth, but rather from a layer a few centimeters thick. In fact, the samples from the upper two points consist partly of supernatant. This means that, without corrections, wrong concentration gradients may be gained, especially where real gradients are steep.

For non-conservative species, the concentration changes during transport from the initial location in the core to the sampling point, because of chemical equilibration. Hence, some of the original differences in pore water quality will be lost. The effect of chemical reactions on the final concentrations in a sample is dependent on the kinetics of these reactions and the rate at which pore water is extracted. When time needed for sampling is much longer than that for equilibration, measured concentrations will be a good estimate for those at the intake depth. A rapid procedure, however, will give less good results. In this case (Lake Veluwe), the rate constant for phosphate equilibration in the interstitial water is about 10 hr^{-1} (Brinkman et al, 1984). It is therefore concluded that sampling time should at least be one day.

A second conclusion from fig. (2) is that supernatant may infiltrate into the upper centimeters of the sediment. Sampling of interstitial water during the release experiments will therefore influence the measured fluxes, comparable to the effect of natural downward seepage. For this reason we only extracted pore water just before and after the experiments.

RESULTS AND DISCUSSION

Cores were taken from three representative locations in Lake Veluwe (table 1). The samples 1 and 2 were withdrawn from the bottom of the shipping channel, the main area of accumulation (covering 5% of the sedimentsurface). Core 4 and 5 originated from the erosive part of the lake (50%), and 3 and 6 from the intermediate zone (45%). Sediment from the channel showed a much higher LOI compared to material from the other locations. Chemical analysis also resulted in higher phosphorus, calcium and iron contents (table 2). Lowest values were found in material from core 4 and 5. On average in the sediment, contents decreased slightly with increasing depth.

TABLE 1: Main Properties of the Different Sampling Locations

| core (location) | waterdepth (m) | sediment type | porosity (%) | LOI (mg/g) |
|--------------------|-------------------|------------------|-----------------|---------------|
| 1,2 | 4 | mud + clay | 65 | 100 |
| 3,6 | 2 | sand + clay | 63 | 15 |
| 4,5 | 0.75 | sand | 35 | 5 |

Data of phosphate and calcium concentrations in the interstitial water were evaluated according to the theory described in the previous section. After calculation of the drainage area for each sampling point, this area was divided in layers of 5 mm. Using eq. [11], the average retention time in these slices was estimated. Assuming first order reaction and a rate constant in the order of 10 hr^{-1} (Brinkman et al, 1984), it was concluded that measured concentrations were representative for those at the sampling depth. Examples of two concentration profiles are given in fig. 3. Highest phosphate concentrations were found in core 1 and 2 ($200\text{-}500 \mu\text{g P.l}^{-1}$), lowest in core 4 and 5 ($50\text{-}150 \mu\text{g P.l}^{-1}$). The other two cores showed intermediate values: $100\text{-}200 \mu\text{g P.l}^{-1}$. Concentrations mostly increased

with increasing sampling depth. In each core, the calcium content of the porewater reached values about $160 \text{ mg} \cdot \text{l}^{-1}$. There was little variation with depth. On average, pH-values were between 7 and 8.

TABLE 2: Results of Chemical Analysis of Sedimentcores
Values are averages of two cores

| core | depth (cm) | P (mg/g) | Ca (mg/g) | Fe (mg/g) |
|------|------------|----------|-----------|-----------|
| 1, 2 | 0-1 | 0.78 | 43 | 19 |
| | 1-2 | 0.79 | 45 | 30 |
| | 2-5 | 0.76 | 42 | 33 |
| | 5-10 | 0.67 | 34 | 25 |
| 3, 6 | 0-1 | 0.58 | 55 | 18 |
| | 1-2 | 0.51 | 49 | 17 |
| | 2-5 | 0.45 | 21 | 12 |
| | 5-10 | 0.30 | 17 | 16 |
| 4, 5 | 0-1 | 0.06 | 15 | 5 |
| | 1-2 | 0.06 | 10 | 4 |
| | 2-5 | 0.09 | 11 | 5 |
| | 5-10 | 0.14 | 10 | 7 |

Experiments in a CSTR were run with core 1 and 2. To simulate conditions with low calcium concentrations in the overlaying water, distilled water (NaCl added) was used as bulkwater. The supernatant in core 1 was 75% saturated with oxygen, while number 2 was kept anaerobic. Both showed a pH-value between 7.0 and 7.5. Phosphorus and calcium concentrations reached a steady state within 4 days (table 3). In this stationary phase phosphate fluxes were $7.5 \text{ mg P.m}^{-2} \cdot \text{day}^{-1}$ in core 1 and $17 \text{ mg P.m}^{-2} \cdot \text{day}^{-1}$ in core 2. Calcium fluxes were 2.4 and $2.0 \text{ g.m}^{-2} \cdot \text{day}^{-1}$ respectively.

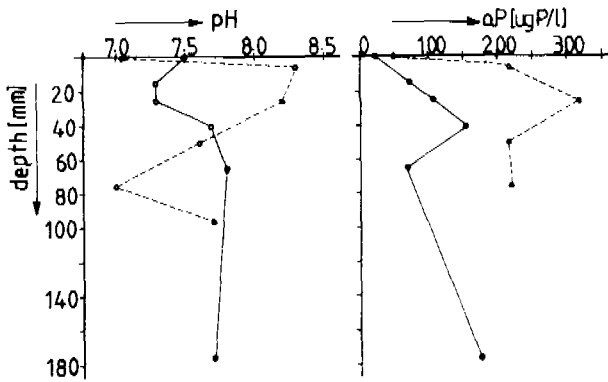


Fig. 3: pH and phosphate concentration (in $\mu\text{g P.l}^{-1}$) in interstitial water.
solid lines: core 1
dashed lines: core 4

TABLE 3: Steady State Concentrations of Phosphate and Calcium during the Flux Experiments

| core | [o-P] _{max} ug P.l ⁻¹ | [Ca] _{max} mg Ca.l ⁻¹ |
|------|--|--|
| 1 | 80 | 25 |
| 2 | 210 | 25 |
| 3 | 40 | 300 |
| 4 | 45 | 170 |
| 5 | 30 | 150 |
| 6 | 45 | 170 |

* CSTR

* BR

BR-experiments were run with core 3 to 6. Seepage, about 3 mm.day^{-1} , was induced in core 5 and 6. Overlaying water (phosphorus free lake water) was almost 100% saturated with oxygen and had a pH between 7.5 and 8.0. An example of the phosphate flux and concentration during the experiments is given in fig. 4. The phosphate flux F_p dropped rapidly to a value below $0.2 \text{ mg P.m}^{-2}.\text{day}^{-1}$, where the concentration reached a maximum. Same results were found in the other experiments (table 3). Calcium-concentration and fluxes showed a similar pattern. Influence of the induced seepage could not be demonstrated.

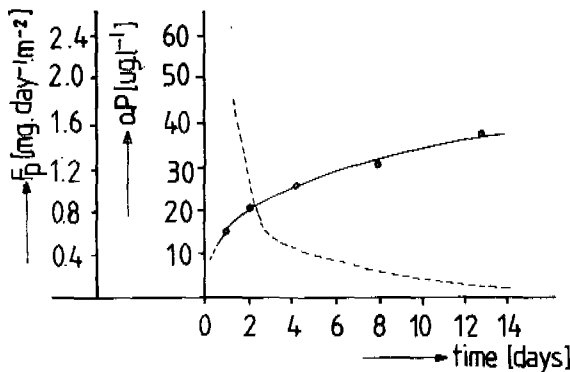


Fig. 4: Phosphate concentration and flux (F_p) in core 3.
solid line: phosphate concentration ($\mu\text{g P.l}^{-1}$)
dashed line: phosphate flux ($\text{mg P.m}^{-2}.\text{day}^{-1}$)

Theoretically the flux F of a species across the sediment water interface is expressed by Fick's law:

$$F = -D_{\text{eff}} \cdot \left(\frac{\partial C}{\partial z} \right)_{z=0} \quad [12]$$

where D_{eff} is the effective diffusion coefficient, depending on the molecular diffusion coefficient and the sediment properties, and C denotes the concentration in the interstitial water. The value of D_{eff} can be calculated, according to Li & Gregory (1974) and Krom & Berner (1980), to be about $10^{-10} \text{ m}^2.\text{s}^{-1}$. The con-

centration gradient is dependent on diffusion, seepage and chemical reactions. A mass balance in a sediment layer yields:

$$\frac{\partial C}{\partial t} = D_{\text{eff}} \cdot \left(\frac{\partial^2 C}{\partial z^2} \right) + q_s \cdot \left(\frac{\partial C}{\partial z} \right) - k_r \cdot (C - C_{\text{eq}}) \quad [13]$$

where q_s is the rate of seepage (in m.s^{-1}), k_r denotes the first order rate constant of the chemical reaction (in s^{-1}) and C_{eq} indicates the concentration at chemical equilibrium. It is assumed that C_{eq} does not change during the experiments. Solutions of eq. [13] have a rather complicated character, depending on the boundary conditions. In case of steady state however, as during the CSTR-experiments, a solution is easily obtained:

$$C - C_{\text{eq}} = (C_0 - C_{\text{eq}}) \cdot \exp(\theta \cdot z) \quad [14]$$

where

$$\theta = (-q_s - (q_s^2 + 4 \cdot D_{\text{eff}} \cdot k_r)^{1/2} \cdot (2 \cdot D_{\text{eff}})^{-1})$$

and C_0 is the concentration at $z = 0$. Taking $D_{\text{eff}} = 10^{-10} \text{ m}^2 \cdot \text{s}^{-1}$, $q_s = 3.5 \cdot 10^{-8} \text{ m.s}^{-1}$ and $k_r = 10 \text{ hr}^{-1} = 2.8 \cdot 10^{-3} \text{ s}^{-1}$, evaluation of eq. [14] leads to the conclusion that the seepage does not influence the concentration gradient. Hence, the flux at $z > 0$ (eq. [12]) is determined by reaction and diffusion only. Secondly, it followed that 99% of the material transported across the interface originates from the upper millimeter of the sediment. This means that the fluxes are not fed by diffusion from deeper layers, but rather by chemical reaction at or just below the interface.

The transport coefficient k_m is defined as:

$$k_m = F \cdot (C_{\text{eq}} - C_0)^{-1} \quad [\text{m.s}^{-1}] \quad [15]$$

A first estimate of C_{eq} is based on the measured pore water concentrations. From the end values during the BR-experiments (table 3), however, it must be concluded that the equilibrium concentrations at or just below the interface are much lower than concentrations at a depth of 10 mm in the sediment. For cores 3 to 6, data from table 3 were used as an estimation of C_{eq} . Values for the other two cores were calculated by interpolation between overlaying water and pore water data. Transport coefficients were obtained from eq. [15] and are summarized in table 4. It is clear that sediments from cores 3 to 6 have coefficients within the same order, while those of core 1 and 2 are at least two times higher. The high value of C_{eq} in core 2 is caused by the anaerobic conditions. Differences in C_{eq} between core 1 and the last four cores may be due to the chemical properties of the sediments (table 2) and the use of calcium free bulk water.

Further, using eq. [12], [14] and [15], a theoretical value of k_m can be calculated from:

$$k_m = (k_r \cdot D_{\text{eff}})^{1/2} \quad [16]$$

Taking the previous mentioned values, this yields $k_m = 5.5 \cdot 10^{-7} \text{ m.s}^{-1}$, which is in good agreement with the experimental results.

In field situations, phosphate concentrations in the overlaying water of 15 $\mu\text{g P.l}^{-1}$ are rather common (Hosper, 1980). Applying the mentioned value for k_m and an equilibrium concentration of 45 $\mu\text{g P.l}^{-1}$ yields a flux of about 1.3 $\text{mg P.m}^{-2} \cdot \text{day}^{-1}$. Balance studies of Lake Veluwe showed P-fluxes to be 1.1 $\text{mg P.m}^{-2} \cdot \text{day}^{-1}$ during summer months (Hosper, 1980), which is of the same order. Fluxes from the sediment of the shipping channel may be much higher. So, in Lake Veluwe, phosphorus fluxes can be explained completely by assuming a direct exchange at the sediment water interface.

From the experiments it is concluded that a good interpretation of measured fluxes is only possible when a good estimation can be gained about the kinetics of the chemical reactions in the sediment. Therefore core experiments should be accompanied by such analysis. Further, values for the equilibrium concentration are needed, which can best be obtained from batch experiments. Final conclusion is that core experiments can be useful in studying the transport of solutes across the sediment water interface.

TABLE 4: Estimated Equilibriumconcentrations of Phosphate($C_{eq,P}$) and calcium ($C_{eq,Ca}$) in the top layers of the sedimentcores and calculated transport-coefficient for phosphate (k_m,P) and calcium (k_m,Ca)

| core | $C_{eq,P}$ [$\mu\text{g P.l}^{-1}$] | $C_{eq,Ca}$ [mg Ca.l^{-1}] | k_m,P [10^{-7} m.s^{-1}] | k_m,Ca [10^{-7} m.s^{-1}] |
|------|--|--|---|--|
| 1 | 100 - 200 | 30 - 150 | 10 - 45 | 2 - 55 |
| 2 | 250 - 400 | 30 - 170 | 10 - 50 | 1 - 50 |
| 3 | 40 | 300 | 6 | 5 |
| 4 | 45 | 170 | 3 | 7 |
| 5 | 30 | 150 | 4 | 10 |
| 6 | 45 | 170 | 3 | 5 |

REFERENCES

- Batchelor, G.K. (1967). An introduction to fluid dynamics. Cambridge Univ. Press, pp. 71-130
- Brinkman, A.G., van Raaphorst, W. and Lijklema, L. (1982). In situ sampling of interstitial water from lake sediments. *Hydrobiologica* 92, 659-663
- Brinkman, A.G., van Raaphorst, W. and Jol, A. (1984). Influence of suspended matter on lake water composition. Int. Symp. on Hydrochemical Balances of Fresh Water Systems, Uppsala 1984
- Fillos, J. and Molof, A.H. (1972). The effects of benthal deposits on oxygen and nutrient economy of flowing water. *J. Water Poll. Control Fed.* 44, 644-662
- Hieljes, A.H.M. (1980). Eigenschappen en gedrag van fosfaat in sedimenten (thesis). Twente University of Technology
- Holdren, G.C. and Armstrong, D.E. (1980). Factors affecting phosphorus release from intact lake sediment cores. *Env. Sci. Techn.* 14, 79-87
- Hosper, S.H. (1980). Resultaten doorspoeling Veluwemeer in het winterhalfjaar 1979-1980. Rijksinstituut Zuivering van Afvalwater, nota 80.400, pp. 1-35
- Kamp-Nielsen, L. (1974). Mud water exchange of phosphate and other ions in undisturbed sediment cores and factors affecting the exchange rates. *Arch. Hydrobiol.* 73, 218-237
- Krom, M.D. and Berner, R.A. (1981). The diffusion coefficients of sulfate, ammonium and phosphate ions in anoxic sediments. *Limnol. Oceanogr.* 25, 327-337
- Li, V.H. and Gregory, S. (1974). Diffusion of ions in seawater and deepsea sediments. *Geochim. Cosmochim. Acta* 38, 703-714
- Morse, Ph.M. and Feshbach, H. (1953). Methods of theoretical physics. McGraw-Hill book comp., NY, pp. 1173-1330
- Murphy, J. and Riley, J.P. (1962). A modified single method for the determination of phosphate in natural water. *Anal. Chim. Acta* 27, 31-36
- Rippey, B. (1977). The behaviour of phosphorus and silicon in undisturbed cores of Lough Neagh sediments. In: Golterman (Ed.); Interactions between sediments and freshwater. Junk publ., The Hague, pp. 348-353

- Van Liere, L. and Mur, L.R. (1982). The influence of simulated groundwater movement on the phosphorus release from sediments, as measured in a continuous flow system. Hydrobiologia 92, 511-518
- Van Liere, L., Peters, J. and Mur, L.R. (1982). Release of sediment phosphorus, and the influence of algal growth on this process. Hydrobiol. Bull. 16, 191-200

MODELLING WATER QUALITY

STREAM MODELING OF NON-CONVENTIONAL WATER QUALITY PARAMETERS: PHENOL, CYANIDE, AMMONIA, OIL AND GREASE

Abul Basher M. Shahalam* and Dennis A. Burke**

**Civil Engineering Department, Yarmouk University, Irbid, Jordan*

***Bradford Woods, Pennsylvania, U.S.A.*

ABSTRACT

Due to complexities in the water uses of the modern time, the water quality management often needs much information in addition to the traditional DO and BOD data, to impose any kind of control on the industrial and municipal discharges into natural streams. The simplistic Monod type of substrate limiting kinetics are not sufficient to express the fate of complex chemicals such as phenol, cyanide, ammonia, oil and grease.

This paper presents the kinetics of physical and biological degradation and transformation of such chemicals in the natural waters. The kinetics were developed through the multiple regression analysis using the data monitored over a year from a river in Pennsylvania, USA. The conventional unidirectional hydraulic transport and mass balance equations were then combined with these kinetics to predict the steady state water qualities in various reaches of the river under a specific set of known external discharges. When compared to the monitored water quality data under that specific set of external discharges, the predictions were found to be satisfactory. Some disagreement was observed in cyanide concentrations in the most down stream section of the 25 mile stretch of river.

KEYWORDS

Model, Industry, Waste, Cyanide, Phenol, Ammonia, Oil, Grease, Natural-Stream.

INTRODUCTION

Unlike our engineering predecessors who were responsible for the sanitary revolution of the 1850's, engineering decision making today and the tools of the environmental profession are highly complex. The basic decision-making tool is the model or algorithm which can quantitatively establish the consequences of a particular action. The model, by its very nature and structure, establishes cause and effect relationships. Today, most complex engineering decisions are made with the aid of models. Thousands of models are in use describing water supply, waste treatment, air quality, flood control, groundwater flow, and water quality. A 1974 survey of aquatic ecosystem models by the Institute of Ecology (1) established that well over 100 water quality models existed at that time. Of those, only one

was reported to address non-traditional water quality parameters.

As research continues to reveal the contribution of environmental factors to public health problems, the need to accurately define and describe the behavior of potential etiological factors in the environment will become increasingly acute. Water quality models of toxic materials represent important, useful, and efficient tools in gaining this understanding. The major benefits which can be achieved by toxic materials water quality models include:

1. Definition of the Sources, Transformations and Effects of Toxic Materials Discharges.

As will be pointed out later, the effect of toxic wastes within riverine systems is not totally a function of the concentration of the toxicant alone. The process of defining the sources, transformations, and effects allows one to integrate current scientific knowledge in a logical, orderly fashion.

2. Systems Optimization.

In an era of concern over inflation and the general economy of the nation, trade-offs will have to be made between economic and environmental goals. A model allows one to optimize the system and determine the incremental costs and benefits associated with restricting or allocating waste loads.

3. Non-Point Source Waste Load Control.

Those associated with 208 planning or who have had past experience with controlling non-point sources of pollution in USA are painfully aware of the lack of decision-making criteria available for restraining non-point source loads. Although the total mass of indicator pollutants originating from non-point sources may be great, their adverse consequences are difficult if not impossible to discern. The definition of specific toxic pollutants, their sources, transformations and effects could provide a means for logically controlling diverse sources of pollution and measuring their effect on the aquatic system.

TOXIC MATERIALS MODELS

By its very nature the aquatic system is complex. A toxic materials model must reflect those complexities. Figure 1 presents in a simplistic manner the various system components. The system can be described through aquatic chemical, physical, biological, and environmental variables. The chemical and environmental variables are, in turn, controlled by external waste loads and external environmental conditions. Those descriptive variables determine the rate of degradation of a toxicant and are also influenced by such degradation. In addition, while being degraded, the total mass of toxic material must be transported throughout the system in the traditional manner (Figure 2).

The requirements for modeling each of the major system components presented in Figures 1 and 2 will be described in this paper through the use of examples from a 1974 through 1977 study of the toxic pollutants found in the Lower Monongahela River(2). Figures 3 through 5 present typical variations found in the Monogahela River. Figures 6 and 7 present corresponding variations in the concentration of cyanide and phenol at the same monitoring locations. Figure 8 presents the stream segment and Table 1 lists the number of discharges by type. The principal sources of phenol were industrial discharges followed by industrially induced non-point sources, municipal discharges, storm runoff and combined sewer overflows. The principal sources of cyanide A (amenable to chlorination) were industrial discharges and perhaps the aquatic system itself.

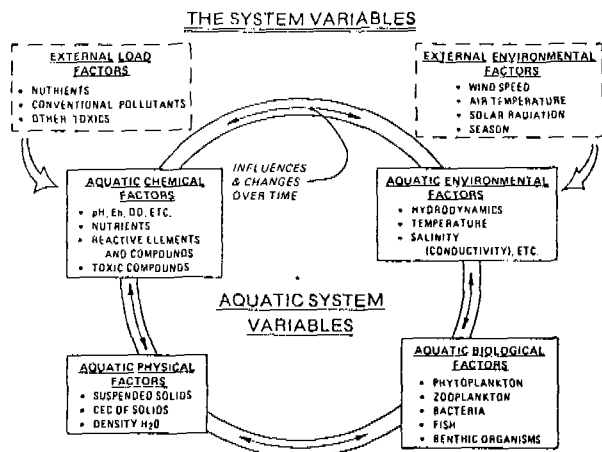


Fig.1. Aquatic System Variables Pertinent to Toxic Material Models

THE SYSTEM TO BE MODELED

THE WATER ELEMENT

- Advection(in-out)
- Dispersion
- Degradation within
- (in-out)

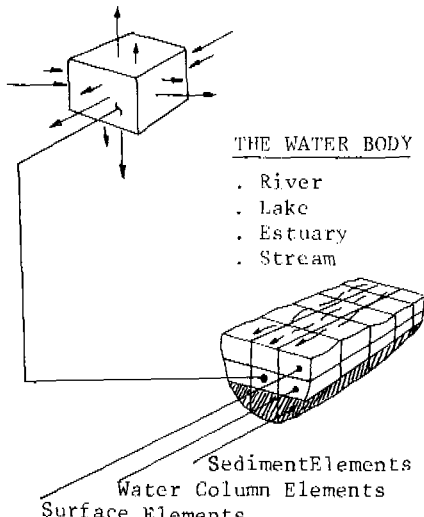


Fig.2. Pictorial Representation of the System

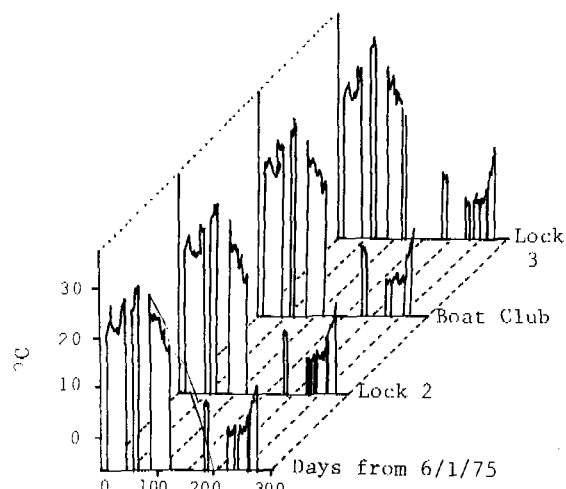


Fig. 3. Monongahela River Temperature at Continuous Monitoring Stations

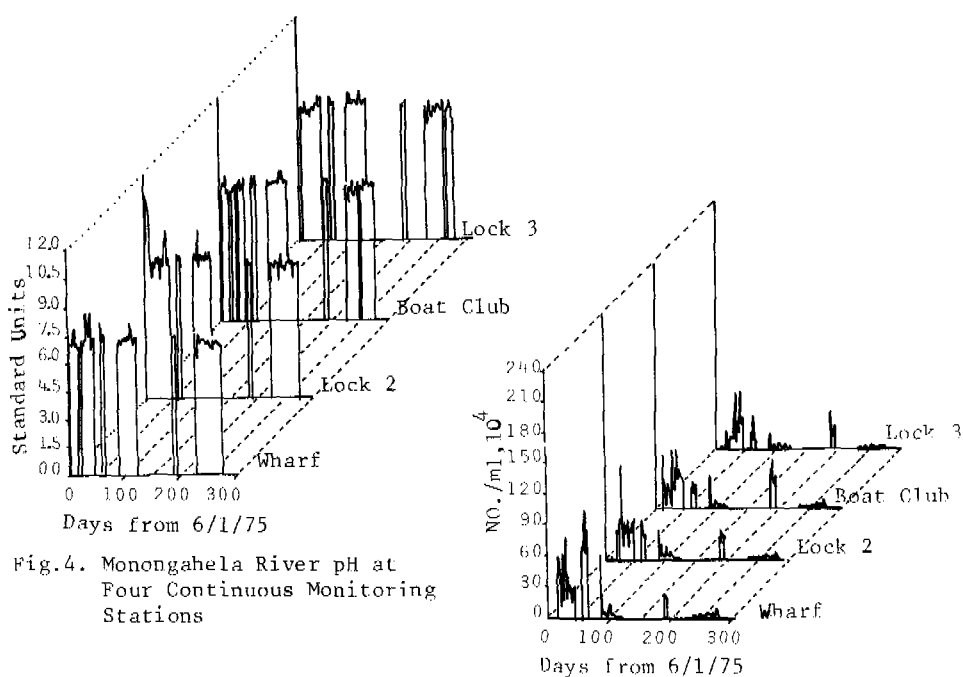


Fig.4. Monongahela River pH at Four Continuous Monitoring Stations

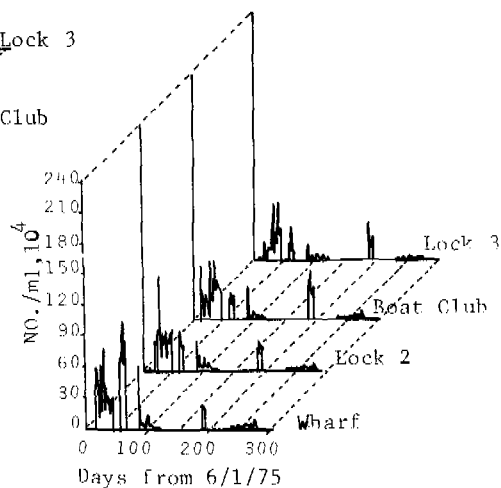


Fig.5. Monongahela River Total Bio-mass(ATP) at Four Continuous Monitoring Stations

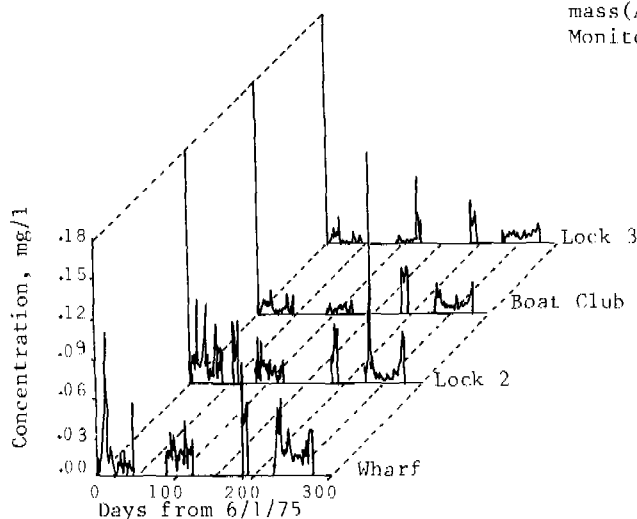


Fig.6. Monongahela River Total Cyanide at Four Continuous Monitoring Stations

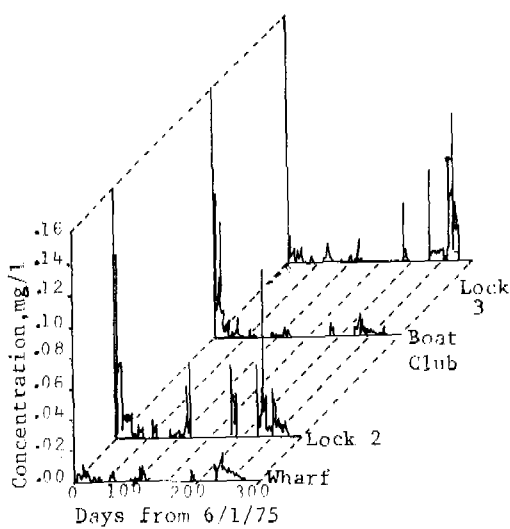


Fig. 7. Monongahela River Phenol at Four Continuous Monitoring Stations

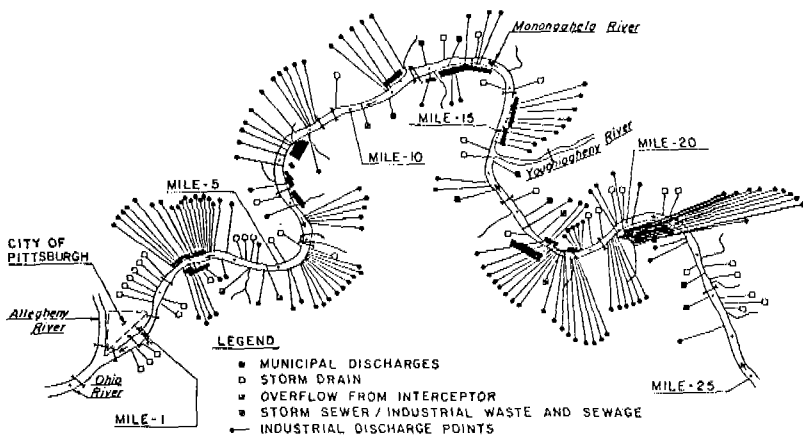


Fig. 8. Lower Monongahela River Discharges

TABLE 1
DISCHARGES TO LOWER 23 MILES
OF MONONGAHELA RIVER

| <u>TYPE OF DISCHARGE</u> | <u>NUMBER OF DISCHARGES</u> |
|--------------------------|-----------------------------|
| Industrial | 132 |
| Storm Sewers | 40 |
| Tributary Streams | 14 |
| Combined Sewer Overflows | 2 |
| Storm Sewers with Wastes | 3 |
| Municipal Discharges | 8 |
| TOTAL | 199 |

In addition to the necessity for identifying all possible sources, dependable modeling requires that the variation of waste loads be identified. Experience obtained during the Lower Monongahela River Study has established the need for identifying the total waste loads, over extended time intervals, through long-term and intensive short-term sampling. All samples obtained by the industries, the Pennsylvania DER, and the EPA for all industrial discharges were subjected to a statistical analysis, resulting in the development of frequency distributions. Figures 9 and 10 display typical frequency distributions. The median values for waste discharges and tributary streams were then utilized to construct typical mass loading curves shown in Figures 11 through 13.

DEVELOPMENT OF DATA BASED KINETICS

The aquatic physical, biological, and environmental variables presented in Figure 1 control the rate of degradation of toxic materials within riverine systems. They are also directly affected by the presence of the toxicant. Traditional DO/BOD water quality models have been simplistically constructed. They merely transport the BOD throughout the system, degrade the BOD as a function of time and concentration alone, and correspondingly deplete the dissolved oxygen of the system. First order degradation kinetics utilized in DO/BOD models cannot be effectively utilized in modeling toxic materials. First order kinetics cannot be utilized since the degradation of toxic compounds is a function of a variety of physical, environmental, and biological factors. Figures 14 and 15 present typical first order degradation rates calculated from samples obtained from the Monongahela River. In some cases, first order rates can be correlated to temperature. However, water or incubation temperature alone cannot explain the difference in the observed degradation rates.

Not only do traditional modeling approaches fail to adequately explain degradation rates, they also fail to explain the ultimate fate of the toxicant, the degradation products, and the consequences of such degradation. Therefore, more descriptive degradation functions must be utilized to describe the decay of a toxicant, its byproducts and its ultimate fate.

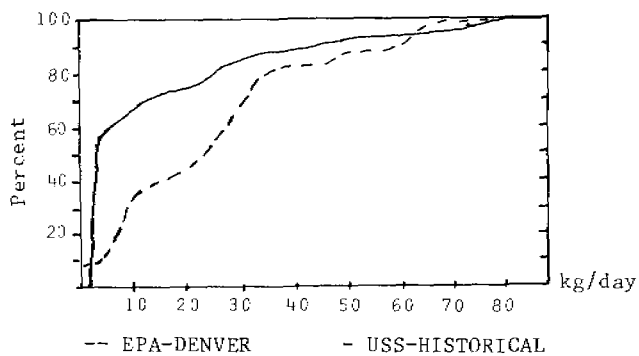


Fig.9. Frequency Distribution of Phenol Loads from a Typical Industrial Outfall to the Monongahela

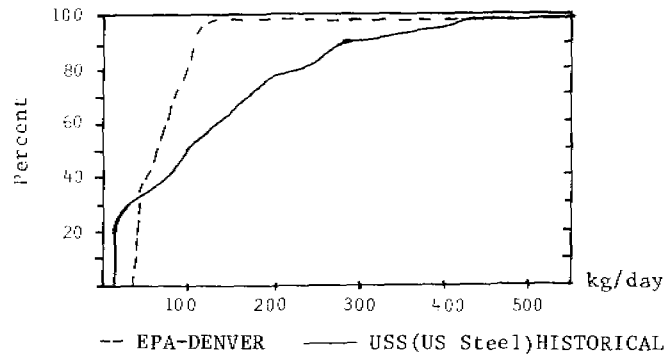
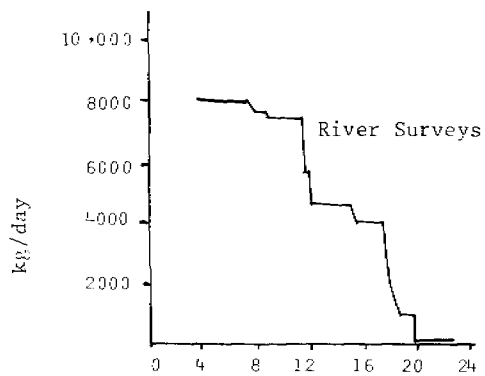
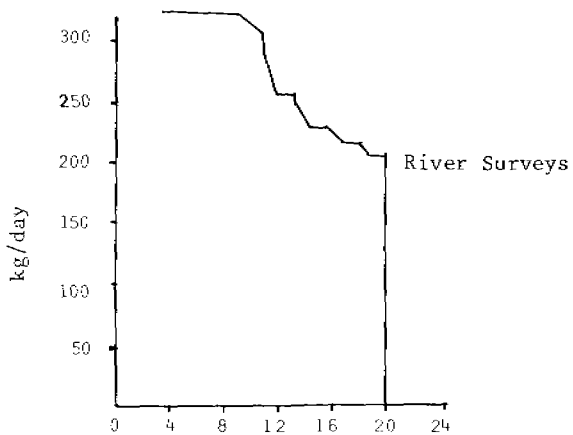


Fig.10. Frequency Distribution of Cyanide from an Industrial Outfall to the Monongahela River



Rivermile [1 mile=1.609 Km]
Fig.11. Mass Load of Oil and Grease by Rivermile



Rivermile [1 mile=1.609 Km]
Fig.12. Mass Load of Phenol by Rivermile

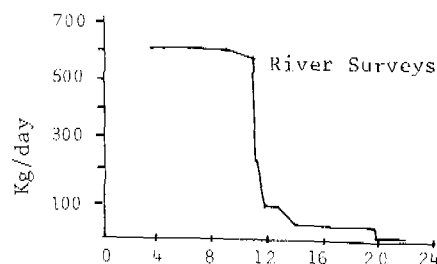


Fig. 13. Mass Load of Total Cyanide by River Mile

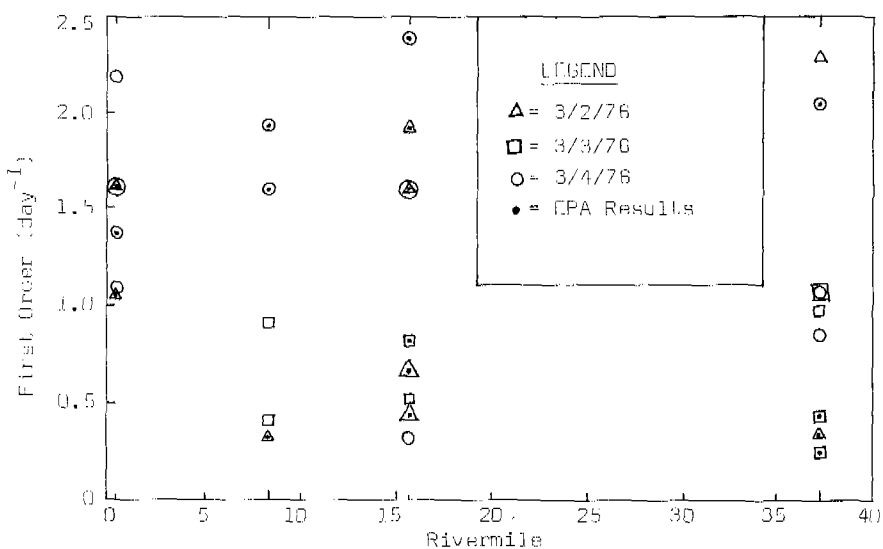


Fig. 14. Phenol Bottle First Order Degradation Rates From Samples Collected Over a Three Day Period At Four River Locations.

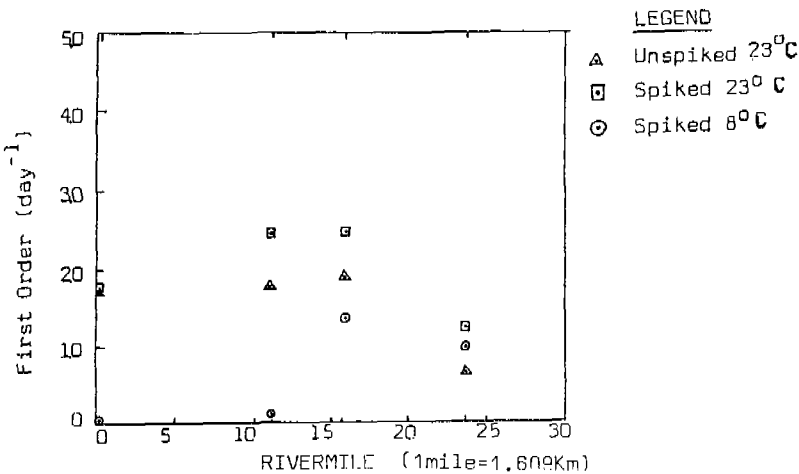


Fig. 15- Cyanide Bottle First Order Degradation Rates From Samples Collected At Four River Locations and Incubated at Different Temperatures

The transformation of a toxicant or its degradation is the sum of a number of mechanisms. Those mechanisms include volatilization, hydrolysis, photolysis, sorption on solids or microbial flocs, chemical oxidation and biodegradation. General expressions have previously been developed which can adequately characterize the rate of anticipated conversion as a function of physical, chemical, biological and environmental factors. If all of the defined mechanisms are operable on a particular toxicant, a great amount must be known about the water body. All of the variables influencing or controlling those removal mechanisms must be modeled.

Fortunately, not all degradation mechanisms are of primary concern. The Monongahela River Study established that phenol loss was primarily controlled by biodegradation. Hydrolysis, volatilization, sorption, and photolysis did not significantly affect the removal of phenolic compounds. Biological degradation was adequately characterized through Monod expressions. Cyanide loss was more complex. Its degradation was a function of biodegradation, volatilization, and hydrolysis. The byproduct of hydrolysis was ammonia which was also modeled. Oil and grease was lost through sorption on suspended solids which required a solids transport model. The expressions utilized for modeling the degradation of phenol, cyanide, and oil and grease within the Monongahela River are shown in Table 2.

MODEL VERIFICATION AND DISCUSSION

The use of those expressions coupled with conventional advection and dispersion functions resulted in the successful simulation of steady-state conditions. Figures 16 through 18 present the verification simulations in conjunction with river survey analytical data. The model simulations were impressive, especially

TABLE 2

DEGRADATION EQUATIONS UTILIZED IN THE
LOWER MONONGAHELA RIVER TOXIC MATERIALS MODEL

| <u>CHEMICAL CONSTITUENT</u> | <u>RATE EQUATION</u> | <u>VARIABLE DESCRIPTION</u> |
|-------------------------------------|---|---|
| Phenol Removal Rate | $\frac{ds}{dt}/_X = (3.16e^{-7.46/T})S$ | $\frac{ds}{dt}$ = differential change in phenol S = concentration of phenol, mg/l X = concentration of phenol degrading microbes, mg/l T = temperature, °C |
| Phenol Degrading Microbes | $\frac{dx}{dt}/_X_T = (1.125 - 0.023T) \cdot (3.16e^{-7.46/T})S - (0.0005 + 0.0003T)$ | $\frac{dx}{dt}/_X_T$ = net specific growth rate at temperature T, °C S = concentration of phenol, mg/l X = phenol degrading microbes, mg/l |
| Cyanide Removal Rate Volatilization | $(\frac{dn}{dt})_V = 0.142 (0.874)^{20-T} (n)$ | $(\frac{dn}{dt})_V$ = loss of cyanide due to volatilization (per square meter of surface area) n = concentration of cyanide, mg/l |
| Hydrolysis | $(\frac{dn}{dt})_H = 0.0029 (0.959)^{20-T} (n)$ | $(\frac{dn}{dt})_H$ = differential change in cyanide n = concentration of cyanide, mg/l |
| Biological Removal | $\frac{dn}{dt}/_X = 0.01(n)^{(1.49-0.0333T)}$ | n = concentration of cyanide, mg/l X = cyanide degrading microorganisms concentration, mg/l |
| Cyanide Degrading Microbes | $\frac{dx}{dt}/_X_T = (37.8 + 0.4166T) \cdot \{0.01(n)^{(1.49-0.0333T)}\}$ | $\frac{dx}{dt}/_X_T$ = net specific growth rate at temperature T, °C n = concentration of cyanide, mg/l |
| Ammonia Effect of Cyanide Removal | $\frac{d(NH_4)}{dt} = (0.00156 (0.959)^{20-T})n$ | $\frac{d(NH_4)}{dt}$ = differential change of ammonia n = concentration of cyanide, mg/l |
| Oil and Grease | $\frac{A}{SS} = (0.009 - 6.3 \times 10^{-6} SS) S^{0.475}$ | A = concentration of oil and grease adsorbed SS = concentration of solids, mg/l S = equilibrium concentration of oil and grease, mg/l |

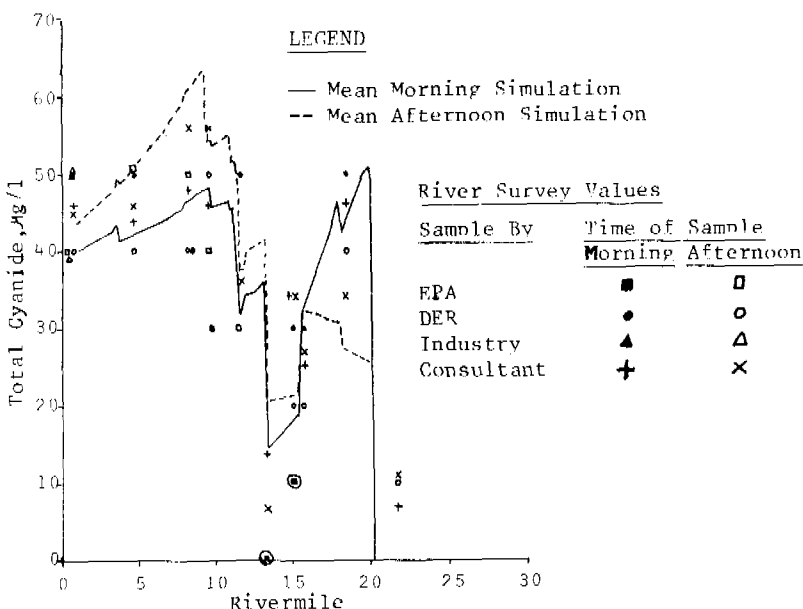


Fig.16. Monongahela River Total Cyanide Model Verification with March 4, 1976 River Survey Data

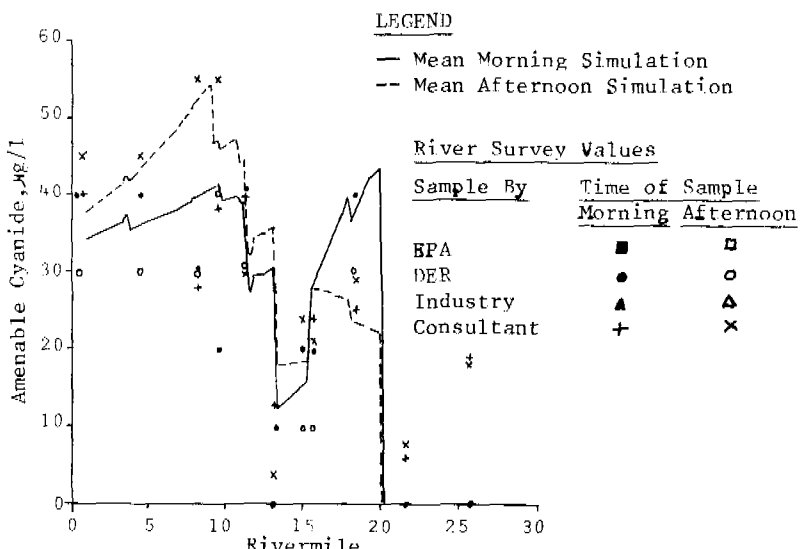


Fig.17. Monongahela River Amenable Cyanide Model Verification with March 4, 1976 River Survey Data

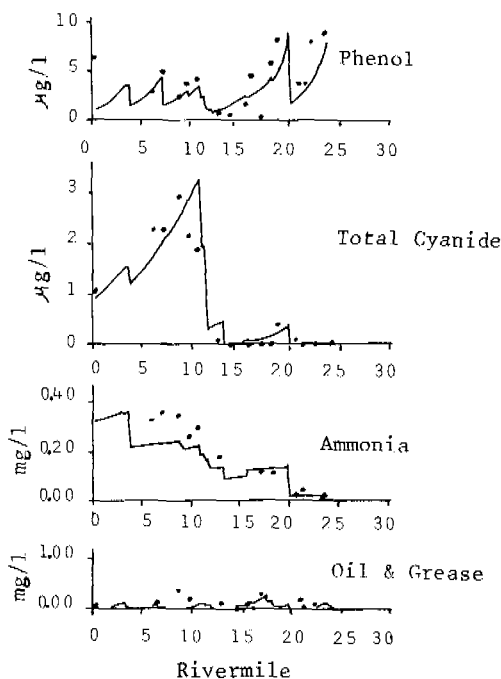


Fig.18. Monongahela River Phenol, Cyanide, Ammonia, and Oil & Grease Simulations for July, 1975 River Survey Condition

since arbitrary source and sink terms were not utilized. However, the simulations were conducted under steady-state conditions with known point and non-point waste loads, river temperature, flow, boundary conditions, etc.

Traditional water quality modeling efforts are normally considered adequate after successful calibration and verification. Calibration and verification are generally conducted with two independent sets of water quality and waste load information. Those sets of data are normally acquired under similar environmental conditions (summer or fall steady-state conditions). Given the flexibility associated with source and sink terms, benthic oxygen demand terms, rate constants, etc. and the similarities under which the calibration and verification simulations are conducted, the modeling effort often results in a curve fitting exercise. The models are rarely ever tested over long periods of time to establish the effect of changing environmental conditions such as water temperature, flow and sediment movement, or the effect of events preceding the steady-state simulations.

The true test of a water quality model's adequacy is its ability to simulate the variables which describe the aquatic environment as a function of time and

distance. Time in this context includes seasonal and environmental variations. Environmental variations could include precipitation events causing the increased delivery of nutrients, waste loads, sediment, and microorganisms; or cold weather conditions and its effects on water temperature and the reduced delivery of microorganisms because of frozen ground conditions. The delivery and relative population of specific microorganisms capable of degrading a toxic material is of extreme importance in developing toxic material water quality models. The kinetics developed for this model (Table 2) are responsive to the dynamic changes of variable factors. The comparison of the predicted vs. observed phenol concentrations was considered adequate. The cyanide and ammonia results were generally satisfactory in the upper reaches but diverged periodically in the lower reaches of the river. A multivariate statistical analysis of the differences between predicted and observed values indicated that a number of undefined mechanisms were the causative factors. One of the more basic problems was the fact that phenol, cyanide and ammonia were generally degraded by the same microorganism, *P. aeruginosa*.

One possible explanation of the variation in cyanide concentration, which was linked statistically to biomass, is the unique characteristics of the microorganism responsible for the degradation of phenol and cyanide. Recent research studies (3) have established that *P. aeruginosa*, one of the few microorganisms capable of breaking a benzene ring, produce substantial quantities of cyanide during respiration. If studies would confirm such an occurrence in riverine systems, it would explain the production of cyanide within the Monongahela River and other mysterious occurrences of cyanide within the Ohio River system.

However, the most significant problem associated with toxic materials models is the lack of sediment quality criteria. Many slightly soluble or insoluble toxic chemical compounds will be removed from the water column by sorption on biological flocs or particulate matter. Those chemical compounds adsorbed to biological flocs will ultimately settle and may become incorporated into the benthic communities food chain. Those toxic chemicals associated with inert material will ultimately settle, and undergo aerobic decomposition, anaerobic decomposition, or accumulate to a level which inhibits the viability of the benthic community. In order for toxic materials models to be utilized, the limiting concentration of toxic chemical compounds delivered to the sediments through partitioning within the water column and ultimate settling must be established.

CONCLUSION

The discharge of toxic materials into the aquatic system has the potential to produce a wide variety of effects, many of which are presently poorly defined. It is also apparent that the long-term human health consequences of such discharges constitutes a more serious unanswered question. The unlikely elimination of the numerous sources of toxic materials, the efficient delivery of such materials through the water route, and the general health problems of our time dictate the need to develop complex decision-making tools to control the sources of toxic materials. The development of those tools or toxic materials models will require the following:

1. Refined physical/chemical characterization of pollutants.
2. Definition of all sources including industrial, municipal, non-point, and the natural environment.
3. Delineation of all effects including those directly attributed to the transformation of substances.

4. Description of the degradation pathways of the toxic material alone and in conjunction with other pertinent chemical compounds.

Succinctly stated, the characteristics, sources, effects, and degradation of each prominent toxic material must be defined. Clearer definition of those factors will provide a rational basis for the control of toxic materials.

It may be concluded that although much has been learned in recent years concerning the modeling of toxic materials with riverine systems and their sources, effects and degradation, the system is extremely complex and requires further study. Toxic materials must be characterized properly. The possible point and non-point sources must be defined in terms of their variation. In addition, the degradation mechanism and the effects of degradation must be determined. In short, the characteristics, sources, effects, and degradation of all toxic pollutants must be known.

ACKNOWLEDGEMENT

At the time when the paper was in preparation, the authors were associated with The Chester Engineers, Coraopolis, Pennsylvania; A.B. Shahalam is currently associated professor of Civil Engineering, University of Yarmouk, Irbid, Jordan.

REFERENCES

1. Parker, R., "Survey of Aquatic Ecosystem Models," The Institute of Ecology, Logan Utah, 1974.
2. Burke, D. A., et al, "Report on the Lower Monongahela River Study, Water Quality Conditions, Point and Non-Point Source Waste Loads and Waste Load Allocation," January 1977.
3. Kracik, C. A., "Some Genetic and Physiological Aspects of Cyanide Production in Pseudomonas Aeruginosa. M.S., Duquesne University, Biology, 1977.

MODELLING OF OXYGEN DEPLETION IN COASTAL WATERS

A. Malmgren-Hansen,* P. Mortensen** and Bo Møller*

**Water Quality Institute, Agern Alle 11, DK-2970 Horsholm, Denmark*

***Danish Hydraulic Institute, Agern Alle 5, DK-2970 Horsholm, Denmark*

ABSTRACT

The relative importance of nutrient loadings and hydrographical and meteorological conditions for oxygen conditions in the Thisted Bredning, Denmark were evaluated by intensive survey and model calculations. The influence of wind speed on the vertical mixing in the unstratified shallow waters was quantified and tested in an oxygen model. The significance of oxygen consuming biological processes on the oxygen conditions were tested. By the use of a eutrophication model, the influence of local discharges of sewage on the size of the oxygen producing and oxygen consuming processes in the Thisted Bredning was calculated. Calculations showed that only a minor increase in rates of the oxygen consuming processes result in a drastic rise in the probability of oxygen depletion.

KEYWORDS

Oxygen depletion, Eutrophication, Loadings, Meteorological Conditions, Hydrographical Conditions, Modelling.

INTRODUCTION

Over the last decades, eutrophication has become an increasing problem in Danish coastal waters. One of the most drastic results is seen every year in the Limfiord in the northern part of Jutland. Large areas of this fiord are struck by severe oxygen depletion in the bottom waters causing mass kill of the bottom fauna and fish. Figure 1 shows the Limfiord. The areas known to suffer from oxygen depletion are shown.

It has been a matter of discussion whether the occurrence of oxygen depletion is a natural phenomenon or is caused by human activity.

This paper deals with a study carried out in the Thisted Bredning, one of the areas in the Limfiord, where oxygen depletion occurs once or more every year. The aim of the study was to examine the relative importance of nutrient loadings, and the hydrographical and meteorological conditions for oxygen conditions in the Thisted Bredning and the Limfiord in general.

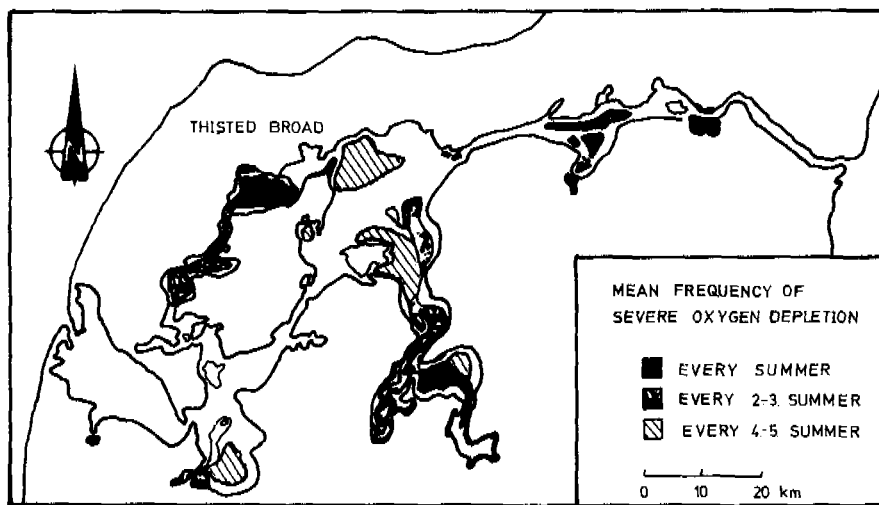


Fig. 1. The Limfiord in the northern part of Jutland, Denmark. Areas liable to oxygen depletion are shown.

The investigation was carried out in 1980 by the Water Quality Institute and the Danish Hydraulic Institute for the Committee of the Limfiord comprised of the environmental departments in the Countries of Northern Jutland, Ringkøbing and Viborg.

HYDRAULIC CONDITIONS

The Limfiord is a 'fiord' connected to the sea by two tidal inlets i.e. to the North Sea in the west and to the Kattegat at the eastern end of the fiord.

Dominant western winds produce a residual east-going current. Because of the salinity difference between the North Sea and the Kattegat and the fresh water run off, pronounced salinity gradients exist throughout the fiord system.

The Limfiord is quite shallow and can normally be considered as a well mixed system. The part of the fiord system in question, Thisted Bredning, can be characterized as a shallow basin connected to the rest of the fiord system by narrow sounds.

The general hydraulic behaviour of the fiord system was known from a previous study (The Limfiord Committee 1976). A depth integrated mathematical model in that study was set up and calibrated for the whole system. The detailed horizontal and vertical mixing processes of the Thisted Bredning were studied on the basis of a field programme including measurements of current and wind continuously and vertical and horizontal distribution of salinity and temperature. The measurements revealed that horizontal salinity gradients up to 2 ppt exist from the southwest end to the northeast end of the basin, and that normally the basin is well mixed vertically. In some situations a certain vertical stratification can develop and exist for some time if followed by calm weather conditions. However, the turbulent energy supplied by a following wind will again establish vertical mixing of the water body.

Based on the field measurements and the previous general hydraulic model study a

simplified hydraulic model including vertical segmentation was set up and calibrated for the Thisted Bredning.

WATER QUALITY

The loadings of organic matter, nitrogen and phosphorus from air and land to the Thisted Bredning were measured throughout the year of 1980. At the same time, the concentration of the same constituents were measured in the two narrow sounds through which Thisted Bredning is connected with the rest of the Limfiord. In the Thisted Bredning itself, measurements of nutrient concentrations, chlorophyll-a and primary production as well as sedimentation of organic matter were carried out simultaneously.

The horizontal and vertical variation in the oxygen concentration was measured a number of times with the highest frequency in July and August. This is the time of maximum probability of oxygen depletion. Measurements were carried out at the positions shown in Fig. 2 at intervals of 2 meters depth down to half a meter above the bottom.

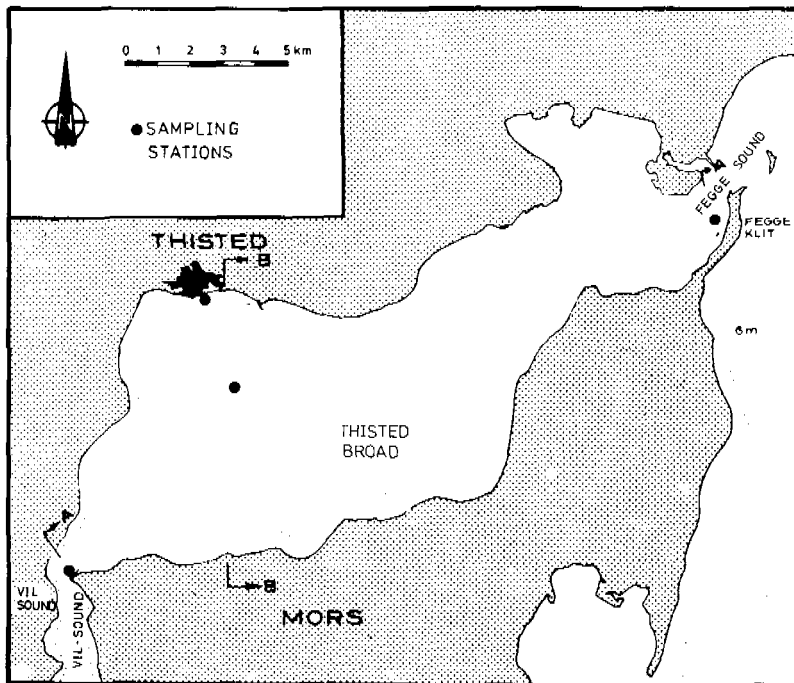


Fig. 2. Sampling stations in the Thisted Bredning.

Continuous measurement of oxygen concentrations at four depths at one position in the middle of the Thisted Bredning was carried out from the 12th to the 27th of August. At the same time sedimentrespiration in undisturbed cores from the same location was measured in the laboratory. From July to September the sedimentation was measured in sediment traps.

Based on the water quality data and in combination with measurements of water flow in the sounds, a mass balance for organic matter, total nitrogen and total phosphorus from the 1st of July to the 1st of October was established.

During the survey samples of phytoplankton were collected. There were no blue-green algae in these samples indicating that nitrogen fixation by algae probably was insignificant in the mass balance for nitrogen. The rate of denitrification was not measured, but estimated from other measurements in the Limfiord. (HenrikSEN and Blackburn, 1979).

HYDRAULIC MODEL

A mathematical model of transport and mixing was set up for the Thisted Bredning and the adjacent sounds. The model was based on a box-model principle and assumed well mixed conditions in the sounds but allowed for vertical density variations in Thisted Bredning. The model is outlined in Fig. 3.

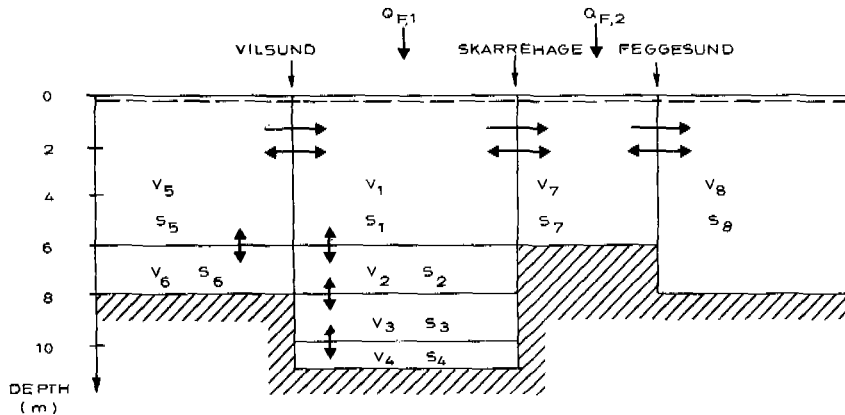


Fig. 3. Sketch of box-model of Thisted Bredning. $v_1 - v_8$ are box volumes. $s_1 - s_8$ are mean salinities of individual boxes and $Q_{F,1}$ and $Q_{F,2}$ are fresh water inflow volumes.

The first step of the model set-up involved a calibration of horizontal flows and mixing characteristics based on simulation of measured horizontal salinity profiles throughout a 3 month period. Time step was 1 day.

The next step was to select periods characterized by a reduced horizontal water exchange. Simulation of the vertical mixing in these periods was carried out with a time step of 3 hours and with measured horizontal and vertical density profiles as initial conditions. The vertical diffusion coefficient D_z was calculated from the formula:

$$D_z = 2 \cdot 10^{-9} \frac{w_{10}^3}{y \cdot N^2} \quad [m^2/s] \quad (1)$$

where

w_{10}^3 = mean of wind velocity 10 m above sea surface to third power [m^3/s^3]

y = water depth

N^2 = vertical stability parameter

$$N^2 = \frac{g}{\rho} \cdot \frac{dp}{dz}$$

Calculated vertical diffusion coefficients are shown in Fig. 4. A verification of the vertical diffusion coefficients has been carried out for the selected periods on the basis of consecutive oxygen profiles as described in the next section.

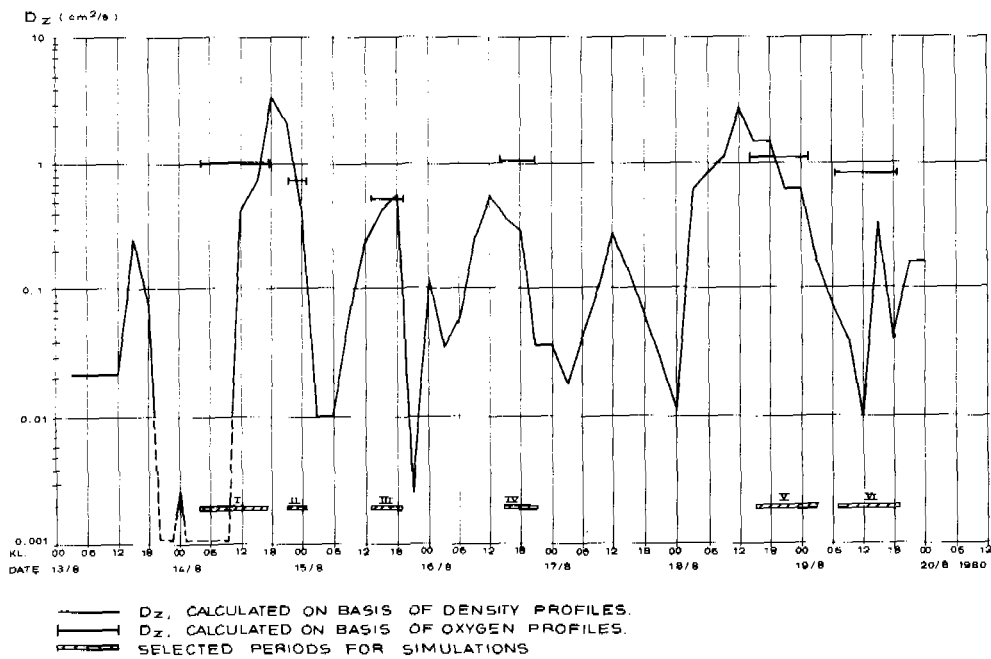


Fig. 4.

OXYGEN MODEL

A model was set up to describe the oxygen conditions in the central deep part of the Thisted Bredning as described in the previous section. The model consisted of 4 boxes in the vertical as shown in Fig. 5.

In the oxygen model it is assumed, that in short periods, the oxygen conditions in the central part of the model area are horizontally uniform and only influenced by internal processes and vertical mixing generated by the wind. The variation in the oxygen concentration is generally described as follows:

$$\frac{dc}{dt} = P_r - R_e + K(C_s - c) - S_r \quad (2)$$

where

c = oxygen concentration

t = time

P_r = production of oxygen

R_e = respiration in water

K = reaeration constant

C_s = saturation concentration of oxygen

S_r = sediment respiration.

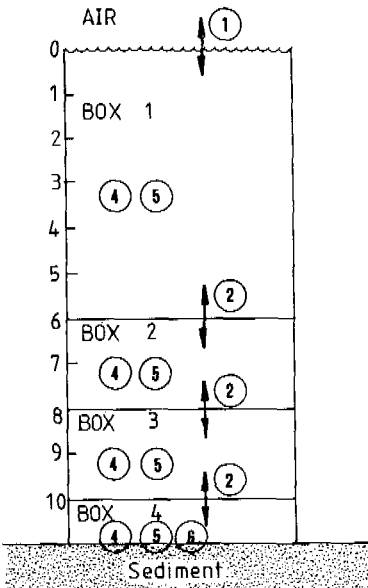


Fig. 5. The composition of the vertical oxygen model.

- Processes:
1. Exchange of oxygen air/water.
 2. Vertical mixing.
 4. Production of oxygen.
 5. Respiration in water.
 6. Respiration in sediment.

The model was first used to verify the description of the vertical mixing. Measured and simulated oxygen concentrations at 4 depths coinciding with the centers of the boxes in the model were compared. From continuously measured oxygen concentrations and respiration in water and sediment through six short periods, the vertical mixing coefficients in these periods were calculated and compared with the calculated mixing coefficients based on the wind speed and vertical density profile using equation (1). The results of the verification are shown in Fig. 4.

A reasonably good agreement between the dispersion coefficients estimated from the oxygen measurements and from theoretical calculations was found.

The ability of the model to simulate variations in the oxygen concentration in the Thisted Bredning was tested for the three periods 1/7-8/7, 22/7-29/7 and 12/8-26/8 1980. In the first two periods measurement of the oxygen concentration was carried out at the beginning and at the end. In the last period the oxygen concentration was measured continuously at depth of 9.5 m. The results of the verification of the model are shown in Figs. 6 and 7.

The agreement between measured and calculated values in the three periods are generally good. Unfortunately the variation in the oxygen concentration from the 12th to the 26th of August was very modest, giving a poor opportunity for strong verification of the model.

As can be seen from Fig. 7, the model was not able to describe the daily variations due to the variation in radiation from the sun. Only daily mean values of

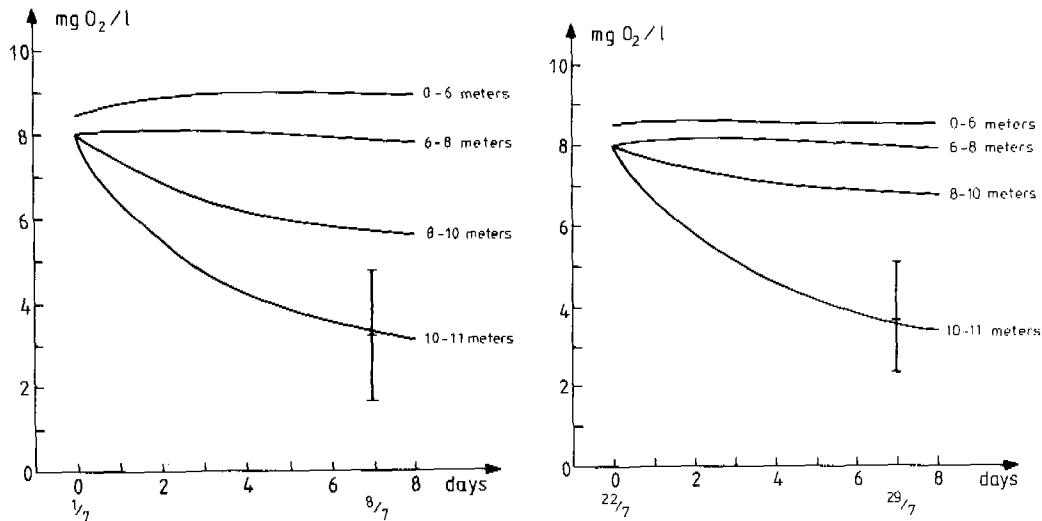


Fig. 6. Calculated oxygen concentrations in two test periods (1-8 and 22-29 July, 1980). The measured oxygen concentration at the bottom at the end of each test period is shown as mean and with an indication of the standard deviation.

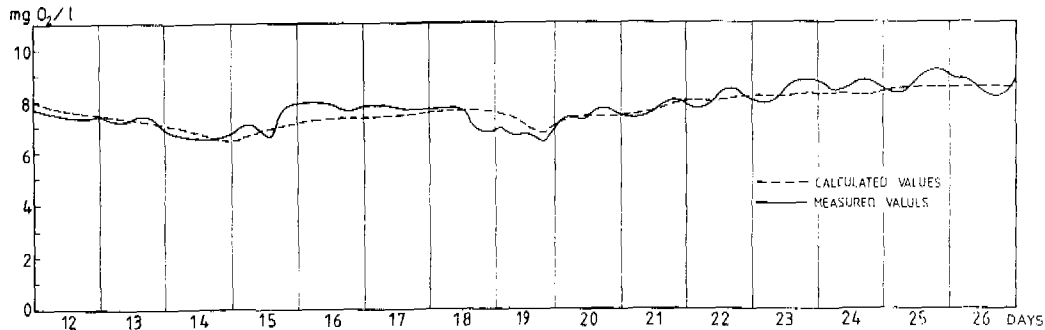


Fig. 7. Calculated and measured oxygen concentration at 9.5 meters depth in the period 12-26 of August, 1980 in the central part of Thisted Bredning.

wind speed, primary production, respiration and temperature were used in the model. This caused the model to react slowly in situations where wind speed changed rapidly e.g. on the 15th and 18th of August.

SENSITIVITY ANALYSIS

The oxygen concentration at the bottom is sensitive to two main factors; the vertical mixing and the biological processes producing and consuming oxygen. The sensitivity of the oxygen concentration in the model was tested for these two factors, firstly by varying the wind speed and keeping the biological processes constant and secondly by keeping the wind speed constant and varying the biological processes. The results are shown in Fig. 8 and Fig. 9.

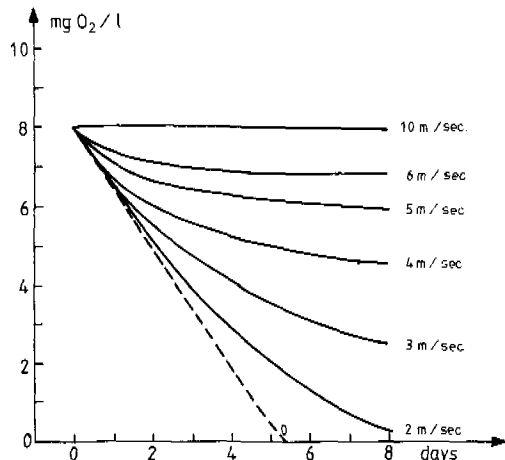


Fig. 8. Oxygen concentration at the bottom calculated at different wind speeds.

In the example shown in Fig. 8 the primary production in the upper 6 meters was constant at 5.5 g O₂/m²/day, the respiration in free waters 0.40 g O₂/m²/day and the sediment respiration 1 g O₂/m²/day. From a situation with complete mixing the oxygen concentration was calculated on the following eight days at different wind speeds. In the second example in Fig. 9 the production and respiration varied but the wind speed was kept constant at 3 m/sec.

The sediment respiration was kept at a constant level, as the consumption in the sediment is mainly governed by the diffusion of oxygen from the over-lying waters and down in the sediment, and to a minor degree by the production of organic matter in the overlying waters. The sediment respiration had a value of 1 mg O₂/m²/day as in the example shown in Fig. 8.

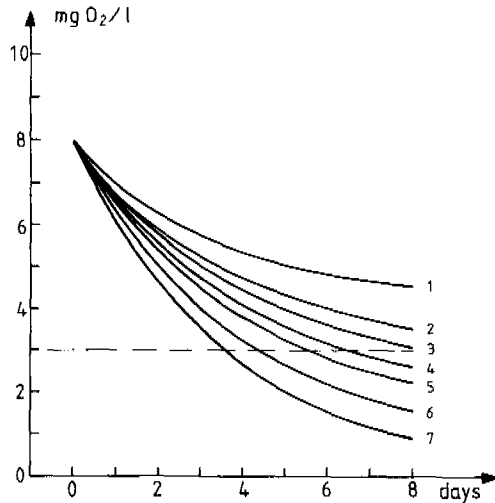


Fig. 9. Oxygen concentration at the bottom calculated at different process rates.

| | 1 | 2 | 3 | 4 | 5 | 6 | 7 | g O ₂ /m ² /day |
|-------------|-----|-----|-----|-----|-----|-----|-----|---------------------------------------|
| Production | 2.5 | 4.5 | 5.5 | 6.5 | 7.5 | 10 | 12 | g O ₂ /m ³ /day |
| Respiration | 0.1 | 0.3 | 0.4 | 0.5 | 0.6 | 0.8 | 1.0 | |

PRIMARY PRODUCTION MODEL

The effect of the outlet of sewage to the Thisted Bredning was described by a primary production model. A short description of the model is given in the following. For a detailed description see Dahl-Madsen, 1978.

Model Description

The model describes the variation of carbon, nitrogen, and phosphorus in:

Phytoplankton
Zooplankton
'Detritus'
Sediment
Inorganic nutrients
Benthic vegetation.

Important biological and chemical processes are:

Growth of phytoplankton
Grazing by zooplankton
Sedimentation of phytoplankton and 'detritus'
Mineralisation of organic matter in sediment
Mineralisation of 'detritus'
Growth of benthic vegetation.

The growth of phytoplankton is related to intracellular concentrations of nitrogen and phosphorus (Nyholm, 1975). This is different from most eutrophication models. The state variables and processes in the model are shown as a flow diagram in Fig. 10.

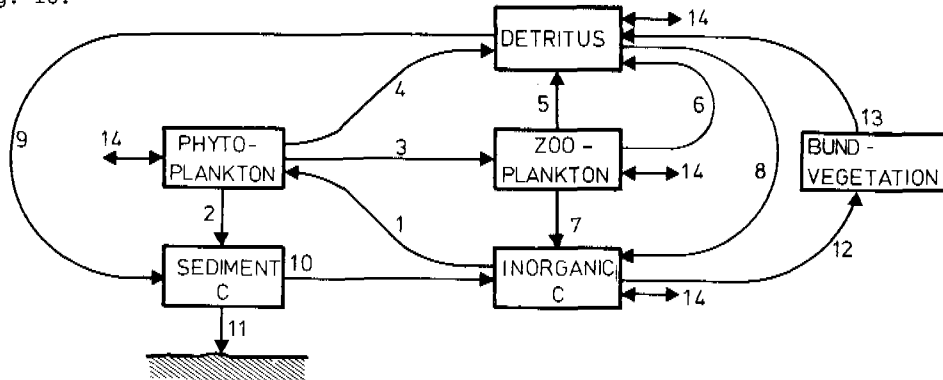


Fig. 10. State variables and processes in the primary production model.
Numbers in the figure refer to the following processes:

- | | |
|---|---------------------------------------|
| 1. production, phytoplankton | 9. sedimentation of detritus |
| 2. sedimentation, phytoplankton | 10. mineralisation of detritus |
| 3. grazing | 11. accumulation in sediment |
| 4. extinction, phytoplankton | 12. production, benthic |
| 5. excretion, zooplankton | vegetation |
| 6. extinction, zooplankton | 13. extinction, benthic |
| 7. respiration, zooplankton | vegetation |
| 8. mineralisation of suspended detritus | 14. exchange with surrounding waters. |

The forcing functions in the model are:

Surface light intensities
Water temperature
Hydraulic conditions.

The water exchange in the gauging period was simulated in the simple box model shown in Fig. 3. This hydraulic model was coupled with the primary production model.

Model Calibration

The primary production model consists of a series of equations including a number of parameters. The value of these parameters were estimated through:

Direct measurements
Literature studies
Laboratory experiments
Calibration.

Measured concentrations of nutrients, phytoplankton and zooplankton as well as the measured sedimentation rates, primary production and respiration rates were used in the calibration of the model.

The results of the calibration are shown in Fig. 11.

Generally there is an acceptable agreement between measured and calculated values.

MODELLING RESULTS

The consequences on the primary production and on the respiration in the Thisted Bredning was calculated in the three alternative situations:

1. No outlet of sewage
2. Present outlet of sewage
3. 2 x present outlet of sewage.

The calculations carried out for the period from 15th May to 1st of October gave the results shown in Table 1.

TABLE 1

| | Primary prod. g C/m ² | Primary prod. g C/m ³ /d |
|---------------------------------|----------------------------------|-------------------------------------|
| 1. No outlet of sewage | 166 | ~ 5.0 |
| 2. Present outlet of sewage | 179 | 5.5 |
| 3. 2 x present outlet of sewage | 190 | ~ 6.0 |

Using the oxygen model with the estimated rates of primary production and respiration in a situation with a wind speed constantly at 3 m/sec and with no density stratification gives the results shown in Fig. 12.

If 3 mg O₂/l is chosen as a critical value to fish it is seen that this value will be reached in seven to nine days depending on the loadings.

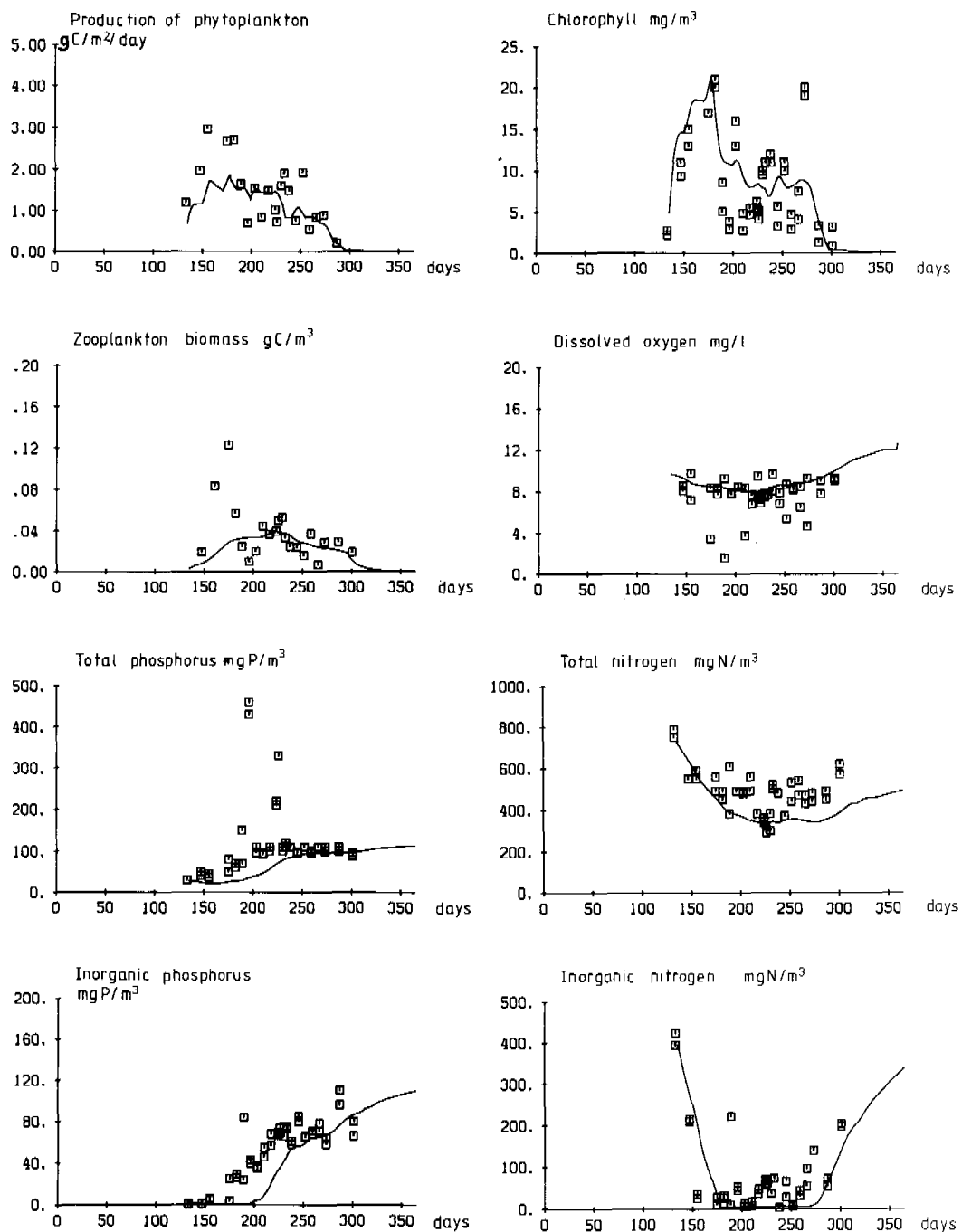


Fig. 11. Calibration results. Calculated values (lines) compared with measured values (squares) for box 1.

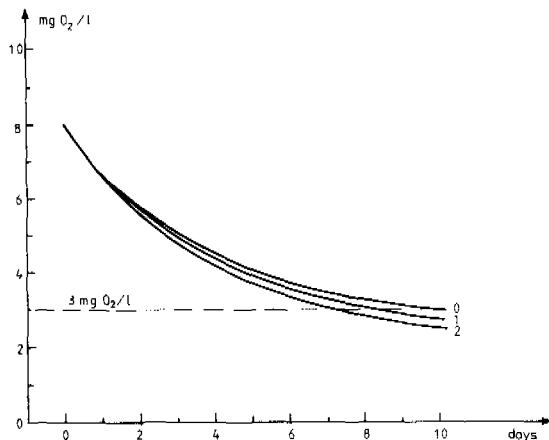


Fig. 12. Oxygen concentration at the bottom in Thisted Bredning at different loadings and with a constant wind speed at 3 m/sec and no stratification.

From analysis of the duration of periods with low wind speed (The Limfiord Committee, 1982) it was found that in the northern part of Jutland, periods with wind speeds at or below 3 m/sec during 7, 8 and 9 days periods are expected to occur 4, 2 and 1 times respectively every 10th year.

CONCLUSION

The model calculations show that a minor increase in phytoplankton production results in oxygen depletion in a shorter time. This is due to the increased oxygen consumption from mineralisation of produced organic material. In the example shown, oxygen depletion occurs after 7 days if loadings are doubled instead of after 8 days if loadings are unchanged. Statistical analysis of wind speed measurements shows that the duration of periods with low wind speed is inversely proportional to the logarithm of the number of events. This means that the number of periods with oxygen depletion will increase exponentially with the rates of the oxygen consuming processes.

REFERENCES

- The Limfiord Committee (1982). Iltsvindsundersøgelse i Thisted Bredning. Hydrografiske målinger og modelundersøgelser. (Report in Danish).
- Henriksen, K. and Blackburn, T. (1979). Nutrients from Sediments. Vand, 4, (in Danish).
- Dahl-Madsen, K.I. (1978). Mathematical Modelling of Eutrophied Coastal Areas. Prog. Wat. Tech., 10, Nos 5/5, 217-235.
- Nyholm, N. (1975). Kinetics of Nitrogen-Limited Algae Growth. Paper presented at the Conference on Nitrogen as a Water Pollutant, Vol. 2 IAWPR specialized Conference. Copenhagen.
- The Limfiord Committee (1976). Limfjordsundersøgelsen 1973-75, Samlerapport. (Report in Danish).

WATER QUALITY MODELING OF THE LOWER HAN RIVER, KOREA

L. F. Tischler,* R. M. Bradley,* S. J. Park** and
D. G. Rhee***

*Engineering-Science, Inc. 911 W. Huntington Dr., Arcadia, California 91006, U.S.A.

**Hyundai Engineering Co., Ltd., Seoul, Korea

***Office of Environment, Seoul, Korea

ABSTRACT

The Han River Basin in the Republic of Korea covers an area of about 27,000 sq km south of the Demilitarized Zone, almost one quarter of the total area of the country. The total population in the basin is of the order of 13 million, of which more than 80 percent are concentrated in the urban conurbation of Greater Seoul alongside the Lower Han River. Within the vicinity of Seoul the river is used extensively for water supply, irrigation and both contact and non-water contact recreation. Treated nightsoil, untreated sludge, partially treated sewage and industrial wastes generated in the urban areas are also discharged to the river which is heavily polluted in the downstream reaches as a result. The finite difference water quality model QUAL-II was adapted to the Lower Han River using data obtained from extensive field water quality surveys especially designed to provide the necessary calibration and verification data base. Hydraulic data for the model were obtained from operation of the U. S. Army Corps of Engineers HEC-II computer model. Model calibration and verification was confirmed by statistical comparison of model simulations with the field data. The calibrated model was used to evaluate a number of different treatment alternatives for two different future years. Extensive model sensitivity analyses were run on both the key model parameters and the treatment alternatives to quantify the reliability of the prediction.

KEYWORDS

Han River, water quality modeling; mathematical modeling; QUAL-II.

LOWER HAN RIVER CHARACTERISTICS

The Lower Han River drains an area of about 2000 sq km from the Paldang Dam to the confluence with the Imjin River 80 km downstream. About 60 percent of the drainage area is within the Greater Seoul urban and periurban area, with the 1983 population in the basin approaching 10.25 million. Residential land use represents 263 sq km with commercial, institutional and industrial land uses accounting for an additional 83 sq km. The population draining the river is anticipated to increase to almost 14 million by the year 2001, when the total urban land use will have increased by almost one-third to 460 sq km.

At the upstream end of the Lower Han River the river flow is controlled by the Paldang Dam which provides the main water source for the Seoul-Incheon area. The average flow at Paldang is 530 cu m/s; the average minimum flow during the dry season (October-June) being 125 cu m/s. The Chungju regulation dam, which is currently under construction on the South Han River, will increase the average minimum flow from Paldang to about 200 cu m/s during dry weather conditions.

The lower portion of the river is tidal, the tidal range decreasing rapidly from 8.8 m south of the river mouth near Incheon to zero near the Third Han River Bridge in Seoul (river km 47). Throughout most of the urbanized river reach the tidal variation is less than 2.0 m.

The Lower Han River currently receives about 390 tonne/d BOD from domestic, commercial, institutional and industrial sources, the major proportion of this load being from domestic sources. The total dry weather flow from all sources averages about 35 cu m/s, or about 50 percent of the average flow in the major urban area tributaries. The desired uses of the Lower Han River are domestic water supply (in the area about Seoul City), irrigation supply, non-contact recreation and minimal protection of fish and wildlife.

WATER QUALITY MONITORING

The basic objective of the program was to collect an adequate number of samples and flow measurements in the main river and major discharges in order to produce a representative picture of pollution loads and resulting river quality over as wide a range of conditions as budget and time conditions would permit. The program was specifically designed to collect data suitable for calibration and verification of a water quality model.

Locations of monitoring sites in the main river and major tributaries are shown in Figure 1. In each case the sites were selected on the basis of compatibility with historic sites, ease of access during different river flows and weather conditions, optimum conditions of mixing in the water body and, whenever possible, proximity to flow gauging stations. It was not possible to monitor conditions in the estuarine portion of the river downstream of Jeonryu because of restrictions on access.

Six surveys were carried out, one each month from July to December 1982. This period covered both the wet summer period and the low temperature winter period and was, therefore, representative of typical annual variations. On each occasion the main river sampling was arranged so that as far as possible the same body of water was sampled as it moved downstream. Tributaries were sampled in accordance with the main river program and flows were either obtained from gauging stations or measured using the cross section and velocity method. The time of travel down the river was derived from a knowledge of the planned release from Paldang Dam and the flow velocities computed from the HEC-II Water Surface Profiles Model. For the flow range experienced during the monitoring program the travel time from Paldang to Jeonryu varied from about 2 to 5 days. All sampling in the tidally-effected reaches was conducted on the ebb tide in order to ensure that the data represented the free-flowing river condition. This timing was of particular importance for the tidally-influenced tributaries since sampling and flow measurement under a backwater influence would have produced misleading results.

Over the six-month monitoring period the flow at Paldang ranged from 124 to 1154 cu m/s and the water temperature from 1 to 28 degree C. This temperature range represents the typical extremes over an annual cycle. The maximum flow recorded was double the annual average flow and about five times greater than the flow exceeded 50 percent of the time. Most of the survey flows were in the low range

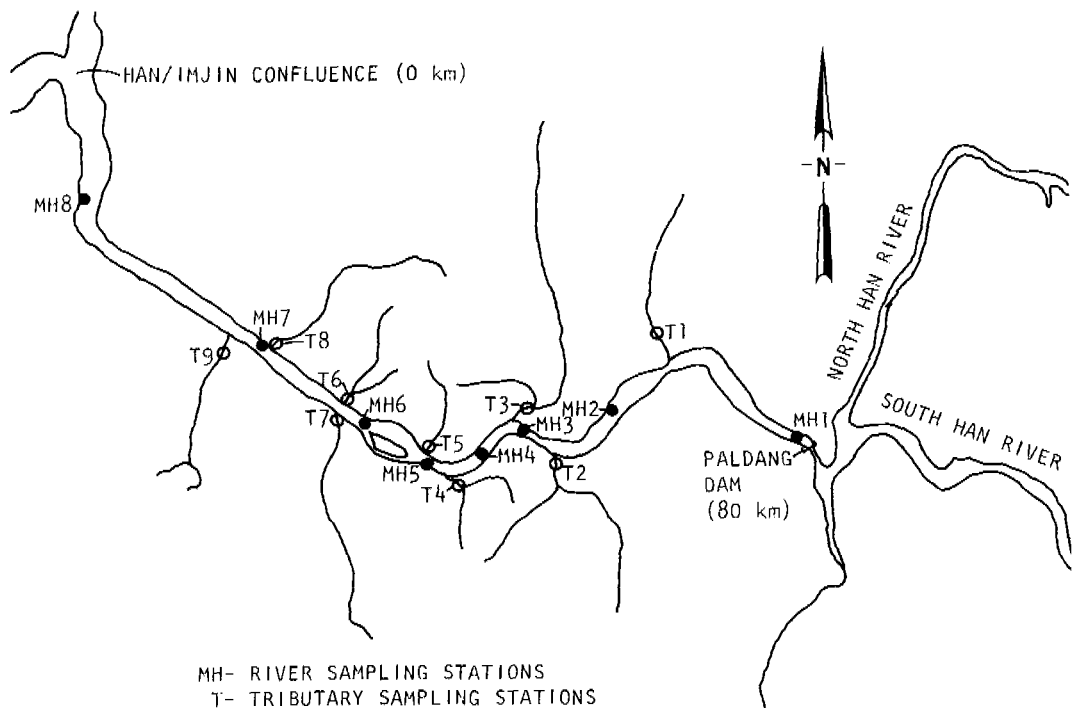


Fig. 1. Location of river and tributary monitoring stations in the lower Han River basin

which represent typical minimum release rates from Paldang and which occur frequently outside the summer wet season. A total of almost 2000 analyses were performed on the main river and tributary samples.

The validity of the surveyed tributary pollution levels was verified by comparing them with calculated values based on land use, population and point-source pollution loads in each tributary catchment area. The pollution loads for residential, commercial, institutional and industrial discharges were based on detailed field surveys of a range of socio-economic residential/commercial areas and industrial establishments, involving almost 1000 analyses. The comparison showed that the calculated BOD loads were in close agreement with the survey data. The nine main tributaries covered by the monitoring program account for about 85 percent of the total BOD load discharged to the main river from the Greater Seoul area.

WATER QUALITY MODELING

The primary objective of modeling the Lower Han River was to provide a tool for water quality management purposes which would enable the relationships between waste loadings and resulting water quality to be evaluated. The QUAL-II modeling system was selected for use in simulating the Lower Han River. This computer code is the most advanced version of the series of models derived from the QUAL-I model developed by the Texas Water Development Board and F. D. Masch and Associates (Texas Water Development Board, 1970). It was updated by Water Resources Engineers (1977) for the U. S. Environmental Protection Agency. For this application the model was run on an IBM 4341 computer at Hyundai Construction Company, Seoul.

QUAL-II can simulate up to 13 water quality constituents in any combination desired by the user. The model is applicable to dendritic (branched) streams which are well-mixed. It assumes that the major transport mechanisms, advection and dispersion, are significant only along the main direction of flow (longitudinal axis of the stream or canal). It allows for multiple waste discharges, withdrawals, tributary flows, and incremental inflow. The basic theory and mechanics of QUAL-II are fully described in the Program Documentation Manual (Water Resources Engineers, 1977).

The Lower Han River model was designed to extend from Paldang Dam (km 79.3 above the Imjin River-Han River confluence) to Jeonryu (km 9.9). Waste loads for each of the major tributaries were modeled as a single large source entered at the location where tributary flow measurements and water quality samples were obtained. A computational element length of 500 meters was selected to give the high degree of resolution needed for the Lower Han River. A total of 59 reaches was used with the total number of computational elements in the system being 411. A total of 64 separate point sources and sinks was used in the model.

Hydraulic and geometric input data required by QUAL-II were derived from the application of the U.S. Army Corps of Engineers, Hydrologic Engineering Center, Water Surface Profiles (HEC-II) Model. The HEC-II model was operated at a number of different river flow rates in the range of 125 to 1500 cu m/s to define stage-discharge and velocity discharge relationships for both existing and future conditions.

Calibration and Verification

Before a water quality model can be used for simulation with confidence, calibration and verification of the model using measured responses of the receiving water body is necessary. Calibration represents estimation of model parameters using measured waste loadings, streamflows and water quality data. The term verification is used to describe the situation where a model calibrated at one set of source inputs and receiving water conditions successfully predicts observed water quality under a different set of waste load and receiving water conditions. In practice, the calibration and verification process is an interactive procedure with the model coefficients being adjusted until the best fit of all available receiving water quality data sets is obtained.

The water quality monitoring results from the six main river surveys were used for calibration and verification. The water quality data used to characterize the waste inputs and receiving water quality included BOD₅, dissolved oxygen, temperature, ammonia-nitrogen, nitrate/nitrite nitrogen, fecal coliforms and chlorides. Since algae were not significant in the Lower Han River because of the high level of pollution, these were not modeled.

Calibration of the Lower Han River model was initiated using the data from survey 4, performed from October 20 to 22, 1982. In the calibration procedure, both the receiving water quality and source data were evaluated and adjustments made to the appropriate coefficients within accepted ranges for each until the best fit was obtained.

The downstream reaches of the river are tidally-affected and below Jeonryu the river is best represented by an estuary model. Upstream of Jeonryu measurements of chloride concentration showed a steep concentration gradient, reflecting advective transport as the dominant transport mechanism. It was concluded that the internally calculated dispersion coefficients used by QUAL-II were sufficient to

represent the measured dispersion in the Lower Han River and to achieve satisfactory calibration.

At the beginning of calibration, the Langbien and Duram (1967) equation was used to calculate reaeration coefficients (K_2) in all reaches. It was found that this equation, and all others available in the model, did not adequately account for observed levels of atmospheric reaeration in many of the reaches. It was, therefore, necessary to estimate reaeration coefficients for these reaches to achieve observed dissolved oxygen concentrations. There are several reasons which can account for observed reaeration being higher in the Lower Han River than that predicted by the commonly-used equations: (1) in the tidal zone the average tidal velocity, which drives reaeration, is much higher than the net advective velocity used by QUAL-II; (2) a very large surface area-to-depth ratio is present throughout the river; and (3) numerous riffles and shallow flats in the non-tidal zone were not adequately represented in the hydraulic coefficients from HEC-II.

Although it is theoretically possible that in the upper reaches of the river photosynthesis is a contributor to net reaeration, diurnal dissolved oxygen studies conducted during the water quality data collection program did not show significant photosynthetic action. It was concluded that photosynthetic effects were relatively minor and were not believed to represent a major dissolved oxygen component in the Lower Han River under current loadings.

After a good calibration was obtained on the survey 4 data base, the model was then applied, using the derived coefficients, to the water quality data from Surveys 1, 2, 3, 5 and 6. Once the coefficients were adjusted to achieve a "best fit", the model was rerun using the final set of coefficients for all survey conditions. Acceptable calibration was demonstrated by statistically analyzing the relationship between predicted and observed concentrations for selected pollutants.

A linear regression between simulated (predicted) concentrations and observed concentrations for dissolved oxygen is shown in Figure 2. Also shown in Figure 2 is the 95 percent confidence interval on simulated dissolved oxygen concentration which can be interpreted to mean that the simulated dissolved oxygen concentrations for the calibration period were within the range of the observed concentrations for 95 percent of the measurements, an excellent degree of predictive ability given the expected natural variability in observed concentrations for this constituent. A probability analysis of the prediction error of the individual observed and predicted dissolved oxygen values showed that out of the 47 values, 57 percent had an error less than plus or minus 1.0 mg/l and 98 percent had an error less than plus or minus 2.0 mg/l.

BOD data were analyzed in a similar manner. A probability analysis of the prediction error of the individual observed and predicted BOD values showed that out of the 32 values, 63 percent had an error less than plus or minus 3.0 mg/l, indicating a good degree of BOD calibration.

The results of the analysis of calibration/verification of the Lower Han River model demonstrated that a very high degree of predictive capability was attained. The model was thus acceptable for analyzing a wide range of wastewater management alternatives to determine the water quality impacts associated with their implementation.

Sensitivity Analysis

Parameter sensitivity in a water quality model is defined as the response of an output variable such as dissolved oxygen or BOD to change in a single input

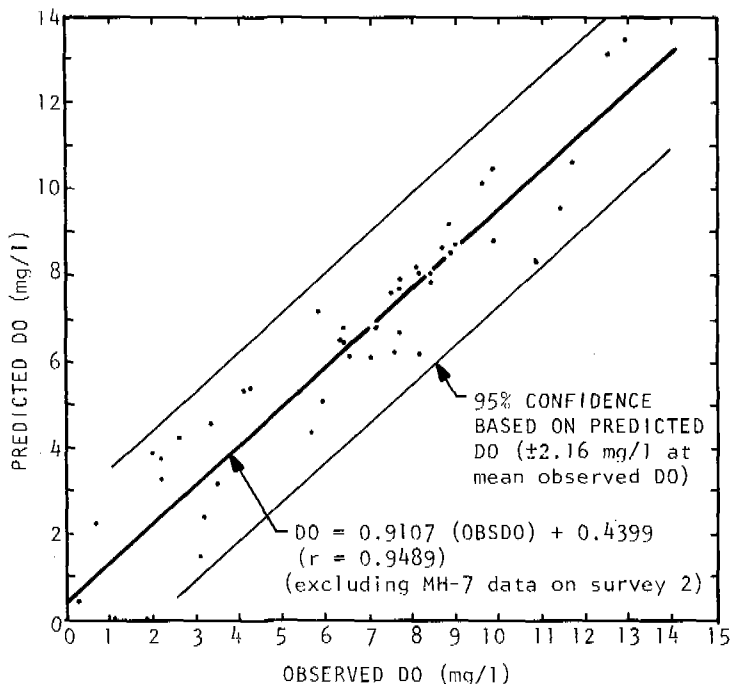


Fig. 2. Correlation between predicted and observed dissolved oxygen concentrations - all surveys

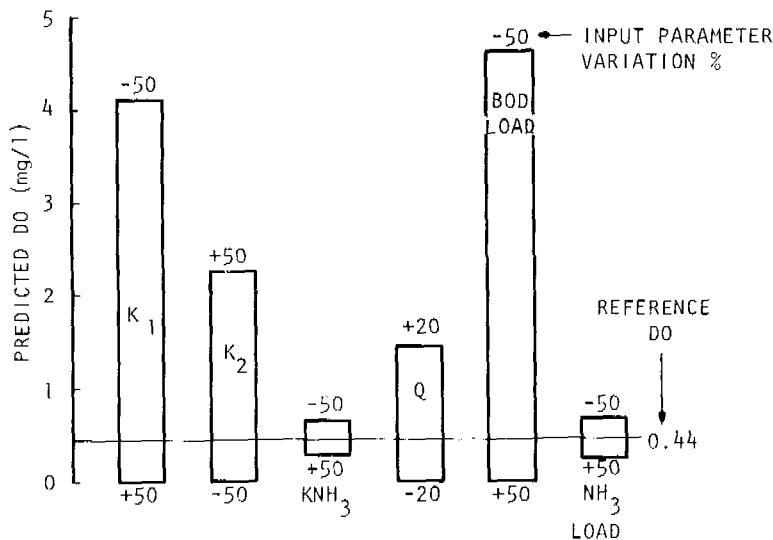
variable. The objective of such an analysis is to gain an understanding of model response to the major input variables and to provide a measure of the possible effect on simulated concentrations of a particular water quality constituent of uncertainty in the estimates of important input variables.

The sensitivity analysis was performed by varying one input parameter from the calibration value by a constant amount while holding all other input variables constant. In general, the variation selected was intended to represent the perceived uncertainty associated with that input parameter.

The sensitivity of simulated dissolved oxygen concentrations at each of the sampling stations on the Lower Han River was determined for the following input variables: (1) BOD removal coefficient; (2) reaeration rate coefficient; (3) ammonia removal coefficient; (4) flow from Paldang Reservoir; (5) BOD loading discharged to river; and (6) NH_3 loading discharged to river.

All input parameters except flow from Paldang Reservoir, which was varied plus or minus 20 percent, were varied by a range of plus or minus 50 percent. Typical results of these sensitivity analyses of simulated dissolved oxygen concentration are presented in Figure 3 for sample station MH-7.

A review of the sensitivity analysis results for dissolved oxygen concentrations showed the following. (1) Dissolved oxygen sensitivity to all associated input parameters increased in the downstream direction, as pollutant concentrations increased and in-stream dissolved oxygen concentrations decreased. (2) In general, simulated dissolved oxygen concentrations were sensitive to the input parameters in the following order from most sensitive to least: BOD loading, BOD



BASED ON SURVEY 5 DATA

K_1 = CARBONACEOUS BOD DECAY RATE (1/day)

K_2 = REAERATION RATE (1/day)

KNH_3 = NH_3 -N OXIDATION RATE (1/day)

Q = RIVER FLOW AT PALDANG (m^3/s)

BOD LOAD = BOD₅ LOAD DISCHARGED TO RIVER

NH_3 LOAD = NH_3 -N LOAD DISCHARGED TO RIVER

Fig. 3. DO sensitivity at MH-7 (Haengju)

removal coefficient, reaeration rate, river flow, ammonia load and ammonia removal coefficient. The only exceptions were at MH-8, Jeonryu, where the dissolved oxygen concentration was slightly more sensitive to reaeration rate than to BOD removal rate and at MH-1 and MH-2 where reaeration rate was the most significant parameter. (3) The relatively low sensitivity of dissolved oxygen to ammonia concentrations at all river stations indicated that nitrification was not an important oxygen sink under current conditions.

The results of the dissolved oxygen sensitivity analysis, in addition to providing a perspective on the possible uncertainty of model results as a function of input uncertainty, provided a basis for estimating how changes in these parameters due to external influences could change dissolved oxygen concentrations in the river. For example, changes in river channel configuration which tend to reduce the reaeration coefficient would have a potentially major impact on dissolved oxygen concentration in all reaches.

Similar sensitivity analyses were performed on simulated BOD, ammonia and fecal coliform concentrations. The results of these analyses showed that the sensitivity of instream concentrations of each pollutant was primarily a result of the loadings for the respective pollutant, as expected. The sensitivity of fecal coliform concentration to coliform die-off rate was very high, and in fact, was more important than coliform loading in determining in-stream concentration.

WATER QUALITY SIMULATION

The use of the calibrated/verified QUAL-II model to simulate the water quality impacts of alternative wastewater management plans and physical changes in the Lower Han River channel was the primary objective of the modeling activity. Approximately 100 separate simulations were made to evaluate different combinations of treatment and channel changes.

The primary water quality objective to be met for the Lower Han River is to prevent the occurrence of anaerobiosis (zero dissolved oxygen) in any section of the river downstream of Paldang. To assure that this objective is met at all times, a dissolved oxygen target concentration of a minimum of 2.0 mg/l in all river segments was used to evaluate treatment and disposal alternatives.

Land constraints and topographic considerations effectively reduced the possible number of sewage treatment plant locations to five. In terms of water quality impact analysis the possible treatment alternatives were reduced to two, namely to convey all wastes to two downstream plants at Nanjido and Kimpo (or Kimpo and Gulpo), or to treat the wastes from the eastern areas at Jungrang (site of the existing plant) and Tan.

Changes in river regime could also have an impact on water quality. A project is now underway to provide a more uniform channel cross section between river km 27.1 and km 62.2. The modified channel sections will, in general, be wider and deeper than the existing channel. These changes will reduce the mean velocities in the river sections affected, increase travel time and reduce the atmospheric reaeration coefficients which are directly proportional to velocity and inversely related to depth. The decreased velocities will also increase the BOD removal by sedimentation and possibly increase the sediment oxygen demand.

A project has also been proposed to construct two low dams; one at Jamsil (55.5 km) and one between Changneung and Gulpo tributaries at 28.5 km ("Seoul Dam"). These dams would cause the same types of effects on stream hydraulics and reaeration as described for the channel modifications, only to a much greater extent. The construction of the dams would also increase the potential for growth of algae and consequent water quality effects associated with nutrient enrichment. This phenomenon would be more likely to be significant after the implementation of planned waste treatment plants, since the current waste loadings would result in a very low dissolved oxygen concentration behind the dams which would not be conducive to the growth of most algae.

A major effect of the Seoul Dam would be the elimination of tidal dispersion effects on upstream reaches at low stream flows, since at stream flows below approximately 300 cu m/s there would be a free flow over the Seoul Dam under most tidal conditions. As a result, wastewaters discharged downstream of the Seoul Dam would not affect dissolved oxygen concentrations in the upstream reaches, which they do under current conditions due to tidal mixing and dispersion. A negative aspect of this effect, however, is that the tidal flushing and mixing which currently affects the tidally-influenced reaches upstream of Seoul Dam and reduces pollutant concentrations would also be eliminated.

Since the reaeration coefficients would change when the hydraulic modifications were completed, it was necessary to modify the values used for model calibration/verification. A review of the HEC-II model output for the modified channel reaches indicated that the new velocity and depth expected under low flow conditions were best represented by the O'Connor and Dobbins (1958) equation for reaeration coefficients. This reaeration coefficient equation was used in reaches

subject to hydraulic modification, the reaeration coefficients were adjusted in proportion to the observed changes in net velocity. For those reaches unaffected by the hydraulic modifications the calibration phase reaeration coefficients were used.

The BOD removal rate due to sedimentation, k_3 , was adjusted in those reaches affected by hydraulic modification and which received the highest suspended solids loadings. The adjustment to k_3 was proportional to the reduction in velocity caused by the channel modification. This was only done for simulations using waste loads from sources without primary or higher level treatment.

The simulations represented the critical conditions in terms of water quality, as substantiated by the water quality monitoring surveys. In addition, they also represented the conditions observed during the time of the year most suitable for water-based recreation.

Flows in the tributaries were estimated by taking the differences between measured dry weather flows and calculated wastewater contributions. Water quality in those tributaries from which wastewater would be diverted to the treatment plants (Tan, Jungrang, Anyang, Banpo, Ug, Hongje and Gulpo) was based on survey data and the assumption that some sewage discharges would continue even after implementation of the treatment plants. The waste loads in Wansug and Changneung tributaries represented projected loadings and no treatment since they were not included in the regional treatment alternatives.

All simulations were conducted for all water quality constituents incorporated in the calibrated model, that is BOD, dissolved oxygen, ammonia, nitrate and fecal coliforms. Comparison of wastewater management alternatives, however, was done using only the simulated dissolved oxygen concentration. In the Lower Han River, the water quality data clearly showed dissolved oxygen to be the most critical water quality parameter, in terms of current future water uses, and it was also highly correlated, as expected, to other water quality constituents such as fecal coliforms and ammonia nitrogen.

The treatment simulations considered preliminary, primary, secondary and tertiary levels of treatment and were carried out for projected 1991 and 2001 waste loads. Simulations were also performed for future loads assuming no change in the existing sewerage and treatment facilities. Nightsoil facilities were assumed to be replaced by flush toilets and sewers by the year 2001.

The simulations for no change in existing waste collection and disposal practices showed that under summer low flow conditions the dissolved oxygen level under 1991 loads would be below 1.0 mg/l from river km 42 to km 16. By 2001 the level would be below 1.0 mg/l downstream from river km 46 and zero from river km 43 (Indogyo) to Jeonryu, the model boundary. These simulations clearly demonstrated that, if growth in the Seoul area continued as projected and no additional treatment was to be provided, adverse water quality would result and these conditions would be obvious within the city itself, from the confluence with Jungrang tributary downstream.

The effect of different degrees of treatment on dissolved oxygen levels in the main river under 2001 loading conditions are shown in Figure 4 for the two basic alternatives of treatment of all wastes downstream at Nanjido and Kimpo and treatment in four plants at Nanjido, Kimpo, Jungrang and Tan. The simulations showed that regardless of the effluent discharge locations, secondary treatment would be necessary to achieve the target dissolved oxygen level of 2.0 mg/l throughout the whole river reach.

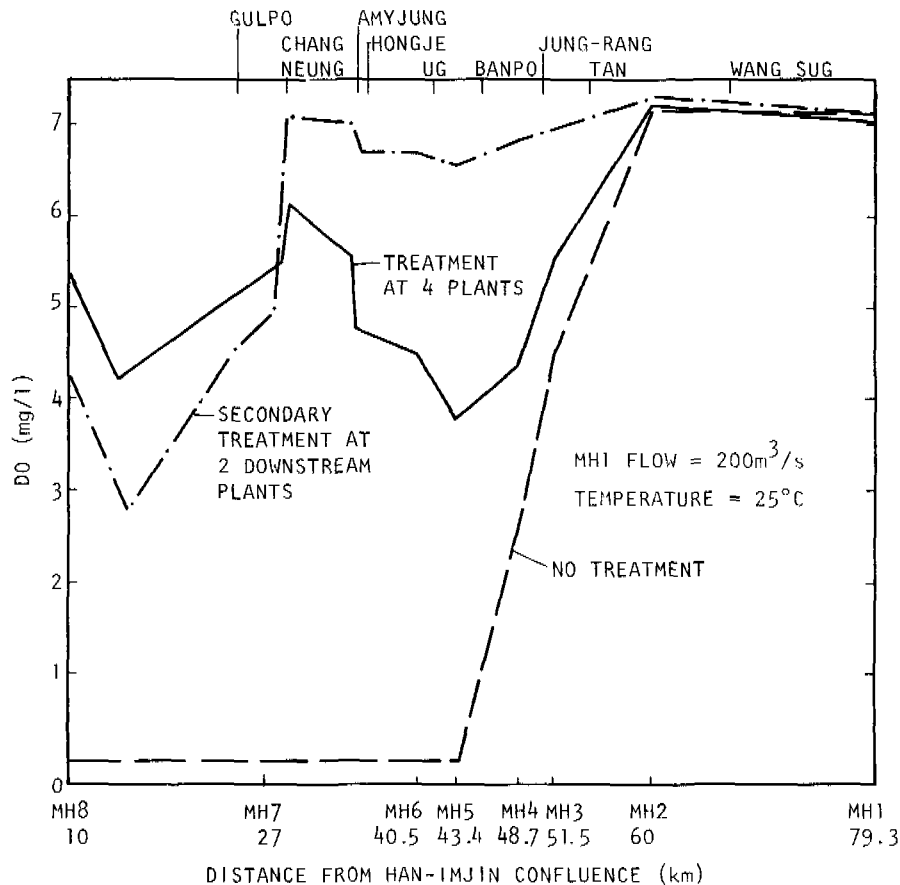


Fig. 4. DO simulation for year 2001 conditions

The predicted concentrations of dissolved oxygen, BOD, ammonia nitrogen, and fecal coliforms at selected river sampling stations from MH-1 to MH-7 under 2001 loading conditions for all treatment alternatives are presented in Table 1. The correspondence between low dissolved oxygen concentrations and high concentrations for other key water quality constituents is evident from these data, demonstrating that dissolved oxygen is a good surrogate parameter for overall water quality conditions. The highest predicted concentrations of BOD, ammonia, and fecal coliforms occurred at Haengju (MH-7) with the alternative of two downstream plants. This is a direct result of concentrating all treated discharges at essentially one location on the river. The predicted ammonia concentration of 2.05 mg/l could be toxic to sensitive species of fish at low flow, high temperature and high pH conditions. At all other locations water quality was generally acceptable for tolerant fish species.

For all stations upstream of MH-7 the simulation showed significantly better water quality with the two-plant alternative. The fecal coliform numbers would meet the recommended criterion for contact recreation of 1000 organisms/100 ml all of the way from Paldang Dam to Seonyu (MH-6), a distance of 39 km. The four plant alternatives would provide water quality acceptable for contact recreation only from Paldang to Dugdo (MH-3), a distance of 28 km. The dissolved oxygen level would

TABLE 1 Water Quality Impacts of Alternatives 1 and 2
(Under 2001 Loads)

| Parameter | Water Quality Constituent Concentrations at Designated Locations for Each Alternative | | | | | | | |
|------------------------------|---|------|------------|------|--------------|------|--------------|------|
| | Paldang MH-1 | | Dugdo MH-3 | | Indogyo MH-5 | | Haeneju MH-7 | |
| | 1 | 2 | 1 | 2 | 1 | 2 | 1 | 2 |
| DO (mg/l) | 7.08 | 7.08 | 5.61 | 6.91 | 3.83 | 6.50 | 5.28 | 4.85 |
| BOD ₅ (mg/l) | 1.30 | 1.30 | 2.44 | 1.48 | 1.70 | 0.79 | 2.38 | 4.39 |
| NH ₃ -N (mg/l) | 0.18 | 0.18 | 0.38 | 0.08 | 0.60 | 0.10 | 1.55 | 2.50 |
| Fecal Coliforms (no./100 ml) | 1.09 | 1.09 | 7.49 | 1.04 | 2.08 | 1.38 | 1.03 | 2.01 |
| | E3 | E3 | E2 | E1 | E3 | E2 | E4 | E4 |

Alternative 1 is treatment at Jungrang, Tan, Nanjido and Kimpo (\pm Gulpo)

Alternative 2 is treatment at Manjido and Kimpo (\pm Gulpo)

be less than 6.0 mg/l over a length of 17 km for the two-plant alternative, compared to 45 km with four plants.

The effect of construction of Seoul Dam was also simulated. The dam would have the most adverse impact on dissolved oxygen concentrations with the adoption of four treatment plants because of the discharge of effluent to the pool behind the dam. Even with the tertiary treatment at the two upstream plants the target dissolved oxygen level of 2.0 mg/l would probably not be achieved. If the dam is constructed, special operating conditions such as the ability to flush the river at low flows will be necessary.

Simulations were also conducted to determine the sensitivity of the dissolved oxygen and BOD concentrations resulting from implementation of the four plant alternatives (the selected regional plan) to changes in the projected 2001 BOD loadings. A plus or minus 20 percent BOD loading for each of the four discharge points was compared to base case year 2001 loads under low flow, high temperature conditions in the Lower Han River. As shown by the concentration distributions for dissolved oxygen and BOD, the receiving water quality was quite insensitive to increases and decreases in loading at the four (or five) treatment plants. It could be concluded from this analysis that the water quality impacts of the selected plan were very insensitive to uncertainty in the BOD load; in fact, the estimates could be incorrect by as much as 100 percent and the minimum dissolved oxygen target of 2.0 mg/l would still not be jeopardized.

CONCLUSIONS

The adaption of the QUAL-II and HEC-II models to the Lower Han River provided a reliable tool to assist in the evaluation of water pollution control strategies for the Greater Seoul urban area. An excellent degree of reliability was achieved based on calibration against six major water quality monitoring surveys, and the sensitivity analyses showed that the simulation predictions were entirely acceptable within the expected range of accuracy of such input parameters as BOD loads, river flows and reaeration coefficients.

The model was used extensively to evaluate the cost-effectiveness of various treatment plant options and enabled estimates to be made of improved water quality benefits such as enhanced water-based recreation opportunities and reductions in health risks resulting from an improved quality of potable water intakes.

ACKNOWLEDGEMENTS

The modeling work described in the paper was carried out during the period 1982 to 1983 as part of the Han River Basin Environmental Master Plan project, a joint Korean Government-Asian Development Bank-funded project carried out by Engineering-Science, Inc. in association with Hyundai Engineering Co. Ltd. for the Office of Environment of the Republic of Korea. Dr. Tischler and Dr. Bradley were associated with the project as Water Quality Consultant and Water Quality Division Manager, respectively. Mr. Park was responsible for the implementation of the water quality surveys and modeling tasks.

The authors gratefully acknowledge the agreement of the Office of Environment to the publication of the results of the modeling.

REFERENCES

- Kramer, R. H. (1970). A search of the literature for data pertaining to bioenergetics and population dynamics of freshwater fishes, Desert Biome Aquatic Program, Utah State University.
- Langbien, W. B. and Duram, W. H. (1967). The aeration capacity of streams. U. S. Geol. Survey Circ., 542.
- O'Connor, D. J. and Dobbins, E. W. (1958). Mechanism of reaeration in natural streams. Trans. Amer. Soc. Civ. Engrs., 123.
- Texas Water Development Board (1970). Simulation of water quality in streams and canals. Program Documentation and User's Manual.
- Water Resource Engineers (1977). Computer program documentation for stream quality model (QUAL-II), U. S. Environmental Protection Agency Center for Water Quality Modeling, Athens, GA.

DISPERSION IN ESTUARIES

A ROLE FOR A SIMPLE DISCRETE-TIME MODEL TO DESCRIBE DISPERSION IN AN ESTUARY

T. Wood

*Department of Chemical Engineering, The University of Sydney,
NSW 2006, Australia*

ABSTRACT

A simple discrete-time model is proposed to describe dispersion in an estuary, based on tidal exchanges between neighbouring segments. A procedure for parameter estimation and model validation is described which can be implemented with a minimum of field measurements; and the application of the model is demonstrated with data collected from the Hawkesbury River system, near Sydney. The results indicate that the modelling procedure described is capable of producing useful predictions of the response of salinity distribution to changes in fresh water input and tidal amplitude. The method could be most useful in circumstances where limitations on experimental resources preclude the undertaking of a more detailed investigation.

KEYWORDS

Diffusion-advection models; dispersion; exchange coefficients; mixing; models; tidal prism.

INTRODUCTION

This paper describes work resulting from the author's continued interest in the application of simple models to describe dispersion in an estuary. The case for their use has been put forward in two previous papers (Wood, 1978, 1980), and so only a brief resumé of the arguments is presented here. The author's view is that the remarkably simple concepts developed by Ketchum (1951a, 1951b, 1955) to describe salinity dispersion in terms of tidal prism exchanges between neighbouring segments of an estuary were prematurely abandoned before their potential had been fully explored. A major factor was the advent of the high-speed computer in the middle 1950's which opened up the possibility of using the space-time continuum equations of momentum, energy and mass transport. The serious limitation of spatially-averaged properties within a segment was an evident problem, so that the intrinsic advantages of the more precise description of the continuum-based model seemed obvious enough. Over the next two decades, this was (and still is) the dominant approach.

Approaches to Modelling

The approach adopted to modelling must clearly be identified with the purpose of the study, and it is not the intention in this paper to argue that a simple approach is always to be preferred to a more complex one. Estuarine hydrodynamics is in itself extraordinarily complex, as Officer(1980) points out in a recent review; so that if the objective of the study is a detailed understanding of the physical mechanisms of circulation, mixing, and dispersion, then clearly a continuum-based analysis is called for, as evidenced by many notable advances in these areas. When chemical, biological or geological factors must also be considered, though, the problem is often further compounded by a relatively incomplete description of their associated physics-chemical mechanisms. The coupled description of hydrodynamics and these other aspects presents something of a modelling dilemma which is still unresolved: it centres around a trade-off between the accuracy of the model description, and subsequent problems encountered in mathematical solution and validation. Suffice it to say here that the principal reasons for pursuing the simpler approach are to minimize the considerable effort involved in continuum model computation, and to explore the use of model identification and validation techniques which the simpler models would appear to permit.

Objectives of the Study

The study originated in the following problem: given the minimal information listed below, is it possible to devise a simple model which is capable of providing a useful description of the response of the high and low tide salinity distributions in an estuary to changes in fresh water inputs and tidal conditions?

- (a) A limited sequence of high and low tide salinity measurements at a few specified locations in the estuary.
- (b) Tidal information.
- (c) Fresh water information as a cumulative input from all monitored sources over 24 hour periods of time.

The rather stringent limitation on available information was chosen deliberately to be the absolute minimum that would be required in order to make any progress at all. In practical terms this could have important consequences: there may often not be sufficient resources of manpower, equipment or money to mount an extensive data collection exercise that a sophisticated modelling study might require, and in these circumstances a more limited study based on minimal information might still yield worthwhile results.

The basis of the proposed model is first described, and the relevant equations are deduced. Then the method of state and parameter estimation using the measured data is explained; and finally the model is evaluated using data collected on the Hawkesbury River system, which is an important estuary near the city of Sydney.

THE PROPOSED MODEL

The estuary is divided into five segments as shown in Fig. 1. The geometry of each segment is characterized by surface area, and a datum depth from which tidal heights are measured; a tidal attenuation factor allows for variations in tidal amplitude along the estuary. Transport of salinity occurs through the mechanism of exchanges between neighbouring segments during the tidal cycle, and the overall effect can be interpreted as a combined process of fresh-water advection and tidal dispersion as explained in an earlier paper (Wood, 1978).

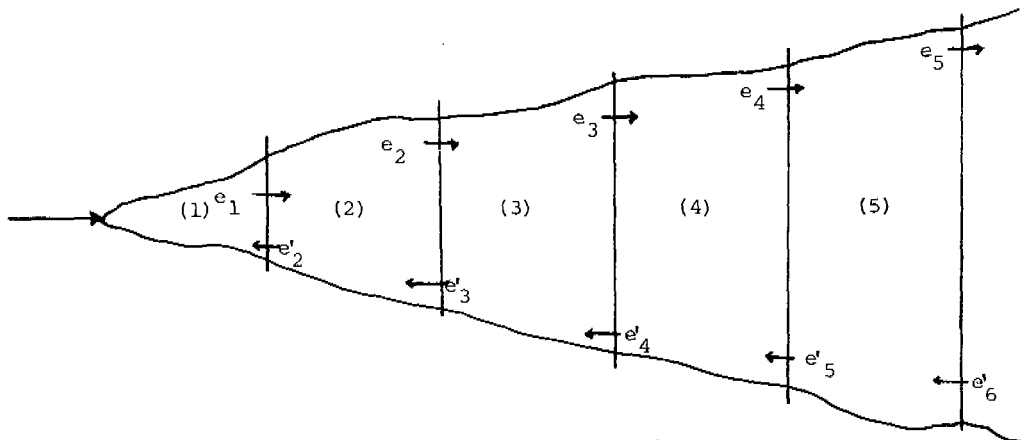


Fig. 1 Five-Segment Estuary Model Showing Exchanges Between Segments

Derivation of Model Equations

Ebb flow exchanges.

$$e_i = e_{i-1} + a_i \lambda_i (T_2 - T_1) \quad (1)$$

Flood flow exchanges.

$$e'_2 = -e'_0 + a_1 \lambda_1 (T_2 - T_1) \quad (2a)$$

$$e'_i = e'_{i-1} + a_{i-1} \lambda_{i-1} (T_2 - T_1) \quad (i = 3 \text{ to } 6) \quad (2b)$$

Low tide segment volumes.

$$L_i = a_i (d_i + \lambda_i T_1) \quad (i = 1 \text{ to } 5) \quad (3)$$

High tide segment volumes.

$$H_i = a_i (d_i + \lambda_i T_2) \quad (i = 1 \text{ to } 5) \quad (4)$$

Salinity changes (high tide to low tide).

$$s'_1 = s_i - c_i (s_i - s_{i-1}) \quad (i = 1 \text{ to } 5) \quad (5a)$$

$$\text{where: } c_i = e_{i-1} / L_i \quad (5b)$$

Salinity changes (low tide to high tide).

$$s_1 = s'_1 + c'_1 (s'_2 - s'_1) - c'_0 - s'_1 \quad (6a)$$

$$s_i = s'_i + c'_i (s'_{i+1} - s'_i) \quad (6b)$$

$$\text{where: } c'_0 = e'_0 / H_1 ; c'_2 = e'_{i+1} / H_i \quad (i = 1 \text{ to } 5) \quad (6c)$$

PARAMETER ESTIMATION

Problem Statement

The problem consists in finding the 'best' set of unknown parameters from the available set of field measurements. The measured variables, unknown variables, and the unknown parameters are listed below.

Measured variables: High tide and low tide salinities in segments 2, 3 and 4; high and low tide heights; cumulative fresh water input over 24 hr intervals.

Unknown variables: High and low tide salinities in segments 1 and 5.

Unknown parameters: Areas; base depths; tidal attenuation factors; for each segment.

The measured variables themselves are subject to errors of measurement, and in the case of the fresh water input the error is expected to be considerable. It is therefore necessary to use established non-linear state/parameter estimation theory (Extended Kalman Filter) to solve the stated problem. It is not appropriate here to describe the state/parameter estimation procedure in detail, but a previous paper contains an account of the relevant background material and references (Wood, 1980).

The Augmented State Vector

An augmented vector is produced by combining salinities, geometrical parameters, and fresh water input. In effect, each factor influencing the behaviour of the simulated estuary is treated as a 'state'; and filtered state estimates are then produced for each element of the augmented vector from noise-corrupted measurements of four of the states (salinities in segments 2, 3, 4; fresh water input), taken sequentially at high and low tide marks. To simplify the dimensionality of the vector, the terms involving $a_i \lambda_i$ and d_i / λ_i are treated as single 'attenuated' variables, as an examination of equations (3) and (4) show. In addition the attenuated area and datum depth parameters for segments 1 and 5 are set at known values, for reasons which are explained in the section describing the Hawkesbury River case study. By this means, the dimension of the augmented vector \underline{x} is reduced to (12x1), made up of the segment salinities (5x1); the attenuated areas for segments 2, 3, 4 (3x1); the modified datum depths for segments 2, 3, 4 (3x1); and the fresh water input (1x1).

Mathematical Statement of the Problem

Model equation: $\underline{x}(k) = f(\underline{x}(k-1)) + \underline{w}(k-1)$ (7)

Measurement equation: $\underline{z}(k) = G\underline{x}(k) + \underline{v}(k)$ (8)

The first five elements of the augmented vector \underline{x} , describing salinity in the segmented estuary, are modelled by equations (1) to (6), where the symbols ($x_1, x_2, \dots, x_{11}, x_{12}$) are substituted in place of salinities, parameters and fresh water input, as described above. The area and depth parameters, assumed constant are modelled by -

$$x_i(k) = x_i(k-1) \quad (i = 6 \text{ to } 11) \quad (9)$$

The final element, x_{12} , representing fresh water input is modelled by -

$$x_{12}(k) = x_{12}(k-1) + w_{12}(k-1) \quad (10)$$

The four elements of the measurement vector \underline{z} are the salinity observations on segments 2, 3, 4; and the fresh water input.

The vectors w and v are the noise components associated with the modelling and measurement processes, respectively; the statistical properties are specified, as required, in the next section.

HAWKESBURY RIVER CASE STUDY

The Region

The Hawkesbury-Nepean basin occupies an area of about 2.1 million hectares to the northwest and southwest of Sydney. A considerable variation exists in topography, vegetation, climate; and in the levels of industrial and urban development. The tributary watersheds to the north and west are largely undeveloped, rugged and forested, while flatter terrain to the west and southwest of Sydney, which used to be pastoral and agricultural, now accommodates the greater proportion of the population of the basin - about 500,000 people. Much of the available land for expansion of the Sydney urban area lies within the Hawkesbury-Nepean basin, and the region also is a major recreational resource for the existing population of Sydney. So great are the potential environmental stresses on the region that it has been the subject of detailed studies by two New South Wales Government Authorities: the Department of Environment (1973) and the State Pollution Control Commission (1977, 1983).

The Hawkesbury River is the tidal section of system which extends from Broken Bay to the confluence of the Nepean and Grose Rivers - Some 140 km in length. The Nepean River system includes the mainstream and tributaries above the Grose River confluence. Large variations occur in fresh water flow in the Nepean system, and in significant tributaries entering the tidal region (the Colo and MacDonald Rivers); they can range from extreme flood to extreme drought conditions over relatively short periods of time. Irrigation requirements during summer months greatly reduce the fresh water flow, and dry weather flows are sometimes augmented by releases from upstream dams, from groundwater sources, and from sewage treatment works effluents. Because of its importance, the Hawkesbury River system was chosen for this study. A schematic diagram of the relevant features is shown in Fig. 2.

Data Used in the Study

Table 1 summarizes the data used in the study. The time index k is chosen to coincide with high tide (k even) and low tide (k odd). Tidal heights were taken from published charts for Fort Denison in Sydney Harbour. The salinity values were obtained from a sequence of observations obtained at the locations shown in Fig. 2, using a sampling frequency of 40 min over a period of 14 days; from these records the high tide and low tide salinity values were taken. The fresh water information was available as cumulative volumes over 24 hour periods for the major tributaries: the Nepean, Grose, Colo and MacDonald Rivers. These readings were combined and the proportional volume inputs, corresponding to the high and low tide marks, were calculated. The data sequence was chosen to cover an approximately two-fold variation in tidal range and a four-fold variation in fresh water flow.

TABLE 1 Hawkesbury River Study Data

| k | Tide | Salinity (2) | Salinity (3) | Salinity (4) | Fresh Water |
|----|------|--------------|--------------|--------------|-------------|
| 0 | 1.40 | 3.8 | 14.9 | 24.2 | 1.31 |
| 1 | 0.54 | 0.5 | 10.0 | 18.5 | 1.40 |
| 2 | 1.30 | 4.0 | 15.1 | 24.6 | 1.29 |
| 3 | 0.45 | 0.5 | 10.1 | 18.0 | 1.31 |
| 4 | 1.49 | 5.0 | 15.8 | 25.0 | 0.71 |
| 5 | 0.48 | 0.7 | 11.5 | 18.5 | 0.76 |
| 6 | 1.25 | 4.3 | 15.1 | 24.1 | 0.66 |
| 7 | 0.47 | 0.7 | 11.7 | 19.6 | 0.76 |
| 8 | 1.63 | 6.0 | 16.9 | 25.6 | 0.41 |
| 9 | 0.54 | 1.5 | 11.6 | 19.4 | 0.35 |
| 10 | 1.34 | 5.1 | 15.2 | 24.3 | 0.35 |
| 11 | 0.42 | 1.4 | 11.9 | 10/2 | 0.40 |
| 12 | 1.69 | 7.0 | 16.9 | 25/9 | 0.38 |
| 13 | 0.39 | 1.6 | 9.4 | 19.2 | 0.33 |
| 14 | 1.28 | 5.0 | 15.1 | 23.9 | 0.32 |
| 15 | 0.38 | 1.5 | 8.9 | 18.4 | 0.36 |
| 16 | 1.78 | 7.4 | 15.8 | 26.1 | 0.36 |
| 17 | 0.27 | 1.9 | 9.1 | 19.6 | 0.31 |
| 18 | 1.39 | 6.2 | 15.2 | 24.3 | 0.32 |
| 19 | 0.37 | 1.7 | 8.9 | 19.1 | 0.33 |
| 20 | 1.89 | 7.9 | 16.9 | 27.3 | 0.36 |
| 21 | 0.18 | 1.8 | 8.4 | 19.7 | 0.30 |
| 22 | 1.49 | 6.5 | 15.3 | 25.1 | 0.30 |
| 23 | 0.28 | 1.5 | 9.0 | 19.8 | 0.32 |
| 24 | 1.95 | 8.1 | 17.0 | 27.2 | 1.32 |
| 25 | 0.10 | 1.5 | 8.4 | 20.4 | 1.21 |
| 26 | 1.53 | 6.4 | 15.4 | 25.7 | 1.09 |
| 27 | 0.27 | 1.6 | 8.5 | 20.4 | 1.27 |
| 28 | 2.05 | 7.7 | 18.9 | 27.8 | 0.71 |
| 29 | 0.10 | 1.2 | 8.7 | 20.5 | 0.67 |
| 30 | 1.67 | 5.9 | 15.7 | 26.3 | 0.64 |
| 31 | 0.30 | 1.0 | 8.4 | 20.5 | 0.68 |

Column 1: Time index: high tide, low tide sequence

Column 2: Tidal height (metres)

Columns 3, 4, 5: Salinity in segments 2, 3, 4 (parts per thousand)

Column 6: Fresh water input during interval k to k+1 ($m^3 \times 10^{-6}$)

Data Analysis

The data listed in Table 1 were used in conjunction with the Extended Kalman Filter to produce filtered estimates of the salinities in the five segments, the area and depth parameters for each segment, and the fresh water inputs. The Extended Kalman Filter produced two estimates of the elements of the augmented (12 x 1) vector: the first is an estimate for time k based on all measurements collected up to and including time k - 1 (pre-estimate), and the second is an estimate for time k based on all measurements received up to and including time k (post-estimate). The first of these estimates can be regarded as a test of the predictive power of the model. In this study the sum of the squares of the

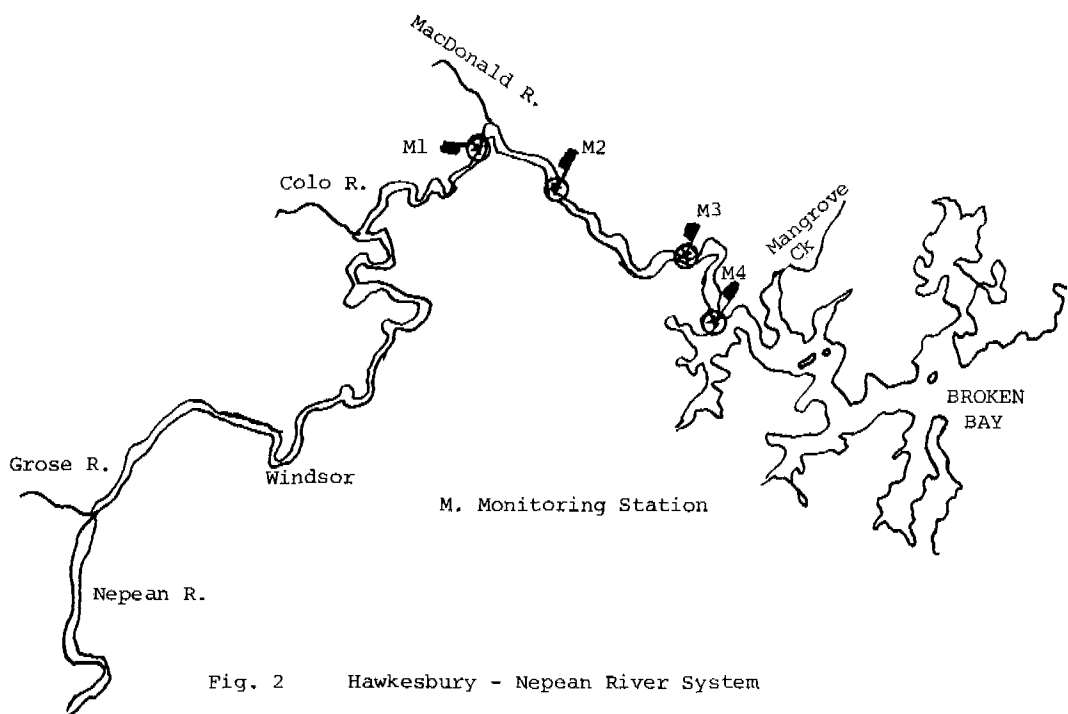


Fig. 2 Hawkesbury - Nepean River System

residual difference between the measured salinity and the first estimate of salinity, in segments 2, 3 and 4, is used as an indicator of the model's predictive capability. The sum of squares had a mean value of 4.53 for the total sequence of 31 sampling instants, indicating that on average the predictions given by the model are reliable to ± 1.2 ppt. Table 2 shows examples for a typical range of model performance.

TABLE 2 Examples of Model Predictions

| Sampling Instant k | Predicted Salinity | | | Measured Salinity | | | Sum Squares of Residuals |
|--------------------|--------------------|---------|---------|-------------------|---------|---------|--------------------------|
| | seg (2) | seg (3) | seg (4) | seg (2) | seg (3) | seg (4) | |
| 2 | 3.8 | 13.1 | 23.7 | 4.0 | 15.1 | 24.6 | 4.64 |
| 7 | 2.2 | 10.8 | 19.9 | 0.7 | 11.7 | 19.6 | 3.27 |
| 12 | 7.2 | 15.8 | 27.2 | 7.0 | 16.9 | 25.8 | 3.39 |
| 17 | 0.1 | 9.0 | 18.2 | 1.9 | 9.1 | 19.6 | 6.02 |
| 22 | 6.2 | 16.6 | 26.8 | 6.5 | 15.3 | 25.1 | 4.98 |
| 27 | 2.5 | 10.6 | 21.2 | 1.6 | 8.5 | 20.4 | 5.82 |

The post-estimates for the geometric parameters (area, depth) for segments 2, 3 and 4 are listed in Table 3, together with the assumed values for segments 1 and 5.

TABLE 3 Geometrical Parameter Estimates

| Segment | 'Attenuated' Area (m^2) | 'Attenuated' Depth (m) |
|---------|-----------------------------|------------------------|
| 1 | 9.52×10^6 | 7.40 |
| 2 | 3.64×10^6 | 5.77 |
| 3 | 4.46×10^6 | 6.75 |
| 4 | 7.06×10^6 | 6.53 |
| 5 | 32.90×10^6 | 8.71 |

The post estimates for the fresh water flow inputs are shown in Fig. 3.

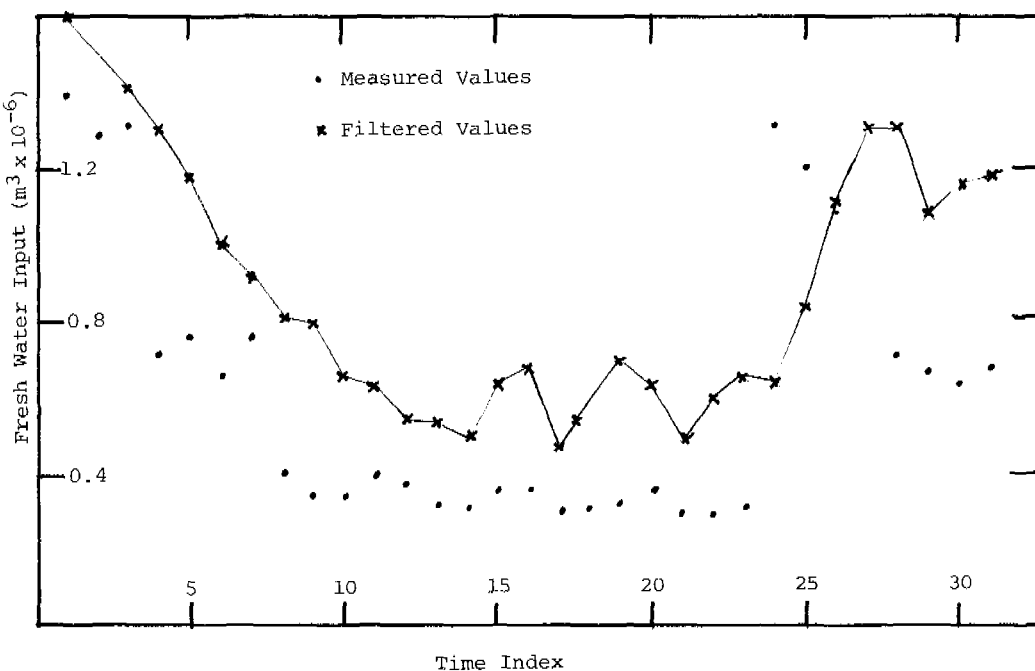


Fig. 3 Measured Values and Filtered Values of Fresh Water Input
Salinity Predictions

The simple five-segment model of an estuary proposed to describe the salinity response to changes in fresh-water input and tidal height, has been shown to be capable of providing estimates to within an average of ± 1.2 ppt of the measured values at 3 locations. The extra segments (1) and (5) were added to account for the large volumes of water known to exist between the tidal head and segment (2) and between segment (4) and the ocean. The geometrical parameters for these segments were chosen to give realistic values of the high and low tide salinity values. In both segments the salinity values are known to lie close to the extreme values of 0 ppt (fresh water) and 35 ppt (sea water) and the range between low and high tide readings is known to be small. Although the choice was of necessity arbitrary, the values are consistent with available hydrographic data

(which unfortunately is rather out of date and consequently of unknown accuracy).

Bearing in mind the limited amount of information on which the modelling is based, the outcome of the exercise is encouraging, and would appear to justify further work along these lines. The original plan was to have salinity monitored in segments (1), (2), (3), (4); but an equipment mal-function, which was not discovered until the data was read-back at the end of the field work, prevented the use of this valuable extra information in segment (1).

The parameter estimates for area and depth, although consistent with the available hydrographic information, cannot be claimed to be 'optimal' in any strict sense of this term. This is partly due to limitations inherent in the Extended Kalman Filter and partly due to the limited accuracy of field measurements. In particular, it is very apparent that the fresh water input values are highly irregular. This is demonstrated in Fig. 3 where the filtered estimates are, for the most part, significantly greater than the measured values. The discrepancy could be due to significant inputs from sources other than the ones mentioned or to inaccuracies in monitored flows, or to both. This aspect is being examined further since it clearly affects the predictive capability of the model.

Potential Uses of the Model

The main purpose of this exercise was to examine whether it was feasible to devise a simple model of an estuary from limited information which would be capable of making useful predictions on the response of salinity to changes in fresh water input and tidal height. The purpose was not to argue against more elaborate modelling approaches, since the circumstances inherent in any given study must dictate which approach must be taken. From this study it seems that a simple model can be devised from limited information. The role for such a model would exist where there are constraints in available resources - manpower, equipment, time.

The information to be gained from a simple model must of necessity also be limited. Three potential applications appear to be possible:-

- (i) To assess exchanges of water between regions of an estuary for pollutant distribution studies.
- (ii) To estimate unknown fresh water inputs to an estuary.
- (iii) To set up monitoring schemes for an estuary.

NOMENCLATURE

| | |
|--------|---|
| a_i | area of segment (i) (m^2) |
| d_i | datum depth of segment (i) (m) |
| e_i | ebb exchange volume from segment (i) to (i+1) (m^3) |
| e'_i | flood exchange volume from segment (i) to (i+1) (m^3) |
| f | non linear vector function |
| G | measurement matrix |
| H | high hole volume (m^3) |
| k | time index |
| L | low tide volume (m^3) |
| s_i | high tide salinity (ppt) |

| | |
|-----------------|-------------------------|
| s'_i | low-tide salinity (ppt) |
| T_1 | low-tide (m) |
| T_2 | high tide (m) |
| v_w | noise parameters |
| \underline{x} | augmented vector |
| \underline{z} | measurement vector |
| λ_i | tidal attenuation |

REFERENCES

- Ketchum, B.H. (1951a). Journal of Marine Research, 10, 18-38
- Ketchum, B.H. (1951b). Sewage and Industrial Wastes, 23, 198-290
- Ketchum, B.H. (1955). Sewage and Industrial Wastes, 27, 1288-1296
- New South Wales Dept. of Environment (1973). The Hawkesbury River Valley Environmental Study Background Report. NSW, Australia
- New South Wales State Pollution Control Commission (1977). The Quality of Sydney's Waterways in Relation to its Growth. NSW, Australia
- New South Wales State Pollution Control Commission (1983). Water Quality in the Hawkesbury-Nepean River. NSW, Australia
- Officer, C.B. (1980). in Estuarine and Wetland Processes. Plenum Press, New York
- Wood, T. (1978). Estuarine and Coastal Marine Science, 7, 339-347
- Wood, T. (1980). Discrete-time modelling of dispersion in estuaries. Proceedings 17th International Conference on Coastal Engineering, Sydney, Australia.

TIDAL VARIATION OF SALT FLUX AND DISPERSION IN A POLLUTED ESTUARY

J. K. Park and A. James

Department of Civil Engineering, University of Newcastle upon Tyne, U.K.

ABSTRACT

Velocity and salinity data collected during the summer of 1983 in the Tyne estuary are used to investigate the dominant mechanisms for the flux of salt and dispersion. The instantaneous salt flux arises mainly from the combination of velocity fluctuation with the tidal mean salinity, and the instantaneous dispersion results almost entirely from the combination of vertical oscillatory velocity and steady salinity. Of the net downstream salt flux, 92.4% is accounted for by the river discharge. The non-tidal drift appears to be of most importance in the net upstream salt flux. The estuary has a strong vertical salinity gradient and due to the strong secondary flow, has a uniform transverse gradient; thus, the dominant factor in the longitudinal dispersion arises from the vertical shear in the oscillatory tidal current. The dispersion coefficient is highly time-dependent within the tidal cycle as well as a function of distance. The importance of time-varying longitudinal dispersion coefficients are demonstrated in a water quality model by using the sensitivity analysis.

KEYWORDS

Decomposition, Estuary, Longitudinal Dispersion, Mixing, Pollution, Salt Flux, Water Quality Model.

INTRODUCTION

Pollutants discharged into estuaries appear to be mixed by the same processes as those which mix the salt since the natural mixing is characterised by the tidal movement and a gravitational circulation due to the salinity gradient from the head to the mouth of the estuary. So detailed information on salinity and velocity may provide some insight into the mass transport of a pollutant as well as salt.

The tidally induced velocities are larger than velocities due to the freshwater flow, and the vertical salinity profile as well as the velocity profile vary considerably within a tidal period; thus, the mixing mechanisms are highly time dependent. Pritchard (1954) found that the vertical non-advection flux of salt increased with the increase in the tidal velocity in the James River estuary. A quantitative study of the variation of the mixing rate in the Mersey Narrows by Bowden (1960), showed that the maximum values of the vertical eddy diffusivity, occurred at maximum tidal velocities and were three to five times larger than the

tidal mean value.

In much of the earlier study of the longitudinal dispersion in estuaries, variations within the tidal cycle were eliminated by taking averages over the tidal period and applying the mean values to the one-dimensional mass balance equation. In a dynamic water quality model it is unrealistic to take the constant longitudinal dispersion coefficient in time. It is reasonable to expect that the coefficient will depend on the magnitude of the mean velocity, the depth of water and dimensionless parameters such as Richardson number or an estuarine number.

The one-dimensional mass balance equation for the mean concentration of a conservative material is given by Okubo (1964).

$$\frac{\partial \bar{c}}{\partial t} + \frac{\partial u\bar{c}}{\partial x} = \frac{1}{A} \frac{\partial}{\partial x} (\varepsilon_x A \frac{\partial \bar{c}}{\partial x} - \int_A u' c' dA) \quad (1)$$

Molecular diffusion can be neglected since its effects are several orders of magnitude smaller than those of turbulent diffusion in most cases. The flux $u'c'$ is found to be proportional to the longitudinal gradient of c , so that the longitudinal dispersion coefficient ε_x may be defined by

$$\int_A u' c' dA = - \varepsilon_x A \frac{\partial \bar{c}}{\partial x} \quad (2)$$

If the velocity and salinity profiles are known from the field observations, ε_x can be estimated directly.

Velocity and salinity may be decomposed to investigate the contributing factors of the shear effect and the salt flux in an estuary. Hansen (1965) recognized the importance of the variation over the whole cross-section not only in the vertical direction, and showed the importance of the correlation of the tidal fluctuations in velocity and salinity to the salt flux. Fischer (1972) considered the separate contributions of transverse and vertical variations, and decomposed the velocity giving the priority to the transverse deviations as follows:

$$u(x,y,z,t) = u_0(x) + u_1(x,t) + u_{st}(x,z) + u_{sv}(x,z,t) + u_{sv}(x,y,z) + u_{vt}(x,y,z,t) \quad (3)$$

where u_0 is the tidal mean of the cross-sectional average, u_1 is the deviation of the cross-sectional average from u_0 , u_{st} is the tidal mean over the local depth of the deviation from the cross-sectional average, u_{sv} is the tidal mean of the deviation of the local value from the depth mean value, and u_{vt} and u_{sv} are the deviations from the tidal average values u_{st} and u_{sv} . Hughes and Rattray (1980) modified the components by taking u_{sv} as the tidal mean over the width of the deviation from the cross-sectional average and u_{vt} as the remaining difference from the cross-sectional deviation. They showed that 65% of the upstream salt flux was due to the correlation of the tidal fluctuations of the cross-sectional mean salinity and velocity and 20% was due to the vertical oscillatory shear at the high discharge in the Columbia River estuary. Lewis and Lewis (1983) found in the narrow and partially stratified Tees estuary that relative contribution of the salt flux terms to the net upstream transport varies along the estuary. Their results strongly indicate the possible variation of contributing factors in a cross-section within the tidal cycle according to the hydrodynamic changes. A large number of studies were done using decompositions that have helped understanding the mass transport mechanisms in estuaries. However, all of these failed to give enough information within the tidal period and the data interpretations were limited to the tidal average values.

Variation of each component within the tidal cycle was examined using the field data collected during the summer of 1983 in the estuary of the River Tyne. A numerical analysis was tried to find the reasonable number of points based on the contours of salinity and velocity at each lunar hour. Transverse partitioning and vertical partitioning were also compared to find the better way of understand-

ing the transport mechanism.

COMPONENTS OF THE NET LONGITUDINAL SALT FLUX

The net longitudinal salt flux through a cross-section in an estuary can be decomposed into three terms: due to the tidal mean of velocity and salinity, due to the correlations between fluctuations of velocity, salinity and cross-sectional area, and due to short period fluctuations. The first term arises from the freshwater flow and the second term results from the spatial correlations of the transverse and of the vertical deviations in velocity and salinity, the so-called shear effect, derived from Taylor (1954).

Hansen (1965) considered each variable as the sum of a tidal mean, a tidal fluctuation and a turbulent term to obtain the equation:

$$\langle F_s \rangle = \underbrace{\langle A_0 u_0 s_0 \rangle}_1 + \underbrace{\langle \bar{s}_0 \rangle \langle \bar{A}_0 \bar{u}_0 \rangle}_2 + \underbrace{\langle \bar{u}_0 \rangle \langle \bar{A}_0 \bar{s}_0 \rangle}_3 + \underbrace{\langle \bar{A}_0 \bar{u}_1 \bar{s}_1 \rangle}_4 + \underbrace{\langle \bar{A}_1 \bar{u}_2 \bar{s}_2 \rangle}_5 \quad (4)$$

where the angle brackets denote the average over the tidal cycle and the bar denotes the cross-sectional average, and in which

$$u(x, y, z, t) = u_0(x) + u_1(x, t) + u_2(x, y, z, t) \quad (5)$$

$$s(x, y, z, t) = s_0(x) + s_1(x, t) + s_2(x, y, z, t) \quad (6)$$

$$A(x) = A_0(x) + A_1(x, t) \quad (7)$$

Dyer (1974) included a fluctuation of cross-sectional area over the tidal period to obtain eleven components contributing to the net salt flux based on Fischer's decompositions as follows:

$$\begin{aligned} \langle F_s \rangle = & \underbrace{\langle \bar{A}_0 \rangle \langle \bar{u}_0 \rangle \langle \bar{s}_0 \rangle}_1 + \underbrace{\langle \bar{A}_1 \bar{u}_1 \rangle \langle \bar{s}_0 \rangle}_2 + \underbrace{\langle \bar{A}_0 \rangle \langle \bar{u}_1 \bar{s}_1 \rangle}_3 + \underbrace{\langle \bar{A}_1 \bar{s}_1 \rangle \langle \bar{u}_0 \rangle}_4 + \underbrace{\langle \bar{A}_1 \bar{u}_1 \bar{s}_1 \rangle}_5 \\ & + \underbrace{\langle \bar{A}_0 \rangle \langle \bar{u}_{st} \rangle \langle \bar{s}_{st} \rangle}_6 + \underbrace{\langle \bar{A}_0 \rangle \langle \bar{u}_{sv} \rangle \langle \bar{s}_{sv} \rangle}_7 + \underbrace{\langle \bar{A}_0 \rangle \langle \bar{u}_{st}^! \bar{s}_{st}^! \rangle}_8 + \underbrace{\langle \bar{A}_0 \rangle \langle \bar{u}_{sv}^! \bar{s}_{sv}^! \rangle}_9 \\ & + \underbrace{\langle \bar{A}_1 \bar{u}_{st}^! \bar{s}_{st}^! \rangle}_{10} + \underbrace{\langle \bar{A}_1 \bar{u}_{sv}^! \bar{s}_{sv}^! \rangle}_{11} \end{aligned} \quad (8)$$

The instantaneous flux of salt through a cross-section can be expressed in a tabular form (Table 1) to consider the possible contributing factors.

Table 1. Components of salt flux.

| | u_0 | u_1 | u_{st} | $u_{st}^!$ | u_{sv} | $u_{sv}^!$ |
|------------|----------|----------|----------|------------|----------|------------|
| s_0 | F_{11} | F_{12} | F_{13} | F_{14} | F_{15} | F_{16} |
| s_1 | F_{21} | F_{22} | F_{23} | F_{24} | F_{25} | F_{26} |
| s_{st} | F_{31} | F_{32} | F_{33} | F_{34} | F_{35} | F_{36} |
| $s_{st}^!$ | F_{41} | F_{42} | F_{43} | F_{44} | F_{45} | F_{46} |
| s_{sv} | F_{51} | F_{52} | F_{53} | F_{54} | F_{55} | F_{56} |
| $s_{sv}^!$ | F_{61} | F_{62} | F_{63} | F_{64} | F_{65} | F_{66} |

Note : $F..$ stands for the cross-product of $u..$ and $s..$.

The integration and sum of the values in Table 1 give the tidal mean transport of salt. F_{11} corresponding to term 1 in Eq.8 is due to the river discharge and F_{12} (term 2 in Eq.8) results from the compensation flow for the inward transport on the progressive tidal wave, both of which are associated with the 'non-tidal drift'. F_{21} (term 4 in Eq. 8) is due to the correlation between tidal velocity variation and mean salinity, and F_{22} (term 3 plus 5 in Eq. 8) the third-order correlation of tidal variations of mean salinity and velocity. $F_{3-6}, 3-6$ are due to the shear effect: F_{33} (term 6) the transverse gravitational net circulation, F_{44} (term 8 plus 10) the transverse oscillatory shear, F_{55} (term 7) the vertical gravitational

net circulation, and F_{66} (term 9 plus 11) the vertical oscillatory shear. F_{43} arises from the non-zero correlation of the transverse steady velocity and the oscillatory salinity and F_{65} from the non-zero correlation of the vertical steady velocity and the oscillatory salinity.

FIELD OBSERVATIONS AND DATA TREATMENT

The river Tyne is relatively narrow and falls in classes 2a or 2b of the Hansen and Rattray classification system (Hansen and Rattray, 1966) depending on the location and the river discharge. The tidal limit of the Tyne is near the Wylam bridge which is approximately 32 km inland from the mouth of the estuary. The annual mean freshwater flow is estimated to be 45 m³/sec and ranges from 7 m³/sec at low flow (10 percentile) to 120 m³/sec at high flow (95 percentile).

Velocity and salinity measurements were carried out on 27-28 July and 1 September, 1983 at Hebburn, and on 16 August, 1983 near the Swing Bridge (Fig.1). One boat remained stationed at one reference point taking vertical measurements every hour during one complete tidal cycle while the other boat moved from position to position to measure the velocity and salinity distributions in the vertical plane. Each run at a position took five to seven minutes at four different depths: 0.5 m below the surface, two points in the middle, and 0.5 m above the bottom. It was possible to measure velocity and salinity at four positions with one boat within an hour interval. After the measurement at the bottom, the surface velocity was measured for a second time to correct the measured velocity to the same instance (British Standards Institution, 1973). At the reference position, measurements were made over a one minute interval at each of five depths while at the other positions four points and 30 seconds were used. A third boat was mobilised to estimate the salinity gradients between two sections, 700 m upstream and downstream from the velocity measurement section. Dye tests were also carried out at the same time at high tide, mid-tide on ebbing and low tide at the two stations to measure the transverse and vertical eddy diffusion coefficients.

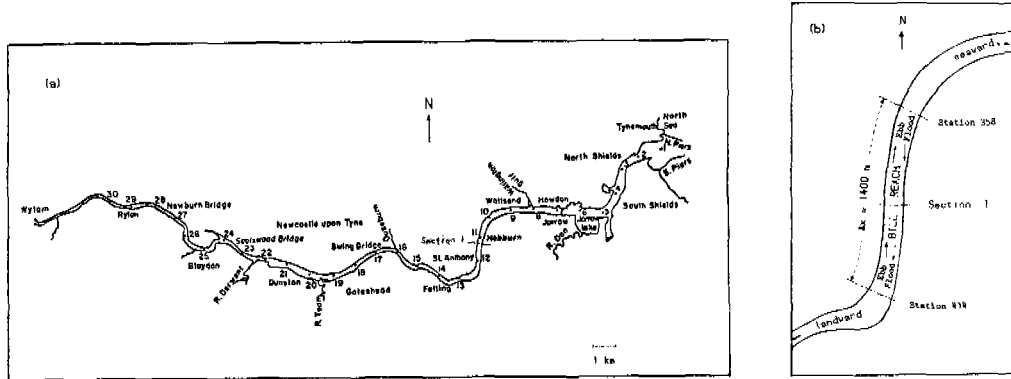


Fig.1 (a) Map of the Tyne estuary, (b) Bill reach selected for velocity and salinity observation.

The velocity and salinity data at four or five different depths were interpolated or extrapolated to 11 points (Kjerfve, 1979) and were fitted to the sinusoidal equations:

$$u = u_0 + u_1 \cos (\omega t + \phi_u) \quad (9)$$

$$s = s_0 + s_1 \cos (\omega t + \phi_s) \quad (10)$$

Those equations at five positions were entered into the computer to generate a 105 x 50 grid over the cross-section and to draw contours at each lunar hour using

SURFACE II (Sampson, 1978). 105 x 50 matrix was reduced to the required size in order to estimate the decomposed components in Table 1.

METHODS OF ANALYSIS

The total cross-section was broken into sub-areas and each sub-area was designed to change due to the tidal fluctuation (Fig.2). The transverse partitioning and the vertical partitioning are used to estimate each component contributing to the salt flux. Rattray and Dworski (1980) concluded that the procedure of using proportional depth (Fig.2) did not reflect the important effect of gravity based on two-way analysis of variance technique. However, the model seems to be best to describe inter-tidal variation of contributing factors for the salt flux since data points can be expressed as a function of time. Using row indices i to denote depth, column indices j to denote transverse position, and $s..$ and $u..$ to denote the average value of salinity and velocity, this may be written as:

$$s_{ij} = \frac{1}{A_{ij}} \sum_i s_{ij} \Delta A_{ij} \quad (11)$$

$$s_{i..} = \frac{1}{A_{i..}} \sum_j s_{ij} \Delta A_{ij} \quad (12)$$

and $s_{..} = \bar{s} = \frac{1}{A} \sum_i \sum_j s_{ij} \Delta A_{ij} \quad (13)$

in which $A_{ij} = \sum_i \Delta A_{ij} \quad (14)$

$$A_{i..} = \sum_j \Delta A_{ij} \quad (15)$$

$$A_{..} = \sum_i \sum_j \Delta A_{ij} = \sum_i A_{i..} = \sum_j A_{..j} \quad (16)$$

$$\langle \Delta A_{ij} \rangle = (1/T) \sum_t \Delta A_{ij} \quad (17)$$

and $\langle A \rangle = \sum_i \sum_j \langle \Delta A_{ij} \rangle \quad (18)$

Velocity may be written in a similar way. Each component in Table 1 can be expressed:

$$F_{33} = \frac{1}{\langle A \rangle} \sum_j (u_{st})_{ij} (s_{st})_{ij} \langle A_{ij} \rangle \quad (19)$$

$$F_{44} = \frac{1}{A} \sum_j (u_{st}^t)_{ij} (s_{st}^t)_{ij} A_{ij} \quad (20)$$

$$F_{55} = \frac{1}{\langle A \rangle} \sum_j \sum_i (u_{sv})_{ij} (s_{sv})_{ij} \langle \Delta A_{ij} \rangle \quad (21)$$

$$F_{66} = \frac{1}{A} \sum_j \sum_i (u_{sv}^t)_{ij} (s_{sv}^t)_{ij} \Delta A_{ij} \quad (22)$$

$$F_{34} = \frac{1}{\sum_j \langle A_{ij} \rangle} \sum_j (u_{st})_{ij} (s_{st}^t)_{ij} \langle A_{ij} \rangle A_{ij} \quad (23)$$

$$F_{35} = \frac{1}{\sum_i \sum_j \langle A_{ij} \rangle \langle \Delta A_{ij} \rangle} \sum_i \sum_j (u_{st})_{ij} (s_{sv})_{ij} \langle A_{ij} \rangle \langle \Delta A_{ij} \rangle \quad (24)$$

$$F_{36} = \frac{1}{\sum_i \sum_j \langle A_{ij} \rangle \Delta A_{ij}} \sum_i \sum_j (u_{st})_{ij} (s_{sv}^t)_{ij} \langle A_{ij} \rangle \Delta A_{ij} \quad (25)$$

$$F_{46} = \frac{1}{\sum_i \sum_j A_{ij} \Delta A_{ij}} \sum_i \sum_j (u_{st}^t)_{ij} (s_{sv}^t)_{ij} A_{ij} \Delta A_{ij} \quad (26)$$

The other components were described in a similar way.

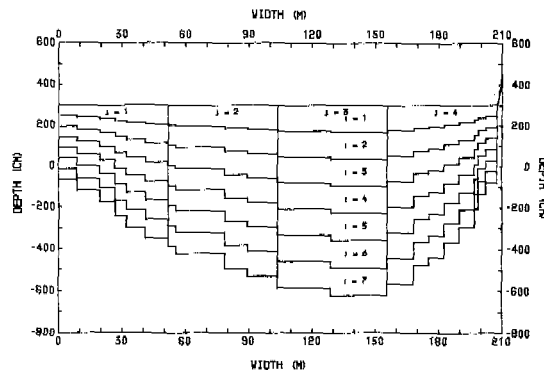


Fig.2 Decomposed sub-areas over the cross-section at Hebburn

VELOCITY AND SALINITY PATTERNS

Bill reach (section 1, Fig.1 (b)) was used to investigate the salt balance and the shear effect during the low discharge stage of the river Tyne. The study reach was described as hydraulically simple by Allen (1962). The variations of current and salinity are illustrated over the tidal period in different ways in Figs. 3, 4 and 5. Fig.3 shows the velocity fluctuations in the mid-channel. Interaction of tidal movement and river discharge caused the phase lag over a depth. There is a very small phase shift between the actual and the predicted tides in the bottom layer because of the strong tidal movement and due to friction with the bed. However, there is some phase lag at the surface layer which can be easily affected by the freshwater flow, and wind or other physical factors such as stratification.

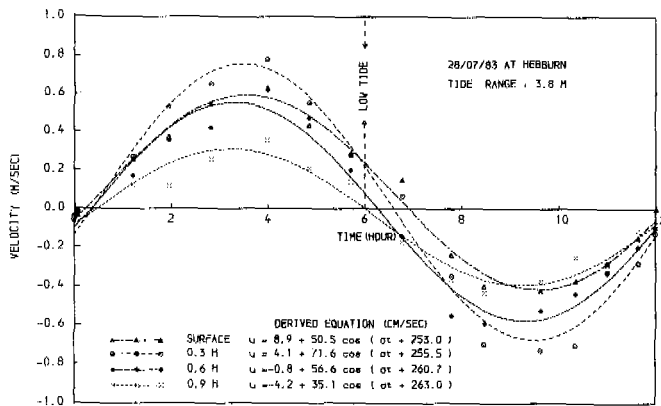
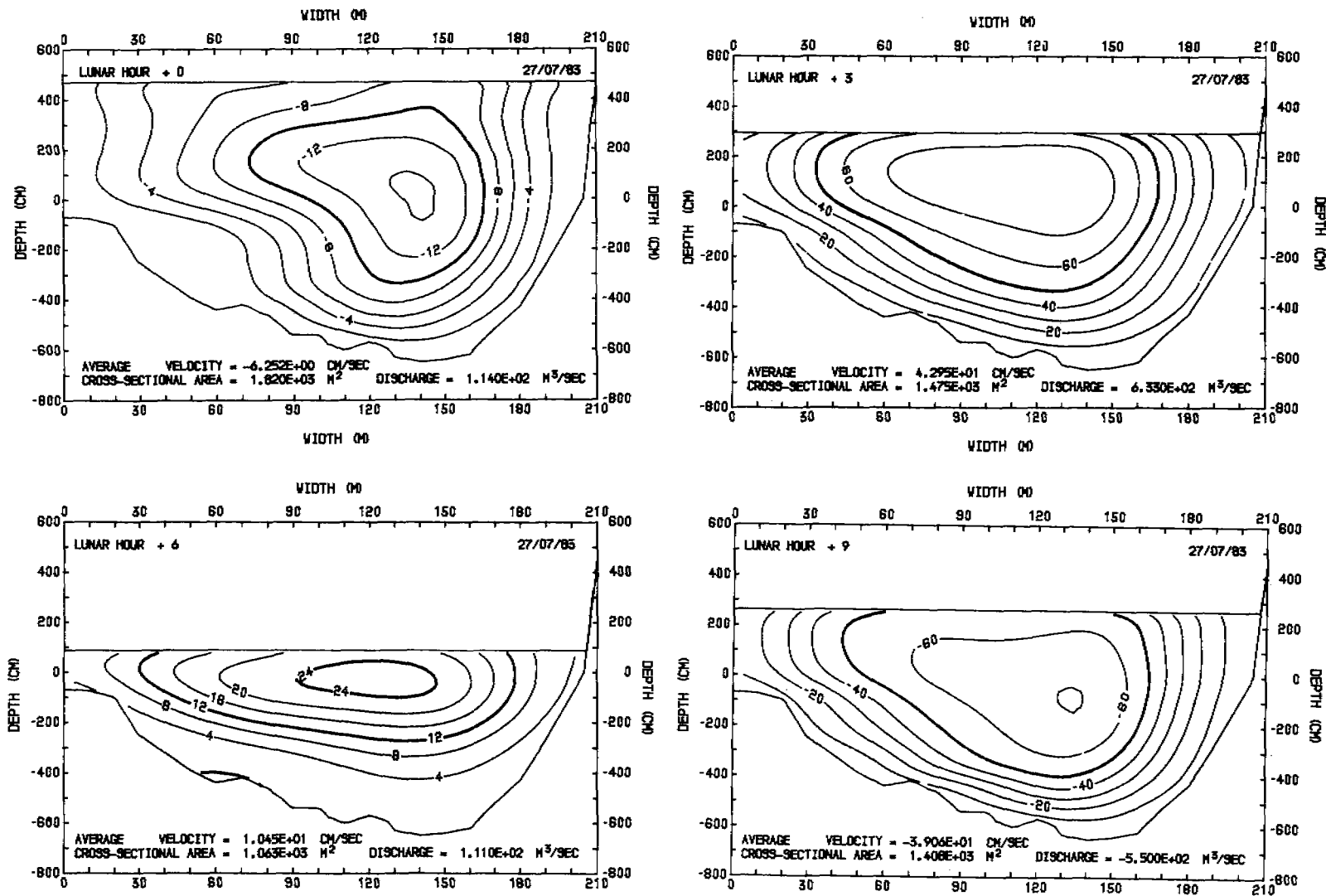


Fig. 3 Phase shifts of current in different depths at Hebburn

The variation of the phase over the depth was observed at each position. Current and salinity distributions over a cross-section at each lunar hour are shown in Figs. 4 and 5. Salinity variation at the transverse direction seems to be small compared with those in the vertical direction. Areas of high velocity move from the north at mid-tide on ebbing to the south at mid-tide on flooding due to the bending at both ends of the reach (Fig. 1 (b)). Fig. 6 shows that net downstream flow occurs at the surface layer (60% of the cross-sectional area), while net upstream flow occurs in the bottom layer.

River discharge was obtained by integrating the speed over the cross-sectional area at each lunar hour and averaging the instantaneous discharge through the tidal cycle. The estimated river discharge rate was 19.0 m³/sec and average cross-



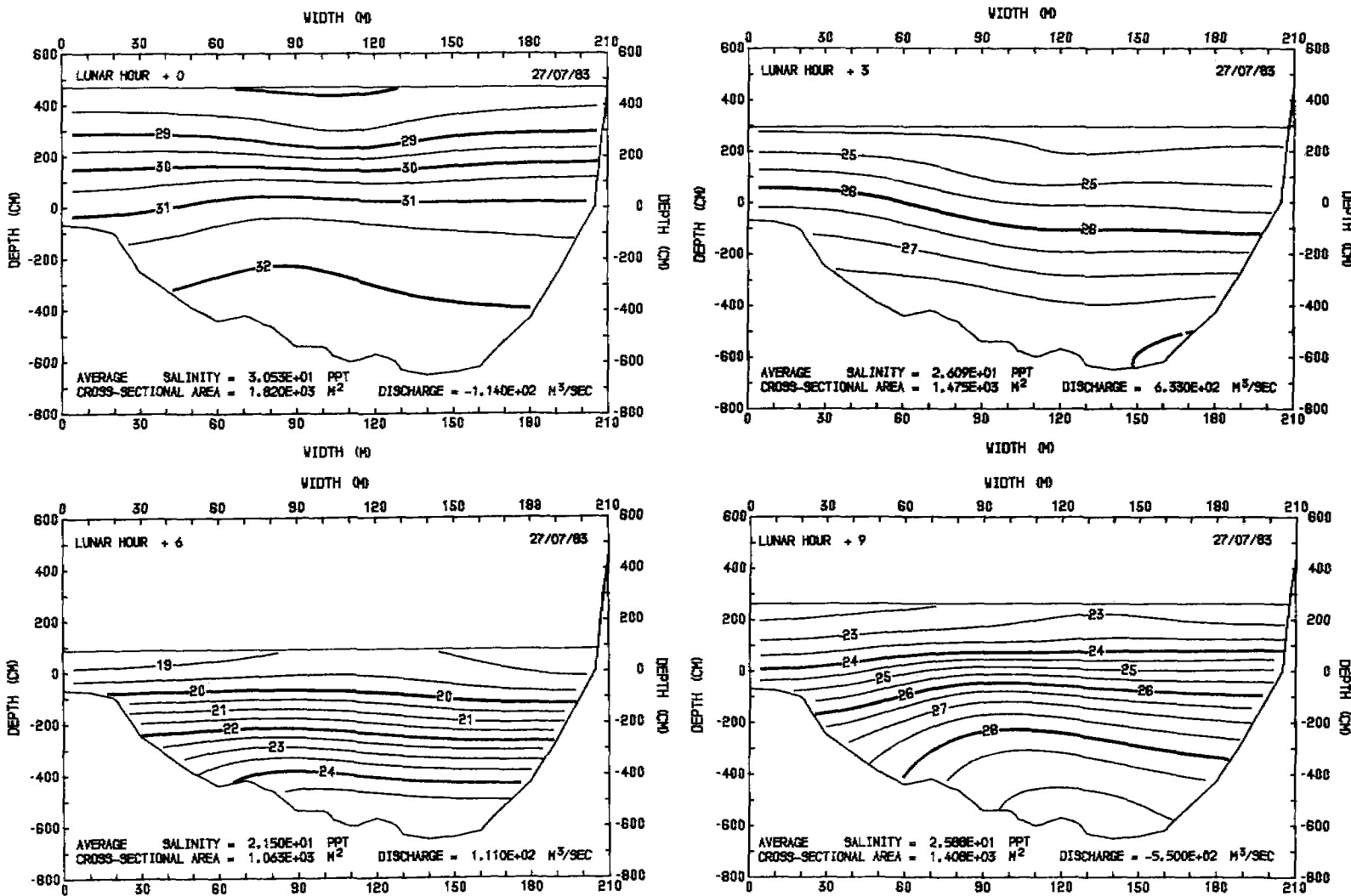


Fig. 5. Isosalts at high tide, mid-tide on ebbing, low tide, and mid-tide on flooding.

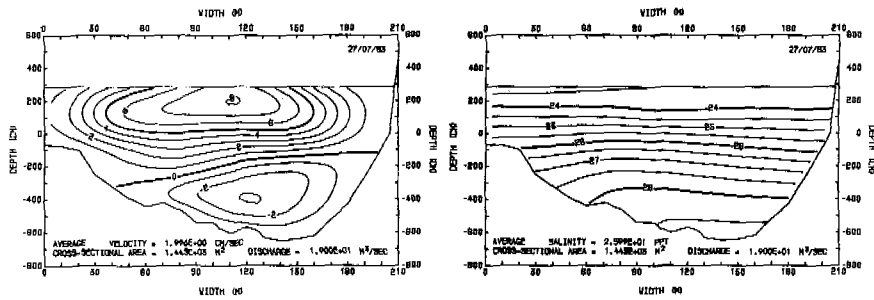


Fig.6 Residual velocity and salinity distributions at Hebburn

sectional area was 1443 m^2 . The equations derived from the field data at Hebburn are as follows:

$$\bar{u} = 2.00 + 41.64 \cos(\sigma t + 258.5) \quad (\text{cm/sec}) \quad (27)$$

$$\bar{s} = 26.0 + 4.53 \cos(\sigma t + 358.6) \quad (\text{ppt}) \quad (28)$$

$$A = 1443 + 377.3 \cos(\sigma t + 354.6) \quad (\text{m}^2) \quad (29)$$

and $Q = 19.0 + 602.6 \cos(\sigma t + 281.3) \quad (\text{m}^3/\text{sec}) \quad (30)$

TRANSPORT OF SALT

A matrix having 105 points over the depth and 50 points over the width was generated to estimate the cross-sectional average of each variable and to draw contours (Figs.4, 5 and 6), and was reduced in size to find the optimal grid. The difference between the direct estimation and each matrix was tested. The test results are summarised in Table 2. 7 \times 4 and 11 \times 8 matrices are thought to be suitable for the computation of the salt flux and dispersion, respectively. Thus, all computations were done based on those matrices. Of eight matrices, only two were acceptable at the 10% significance level of two-tailed tests during the estimates of shear effect terms from vertical partitioning, even though the salt flux terms are computed more accurately than from transverse partitioning. Vertical partitioning is inclined to reducing the vertical effects, which is contrary to the results of Hughes and Rattray (1980).

Increasing the number of points over the width did not give good results. This seems to be due to a low correlation of the transverse variation. Great care, however, should be taken of the selection of the width partitioning positions since the averaged values from the partitioning positions may distort the results, especially when the velocity profiles over a cross-section are complicated. On the other hand, increase in the number of points over the depth gave better results. This may imply that the vertical effects are dominant in this estuary. Variation of the components within the tidal cycle is plotted in Fig. 7. Six terms in Table 1 appear to be important: F_{11} due to the mean current corresponding to river discharge, F_{12} and F_{21} due to the non-zero correlation between the tidal mean velocity/salinity and the deviation of an instantaneous cross-sectional mean from the tidal mean, F_{55} due to the vertical gravitational circulation, F_{65} due to the non-zero correlation of the vertical oscillatory velocity and steady salinity, and F_{66} due to the vertical oscillatory shear. F_{12} is the most significant factor for the instantaneous net upstream and downstream flux of salt.

It is natural that F_{22} has a semi-tidal period. The tidal average over the cross-section occurs at the mid-tide in salinity and near low and high water in velocity. This product causes the semi-tidal cycle. The correlation of the vertical oscillatory velocity and steady salinity leads to upstream salt flux during flooding tide and to downstream salt flux during ebbing tide. F_{11} is the steady source of the downstream salt flux.

Table 2. Comparison of test results.

unit : $10^{-2} \text{ kg/m}^2/\text{sec}$

| | | | | | | | | | Direct Estimation from 105x50 grids |
|--------------------------------------|--------|--------|--------|--------|--------|--------|--------|--------|--|
| 7 x 4 | 7 x 8 | 7 x 16 | 7 x 24 | 11x 8 | 21x 8 | 11X16 | 21X24 | | |
| (a). Transverse partitioning. | | | | | | | | | |
| $\sum_1^6 \sum_1^6 F_{ij}$ | 3.065 | 3.048 | 3.046 | 3.038 | 3.037 | 3.038 | 3.037 | 3.033 | 3.089 |
| T-test | 0.24 | 0.49 | 0.54 | 0.66 | 0.51 | 0.46 | 0.55 | 0.57 | - |
| $\sum_3^6 \sum_3^6 F_{ij}$ | -0.414 | -0.422 | -0.423 | -0.431 | -0.433 | -0.431 | -0.432 | -0.435 | -0.433 |
| T-test | -0.23 | -0.23 | -0.27 | -0.05 | 0.01 | -0.02 | -0.02 | 0.03 | - |
| (b). Vertical partitioning. | | | | | | | | | |
| $\sum_1^6 \sum_1^6 F_{ij}$ | 3.079 | 3.081 | 3.084 | 3.075 | 3.080 | 3.081 | 3.082 | 3.079 | 3.089 |
| T-test | 0.11 | 0.15 | 0.10 | 0.27 | 0.15 | 0.11 | 0.12 | 0.17 | - |
| $\sum_3^6 \sum_3^6 F_{ij}$ | -0.400 | -0.389 | -0.385 | -0.394 | -0.392 | -0.388 | -0.386 | -0.389 | -0.433 |
| T-test | -0.44 | -4.29 | -2.94 | -2.12 | -1.93 | -1.31 | -4.07 | -2.11 | - |

Note : $H_0 : \mu_{1j} = \mu_{2j}, t_{0.05,11} = 1.796, P(|t| < 1.796) = 0.1$
 Matrix has (depth x width) points throughout the tidal period.

Tidally averaged values of each component are illustrated in Table 3. The net longitudinal flux of salt was estimated to be $3.08 \times 10^{-2} \text{ kg/m}^2/\text{sec}$. The magnitudes of ten terms are divided into two parts: upstream salt flux and downstream salt flux (Table 4).

The cross-product terms other than F_{12}, F_{13}, F_{14} , and F_{21} became zero (Table 3). The correlation between the steady transverse velocity and tidal mean salinity (F_{13}) contributes to upstream salt flux. F_{13} appears to arise from the bathymetry of the study reach (Fig. 1 (b)). The energy available from the tidal currents induced by the channel topography drives the steady circulation which is an important mechanism for the upstream transport of pollutants and salinity against the river discharge and is referred to as the tidal pumping.

It is evident that the estuary did not reach a stage of true salt balance. In the real estuary, a steady state seldom occurs in which upstream dispersive flux is exactly balanced by downstream advective flux since freshwater flow rate, tide range, or boundary geometry are not constant for many tidal periods. In the steady state, integrating Eq.1 in terms of distance gives:

$$\int_A u c dA = \int_A E_x \frac{\partial c}{\partial x} dA \quad (31)$$

The net dispersive salt flux in the steady state is numerically equal to the advective salt flux but opposite in sign (Eq. 2) (Murray and Siripong, 1978). Thus, of the total upstream salt flux, $5.40 \times 10^{-2} \text{ kg/m}^2/\text{sec}$, $3.08 \times 10^{-2} \text{ kg/m}^2/\text{sec}$, or 57% is accounted for by non-advective or dispersive processes. In a rectangular, laterally homogeneous estuary, Hansen and Rattray (1966) had a steady state equation using the similarity theories from the two-dimensional equation:

$$\epsilon_x \frac{\partial \bar{c}}{\partial x} = \gamma u_r \bar{c} \quad (32)$$

where ϵ_x denotes the longitudinal turbulent diffusivity and γ denotes the fraction of the upstream salt flux induced by all dispersion other than the density driven circulation to the net longitudinal salt flux. From Eqs. 27 to 30 and Table 4, we have:

$$\gamma = \frac{\text{Upstream salt flux} - (F_{13} + F_{33} + F_{55})}{\text{Net longitudinal salt flux}} = 0.58 \quad (33)$$

This value means that 58% of the salt balance is maintained by mechanisms other than density driven circulation in the Tyne estuary. The estuarine Richardson number, $R = 0.105$ and the bulk densimetric Froude number, $F_m = 0.031$ yield $\gamma = 0.65$ and $ds/s = 0.15$ in the stratification-circulation diagram. These results are close to $\gamma = 0.58$ from Eq. 33 and $ds/s = 0.16$ from Fig. 6.

Table 3. Tidally averaged values of each component at Hebburn.

unit : 10^{-2} kg/m²/sec

(a). Transverse partitioning.

| | u_0 | u_1 | u_{st} | u'_{st} | u_{sv} | u'_{sv} |
|-----------|-------|-------|----------|-----------|----------|-----------|
| s_0 | 4.99 | 0.21 | -0.06 | 0.07 | 0.0 | 0.0 |
| s_1 | -0.02 | -1.70 | 0.0 | 0.0 | 0.0 | 0.0 |
| s_{st} | 0.0 | 0.0 | -0.01 | 0.0 | 0.0 | 0.0 |
| s'_{st} | 0.0 | 0.0 | 0.0 | -0.08 | 0.0 | 0.0 |
| s_{sv} | 0.0 | 0.0 | 0.0 | 0.0 | -0.45 | 0.0 |
| s'_{sv} | 0.0 | 0.0 | 0.0 | 0.0 | 0.0 | 0.13 |

(b). Vertical partitioning.

| | u_0 | u_1 | u_{st} | u'_{st} | u_{sv} | u'_{sv} |
|-----------|-------|-------|----------|-----------|----------|-----------|
| s_0 | 4.99 | 0.21 | -0.06 | 0.07 | 0.0 | 0.0 |
| s_1 | -0.02 | -1.70 | 0.0 | 0.0 | 0.0 | 0.0 |
| s_{st} | 0.0 | 0.0 | -0.02 | 0.0 | 0.0 | 0.0 |
| s'_{st} | 0.0 | 0.0 | 0.0 | -0.10 | 0.0 | 0.0 |
| s_{sv} | 0.0 | 0.0 | 0.0 | 0.0 | -0.43 | 0.0 |
| s'_{sv} | 0.0 | 0.0 | 0.0 | 0.0 | 0.0 | 0.15 |

Note : Those values less than 1×10^{-4} are written as zero.

Table 4. Downstream and upstream salt flux (transverse partitioning).

unit : 10^{-2} kg/m²/sec

| | F_{11} | F_{12} | F_{14} | F_{66} | Sum | | |
|------------|----------|----------|----------|----------|----------|----------|-------|
| Downstream | | | | | | | |
| Salt Flux | 4.99 | 0.21 | 0.07 | 0.13 | 5.40 | | |
| Percentage | 92.4 | 3.9 | 1.2 | 2.5 | 100.0 | | |
| | F_{13} | F_{21} | F_{22} | F_{33} | F_{44} | F_{55} | Sum |
| Upstream | | | | | | | |
| Salt Flux | -0.06 | -0.02 | -1.70 | -0.01 | -0.08 | -0.45 | -2.32 |
| Percentage | 2.5 | 0.8 | 73.2 | 0.6 | 3.6 | 19.3 | 100.0 |

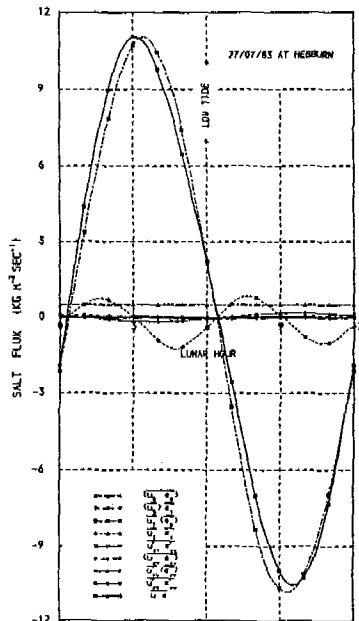


Fig. 7. Variation of the components of the net longitudinal flux of salt during the tidal cycle.

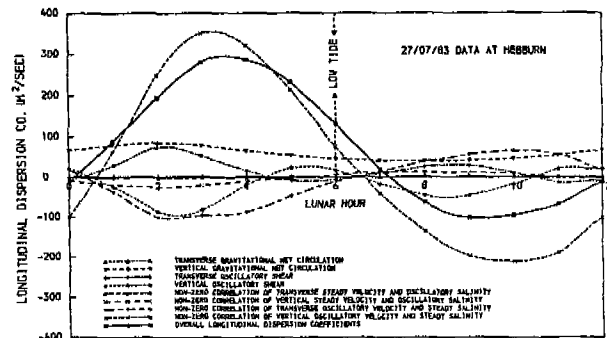


Fig. 8. Variation of decomposed longitudinal dispersion coefficients during the tidal cycle from the observed data at Hebburn.

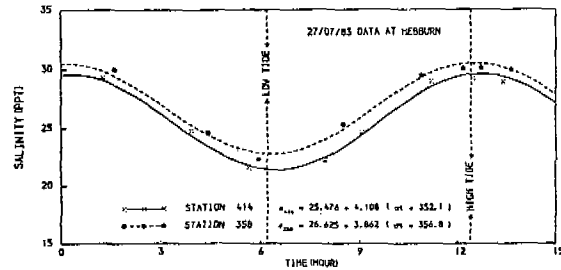


Fig. 9. Salinity changes during the tidal cycle at two stations, 358 and 414.

LONGITUDINAL DISPERSION

The time-dependent longitudinal dispersion coefficients are estimated from Eq. 2 and Fig. 9. Variation of longitudinal dispersion coefficients and each component by the shear effect is shown in Fig. 8. The tidal velocity is several orders of magnitude larger than the freshwater flow and accounts for the main shear effect. The fluctuation of the dispersion coefficients seems to be mainly due to the non-zero correlation of vertical oscillatory velocity and steady salinity. The vertical gravitational circulation is the steady source of the dispersion while the transverse gravitational circulation seems to be negligible. It is noted that the transverse and vertical oscillatory shears interact, thereby reducing the actual dispersion. The mixing caused by the transverse oscillatory shear is thought to arise from the topography of the study reach. The strong tidal current causes higher value of vertical eddy diffusion coefficient, leading to a lower degree of stratification. Bowden (1968) found that E_x is inversely proportional to the magnitude of the vertical eddy diffusion coefficient, other factors being equal. This may support the reason for the negative effect of vertical oscillatory shear. The dispersion resulting from the transverse and vertical steady velocity is small because of the small magnitude of the steady current. E_x at Hebburn can be expressed as the following equation:

$$E_x(t) = 73.6 + 198.8 \cos(\omega t + 249.5) \quad (\text{m}^2/\text{sec}) \quad (34)$$

$E_x(t)$ may be expressed as root mean square to represent a steady state coefficient. The tidally averaged E_{xT} derived from the steady state equation (Eq. 31) is approximately three times larger than E_{xT}^{rms} (Eq. 34). It should be noted that E_{xT} will be larger than E_x from Eq. 1 since Eq. 1 does not include the longitudinal spreading action of velocity gradients throughout the tidal cycle. Furthermore,

the longitudinal dispersion coefficient, E_{xTS} at a slack-tide steady state (Harleman, 1964) is not the same as E_{xTL} for the long-term tidal average condition nor E_x^{rms} from Eq. 34. Table 5 shows the variation of the tidally averaged E_x^T derived from different conditions.

Table 5. Comparison of longitudinal dispersion coefficients at different conditions.

| | | | | | | unit : m ² /sec |
|----------------|----------------------|-------------------|--------------------|-----------|-----------|----------------------------|
| E_x (Eq. 34) | E_x^{rms} (Eq. 34) | E_{xt} (Eq. 31) | E_{xt}' (Ref. 5) | E_{xTS} | E_{xTL} | |
| -110 - 250 | 145 | 375 | 500 | 417 | N.A. | |

APPLICATION OF DISPERSION COEFFICIENTS TO A WATER QUALITY MODEL

The modelling of dissolved oxygen in estuaries necessitates the evaluation of several coefficients which are difficult to measure. A sensitivity analysis of dissolved oxygen to variations in these coefficients was performed using the dissolved oxygen model of the river Tyne. The basic parameter set (BPS) of values for the coefficients was determined by field observation, laboratory experiment and curve fitting. Table 6 shows the effect of variations in the range from 50% to 150% of BPS. It would appear that reaeration has the major impact on DO but when the possible range of variation in coefficient values is considered, reaeration only has a range of 4x compared with 80x for the dispersion coefficient. In the model calibration, it is therefore vitally important that a good estimate should be obtained of the dispersion coefficient.

In a laterally homogeneous estuary, the time-dependent longitudinal dispersion coefficient may be expressed:

$$E_x(x,t) = C_1 u_f(x) \{d(x,t)\}^{P_1} + C_2 \{s(x,t)/s_g\}^{P_2} + C_3 u_t(x) \cos(\omega t + \phi) \{d(x,t)\}^{P_3} \quad (35)$$

in which u_f denotes the freshwater flow, u_t the amplitude of tidal current, and d the river depth. Term 1 is the shear effect due to the freshwater flow, term 2 the gravitational shear effect and term 3 oscillatory tidal shear effect. The constants are decided empirically in m-sec units as follows: $C_1 = 13500$, $P_1 = -0.75$, $C_2 = 116$, $P_2 = 1.5$, $C_3 = 13.7$ and $P_3 = 1.25$. Fig. 10 shows the change of DO profile due to the change of longitudinal dispersion coefficients along the estuary. In Fig. 10, the constant E_x is a function of distance and may be expressed as:

$$\begin{aligned} E_x(x) &= 150 + 100 (25,000 - x)/25,000 \text{ (m}^2/\text{sec)} & ; & & x \leq 25 \text{ km} \\ E_x(x) &= 150 + 100 (x - 25,000)/7,000 \text{ (m}^2/\text{sec)} & ; & & 25 \text{ km} < x < 32 \text{ km} \end{aligned} \quad (36)$$

CONCLUSIONS

Fluctuation in the tidal velocity is the most significant factor contributing to the instantaneous salt flux within the tidal cycle. The third-order correlation of the tidal variations of mean velocity and salinity has a quarter-diurnal period, which is the major factor to the tide average upstream salt flux (73.2%). Of the upstream salt flux, 4.2% is accounted for by the transverse variation and 19.3% by the vertical variation. The river discharge accounts for 92.4% of the tide average downstream salt flux. Minor factors are the terms due to the non-tidal drift, due to the vertical oscillatory shear and induced by the channel topography.

Table 6. Sensitivity analysis of DO to parameters and possible range of parameters in estuaries.

| | Average value used in model | Possible variation of parameter in estuaries | Σ (Modified BPS/BPS) 50 % | Σ (Modified BPS/BPS) 150 % |
|---|-----------------------------|--|----------------------------------|-----------------------------------|
| Dispersion coefficient (m^2/sec) | 118.7 | 15 - 1200 | -10.1 | 8.6 |
| Reaeration coefficient (1/day) | 0.23 | 0.1 - 0.48 | -31.2 | 19.7 |
| Benthic uptake rate ($g O_2/m^2/day$) | 2.54 | 1.0 - 3.0 | 21.5 | -11.1 |
| Deoxygenation coefficient (1/day) | 0.21 | 0.12 - 0.47 | 13.2 | -7.1 |

The main shear effect arises from the tidal current. The oscillatory shear effect due to bottom friction on the tidal current corresponding to F_{65} is of most importance in mixing salt or pollutants over intervals of less than tidal cycle, though this effect becomes negligible when averaged over the tidal period. Dispersion resulting from vertical oscillatory shear causes negative effect on the actual dispersion since E_x is inversely proportional to the magnitude of vertical eddy diffusivity. Time-varying dispersion coefficients within the tidal cycle may be expressed as a sinusoidal function having such terms as the tidal current, depth, salinity, freshwater flow rate, etc. Eq. 35 is very adaptable in predicting dispersion coefficients of the different types of estuaries since it considers the possible components contributing to the dispersion mechanism. It is desirable that the constants in Eq. 35 should be decided by theoretical as well as empirical approaches. Estimates of the dispersion coefficient vary by a factor of three to four depending on the particular conditions on which the equation is based. Sensitivity analysis has shown the strong dependence of dissolved oxygen concentration on the value of the dispersion coefficient. Because of the wide range of possible values (80x) compared with the range for other coefficient (4x), longitudinal dispersion is the most important coefficient to estimate accurately.

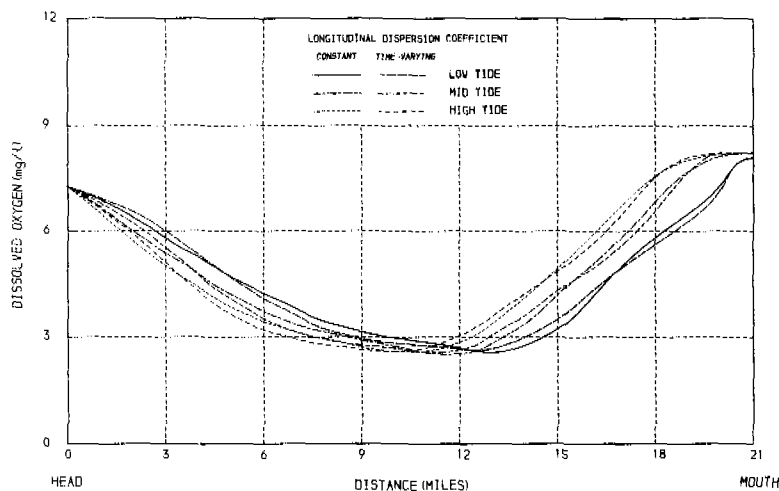


Fig. 10. Variation of dissolved oxygen distributions due to change of dispersion coefficients.

ACKNOWLEDGEMENTS

The authors wish to thank Dr. R.E. Lewis, ICI PLC, Brixham for his advice during the early stages of this study, and Mr. D. Elliott and Mr. J. Hamilton, Department of Civil Engineering, University of Newcastle upon Tyne for their advice and assistance during the surveys and the investigation. The field surveys were partly supported by the Northumbrian Water Authority. Finally, the first author would like to thank the British Council for the financial support to make this research possible.

REFERENCES

- Allan, J.H. (1962). Hydraulic Studies in the Estuary of the River Tyne, PhD Thesis, Dept. of Civil Engineering, University of Newcastle upon Tyne.
- Bowden, K.F. (1960). Circulation and Mixing in the Mersey Estuary, Int. Association for Scientific Hydrology, Committee on Surface Waters.
- Bowden, K.F. (1965). Horizontal Mixing in the Sea due to a Shearing Current, Jour. Fluid Mechanics, 21, 83-95.
- British Standards Institution (1973). Measurement of Flow in Tidal Channels, B.S. 3680, Part 6, British Standards Institution.
- Dyer, K.P. (1974). The Salt Balance in Stratified Estuaries, Estuarine and Coastal Marine Science, 2, 273-281.
- Fischer, H.B. (1972). Mass Transport Mechanisms in Partially Mixed Estuaries, Jour. Fluid Mechanics, 53, 671-687.
- Hansen, D.V. (1965). Currents and Mixing in the Columbia River Estuary, Transactions Joint Conference on Ocean Science and Ocean Engineering, 943-955.
- Hansen, D.V. and Rattray, M. Jr. (1966). New Dimensions in Estuary Classification, Limnology and Oceanography, 11, 319-325.
- Harleman, D.R.F. (1964). The Significance of Longitudinal Dispersion in the Analysis of Pollution in Estuaries, Proceedings of the 2nd Int. Conf., Tokyo, 279-306.
- Hughes, F.W. and Rattray, M. Jr. (1980). Salt Flux and Mixing in the Columbia River Estuary, Estuarine and Coastal Marine Science, 10, 479-493.
- Kjerfve, B. (1979). Measurement and Analysis of Water Current, Temperature, Salinity and Density, Estuarine Hydrography and Sedimentation, Edited by K.R. Dyer, Cambridge University Press, 186-216.
- Lewis, R.E. and Lewis, J.O. (1983). The Principal Factors Contributing to the Flux of Salt in a Narrow, Partially Stratified Estuary, Estuarine and Coastal Marine Science, 16, 599-626.
- Murray, S.P. and Siripong, A. (1978). Role of Lateral Gradients and Longitudinal Dispersion in the Salt Balance of a Shallow, Well-Mixed Estuary, Estuarine Transport Processes, Edited by Kjerfve, B., Univ. of South Carolina Press, Columbia, South Carolina, 113-124.
- Okubo, A. (1964). Equations Describing the Diffusion of an Introduced Pollutant in a One-Dimensional Estuary, Studies in Oceanography, Tokyo, 216-226.
- Pritchard, D.W. (1954). A Study of the Salt Balance in a Coastal Plain Estuary, Jour. Marine Research, 13, 133-144.
- Rattray, M. Jr. and Dworski, J.G. (1980). Comparison of Methods of Analysis of the Transverse and Vertical Circulation Contributions to the Longitudinal Advection Salt Flux in Estuaries, Estuarine and Coastal Marine Science, 11, 515-536.
- Sampson, R.J. (1978). SURFACE II Graphics System, Kansas Geological Survey, Kansas, 240p.
- Taylor, G.I. (1954). The Dispersion of Matter in Turbulent Flow through a Pipe, Proceedings of the Royal Society of London, Series A, 223, 446-468.

PHYSICAL/CHEMICAL TREATMENT

FACTORS AFFECTING THE ADSORPTION OF COMPLEXED HEAVY METALS ON HYDROUS Al_2O_3

H. A. Elliott* and C. P. Huang**

**Department of Agricultural Engineering and Environmental Engineering Program, Department of Civil Engineering, University of Delaware, Newark, DE 19716, U.S.A.*

ABSTRACT

Factors influencing the adsorption behavior of heavy metals, viz Cu(II), Zn(II), Cd(II), Pb(II) and Ni(II), onto Al_2O_3 from aqueous solutions containing complexing ligands were investigated using batch adsorption experiments. For the Cu(II)/NTA/ $\gamma\text{-Al}_2\text{O}_3$ system, increasing the system ionic strength reduced Cu adsorption through activity coefficient and surface electrical double layer effects. The presence of alkaline earth cations (Ca(II) and Mg(II)) also reduced Cu removal from solution by lowering the ability of NTA to prevent $\text{Cu}(\text{OH})_2$ precipitation and through specific adsorption to the alumina surface. The adsorption of the heavy metals on Al_2O_3 from solutions containing NTA followed the sequence: Cu > Zn > Cd > Pb ≈ Ni. Increase in system temperature tended to decrease metal adsorption.

KEYWORDS

Adsorption; Heavy metals; Complex formation; Al_2O_3 .

INTRODUCTION

The dramatic increase in the use of heavy metals over the past few decades has inevitably resulted in an increased flux of metallic substances to the aquatic environment. The public awareness of the detrimental environmental effects has led to much research aimed at elucidating the mechanisms and processes governing the transformation and fate of heavy metals in natural bodies of water.

This effort to understand the aqueous chemistry of heavy metals is complicated by the presence of organic substances capable of combining with the metals to form soluble complexes and chelates. The role of complexation in heavy metal interactions with particulate hydrous oxides has been studied in the laboratory (Davis and Leckie, 1978; Elliott and Huang, 1979) and a semiquantitative model has been developed (Benjamin and Leckie, 1981) to describe these phenomena. More recently, Chubin and Street (1981) and Elliott and Denneny (1982) have studied the effect of organic substances on cadmium adsorption on some natural colloids, i.e. clays and soils. A variety of system parameters influence these adsorption processes which, in turn, affect the environmental impact of heavy metal pollution. The objective of this study was, therefore, to investigate the role of ionic strength, temperature, presence

of alkaline earth cations, and the effect central metal atom on the adsorption of complexed heavy metals by Al_2O_3 , an important naturally occurring adsorbent.

MATERIALS AND METHODS

Solids: A commercial aluminum oxide, "Aluminum oxide C" (Degussa, Inc.) was the predominant solid used in this study. It is an extremely fine powder of primarily $\gamma\text{-Al}_2\text{O}_3$ structure and the average particle size is given as $0.02 \mu\text{m}$. The specific surface area is $100 \pm 15 \text{ m}^2\text{g}^{-1}$.

Chemicals: All metal solutions were prepared from perchlorate salts and sodium perchlorate (Pfaltz & Bauer, Inc.) was used as the inert electrolyte for maintaining constant ionic strength. Perchlorate anions were used as "neutral" ions because of their tendency to remain uncoordinated with metal ions in aqueous solution. The organic chemicals were obtained from a variety of sources, most often from Fisher Scientific Co. or Eastman Kodak Co.

All solutions were prepared using distilled-deionized water and standard acid (HClO_4) and base (NaOH) were used for pH adjustments.

Adsorption Experiments. Appropriate quantities of the ionic solution (NaClO_4), distilled-deionized water, organic ligand, and metal solutions were added to a 125-ml polyethylene bottle. The solids were then added from stock solutions of 10, 25 or 125 g ml^{-1} which had been prepared at least 48 hrs. prior to use. Solids addition was made just prior to initial pH adjustment with 1.0 and 0.1 M HClO_4 and/or NaOH using an Orion model 901A pH meter. The initial sample pH was systematically varied from a value of 3 upto approximately 10.5. After pH adjustment, the samples were shaken on an American Optical temperature - controlled shaking machine where the sample temperature was maintained at $25 \pm 1^\circ\text{C}$. A three hour shaking time was found adequate to reach equilibrium. A portion of the sample was retained for pH measurement, and the solids were removed by centrifugation at 15,000 rpm (25,000 g) for 15 minutes with a DuPont - Sorvall temperature - controlled centrifuge.

Metal analysis of the supernatant was performed by means of flame atomic absorption spectroscopy using a Jarrell-Ash Model 810 Atomic Absorption Spectrophotometer. Calibration standards of similar ionic strength were prepared in order to avoid matrix interference effects.

RESULTS AND DISCUSSION

Influence of Ionic Strength

The influence of ionic strength on the adsorption of CuNTA^- complexes on $\gamma\text{-Al}_2\text{O}_3$ is shown in Figure 1. The data indicate that, in general, increasing concentrations of supporting electrolyte ions lead to progressively smaller amounts of metal complex adsorption. A similar trend has been reported or suggested for the metal ions (O'Connor and Kester, 1975; Garcia-Miragaya and Page, 1976; James and Healy, 1972; Rohatgi and Chen , 1975) and for ligand substances (Graham, 1976) alone. Factors which influence complex adsorption as a result of ionic strength variations can be broadly grouped into two categories: (1) those which affect the solution metal composition (i.e., changes in activity of the principal adsorbate species) and, (2) those which modify the affinity of the adsorbate species for the surface by altering some component of the overall free energy of adsorption ($\Delta G^\circ_{\text{ads}}$).

As the concentration of supporting electrolyte is increased, the activity of the adsorbate ions will be reduced because of long-range electrostatic interactions

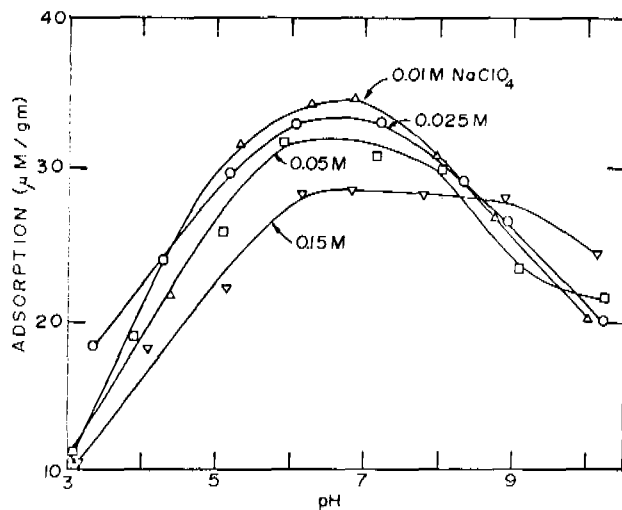
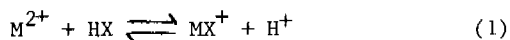


Fig. 1. The Effect of Ionic Strength (NaClO_4) on $\text{Cu}(\text{II})$ Adsorption in the $\text{Cu}(\text{II})/\text{NTA}/\gamma\text{-Al}_2\text{O}_3$ System.

Conditions: $\text{Cu}_T + \text{NTA}_T = 10^{-4}$ M, 2.5 gm l⁻¹ solids, 25° C, I = 0.01 → 0.15 M NaClO_4 .

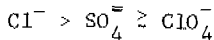
with oppositely charged electrolyte ions (Butler, 1964). This fact has led O'Connor and Kester (1975) to conclude, on the basis of equilibrium principles, that increasing ionic strength should diminish metal adsorption. For example, they propose the following equation for the adsorption of a metal, M, onto a clay surface, X:



As the activity of M is reduced, the equilibrium is shifted to the left with the accompanying reduction in the extent of adsorption. For the system depicted in Figure 1, the adsorbing species is the monovalent anionic CuNTA^- complex. Based on activity coefficients calculated from the Davies equation, if the concentration of CuNTA^- is 1×10^{-4} M, its activity is 9.2×10^{-5} M at I = 0.01 M and 7.5×10^{-5} M at I = 0.15 M. Thus, the adsorbate activity at the highest ionic strength used (I = 0.15 M) is about 81% of its value at I = 0.01 M, the lowest ionic strength value used. For the pH range of 5 to 8, where certain complicating effects associated with the more acid or alkaline conditions are not encountered, the adsorption for the 0.15 M system drops to about 80% of that observed in the 0.01 M system. Thus, changes in solute activity coefficient provide a semiquantitative explanation of the antagonistic effect of increasing NaClO_4 concentration on CuNTA^- adsorption.

Besides activity coefficient-related changes, supporting electrolyte ions may actually form complexes with Cu^{2+} and NTA^{3-} , the constituents of the adsorbed complex. This effect has indeed been suggested (Garcia-Miragaya and Page, 1976; Rohatgi and Chen, 1975) when the anion of the electrolyte is chloride, which readily complexes certain metal ions. However, in the systems studied, such an effect is probably of little import, in view of the propensity of the perchlorate ion (ClO_4^-) to remain

uncoordinated in aqueous solutions (Johansson, 1974). This is consistent with the observed order in which anions reduced adsorption of Cd on montmorillonite (Garcia-Miragaya and Page, 1976):



Furthermore, the likelihood of Na^+ (aq) successfully competing with Cu^{2+} (aq) for the soluble NTA is remote, inasmuch as the stability constant for NaNTA^{2-} is twelve orders of magnitude less than that of CuNTA^- (Sillen and Martell, 1964).

At the highest ionic strength (0.15 M) and the most alkaline conditions of this study, the "adsorption" apparently begins to increase. This is attributed to the fact that both $\text{Cu}(\text{OH})_2(s)$ solubility and complex formation depend on, though to differing degrees, the concentration of supporting electrolyte. If the electrolyte contains no ions common to the lattice of the solid precipitate, increasing electrolyte will enhance solubility as a result of activity coefficient considerations. Based on the Davies equation activity coefficients, the solubility product at $I = 0.15$ M is about 5-6 times its infinite dilution value. However, this enhanced solubility is more than offset by the reduced tendency of complex formation with increasing ionic strength. Specifically, the CuNTA^- stability constant at $I = 0.15$ M is 8.5×10^{12} compared to its zero ionic strength value of 2.5×10^{14} . Thus, decreasing copper's ability to be sequestered by NTA in solution rendered it more susceptible to precipitation as a hydroxide phase. Enhanced removal at pH 9-10 for the 0.15 M solution is a manifestation of precipitation, in addition to complex adsorption at the alumina interface.

Besides variation in the adsorbate bulk solution activity, ionic strength changes can also modify the tendency of the adsorbate to preferentially accumulate at the solid/solution interface. Of the various contributions to the overall energy of adsorption ($\Delta G^\circ_{\text{ads}}$), two which depend on the ionic strength are the electrostatic, $\Delta G^\circ_{\text{elect}}$, and the solvation, $\Delta G^\circ_{\text{solv}}$, free energy contributions (James and Healy, 1972).

According to the Stern refinement of the Gouy-Chapman double-layer model, the electrostatic term of the standard free energy of adsorption is:

$$\Delta G^\circ_{\text{elect}} = zF\psi_d \quad (2)$$

where z is the ionic valence, F is Faraday's constant, and ψ_d is the potential drop (including algebraic sign) between the Stern layer and infinite distance from the charged surface (Stumm and Morgan, 1981). Since compression of the double-layer with increasing ionic strength reduces ψ_d , it will accordingly lower the electrostatic free energy of adsorption (James and Healy, 1972). Coulombic adsorption has previously been shown to play a decisive role in the CuNTA^- uptake (Elliott and Huang, 1979); hence, this may explain, in part, the antagonistic effect of ionic strength on adsorption. In addition to electrolyte ions acting "indifferently" to alter surface charge characteristics, Davis and Leckie (1978), suggest that, at moderate or high concentrations of supporting electrolyte, the electrolyte ions themselves react with surface sites and alter the surface charge. This will also change ψ_d and the observed adsorption.

The solvation free energy, $\Delta G^\circ_{\text{solv}}$, represents a barrier to adsorption inasmuch as work must be expended to remove the secondary solvation sheath of water with a dielectric constant equal to that of the bulk water (ϵ_{bulk}), and replace it with

interfacial water of a much lower dielectric constant (James and Healy, 1972). With increasing ionic strength, the electric field, $d\psi/dx, |$ at any point near the surface will increase. This lowers the dielectric constant near the surface (ϵ_{int}) as the interfacial water molecules experience increased electrical saturation. The lower the ϵ_{int} compared to ϵ_{bulk} , the more work required in moving the adsorbate to the surface. The adsorption free energy is somewhat more positive and the extent of adsorption is correspondingly lowered.

The Influence of Competing Alkaline-Earth Cations

The existence of soluble organically-bound metal species at appreciable concentrations in natural aquatic systems is a subject of considerable controversy (Stumm and Bilinski, 1972; Manahan, 1972; Stumm and Morgan, 1981). The evidence in favor is indirect and partially rests on the observation that metal concentrations found in natural waters often represent oversaturated conditions with respect to the least soluble metal precipitates. The case against their existence is based, in part, on the fact that alkali and alkaline-earth elements are present at concentrations several orders of magnitude greater than trace elements capable of strong complex formation. It is argued that, despite their meager complexing ability, the much more abundant major ions (especially Mg(II) and Ca(II)) can outcompete the trace metals (e.g., Cu(II), Ni(II)) for the available organic material.

The extent of this competition, and its influence on metal adsorption, was investigated for the Cu(II)/NTA/ γ -Al₂O₃ system. Major cation concentrations equimolar (10^{-4} M) as well as 10 times and 100 times the soluble Cu(II) value were studied. The results are presented in Figures 2a and 2b for Ca(II) and Mg(II), respectively. The salient feature of this data is the marked deviation of the removal of Cu(II) at alkaline pH values caused by the presence of Ca(II) and Mg(II). In both cases,

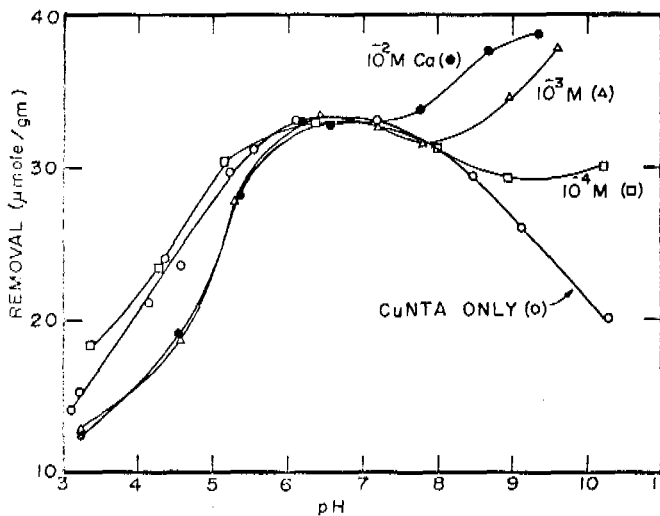


Fig. 2a. The influence of Ca(II) on Cu(II) Adsorption in the Cu(II)/NTA/ γ -Al₂O₃ System. Conditions: $C_{UT} = NTA_T = 10^{-4}$ M, $C_{AT} = 10^{-4} \rightarrow 10^{-2}$ M, 2.5 g L^{-1} solids, 25°C, $I = 0.025$ M.

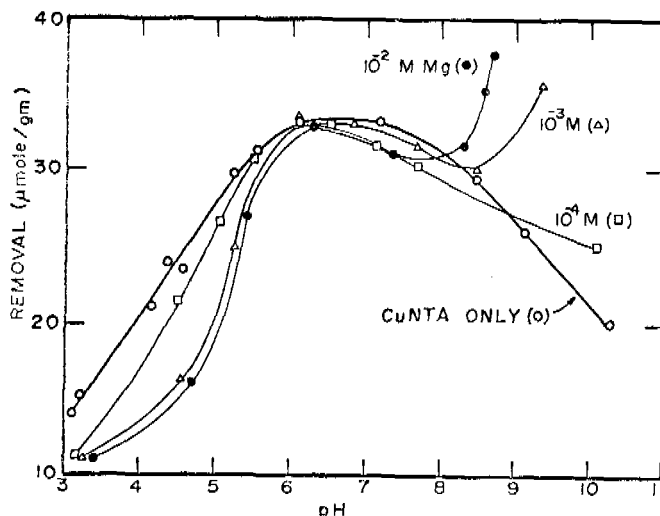


Fig. 2b. The Influence of Mg(II) on Cu(II) Adsorption in the Cu(II)/NTA/ γ -Al₂O₃ System. Conditions: Cu_T = NTA_T = 10⁻⁴ M, Mg_T = 10⁻⁴ → 10⁻² M, 2.5 g l⁻¹ solids, 25°C, I = 0.025 M.

this deviation becomes more pronounced with increasing major ion concentration. This fact can be explained by considering the theoretical calculations for the effect of Ca(II) and Mg(II) on the solubility of Cu(OH)₂(s) in the presence of 10⁻⁴ M NTA (Figures 3a and 3b). From these figures, it is clear that in the absence of major cations, NTA is capable of maintaining a 10⁻⁴ M Cu(II) solution undersaturated with respect to the copper hydroxide phase, up to pH values in excess of ten. Yet, in the presence of excess alkaline earth cations, even a powerful chelating agent like NTA is incapable of preventing Cu(OH)₂(s) precipitation at mildly alkaline conditions. Note the uncanny agreement between the predicted pH of incipient Cu(OH)₂(s) precipitation at 10⁻⁴ M Cu(II) and various Ca(II) or Mg(II) molar concentrations (Figures 3a and 3b) and the pH values for the point of departure from the "CuNTA only" curves (Figures 2a and 2b). Also concordant with this interpretation is the observation that the effect of Ca(II) in this regard is greater than for equimolar concentrations of Mg(II). Because the formation constant for CaNTA⁻ is an order of magnitude larger than that for MgNTA⁻ (Table 1), Ca(II) can more effectively compete with Cu(II) for the NTA ligand.

A feature of the data that does not conform to the concept that the major cations successfully compete for NTA with the copper is the reduced adsorption in the pH 3-6 range. The fact that the retardant effect of Mg(II) is greater than Ca(II) makes the competition argument untenable. Besides, predictions based on thermodynamic stability constants indicate that neither Ca(II) or Mg(II) significantly alter the Cu(II) speciation picture in this range (this is evident from the convergence of the various Ca(II) and Mg(II) concentration curves at low pH values in Figures 3a and 3b.)

The observed displacement of the adsorption curves at low pH values must be a result of the interaction of the alkaline-earth ions with the adsorbent, since under

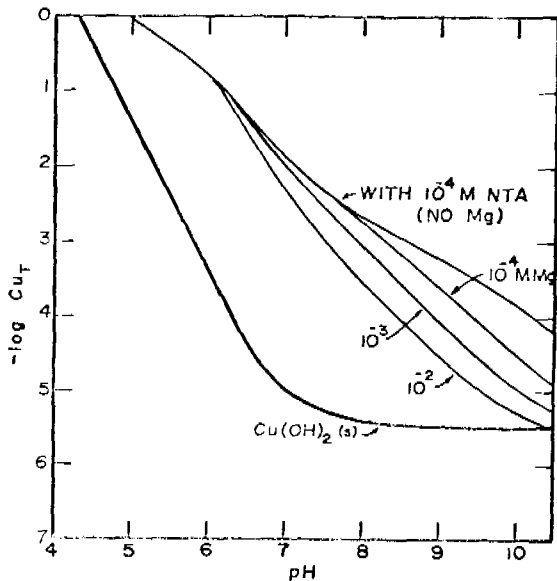


Fig. 3a. Effect of Ca(II) and NTA on $\text{Cu}(\text{OH})_2(\text{s})$ Solubility
Conditions: $\text{Ca}(\text{II})_T = 10^{-2} - 10^{-4} \text{ M}$, $I = 0.025 \text{ M}$,
 25°C , 10^{-3} M total carbonates. Figure constructed
from equilibrium constants given in Table 1.

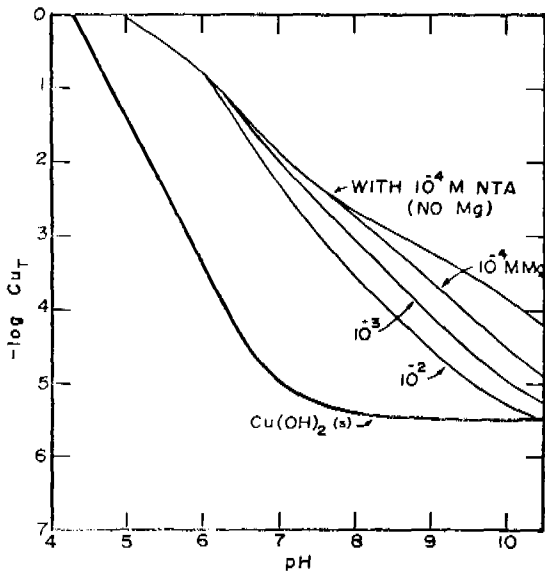


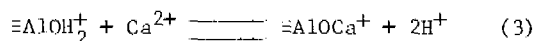
Fig. 3b. Effect of Mg(II) and NTA on $\text{Cu}(\text{OH})_2(\text{s})$ Solubility
Conditions: $\text{Mg}(\text{II})_T = 10^{-2} - 10^{-4} \text{ M}$, $I = 0.025 \text{ M}$,
 25°C , 10^{-3} M total carbonates. Figure constructed
from equilibrium constants given in Table 1.

TABLE 1. EQUILIBRIUM CONSTANTS (25°C, I = 0)
RELEVANT TO SYSTEM STUDIED

| Species | Log Constant * | Species | Log Constant* |
|-----------------------------------|-----------------------|-----------------------------------|----------------------|
| CuOH ⁺ | *K ₁ -8.0 | CuNTA ⁻ | K ₁ 14.4 |
| Cu(OH) ₂ ⁰ | *β ₂ -13.7 | Cu(NTA) ₂ ⁻ | K ₂ 2.3 |
| Cu(OH) ₃ ⁻ | *β ₃ -26.3 | AlNTA ⁰ | K ₁ 13.74 |
| Cu(OH) ₄ ²⁻ | *β ₄ -39.4 | CaNTA ⁻ | K ₁ 7.62 |
| CaOH ⁺ | *K ₁ -12.5 | MgNTA ⁻ | K ₁ 6.52 |
| MgOH ⁺ | *K ₁ -11.4 | NiNTA ⁻ | K ₁ 12.89 |
| | | PbNTA ⁻ | K ₁ 12.82 |
| | | ZnNTA ⁻ | K ₁ 11.78 |
| | | CdNTA ⁻ | K ₁ 11.35 |

*Obtained from references (Sillen and Martell, 1964, 1976; Baes and Messmer, 1976).

these conditions it does not influence the adsorbate solution properties to any significant extent. Specific interaction of alkaline-earth cations with the alumina surface has been documented (Jacob, 1966; Huang and Stumm, 1973). Jacobs (1966) found that the magnitude of attractive forces between alumina and alkaline-earth cations exceeded predictions based solely on the Couy-Chapman theory. Huang and Stumm (1973) reported that specific adsorption of the alkaline-earth cations, at least at higher pH values, could be described as an ion exchange reaction with the γ-Al₂O₃ surface. At these low pH values, where the AlOH₂⁺ sites dominate the surface distribution, the appropriate surface exchange reaction would be:



Since this equation represents an electrically equivalent exchange, the surface charge and hence the ΔG°_{elect} contribution to the adsorption free energy does not change. However, removal of protons from surface sites precludes the possibility of AlOH₂⁺....NTACu hydrogen bond formation (Elliott and Huang, 1979). Thus, the ΔG°_{chem} term becomes more positive and a corresponding suppression of the Cu(II) adsorption results. Since Mg(II) exerted a larger effect than Ca(II), its specific interactions with the surface must be stronger. This is consistent with the affinity sequence of alkaline-earth cations for γ-Al₂O₃ found by Huang and Stumm (1973): Mg²⁺ > Ca²⁺ > Sr²⁺ > Ba²⁺.

Effect of Central Metal on Metal-NTA Complex Adsorption

In order to investigate the influence of the central metal atom, various metal-NTA complexes were adsorbed from aqueous solution onto γ-Al₂O₃. The results in Figure 4 illustrate that the nature of the metal ion does indeed affect the extent of complex adsorption, as evidenced by the affinity series for the γ-Al₂O₃ surface:
 Cu > Zn > Cd > Pb ≈ Ni.

Because all the metals used are divalent, both the electrostatic and solvation free energies of adsorption should be identical for the sequence. The notably larger CuNTA uptake at low pH values hints that the difference for the metals may be related to the strength of the metal-NTA complexes. Table 1 shows that the NTA

formation constant for Cu(II) is approximately 2-3 orders of magnitude larger than for the other metals. The downturn in adsorption for $\text{pH} < \text{pH}_{\text{max}}$ was attributed to competition by dissolved Al(III) for the NTA (Elliott and Huang, 1979) since the AlNTA complex is very stable ($\log K = 13.74$). These other metals would be even less able to compete for NTA with Al(III) than the Cu(II). Even the lower concentrations of Al(III) dissolved in the neutral and alkaline pH ranges are important for the Zn(II), Cd(II), Pb(II) and Ni(II) systems since the Al(III) forms stronger complexes with NTA than any of them. Hence, their adsorption is less pronounced than Cu(II) over essentially the entire pH range.

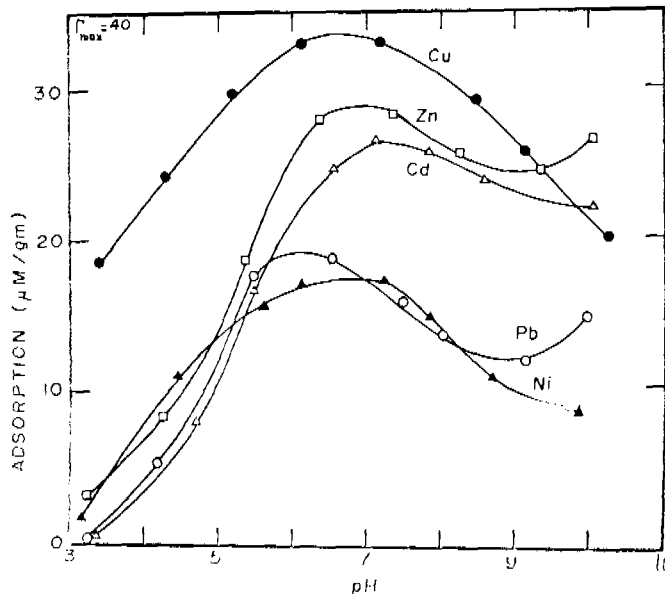


Fig. 4. Adsorption of Various Metals onto $\gamma\text{Al}_2\text{O}_3$ from 10^{-4} M NTA Solutions. All metals prepared from perchlorate salts. Conditions: $\text{M}_{\text{T}} = \text{NTA}_{\text{T}} = 10^{-4}$ M, 2.5 gm l^{-1} , $I = 0.025$ M NaClO_4 , 25° C .

Clearly the observed affinity sequence is not totally consistent with the foregoing interpretation since at neutral pH values it does not follow the ranking with decreasing tendency to form stable complexes: $\text{Cu} > \text{Ni} \approx \text{Pb} > \text{Zn} > \text{Cd}$. A second factor must be involved which influences the $\Delta G^{\circ}_{\text{chem}}$ component of the adsorption free energy. Since hydrogen bonding dominates $\Delta G^{\circ}_{\text{chem}}$ for the metal-NTA complexes, the electronegativity of the central metal is an influential parameter. The greater the electronegativity or "electron-pulling" (Sienko and Plane, 1961) ability of the metal, the less nucleophilic the NTA oxygen atoms become. Concomitantly, the ability of the complex to H-bond to the surface is diminished. For the non-copper metals the ranking with decreasing electronegativity $\text{Zn} > \text{Cd} > \text{Pb} = \text{Ni}$ also precisely defines the adsorption sequence as well. The cupric ion should have the highest electron withdrawing ability, yet its adsorption was the greatest because, as noted previously, it contends most favorably with Al(III) in binding the soluble NTA.

Thus, the extent of metal uptake depends chiefly on a balance between two counter-acting effects. First, soluble Al(III) from alumina dissolution competes with the metal for NTA. This has an antagonistic influence on metal adsorption since it reduces the bulk concentration of the adsorbate. An index of this competition is the metal-NTA stability constant (K); with increasing (K), adsorption should increase. Secondly, once formed, the metal-NTA complexes can hydrogen bond to the alumina surface to a greater or lesser extent. The electronegativity of the central atom determines the electron-rich character of the ligand donor groups which directly influence the ability of the complex to H-bond to the protonated surface sites. With increased electronegativity, adsorption should decrease.

Temperature Effect

The effect of system temperature on the $\gamma\text{-Al}_2\text{O}_3$ adsorption of CuNTA^- complexes is shown in Figure 5. An inverse relationship was observed between temperature and the extent of adsorption. Thermodynamically, adsorption must be exothermic. This follows, since a decrease in entropy accompanies a confining of the adsorbate to a two dimensional surface layer (Hayward and Trapnell, 1964) and adsorption proceeds due to a negative $\Delta G_{\text{ads}}^{\circ}$.

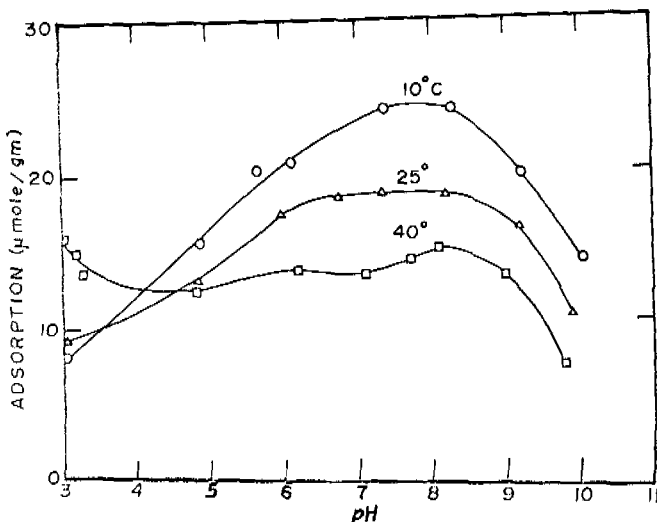


Fig. 5. The Temperature Dependence of CuNTA^- Adsorption on $\gamma\text{-Al}_2\text{O}_3$. Conditions: $\text{Cu}_T = 10^{-4}$ M, $\text{NTA}_T = 5 \times 10^{-4}$ M, 2.5 gm l⁻¹ solids, I = 0.025 M, 10 - 40°C.

A somewhat puzzling feature of the data is the apparent reversal in the temperature dependence of adsorption under the most acidic conditions. It is unlikely that adsorption at these acidic pH values increased with elevated temperatures, since no examples of endothermic adsorption are known (Hayward and Trapnell, 1964). Such an effect must be related to the non-adsorption processes peculiar to acidic pH values, namely dissolution of the alumina substrate and the related competition between Al(III) and Cu(II) for the NTA.

An exhaustive search of the literature failed to provide any conclusive evidence

regarding the temperature dependence of $\gamma\text{-Al}_2\text{O}_3$ dissolution, although the rate of dissolution under alkaline conditions increases roughly three-fold with a 15°C temperature rise (Packter and Dhillon, 1970). Documentation of the solubility-temperature relation for $\text{Al}(\text{OH})_3(s)$ is also rare. The compilation of Seidell (1958) included one reference indicating an increasing extent of dissolution with temperature; the solubility product ($\log K_{\text{so}}$) being -32.9 at 20°C and -31.7 at 30°C. However, one reference reported the opposite effect, although at a different ionic strength (Seidel and Linke, 1958).

An alternate explanation is that the temperature change disproportionately effects the competition between AlNTA^0 and CuNTA^- formation. Chelation reactions between similar metals can have dramatically different enthalpy changes. For example, the formation of CaEDTA^{2-} complexes is exothermic ($\Delta H = -8 \text{ kcal mole}^{-1}$) whereas MgEDTA^{2-} is endothermic ($\Delta H = +2 \text{ kcal mole}^{-1}$) (Stumm and Morgan, 1981). Tabulated thermodynamic data (Sillen and Martell, 1964, 1971) indicates that the formation of CuNTA^- is slightly exothermic; ΔH values of -1.1 and $-1.84 \text{ kcal mole}^{-1}$ were found. In order to sufficiently explain the observed behavior, ΔH values for AlNTA^0 formation must be more exothermic than for CuNTA^- so that a rise in temperature would reduce the tendency of AlNTA^0 formation to a greater extent. However, since the temperature dependence of AlNTA^0 formation was not available, this conjecture remains unverified.

SUMMARY

A variety of factors are important in determining the extent of metal adsorption in the presence of complex-forming ligands. The pH-dependence of metal adsorption is inseparably related to the specific chemical form of the metal prevailing under existing conditions. Changes in system ionic strength and temperature, the presence of competing cations, and the nature of the central metal atom all influence, to various degrees, the adsorption process.

Increasing the concentration of supporting electrolyte, in general, decreased the extent of CuNTA^- adsorption. Ionic strength has a dual tendency to reduce adsorption. First, reduction in the activity coefficient of the principal adsorbate, CuNTA^- , lowered its effective bulk concentration. Second, increasing ionic strength compressed the $\gamma\text{-Al}_2\text{O}_3$ double layer, reducing the potential and increasing (more positive direction) the potential dependent $\Delta G_{\text{elect}}^{\circ}$ and $\Delta G_{\text{solv}}^{\circ}$ contributions to the free energy of adsorption. For conditions that are marginally undersaturated with respect to $\text{Cu}(\text{OH})_2(s)$, increasing ionic strength may preferentially favor precipitation over complex formation, causing an apparent adsorption increase.

The presence of alkaline-earth ions, Ca(II) and Mg(II) , altered the extent of CuNTA^- adsorption in two distinct pH regions: 3-6 and 7.5-10. Two separate mechanisms are involved since at high pH values $\text{Ca(II)} > \text{Mg(II)}$ in its ability to influence uptake; in the acidic range $\text{Mg(II)} > \text{Ca(II)}$. Under mildly alkaline conditions, the competitive influence of Ca(II) and Mg(II) on CuNTA^- formation induced $\text{Cu}(\text{OH})_2(s)$ precipitation. In the pH 3-6 range, specific adsorption of Mg(II) and Ca(II) impeded hydrogen bonding of CuNTA^- to the alumina surface.

The adsorption of NTA complexes of Zn(II) , Cd(II) , Pb(II) , and Ni(II) exhibited a similar pH dependence as that of CuNTA^- , although the magnitude of adsorption was less. Cu(II) binds NTA much more strongly than the other metals, so that the presence of dissolved aluminum is of no consequence, except at low pH values. The adsorption sequence, $\text{Zn} > \text{Cd} > \text{Pb} \approx \text{Ni}$, corresponded directly to the central ion electronegativity, i.e., the least electronegative metal was the most adsorbable. The more electronegative the central metal ion, the weaker the hydrogen bonding of the complexes to the surface.

The uptake of CuNTA⁻, like most adsorption reactions, decreased with increasing temperature. The apparently anomalous trend at the most acidic pH values is related to the temperature dependence of alumina dissolution and/or Cu(II)/Al(III) NTA complex formation.

ACKNOWLEDGEMENT

This work was supported by Grants ENG-77-27379 and ENG-79-10483 from the Water Resources, Urban and Environmental Engineering Program of the National Science Foundation.

REFERENCES

- Baes, C.F., and R. E. Messmer (1976). The Hydrolysis of Cations. Wiley-Interscience, New York.
- Benjamin, M. M., and J. O. Leckie (1981). Environ. Sci. Technol., 15, 1050-1057.
- Butler, J. N. (1964). Ionic Equilibrium. Addison-Wesley, Reading, MA.
- Chubin, R. C., and J. J. Street (1981). J. Environ. Qual., 10, 225-228.
- Davis, J. A., and J. O. Leckie (1978). Environ. Sci. Technol., 12, 1309-1315.
- Elliott, H. A., and C. M. Denneny (1982). J. Environ. Qual., 11, 658-662.
- Elliott, H. A., and C. P. Huang (1979). J. Colloid & Interface Sci., 70, 29-45.
- Garcia-Miragaya, J., and A. L. Page (1976). Soil Sci. Soc. Am. J., 40, 599-612.
- Graham, W. S., The Adsorption Characteristics of Free Amino Acids and Protein at the Solid-Solution Interfaces (1976). M. S. Thesis Univ. of Delaware, Newark, DE.
- Hayward, D. O., and B. M. W. Trapnell (1964). Chemisorption, Butterworth, MA.
- Huang, C. P., and W. Stumm (1973). J. Colloid & Interface Sci., 43, 409-423.
- Jacob, D. G. (1966). Health Physics, 12, 1565-1572.
- James, R. P., and T. W. Healy (1972). J. Colloid & Interface Sci., 40, 42-75.
- Manahan, S. E. (1972). Environmental Chemistry, Willard Grand Press, Boston.
- O'Connor, T. P., and D. R. Kester (1975). Geochim Cosmochim Acta, 39, 1531-1546.
- Packter, A., and H. S. Dhillon (1970). J. Chem. Soc., 1266-1275.
- Rohatgi, N., and K. Y. Chen, J. Wat. Poll. Cont'l Fed., 47, 2298-2311.
- Seidell, A., and W. F. Linke (1958). Solubilities, Inorganics and Metal-Organic Compounds. 4th Edn, Van Nostrand, Princeton.
- Sienko, M. J., and R. A. Plane, Chemistry (2nd Ed.) (1961). McGraw-Hill, New York.
- Sillen, L. G., and A. E. Martell (1964). Stability Constants, Sp. Pub. No. 17, The Chem. Soc., London.
- Sillen, L. G., and A. E. Martell (1971). Stability Constants, Sp. Pub. No. 25.
- Stumm, W., and H. Bilinski (1972). Pror. 6th Int'l Conf. Water Pollut. Res., 39-56, Pergamon Press, New York.
- Stumm, W., and J. J. Morgan, Aquatic Chemistry, (1981). John Wiley Pub. Co.

INFRARED THERMAL REGENERATION OF SPENT ACTIVATED CARBON FROM WATER RECLAMATION

B. M. van Vliet and L. Venter

National Institute for Water Research, Council for Scientific and Industrial Research, P.O. Box 395, Pretoria 0001, South Africa

ABSTRACT

An infrared conveyor-belt furnace was evaluated and utilized to conduct a parametric study on the effects of temperature and residence time on spent granular carbon intraparticle structure and concomitant regeneration efficiencies, incorporating an appraisal of the efficacy of low-temperature long-residence-time regeneration conditions. In addition, a virgin carbon of the same type and particle size fraction as was used in the above regeneration study, was subjected to equivalent temperature and residence time conditions to serve as a control experiment designed to shed light on the effects of regeneration conditions on the activated carbon *per se*. The infrared furnace proved to be an effective system for the regeneration of spent carbon; and an optimum operating region of 800 °C/10 min to 850 °C/5 min was identified. Temperatures in excess of 850 °C, regardless of residence time, must be avoided since excessive structural and pore volume distribution degradation is effected.

KEYWORDS

Activated carbon; infrared; pore volume distribution; regeneration; water reclamation.

INTRODUCTION

This paper is aptly introduced by quoting part of a Theme Introduction entitled 'Controlling organics: Research update', which recently appeared in *Journal of the American Waterworks Association* (Sayre, 1982):

'Although the effectiveness of activated carbon in adsorbing organics is gradually being acknowledged, the economic feasibility of the technique continues to be discouraging. The cost of regenerating carbon constitutes such a large percentage of the operating and maintenance costs of facilities using the technique that research on this aspect of the procedure is necessary before it can be fully accepted.'

Cairo *et al.* (1982) and Clark (1983) present adsorption and regeneration cost information which is essentially in agreement with the above sentiments, underscoring the need for systematic regeneration-related research.

A study was initiated to -

- evaluate the performance and effectiveness of an infrared conveyor-belt furnace for regeneration of water reclamation derived spent granular activated carbon.
- conduct a parametric study with respect to the effects of temperature and residence time on carbon intraparticle structure and concomitant regeneration efficiencies, incorporating an appraisal of the efficacy of low-temperature long-residence-time regeneration conditions.
- subject a virgin carbon (of the same type and particle size as used in the above regeneration study) to equivalent temperature and residence time conditions to serve as a control experiment designed to shed light on the effects of regeneration conditions on the activated carbon *per se*. (It is normally very difficult to distinguish between oxidative loss of adsorbate or pyrolyzed adsorbate, and a similar loss of activated carbon matrix whilst regenerating spent carbon.)
- optimize the selection of regeneration conditions, with due cognizance of the type of (thermal) regeneration equipment used.

EXPERIMENTAL

Infrared Furnace System

The 3 kg/h (12 kW) infrared conveyor-belt furnace (Shirco, Inc., Texas) used in this study is depicted schematically in Fig. 1. The furnace system is fed by a variable speed dewatering screw (not included in the original assembly supplied by the vendor) made of 316 stainless steel. A clearance, just exceeding the upper limit of carbon particle size, has been allowed between the screw and its casing to minimize carbon attrition during conveyance. The equalizer subsection effects a carbon layer of uniform thickness (2 cm for this study) through the action of a level-adjustable spreading screw operating parallel to a small rubber belt which transfers the carbon onto the main furnace conveyor-belt. The drive mechanisms for both belts are interlinked and thus synchronized. Linear belt speed is continuously variable to quantitatively effect residence times ranging from 5 to 60 min.

The main conveyor-belt is of woven design and made of heat resistant stainless steel. Its width is 30 cm and effective length (from carbon acceptance to discharge) 97 cm. At the nominal carbon feed rate of 3 kg/h and for a residence time of 30 min with a layer thickness of 2 cm, the corresponding width of the layer is about 15 cm. Infrared radiant thermal energy is generated by five silicon carbide heating elements. Temperatures are recorded at the points indicated in Fig. 1, using mineral-insulated thermocouples. Temperature control is effected simply and effectively (± 5 °C of setpoint) by means of a proportional controller.

Saturated steam at about 100 °C is introduced at four points in between the upper and lower segments of the main conveyor-belt, which provides for intimate steam-carbon contact during passage through the adsorbent layer. Regenerated, or heat-treated carbon is discharged directly into a quench tank, which also maintains a water seal to prevent inward leakage of air. The furnace shell is constructed of 304 stainless steel, and lined internally with a 12 cm ceramic fibre insulation blanket.

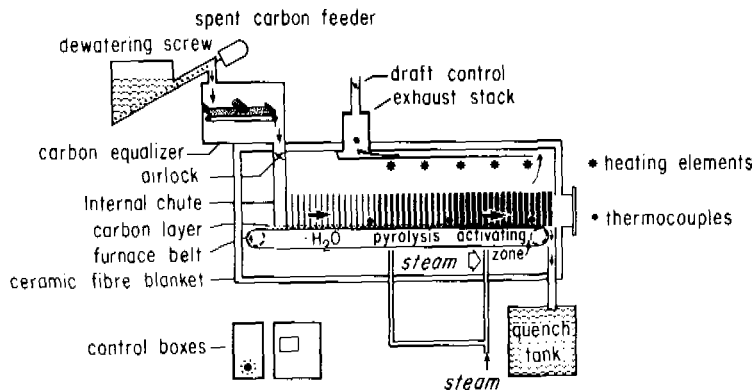


Fig. 1. Schematic diagram of infrared conveyor-belt carbon regeneration furnace

Spent and New Carbon Feed Stocks

Samples of the spent columns of a typical water reclamation plant (National Institute for Water Research, 1981) were taken and analysed to locate a column segment (containing spent 8 x 30 mesh bituminous coal based activated carbon) that would provide about 4 m³ of highly and uniformly saturated carbon. This carbon, used in the reclamation of potable water from secondary treated wastewater, had previously undergone three adsorption-regeneration cycles. The spent carbon was sieved to yield a symmetrically distributed 0.5 to 2.0 mm size fraction, to further increase the uniformity of the feed stock with a view to increasing the validity of comparisons between different regeneration conditions or methods. Some 150 woven polypropylene bags were filled with approximately 20 kg each of the sieved spent carbon, and stored. A consignment of new carbon of the same type was also sieved to yield a 0.5 to 2.0 mm size fraction. This feed stock was used for all new carbon furnace runs. Prior to a furnace run, the relevant feed stock was soaked overnight in tap water in the screw conveyor's holding tank.

Parametric Study

The experimental conditions for the parametric studies were as follows:

Spent carbon. All possible combinations of the temperatures 700, 750, 800, 850, 900 and 950 °C, with the residence times 0 (spent), 5, 10, 15, 20, 25, 30, 35, 40, 45, 50, 55 and 60 min were evaluated. The furnace atmosphere was steam (apart from a small fraction of volatilized adsorbate) in all cases.

New carbon. The same conditions were applied, except that the residence time intervals were increased to 10 min and the 700 °C run was not included. Experience with spent carbon had shown that this could be done without seriously detracting from the usefulness and scope of the data.

Procedures and analyses. Quenched product samples (approx. 2 l) were taken for each combination of operating conditions. At least two residence times were provided at steady state conditions prior to each sampling session. Samples were labelled, dried for 24 h at 110 °C and stored in sealed containers. Analyses were conducted on representative (riffled) portions in respect of pore volume distributions, iodine number and apparent density (the latter two according to the AWWA Standard for Granular Activated Carbon, 1974). (Continuing studies on the above samples are to include other adsorptive and kinetic evaluations.)

The pore volume distributions (including particle density) were determined by means of mercury porosimetry and helium pycnometry (Autopore 9200 and Autopycnometer 1320 respectively, Micromeritics, Inc., Georgia). These determinations were carried out at 20 °C, using a mercury-carbon contact angle of 130 ° and a surface tension of 0.484 N/m.

RESULTS AND DISCUSSION

Infrared Furnace System

Various mechanical modifications and additions were made to the regeneration system during the commissioning stages, in order to ensure its proper and reliable functioning. These included the installation of a 316 stainless steel chimney stack with a built-in draft control mechanism. The draft control damper was fitted with a precise indicator of degree of opening, to enable reproducible control during different regenerations. A dewatering screw/carbon feeder assembly was also installed. The feed chute between the dewatering screw and equalizer assembly became blocked at times and was therefore redesigned to a conical form. The carbon equalizer subsystem blocked repeatedly and had to be redesigned to prevent this from recurring. The temperature recorder was rectified to print thermocouple numbers, and was also calibrated. Steam addition points were installed, together with a safety control valve to prevent water from accidentally entering the furnace. The internal chute which feeds directly onto the main conveyor-belt was modified in order to prevent carbon from spilling off the belt. Extensive resealing of flanges on the furnace shell, using ceramic fibre blanket gaskets or silicon rubber sealant, was required to arrest inward leakage of air.

Useful experience was gained in performing the necessary adjustments to keep the main furnace conveyor-belt correctly tracked. The furnace belt was replaced owing to mechanical distortions which accompanied initial tracking problems. The initial set of five heating elements (the power generation level of which seems to have been stoichiometrically specified) also had to be replaced, because of the invariable decrease in heating capacity resulting from a gradual increase in electrical resistance with usage. Any new heating element system, or replacement elements, should be overdesigned by a considerable factor to ensure a longer and more economically useful life.

Considerable experience was also gained in operating the infrared regeneration system. Factors strongly in favour of this type of furnace, as borne out by local experience, are -

- Rapid heating-up and cooling-down times (approx. 1.5 h each), without any discernible detrimental effect on the ceramic fibre blanket insulation or other internal structures, or excessive energy requirements. The daily runs that were conducted may have adversely affected the useful life of the heating elements, but a compromise operating schedule in practice would be likely to be a five-day working week with shut-down over weekends, especially for a relatively small user not geared to fully continuous supervision.
- Residence time control, owing to the plug-flow nature of a conveyor-belt furnace, was quantitative (compared to the plug-flow-with-dispersion type flow in a multiple hearth furnace, and the dispersed flow in a fluidized-bed furnace).
- Temperature control was excellent, the critical (maximum) temperature normally being controlled to within ± 5 °C of the setpoint.

- Furnace atmosphere control, in the absence of the comparatively large quantities of flue gases associated with fired systems, is simple. Co-currently moving evaporated water, resulting from the initial heating of wet carbon entering the furnace, largely makes provision for the required steam atmosphere. The nominal amount of steam additionally introduced below the layer of carbon on the conveyor-belt ensures good steam-carbon contact and effects a slight over-pressure in the furnace, so as to suppress any inward leakage of air. Klei *et al.* (1975) have shown that the carbon-steam reaction is relatively insensitive to gas (steam) flow rate around the particles and that the external mass transfer rate therefore does not control overall dynamics. This implies that the actual flow rates and flow patterns of steam around the particles are not of primary importance (provided sufficient steam is present). However, the carbon-steam reaction rate was found by Klei *et al.* to vary with the 0.58 power on the steam concentration, emphasizing the distinct benefit that an electrically heated furnace (e.g. infrared) has over gas- or oil-fired furnaces, in that a true steam atmosphere can be attained.

The most important operating complication, based on local experience with the infrared furnace system, was the difficulty (albeit not insurmountable) associated with the proper tracking of the main conveyor-belt.

Pore Size Distributions

Pore volume distributions (micro-, meso- and macropores) were calculated on the basis of pore volume/unit volume of particle, being the most realistic way to compare different carbons under various operating conditions. [During regeneration, intraparticle matter is volatilized/gasified, with a concomitant decrease in particle density. If a unit mass of carbon were to be used as basis, different quantities (volumetrically speaking) would then be involved in comparisons, which would be misleading.]

The following pore size intervals are defined:

Macropore volume (V_{ma}): $60 < D_p \leq 10\,000$ nm, cm^3/cm^3 particle

Mesopore volume (V_{me}): $3 < D_p \leq 60$ nm, cm^3/cm^3 particle

Micropore volume (V_{mi}): $D_p \leq 3$ nm, cm^3/cm^3 particle

Where: D_p = pore diameter, nm.

V_{ma} and V_{me} result directly from mercury porosimetry determinations (Rootare and Prenzlow, 1967), and V_{mi} is calculated as follows:

$$V_{mi} = V_t - V_{ma} - V_{me}$$

Where: V_t = total pore volume ($D_p \leq 10\,000$ nm), cm^3/cm^3 particle
 $= (1 - \rho_p / \rho_s)$

With: ρ_p = particle density via mercury displacement, with pores exceeding 10 000 nm excluded

And: ρ_s = skeletal density via helium displacement

In the most general sense, adsorption will take place predominantly within micropores, the macro- and mesopores serving essentially as transport routes

connecting the external fluid phase with the adsorption sites. Mesopores, however, also serve to adsorb higher molecular mass molecules, most notably humic and fulvic compounds.

Mesopores. Lee *et al.* (1981) have shown that activated carbon pore size distribution is an important parameter relative to the carbon's adsorption capacity and rate of uptake of humic compounds. Pore volume in pores with a diameter of less than 14 nm correlated well with the adsorption capacity of activated carbon for commercial humic acid and peat fulvic acid with a molecular mass of less than 1 000. Pore volume in pores with a diameter of less than 80 nm correlated well with the adsorption capacity of activated carbon for peat fulvic acid with a molecular mass of more than 50 000. Black and Christman (1963) found particle sizes of humic substances extracted from coloured surface waters to be in the range 3.5 to 10 nm in diameter, and some of the smaller pores in carbon would not be accessible for these compounds. Snoeyink *et al.* (1980) also concluded that the smaller pores in high activity bituminous activated carbons are not generally available to the molecules that make up commercial humic acid.

By and large, therefore, the mesopore size range (~3 to 60 nm) emerges as being of particular importance for the removal of humic compounds. [The potential toxicological implications of humic compounds, in that they can act as precursors to the formation of trihalomethanes and other halogenated organic compounds during chlorination of water supplies have been discussed, *inter alia*, by Rook (1974) and Symons (1975). Oliver and Visser (1980), for example, have shown further that humic compounds, particularly in the molecular mass range 20 000 to 30 000, act as precursors for chloroform formation].

Micropores. Pore size ranges of importance in adsorption of lower molecular mass organic compounds have been estimated by Hözel and Sontheimer (1979) as follows: Crystal violet >1.2 nm, iodine >1 nm, naphthalenedisulfonic acid >0.8 nm, benzoic acid >0.6 nm and paranitrophenol >0.5 nm. Johula (1977) correlated iodine number with the surface area of carbon pores larger than 1 nm diameter and molasses number with the surface area of pores larger than 2.8 nm diameter. The key role that micropores play in respect of adsorption of relatively low molecular mass compounds, is supported further by extensive gas-phase adsorption experience with solvent vapours (e.g. Dubinin, 1966; Urano *et al.*, 1982).

Optimization Objective

A comparison of spent (averages for 12 analyses) and virgin (averages for 5 analyses) carbon pore volume distributions, presented in Table 1, shows that both V_{me} and V_{ma} in the spent state, are already greater than in the virgin state. This is because the spent carbon in question had previously undergone three adsorption-regeneration cycles (in a water reclamation context, with multiple-hearth furnace regeneration), and progressive pore enlargement had accordingly taken place. Although it is intended as the topic of later investigation, this study provided sufficient qualitative evidence to support the notion that excessive meso- and macropore volume increases, over and above those present in virgin carbon, will cause a rapid and undesirable decrease in particle hardness and abrasion resistance. On the other hand, since adsorption takes place primarily in the micropores, V_{mi} must be maximized during regeneration.

A natural course of events during regeneration would be the removal (volatilization, gasification) of adsorbate plus possible structural damage to the activated carbon matrix *per se*, which would manifest as a progressive increase in pore size, with a concomitant decrease in V_{mi} and/or an increase in V_{me} and V_{ma} .

TABLE 1 Pore Size Distributions for New and Spent Carbon
(0.5-2.0 mm Particle Size Fraction)

| Parameter | New carbon | Spent carbon |
|---|------------|--------------|
| Micropore volume ¹ , V _{mi} | 0.290 | 0.135 |
| Mesopore volume ¹ , V _{me} | 0.161 | 0.180 |
| Macropore volume ¹ , V _{ma} | 0.187 | 0.201 |
| Total pore volume ¹ , V _t | 0.638 | 0.516 |
| Particle density ² , ρ _p | 0.790 | 0.920 |

¹cm³/cm³ particle ²g/cm³ particle (via mercury displacement)

The optimization objective was therefore to attempt to maximize V_{mi}, with as little as possible increase in V_{me} and V_{ma}, except for an initial restoration, if applicable, of V_{me} and V_{ma} to new carbon levels. In any event, although V_{me} is important for humic compound adsorption, such volume should not be developed at the expense of V_{mi}.

Parametric Study - Spent Carbon

Pore size distribution results for the parametric study with regard to temperature and residence time, for spent carbon regeneration, are presented in Fig. 2. The respective graphs for micropore volume and meso- plus macropore volume (both in cm³ pore volume/cm³ particle) each represent the experimental matrix of six temperatures by 13 residence times, with additional smooth interpolation lines between data lines to facilitate 3-D representation.

The general trend for (V_{me} + V_{ma}) is to increase with increasing temperature and residence time. At low temperatures (700 to 800 °C), (V_{me} + V_{ma}) does not increase extensively, but at higher temperatures a very distinct increase occurs, with both temperature and residence time. The general trend for V_{mi} is not consistently monotonic as for V_{me} and V_{ma}, but entirely different (strictly non-linear) shapes are adopted for different temperatures. The non-linearity and often non-monotonic nature of the V_{mi} curves are of crucial importance in optimizing procedures, since maximization of V_{mi} is a major objective and simple interpolations with regard to temperatures or residence times would be unsuitable.

The overall optimum point (800 °C/8 min) is evident from Fig. 2, where V_{mi} is maximized with hardly any (V_{me} + V_{ma}) increase. The optimum extent of V_{mi} recovery at 800 °C/8 min was almost double the peak recovery achievable for 950 °C regeneration (at 5 min), illustrating that regeneration at very high temperatures for brief periods is not a viable route at all. The notion, however, of operating at low temperature (~700 °C) for an extended residence time appears to be a technically feasible route to achieving extensive restoration of pore size distribution properties. However, a residence time on the order of one hour will require a substantially greater capital investment than the more conventional times of about 10 min and economic factors also require consideration before selection of actual design conditions. The 100 degree favourable decrease in temperature (800 → 700 °C) though, is not likely to offset the increased residence time requirement (10 → 60 min).

The new-carbon level for V_{mi} was not approached at any combination of temperature or time. (Figs 2 and 3; Table 1). This is not surprising, since a fourth-cycle spent carbon was being used and a measure of pore enlargement (with the concomitant irreversible decrease in V_{mi} and increase in V_{me} and V_{ma}) would have

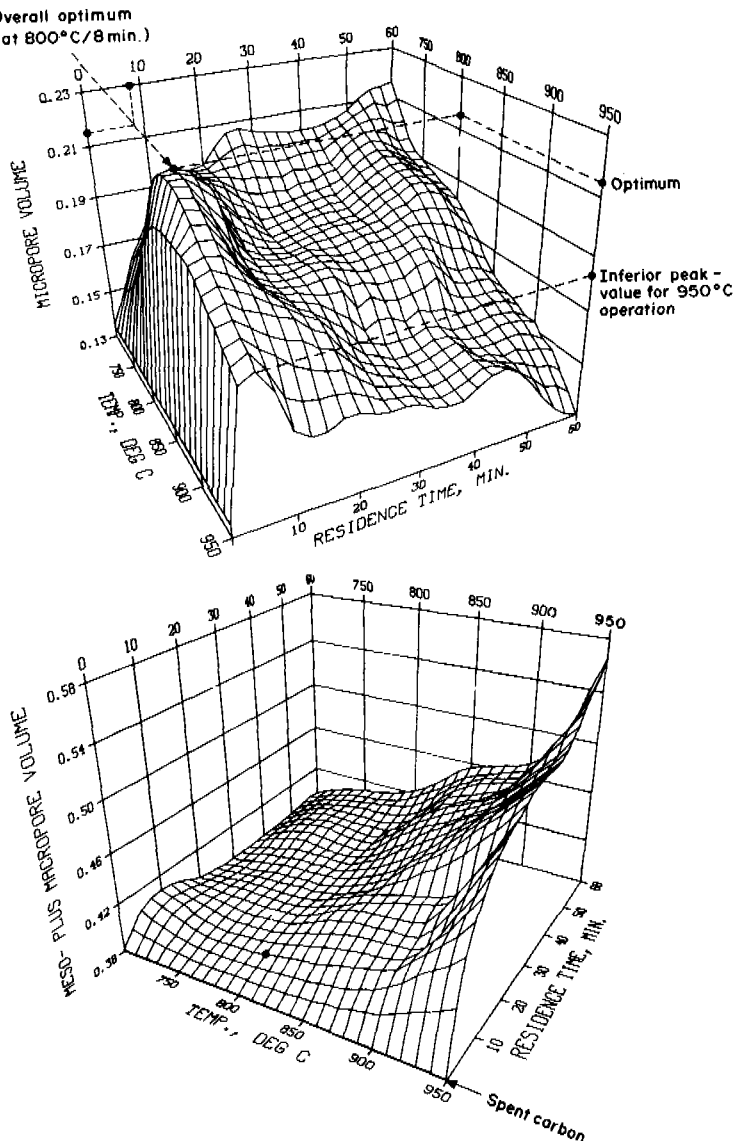


Fig. 2. Regeneration of spent carbon: Effect of temperature and residence time on micropore and meso- plus macropore volumes (in cm^3 pore volume/ cm^3 particle)

previously taken place. It would therefore not be a realistic objective, in practice, to strive at regaining new-carbon status in all respects during regeneration, but to accept the given spent carbon and then improve its quality in accordance with the objectives defined earlier. The hazards of attempting to regenerate at high temperatures (900 to 950 °C), even by using very short residence times, have been demonstrated: Maximum achievable V_{mi} levels are considerably below those reached at lower temperatures, and V_{me} and V_{ma} are excessively high. The value of V_{mi} reaches an all-time low, which is even less than the spent carbon value, for regeneration at 950 °C/60 min. Cairo *et al.* (1982),

evaluating regeneration efficiency by conducting column breakthrough curves, similarly found that carbon which had been regenerated at 962 °C was performing below par; the authors speculated that intraparticle structural changes may have been responsible, which is likely to have been the case. Furthermore, although the determination of hardness and abrasion resistance of samples for the various regeneration conditions is still pending, it was qualitatively obvious that the 950 °C/30 min+ carbons had become impractically soft.

Fig. 3 highlights the different shapes of V_{mi} curves obtained at different temperatures. A peak appears to start developing at a residence time of 25 min for 700 °C regeneration. This peak V_{mi} -value shifts to the left as temperature increases to about 800 °C (logically, reaction rates increase, requiring shorter reaction times) and upward to effect improved restoration of micropore volume. Above 800 °C, the V_{mi} peak becomes more narrow (which would make control of operations at precisely those conditions more difficult), and drops rapidly as temperature increases to 950 °C. The 800 °C/10 min to 850 °C/5 min range of operating conditions in any event, represents the optimum area of interest. Meso- and macropores are not significantly affected in this range (Figs. 2 and 3), also conforming well to the optimization objective.

Fig. 4 presents data similar to those of the previous figure, but using residence time as parameter and temperature as independent variable. The non-linear influence of operating conditions on V_{mi} and regeneration efficiency is apparent. A minimal increase in ($V_{me} + V_{ma}$) takes place up to about 850 °C, making this temperature range (<850 °C), desirable. Above 850 °C, and especially at 950 °C, extensive ($V_{me} + V_{ma}$) increases occur, with a concomitant (qualitatively observed) reduction in mechanical strength. Long residence times (~ 60 min) may only be selected for very low temperatures (e.g. 700 °C), since a rapid increase in ($V_{me} + V_{ma}$) takes place with increasing temperature (i.e. at prolonged residence time). At 800 °C, a residence time of 20 min should not be exceeded, and at 850 °C, 5 min should not be exceeded.

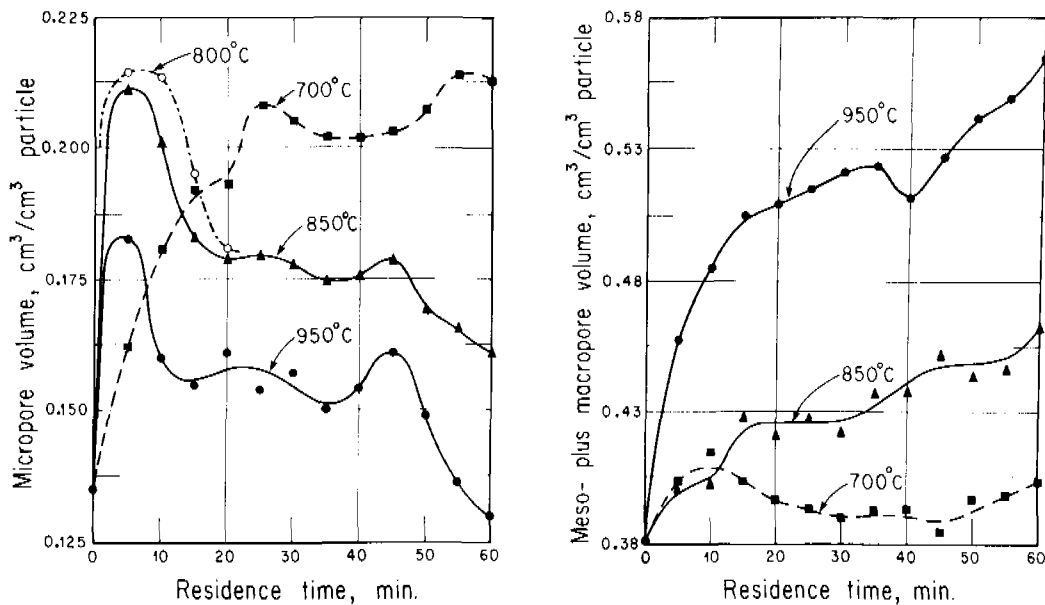


Fig. 3. Regeneration of spent carbon: Comparative temperature effects on intraparticle structure

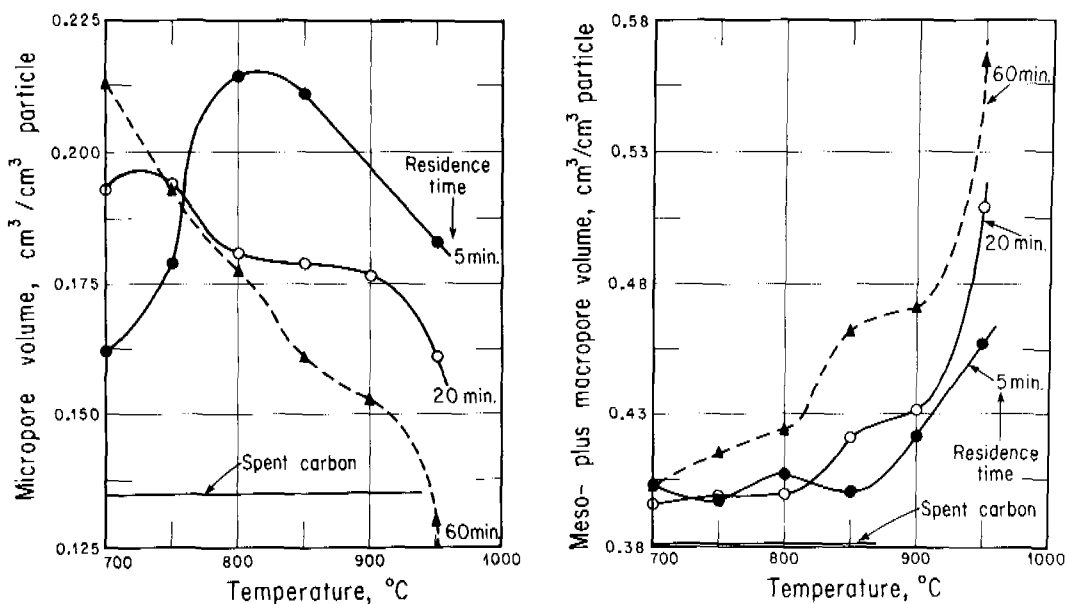


Fig. 4. Regeneration of spent carbon: Comparative residence time effects on intraparticle structure

Parametric Study - New Carbon

A limitation in the interpretation of results pertaining to an adsorbate-free system is that adsorbate within the porous structure of a spent activated carbon could, in principle, have different effects on the activated carbon matrix during regeneration. For example, organic adsorbate, or carbonized adsorbate might well form a protective layer which could retard damage to the matrix; however, adsorbed inorganic constituents (e.g. metals) could well catalyze the oxidative loss of the activated carbon. Nevertheless, knowledge of the effects of regeneration conditions on the carbon matrix remains useful in that broad operating regions that are acceptable, or should be avoided, can be delineated.

Fig. 5 depicts pore volume distribution results for the thermal treatment of new carbon between 750 to 950 °C, and 0 (spent) to 60 min residence time. (Smooth extrapolations have been made down to 700 °C, to facilitate comparison with the corresponding graphs for spent carbon.) Up to about 850 °C, intraparticle structural changes are, by and large, marginal. Above 850 °C, temperature plays an increasingly important role; the effects being similar to that experienced with spent carbon, i.e. micropore volume is lost and meso- plus macropore volume progressively gained, with increasing residence time and temperature.

The results for the thermal treatment of new carbon study can also be seen from Fig. 6. The curves for micropores, and meso- plus macropores at 850 °C treatment, are largely representative of the effects of treatment at between 750 and 850 °C. In this region (750 - 850 °C/0 - 60 min), damage to the porous structure is only marginal. The previously selected optimum operating region for regeneration of spent carbon therefore lies within the acceptable boundaries for thermal treatment of activated carbon *per se*. Above 850 °C, and especially for residence times exceeding 20 min, structural damage (decreasing V_{mi} , and increasing V_{me} plus V_{ma}) occurs to an unacceptable degree.

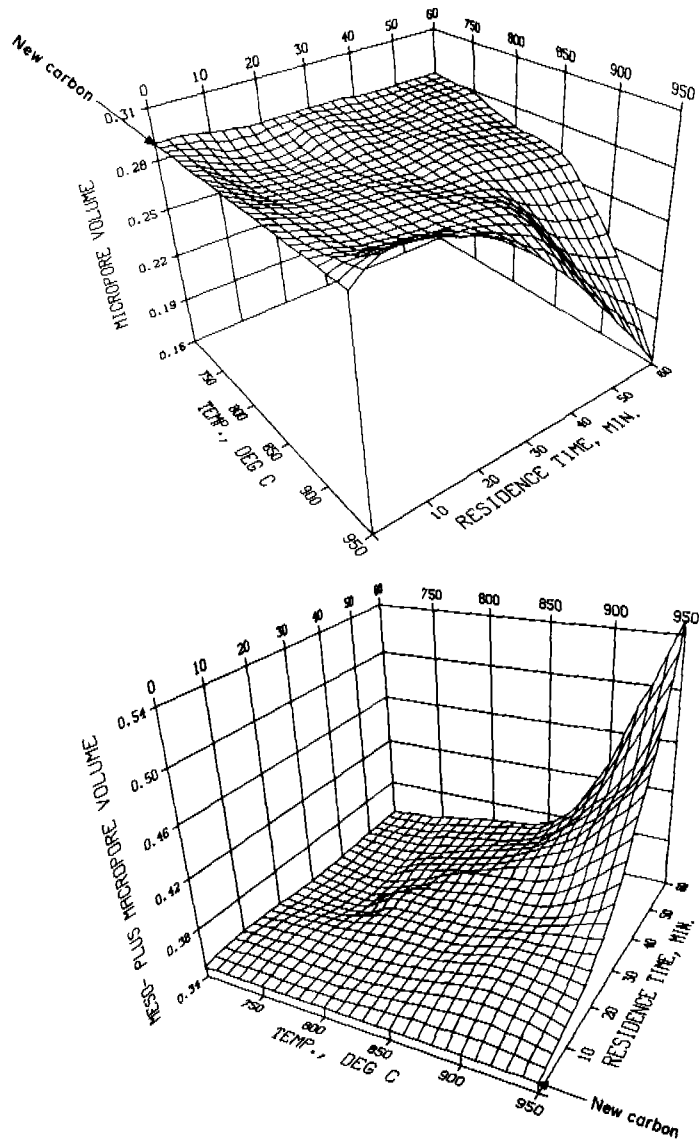


Fig. 5. Thermal treatment of new carbon: Effect of temperature and residence time on micropore and meso- plus macropore volumes (in cm^3 pore volume/ cm^3 particle)

The various sequential reactions typical of thermal treatment of porous activated carbon are illustrated in Fig. 7, which pertains to a temperature of 950 °C. During the first 10 min of treatment, initial small increases in micropore and macropore volumes are observed. This could be the result of removal of small amounts of substances adsorbed during transport and storage, and/or a further refinement in the degree of activation of the raw material. During the residence time interval 10 to 30 min, an almost stoichiometric conversion of micropores to mesopores takes place, with macropores being largely unaffected. The slight increase in total pore volume during this period is likely to be the result of

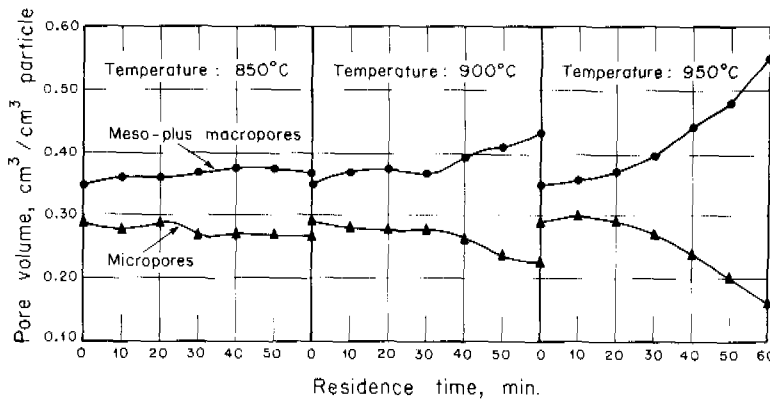


Fig. 6. Thermal treatment of new carbon: Comparative temperature effects on intraparticle structure

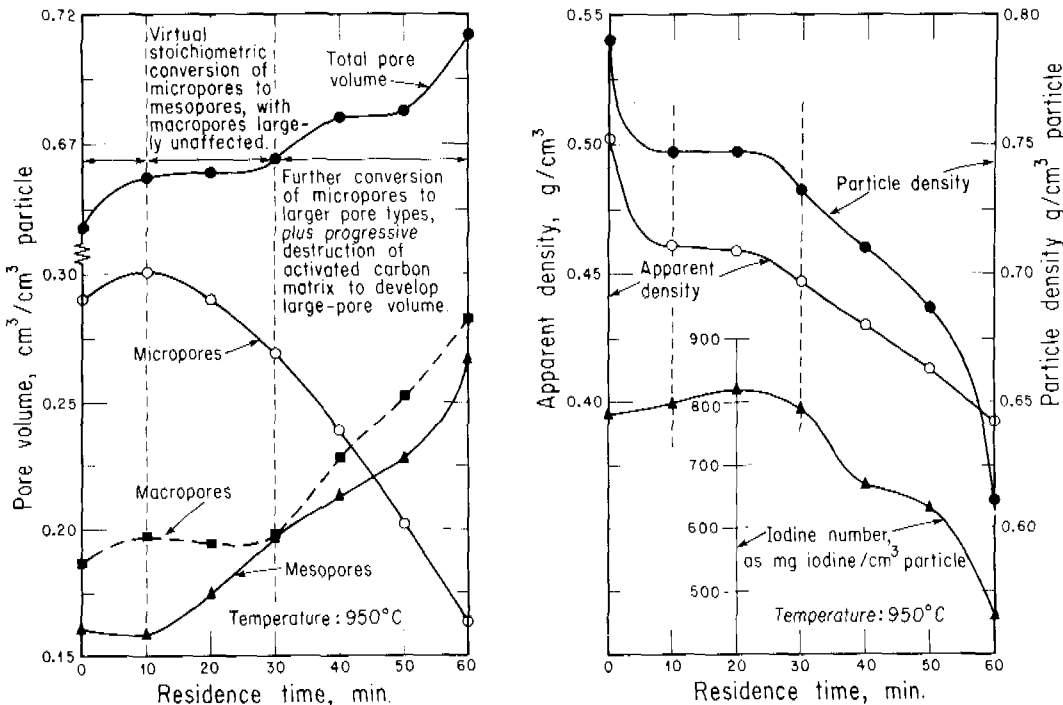


Fig. 7. Thermal treatment of new carbon: Stages of intraparticle structural change

inter-micropore matrix erosion. Beyond 30 min residence time a further conversion of micropores to larger pore (meso- and macro-) types occurs, plus a progressive destruction of activated carbon matrix to develop additional large-pore volume. The net result is an extensive loss of V_{mi} , and the enlargement of V_{me} and V_{ma} , with a concomitant diminishing degree of mechanical strength. Consideration of total pore volume only, would therefore be very misleading since the net effect of substantial intraparticle changes is reflected in V_t ; micropore volume decreases by 44% during the full 60 min residence time, and meso- and macropore volumes increase by 66% and 50%, respectively. This aspect has

important practical implications, particularly in respect of operation within 10 to 30 min residence time, as supported by the data for particle density, apparent density and iodine number (Fig. 7). None of the latter properties, nor total pore volume changes much here, and yet micropores are rapidly being converted to mesopores. The desired 'endpoint' (i.e. at about 10 min residence time) is in this case not sensitive to the routinely monitored apparent density (or particle density) and iodine number, and the on-line monitoring of an additional quality index is therefore desirable.

CONCLUSIONS

The infrared conveyor-belt furnace proved to be an effective system for the regeneration of spent carbon, with quantitative residence time, temperature and furnace atmosphere control capability. Rapid heating-up and cooling-down times facilitate intermittent operating schedules; however, proper conveyor-belt tracking requires special attention.

Optimization objectives relating to the intraparticle structure of carbon were formulated, comprising the maximization of micropore volume with as little as possible enlargement of meso- and macropore volumes.

The micro-, meso- and macropore volume relationships as a function of regeneration temperature and residence time are strictly non-linear, and often non-monotonic (especially V_{mi}). This is of crucial importance in optimizing procedures, since maximization of V_{mi} is a major objective and simple interpolations with regard to temperatures and residence times would be unsuitable, except within a narrow range of optimum operating conditions.

Regeneration temperatures in excess of 850 °C (regardless of residence time) must be avoided since excessive meso- and macropore enlargement occurs, and the extent of micropore restoration is greatly diminished. It was impossible to effectively regenerate spent carbon at 900 to 950 °C, even by using very short residence times: Maximum achievable V_{mi} levels were considerably below those reached at lower temperatures. Furthermore at 950 °C/30 min+, the mechanical strength of the granules becomes severely impaired.

Within the acceptable regeneration temperature range <850 °C, an optimum operating region was identified, namely 800 °C/10 min to 850 °C/5 min. It was confirmed that low-temperature long-residence-time regeneration (700 °C/60 min) is indeed technically effective; however, a considerable capital investment would be required to accommodate the prolonged in-furnace residence, and the former operating region is therefore more attractive. Within this region, the 850 °C/5 min regeneration approach would be poised at a comparatively sharp V_{mi} peak, requiring the quantitative process control capability of, for example, a conveyor-belt furnace, but which may pose difficulties in the case of, for example, a fluidized-bed furnace (with dispersed flow). All matters considered, regeneration at 800 °C/8 - 10 min emerges as most desirable.

The equivalent parametric study with regard to new carbon showed that intraparticle structural damage manifests in the 850 °C+/20 min+ region, indicating that the previously selected optimum operating region for regeneration of spent carbon lies within the acceptable boundaries for thermal treatment of activated carbon matrix *per se*.

This study has shed light on the various steps that occur during thermal treatment of porous activated carbon, including the conversion of small to larger pore types, with the concomitant intraparticle structural changes as a function of reigning treatment conditions.

ACKNOWLEDGEMENTS

Mr J. Streeter contributed to the 3-D plotting of data, and the late Mr E. Motau assisted proficiently with the experimental work. The substantive financial support of this work by the Water Research Commission is gratefully acknowledged. This paper is published by permission of the Chief Director of the National Institute for Water Research, CSIR.

Mention of commercial products or trade names does not constitute endorsement or recommendation for use.

REFERENCES

- AWWA Standard for Granular Activated Carbon* (1974). AWWA B604-74 (first edition). *J. Am. Wat. Wks Ass.*, 66, 672-681.
- Black, A.P. and Christman, R.F. (1963). Characteristics of colored surface waters. *J. Am. Wat. Wks Ass.*, 55, (6), 753.
- Cairo, P.R., Coyle, J.T., Davis, J.J., Neukrug, H.M., Suffet, I.H. and Wicklund, A. (1982). Evaluating regenerated activated carbon through laboratory and pilot-column studies. *J. Am. Wat. Wks Ass.*, 74, (2), 94-102.
- Clark, R.M. (1983). Optimising GAC systems. *J. environ. Engng.*, 109, (1), 139-156.
- Dubinin, M.M. (1966). In: *Chemistry and Physics of Carbon*, P.L. Walker, Jr, (Ed.), Vol. 2, Marcel Dekker, New York.
- Hölzel, G. and Sontheimer, H. (1979). Untersuchungen zur Optimierung der Aktivkohleanwendung bei der Trinkwasseraufbereitung am Rhein unter besonderer Berücksichtigung der Regeneration nach thermischen Verfahren. Heft 12, *Veröffentlichungen des Bereichs und Lehrstuhls für Wasserchemie*, University of Karlsruhe.
- Juhola, A.J. (1977). Manufacture, pore structure and application of activated carbons, Part II. *Kemia-Kemi*, 4, (12), 653.
- Klei, H.E., Sahagian, J. and Sundstrom, D.W. (1975). Kinetics of the activated carbon steam reaction. *Ind. & Eng. Chem. Process Des. & Dev.*, 14, (4), 470-473.
- Lee, M.C., Snoeyink, V.L. and Crittenden, J.C. (1981). Activated carbon adsorption of humic substances. *J. Am. Wat. Wks Ass.*, 73, (8), 440-446.
- National Institute for Water Research (1981). *Manual for Water Renovation and Reclamation*, 2nd ed., CSIR Technical Guide K42, Pretoria.
- Oliver, B.G. and Visser, S.A. (1980). Chloroform production from the chlorination of aquatic humic material: The effect of molecular weight, environment and season. *Wat. Res.*, 14, (8), 1137-1141.
- Rook, J.J. (1974). Formation of haloforms during chlorination of natural waters. *Wat. Treat. & Exam.*, 23, (2), 234.
- Rootare, H.M. and Prenzlow, O.F. (1967). Surface areas from mercury porosimeter measurements. *J. phys. Chem.*, Ithaca, 71, 2733-2736.
- Sayre, I.M. (1982). Theme introduction - controlling organics: Research update. *J. Am. Wat. Wks Ass.*, 74, (2), 57.
- Snoeyink, V.L., Chudyk, W.A., Beckman, D.D., Boening, P.H. and Temperly, T.J. (1980). *Bench-Scale Evaluation of Resins and Activated Carbons for Water Purification*. Report no. ISU-ERI-AMES 80091, Iowa State University, Ames, Iowa.
- Symons, J.M., Bellar, T.A., Carswell, J.K., De Marco, J., Kropp, K.L., Robeck, G.G., Seeger, D.R., Slocum, C.J., Smith, B.L. and Stevens, A.A. (1975). National organics reconnaissance survey for halogenated organics. *J. Am. Wat. Wks Ass.*, 67, (11), 634-648.
- Urano, K., Omori, S. and Yamamoto, E. (1982). Prediction method for adsorption capacities of commercial activated carbons in removal of organic vapors. *Environ. Sci. & Technol.*, 16, (1), 10-14.

ORGANIC REMOVAL MECHANISMS IN BIOPHYSICAL TREATMENT SYSTEMS

J. R. Schultz* and T. M. Keinath**

**Department of Civil Engineering, University of Utah, Salt Lake City, Utah, 84112, U.S.A.*

***Department of Environmental Systems Engineering, Clemson University, Clemson, South Carolina, 29631, U.S.A.*

ABSTRACT

An experimental program was conducted to evaluate the significance of enhanced biodegradation, bioregeneration, and metabolic end product (MEP) adsorption in a bench-scale biophysical reactor using phenol as the substrate. Radiotracer methods and a desorption-extraction procedure that measures the amount of adsorbed phenol were used to discriminate between the various mechanisms. The results showed the major benefit of PAC addition under steady-state conditions to be MEP adsorption. Furthermore, adsorption reversibility was established as the controlling mechanism for bioregeneration. Reversibly adsorbed phenol could be desorbed to regenerate the PAC, but irreversibly adsorbed MEP could not. PAC, therefore, acts as a storage reservoir during shock loads via an adsorption-desorption sequence.

KEYWORDS

Activated carbon; activated sludge process; organics removal; adsorption; desorption; biodegradation; biological regeneration.

INTRODUCTION

One method of using activated carbon in wastewater treatment is the addition of powdered activated carbon (PAC) to the aeration basin of an activated sludge system. The PAC and biomass combine to form a dark sludge with good settling properties. This process has become known as the DuPont PACT or biophysical treatment process. Early developmental work by Grulich et al. (1973) showed that PAC addition may provide several benefits including improved organic removals. Further work has suggested that the improved organic removals may not be explained by adsorption alone and that interactions between the PAC and biomass play an important role in the removal of organics by PACT systems. These interactions can be grouped into three different phenomena: enhanced bioactivity, bioregeneration of the PAC, and metabolic end product (MEP) adsorption.

Enhanced bioactivity is the ability of PAC to increase the biological assimilation of organics by an activated sludge system. This phenomenon may be due to a number of separate mechanisms including increased organic concentrations at the PAC

surface (Kalinske, 1972), extended contact time between the biomass and adsorbed organic compounds (Flynn, 1975), increased oxygen concentrations at the PAC surface (Ying and Weber, 1979), adsorption of toxic compounds (Thibault et al., 1977), and alterations of the microbial population (Robertaccio, 1976). To date, the only mechanism that has definitively been shown to be operative is protection of the microbial population by the adsorption of toxic compounds (Nayar and Sylvester, 1979; Sundstrom et al., 1979). Enhanced bioactivity in the absence of toxic compounds, however, has not been unequivocally established. Studies (Flynn, 1975; Robertaccio, 1976; DeWalle and Chian, 1977; Lee and Johnson, 1979) based on measuring the amount of substrate remaining in the liquid phase suggest that PAC enhances both the rate and extent of biological activity, but these results are difficult to interpret because the experiments do not effectively discriminate between adsorption and biological assimilation mechanisms. Another approach has been to compare the oxygen consumption during batch biodegradation tests with and without PAC (Scaramelli and DiGiano, 1973; Hals, 1974). Although no evidence of enhanced bioactivity has been observed in these experiments, the extent of adsorption of dissolved oxygen onto the PAC (Prober et al., 1975) has not always been considered. It is obvious that further research must be conducted to define the fundamental operative mechanisms.

Bioregeneration is the process by which adsorbed organics become available for biodegradation, thereby renewing the PAC surface for further adsorption. Adsorbed organics may be removed from the PAC surface either by desorption, direct bacterial assimilation, or exoenzymatic attack. The results of oxygen uptake (Hals, 1974) and repeated feeding experiments (Flynn, 1976; McShane and Rao, 1981) indicate that a reversibly adsorbed substrate (phenol) can be removed from the carbon surface. For more complex substrates, however, the extent of bioregeneration appears to be limited (Maqsood and Benedek, 1977). Since complex substrates are likely to be irreversibly adsorbed, Flynn et al. (1976) and Benedek (1980) have suggested that bioregeneration is controlled by the reversibility of adsorption, but further research is needed to verify this claim.

Previous work (Daigger and Grady, 1979) has established that a major portion of the residual organics in the effluent of activated sludge systems is not the original substrate, but is MEP synthesized by the biomass. Several studies (Kim et al., 1976; Martin and Iwugo, 1980; Tsezos and Benedek, 1980) have shown that a significant fraction of the MEP is adsorbable. Adsorption of MEP, therefore, may account for the increased organic removals that result from PAC addition. Furthermore, although MEP are generally considered to be nonbiodegradable, work by Chudoba et al. (1969) and White (1981) indicates that concentrated MEP can be biologically assimilated. This suggests that PAC may enhance the biodegradation of MEP if the concentration of MEP at the PAC surface is increased by adsorption. Since many previous studies on PACT systems have failed to consider the possible role of MEP adsorption and biodegradation mechanisms, further research is necessary to clarify the fate of MEP in these systems.

The research program reported herein was undertaken to meet the overall objective of evaluating the importance of the various proposed mechanisms that may be involved in the removal of a simple substrate that is both adsorbable and biodegradable in a biophysical system. This objective is obviously very broad in scope and was reduced to six specific objectives: (1) determine whether PAC addition results in enhanced biodegradation; (2) determine the extent of bioregeneration of adsorbed substrate; (3) determine the relative importance of desorption and displacement mechanisms in the removal of adsorbed substrate; (4) determine the importance of MEP adsorption and desorption mechanisms; (5) determine the extent of biodegradation of MEP due to PAC addition; and (6) determine the extent of bioregeneration of adsorbed MEP.

The major difficulty in meeting these objectives is the development of an experimental methodology that effectively discriminates between the various mechanisms. One technique that has the potential for accomplishing this is the use of ^{14}C radiotracers. This technique consists of introducing a ^{14}C -labeled compound into a reactor and subsequently measuring the ^{14}C in the various components of the system with time. The major advantage of radioisotopes is their ability to trace dynamic mechanisms that often cannot be studied by other methods. In addition, the detection sensitivity of radiotracers far exceeds that of most other chemical or physical methods.

To aid in planning experiments, a conceptual model of a biophysical system was developed as shown in Figure 1. The model divides the liquid-phase carbon into substrate and MEP components, the solid-phase carbon into biomass and PAC components, and the evolved CO_2 into solution-phase and gaseous-phase components. The transfer rates between the various components represent many of the interactions that may occur between the biomass and PAC. Thus, a soluble substrate that is both adsorbable and biodegradable can be removed from solution by either biological assimilation or adsorption on the PAC. Once the substrate has been assimilated by the biomass, the carbon atoms can be evolved as CO_2 , excreted as MEP, or synthesized into biomass. The adsorbed substrate may be removed from the PAC surface by either desorption or direct bacterial attack. The soluble MEP may then be adsorbed on the PAC or reassimilated by the biomass via the proposed concentration enhancement mechanism.

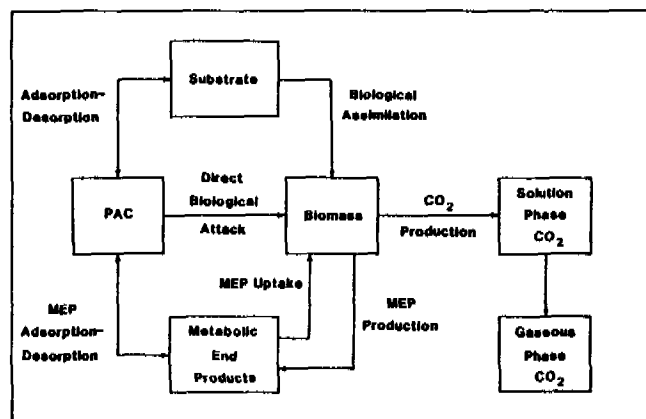


Fig. 1. Biophysical process mechanisms

MATERIALS AND METHODS

Stock cultures. The microorganisms used throughout this study were obtained from parallel biological and biophysical stock cultures maintained in the laboratory. The 5-l cultures were operated on a fill-and-draw basis with a solids residence time of 5 days. Phenol was used as the sole carbon source in the nutrient growth medium except during a two-week start-up period when a mixture of glutamic acid and phenol was used to acclimate the cultures to phenol. Phenol was used because it is both adsorbable and biodegradable, which allows study of the interactions between the PAC and biomass. Two grams of PAC (Westvaco Nuchar SA-15) were added daily to the biophysical culture to maintain a mixed liquor PAC concentration of 2000 g/m^3 . This concentration ensured that approximately 50 percent of the phenol added to the biophysical culture was immediately adsorbed and that the PAC would

be entrapped by the biological flocs during settling. The stock cultures were monitored weekly for suspended solids, pH, and soluble organic carbon (SOC) by taking samples immediately before sludge wasting. A nitric acid solubilization technique (Lee, 1977) was used to determine the relative amounts of PAC and biological solids in the biophysical culture. Both cultures were acclimated for 30 days (6 solids residence times) before the subsequent experiments were performed.

Radiotracer batch experiments. The reactor used for the radiotracer studies (Figure 2) consisted of a one-liter beaker sealed with a rubber stopper. The exhaust gas was routed through a series of three traps. The first trap was used to remove any water in the exhaust stream. The next two traps contained 15 ml of a carbon dioxide adsorbing solution consisting of a 1:2 v/v ethanolamine: ethylene glycol monomethyl ether (EGME) mixture.

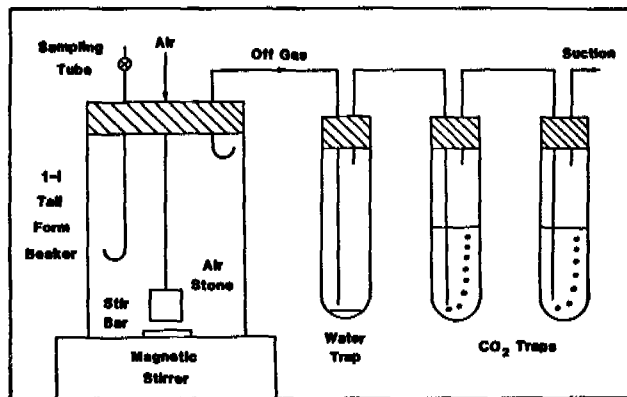


Fig. 2. Experimental apparatus used for ^{14}C batch studies

The ^{14}C batch experiments were conducted with waste sludge obtained from the acclimated stock cultures. The procedure consisted of placing 750 ml of sludge into the reactor and allowing the sludge to settle for one hour before removing 600 ml of supernatant by vacuum. A 600-ml aliquot of the nutrient growth medium containing 2.0 μCi of ^{14}C -phenol was then added to the settled sludge. Make-up PAC was also added to the biophysical culture. The reactor was then quickly sealed and aeration initiated to start the experiment. Samples were taken by replacing the CO_2 traps containing the ethanolamine solution and withdrawing a 3-ml portion of the reactor contents through the sampling tube. Immediately after collection, the mixed liquor samples were filtered to separate the liquid and solid-phase components. The filtrates were then acidified with HCl and purged with N_2 to separate the liquid-phase ^{14}C into organic and inorganic (CO_2) components. An ethanolamine-EGME solution was used to trap the purged $^{14}\text{CO}_2$ for subsequent radioassay.

The amount of ^{14}C in the various components was determined by liquid scintillation counting. The ^{14}C in solid-phase samples was converted to $^{14}\text{CO}_2$ using a wet combustion procedure (Jeffay and Alvarez, 1961). Aqueous samples were prepared for counting by pipetting 2 ml of the purged filtrates into a vial containing 15 ml of a dioxane-based solution. Counting was performed using a Beckman LS 7500 instrument. Quench corrections were performed by the internal standardization method using a certified ^{14}C toluene solution.

Adsorbed phenol batch experiments. The extent of bioregeneration was examined by developing a procedure that measures the amount of phenol adsorbed on the PAC in a

biophysical culture. This technique consisted of desorbing the adsorbed phenol using a 100-ml nutrient salt solution wash. A preliminary experiment established that the efficiency of the desorption wash procedure was 85 percent. The desorption technique was employed in several batch experiments conducted with both stock cultures. The experiments with the biological culture were used to ensure that the phenol recovered from the desorption washes of the biophysical culture was derived from the PAC surface and not the biomass. Samples were taken from the cultures at various times after nutrient addition and filtered through a prewetted glass fiber filter. The filter, which contained the solids, was then transferred to a clean filter apparatus and washed with 100 ml of the nutrient salt solution to desorb the phenol. A direct acetylation-extraction-chromatography procedure (Mathew and Elzerman, 1981) was used to determine the amount of phenol in the washes.

Phenol desorption-displacement experiments. Two experiments were conducted to evaluate the effects of MEP on the adsorption-desorption characteristics of phenol. The first was performed to elicit the competitive adsorption interactions between MEP and phenol. Two sets of isotherm bottles were prepared. The first was prepared with the nutrient growth medium while the second was prepared with filtered biological stock culture supernatant (MEP source) spiked with phenol. After agitation, samples were withdrawn and centrifuged to remove the PAC. The supernatants were then analyzed for phenol by direct aqueous-injection gas chromatography. A second experiment was conducted to develop desorption isotherms for phenol in the presence and absence of MEP. Portions of the bottles from the previous competitive isotherm experiment were diluted with 10 ml of either the nutrient salt solution or filtered biological stock culture supernatant. The bottles were then equilibrated and a sample withdrawn for analysis of residual phenol. The dilution procedure was repeated until 3 samples were taken from each bottle.

¹⁴C MEP synthesis. Radioactive MEP was synthesized via batch biodegradation of ¹⁴C phenol using the same procedure described for the ¹⁴C batch experiments, with the exception that 20 µCi of ¹⁴C phenol was added to the culture. The large amount of radioactivity was used because only 2 percent of the ¹⁴C added ultimately is transformed to ¹⁴C MEP. After the culture was aerated for 24 hours, the sludge was allowed to settle before the supernatant was filtered through a glass fiber filter. The radioactivity remaining in the filtrate was assumed to be entirely in the form of metabolic end products. This assumption was based on the results of the batch studies which showed that the phenol remaining in solution after 6 hours of aeration was negligible.

MEP batch removal experiment. To examine the possibility of enhanced biodegradation of MEP, ¹⁴C-labeled MEP was added to a sample of biophysical sludge and the fate of the ¹⁴C was monitored with time. Procedurally, this experiment was similar to the previous batch experiments except that synthesized ¹⁴C-MEP was added instead of the nutrient growth medium.

MEP adsorption-desorption experiments. To evaluate the adsorbability of MEP, an adsorption isotherm for MEP was developed using the bottle technique used to develop the phenol isotherms. Two desorption experiments were also performed. One consisted of dilution with a nutrient salt solution to determine the extent of desorption by dilution. The other consisted of dilution using a nutrient salt-phenol solution to determine the extent of desorption via displacement by phenol. Procedurally, these experiments were similar to those conducted for phenol.

Adsorbed MEP biodegradation experiment. Direct biodegradation of adsorbed MEP was examined by adding PAC with adsorbed ¹⁴C MEP to a sample of biophysical sludge and

monitoring the fate of the ^{14}C . PAC with adsorbed ^{14}C MEP was prepared by adding a 100-ml aliquot of the ^{14}C MEP to an isotherm bottle containing 0.2 g of PAC. The bottle was agitated for 24 hours before its contents were centrifuged. The centrate was then carefully decanted to leave a PAC pellet with adsorbed ^{14}C MEP which was transferred to the biophysical sludge to initiate the experiment.

RESULTS AND DISCUSSION

Radiotracer batch experiments. The ability of PAC to enhance the biodegradation of phenol was evaluated by comparing the relative amounts of $^{14}\text{CO}_2$ evolved during the ^{14}C batch experiments as shown in Figure 3. Although the evolution of $^{14}\text{CO}_2$ from the biological culture exhibited a short lag period that was not observed in the PACT culture experiment, the rate of $^{14}\text{CO}_2$ evolution during the period of rapid substrate assimilation (1 to 4 hours after phenol addition) was almost identical in both experiments. After four hours, the $^{14}\text{CO}_2$ evolution continued, but at a much slower rate. This slow evolution of $^{14}\text{CO}_2$, due to the endogenous respiration of the bacterial cells, was also nearly identical in both cultures. The total amount of $^{14}\text{CO}_2$ evolved by the PACT culture was 11 percent less than the biological culture (1.035 μCi vs. 1.168 μCi). Although this difference may be due to adsorbed phenol which may not be available for biodegradation, it may also be due to the error which is inherent in the radiotracer experiments. Accordingly, it was concluded that PAC addition did not significantly affect either the rate of biological assimilation or endogenous respiration by the biomass.

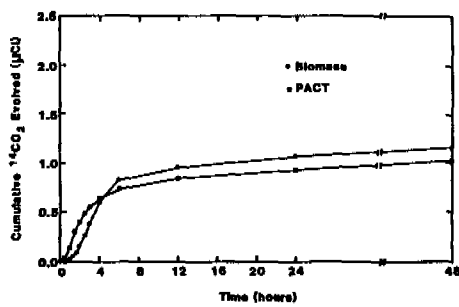


Fig. 3. $^{14}\text{CO}_2$ evolved during batch aeration of ^{14}C phenol in biophysical and biomass cultures

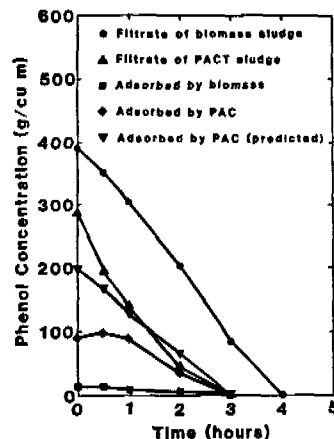


Fig. 4. Fate of phenol in biophysical and biomass batch experiments

These conclusions support those of Hals (1974) who observed that PAC addition did not enhance either the rate or extent of oxygen consumption during batch biodegradation of phenol. In contrast, the $^{14}\text{CO}_2$ data do not support the conclusion of Robertaccio (1976) who claimed that PAC addition enhances the biological assimilation rate of phenol. His conclusion, however, was based on an analysis in which the amount of phenol adsorbed on the PAC surface was calculated by assuming that only 70 percent of the PAC was effective as an adsorbent and that the adsorbed and solution phases were in equilibrium. Both of these assumptions may not be valid because the biofilm surrounding the PAC may decrease the rate of mass transfer to the PAC surface and prevent attainment of adsorption equilibrium.

These assumptions were evaluated using the data obtained in the batch experiments in which the amount of adsorbed phenol was measured using the desorption wash procedure.

Adsorbed phenol batch experiments. The concentrations of phenol measured in the desorption washes and the mixed liquor filtrate samples for one of the adsorbed phenol experiments are presented in Figure 4. The results of the desorption washes were expressed as an equivalent phenol concentration in the solution phase, for comparison purposes. Although a small amount (10 to 20 g/m³) of phenol was recovered from the solids of the biological control culture, this amount is relatively small compared to the phenol recovered from the desorption washes of the biophysical culture samples. This large difference supports the validity of the wash procedure for determining the mass of phenol adsorbed on the PAC surface.

The desorption washes of the biophysical culture samples indicated a rapid initial adsorption of phenol onto the PAC surface. The first sample, taken 30 seconds after nutrient addition, showed that 90 g/m³ of phenol had already been adsorbed on the PAC. This rapid initial adsorption of phenol was supported by the biophysical culture filtrate data which showed the phenol concentrations in the first filtrate samples to be 110 to 120 g/m³ below those observed in the biological culture. After the large initial adsorption, the amount of adsorbed phenol increased slightly during the first half-hour suggesting that a small amount of adsorption continued to occur. After one hour, however, a rapid decrease in the adsorbed phenol concentration was observed until an undetectable concentration was attained two hours later. These results clearly demonstrate that phenol was removed from the PAC surface; i.e., bioregeneration occurred and was essentially complete. This supports the observations of Robertaccio (1976) which showed that the PAC surface could be completely renewed for further adsorption of phenol. On the other hand, the results disagree with previous oxygen consumption observations (McShane and Rao, 1981) which indicated incomplete bioregeneration of GAC when a phenol substrate was used.

One hypothesis advanced to explain this conflict is that bioregeneration is controlled by the reversibility of adsorption (Flynn et al., 1976; Benedek, 1980). According to this hypothesis, activated carbon can be bioregenerated if the adsorbed compounds can be desorbed from the PAC surface, but cannot if the compounds are irreversibly adsorbed. The results of the experiments with phenol support this hypothesis because the preliminary desorption experiment demonstrated that phenol could be completely desorbed from the PAC. Similar results were obtained by Robertaccio (1976). It should be noted that the reversibility of phenol adsorption prevents experiments that examine the direct biodegradation of phenol from being conducted. Such experiments, however, were conducted with irreversibly adsorbed MEP and will be discussed later in this paper.

It is important to note that the measured adsorbed phenol concentrations shown in Figure 4 are lower than those predicted on the basis of adsorption equilibria. Equilibrium between the adsorbed and solution phases, therefore, was not obtained during the experiments. Since a preliminary adsorption rate study showed that the adsorption of phenol onto PAC is extremely rapid, it appears that the biomass in the biophysical culture impedes the transfer of phenol to the PAC surface. Consequently, the application of adsorption isotherms to calculate the amount of adsorbed substrate is not valid unless mass transfer through the biological flocs is considered. This requires the use of complex mass transfer models that are presently being developed for GAC contactors (Ying and Weber, 1979) but have not been considered by researchers working with biophysical systems.

Phenol desorption-displacement experiments. The results of the competitive adsorption experiment are presented in Figure 5. No significant differences

between the isotherms were evident indicating that competitive adsorption interactions between MEP and phenol were not significant. This result was anticipated, since White (1981) showed that the majority of MEP have molecular weights greater than 1600 and would not be expected to compete for the same adsorption sites as the comparatively low molecular weight phenol (mol wt = 94).

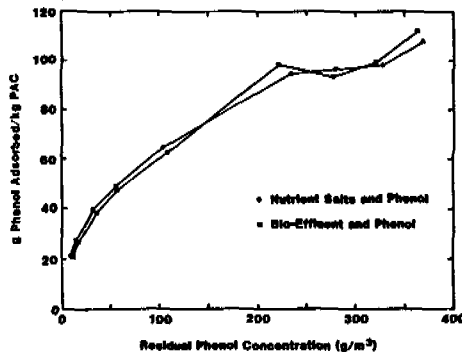


Fig. 5. Adsorption isotherm for phenol with and without metabolic end products

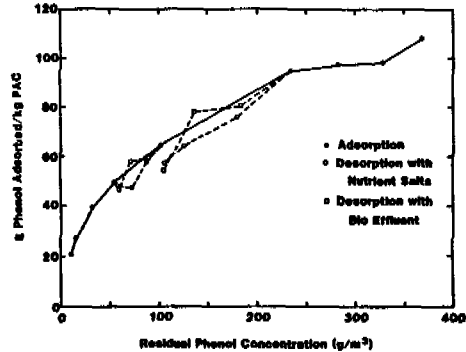


Fig. 6. Desorption isotherms for phenol with and without metabolic end products

The desorption isotherms developed for phenol in the presence and absence of MEP are given in Figure 6. The adsorption isotherm for phenol as a single solute is also presented for comparison purposes. Although the desorption isotherms lie slightly below the adsorption isotherm, the minor variations from the adsorption isotherm are not considered significant. The data verifies that phenol adsorption is completely reversible as observed in earlier studies and demonstrates that hysteresis is not significant. In addition, the desorption isotherm developed in the presence of MEP was not significantly different from the desorption isotherm developed solely with the nutrient salt solution. Displacement by MEP, therefore, does not appear to be an important mechanism for the removal of adsorbed phenol from PAC at the concentrations of MEP experienced in biological cultures.

MEP batch removal experiment. The ^{14}C measured in each component of the system during the MEP batch removal experiment is shown in Figure 7. Approximately 47 percent of the ^{14}C MEP added was immediately incorporated into the solid phase. Although removal from the liquid phase is a combination of adsorption and biological assimilation, the major mechanism that accounts for this rapid removal is thought to be adsorption. This conclusion is supported both by the rate at which the removal occurred (the first sample was taken 30 seconds after the ^{14}C MEP was added) and the relatively small amount of ^{14}C evolved as CO_2 during this period. These results demonstrate that MEP adsorption is significant in biophysical systems and should not be ignored in the analysis of such systems.

Relative to biodegradation, Figure 7 shows that approximately 20 percent of the ^{14}C added was evolved as $^{14}\text{CO}_2$ with over half being evolved during the first 30 minutes. Although a parallel experiment examining the biodegradability of ^{14}C MEP in a biological control culture was not performed, the amount of MEP biodegraded by the PACT culture in the present study was less than that observed in previous work (White, 1981) which showed that 30 percent of the MEP could be biodegraded by the same culture that produced it. PAC addition, therefore, does not appear to significantly enhance the biodegradation of MEP.

MEP adsorption-desorption experiments. The adsorption and desorption isotherms

developed using ^{14}C -labeled MEP are presented in Figure 8. The ^{14}C loading on the PAC and the residual concentrations were expressed as organic carbon using the estimated specific activity of the ^{14}C MEP solution (0.05 $\mu\text{Ci}/\text{mg TOC}$). Although the isotherm appears to be unfavorable at low MEP concentrations, high PAC concentrations were not required to adsorb a significant amount of the MEP. PAC concentrations of 200 and 1000 g/m^3 adsorbed 42 and 62 percent of the MEP, respectively. Extrapolation of the isotherm to an infinite carbon dose (zero MEP loading) indicates that 25 percent of the ^{14}C MEP (2 g/m^3 as TUC) was nonadsorbable. This observed nonadsorbable fraction agrees with the results of Martin and Iwugo (1980) which also showed a nonadsorbable MEP fraction produced during the batch biodegradation of a variety of pure compounds. The observed results, however, disagree with those of Tsezos and Benedek (1980) and Trgovcich et al. (1981) which indicated complete adsorptive removal of the MEP produced from phenol and succinic acid substrates, respectively. Possible explanations for this conflict include differences in substrates, activated carbons, and microbial populations used in the various studies.

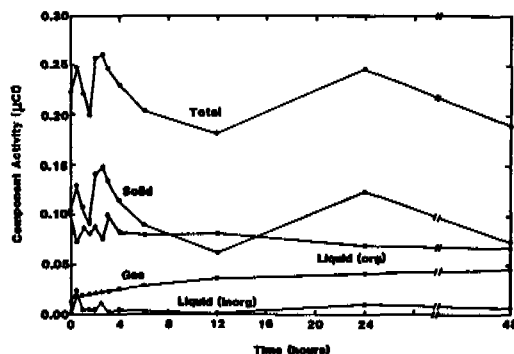


Fig. 7. Fate of ^{14}C MEP during aeration in a biophysical culture

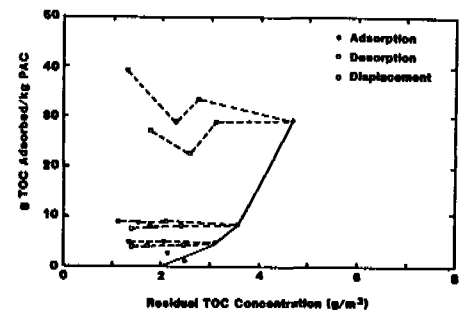


Fig. 8. Adsorption and desorption isotherms for metabolic end products

The desorption tests showed that ^{14}C MEP was essentially irreversibly adsorbed, since no change in the MEP loading on the PAC was observed as the solution concentration was decreased by dilution. In addition, the displacement of MEP by phenol was insignificant. The highest phenol concentration used, 806 g/m^3 , displaced only 7 to 16 percent of the adsorbed MEP. These results offer an explanation for the conflicting observations on bioregeneration. If desorption is the controlling mechanism for bioregeneration of the PAC surface, the fact that MEP is irreversibly adsorbed explains, in part, the incomplete bioregeneration observed in several studies (McShane and Rao, 1981; Flynn et al., 1976; Maqsood and Benedek, 1977). An experiment in which one examines the removal of adsorbed MEP by direct bacterial or enzymatic attack is required, however, before a final conclusion can be drawn.

Adsorbed MEP Biodegradation Experiment. Direct biodegradation of adsorbed MEP was examined by adding PAC with adsorbed ^{14}C MEP to a sample of PACT sludge and monitoring the fate of the ^{14}C with time. Table I presents the distribution of ^{14}C in the various components of the biophysical culture immediately after addition of the preloaded PAC and after 24 hours of aeration. Two points are noteworthy regarding these results. First, 10.2 percent of the ^{14}C added appeared in the liquid phase of the initial sample. This could be due to the desorption of MEP, incomplete decanting of the centrate in the centrifuge tubes, or to interstitial water. Second, only 4.1 percent of the added ^{14}C was evolved as $^{14}\text{CO}_2$.

demonstrating that adsorbed ^{14}C MEP was not assimilated by direct bacterial or exoenzymatic attack and subsequently evolved as $^{14}\text{CO}_2$.

TABLE I. Fate of ^{14}C MEP Initially Adsorbed on PAC
During Aeration in a PAC Culture

| Time (hrs) | Total Activity in Component | | | Total Activity Recovered (μCi) |
|---------------|--|---|--|--|
| | Cumulative Activity Evolved as $^{14}\text{CO}_2$ (μCi) | Liquid Phase Activity (μCi) | Solid Phase Activity (μCi) | |
| 0 | 0.000 | 0.005 | 0.044 | 0.049 |
| 24 | 0.002 | 0.004 | 0.043* | |

*Calculated by difference

The fact that adsorbed MEP was not removed from the PAC surface supports the hypothesis that the reversibility of adsorption controls the bioregeneration process rather than direct bacterial or enzymatic attack. This suggests that several of the proposed mechanisms which depend on the ability of the biomass to directly remove substrate adsorbed on the PAC surface, such as concentration enhancement or slow contact degradation, probably do not have a significant role in the removal of organic compounds in biophysical systems.

SUMMARY AND CONCLUSIONS

An experimental program was conducted to evaluate the significance of enhanced bioactivity, bioregeneration, desorption, and metabolic end product adsorption in a laboratory-scale biophysical reactor maintained with a phenol substrate. Radiotracer methodology and a desorption-extraction procedure that measures adsorbed phenol were used to discriminate between the various mechanisms. The results of the experimental program led to the following conclusions:

No significant differences in the extent or rate of $^{14}\text{CO}_2$ evolution from acclimated biophysical and biomass cultures were found. This refutes the hypothesis that PAC addition enhances the rate or extent of biodegradation of phenol.

All of the phenol initially adsorbed was eventually removed from the PAC surface. This indicates that bioregeneration does indeed occur and was essentially complete for the phenol substrate.

The experimental values for adsorbed phenol were smaller than the corresponding values predicted by adsorption equilibria. This implies that equilibrium between the adsorbed and liquid phases was not obtained and that mass transfer through the biofilm had a significant effect on the rate of substrate removal by adsorption.

A desorption experiment showed that adsorption of phenol was completely reversible. This implies that the controlling mechanism for bioregeneration is desorption by a lowering of the liquid-phase phenol concentration and not direct bacterial or enzymatic attack.

Since 62 percent of the MEP could be adsorbed by the PAC at a concentration of

1000 g/m³, MEP adsorption may explain the increased organic removals observed in biophysical systems.

Approximately 20 percent of the radioactivity in ¹⁴C MEP was converted to ¹⁴CO₂ by a biophysical sludge. Since previous work has shown that up to 30 percent of the MEP produced can be biodegraded, PAC addition does not appear to enhance the biodegradation of MEP.

Adsorbed MEP was not significantly desorbed by dilution or displaced by phenol. The irreversible adsorption of MEP explains the incomplete bioregeneration observations of previous studies and supports the hypothesis that reversibility of adsorption is the controlling mechanism for bioregeneration.

Only 4 percent of the adsorbed ¹⁴C MEP was converted to ¹⁴CO₂ by the biophysical sludge. This demonstrated that MEP cannot be removed from the PAC surface by direct biological or exoenzymatic attack.

REFERENCES

- Benedek, A., (1980). Simultaneous Biodegradation and Activated Carbon Adsorption--A Mechanistic Look. In Activated Carbon Adsorption of Organics from the Aqueous Phase Vol. II, M.J. McGuire and I.H. Suffet (Ed.), Ann Arbor Science Pub., pp 273-302.
- Chudoba, J., Cervenka, J., and Zima, M. (1969). Residual Organic Matter in Activated Sludge Process Effluents: IV. Treatment of Municipal Sewage. Technology Water, 14, 5-19.
- Daigger, G.T., and Grady, C.P.L., (1979). A Model for the Bio-Oxidation Process Based on Product Formation Concepts. Water Research, 11, 1049-1057.
- DeWalle, F.B. and Chian, E.S.K., (1977). Biological Regeneration of Powdered Activated Carbon Added to Activated Sludge Units. Water Research, 11, 439-446.
- Flynn, B.P., (1975). A Model for the Powdered Activated Carbon--Activated Sludge Treatment System. Proc. 30th Purdue Ind. Waste Conf., 233-252.
- Flynn, B.P., Robertaccio, F.L., and Barry, L.T., (1976). Truth or Consequences: Biological Fouling and Other Considerations in the Powdered Activated Carbon--Activated Sludge System. Proc 31st Purdue Ind. Waste Conf. 855-862.
- Grulich, G., Hutton, D.G., Robertaccio, F.L., and Glotzer, H.L., (1973). Treatment of Organic Chemicals Plant Wastewater with the DuPont PACT Process." Water-1972 Am. Inst. Chem. Eng. Symp. Series No. 129, 69, 127-134.
- Hals, O., (1974). Simultaneous Biological Treatment and Activated Carbon Adsorption. M. Eng. Thesis, Dept. of Chem. Eng., McMasters Univ.
- Jeffay, H., and Alvarez, J., (1961). Liquid Scintillation Counting of Carbon-14: Use of Ethanolamine-Ethylene Glycol Monomethyl Ether-Toluene. Anal. Chem., 33, 612-615.
- Kalinske, A.A., (1972). Enhancement of Biological Oxidation of Organic Wastes Using Activated Carbon in Microbial Suspensions. Water and Sewage Works, 119 (6), 62-64.
- Kim, B.R., Snoeyink, V.L., and Saunders, F.L. (1976). Influence of Activated Sludge CRT on Adsorption. J. Envir. Engrg. Div ASCE, 102, 55-70.
- Lee, J.S., (1977). A Dynamic Model of Nitrification-Denitrification in the Activated Sludge System with Powdered Activated Carbon. Ph.D. Thesis, Univ. of Minnesota.
- Lee, J.S., and Johnson W.K., (1979). Carbon-Slurry Activated Sludge for Nitrification-Denitrification. J. Water Poll. Control Fed., 51, 111-126.
- Maqsood, R., and Benedek, A., (1977). Low Temperature Organic Removal and Denitrification in Activated Carbon Columns. J. Water Poll. Control Fed., 49, 2107-2117.
- Martin, R.J. and Iwugo, K.O., (1980). Studies on Residual Organics in Biological

- Plant Effluents and their Treatment by the Activated Carbon Adsorption Process. In: Activated Carbon Adsorption of Organics from the Aqueous Phase Vol. II. M.J. McGuire and I.H. Suffet (Ed.), Ann Arbor Science Pub., pp. 385-404.
- Mathew, J., and Elzerman, A.W., (1981). Gas-Liquid Chromatographic Determination of some Chloro- and Nitrophenols by Direct Acetylation in Aqueous Solution. Analyt. Lett., 14, 1351-1361.
- McShane, S.F., and Rao, P.B.V., (1981). Microbial Degradation of Organics Adsorbed on Granular Activated Carbon. J. New England Water Poll. Control Assoc., 15, 87-104.
- Nayar, S.C., and Sylvester, N.D., (1979). Control of Phenol in Biological Reactors by Addition of Powdered Activated Carbon. Water Research, 13, 201-205.
- Prober, R., Pycha, J.J., and Kidon, W.E., (1975). Interaction of Activated Carbon with Dissolved Oxygen. J. Am. Inst. Chem. Eng., 21, 1200-1204.
- Robertaccio, F.L., (1976). Powdered Activated Carbon Addition to Biological Reactors. Ph.D. Thesis, Univ. of Delaware.
- Scaramelli, A.B. and DiGiano, F.A., (1973). Upgrading the Activated Sludge System by Addition of Powdered Carbon. Water and Sewage Works, 120 (9), 90-94.
- Sundstrom, D.W., Klei, H.E., Tsui, T., and Nayar, S., (1979). Response of Biological Reactors to the Addition of Powdered Activated Carbon. Water Research, 13, 1225-1231.
- Thibault, G.T., Tracy, K.D., and Wilkinson, J.B., (1977). PACT Performance Evaluated. Hydrocarbons Proc., 56, 143-146.
- Trgovcich, B., Kirsch, E.J., and Grady, C.P.L., (1981). Organic Microbial By-Products in Activated Sludge Effluents -I- Effects of Operational Conditions and Breakpoint Chlorination. Paper presented at the 54th Annual Conference of the Water Pollution Control Federation, Detroit, MI.
- Tsezos, M., and Benedek, A. (1980). Removal of Organic Substances by Biologically Activated Carbon in a Fluidized-Bed Reactor. J. Water Poll. Control Fed., 52, 578-586.
- White, S.C., (1981). Characteristics of Soluble Organic Carbon in Biological Reactor Effluents. Ph.D. Dissertation, Clemson Univ., Clemson, SC.
- Ying, W., and Weber, W.J. Jr., (1979). Bio-Physicochemical Adsorption Model Systems for Wastewater Treatment. J. Water Poll. Control Fed., 51, 2661-2677.

OZONE ENHANCED BIOLOGICAL ACTIVATED CARBON FILTRATION AND ITS EFFECT ON ORGANIC MATTER REMOVAL, AND IN PARTICULAR ON AOC REDUCTION

J. G. Janssens,* J. Meheus* and J. Dirickx**

**Study Syndicate for Water Research (S.V.W.) c/o I.H.E., Juliette Wytsmanstraat 14, B-1050 Brussels, Belgium*

***General Manager, Antwerp Waterworks (A.W.W.) Mechelsesteenweg 64, B-2018 Antwerp, Belgium*

ABSTRACT

Ozonation prior to GAC filtration is evaluated in relation to organic matter removal, and in particular to AOC (assimilable organic carbon) reduction. In terms of TOC removal, experimental results on pilot plant scale showed an increase of filter service time with about 60 % to 65 %. A dosage higher than 2 mg ozone/l had no additional effect. The extent to which this increase of service time was predominantly due to enhanced biological activity or to long term cumulative slow adsorption is not yet clear.

Ozonation caused a very significant increase of AOC. This increase was a function of the applied ozone dosage. First experimental results suggested a relation between ozonation and an early "breakthrough" of AOC with GAC filters fed with ozonated water.

KEYWORDS

Water treatment, activated carbon, ozone, biological activated carbon filtration, assimilable organic carbon (AOC).

INTRODUCTION

Ozonation of organic compounds in water usually produces oxygenated organic byproducts that are more readily biodegradable. When it is assumed that the same relationship between the organic load curve and the breakthrough curve is maintained in the case of biological activated carbon filtration, it is theoretically possible, as is shown in figure 1, to derive breakthrough curve 2 (with ozonation) from load curves 1 and 2 as far as breakthrough curve 1 (without ozonation) is known under equal process conditions.

As is illustrated in figure 2, increasing ozone dosages may result in breakthrough curves with a different pattern. It is hereby generally assumed that with higher ozone dosages the fraction of biodegradable organic compounds increases, but that at the same time low molecular and polar oxidation products of ozonation are formed which are less adsorbable, yet with a moderate concentration so that biodegradation can readily proceed at the carbon surface.

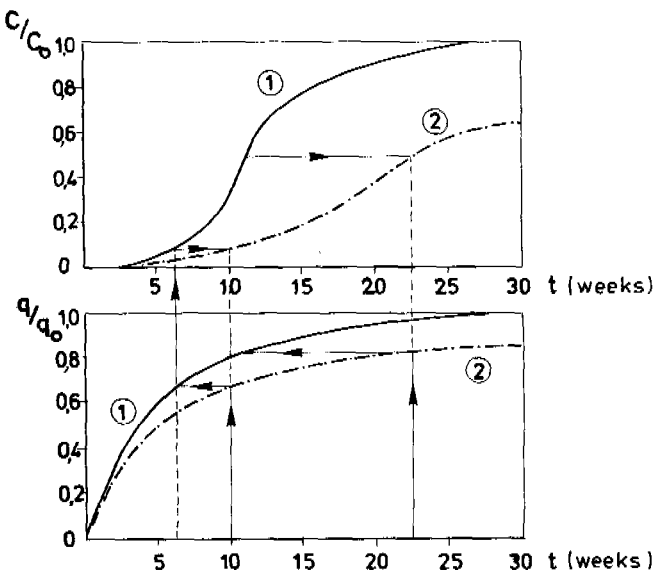


Fig. 1. Conceptual breakthrough curves of a GAC filter without (1) and with (2) biological enhancement
(after Sontheimer (1979))

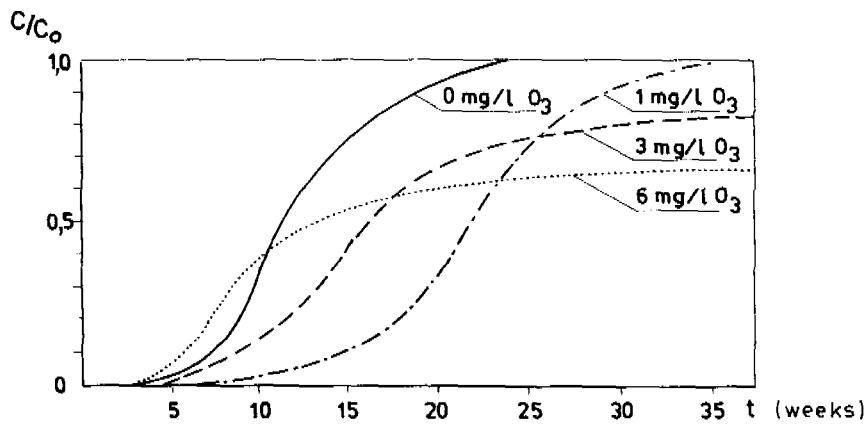


Fig. 2. Conceptual breakthrough curves of a GAC filter at different ozone dosages
(after Sontheimer (1979))

Recent studies (Fiessinger et al., 1983; Maloney et al., 1983) have shown that bacteria do not appear able to utilize most of the organics adsorbed on GAC, and that the long term organic removal observed in carbon columns is mostly due to slow adsorption kinetics. Nevertheless, ozone has been reported to enhance greatly the efficiency of GAC filters by increasing the fraction of biodegradable organic compounds and by extending service time between two reactivations.

Benedek (1979, 1980) and Mallevialle (1980) however, concluded from their investigations that the effect of ozone is relatively small and that the most significant operating mechanism which determines long term activated carbon efficiency is slow adsorption and not biodegradation.

It may however be argued that these conclusions are specific and cannot therefore automatically be extrapolated to other waters to be treated.

PURPOSE AND SCOPE

Within the S.V.W. (Study Syndicate for Water Research, Belgium), much attention is being paid to the investigation of ozonation not only as to its efficiency, but also in relation to other treatment processes and more in particular to activated carbon filtration (Janssens, 1983).

In this paper, experimental results on pilot plant scale are reported in relation to biologically enhanced GAC filtration and first results on the effect of ozonation prior to GAC filtration on AOC reduction are discussed.

DESCRIPTION OF PILOT PLANT AND EXPERIMENTAL CONDITIONS

The pilot plant for studying the ozone-activated carbon filtration process was operated at the Antwerp Waterworks' production centre Notmeir. It was fed with the filtrate of the direct-filtration plant, after dechlorination and before pH-correction with NaOH (cf. figure 3), (Dirickx, 1981).

A survey of the water quality at the entrance of the pilot plant is given in table 1.

The experimental plant was composed of four parallel treatment lines with dosages of 2, 4 and 8 mg ozone/l added and a zero dosage line as a reference. One parallel line was composed of two contact columns, one contact reservoir and one GAC filter unit (cf. figure 4).

The contact reservoir (contact time ca. 0.5 h) between ozonation and GAC filtration provided a zero residual ozone concentration in the influent of the activated carbon filter.

The working conditions of the pilot installation are summarized in table 2.

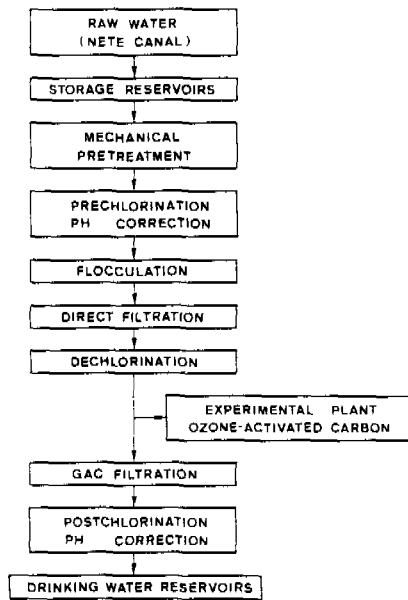


Fig. 3. A.W.W. Production Centre Notmeir with experimental plant ozone - GAC filtration

| PARAMETER | UNIT | \bar{x} | s_x | Xmin | Xmax |
|--------------------------|---------------------------|-----------|-------|------|------|
| temperature | °C | 15.5 | 5.7 | 2.5 | 22.4 |
| pH | - | 7.5 | 0.2 | 7.1 | 7.8 |
| turbidity | NTU | 0.2 | 0.7 | 0.1 | 0.3 |
| free residual chlorine | $\mu\text{g/l}$ | 273 | 151 | 60 | 500 |
| total residual chlorine | $\mu\text{g/l}$ | 538 | 258 | 200 | 1030 |
| <hr/> | | | | | |
| ORGANIC MATTER | | | | | |
| TOC | mg/l | 2.7 | 0.4 | 2.0 | 3.7 |
| UV-ext.(254 nm) | $.\text{m}$ | 4.8 | 1.2 | 2.5 | 8.0 |
| (UV-ext.)/TOC | $(.\text{m})/\text{mg/l}$ | 1.8 | 0.4 | 1.1 | 2.4 |
| KMnO_4 - demand | mg/l | 8.2 | 1.8 | 3.5 | 11.7 |
| 1THM | $\mu\text{mol/l}$ | 0.4 | 0.2 | 0.2 | 0.8 |

Table I. Water quality of influent of pilot plant ozone - GAC filtration

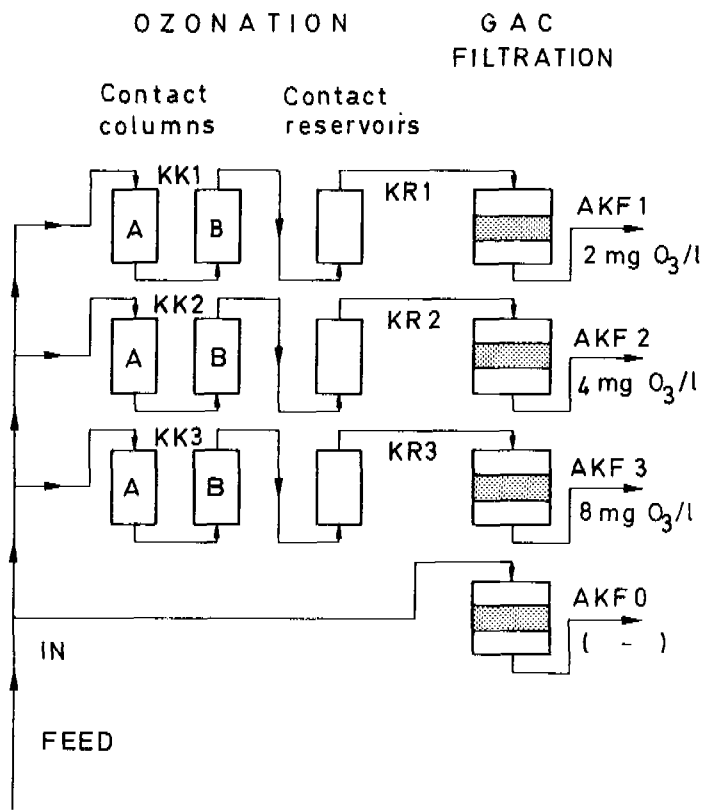


Fig. 4. Configuration of ozone - GAC filtration pilot plant

| GAC FILTRATION WORKING CONDITIONS (Experimental Period I) | COLUMN 0 AKF0 | COLUMN 1 AKF1 | COLUMN 2 AKF2 | COLUMN 3 AKF3 |
|---|------------------|------------------|------------------|------------------|
| OZONE DOSAGE ADDED (mg/l) | 0 | 1.9 ± 0.2 | 3.8 ± 0.5 | 7.6 ± 0.9 |
| GAC FILTER DIAMETER (m) | 0.144 | 0.144 | 0.144 | 0.144 |
| BEDVOLUME (l) | 23.14 | 23.37 | 23.91 | 23.93 |
| BEDHEIGHT (m) | 1.42 | 1.44 | 1.47 | 1.47 |
| GAC FILTRATION (mean values) | | | | |
| FLOW RATE (l/h) | 133.3 | 171.4 | 158.0 | 158.4 |
| VELOCITY (m/h) | 8.3 | 10.7 | 9.9 | 9.9 |
| E.B.C.T. (min) | 10.2 | 8.0 | 8.9 | 8.9 |

Table 2. Working conditions of pilot plant ozone - GAC filtration

EXPERIMENTAL RESULTS AND DISCUSSION

Biologically enhanced GAC Filtration

The effect of ozonation on the performance of activated carbon filtration in relation to reduction of organic matter was always statistically significant. Nevertheless, within the range of 2 to 8 mg ozone/l added, the effect of different ozone dosages on the final water quality was not always clear.

Experimental results however indicated that TOC must be preferred to UV-extinction for the evaluation of ozonation combined with GAC filtration performance, since a reduction of UV-extinction mainly shows a modification of organic matter, rather than a real removal, when an oxidation process is involved. The mean level of the ratio UV/TOC before and after GAC filtration showed a decreasing trend with increasing ozone dosages, since higher amounts of ozone applied gave rise to more saturated organic compounds that do not show UV-extinction at 254 nm (cf. figure 5).

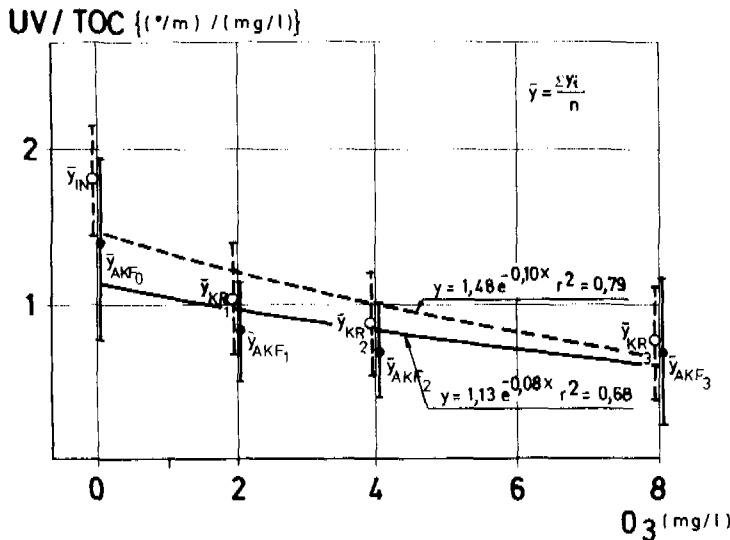


Fig. 5. Effect of ozonation on the ratio
UV-extinction/TOC before and after
GAC filtration

Gomella (1973, 1975) and Belle (1979) developed equation (1) based on pilot and industrial plant scale investigations. This model was used to fit the experimental data concerning TOC.

$$\log \left(\frac{C}{C_0} \right)_t = \alpha \int_0^t Q \cdot (C_0 - C) \cdot dt + \beta$$

$$= \alpha \cdot M_t + \beta \quad (1)$$

where M_t = total organic matter removed by adsorption at time t
 C, C_0 = outlet and inlet concentration of organic matter at time t

With $C = C_0$, the total organic matter removed at saturation of the GAC column, M_s , can be derived, i.e.,

$$\begin{aligned} M_s &= \int_0^{t_s} Q \cdot (C_0 - C) \cdot dt \\ &= - \frac{\beta}{\alpha} \end{aligned} \quad (2)$$

Calculated results based on equations (1) and (2) are summarized in table 3. The agreement of the experimental results with the given regression equation was acceptable although only 0.42 and 0.51 were obtained for R^2 in the case of 2 and 4 mg ozone/l.

| GAC filtration | Regression equation | R^2 | M_s/BV (kg TOC/m ³ AC) | |
|---------------------------------|--|-------|-------------------------------------|---------------|
| AKF 0 (without O ₃) | $Y = 8.05 \cdot 10^{-5} \cdot X + 1.63$ | 0.77 | 20.25 | 100 % |
| AKF 1 (2 mg O ₃ /l) | $Y = 3.26 \cdot 10^{-5} \cdot X + 1.06$ | 0.51 | 32.52 | 161 % |
| AKF 2 (4 mg O ₃ /l) | $Y = 3.50 \cdot 10^{-5} \cdot X + 0.98$ | 0.42 | 28.00 | 138 % |
| AKF 3 (8 mg O ₃ /l) | $Y = 5.12 \cdot 10^{-5} \cdot X + 1.50$ | 0.65 | 29.30 | 145 % |
| | | | | AVERAGE VALUE |
| | | | | 29.9 ± 2.3 |
| | | | | (148 ± 12)% |
| | $\frac{C_t}{C_0} = \log \frac{C_0}{C_t}$ | | $(C) = \text{mg TOC/l}$ | |
| | $X = \frac{M_t}{BV} = \sum_t \left[\frac{\Delta \text{TOC}_t \cdot Q_t \cdot \Delta t}{BV} \right]$ | | $(X) = \text{g TOC/m}^3 \text{ AC}$ | |
| | | | $(BV) = \text{treated bed volume}$ | |

Table 3. Results of regression analysis

$$\log \left(\frac{C}{C_0} \right)_t = \alpha M_t + \beta$$

Calculated M_s -values of GAC filters fed with ozonated water were shown to exceed to an average of 48 % the M_s -value of the GAC filter fed with non-ozonated water. No significant effect however between the different ozone dosages applied could be shown hereby. When the logistic model (Oulman, 1980) to fit the experimental data was applied, calculated values for the adsorption rate coefficient K decreased as a result of ozonation, whereas calculated values for the adsorption capacity coefficient N increased, as could be expected.

The higher M_s -values for GAC filters fed with ozonated water correspond with the observed longer service time of these filters. To determine filter service time, a TOC removal equal to 1 mg/l was taken as a criterion, which corresponded to a TOC reduction of 40 % with the given water quality. Experimental results indicated that with this criterion, ozonation indeed resulted in a 63 % increase of the operating time of a GAC filter. However, a higher ozone dosage than 2 mg/l added had no additional effect (cf. figure 6). The extent to which this increase of service time was predominantly due to enhanced biological activity or to long term cumulative slow adsorption, is not clear.

Within the range of ozone dosages studied, no significant dose-response relationship was observed concerning cumulative removal of TOC as a function of TOC applied (cf. figure 7).

On the other hand, the assumption that a more intense biological activity developed within the activated carbon bed, is sustained by the higher specific oxygen demands in the GAC filters fed with ozonated water as is shown in table 4.

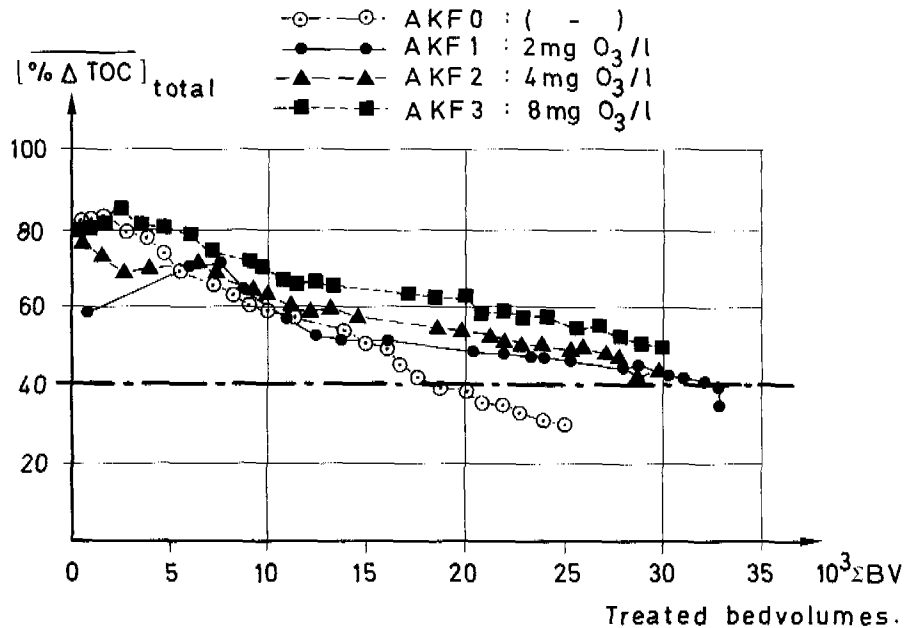


Fig. 6. Influence of ozonation prior to GAC filtration on overall % reduction of TOC concentration

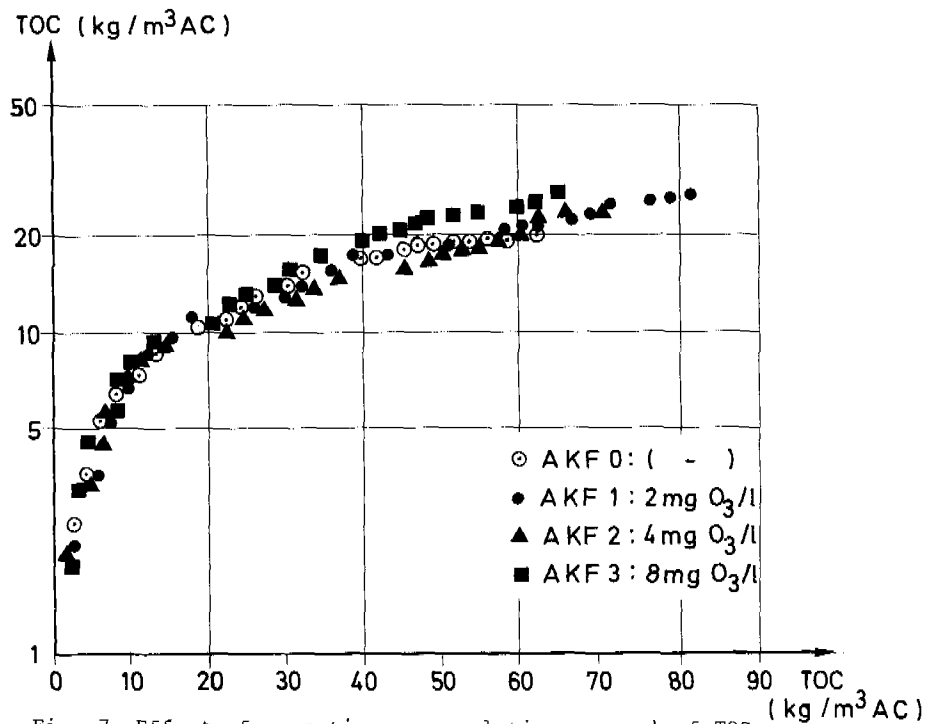


Fig. 7. Effect of ozonation on cumulative removal of TOC as a function of applied TOC

| D_v (g/m ³ AC.h) | 0mg ozone/l (AKF0) | | 2mg ozone/l (AKF1) | | 4mg ozone/l (AKF2) | | 8mg ozone/l (AKF3) | |
|----------------------------------|-----------------------|-----|-----------------------|-----|-----------------------|-----|-----------------------|-----|
| | \bar{x} | s | \bar{x} | s | \bar{x} | s | \bar{x} | s |
| Experimental Period I | 5.2 | 2.6 | 8.6 | 3.5 | 9.6 | 1.9 | 9.8 | 3.4 |
| Experimental Period II | 6.2 | 3.4 | 7.5 | 1.9 | 9.1 | 3.4 | 10.4 | 2.7 |

Table 4. Biological GAC filtration : Effect of ozonation on specific oxygen demand D_v

Effect of Ozonation prior to GAC Filtration on AOC Reduction

Sontheimer as well as Lavagne (1978) reported a possible relation between a decrease of the ratio UV-extinction to NVTOC (non-volatile TOC), and an increase of biodegradability of organic matter. The nature of this relation however proved to be dependent on the type of water, on the water treatment system applied and on the mode of ozonation. Also this relation may be a necessary but not sufficient condition for microbial regrowth. It may therefore be argued that unambiguous conclusions concerning potential microbial regrowth cannot be derived from TOC or UV-extinction data.

The determination of easily assimilable organic carbon (AOC), as introduced by Van der Kooij (1979), may give more quantitative information on potential microbial regrowth. Since the concentration of AOC cannot be assessed by simple chemical methods as a consequence of the complexity of the compounds gathered in the term AOC and because of many of its compounds are difficult to detect at low concentrations, an indirect microbiological method was developed. The method is based on the growth of fluorescent pseudomonads as a function of the concentration of easily assimilable organic carbon (AOC) in water. Van der Kooij (1979, 1981, 1982) gives a detailed description of the methodology of the AOC measurement and its application.

Since the reduction of concentration of biodegradable compounds in water to sufficiently low levels is important to control microbial regrowth, valuable information can be obtained by means of the AOC measurement about the efficiency of various unit operations in water treatment for the removal of the total assimilable organic carbon content in water.

Results of AOC measurements and of colony counts in situ are summarized in table 5. All data are averages of duplicate determinations.

A longer generation time G points to a slower growth of Pseudomonas fluorescens P17. A relation does exist between generation time on the one hand, and concentration and biodegradability of organic matter in water on the other hand. At low concentrations, longer generation time values indicate the presence in the water sample analysed, of organic compounds that are less biodegradable. As may be seen from table 5, higher G values were observed for the influent of the pilot plant and the effluent of the GAC filter fed with non-ozonated water.

| GENERATION TIME G (h) | | | | MAXIMUM GROWTH N _{max} ((CFU/ml)) | | | AOC (µg/l) | | | COLONY COUNT (IN SITU N _{sit} ((CFU/ml))) | | |
|-------------------------|------------|------------|------------|--|---------------------|---------------------|------------|------------|------------|---|---------------------|---------------------|
| SAMPLING DATE | 06.03 1981 | 11.08 1981 | 09.12 1981 | 06.03 1981 | 11.08 1981 | 09.12 1981 | 06.03 1981 | 11.08 1981 | 09.12 1981 | 06.03 1981 | 11.08 1981 | 09.12 1981 |
| INFILTRATION PLANT | 11.3 | 15.9 | 17.9 | 4.4x10 ⁴ | 8.3x10 ⁴ | 9.4x10 ⁴ | 10.5 | 20 | 22 | - | 330 | 87 |
| AFTER OZONATION | | | | | | | | | | | | |
| + 2 mgO ₃ /l | | 7.3 | 11.6 | | 3.1x10 ⁵ | 2.4x10 ⁵ | | 74 | 56 | | 7 | 15 |
| + 4 mgO ₃ /l | 8.9 | | 8.9 | 4.1x10 ⁵ | | 3.8x10 ⁵ | 97 | | 91 | - | | 7 |
| AFTER GAC FILTRATION | | | | | | | | | | | | |
| + 0 mgO ₃ /l | 44.6 | 89 | 30.8 | 1.9x10 ⁴ | 2.4x10 ⁴ | 5.0x10 ⁴ | 4.6 | 5.7 | 11.8 | - | 6.8x10 ³ | 6.5x10 ⁵ |
| + 2 mgO ₃ /l | 14.2 | 24.9 | 17.8 | 3.6x10 ⁴ | 8.7x10 ⁴ | 1.2x10 ⁵ | 8.6 | 21 | 29 | - | 5.8x10 ⁴ | 3.7x10 ⁴ |
| + 4 mgO ₃ /l | 21.4 | | | 2.8x10 ⁴ | | | 6.7 | | | - | | |
| + 8 mgO ₃ /l | 24.3 | | 16.2 | 2.7x10 ⁴ | | 1.3x10 ⁵ | 6.5 | | 31 | - | | 1.1x10 ⁵ |

Table 5. AOC measurements : experimental results

Table 5 also shows that a higher AOC load on GAC filtration resulted in higher colony counts in situ of the GAC filtrate.

Ozone itself has no direct biological action. Ozone is a strong oxidant with a strong bactericidal action, and it is certain that micro-organisms cannot develop in the presence of ozone. Nevertheless, partial oxidation and fragmentation of organic matter by ozonation leads to the formation of biodegradable products, thus stimulating biological activity in subsequent treatment steps. As could be expected, ozonation therefore caused a marked increase of the AOC concentration : + 370 % to + 540 % depending on the ozone dosage applied (cf. figure 8). These results indicate that ozonation has in fact not removed any biodegradable matter at all, and on the contrary only leads to incomplete oxidation and fragmentation of the organic compounds present in water. This is well illustrated by the differing effect of ozonation on organic matter according to its characterization by TOC, UV-extinction (254 nm) or KMnO₄ - demand, as was also observed in this investigation (cf. table 6).

As may be seen from table 7, an inverse relationship was shown to exist between the influent AOC concentration and the efficiency of GAC filtration with regard to AOC reduction.

Ozone enhanced biological GAC filtration could indeed be expected to show a high performance in removal of AOC. Nevertheless, under equal working conditions, GAC filtration of non-ozonated water gave the lowest AOC values in its effluent (cf. figure 8). This however must be due to the lower absolute AOC levels in the GAC influent, while % removal was lower.

Also, figure 9 suggests a relation between ozonation and an early "breakthrough" of AOC with GAC filters fed with ozonated water. When an AOC limit value should be applied as a criterion for filter operating time, ozonation prior to GAC filtration therefore would result in a significant shortening of the filter service time.

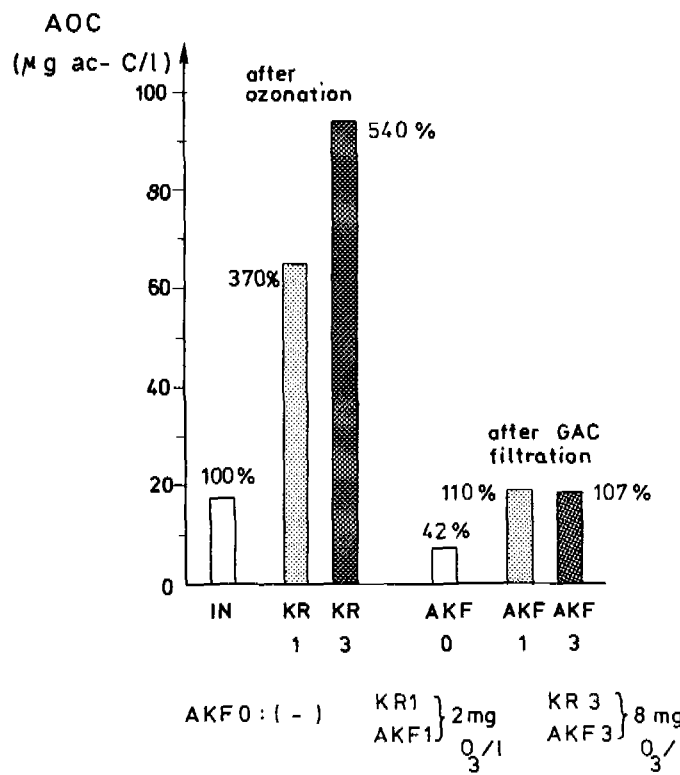


Fig. 8. AOC concentrations after ozonation and after GAC filtration

| SUMPARAMETER OF ORGANIC MATTER CONTENT | % REDUCTION BY OZONATION | | |
|---|--------------------------|-----------------------|-----------------------|
| | 2 mg ozone/l (KR1) | 4 mg ozone/l (KR2) | 8 mg ozone/l (KR3) |
| TOC | (11) | (12) 13 * 3 | (16) |
| UV-ext. (254nm) | 50 | 59 | 64 |
| KMnO ₄ - demand | 17 | 20 | 29 |
| UV/TOC | 48 | 60 | 66 |

Table 6. Mean % reduction of organic matter by ozonation

| OZONATION | GAC FILTRATION | | | | | |
|----------------------------|----------------------------------|-----|----------------------------------|------|--------------------------------------|-------------------|
| | AOC INFLUENT ($\mu\text{g/l}$) | | AOC EFFLUENT ($\mu\text{g/l}$) | | AOC REDUCTION ($\mu\text{g/l}$) | AOC REDUCTION (%) |
| | \bar{x} | s | \bar{x} | s | | |
| 8 mg O_3/l | 94 | 4 | 18.8 | 12.5 | 75.2 | 80 |
| 2 mg O_3/l | 65 | 13 | 19.5 | 10.5 | 45.5 | 70 |
| 0 mg O_3/l | 17.5 | 6.1 | 7.4 | 3.9 | 10.1 | 58 |

Table 7. Influence of ozonation prior to GAC filtration on AOC reduction

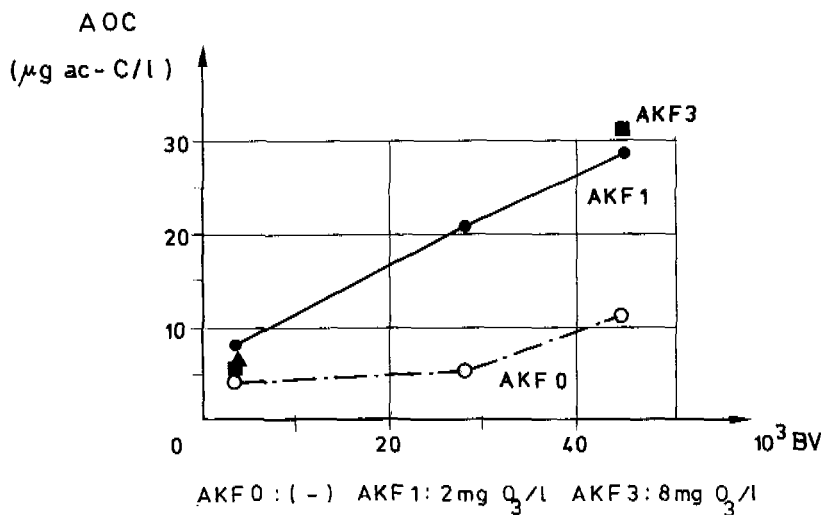


Fig. 9. AOC concentration after GAC filtration as a function of treated bedvolumes

This observation might be explained by a possible desorption effect of the low molecular and polar AOC compounds as byproducts of ozonation, and which on the other hand were incompletely removed by biodegradation in the (rapid) GAC filters under investigation. Additional work is required to assess the existing inter-relationships between contact time, filter operating time, filtration rate and water temperature on the one hand and AOC removal efficiency on the other hand.

CONCLUSIONS

Ozone prior to granular activated carbon filtration resulted in a final water quality with generally a lower organic matter concentration, characterized as TOC, UV-extinction (254 nm) or KMnO_4 -demand.

In terms of a TOC reduction, ozone enhanced GAC filtration resulted in an increase of filter service time with about 60 % to 65 %. A dosage higher than 2 mg ozone/l showed no additional effect.

The extent whether this increase of service time was predominantly due to enhanced

biological activity or to long term cumulative slow adsorption was not clear. An indicative economic analysis showed that the costs, as a result of ozonation, could not be covered by the cost-savings in reactivation of activated carbon.

Ozonation caused a very significant increase of AOC (assimilable organic carbon). This increase was a function of the applied ozone dosage.

Under equal working conditions, GAC filtration of non-ozoneated water gave the lowest AOC values in its effluent.

First experimental results suggested a relation between ozonation and an early "breakthrough" of AOC with GAC filters fed with ozonated water.

When an AOC limit value should be applied as a criterion for filter operating time, ozonation prior to GAC filtration would result in a significant shortening of the filter service time.

ACKNOWLEDGEMENT

This investigation forms part of the program "Ozonation and Activated Carbon" of the Study Syndicate for Water Research (S.V.W.), Belgium. Valuable discussions within the S.V.W. Working Party "Oxidation and Disinfection" are gratefully acknowledged. Determinations of AOC (assimilable organic carbon) were carried out by Van der Kooij and co-workers of the Netherlands Testing and Research Institute (KIWA).

REFERENCES

- Belle, J.P. (1979). Evaluation et critères de contrôle des performances du charbon actif en poudre et en grains. I.W.S.A. Spec. Conf. The Use of Activated Carbon in Water Treatment, Brussels, May 1979.
- Benedek, A. (1979). The effect of ozone on activated carbon adsorption : A mechanistic analysis of water treatment data. *Ozonews*, 6 (1, Part 2), 1-6.
- Benedek, A. and Richard, Y. (1980). Advances in biological treatment. Special Subject 7, 13th I.W.S.A. Congress, Paris, September 1980.
- Buydens, R. (1972). La réviviscence microbienne dans les eaux et particulièrement, dans les eaux ozonées. *La Tribune du CEBEDEAU*, 25 (338), 3-9.
- Dirickx, J. (1981). A century of water for Antwerp. *Aqua*, (3), 10-13.
- Dirickx, J. and Janssens, J. (1982). De actuele betekenis van actieve kool in de drinkwaterbereiding. *Water*, 1 (4), 113-117.
- Fiessinger, F., Mallevialle, J. and Benedek, A. (1983). Interaction of Adsorption and Bioactivity in Full-Scale Activated-Carbon Filters : The Mont Valerien Experiment. In : *Treatment of Water by Granular Activated Carbon*, Chapter 14, pp. 319-336, Mc Guire, M.J. and Suffet, I.H., Editors, *Advances in Chemistry Series 202*, American Chemical Society.
- Fiore, J.V. and Babineau, R.A. (1977). Effect of an activated carbon filter on the microbial quality of water. *Appl. Environ. Microbiol.*, 34 (5), 541-546.
- Gomella, C. (1973). Emploi optimal du charbon actif. *Techniques et Sciences Municipales*, 68 (4), 151-160.
- Gomella, C. and Belle, J.P. (1975). Extraction de micropolluants par le charbon actif. *Techniques et Sciences Municipales*, 70 (5), 195-203.
- Janssens, J.G. (1983). Ozonisatie en actieve koolfiltratie. S.V.W. Report 1983/3, September 1983.
- Kuhn, W., Sontheimer, H., Steiglitz, L., Maier, D. and Kurz, R. (1978). Use of Ozone and Chlorine in water utilities in the Federal Republic of Germany. *Journal AWWA*, 70 (6), 326-331.
- Lamblin, H. (1977). Protection d'un réseau d'eau ozonée vis-à-vis des germes. 3rd I.O.A. Congress, Paris, May 1977.

- Lavagne, J. Ph. (1978). La filtration sur charbon actif et la réviviscence micro-bienne dans les réseaux. La Tribune du CEBEDEAU, 31 (42!), 485-494.
- Mallevalle, J. (1980). The interaction of slow adsorption kinetics and bio-activity in full scale activated carbon filters : The development of a new predictive model. Paper submitted to the Chemviron Award Committee, Feb. 1980.
- Maloney, S.W., Bancroft, K., Suffet, I.H. and Cairo, P.R. (1983). Comparison of Adsorptive and Biological Total Organic Carbon Removal by Granular Activated Carbon in Potable Water Treatment. In : Treatment of Water by Granular Activated Carbon, Chapter 12, pp. 279-302, Mc Guire, M.J. and Suffet, I.H., Editors, Advances in Chemistry Series 202, American Chemical Society.
- Meijers, A.P. (1977). Ozonisatie. H2O, 10 (18), 417-427.
- Miller, G.W., Rice, R.G., Robson, C.M., Scullin, R.L., Kuhn, W. and Wolf, H. (1978) An assessment of ozone and chlorine dioxide technologies for treatment of municipal water supplies - Executive summary. EPA-600/8-78-018, October 1978.
- Oulman, Ch. S. (1980). The logistic curve as a model for carbon bed design. Journal AWWA, 72 (1), 50-53.
- Rice, R.G., Robson, G.M., Miller, G.W. and Hill, A.G. (1981). Uses of ozone in drinking water treatment. Journal AWWA, 73 (1), 44-57.
- Rizet, M. and Coute, A. (1981). Evaluation des micro-organismes des milieux granulaires utilisés pour la filtration des eaux de surface. Techniques et Sciences Municipales, L'eau, Juin 1981, 371-379.
- Rook, J.J., Graveland, A. and Schultink, L.J. (1982). Considerations on organic matter in drinking water treatment. Water Research, 16, 113-122.
- Snoek, O.I. (1970). Enige chemische en bacteriologische aspecten van de toepassing van ozon bij de drinkwaterzuivering. H2O, 3 (7), 108-110.
- Sontheimer, H. (1979). Biologisch-adsorptive Trinkwasseraufbereitung in Aktivkohle Filtern - Das Mülheimer Verfahren. R.W.W., Mülheim a.d. Ruhr und DVGW-Forschungsstelle, Engler-Bunte-Institut, Karlsruhe, February 1979.
- Symons, J.M. (1977). Ozone, Chlorine Dioxide and Chloramines as alternatives to chlorine for disinfection of drinking water. State of the Art. U.S. EPA, November 1977.
- Symons, J.M. (1978). Interim Treatment Guide for controlling organic contaminants in drinking water using granular activated carbon. U.S. EPA, January 1978.
- Van der Kooij, D. (1979). Ontwikkeling van een methode om de nagroeiemogelijkheden van bacteriën in drinkwater te bepalen. H2O, 12 (8), 164-167.
- Van der Kooij, D. (1979). Kwaliteitsverandering van drinkwater als gevolg van de groei van micro-organismen in het distributiesysteem. H2O, 12 (12), 269-273.
- Van der Kooij, D., Hijnen, W.A.M. and Oranje, J.P. (1981). Vermeerdering van bacteriën in drinkwater. H2O, 14 (14), 317-324.
- Van der Kooij, D., Visser, A. and Hijnen, W.A.M. (1982). Determining the concentration of easily assimilable organic carbon in drinking water. Journal AWWA, 74 (10), 540-545.
- Vogt, C. and Regli, S. (1981). Controlling trihalomethanes while attaining disinfection. Journal AWWA, 73 (1), 33-40.
- Zoeteman, B.C.J. (1973). De plaatsing van ozon in de zuivering tot drinkwater. H2O, 6 (2), 47-49.

OZONATION OF NON-IONIC SURFACTANTS IN AQUEOUS SOLUTIONS

Nava Narkis,* Bella Ben-David** and Malka Schneider Rotel*

**Environmental and Water Resources Engineering, Technion, Technion City, Haifa 32000, Israel*

***Advisor on Environmental Quality to the Major, Municipality of Haifa, 14 Bracha Chabas St., Haifa 33393, Israel*

ABSTRACT

The effect of ozone on dilute aqueous solutions of a series of non-ionic surfactants of nonyl phenol ethoxylates, with n=4 to 30 ethylene oxide groups, dinonyl phenol ethoxylate and a polyethylene glycol were investigated. Assuming ozone concentration in solution to remain constant throughout the ozonation, the experiments showed first-order reactions with respect to surfactant concentration, as measured by the Wickbold method, and also with respect to COD & TOC. A linear relationship was established between the first-order reaction rate constants, and between n, the average number of ethylene oxide groups in the ethoxylate chain of the nonyl phenol ethoxylate series.

The oxidation mechanism by ozone of non-ionic surfactant molecules is explained as mainly polyethoxylate chains' cleavage into shorter polyethylene glycols and to a smaller extent oxidation of the aromatic ring. High ozone doses do not convert the non-ionic surfactant completely to CO₂ and H₂O but smaller doses are sufficient to enhance biodegradation.

KEYWORDS

Non-ionic surfactants; nonyl phenol ethoxylates; polyethylene glycol; ozone; kinetics; oxidation; first order reaction; biodegradation.

INTRODUCTION

Non-ionic surfactants, mostly as nonyl and dinonyl phenol ethoxylates, are used world-wide in household and in industry (Non-ionic, 1971). Being nonbiodegradable makes them a potential nuisance to the environment (Narkis et al, 1977). They produce foams on surface waters (Twelfth Progress Report, 1977), interfere with sewage treatment processes, and were proved to be toxic to fish and crops (Horowitz, 1977; Weinberger, 1983). Laws forbidding the use of hard surfactants in Europe, United States and Israel relate only to anionic surfactants, and ignore the existence of non-ionic surfactants. As a result the hard non-ionics are widely dispersed. Their presence in sewage and effluents is likely to create environmental hazards. In Israel, effluents are widely recycled nowadays for industrial use, agricultural processes and in fish ponds. There is a need to find a physico-chemical treatment capable of removing the non-ionic surfactants efficiently from water and from effluents.

The literature survey indicated that little if any work has been carried out on the subject of ozonation of non-ionic surfactants. From research on the ozonation of various organic materials it may be concluded that ozone attacks polyethylene glycols (Suzuki, 1976a; Price and Tumolo, 1964, 1967) and phenols (Evans, 1972; Gilbert, 1976). Simple etheric oxidation by ozone has been reported by Price and Tumolo (1964) who explained the reaction by electrophilic attack of the ozone on hydrogen atoms α to an ether group. The ozonation involves a hydrotrioxide intermediate (Evans, 1972) by a 1.3 - dipolar insertion of ozone, in which there is developing carbonium ion character in the transition state. By these reactions ethers are converted to esters, alcohols, aldehydes and ketones. Price & Tumolo (1967) and Suzuki (1976a,b) investigated the degradation of polyethylene and polypropylene oxides by ozone. As a result of ozonation the polymer chain was found to be cleaved randomly to lower molecular weight products. The production of formic ester, ethylene glycol, diethylene glycol, triethylene glycol and hydrogen peroxide was confirmed by IR, NMR, gas chromatography and chemical analysis.

This paper reports our investigation into ozonation of aqueous solutions of a series of non-ionic surfactants widely used in household and industry (Ben David 1980). For the purpose of comparison, ozonation of polyethylene glycol of MW 1000, PEG 1000, was also investigated. The effect of the surfactant molecular structure and ethoxylate chain length on the kinetics of ozonation was studied.

EXPERIMENTAL

Non-Ionic Surfactants

TABLE 1 Nonyl And Dinonyl Phenol Ethoxylates Characteristics.

| Non-ionic Surfactant | Symbol | Average EO*groups per molecule | Molecular Weight | HLB Value |
|--|----------|--------------------------------|------------------|-----------|
| SYNPONIC NP4 | SNP4 | 4 | 396 | 8.9 |
| MARLOPHEN 86 | M86 | 6 | 484 | 10.9 |
| SYNPONIC NP9 | SNP9 | 9 | 616 | 12.8 |
| MARLOPHEN 810 | M810 | 10 | 660 | 13.3 |
| SYNPONIC NP12 | SNP12 | 12 | 748 | 13.9 |
| SYNPONIC NP20 | SNP20 | 20 | 1100 | 16.0 |
| MARLOPHEN 830 | M830 | 30 | 1540 | 17.1 |
| DI-NONYL PHENOL ETHOXYLATE (BEROL 716) | DNP | 16 | 1029 | 13.7 |
| POLYETHYLENE GLYCOL | PEG 1000 | 23 | 1000 | |

*EO = Ethylene Oxide.

Dinonyl phenol ethoxylate. DNP, Berol 716, product of Berol Kemi AB Sweden, obtained from Vitco, Ltd., Haifa.

Polyethylene glycol. PEG 1000 product of Fluka A.G. Switzerland. MW 1000.

Nonyl phenol ethoxylates. The non-ionic surfactants (NIS) investigated were branched chain nonyl phenol ethoxylates, para substituted with chains ranging from 4 to 30 units ethylene oxide (EO) groups per molecule. The non-ionics are listed in Table 1. These were obtained from two sources: a) Marlophen series (M notation) product of Marl, Chemische Werke Fabrics, Hülls A.G.W., Germany, b) Syneronic series product of I.C.I., England, (SNP notation).

Analytical Procedure.

Two analytical procedures were used for determination of residual non-ionic surfactant concentration after ozonation: a) complexion with cobaltothiocyanate after extraction with benzene and chloroform (Crabb *et al.*, 1964). The benzene extraction separates out only the surfactant whilst the chloroform in addition separates out PEG, and thus this method can identify PEG cleavage in the ozonation products. b) The Wickbold (1972) method, based on complexation with bismuth and potentiometric titration of the complexed bismuth as a measure of the non-ionic surfactant.

Ozonation

Ozone was produced in a Welsbach T-816 generator, fed with oxygen. Ozone concentration in the oxygen stream entering and leaving the reactor was measured by an iodometric procedure (Standard Methods, 1980) to determine the ozone consumed. Ozonation was carried out in a batch reactor with a 5 liter glass column, height 80 cm and diameter 10 cm. In order to minimize foaming the gas flow rate was decreased to 0.2 L/min.

Effect of pH. In studying the effect of different initial pH on the efficiency of ozonation, 2 buffer solutions were used: Phosphate buffer in the pH 7-8 range, prepared from 0.1 M NaOH and 0.1 M KH₂PO₄ and borate buffer for the pH range 8-12, prepared from 0.1 M KCl, 0.1 M NaOH and 0.1 M H₃BO₃. A mother solution containing 40 mg/L SNP12 was used in these experiments and the initial pH fixed by using concentrated H₂SO₄ or 50% NaOH. Ozonation time was 15 minutes.

The efficiency of ozonation was investigated in a pH range from 3 to 12 by registering residual surfactant, as determined by the Wickbold technique, COD, final pH and ozone demand. The experimental results show that the suitable pH, from the standpoint of residual surfactant, is 9, when 15 ml/L borate buffer are added. These results are in keeping with those of Wachs, Narkis *et al.* (1976, 1977, 1978, Schneider, 1976) which showed that effective removal of organic matter, as indicated by COD, was maximum in the pH range 8 to 9.

Kinetics of the reactions. Kinetics of ozonation was investigated in batch experiments of 1 litre solutions containing 40 mg/L surfactant prepared in distilled water, to which 15 ml/L borate buffer were added (pH 9.0), which were changed for each ozonation period. Ozonation periods were between 0 and 30 minutes.

The parameters followed were thus: Concentration of non-ionic surfactant by the Wickbold technique and by complexation with cobaltothiocyanate, residual COD in dilute solution, TOC in a Beckman 915A TOC analyzer and changes in U.V. spectrum at a wavelength of 225 nm in a Spectronic 710 spectrophotometer. At this wavelength, the spectrum of the benzene ring in the non-ionic surfactant is identified.

RESULTS AND DISCUSSIONS

Figs. 1 to 4 indicate the removal of surfactant, COD, TOC and UV absorbance as a function of ozonation time. Generally ozonation effectively reduces surface activity of the aqueous solutions according to the quantity of surfactant removal. This was confirmed by a similar reduction in the foaming, obtained initially when bubbling ozone gas through the solution, and disappearing minutes after initiating ozonation. Fig. 1 indicates that it is possible to achieve up to 100% removal of surfactant with an ozonation period of half an hour on the materials M86, SNP12, SNP20, and M830. In the case of M830, effective removal was greater at all ozonation times than with any other surfactant. SNP4 and DNP were the least affected with only 91.6% removal after a 30 minutes period. The case of SNP4 may be explained by its low ethoxylate chain length and greater hydrophobicity. DNP's behaviour may be explained by the relatively high steric hindrance in the hydrophobic part of the two branched alkyl chains. The fact that non-ionic surfactant concentration was reduced during ozonation indicates ozone attack on the molecules resulted in reaction products of low complexing ability with the bismuth used in the Wickbold method. Figs. 2 & 3 indicate that non-ionic surfactants' removal measured as COD and TOC was incomplete. The percentage COD removal in ozonation of SNP4, M86, SNP9, SNP20 and DNP, reached 40% after 30 minutes ozonation, whilst that of M830 achieved 48% after 25 minutes. In the case of polyethylene glycol, COD removal was the highest at all ozonation times and reached 64% after 30 minutes ozonation.

TOC results were similar to those obtained for COD. TOC removal was greatest for M830 (33% removal after 25 minutes of ozonation) and the only other outstanding result was for SNP9, in which TOC removal of 39% was achieved after 30 minutes. The highest COD removal in the case of PEG 1000 and M830, which was the highest among all surfactants checked, indicates that the ozone effectively attacks the polyethylene oxide structure of the materials, as reported by Suzuki (1976a,b) and Price (1967). Apparently, ozone attack on the polyethylene oxide chain is more effective than that of a surfactant comprising a polyethylene oxide chain plus nonyl phenol or dinonyl phenol group, competing for the ozone, preventing its ability to affect complete break-down of the surfactant molecule. Fig. 4 illustrates percentage removal of U.V. absorption at $\lambda = 225$ nm, which corresponds to the benzene ring in the non-ionic surfactant. During ozonation the strength of absorption is seen to decline, and this indicates that in addition to cleaving the ethoxylate chain, the ozone also attacks the benzene ring. Since the removal of PEG 1000 was the most efficient, the oxidation mechanism by ozone of non-ionic surfactant molecules is explained as mainly polyethoxylate chain cleavage into shorter polyethylene glycols, like ethylene glycol, diethylene glycol, triethylene glycol and formic esters (Suzuki, 1976a) and to a smaller extent oxidation of the aromatic ring.

Ozone treatment of non-ionic surfactants in aqueous solution was effective when the residual was determined by the Wickbold technique and complexation with cobalto-thiocyanate method; however, the surfactant was not completely broken down into CO_2 and H_2O as reflected in the high TOC and COD residual concentrations. Ozonation causes alterations in the surfactant's molecular structure and this results in changes in the material characteristics, such as foaming ability, complexation with bismuth or cobalto-thiocyanate and increased water solubility of the oxidation products. In other words, the non-ionic surfactant still exists in solution in the form of newly created organic materials and although its surface activity has been destroyed by the ozonation, a large organic load remains.

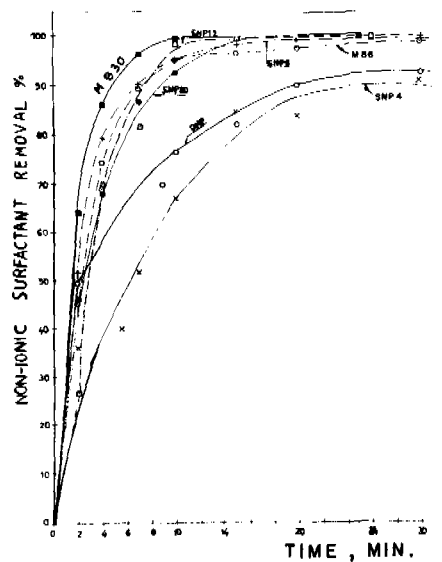


FIG. 1: NON-IONIC SURFACTANTS (WICKBOLD METHOD) REMOVAL EFFICIENCIES BY OZONATION

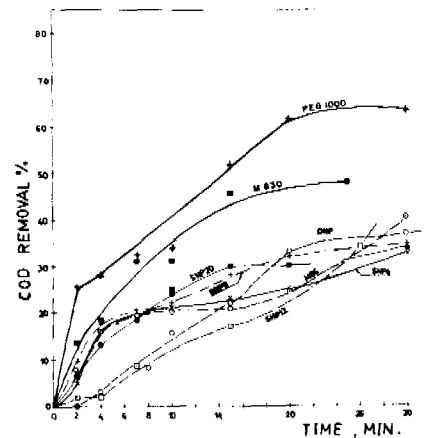


FIG. 2: COD REMOVAL EFFICIENCIES OF NON-IONIC SURFACTANTS AND PEG BY OZONATION

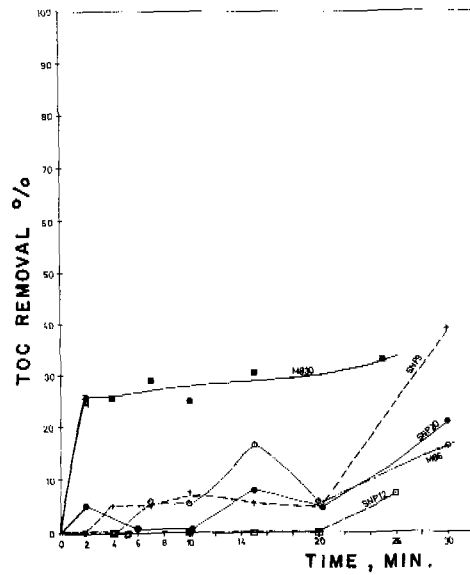


FIG. 3: TOC REMOVAL EFFICIENCIES OF NON-IONIC SURFACTANTS BY OZONATION

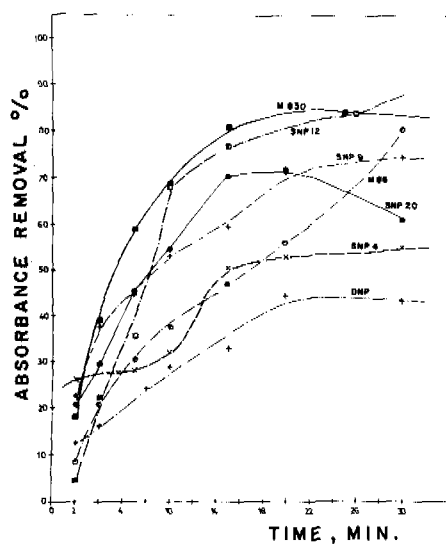


FIG. 4: UV ABSORBANCE REMOVAL EFFICIENCIES OF NON-IONIC SURFACTANTS BY OZONATION ($\lambda = 225 \text{ NM}$)

KINETICS OF OZONATION

The kinetics of the ozonation in aqueous solutions was studied for a series of nonyl phenol ethoxylates ($n=4-30$), dinonyl phenol ethoxylate ($n=16$) and polyethylene glycol ($n=23$) in order to investigate the possible removal of these materials from effluent by ozonation. The kinetics of oxidation by ozone was studied according to the reduction of surfactant concentration in aqueous solution, as determined by the Wickbold method, and the reduction in organic load as reflected in COD and TOC as a function of ozonation time. It was assumed that the rate of surfactant removal resulting from oxidation by ozone was of a first order reaction type according to surfactant concentration, COD and TOC. This assumption is based on the work of Hoigné and Bader (1976), who found that ozonation was a first order reaction according to the substrate concentration in water. The work of Schneider (1976), Wachs and Narkis (1978) determined that the kinetics of the ozonation of organic substrate in lime treated effluent was also of first order type according to COD and TOC. The ozonation experiments were performed batch-wise for 1 litre of non-ionic surfactant solution, with a constant initial concentration of 40 mg/L. Nevertheless, during ozonation the ozone inflow was at a constant rate of 0.2 L/min. through the surfactant solution from the base of the column and exiting through an upper opening. In other words, it can be said that the ozone concentration is always in excess and is maintained at a constant value in solution throughout the process. In these circumstances the rate of surfactant disappearance, resulting from ozonation, is dependent on its solution concentration only. The first order reaction kinetic model may be expressed thus:

$$-\frac{dC}{dt} = K_1 C \quad \text{or} \quad \log C = \log C_0 - K_1 t / 2.3$$

where

K_1 = ozonation reaction rate constant, min^{-1}
 C_0 = initial NIS, COD or TOC concentration, mg/L
 C = concentration of NIS, COD or TOC at time t , mg/L
 t = ozonation time, minutes.

The ozonation first order reaction rate constants, K_1 , refer to the rate of disappearance of NIS, COD and TOC and their values are obtained from the slope of the linear plots of $\log C$ against t . Figures 5 to 9 indicate the linear dependence of $\log C$ against t for the nonyl phenol ethoxylates, dinonyl phenol ethoxylates and PEG 1000.

TABLE 2 First Order Ozonation Reaction Rate Constants, for Non-ionic Surfactant, COD and TOC Concentrations, as a Function of N .

| Non-Ionic Surfactant | n | $K_1(\text{Non-ionic})^*$ min^{-1} | $K_1(\text{COD})$ min^{-1} | $K_1(\text{TOC})$ min^{-1} |
|----------------------|-----|--|--|--|
| SNP4 | 4 | 0.118 | 1.22×10^{-2} | |
| M86 | 6 | 0.220 | 1.54×10^{-2} | 6.0×10^{-3} |
| SNP9 | 9 | 0.246 | 1.80×10^{-2} | 6.0×10^{-3} |
| SNP12 | 12 | 0.260 | 1.77×10^{-2} | 3.0×10^{-3} |
| SNP20 | 20 | 0.284 | 2.40×10^{-2} | 6.5×10^{-3} |
| M830 | 30 | 0.495 | 3.90×10^{-2} | 11.0×10^{-3} |
| DNP | 16 | 0.285 | 2.10×10^{-2} | |
| PEG 1000 | 23 | - | 4.17×10^{-2} | |

* Wickbold Method.

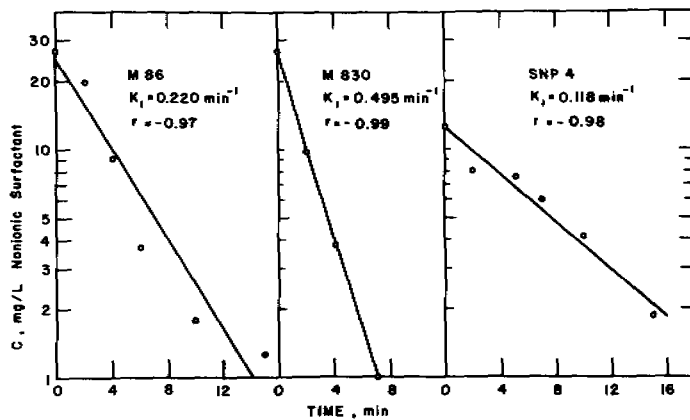


FIG. 5: K_1 FIRST ORDER REACTION RATE CONSTANT BY RESIDUAL NON-IONIC SURFACTANT (WICKBOLD METHOD) FOR SNP4 M86 AND M830

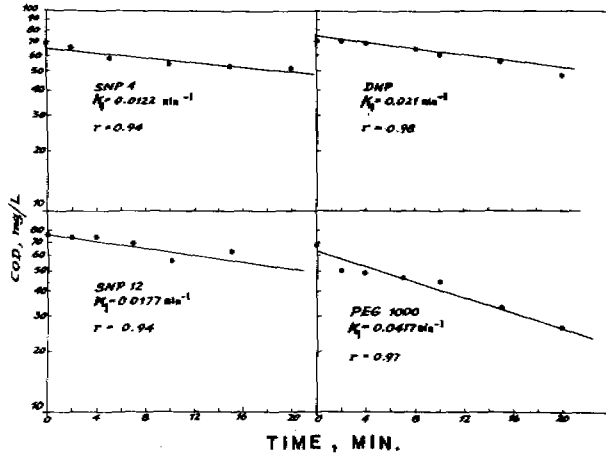


FIG. 7: K_1 FIRST ORDER REACTION RATE CONSTANT BY RESIDUAL COD FOR SNP4, SNP 12, DNP AND PEG 1000

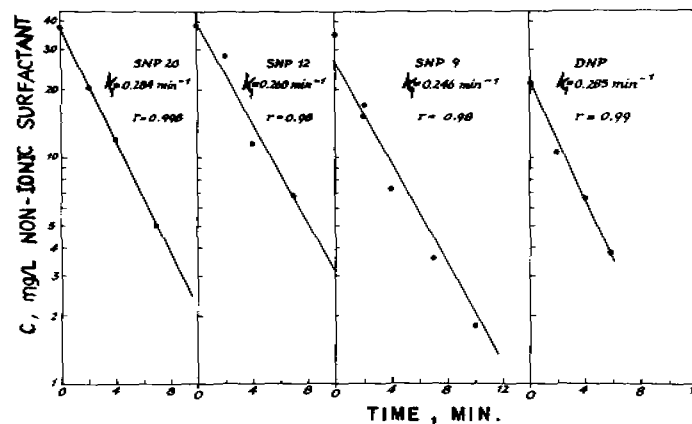


FIG. 6: K_1 FIRST ORDER REACTION RATE CONSTANT BY RESIDUAL NON-IONIC SURFACTANT (WICKBOLD METHOD) FOR DNP, SNP9, SNP12 AND SNP20

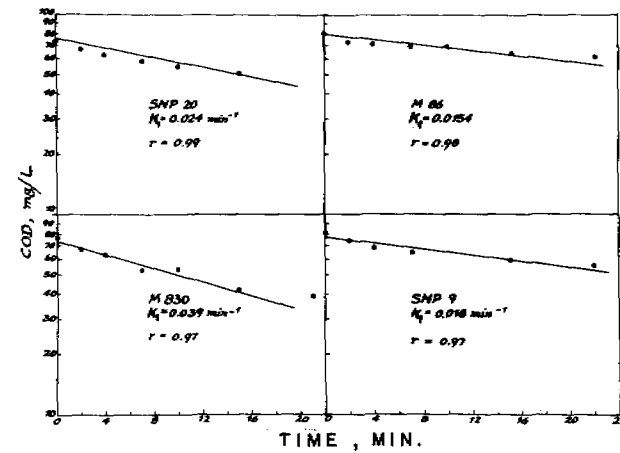


FIG. 8: K_1 FIRST ORDER REACTION RATE CONSTANT BY RESIDUAL COD, FOR M86, SNP9, SNP20 AND M830

The values of K_1 were calculated by linear regression with a correlation coefficient r . Table 2 summarizes the relationship between the first order reaction rate constants, K_1 , and n , the average number of ethylene oxide groups in the ethoxylate chain, of the nonyl phenol and dinonyl phenol ethoxylates and also in the polyethylene glycol investigated. From this table it can be seen that the values of K_1 grow with increasing n in the nonyl phenol ethoxylate series, i.e., ozonation is more effective at higher ethoxylate chain length.

This is graphically illustrated in Figs. 10 & 11. A linear relationship is found between K_1 values, determined by NIS, COD, TOC and n . In the case of DNP (Table 2) the values of K_1 for both NIS & COD are close to those for SNP20 due to the similar numbers of ethylene oxides in both compounds. The value of K_1 for PEG 1000, is near to that evaluated for M830. This tends to show that the effect of ozonation in both cases is similar and that the position of ozone attack is principally on the ethoxylate chain. This theory is substantiated by the values of the rate constants obtained for M830, which are the highest among the non-ionics examined. It should be noted that the polyethylene glycol residual was not determined by the Wickbold method because of difficulties experienced in the ethyl acetate extraction of the very hydrophilic material.

Linear regression was employed to establish a functional dependence of the rate constants on ethoxylate chain length. In the case of NIS in Fig. 10 this can be expressed thus:

$$K_1 = 0.012n + 0.11 \quad \text{where } r = 0.94$$

whilst in the case of COD (Fig. 11) the expression is

$$K_1 = 9.5 \times 10^{-4}n + 8.2 \times 10^{-3} \quad \text{where } r = 0.97$$

and in the case of TOC (Fig. 11)

$$K_1 = 2.28 \times 10^{-4}n + 2.99 \times 10^{-3} \quad \text{where } r = 0.77$$

It should be noted that the order of magnitude of K_1 for NIS is 14 times higher than K_1 for COD and 43 times higher than K_1 for TOC. In other words although COD and TOC concentrations are reduced, it is at a rate of tenths times lower than that for NIS, according to the disability of the ozonation products to complex with bismuth ions, or are too soluble in water and thus not easily extracted and remain undetected by the Wickbold analytical method. All these observations and the indications (Suzuki, 1976a,b) on lower molecular weight ethylene glycol, diethylene glycol and triethylene glycol products can be accounted for by a more favourable ozone attack on the polyethoxylate part of the molecules.

In agreement with the work of Price & Tumolo, (1964, 1967) the data indicate a remarkable activating effect for ozone attack on hydrogen atoms α to ether groups. All the observations seem most logically accounted for by a transition state requiring electron donation to the site of ozone attack, involving a hydrotrioxide intermediate, by a 1,3 - dipolar insertion of ozone, developing carbonium ion character in the transition state (Evans, 1972) to break down to hydroxyl as ethylene glycol, diethylene glycol and triethylene glycol and small polyethylene glycols, esters, acids and aldehydes. The small changes in UV absorption for all the nonyl phenol ethoxylates and DNP, except for SNP12, following ozonation, indicate that in addition to the principal ozone cleavage on the ether linkages the aromatic ring may also be attacked. It appears that the presence of large hydrophobic groups results in a slower ozone attack on the aromatic ring and the polyethoxylate chain of the surfactant.

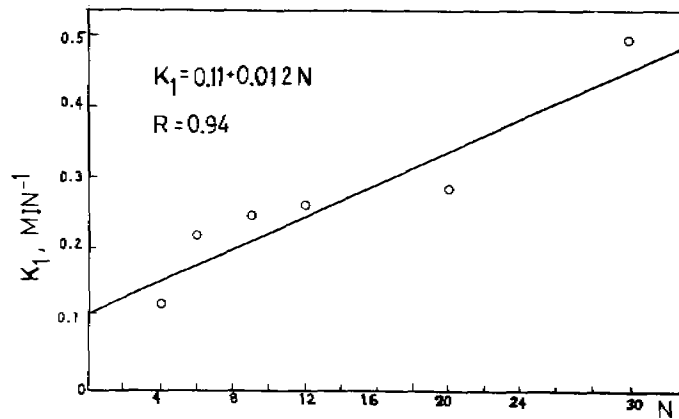
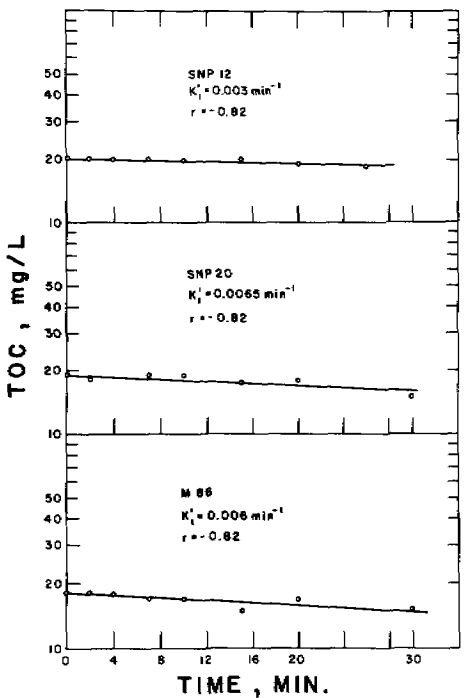


FIG. 10: FIRST ORDER REACTION RATE CONSTANTS K_1 AS A FUNCTION OF N BY WICKBOLD METHOD FOR NONYL PHENOL ETHOXYLATE SERIES

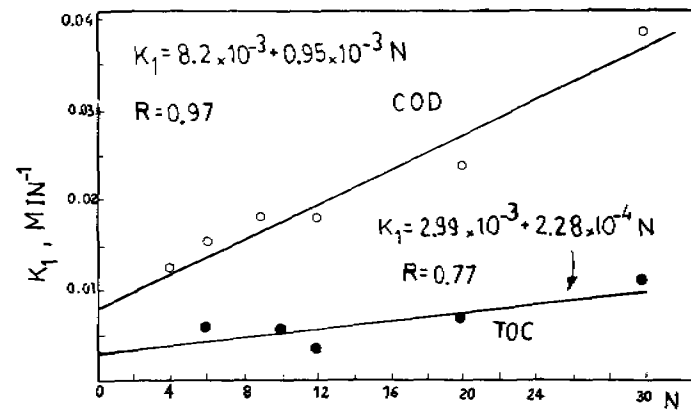


FIG. 11: FIRST ORDER REACTION RATE CONSTANTS K_1 AS A FUNCTION OF N BY COD AND TOC FOR NONYL PHENOL ETHOXYLATE SERIES

BIODEGRADATION

Ozone treatment leads to a reduction in the environmental disadvantages of non-ionic surfactants, such as foaming ability, but does not completely remove the organic content and leaves an organic load, as represented by high COD and TOC residuals. Ozone treatment alone cannot be recommended for total removal of non-ionic surfactants. A more modern approach is to increase the biodegradability of the harder non-ionic surfactant compounds in water by ozonation. In such cases, it may be assumed that the structure of the non-ionic surfactant is adjusted to that which is more amenable to bacteriological break-down and enhance the biodegradative properties of the material. The effect of ozone on biodegradation of a branched chain nonyl phenol ethoxylate ($n=13$), which is considered as a nonbiodegradable non-ionic surfactant, was investigated (Narkis and Schneider, 1980b), using OECD (1971) procedure. Figs 12, 13 & 14 show biodegradability patterns of ozonized surfactant with various ozone doses, based on percentage of non-ionic concentration reduction (Fig. 12) and on residual COD/initial COD (Fig. 13) or residual TOC/initial TOC (Fig. 14) as a function of time. For comparison, biodegradability test curves are also given for non-ozonized non-ionic surfactant and biodegradable LAS, linear alkyl benzene sulfonate anionic surfactant. After ozonation of 1 hour (ozone demand 51 mg/L) 99.3% of the surfactant, 39% COD and 16% TOC were removed just by ozonation. A total removal of 100% NIS, 70.5% COD and 62.5% TOC was effected following biodegradation of the ozonation product as compared to 8-25% COD and 23% TOC removal by biodegradation alone, without ozonation, of the non-ionic surfactant. The improvement in biodegradability is a result of changes in the molecular structure following ozonation which removes inhibitory effects which otherwise retard the breakdown (Narkis and Schneider, 1980a). High ozone doses do not convert the non-ionic surfactant completely to CO_2 and H_2O but smaller doses are sufficient to enhance biodegradation of the pollutant.

ACKNOWLEDGEMENT

This research is partially based on the M.Sc. Thesis of B. Ben David. The research was supported by a grant from the National Council for Research and Development of Israel and the Gessellschaft für Kernforschung (GFK), Karlsruhe, Germany.

REFERENCES

- Ben David, B. (1980). Non-ionic surfactants removal from aqueous solutions by physico-chemical treatment. M.Sc. Thesis, Technion, Haifa, Israel.
- Crabb, N.T. and Presinger, H.E. (1964). The determination of polyoxyethylene non-ionic surfactants in water at the parts per million level. *J. Am. Oil Chem. Soc.* **41**, 752-755.
- Evans, F.L. (1972). Ozone in water and wastewater treatment. Ann Arbor Sci. Publ.
- Gilbert, E. (1976). Reaction of ozone with substituted aromatics and with their oxidation products. Proc. Workshop Ozone Chlorine Dioxide, Oxidation Products of Organic Materials, Cincinnati, Ohio.
- Hoigné, J. and Bader, H. (1976). The role of the hydroxyl radical reactions in ozonation processes in aqueous solutions. *Water Res.*, **10**, 377-386.
- Horowitz, M. (1977). Specific phytotoxicity of surfactants. *Proc. E.W.R.S. Symp. Methods Weed Control and Their Integration*, 79-86.

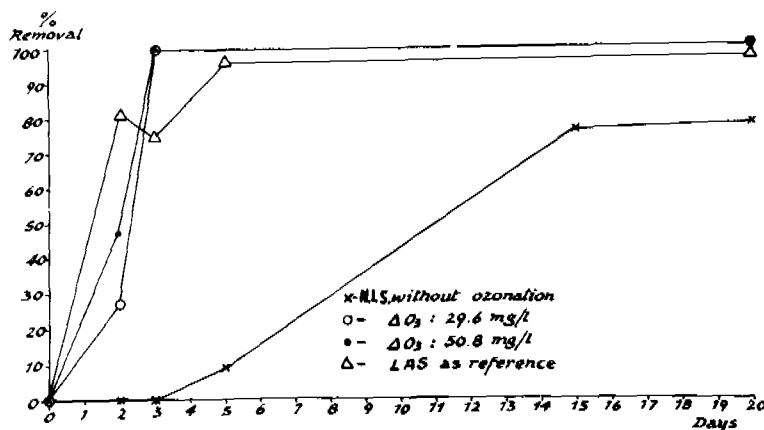


FIG. 12:
EFFECT OF OZONATION
ON BIODEGRADATION OF
NONYL PHENOL
ETHOXYLATE AS
MEASURED BY NIS
CONCENTRATION

FIG. 13:
BIODEGRADABILITY
PATTERN BASED ON
RELATIVE COD
CHANGES

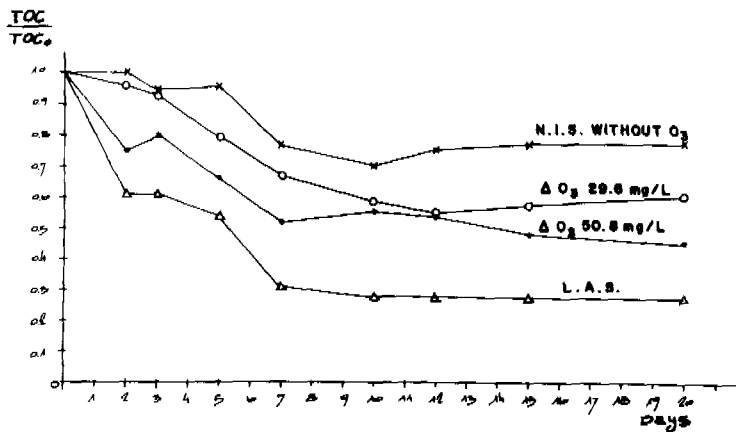
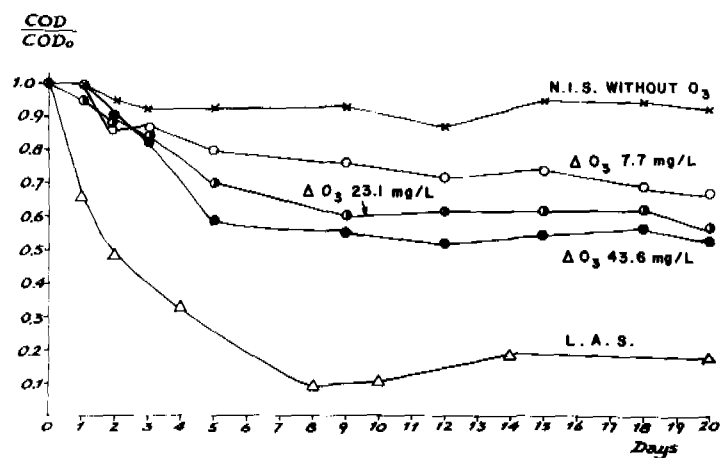


FIG. 14:
BIODEGRADABILITY
PATTERN BASED ON
RELATIVE TOC
CHANGES

- Lacy, W.J. and Rice, R.G. (1977). The status and future of ozone for water and wastewater treatment in the United States. Wasser, Berlin, 77, Int. Symp. Ozone und Wasser, 76-79.
- Narkis, N. and Henefeld-Furie, S. (1977). Israel's use of non-ionic surfactants. Water and Sewage Works, 124, 69-71.
- Narkis, N. and Schneider-Rotel, M. (1980a). Evaluation of ozone induced biodegradability of wastewater treatment plant effluents. Water Res., 14, 929-939.
- Narkis, N. and Schneider-Rotel, M. (1980b). Ozone induced biodegradability of a non-ionic surfactant. Water Res., 14, 1225-1232.
- Non-ionic surfactants production with near anionics level by 1980. European Chemical News, (1971), Oct. 8-10.
- OECD. (1971). Pollution by detergents. Determination of the biodegradability of anionic synthetic surface active agents. Paris.
- Price, C.C. & Tumolo, A.L. (1964). The course of ozonation of ethers. J. Am. Chem. Soc., 86, 4691-4694.
- Price, C.C. & Tumolo, A.L. (1967). Isotactic sequence lengths by ozonation of poly(propylene oxide). J. Polym. Sci., Part A-I, 5, 175-181.
- Schneider, M. (1976). Ozonation of lime treated effluents. M.Sc. Thesis, Technion, Haifa, Israel.
- Standard Methods for the Examination of Water and Wastewater. (1980). A.P.H.A., W.P.C.F. & A.W.W.A., 15th edn. N.Y.
- Suzuki, J. (1976a). Study of ozone treatment of water soluble polymers - I. Ozone degradation of polyethylene glycol in water. J. Appl. Polym. Sci., 20, 93-103.
- Suzuki, J. (1976b). Study on ozone treatment of water-soluble polymers - II. Utilization of ozonized polyethylene glycol by bacteria. J. Appl. Polym. Sci., 20, 2791-2797.
- Twelfth Progress Report on the Standing Technical Committee on Synthetic Detergents. (1970). H.M. Stationery Office, London.
- Wachs, A.M., Narkis, N., Rom, D. and Argaman, Y. (1976). Removal of ammonia and non biodegradable of organic matter by lime treatment, surface stripping and ozonation. Annual Report for the GFK, Ministry of Research and Technology, Federal Republic of Germany.
- Wachs, A.M., Narkis, N., Rom, D. and Argaman, Y. (1977). ibid.
- Wachs, A.M., Narkis, N., Schneider, M. and Wasserstrum, P. (1978). Use of ozone in water renovation - Part I. Removal of organic matter from effluents by lime treatment, ozonation & biological extended carbon adsorption. Int. Conf. IAWPR. Johannesburg, S.A., June 13-17, 1977. Prog. Wat. Technol. 10, 153-161.
- Wickbold, R. (1972). Zur bestimmung nichtionischer tenside in fluss und abwasser. Tenside Detergents, 9, (4), 173-177.
- Weinberger, P. & Ieyngar, S. (1983). Effects of aminocarb, fuel, oil 585 and nonyl phenol on the growth and development of Lemma Minor. Proc. of the International Meeting of the Israel Ecological Society, Jerusalem, Israel. May.

INFLUENCE OF BUBBLE SIZES ON OZONE SOLUBILITY UTILIZATION AND DISINFECTION

Mansoor Ahmad and Shaukat Farooq

*Department of Civil Engineering, University of Petroleum & Minerals,
P.O. Box 144, Dhahran, Saudi Arabia*

ABSTRACT

A disinfection study was carried out in a continuous flow system employing different sizes of ozone bubbles to determine their effects on solubility of ozone, its utilization and inactivation of microorganisms. The bubble sizes were varied by changing the porosity of the diffusers and ozone flow rates through the ozone contactor. Natural bacterial population (standard plate counts) present in the secondary wastewater effluent, was enumerated before and after ozonation. It was found that for a given concentration of ozone at a constant gas flow rate, decrease in bubble sizes resulted in an increase in ozone residual and degree of inactivation of organisms inspite of a decrease in ozone utilization by the wastewater.

KEYWORDS

Ozone, secondary effluent, disinfection, residual, utilization, solubility, correlation coefficients, plate counts.

INTRODUCTION

The degree of inactivation of microorganisms has been reported with respect to applied ozone in the gas phase (Nebel *et al.* 1973; McCarthy and Cecil, 1974; Rosen *et al.* 1974). However, it has been found by Farooq *et al.* (1978) that ozone residual is also one of the major parameters in the inactivation of microorganisms besides applied ozone. In recent years the importance of ozone gas bubbles in microorganism inactivation has also been recognized by several investigators (Ogden, 1970; Rosen *et al.* 1974; Hill and Spencer, 1974; Massachelein *et al.* 1975; Farooq *et al.* 1977). Farooq *et al.* (1976) showed that the presence of ozone bubbles along with ozone residual was more effective in inactivating microorganisms than ozone residual alone. They also pointed out that some inactivation may occur due to the presence of ozone bubbles even in the absence of ozone residual. Hill and Spencer (1974) reported that the inactivation reaction takes place near the surface of the bubbles as free suspended bacteria migrate to the interface due to their surface active properties. Massachelein *et al.* (1975) also emphasized the importance of contact between ozone bubbles and microorganisms.

Recognizing the importance of ozone bubbles in disinfection the present study has been conducted to determine the direct effects of their sizes on ozone residual, ozone utilization and subsequently on disinfection.

MATERIALS AND METHODS

Enumeration Procedure

The procedure for standard plate counts given in the Standard Methods was followed to enumerate the natural population of bacterial colonies in secondary wastewater effluent using the prescribed growth medium. The effluent was obtained from the South Aramco sewage treatment plant. All glassware used in the bacterial analysis was sterilized in a hot air oven at 200°C for 3 hours or more.

Ozone Measurement Technique

The concentration of ozone in the gas phase was determined as described in the Standard Methods, however, the aqueous concentration of ozone, referred to as ozone residual in this study, was not measured by purging the samples. Instead, 3 ml of iodide solution was placed in a beaker in which a 100 ml sample of the ozonated effluent was directly collected, and then titrated against sodium thiosulfate after adding 1 ml of concentrated hydrochloric acid.

Bubbles and Diffusers

Different sizes of ozone bubbles were produced by employing fritted glass diffusers of different porosities, i.e., fine (4-5.5 μ), medium (10-15 μ), and coarse (40-60 μ). Bubble sizes were also varied by changing the gas flow rates for a given diffuser. The actual sizes of the bubbles were measured using a photographic technique. The photographs were taken 1:1 and the bubble sizes were measured with the help of a microscope.

Experimental Technique

The ozone contactor shown in Fig. 1 consisted of a 5.2 cm diameter and 150 cm long Pyrex glass column in which the volume of the reaction mixture (1.3 l) was kept constant throughout the study. Inactivation studies were performed in this continuous flow system using different sizes of diffusers (fine, medium, coarse). Metering pumps were employed to deliver the secondary effluent from a storage tank at a constant rate of flow (250 ml/min) to the bottom of the reactor, while the rate of flow of gas was varied from 0.5 l/min to 2.0 l/min. The ozonator voltage, set by a variac, was used to control the amount of ozone in the gas stream.

The gas was supplied at the bottom of the reactor through a diffuser, and the unreacted gas was exhausted into a hood from the top of the reactor. The effluent was monitored intermittently for ozone residual, and samples were taken for enumerating the surviving organisms after the system had reached a steady state with respect to ozone residual and to surviving organisms in the effluent.

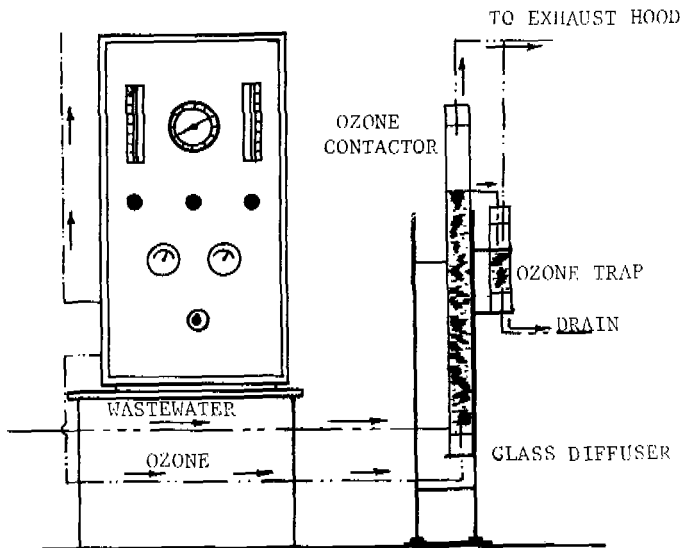


Fig. 1 Experimental set up for disinfection

RESULTS AND DISCUSSION

Effect of Ozone Bubbles on its Solubility

This study was performed to determine the effect of the sizes of ozone bubbles on its solubility in aqueous phase. It was observed that an increase in gas flow rate from 0.5 l/min to 2.0 l/min through a given diffuser (medium porosity) resulted in a slight increase in the size of ozone bubbles from 2.063 mm to 2.695 mm. Further, it was seen that, if the gas flow rate was kept constant at 0.5 l/min and the diffusers were changed from fine to coarse, the bubble size increased from 1.72 mm to 2.382 mm. (Table 1).

TABLE I Variation of Bubble Size with Gas Flow Rate

| Type of Diffuser | Pore Size Microns (μ) | Gas Flow Rate l/min | Bubble Size mm |
|------------------|-----------------------------|---------------------|----------------|
| Fine | 4 - 5.5 | 0.5 | 1.72 |
| Medium | 10 - 15 | 0.5 | 2.063 |
| | | 1.0 | 2.445 |
| | | 1.5 | 2.597 |
| | | 2.0 | 2.695 |
| Coarse | 40 - 60 | 0.5 | 2.382 |
| | | 1.0 | 2.715 |
| | | 1.5 | 2.955 |
| | | 2.0 | 3.250 |

Fig. 2 shows the effect of bubble sizes on residual ozone when the effluent flow rate was kept constant at 250 ml/min and the gas flow rate, G , was varied from 0.5 l/min to 2.0 l/min. As can be seen from Fig. 2, for a constant gas flow rate (0.5 l/min) and ozone input concentration of 2.5 mg/min in gas phase, the residual ozone obtained was 1.1 mg/l for a bubble size of 2.382 mm, which increased to 1.2 and 1.35 mg/l for bubble sizes of 2.063 and 1.72 mm respectively. A similar trend was also found for other gas flow rates.

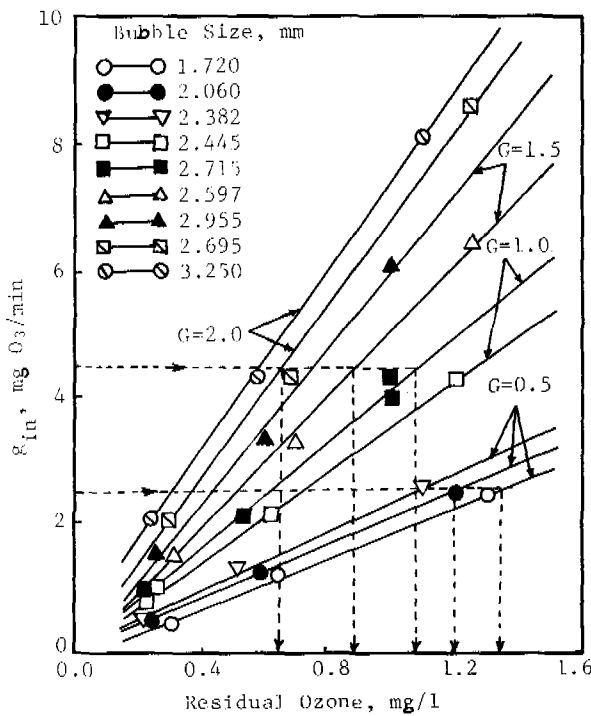


Fig. 2 Effect of bubbles on ozone residual

Since transfer of ozone from one phase to another occurs via diffusion and convective mass transport (Sherwood *et al.* 1975), the two-film theory can be used to explain this phenomenon. Ozone molecules are transferred to a liquid when the liquid is unsaturated with regard to the gas. Gas molecules from the bulk gas phase are continually transferred to the outer gas-film interface by turbulent mixing and diffusion. Through molecular diffusion, they reach the gas-liquid interface when they dissolve into the liquid film. Finally the gas molecules diffuse through this liquid film to the film's outer boundaries where the molecules are transported to the liquid phase by mixing (McCarthy and Cecil, 1974).

The mixing provided by sparging the gas at the bottom of the reactor was kept constant by maintaining steady rate of flow of 0.5 l/min. Therefore, the turbulence caused by mixing being the same in all three types of diffusers, only diffusion was responsible for the change observed in residual ozone. The reduction in bubble size for a given flow rate of gas is known to cause an increase in the number of bubbles resulting in an increase in diffusion area, which most likely is responsible for the higher ozone residual for smaller bubble

sizes. The same trend was observed for other gas flow rates.

When the gas flow rate was not kept constant but was increased, it was noted that there occurred a decrease in the ozone residual irrespective of the type of diffuser and the bubble size. For instance, at gas flow rates of 1.0, 1.5 and 2.0 l/min, with corresponding bubble sizes of 2.715, 2.597 and 2.695 mm, the ozone residuals were 1.1, 0.9 and 0.67 mg/l respectively, for a constant ozone input of 4.5 mg/min in the gas phase (Fig. 2). This decrease in ozone residual at higher gas flow rates may be attributed to a higher degree of ozone decomposition due to the increase in turbulence. Similar observations have been made by Hewes *et al.* (1974). Employing mechanical mixing instead of air-mixing, they demonstrated that the ozone auto-decomposition rate constant increases five-fold when the mixing speed is increased from 548 rpm to 720 rpm.

Effect of Bubble Size on Ozone Utilization

Ozone disinfection experiments were conducted to determine the ozone requirements as expressed by ozone utilization in mg/l for different levels of disinfection. Table 2 shows the ozone input and output in the gas phase and ozone utilization data, along with the data for total counts/ml after ozonation for different gas flow rates. All experiments were duplicated although in some cases the experiments were repeated thrice for better reliability of the data; however, only the average values are reported in Table 2. The data for ozone utilization and total counts after ozonation have been plotted in Figs. 3 and 4 where the lines of best fit, as determined by a power regression analysis ($Y=AX^B$), are shown. Six to nine data points were employed in calculating the correlation coefficient, R, for each line, as reported in the last column of the table.

In most of the cases the correlation coefficient was found within the range of 0.71 to 0.95. This indicates with 90 to 99 percent certainty that the total bacterial reduction is proportional to the ozone utilized. For example it can be seen from Table 2 that, as the ozone utilization increases from 0.48 to 2.4 mg/l, (for a bubble size of 1.72 mm) the bacterial count reduces from 475 to 22/ml. The same trend is shown for other gas flow rates and bubble sizes.

Fig. 3 illustrates that for a gas flow rate of 0.5 l/min and a disinfection level of 10 bacteria/ml, the utilizations for the three bubble sizes of 1.72, 2.063 and 2.382 mm are 5, 6.2 and 9.5 mg/l respectively, indicating that at a constant gas flow rate and a given level of disinfection the amount of ozone utilized is much less for smaller bubble sizes. Similar trends for other gas flow rates at different levels of disinfection can be derived from Figs. 3 and 4.

Effect of Ozone Bubble Sizes on Disinfection

The natural populations of bacteria in secondary wastewater were studied in disinfection experiments to investigate the effects of ozone bubbles on their survival. Table 3 shows the applied ozone, residual ozone, total counts/ml after ozonation and the percent survival of microorganisms for different gas flow rates. The average values of all the experiments conducted in duplicate, or triplicate, have been presented in Table 3. The data for ozone residual and percent survival have been plotted in Figs. 5 and 6 where the lines of best fit, as determined by power regression analysis, are shown. The correlation coefficients for different gas flow rates and bubble sizes are also reported in Table 3.

TABLE 2 Effect of Bubble Sizes on Ozone Utilization

| Gas Flow Rate l/min | Bubble Size mm | Ozone Input mg/l y_1 | Ozone Output mg/l y_2 | Total Count/ml After Ozonation y | Utilization mg/l $\times \frac{G}{Q^*} (y_1 - y_2)$ | Correlation Coefficients, R |
|---------------------|-------------------|------------------------|-------------------------|------------------------------------|---|-----------------------------|
| 0.5 | 1.72 (Fine) | 0.96 | 0.72 | 475 | 0.48 | -0.90 |
| | | 2.40 | 1.68 | 190 | 1.44 | |
| | | 4.80 | 3.60 | 22 | 2.4 | |
| | 2.063 (Medium) | 0.96 | 0.72 | 860 | 0.48 | -0.93 |
| | | 2.40 | 1.68 | 263 | 1.44 | |
| | | 4.80 | 3.6 | 37 | 2.4 | |
| | 2.382 (Coarse) | 0.96 | 0.72 | 1015 | 0.48 | -0.94 |
| | | 2.40 | 1.68 | 340 | 1.44 | |
| | | 4.80 | 3.6 | 65 | 2.40 | |
| 1.0 | 2.445 (Medium) | 0.90 | 0.6 | 340 | 1.2 | -0.95 |
| | | 2.04 | 1.32 | 33 | 2.88 | |
| | | 4.32 | 3.24 | 14 | 4.32 | |
| | 2.715 (Coarse) | 0.88 | 0.57 | 640 | 1.25 | -0.79 |
| | | 2.00 | 1.41 | 201 | 2.35 | |
| | | 4.24 | 3.12 | 36 | 4.48 | |
| 1.5 | 2.597 (Medium) | 0.96 | 0.66 | 106 | 1.80 | -0.89 |
| | | 2.16 | 1.44 | 13 | 4.32 | |
| | | 4.32 | 3.24 | 7 | 6.48 | |
| | 2.955 (Coarse) | 0.92 | 0.61 | 277 | 1.88 | -0.71 |
| | | 2.00 | 1.48 | 71 | 3.12 | |
| | | 4.09 | 2.88 | 28 | 7.28 | |
| 2.0 | 2.695 (Medium) | 0.96 | 0.66 | 85 | 2.4 | -0.85 |
| | | 2.16 | 1.44 | 13 | 5.76 | |
| | | 4.32 | 3.24 | 5 | 8.64 | |
| | 3.250 (Coarse) | 0.92 | 0.64 | 117 | 2.24 | -0.83 |
| | | 2.16 | 1.44 | 35 | 5.76 | |
| | | 4.01 | 2.63 | 16 | 11.04 | |

* Effluent flow rate $Q = 0.25$ l/min

A good correlation in the range of 0.84 to 0.99 has been observed between percent survival of microorganisms and ozone residual, indicating with 95 to 99.9 percent certainty that the survival is a function of ozone residual. An increase in ozone residual from 0.3 to 1.3 mg/l results in a decrease in percent survival from 0.495 to 0.023 percent for a bubble size of 1.72 mm (Table 3). For other gas flow rates and bubble sizes the trend is similar (Table 3).

It can be seen from Table 3 that for bubble sizes of 2.445 and 2.715 mm the corresponding survivals are 0.345 and 0.72 percent respectively, for a given ozone residual of 0.24 mg/l. It is known that the generation of smaller bubbles for a given gas flow rate results in an increase in the number of bubbles, causing an increase in the total contact area. Ogden (1970) has shown that

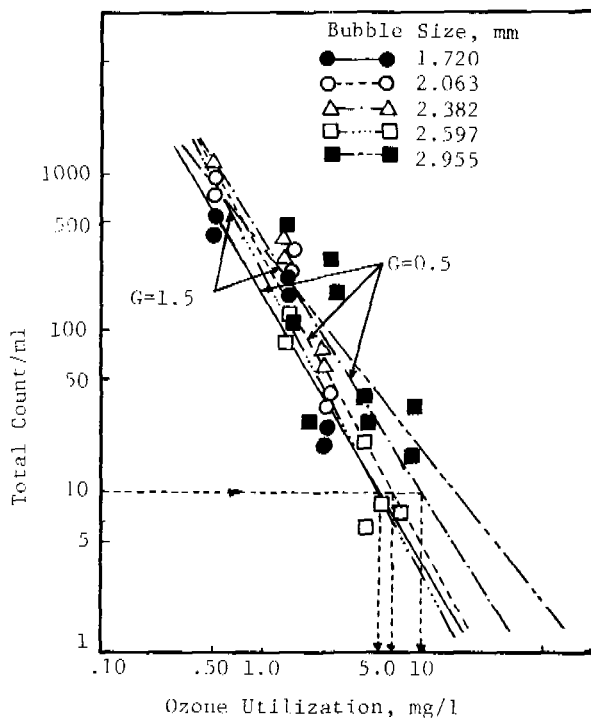


Fig. 3 Effect of bubble sizes on ozone utilization for gas flow rates of 0.5 and 1.5 l/min

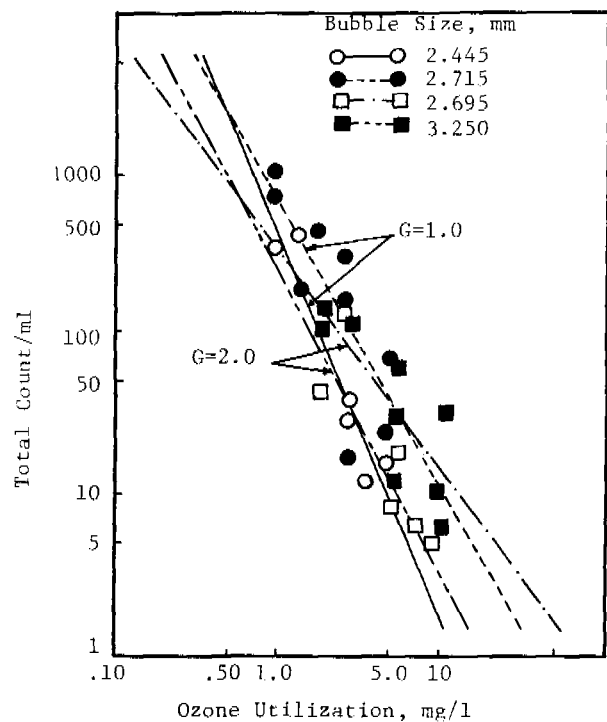


Fig. 4 Effect of bubble sizes on ozone utilization for gas flow rates of 1.0 and 2.0 l/min

bubbles with a diameter of 0.1 cm have nearly 32 times more contact value than those with a diameter of 1.0 cm. The smaller bubble size would, therefore, bring more microorganisms into direct contact with the ozone bubbles, thus providing a higher concentration of ozone and causing a greater amount of kill. Similar trends are observed for other gas flow rates (Table 3).

TABLE 3 Effect of Bubble Sizes on Survival of Microorganisms

| Gas Flow Rate, l/min | Bubble Size | Applied Ozone g/m ³ min | Residual Ozone mg/l | Total Counts/ml After Ozonation | % Survival y | Correlation Coefficients, R |
|----------------------|-------------------|------------------------------------|---------------------|---------------------------------|--------------|-----------------------------|
| G | mm | | x | | | |
| 0.5 | 1.72 (Fine) | 0.48 | 0.3 | 475 | 0.495 | -0.969 |
| | | 1.20 | 0.63 | 190 | 0.198 | |
| | | 2.40 | 1.3 | 22 | 0.023 | |
| | 2.063 (Medium) | 0.48 | 0.26 | 860 | 0.90 | -0.979 |
| | | 1.20 | 0.6 | 263 | 0.27 | |
| | | 2.40 | 1.2 | 37 | 0.385 | |
| | 2.382 (Coarse) | 0.48 | 0.24 | 1015 | 1.06 | -0.99 |
| | | 1.20 | 0.52 | 340 | 0.354 | |
| | | 2.40 | 1.1 | 65 | 0.068 | |
| 1.0 | 2.445 (Medium) | 0.90 | 0.24 | 340 | 0.345 | -0.975 |
| | | 2.04 | 0.62 | 33 | 0.034 | |
| | | 4.32 | 1.2 | 14 | 0.019 | |
| | 2.715 (Coarse) | 0.88 | 0.24 | 640 | 0.72 | -0.93 |
| | | 2.00 | 0.53 | 201 | 0.27 | |
| | | 4.24 | 1.0 | 36 | 0.04 | |
| | 2.597 (Medium) | 1.44 | 0.33 | 106 | 0.487 | -0.916 |
| | | 3.24 | 0.7 | 13 | 0.013 | |
| | | 6.48 | 1.25 | 7 | 0.0077 | |
| 1.5 | 2.955 (Coarse) | 1.38 | 0.25 | 277 | 0.32 | -0.841 |
| | | 3.00 | 0.58 | 71 | 0.076 | |
| | | 6.14 | 0.98 | 28 | 0.035 | |
| | 2.695 (Medium) | 1.92 | 0.3 | 85 | 0.088 | -0.93 |
| | | 4.32 | 0.7 | 13 | 0.013 | |
| | | 8.64 | 1.25 | 5 | 0.0063 | |
| | 3.250 (Coarse) | 1.84 | 0.25 | 117 | 0.141 | -0.86 |
| | | 4.32 | 0.55 | 35 | 0.039 | |
| | | 8.01 | 1.1 | 16 | 0.0175 | |

The above observation is valid only when the gas flow rate, and hence the turbulence, is kept constant and the bubble size is varied only by changing the diffusers. However, when the same porosity diffuser was employed (medium porosity) and the bubble sizes were changed from 2.063 to 2.597 mm by increasing the gas flow rate from 0.5 l/min to 1.5 l/min, the respective microorganism survival for these sizes and gas flow rates were 7.5 and 0.7 percent, at a residual of 0.1 mg/l (Fig. 5). This large kill at higher gas flow rates is

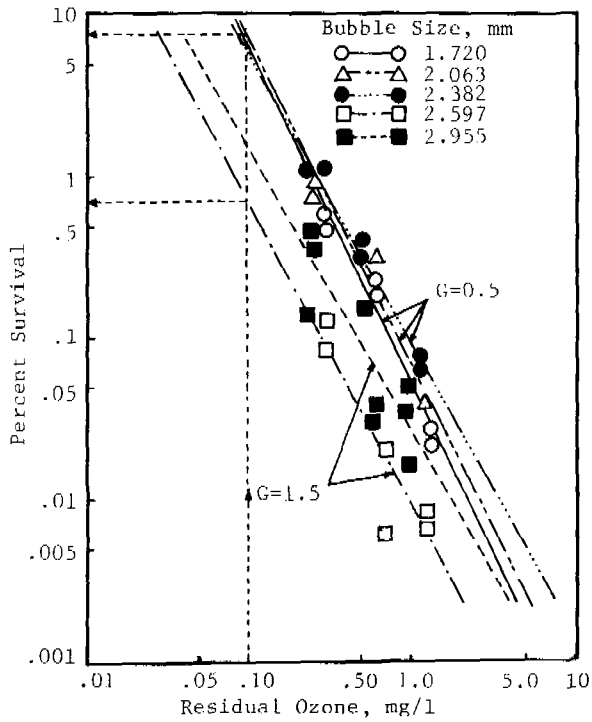


Fig. 5 Effect of bubble sizes on inactivation of microorganisms at gas flow rates of 0.5 and 1.5 l/min

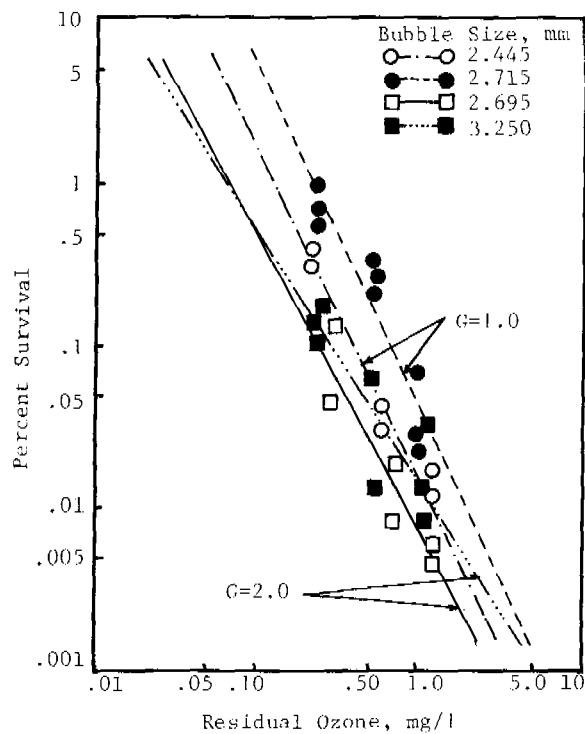


Fig. 6 Effect of bubble sizes on inactivation of microorganisms at gas flow rates of 1.0 and 2.0 l/min

attributed to increased turbulence generated by large bubble sizes. Figs. 5 and 6 show similar trends for other gas flow rates.

CONCLUSIONS

A disinfection study was conducted in a continuous flow system using the natural bacterial population of a secondary treated wastewater effluent. The following specific conclusions may be drawn from this study.

The concentration of ozone in the aqueous phase increases with a decrease in the size of the ozone bubbles for a given gas flow rate, provided the ozone concentration remains constant in the gas phase.

The amount of ozone utilized by the waste water decreases proportionally with the size of the ozone bubbles for the same gas flow rate and for the same level of disinfection.

For a given gas flow rate and ozone residual, the degree of inactivation of microorganisms increases as the size of ozone bubbles decreases.

ACKNOWLEDGEMENT

Authors are grateful to the Department of Civil Engineering and Saudi Arabian Center for Science and Technology for providing all necessary facilities for performing this research.

REFERENCES

- Farooq, S., Engelbrecht, R.S. and Chian, E.S.K. (1977). The effect of ozone bubble on disinfection. Prog. Wat. Tech., 9, 233-247.
- Farooq, S., Engelbrecht, R.S. and Chian, S.K. (1978). Process consideration in design of ozone contactor for disinfection. Jour. of Env. Engg. Div. ASCE, 104, EE5, 835-847.
- Hewes, C.G., Prengle, H.W., Mauk, C.E. and Sparkman, O.D. (1974). Oxidation of refractory organic materials by ozone and ultraviolet light. Final report for U.S. Army Mobility Equipment R & D Center, Fort Belvoir, VA, Contract DAAK02-74-C-0239.
- Hill, A.G. and Spencer, H.T. (1974). Mass transfer in a gas sparged ozone reactor. Presented at the First International Symposium on Ozone for Water and Wastewater Treatment, Washington, D.C., 367-380.
- Massachelein, W., Fransolet, G. and Genot, J. (1975). Techniques for dispersing and dissolving ozone in water Part I, Water and Sewage Works, 122, 12, 57-60.
- McCarthy, J.J. and Cecil, H.S. (1974). A review of ozone and its application to domestic wastewater treatment. Jour. Am. Water Works Assoc., 67.12, 718-725.
- Nebel, C., Gottschling, R.D., Hutchinson, R.L., McBride, T.J., Taylor, D.M., Pavoni, J.L., Spencer, H.E. and Fleischman, M. (1973). Ozone disinfection of industrial-municipal secondary effluents. Jour. Wat. Pol. Control Fed., 45, 12, 2493-2507.
- Ogden, M. (1970). Ozonation today. Ind. Water Engg. 36-42.
- Rosen, H.M., Lowther, F.E. and Clark, R.G. (1974). Get ready for ozone. Water and Waste Engg., 11, 7, 25-31.
- Sherwood, T.K., Pigford, R.L. and Wilke, C.R. (1975). Mass Transfer. McGraw Hill Book Co., New York, pp.718-719.
- Standard Methods for the Examination of Water and Wastewater (1980). 15th ed. Amer. Pub. Health Assoc. Washington, D.C.

THE ROLE OF RAPID MIXING TIME ON A FLOCCULATION PROCESS

R. J. François and A. A. Van Haute

Institute for Industrial Chemistry, Katholieke Universiteit Leuven de Croylaan 2, B-3030 Leuven, Belgium

ABSTRACT

The influence of the duration of rapid mixing on a flocculation process is evaluated by investigating the characteristics of the hydroxide flocs formed under carefully controlled conditions. Two different methods are used for measuring floc dimensions and their distribution. From the experimental results other floc characteristics such as floc strength and size of the flocculi are deduced. Also the reaction constant, the destabilization factor and the growing constant of the coagulation and flocculation process are calculated. Using the influence of rapid mixing time on all floc characteristics and kinetic parameters minimum and maximum limits for the rapid mixing time are deduced.

KEYWORDS

Coagulation kinetics; flocculation kinetics; mixing; hydroxide floc characteristics; floc structure.

INTRODUCTION

A coagulation-flocculation process consists of three steps: coagulation of the suspended solids, flocculation of the destabilized particles and elimination of the floc aggregates formed. Knowledge of the different parameters influencing this process is indispensable. Besides the raw water composition, the process is strongly influenced by kinetic process parameters: duration of rapid mixing and slow mixing steps, and the energy input during the different phases. In this investigation the slow mixing phase was always long enough to form fully grown flocs. The influence of rapid mixing time was investigated and two groups of experiments were developed.

SEDIMENTATION EXPERIMENT

The first group of experiments consisted of sedimentation measurements. Four liters of a prepared suspension were flocculated under carefully controlled conditions of pH, temperature, energy and mixing times. A cylindrical five liter jar was used, without baffles, to reduce the spread of velocity gradients throughout the suspension. Flocculation and sedimentation were studied by means of a flow-through turbidimeter. From the decrease of turbidity as a function of sedimentation time, the floc aggregate equivalent diameters and their distribution were calculated. Newton's law for sedimentation was used. A sphericity for the flocs of 80% was accepted (Tambo *et al.*, 1979), which satisfies the limitations of Newton's law (Foust *et al.*, 1960). For the calculation of floc density an empirical relation drafted by Tambo *et al.* (1979) was used. The sedimentation velocity is influenced by the surface charge of the flocs. A correction formula was published by Booth (1954) and Davies *et al.* (1963), and the resulting non-linear equation was solved for the equivalent diameter by using a Newton-Raphson iteration. Details, together with an extensive discussion and evaluation of the experiments and methodology, were reported by François *et al.* (1982) and a first important conclusion from those experiments is shown in Fig. 1.

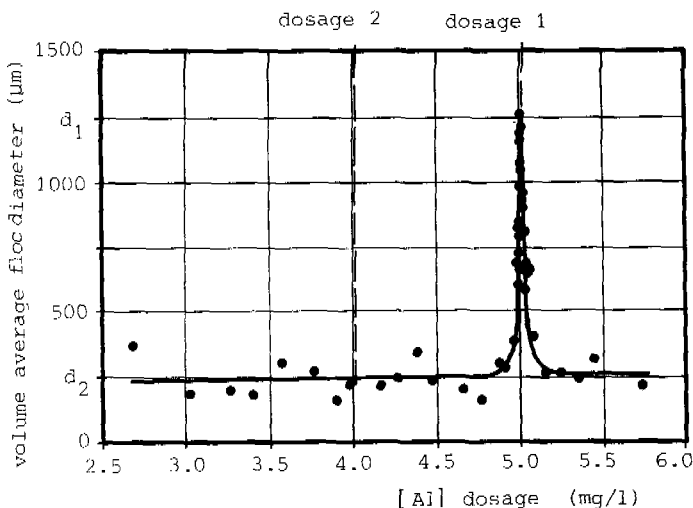


Fig. 1. Influence of coagulant dosage on floc size

For a given set of process parameters one can delimit a small dosage range yielding very large flocs. A change of one of the process parameters causes a shift not only of that small dosage range (dosage 1) but also of diameters 1 and 2, floc build-up time and sludge production. The influence of a change of rapid mixing time on the parameters mentioned is demonstrated in Figs 2 and 3.

Rapid mixing for more than 2 minutes reduced the floc dimensions. A mixing time of 180 seconds required the highest aluminium dosage. Omission of the rapid mixing step ($t = 0$ s) caused discontinuities in the different curves: smaller flocs, a smaller sludge index and a longer floc build-up time. The sludge volume was measured after a sedimentation of 30 minutes in an Imhoff cone. The experimental conditions are summarized in Table 1.

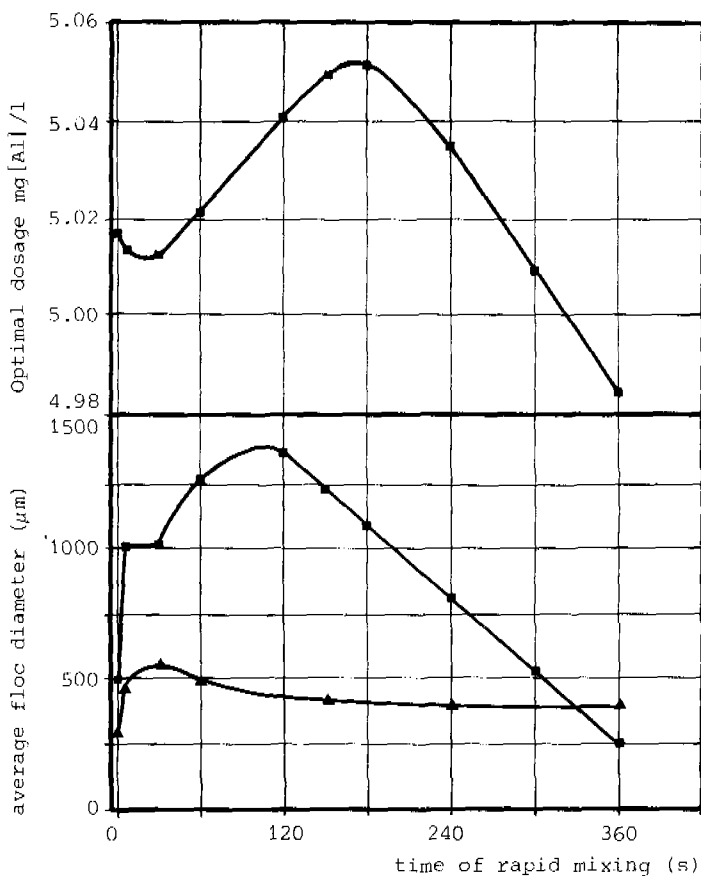


Fig. 2. Influence of rapid mixing time on floc size and "optimal" dosage I

■: results from the sedimentation experiment
 ▲: results measured with a particle sizer

TABLE 1 Experimental Conditions

Raw Water Conditions:

A 75 mg/l suspension of kaolinite in distilled water
 Temperature 25 °C

pH 7.0

Kinetic Conditions:

Velocity gradient during rapid mixing: 329 s⁻¹

Velocity gradient during slow mixing: 34 s⁻¹

Time of slow mixing: until a constant turbidity

Time of rapid mixing: variable

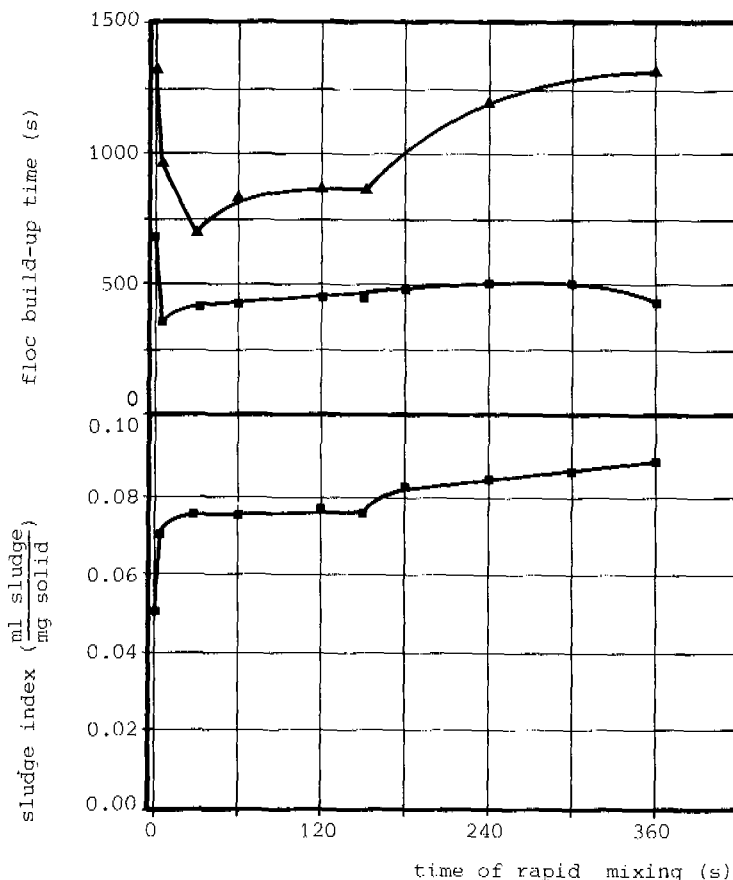


Fig. 3. Influence of rapid mixing time on sludge index and floc build-up time

■: results from the sedimentation experiment
 ▲: results from the experiments with a particle sizer

The influence of other variables such as pH, temperature, quantity of suspended solids, quantity and kind of electrolytes dissolved in the water, energy input during rapid and slow mixing steps are reported elsewhere (François et al., 1982).

EXPERIMENTS WITH A PARTICLE SIZER

For the second group of experiments, the same flocculator as in the previous experiments was used. Thus, the experimental conditions were exactly the same for both investigations. For these experiments dosage 2 was used. This dosage was 80% of the "optimal" dosage 1 because the apparatus was not able to measure diameters larger than 1879.9 μm . The floc diameters and their distribution were measured every 15 seconds with a Malvern Particle Sizer type 2200. The sample

was syphoned from the suspension with a velocity of 5.7 cm per second. In this group three types of experiments were executed. For a given set of process parameters, floc growth was measured first. Two examples are shown in Figs 4 and 5.

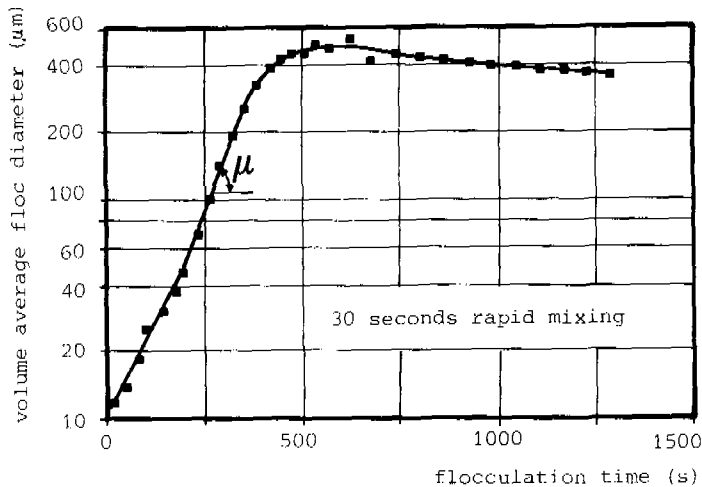


Fig. 4. Floc build-up curve for a rapid mixing time of 30 seconds

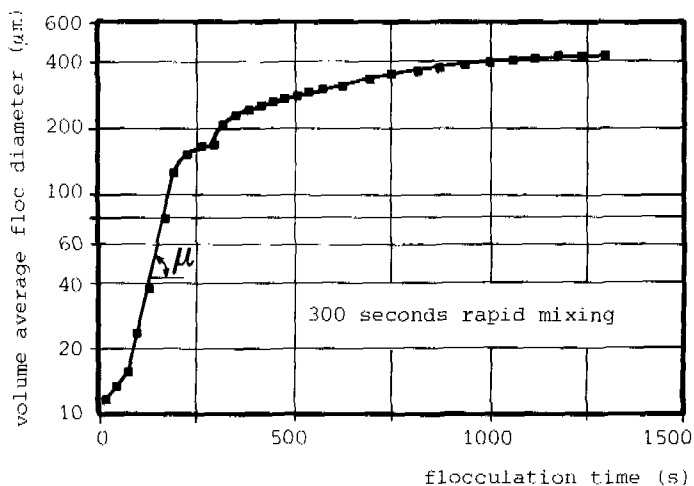


Fig. 5. Floc build-up curve for a rapid mixing time of 300 seconds

From Fig. 5 it is clear that extended rapid mixing can disturb the growth of flocs. The energy from each rapid mixing allows a certain maximum floc diameter. Larger flocs will be ruptured into smaller parts. During flocculation, at a certain moment, there are flocs which reach their maximum allowable size in relation to the G-value of rapid mixing ($\ln d_{\max} = \ln a_0 - b \cdot \ln G$). A rapid mixing time greater than the above mentioned critical time yields smaller flocs because of the temporary rupture of flocs larger than the critical dimension. This phenomenon was also reflected as a discontinuity in the relation of rapid mixing time versus sludge index and floc build-up time (Fig. 3).

From such an experiment one also obtains information about floc build-up time, coagulation kinetics and floc growth. Coagulation and flocculation have first order kinetics (Camp *et al.*, 1943).

$$\frac{dN}{dt} = k \cdot N$$

with $k = -\alpha_0 \cdot 4 \cdot (\frac{du}{dz}) \cdot \phi / \pi$

| | | |
|---------------------|---------------------------------------|--------------|
| $\frac{du}{dz} = G$ | : velocity gradient during the mixing | [s^{-1}] |
| ϕ | : volume fraction of particles | [$-$] |
| N | : number of primary particles | [$-$] |
| t | : coagulation time | [s] |
| k | : reaction constant of coagulation | [s^{-1}] |
| α_0 | : destabilization factor | [$-$] |

The reaction constant is determined as the slope of $\ln(N_i/N_0)$ vs time. From the reaction constant one can easily calculate the collision efficiency or destabilization factor α_0 . For flocculation, the floc growth can be quantified by a growing constant, expressing the rate of increase of the volume median floc diameter.

$$d_i = d_0 \cdot \exp(\mu t)$$

| | | |
|-------|--|-------------|
| d_0 | : volume median diameter of the primary particle | [μm] |
| d_i | : volume median floc diameter on moment i | [μm] |
| μ | : growing constant | |

The influence of rapid mixing time on k , α_0 and μ is graphically presented in Fig. 6 and mathematical relationships are given in Table 2.

TABLE 2 Influence of Rapid Mixing Time on k , α_0 and μ

| | | |
|--------------|-------------------------------|--|
| k : | $5s < t_{\text{rapid}} < 60s$ | $\ln k = 4.5524E - 3 \times t_{\text{rapid}} - 5.838$ |
| | $t_{\text{rapid}} > 60s$ | $\ln k = 4.2032E - 3s^{-1}$ |
| α_0 : | $0 < t_{\text{rapid}} < 240s$ | $\ln \alpha_0 = -7.8293E - 3 \times t_{\text{rapid}} - 6.4652$ |
| | $t_{\text{rapid}} > 240s$ | $\ln \alpha_0 = -2.1534E - 3 \times t_{\text{rapid}} - 7.9715$ |
| μ : | $t_{\text{rapid}} < 150s$ | $\ln \mu = 5.0475E - 3 \times t_{\text{rapid}} - 5.0247$ |
| | $t_{\text{rapid}} > 150s$ | $\ln \mu = 0.0146 s^{-1}$ |

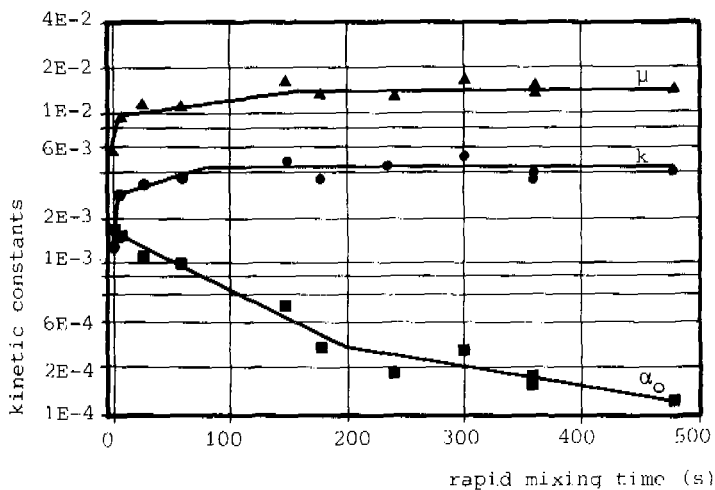


Fig. 6. Reaction constant, destabilization factor and growing constant versus rapid mixing time

$$\begin{aligned} k &= \bullet \\ \alpha_o &= \blacksquare \\ \mu &= \blacktriangle \end{aligned}$$

The effect of the absence of rapid mixing is clearly visible: a smaller reaction constant for coagulation and a smaller growing constant during flocculation. The floc build-up times and the volume median floc diameters measured in these experiments are indicated in Figs 2 and 3.

The smaller floc build-up times measured with the sedimentation experiment are self-evident because they are based on turbidity measurements. When all the particles smaller than 80 μm were grown to larger flocs, then the measured turbidity remained constant. The combination of units greater than 80 μm into larger flocs can still be detected by the particle sizer. This explains the much longer build-up times measured with this instrument, especially for rapid mixing times longer than the critical times. For the same reason partly grown flocs were measured in the sedimentation experiments. This explains the curves for the floc dimensions in Fig. 2.

If the build-up time is known, floc strength can be investigated. Fully grown flocs are broken by known shear stresses, expressed by their velocity gradient. After rupture the fragments are allowed to regrow. A series of such experiments gives an insight into floc strength. Figure 7 shows the results of such a series of experiments on flocs formed after 60 seconds of rapid mixing. In Table 3 the mathematical expressions for the relations $\ln d = \ln a - b \ln G$ are given.

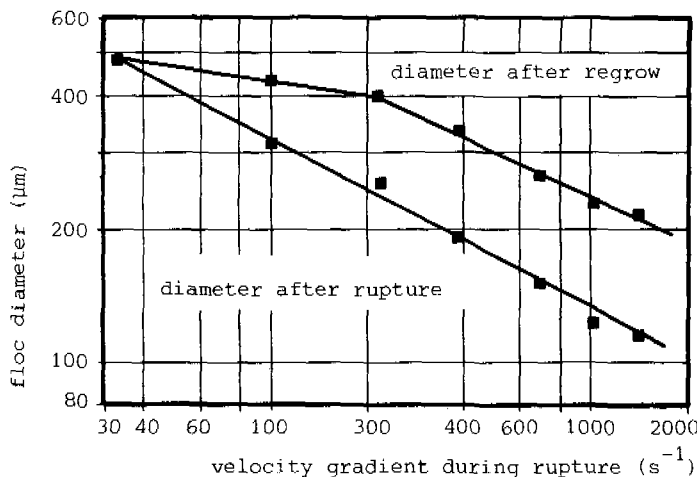


Fig. 7. Influence of the velocity gradient during rupture on the size of the ruptured and regrown flocs

TABLE 3 Relation Between Diameter and G Value $d=a \cdot G^b$

| Time of rapid mixing s | $G < 200 \text{ s}^{-1}$ | | $G > 200 \text{ s}^{-1}$ | |
|------------------------------|--------------------------|-------|--------------------------|-------|
| | a | b | a | b |
| 0 | 778 | .3000 | 653 | .3138 |
| 5 | 1657 | .3793 | 2256 | .4339 |
| 30 | 2162 | .4047 | 1726 | .3752 |
| 60 | 1986 | .3918 | 1986 | .3918 |
| 150 | 1531 | .3630 | 1531 | .3630 |
| 240 | 1250 | .3313 | 1250 | .3313 |
| 360 | 2165 | .4226 | 2165 | .4226 |

A representation of all the diameters after rupture as a function of rapid mixing time and of rupture G-value is given in Fig. 8.

In a previous article, the velocity of a four level organisation of hydroxide floc aggregates was proved (François et al., 1984). The different levels of organisation are: primary particles, flocculi, flocs and floc aggregates. The bonds between the particles are elastic. The flocculi can be regarded as the building stones of the structure and they are formed at those points in the flocculator where the highest velocity gradients exist.

To determine the dimension of a flocculus, a third type of experiment with the particle sizer was developed. In this 'stripping' experiment, fully grown flocs were subjected to a discontinuous increase of the velocity gradient. The fractured parts were measured. Starting from the philosophy that all the measured parts are multiples of the building unit, it is possible to calculate the limits between which the flocculus diameter lies. The influence of rapid mixing time on the flocculus diameter is shown in Table 4 and Fig. 9.

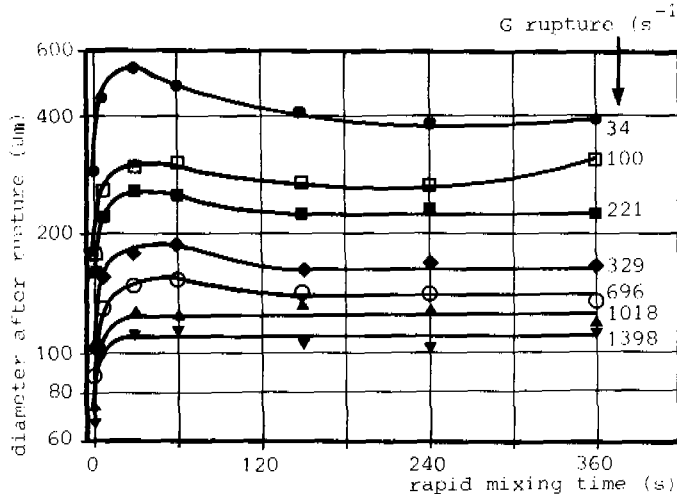


Fig. 8. Diameters of flocs after rupture as a function of rapid mixing time and of rupture intensity

TABLE 4 Influence of Rapid Mixing Time
on the Formation of Flocculi

| Time of rapid mixing (s) | Flocculus diameter (μm) | |
|--------------------------|--------------------------------------|-------------|
| | Lower limit | Upper limit |
| 0 | 5.8 | 6.17 |
| 5 | 7.9 | 11.4 |
| 30 | 15.15 | 18.5 |
| 60 | 14.5 | 15.15 |
| 150 | 11.4 | 11.85 |
| 240 | 10.1 | 11.85 |
| 360 | 7.9 | 10.1 |

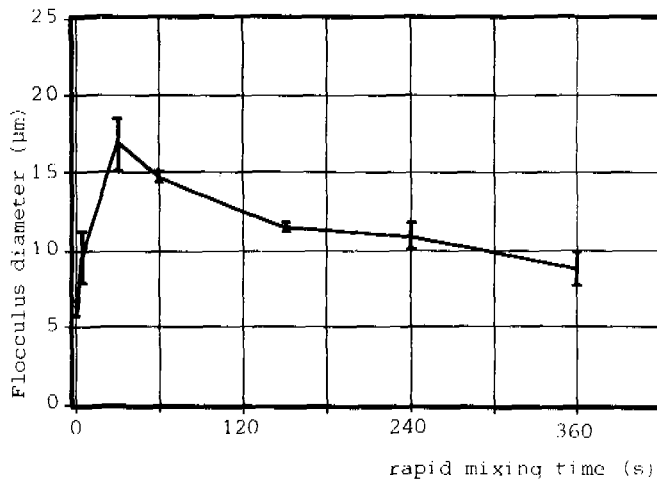


Fig. 9. Diameters of the flocculi in relation to rapid mixing time during floc formation

The curve in Fig. 9 displays a maximum for a rapid mixing time of 30 seconds. Rapid mixing for 30 seconds results in complete formation of flocculi. For longer mixing times, the flocculi are smaller, probably due to erosion during prolonged high mixing intensity. Rapid mixing for less than 30 seconds produces only partially formed flocculi.

The fact that the flocculi are the building stones of the structure is reflected in the similar shape of the relationships between the diameter of the flocs formed and the rapid mixing time (Fig. 2), and between the flocculi diameter and the rapid mixing time (Fig. 9).

GENERAL CONCLUSIONS

A critical time exists for rapid mixing, and mixing for a period longer than that critical time (150 s) leads to a disturbance of floc growth with disadvantageous consequences for the floc characteristics.

The reaction constant for coagulation (k) increases with increasing rapid mixing time. For rapid mixing times longer than 60 seconds, k remains constant.

The destabilization factor (α_0) increases with increasing rapid mixing time. For times longer than 240 seconds, the decrease is smaller.

The growing constant of flocculation (μ) increases if rapid mixing time increases. The rate of floc formation remains constant for rapid mixing times of more than 150 seconds.

The coagulation process cannot be accelerated by using rapid mixing times of more than 60 seconds. On the other hand if a prolonged rapid mixing phase is used, a smaller destabilization of the suspension is sufficient to obtain the same kinetic properties for the coagulation process.

Based on the floc structure model developed, it is possible to determine a minimum rapid mixing time. To obtain a strong structure, flocculi must be formed. This requires a minimum time of 30 seconds.

The largest and most resistant flocs are constructed with the largest flocculi which are the building stones of the structure. A rapid mixing time of 30 seconds seems to be optimal.

An absence of rapid mixing is very disadvantageous for all the characteristics of both flocs and the flocculation process.

Although the conclusions presented are generally applicable for any flocculation unit, the numerical values most probably are not because the raw water parameters differ from plant to plant.

REFERENCES

- Booth, F. (1954). Sedimentation potential and velocity of solid spherical particles. *J. Chem. Phys.*, 22, 956-968.
Camp, T.R. and Stein, P.C. (1943). Velocity gradient and internal work in fluid motions. *J. Bos. Soc. Civ. Engrs*, 30, 219-237.
Davies and Rideal (1963). Sedimentation potentials. In: Interfacial

- Phenomena. Academic Press, New York. pp. 137-140.
- Foust, A.S., Wenzel, L.A., Clump, G. W., Maus, L. and Anderson, L.B. (1960). Phase separation based upon fluid mechanics. In: Principles of Unit Operations, 2nd ed. John Wiley and Sons Inc., New York. pp. 449-453.
- Francois, R.J., Van Haute, A.A. and Winderickx, G.C. (1982). Influence of process parameters on flocculation and floc characteristics. In: Water Filtration, K.VIV, Antwerp. 1.55-1.63 and 1.82-1.83.
- Francois, R.J. and Van Haute, A.A. (1984). Floc strength measurements giving experimental support for a four level hydroxide floc structure. In: Chemistry for the Protection of the Environment, L. Pawlowski and R. Verdier (Eds). Elsevier Scientific Publishers, Amsterdam. 14 pp. (in press).
- Tambo, N. and Watanabe, Y. (1979). The floc density function and aluminium floc. Wat. Res., 13, 409-418.

MANAGEMENT OF URBAN WASTE WATER PHYSICO-CHEMICAL TREATMENT STATIONS: SERVOCONTROL OF REAGENT ADDITIONS AT THE QUIBERON SEWAGE TREATMENT PLANT, FRANCE

P. Marchandise,* J. P. Legendre,* D. Delacroix** and
J. L. Rivoal***

**L.C.P.C., B.P. 19, 44340 Bouguenais, France*

***S.O.B.E.A., rue Louis Brillet, B.P. 11, 56400 Auray, France*

****A.F.B.L.B., 15, rue d'Alger, 44000 Nantes, France*

ABSTRACT

The physico-chemical treatment of sewage requires the addition of costly reagents. The quantities added are generally proportional to the flowrate treated. Recent progress in pollution detectors now makes it possible to measure sewage concentration continuously. This makes it possible to match the quantity of reagent added to the treated-water quality objective set. COD-SM-Turbidity relations have been determined at various sites. An assessment of the performance of a servocontrol device during the summer of 1983 is presented.

KEYWORDS

Physico-chemical treatment; Automatisation.

INTRODUCTION

The physico-chemical treatment of sewage, which is a treatment suited to the liquid wastes of towns of variable population, calls for a judicious choice of reagents, but also for their use in quantities commensurate with the pollution to be eliminated.

The working assumption of a physico-chemical plant is that pollution is proportional to flowrate. In practice, a variation in the characteristics of the pollutant content of the untreated waters results in a deterioration of the quality of treatment (too little reagent or too much). A survey run in 1981 by the Agence Financière de Bassin "Rhône-Méditerranée-Corse" (Unknown, 1981) shows that of the 80 physico-chemical plants counted in France, not one had servocontrol of additions of mineral reagent. The servocontrol developed at the water pollution section of the Laboratoire Central des Ponts et Chaussées makes it possible to add reagent according to pollutant content and to achieve a degree of pollution control chosen in advance on the basis of preliminary jar tests. Its originality lies in the continuous measurement of incoming pollution and immediate reaction on the quantity of reagent. It differs from the automatic flocculation meters similar to programmable automations based on measurement of the characteristics of the treated water following injections of increasing doses of coagulant reagent into a sample of sewage taken at regular intervals.

The installation of the servocontrol module at the treatment plant of Quiberon, France, for the 1983 tourist season provided an opportunity for a full-scale test of the effectiveness of the system.

CONTINUOUS POLLUTION MEASUREMENT

The parameter that was continuously measured, using equipment of original design, was the turbidity. The Monitek turbidimeter functions in accordance with the CLAM (Cleansimatic Liquid Analysis Meter) principle and consists of a stainless-steel measurement probe (1.20 m long) immersed in the liquid to be measured and connected by a multiconductor cable to an electronic unit (fig. 1) giving a direct reading of the measured suspended matter (SM), with a choice of three measurement ranges : 0 to 3,000, 0 to 10,000, and 0 to 30,000.

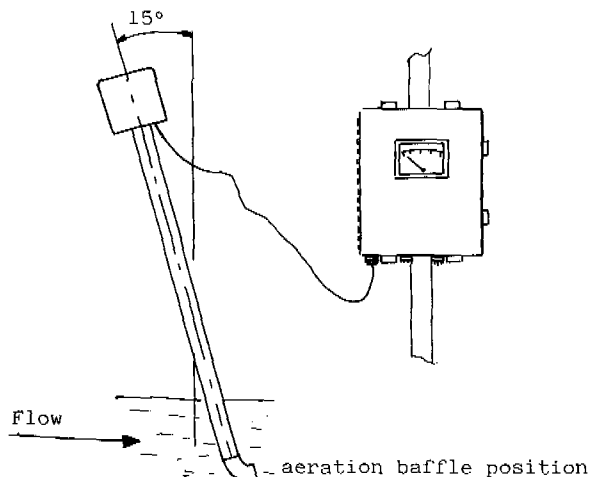


Fig. 1. Turbidimeter

At the end of the probe there is a sensing head (see cutaway view in fig. 2).

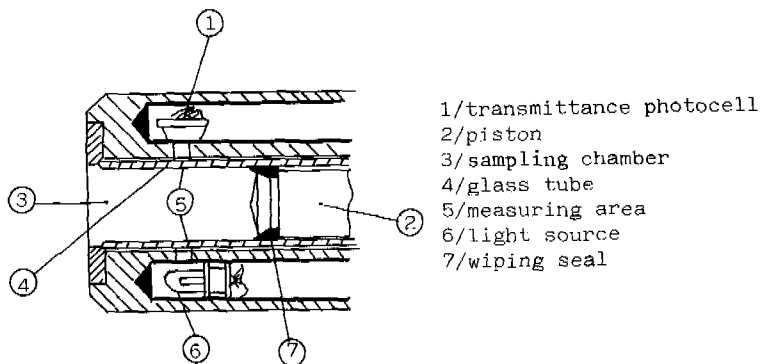


Fig. 2. Sensing head longitudinal cross section

A piston made tight by a scraper ring draws a quantity of liquid waste into the measurement chamber, made of pyrex glass. A photoelectric cell receives the light transmitted through the sample. This signal is stored while the sample is driven back out of the chamber by the piston, the scraper ring of which cleans the optical surface to prevent clogging of the chamber. This operation is repeated every 15 seconds. This procedure provides constant self-cleaning, making it possible to install the turbidimeter at the upstream end of the plant without any special supervision.

This turbidimeter has been tested for long periods with waste waters of different types (urban, urban + agribusiness, industrial) subject to substantial variations in colour, and in particular on waters coloured by iron sulphides resulting from the injection of FeSO_4 .

TABLE 1. Turbidity-COD-SM relations in different types of waste water

| | | | |
|--|-------------|-----------|-----------|
| Industrial waste water | COD = 0.26 | T + 1,407 | r = 0.96 |
| Limay-Porcheville | SM = 0.51 | T + 299 | r = 0.99 |
| Urban + agribusiness | COD = 1.814 | T + 8 | r = 0.968 |
| waste water (Nantes-Sud slaughterhouse) | SM = 1.065 | T - 160 | r = 0.958 |
| Urban sewage with injection of 350 ppm FeSO_4 (St. Jean de Monts) | COD = 0.269 | T - 119 | r = 0.88 |
| | SM = 0.18 | T - 320 | r = 0.93 |

The turbidity-COD-SM correlations given in table 1 for about 50 water samples yield very reasonable correlation coefficients. The coefficients of the relations differ substantially from one site to another because the turbidimeter was adjusted at each site to cover the whole measurement range. Its operation for long periods in greasy or coloured sewage proves that this pick-up can function as a reliable part of a control system.

CONTINUOUS MEASUREMENT OF THE POLLUTION REACHING THE QUIBERON SEWAGE TREATMENT PLANT, St. Pierre, QUIBERON

The turbidimeter was calibrated at 49 spot sampling points covering CODs ranging from 350 to 1,750 mg/l and SMs ranging from 70 to 1,300 mg/l, corresponding to a turbidity range of 200 to 2,700 on the 0-3,000 scale. The correlations obtained are :

$$\begin{aligned} \text{COD} &= 0.4914 \text{ turbidity} + 432 & r &= 0.92 \text{ (fig. 3)} \\ \text{SM} &= 0.4056 \text{ turbidity} + 36.6 & r &= 0.97 \text{ (fig. 4)} \end{aligned}$$

A comparison of simultaneous recordings of turbidity and flowrate shows no direct relationship between the measurements. Analysis of the operating results for the previous year showed COD values varying by a factor of three for the same flowrate. These findings indicate how much there is to be gained by varying the injection of mineral reagent according to the pollutant content to be treated.

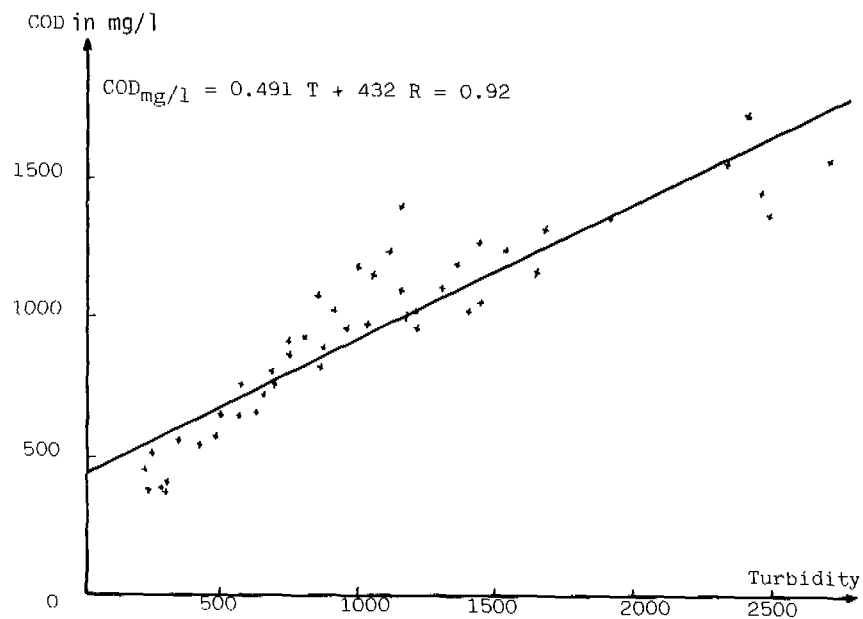


Fig. 3. Quiberon, July 1983 : COD VS. Turbidity

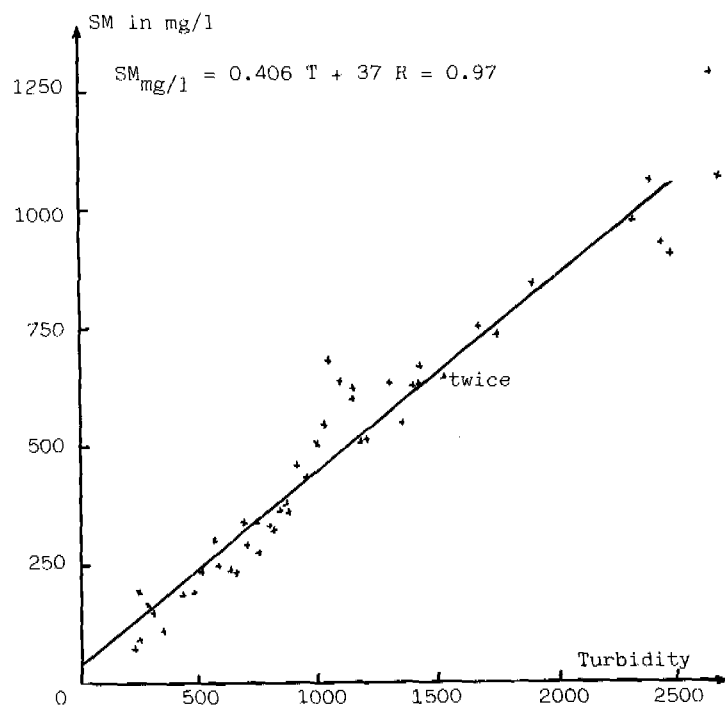


Fig. 4. Quiberon, July 1983 : SM VS. Turbidity

FLOCCULATION TESTS, St Pierre, QUIBERON

In summer operation, a ternary combination is used for treatment :
 $\text{FeSO}_4 + \text{ClFeSO}_4 + \text{anionic polymer}$.

The quantities of these various reagents injected were proportional to the incoming flowrate. The objective of the study is to optimize the addition of the most expensive reagent (ClFeSO_4). Jar tests were carried out on samples of untreated water covering the entire pollution range ; at least six points are necessary.

Eleven jar tests were carried out on the untreated waters during the first week of July 1983. The COD of the samples covered the range from 556 to 1,720 mg/l uniformly. A permanent addition of 100 mg/l FeSO_4 , increasing doses of ClFeSO_4 (0, 250, 375, 500, 625, and 750 mg/l), and a constant injection of 2 mg/l anionic polymer were effected. For all doses of ClFeSO_4 combined, the effectiveness of COD elimination ranged from 16 to 88%.

Analysis of the 66 treatment results yields the curves of foreseeable effectiveness for various types of raw pollution and various doses of ClFeSO_4 . Figure 5 gives the 45 %, 55 %, 65%, 75%, and 85 % COD isoeffectiveness curves and the curves representing the 95% confidence limits.

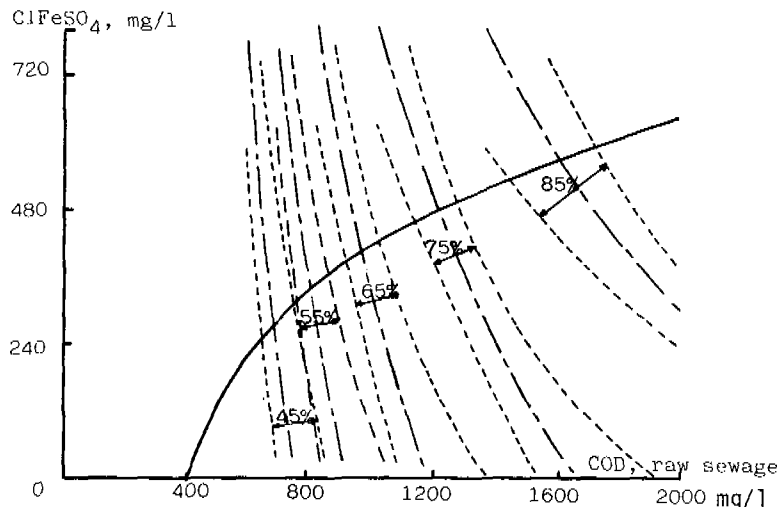


Fig. 5. Efficiency curves

The curve shown by a solid line is the objective set for the treatment, the equation of which is :

$$\text{Dose of } \text{ClFeSO}_4 = 257 \ln (\text{COD} - 262) - 1285$$

This curve was chosen so that little reagent would be added at low levels of pollution, on which the reagent has almost no effect, and pollution peaks would be eliminated.

SERVOCONTROL MODULE FOR THE INTRODUCTION OF ClFeSO₄

The servocontrol module is an improved version of the prototype tested for several months under the supervision of the Agence Financière de Bassin Rhône Méditerranée-Corse during comparative tests at the Nice-Ferber treatment plant. (Unknown, 1981).

The voltage delivered by the turbidimeter is integrated by a logarithmic amplifier in accordance with the effectiveness curve chosen and multiplied at the output by the flowrate information. The resulting voltage is fed to the power amplifier, which controls the armature of the variable-speed motor of the piston-type ClFeSO₄ metering pump (Marchandise et al, 1980).

CHECK OF THE OPERATION OF THE QUIBERON STATION

1) 24-HOUR OPERATING ASSESSMENT, 15 AND 16 AUGUST 1983. The assessment made over the weekend of 15 August, a period during which the number of vacationers on the Quiberon peninsula reached its peak, served as a check of the reliability of the servocontrol with respect to the pollutant content, with continuous hourly samplings of the input and output and checks of ClFeSO₄ consumption. The complete results, given in table 2, show that between noon on 15 August and noon on 16 August the plant took in 7,988 m³ of sewage, 40% more than the nominal flowrate of 6,000 m³ per day.

TABLE 2. 24-hour operating assessment

| | Total for 24 h | Hourly mean | Hourly maximum | Hourly minimum | standard deviation |
|--|-------------------|----------------|-------------------|-------------------|-----------------------|
| Flowrate, m ³ | 7,988 | 333 | 526 | 157 | 123 |
| COD, input, mg/l | | 994 | 3,517 | 413 | 584 |
| COD, output, mg/l | | 313 | 458 | 222 | 59 |
| COD, output, mg/l computed according to assumed efficiency curve | | 370 | 394 | 295 | 29 |
| SM, input, mg/l | | 351 | 1,064 | 156 | 196 |
| SM, output, mg/l | | 34 | 97 | 11 | 23 |
| Consumption of ClFeSO ₄ in mg/l | | 358 | 621 | 6 | 135 |
| Consumption of ClFeSO ₄ in kg | 3,030 | 126 | 237 | 2 | 72 |

The mean elimination effectiveness is 69% for COD and 90 % for SM. A calculation based on incoming pollution indicates that COD discharge should have been 2,677 kg; the assessment gives 2,637 kg.

Figure 6 is a comparison for the 24 hours of actual to anticipated hourly COD output versus incoming COD.

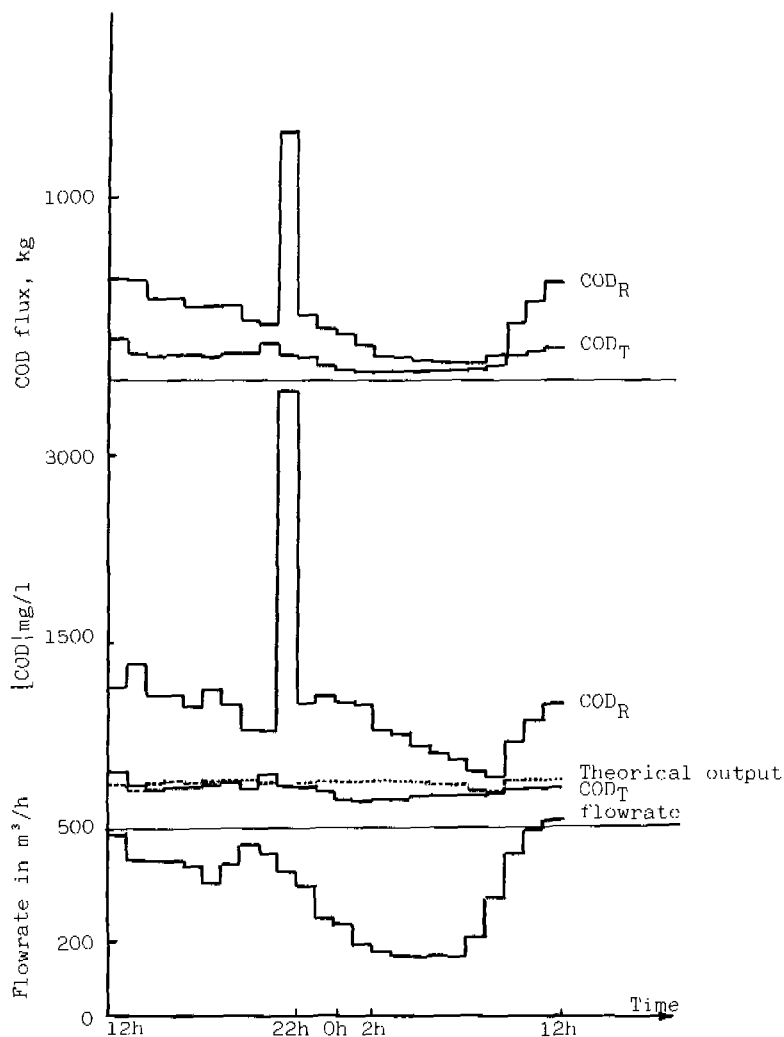


Fig. 6. Quiberon : assessment from 15 to 16/8/83

Figure 7 gives the SM characteristics of the sewage during the assessment.

The hourly mean ratio of in situ efficiency to laboratory efficiency, in terms of COD, for the 24 hours, is 1.15. This shows that the jar tests underestimate COD elimination efficiency.

The relation (for COD) $\frac{\text{in situ eff.}}{\text{laboratory eff.}} = -9.48 \cdot 10^{-4} \text{ flowrate} + 1.47$ $R = 0.70$.

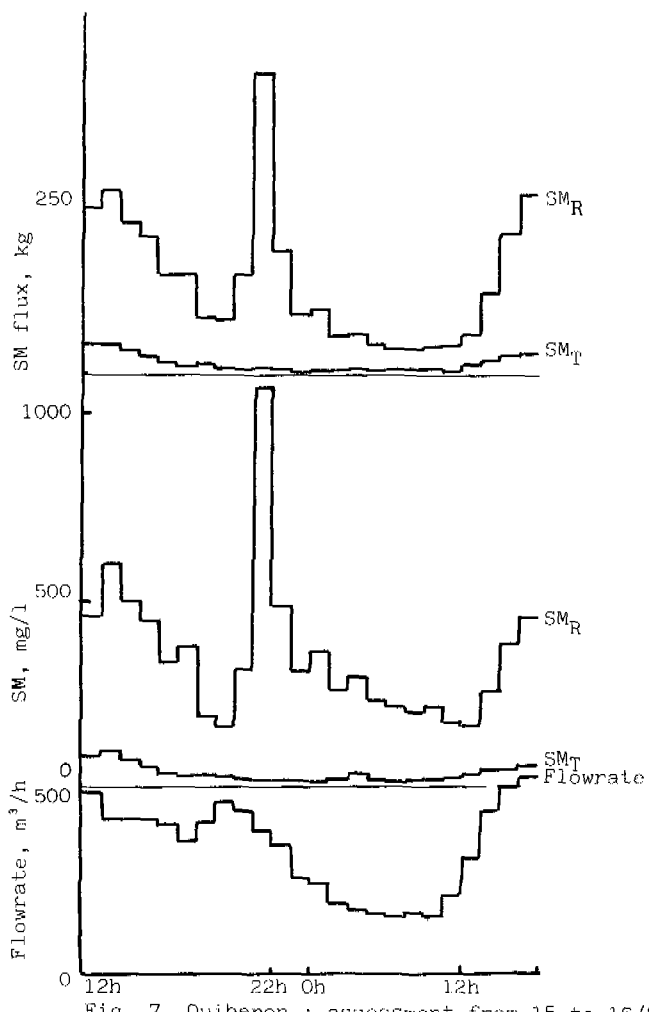


Fig. 7. Quiberon : assessment from 15 to 16/8/83

Figure 8 shows a clear negative effect of flowrate on efficiency.

The influence of the flowrate on the SM level in the treated sewage, for all assessment results, takes the form :

$$SM_{output} \approx 9.75 \times 10^{-5} (\text{flowrate})^{1.99} \quad R = 0.89$$

in kg/h

Figure 9 shows that above $400 \text{ m}^3/\text{h}$ the flowrate has a substantial effect on the degradation of the SM, while between 100 and $400 \text{ m}^3/\text{h}$ the function is linear :

$$SM_{output} \text{ in kg/h} = 0.03 \text{ flowrate} - 1.7; \quad R = 0.85.$$

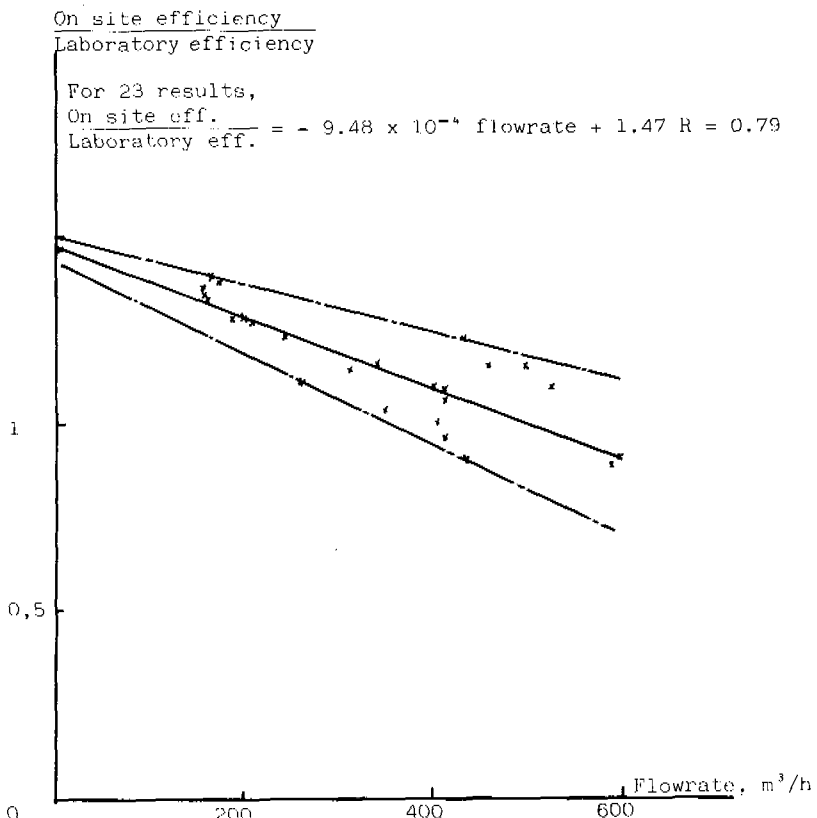


Fig. 8. On site/laboratory efficiency versus flowrate

The quantity of reagent consumed is 3,030 kg of active product or 379 mg/l, corresponding to 6,710 kg of the commercial product. The quantity of reagent consumed in the case of servocontrol based on flowrate only would have been 500 mg of active principle per litre, or 8,862 kg of the commercial product. The servocontrol used accordingly yielded a 24 % saving in reagent consumption.

2) OPERATING ASSESSMENT OF THE SERVOCONTROL FROM 13 July to 31 August 1983. The servocontrol used from 13 July to 31 August 1983 resulted in a mean consumption of ferric chlorosulphate (active principle) of 299 mg/l. Equivalent treatment with the quantity of reagent added controlled by the flowrate only would result in consumption of 500 mg/l. The saving of reagent over one summer holiday season involving the treatment of about 350,000 m³ of sewage was 70 tons of active principle, or $0.685^{70} \times 1.52 = 155$ tons of the commercial product. At the current price of 596,60 F per ton excluding all taxes, the saving on reagents amounted to 110,000 F, all taxes included, a sum equal to the investment made. In other words, the investment made at Quiberon paid for itself in one season's operation.

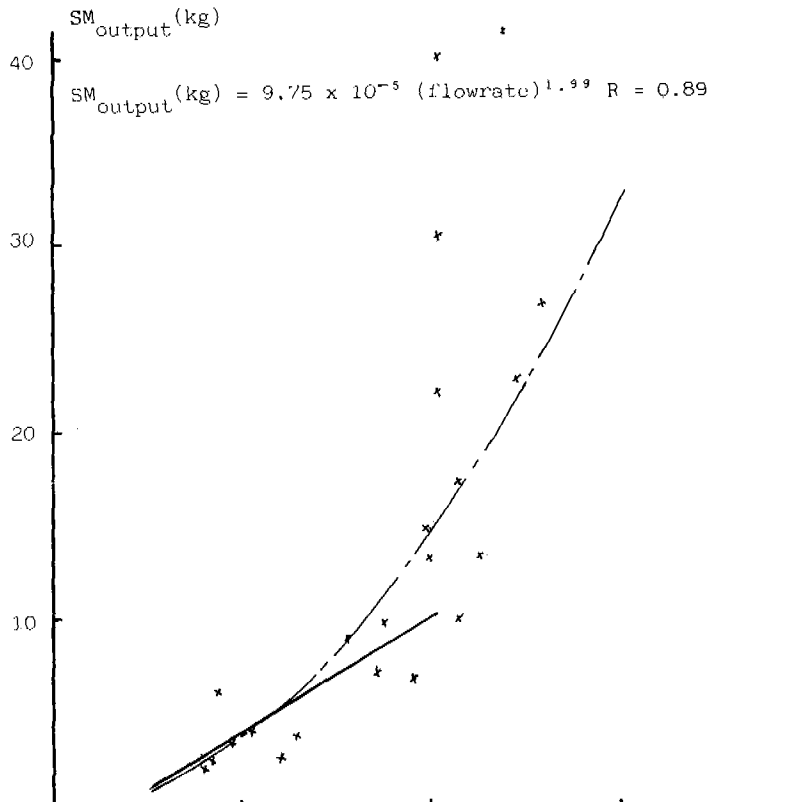


Fig. 9. Relation between SM in treated water and flowrate

CONCLUSION

Controlling the quantities of reagents added according to the pollution load to be treated at a physico-chemical treatment plant has several advantages :

- it is a management aid for the operator ;
- it offers the possibility of setting a treatment objective to be met at all times ;
- it is a means of saving.

The operation of the servocontrol module was tested for one season. The reliability of the system was demonstrated. It was proven to be advantageous, since for equivalent treatment at this 40,000-equivalent-inhabitants plant, the investment was amortized in one season's operation.

REFERENCES

- Procédés physico-chimiques (1981) Epuration des eaux usées urbaines, Etude inter-agence, Agence FBRMC, Ministère de l'Environnement, 5 vols.
 Marchandise, P., J.P. Legendre (1980), Physico-chemical treatment of waste water. Control of reagent by pollutional load to be treated. Progress in water technology 12, 359-369.

MODELLING OF THE COAGULATION- ADSORPTION PROCESS IN TREATMENT SYSTEMS

Andrzej M. Dziubek and Apolinary L. Kowal

*Institute of Environment Protection Engineering, Technical University of
Wrocław, 50-370 Wrocław, Poland*

ABSTRACT

Removal of organics in water or wastewater treatment systems is often described mathematically in the form of Langmuir and Freundlich adsorption isotherms. Using these equations, it is convenient to model, e.g., the removal of organic matter in the adsorption process on an activated carbon bed. In chemical treatment processes, organic substances are frequently removed from the water or wastewater under treatment via an adsorption on the precipitation products.

In this paper presented is a generalized model of the equation of a multilayer adsorption isotherm, which describes TOC removal from a solution during chemical treatment in an alkaline medium. The model also includes the nonremovable concentration of organics.

KEYWORDS

Chemical treatment; adsorption model; coagulation-adsorption; nonremovable concentration.

INTRODUCTION

The contribution of the adsorption process to the removal of organics in water or wastewater treatment by coagulation is often inadequately appreciated when estimating efficiency problems. In engineering practice, the final effect of every water or wastewater treatment system which involves chemical coagulation consists of two contributing factors - the efficiency of coagulation and the efficiency of adsorption. The contribution of both coagulation and adsorption to the final treatment effect depends on the pollutants to be removed and on the properties of the particles which are precipitated due to the addition of reagents. The combined contribution of coagulation and adsorption is particularly obvious in water and wastewater treatment systems involving an alkaline medium.

An earlier report (Thompson *et al.*, 1972) indicates that the adsorption of organics on precipitated calcium-carbonate and magnesium-hydroxide particles has a considerable influence on the total treatment effects. The influence of the adsorption capacity of calcium carbonate and magnesium hydroxide on the degree of TOC removal from municipal sewage was substantiated in another study (Leentvaar and Rebhun, 1982). Recent investigations (Dziubek and Kowal, 1983) showed that chemical treatment of water by coagulation in an alkaline medium involved the coagulating and adsorbing properties of calcium carbonate and magnesium hydroxide which were precipitated in the form of fine-dispersed sediments having a well-developed specific surface. For this reason, it has been suggested that the description and interpretation of phenomena associated with the chemical treatment of water and wastewater in an alkaline medium include the term 'coagulation-adsorption'.

MODEL FORMULATION

To describe the adsorption process in the form of isotherm equations it is necessary to determine the relationship between the quantity of adsorbate removed per unit mass of adsorbent and the concentration of adsorbate which persists in the solution at equilibrium. While a number of models are available for expressing this relationship, the well-known Langmuir and Freundlich equations are still of prime importance to the treatment systems of interest.

The concentration of the pollutant which occurs in an equilibrium state and should be removed from the solution is generally expressed as total organic carbon (TOC), specifically when the medium under treatment is a multicomponent solution. In some treatment processes, a certain portion of the adsorbate determined as TOC is resistant to removal and persists in the solution in the form of nonremovable concentration (C_n). There exist such forms of Langmuir's and Freundlich's isotherm equations that incorporate C_n term. Since the C_n value cannot be obtained by direct measurements, it is necessary to employ another method of determination, e.g. the nonlinear programming technique (Sweeney *et al.*, 1982).

In their study of surface water treatment by coagulation-adsorption with dolomite (Dziubek and Kowal, 1983), the investigators determined the C_n value, using the relationship between TOC concentration and coagulant mass

$$C = \frac{D}{aD + b} , \quad (1)$$

where C is TOC concentration at coagulant dose D , and a, b are parameters which can be evaluated from the linear form of the equation. From Eq. (1) it is obvious that C takes the value of C_n when D tends to infinity. In this way it is possible to determine the nonremovable concentration which persists in the effluent from the coagulation-adsorption process involving calcium carbonate and magnesium hydroxide as adsorbents, and organic compounds included in the term TOC as adsorbate.

Taking into account the specific nature of the coagulation-adsorption process, in which the effect of coagulation and the effect

of adsorption of pollutants are complementary to one another, the multilayer adsorption model (Brunauer *et al.*, 1938) was employed for the mathematical description of associated phenomena. According to the BET model, an adsorbate particle which encounters a covered spot on the available surface area of the adsorbent is ready to form an adsorption complex. As the number of active spots on the adsorbent surface covered by one adsorbate particle continues to decrease, double, triple, etc., adsorption complexes are formed. In the BET model it has been assumed that the Langmuir equation applies to each adsorption layer. The model is widely used to describe adsorption from the gaseous phase and to determine the specific surface of the adsorbents.

Based on the analysis of the adsorption equilibrium, and assuming that there exists a nonremovable concentration of the adsorbate (C_n), the following model was derived.

The total amount of the organics adsorbed (TOC) can be expressed as

$$X = X_m (A_1 + 2A_2 + 3A_3 + \dots) \quad (2)$$

where A_1 , A_2 , A_3 indicate fractions of adsorbent surface covered with single, double, triple, etc., adsorption complexes, and X_m denotes the amount of organic compounds adsorbed in a monolayer.

The equilibrium constants for individual layers (assuming that there occur some nonremovable compounds of a concentration C_n) take the form

$$k_1 = \frac{A_1}{(C_e - C_n) A_0}, \quad k_2 = \frac{A_2}{(C_e - C_n) A_1}, \quad k_3 = \frac{A_3}{(C_e - C_n) A_2} \quad (3)$$

where A_0 denotes the uncovered fraction of the adsorbent surface, and C_e is equilibrium concentration of adsorbate.

As the interaction between adsorbent and adsorbate reduces rapidly with distance from the surface, the value of constant k_1 is much greater than that of constant k_2 . The differences between the value of k_2 and k_3 ; k_3 and k_4 , etc., are much more pronounced than the difference between the value of k_1 and k_2 . Hence, it may be assumed that

$$k_2 \approx k_3 \approx \dots \approx k_L \quad (4)$$

where k_L is equilibrium constant of the last layer. For a system in which some part of the compounds is nonremovable, k_L may be expressed as

$$k_L = \frac{1}{C_0 - C_n} \quad (5)$$

where C_0 denotes initial concentration of the adsorbate.

Transforming Eq. (3) and using Eq. (4), we can write

$$A_1 = k_1 (C_e - C_n) A_o; \quad A_2 = k_2 (C_e - C_n) A_1 = k_L (C_e - C_n) A_1 \quad (6)$$

Combining Eq. (5) and Eq. (6) gives

$$A_2 = -\frac{1}{C_o - C_n} (C_e - C_n) A_1 \quad (7)$$

and

$$A_3 = k_3 (C_e - C_n) A_2 = k_L (C_e - C_n) A_2 = \left(\frac{C_e - C_n}{C_o - C_n} \right)^2 A_1 \quad (8)$$

and so forth.

Substituting Eqs. (6), (7) and (8) into Eq. (2) yields, after suitable transformation,

$$x = x_m k_1 (C_e - C_n) A_o \left[1 + 2 \left(\frac{C_e - C_n}{C_o - C_n} \right) + 3 \left(\frac{C_e - C_n}{C_o - C_n} \right)^2 + \dots \right] \quad (9)$$

Furthermore, we can write

$$A_o + A_1 + A_2 + A_3 + \dots = 1 \quad (10)$$

Combining Eqs. (10), (6), (7) and (8) gives (after transformation) the expression

$$A_o \left\{ 1 + k_1 (C_e - C_n) \left[1 + \left(\frac{C_e - C_n}{C_o - C_n} \right) + \left(\frac{C_e - C_n}{C_o - C_n} \right)^2 + \dots \right] \right\} = 1 \quad (11)$$

Since $\frac{C_e - C_n}{C_o - C_n} \ll 1$, the sum of geometrical progression in Eq. (11) is

$$1 + \left(\frac{C_e - C_n}{C_o - C_n} \right) + \left(\frac{C_e - C_n}{C_o - C_n} \right)^2 + \dots = \frac{1}{1 - \left(\frac{C_e - C_n}{C_o - C_n} \right)} \quad (12)$$

and takes the form

$$1 + 2 \left(\frac{C_e - C_n}{C_o - C_n} \right) + 3 \left(\frac{C_e - C_n}{C_o - C_n} \right)^2 + \dots = \frac{1}{\left(1 - \frac{C_e - C_n}{C_o - C_n} \right)^2} \quad (13)$$

in Eq. (9).

Combining Eqs. (13) and (9), we obtain

$$X = \frac{x_m k_1 (C_e - C_n) A_o}{\left(1 - \frac{C_e - C_n}{C_o - C_n}\right)^2} \quad (14)$$

After substitution of Eq. (12) and after suitable transformation, Eq. (11) becomes

$$A_o = \frac{\frac{C_e - C_n}{C_o - C_n}}{1 + k_1 (C_e - C_n) - \frac{C_e - C_n}{C_o - C_n}} \quad (15)$$

A combination of Eq. (14) and Eq. (15) yields (after simplification)

$$X = \frac{x_m k_1 (C_e - C_n)}{\left(1 - \frac{C_e - C_n}{C_o - C_n}\right) \left(1 + k_1 (C_e - C_n) - \frac{C_e - C_n}{C_o - C_n}\right)} \quad (16)$$

Using Eq. (5), we may write

$$C_e - C_n = \frac{1}{k_L} \frac{C_e - C_n}{C_o - C_n} \quad (17)$$

When the ratio of the equilibrium constant of the first layer to the equilibrium constant of the last layer takes the form

$$\frac{k_1}{k_L} = K \quad (18)$$

and Eqs. (17) and (18) are introduced to Eq. (16), we obtain the following expression

$$X = \frac{x_m K \frac{C_e - C_n}{C_o - C_n}}{\left(1 - \frac{C_e - C_n}{C_o - C_n}\right) \left(1 + K \frac{C_e - C_n}{C_o - C_n} - \frac{C_e - C_n}{C_o - C_n}\right)} \quad (19)$$

After transformation, we obtain the final form of the adsorption isotherm

$$X = \frac{x_m K(C_e - C_n)}{(C_o - C_e) \left(1 + (K - 1) \frac{C_e - C_n}{C_o - C_n} \right)} \quad (20)$$

x_m and K may be determined from the coefficients of the linear form of the isotherm equation

$$\frac{1}{x \frac{C_o - C_e}{C_e - C_n}} = \frac{1}{K x_m} + \frac{K - 1}{K x_m} \frac{C_e - C_n}{C_o - C_n} \quad (21)$$

Assuming that the total amount of organics adsorbed per unit mass of the adsorbent is the ratio of TOC removed to the corresponding dose of the adsorbent (D), we can write

$$x = \frac{C_o - C_e}{D} \quad (22)$$

Combining Eq. (22) and Eq. (21) gives (after transformation)

$$\frac{D(C_e - C_n)}{(C_o - C_e)^2} = \frac{1}{K x_m} + \frac{K - 1}{K x_m} \frac{C_e - C_n}{C_o - C_n} \quad (23)$$

MODEL VERIFICATION

The adsorption-isotherm model (20) was verified by experiments. The experimental study included a surface-water treatment process which involved coagulation-adsorption to remove organic substances (referred to as TOC). Soft-burned and wet-slaked dolomites, containing about 60 percent of calcium hydroxide and some 30 percent of magnesium hydroxide, were used as coagulants.

In the course of the treatment process colloidal particles were coagulated, and organics were adsorbed both on the precipitated calcium carbonate sediment and on magnesium hydroxide added together with the coagulant. The total treatment effect was determined from the measured values of TOC concentration removed per unit mass of the coagulant. Equation (1) was used to calculate the nonremovable concentration value (C_n), the adopted coagulant dose being 1000 gm^{-3} (i.e., four times as high as the optimum doses determined by jar test). The calculations of the K and x_m values involved the linear form of Eq. (23).

Some of the adsorption isotherms, along with respective equations and calculated constant parameters, are given in Figs. 1 and 2. The correlation coefficients of the linear form of the isotherm equation are $r = 0.997$ and $r = 0.976$ for the isotherm of Fig. 1 and Fig. 2, respectively. The difference of the C_n and x_m values between the two figures should be attributed to the differentiated structure

of magnesium hydroxide contained in the two types of the coagulant employed (original and modified). Although the modified coagulant contained the same percent of magnesium hydroxide as did the original one, the specific surface of this constituent in the former was better developed due to peptization which improved its adsorption

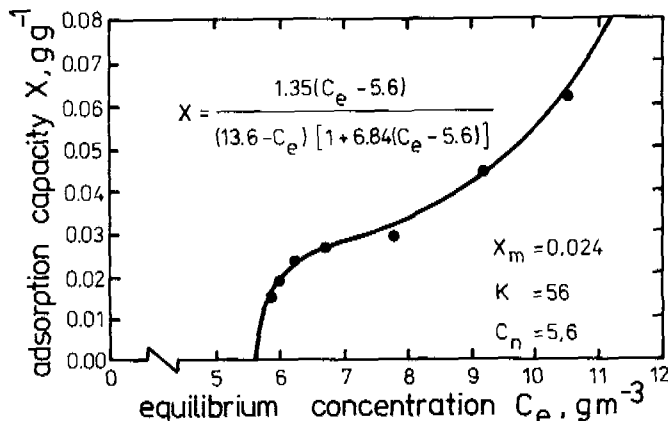


Fig. 1. Adsorption isotherm for TOC removed by coagulation-adsorption with original dolomitic coagulant

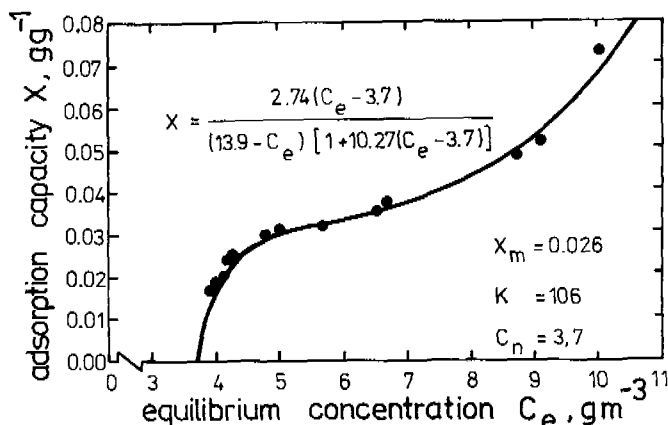


Fig. 2. Adsorption isotherm for TOC removed by coagulation-adsorption with modified dolomitic coagulant

ability. The larger specific surface of magnesium hydroxide contained in the modified coagulant is substantiated by a higher value of X_m as compared to the original coagulant. Consequently, the application of the modified coagulant yields lower values of nonremovable concentration (C_n).

Similar relationships confirming the validity of the adopted model were obtained in the study of a coagulation-adsorption process,

in which the adsorbate concentration was determined as chemical oxygen demand (COD).

CONCLUSIONS

It is shown that the multilayer adsorption model incorporating nonremovable concentration values may be successfully applied to describe the removal of organic compounds in water treatment systems employing coagulation-adsorption in an alkaline medium. Preliminary investigations suggest that this general statement will also be valid for wastewater treatment processes which involve chemical methods and lime as reacting substance.

The experimental verification of the model indicates that adsorption efficiency increases with the increasing initial concentration of the adsorbate. Consequently, the thickness of the adsorption complex is proportional to the initial concentration of the adsorbate.

Investigations are under way in order to verify the adsorption-isotherm model not only in other water or wastewater treatment systems, but also in water renovation.

ACKNOWLEDGEMENT

This paper was developed from a study supported by Government Project No. PR-703.04.02.02.120.

REFERENCES

- Brunauer, S., Emmet, P.H. and Teller, E. (1938). Adsorption of gases in multimolecular layers. J. Am. Chem. Soc., 60, 309-319.
- Dziubek, A.M. and Kowal, A.L. (1983). Water treatment by coagulation-adsorption with dolomite. In: Chemistry for the Environment Protection, L. Pawlowski (Ed.), Elsevier Publishing Company, Amsterdam and New York.
- Leentvaar, J. and Rebhun, M. (1982). Effect of magnesium and calcium precipitation on coagulation-flocculation with lime. Water Res., 16, 655-662.
- Sweeney, M.W., Melville, W.A., Trgovcich, B. and Leslie Grady, C.P.Jr. (1982). Adsorption isotherm parameter estimation. J. Env. Engrg. Div., ASCE, 108, No. EE5, 913-922.
- Thompson, C.G., Singley, J.E. and Black, A.P. (1972). Magnesium carbonate - a recycled coagulant. J. Am. Wat. Wks. Ass., 64, 11-20 and 93-100.

HEXAVALENT CHROMIUM REMOVAL FROM DRINKING WATER

J. M. Philipot,* F. Chaffange** and J. Sibony*

*Centre de recherche de Maisons Laffitte (OTV), Chemin de la Digue,
BP 76-78600 Maisons Laffitte, France

**S.F.D.E. Rue des Chauffours, BP 101-95021 Cergy-Pontoise, France

ABSTRACT

A series of tests were performed with a view to solving the problem of chromium pollution in the Meulan district near Paris, due to the proximity of long-established metal-working plants. It was found that the accumulated pollution not only originated from the groundwater source but also from atmospheric contamination through fall-out from smoke and fumes issuing from local metal-works' stacks. Among the interesting features of this paper is the fact that, since the profound penetration by the pollutant affects potable feedstock, chromium removal studies have been made on potable water for the first time on record.

Several methods are reviewed, among which the only economically feasible one appears to be the reduction of hexavalent chromium by a sufficient quantity of iron sulphate, the problem attached to iron-sulphate overdose being solved by the application of high-rate filtration on very fine sand. This arrests the fine precipitates and reduces the residual ferrous-iron by catalysis. Reliability of the treatment is ensured by a system of continuous metering that automatically controls reagent dosing.

KEYWORDS

Drinking water; hexavalent chromium; origin; removal; iron sulphate; bacteria; pilot plant; true scale.

I BACKGROUND

The Société Française de Distribution d'Eau manages water utilities in the Paris district covering the needs of some 150,000 subscribers and has been licensed as a distributor for the Meulan Water Board. Water supplies for Meulan and neighbouring municipalities, representing about 50,000 inhabitants, were for a long time pumped from wells with a total capacity of $1000 \text{ m}^3 \text{ h}^{-1}$ in a catchment field located over the chalk layer. The wells were sunk in 1929, 1962, 1973 and 1975

respectively, in response to expanding requirements in the vicinity, and notably the supply of water to the new suburban town of Cergy-Pontoise. The quality of the water was such that simple chlorination with gaseous chlorine was the only treatment required before discharging it to the distribution network.

These wells, that are about 125 ft deep, catch the water from the water-bearing chalk layer located under the alluvial deposits forming the bottom of a valley. On top of this lie tertiary formations composing the sides of the valley and the overhanging plateau. Less permeable layers in these covering formations give rise to the existence of springs. The alluvial deposits are made of fine material and peat.

II HISTORICAL DESCRIPTION OF POLLUTION AND HYDRO-GEOLOGICAL SURVEY

Analyses published in February 1981 revealed that the hexavalent chromium content was over the standard for potability (ie. $50 \mu\text{g l}^{-1}$). SFDE at once began work on connections to neighbouring replacement sources. In addition to this preventive action SFDE asked our research centre to send a laboratory truck to the site and proceed with a survey. After about a month's research it was found that the hexavalent chromium could be removed by reducing it with iron sulphate. Fining down the dose rate so as to eliminate the chromium without leaving residual iron led SFDE to ask Montpellier University to make further studies in order to define the precise stoichiometrics of the reduction reaction. Finally, a regular hexavalent and trivalent chromium monitoring system was set up and a series of analyses were carried out on the sediments in the river bed and the alluvion recently deposited in the valley.

From the outset, it was believed that the pollution originated at the local metal works and particularly a surfacing workshop situated about a mile upstream of the catchment wells. The plant was known to have no treatment or storage facilities until 1975 (1978 as regards extractor rejects) and the amounts of hexavalent chromium used since 1935, about 8.4 t year^{-1} , were as follows:

- 20 to 30% (1.7 to 2.5 t) on parts to be chromium plated;
- 15 to 20% (1.3 to 1.7 t) in rinsing water;
- 50 to 60% (4.2 to 5 t) in extractor rejects.

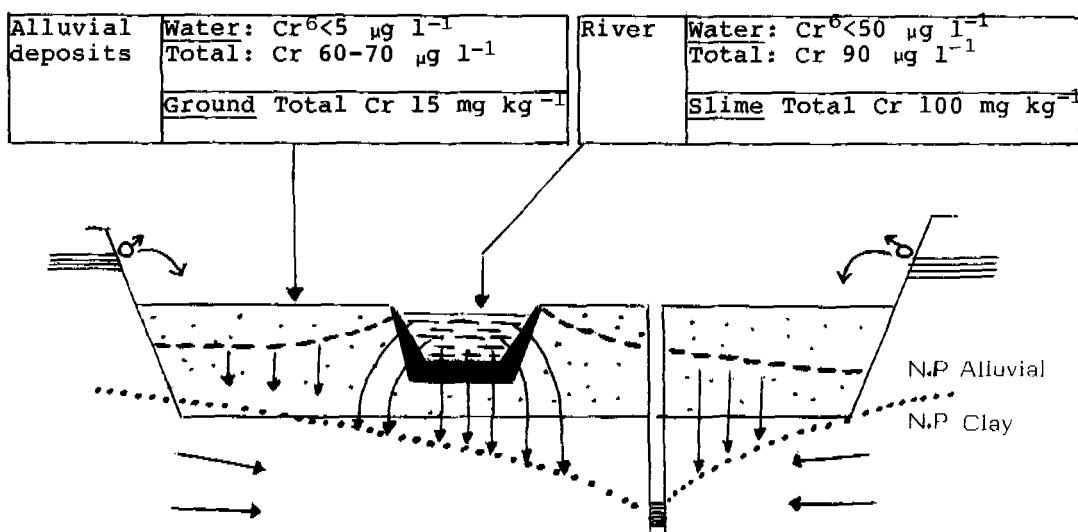
This represents a total of 5 to 7 tons of hexavalent chromium released in the natural environment, most to the atmosphere, and the remainder to one (or two) negative chalk wells. It was therefore not surprising that analysis of the deposits showed:

- no amounts of chromium worth mentioning in deposits sampled upstream of the works concerned;
- abnormally high quantities downstream.

Bearing in mind the different origins of the water feeding the wells, i.e. water from the alluvial and chalk layers, the Seine and other river waters, the following conclusions were suggested:

- contamination by water from the Seine was unlikely;
- there must be significant concentrations of chromium ($60 - 70 \mu\text{g l}^{-1}$ Cr) in the alluvial water layer, at least near the river.

As these concentrations could be due to fall-out from smoke and fumes carrying 50 to 60% of the chromium rejects, it was decided to check the amount of pollution in the springs draining the groundwater table. Unless there is a very big increase in the chromium concentrations as the alluvial water flows into the chalk-layer water depressed by pumping, which is hardly feasible (see sketch), the amount contributed by the alluvial water is not enough to account for the very much stronger concentrations found in the wells.



As regards the part played by the river, it will be noticed that the concentrations of Cr^{6+} in river water are generally less than in the well-water, indicating that water flowing from it into the catchment area is not responsible for the level of chromium in the wells. On the contrary to what has been said about the alluvial layer, there is a possibility that the phenomenon may be due to the release of chromium build-up in river slime that contains quite considerable quantities (100 ppm of total chromium perpendicular to the catchment points).

The most important contribution seems to originate in direct contamination of water from the chalk layer migrating to the wells through preferential flowage paths in the water-bearing layer. In order to check this point, surveys were made to ascertain the piezometric height of the chalk water layer in the valley to detect the preferential passages as far as possible, trying at the same time to determine by analyses of the ground water and storage rock, possible changes in the rate of concentration in relation to distance.

The SFDE then asked BURGEAP, a firm specialized in the development of ground water, to carry out the necessary reconnaissance, by both

drilling and analysis, and make a synthesis of the data collected, in order to determine the transfer mechanism and to forecast developments in pollution. The final report was drafted in April 1982.

Localization and Mechanism of Pollution Transfer

Investigations undertaken by BURGEAP show that: the chromium pollution in the wells comes above all from effluents discharged directly into the chalk and not from widespread atmospheric pollution; it travels via one or several underground preferential flowage paths located approximately by reconnaissance; it is not directly related to the river, the contamination of which is just a general symptom.

Possible Evolution of Pollution

Several unknown factors concerning discharge of pollutants, transfer mechanisms, and the present degree of removal make it impossible to foresee how long contamination will probably persist. However, bearing in mind the high concentrations found in the deposits adjacent to the metalworks 7 years after the discharge of pollution was stopped, it is to be feared that the accumulation effect is considerable and that washout of the stored chromium is likely to continue for many years to come. It was these circumstances that prompted SFDE to study, with the help of OTV, a chromium treatment plant, the general principles of which were defined in March 1981.

III RESEARCH ON PILOT UNIT AND DEFINITION OF TREATMENT LINE

The two most usual states of oxidation are the +6 and +3 states. The maximum contaminant level (MCL), according to European standards, is $50 \mu\text{g l}^{-1}$ expressed as total chromium. No guide level has been fixed.

Hexavalent chromium is the most toxic form of chromium pollution but the standard is expressed in total Cr since trivalent chromium in certain circumstances is quick to oxidize. There is, however, an equilibrium between the two. The dissolved oxygen and the oxidizing agents needed for disinfection oxidize the chromium while organics, on the other hand, help reduce the hexavalent chromium. With organics, and in particular humic and fulvic acids, a stable compound is formed that percolates easily through to the groundwater table.

The trivalent form of chromium is cationic and the resulting hydroxide is insoluble. The hexavalent chromium is anionic, i.e. chromate CrO_4^{2-} and HCrO_4^{2-} , or dichromate $\text{Cr}_2\text{O}_7^{2-}$, both of which are highly soluble.

The commonest method of removal is used in the pretreatment of electroplating effluents. This consists of reducing the soluble hexavalent chromium at an acid pH value by applying a reducing agent, i.e. iron sulphate or sodium bisulphite. Pollution of drinking water by hexavalent chromium is a very exceptional occurrence and therefore there is no specific treatment for such cases. A review of suitable treatments follows, with special reference to removal of the trivalent and hexavalent forms of chromium respectively.

1 Possible Treatments

1.1 Removal During Flocculation

The efficacy of chromium removal during flocculation varies greatly according to the nature of the raw water and the coagulant used. It is certain that flocculation only affects trivalent chromium that has already been precipitated. Hexavalent chromium remains untouched. The factors that determine the effectiveness of trivalent chromium hydroxide flocculation are:

- a) the pH value, the optimum value of which depends on the coagulant: 6 to 9 with aluminium salts;
- b) the ionic environment, especially the presence of anions such as sulphates, phosphates, nitrates, silicates and carbonates;
- c) the organics that have a compounding effect on chromium and some forms of which are soluble.

The curve in Fig. 1 shows the effectiveness of coagulation by WAC (aluminium polychloride) for the precipitation of trivalent chromium in surface water, in this case the Seine at Choisy-le-Roi. The curve represents simulated treatment on a pilot unit (Hamon et al., 1979).

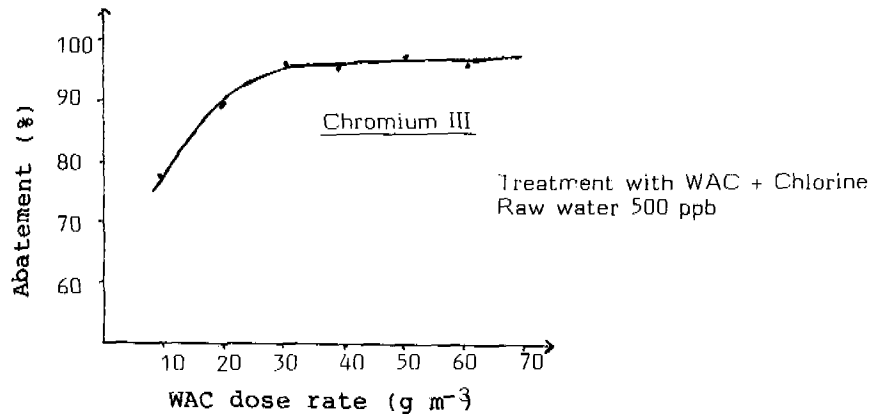


Fig. 1. Removal of Chromium III after treatment with WAC
(after J.L. Hamon)

A certain number of improvements can be made to enhance clarification for the removal of trivalent chromium (and heavy metals in general).

Flocculation additives

Activated silica, alginates and some synthetic polymers improve the elimination of trivalent chromium precipitates because they have an overall positive effect on the clarification process. They also improve the adsorption of chromium oxides and limit desorption effects during the settling process. Some products appear to be specific to the elimination of chromium, e.g. starch xanthate (Morani

and Mezzana, 1981), but are not approved for potabilization purposes. They seem at the moment to be laboratory curiosities and hardly suitable for industrial applications.

Powered Activated Carbon (PAC)

When injected during flocculation, PAC makes possible the adsorption of soluble organo-metallic compounds and substantially contributes to the reduction of the initial concentrations. In the case of Meulan, the proportion of the chromium combined with organic matter is less than 4% of the total chromium and is therefore insignificant (IRCHA analyses).

Clay

One of the main characteristics of clay is its cation exchange capacity resulting from the isomorphic substitutions between silicon and aluminium in a stratified formation. As the dissolved trivalent chromium is in either free cationic form or in a compound form that may be cationic, it will be exchanged and fixed at the surface of the clay particles. The Montmorillonites are the most interesting with regard to the removal of heavy metals. The following chart shows the effectiveness of bentonite used as a flocculating agent when treating water from the Seine to eliminate trivalent chromium and heavy metals (Rauzy, 1980). Hexavalent chromium is not removed by this method.

| Bentonite applied (g m^{-3}) | 0 | 0.5 | 1 | 2.5 |
|---|----|-----|----|-----|
| Percentage removal of Cr III | 50 | 98 | 98 | 96 |

(With aluminium sulphate 70 g m^{-3} and sodium alginate 0.5 g m^{-3} in Rauzy, 1980.)

1.2 Softening with Lime

The results of chromium removal during a softening process are variable, depending on the extent to which the metal is oxidized. As much as 90% of the trivalent chromium can be eliminated by increasing the pH value to 11 with lime. The same does not apply to hexavalent chromium, however, only 10% of which, at the most, can be removed in this way.

1.3 Chromium Reduction

Reduction is the only commonly used chromate removal technique for industrial effluents. The reagents used are sodium bisulphite and iron sulphate at an acid pH value. The precipitates formed are then settled. The adaptation of this treatment to potable water is examined further on in this paper.

1.4 Filtration on Granulated Activated Carbon (GAC)

The removal of chromium by GAC filtration has only recently been described and the mechanisms are still not fully known. There appears to be reduction, adsorption and exchange of the hexavalent chromium at the same time; the relative importance of these effects depending on the pH value. This treatment is an attractive solution for Meulan since percolation on GAC is sufficient to remove the hexavalent chromium.

1.5 Ion Exchange

Anion exchangers can be used for the elimination of chromates and bichromates, e.g. synthetic resins and activated alumina.

1.6 Biological Treatment

There are two methods for the removal of chromium and heavy metals by biological treatment: the metabolism of specialized bacterial systems; and adsorption on membrane-type systems. In both cases the development of the appropriate process would take too long for it to be applicable to Meulan.

Among the different treatment possibilities, we adopted the following for testing on large-scale pilot units:

- a) reduction of precipitable trivalent chromium;
- b) percolation on GAC and activated alumina.

These techniques appeared to be simple to implement in the case of well-water specific to the removal of hexavalent chromium and apparently easy to transpose from pilot scale to the industrial stage.

2 Percolation on GAC and Activated Alumina (Al*)

The aim of the reported tests was not to ascertain the mechanism by which GAC and Al* react on the hexavalent chromium nor to determine the respective roles of adsorption, catalytic reduction and anion exchange. Our purpose was to find the correct practical conditions for using the materials concerned, the correct exhaustion-run time and the optimum conditions for chemical regeneration.

2.1 Percolation on Activated Alumina

We used a 1m layer of crushed alumina media with a grain-size between 0.3 and 1.4 mm. The aluminium was first put through a preliminary acid treatment consisting of percolation with a diluted solution of sulphuric acid. The most meaningful results are given in the following chart. The end of the exhaustion cycle coincided with the appearance in the treated water of a total chromium content of over 50 $\mu\text{g l}^{-1}$.

| Chromium content in raw water $\mu\text{g l}^{-1}$ | Trickle velocity $\text{m}^3 \text{ m}^{-2} \text{h}^{-1}$ | Run time hours |
|---|--|-------------------|
| 350 | 4 | 30 |
| 325 | 4.5 | 30 |
| 400 | 5 | 15 |
| 300 | 8 | 10 |

The quantity of hexavalent chromium fixed per cubic metre of media was between 25 and 35 g m^{-3} per run.

The regeneration stages were as follows: loosening with water; percolation with diluted caustic; water rinse; percolation with diluted sulphuric acid; and water rinse. The chromium was eluted in the basic phase in the form of chromates-bichromates. The loosening water contained only very small amounts of total chromium.

2.2 Percolation by GAC

The carbons used were all highly activated coconut derived (Picactif 70, Chemviron F400, Norit Row Supra). The nature of the carbon, its granulometry and the filtering velocity were the main test factors. The filtration filter bed was 1 m thick.

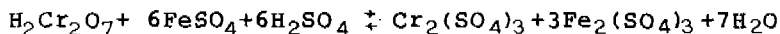
The optimum result was obtained with crushed GAC of which the grain-size distribution was 0.3 to 0.95 mm, for a filtering velocity of 5 $\text{m}^3 \text{ m}^{-2} \text{ h}^{-1}$. The initial hexavalent chromium content in the raw influent was 300 $\mu\text{g l}^{-1}$. The exhaustion run lasted for 48 hours. The quantity of chromium arrested per run and per cubic metre of GAC was 50 to 70 g m^{-3} , in other words twice the capacity observed with activated alumina in identical operating conditions. Regeneration conditions were close to those adopted for activated alumina.

The chromium was eluted in the caustic solution and no trace of the trivalent chromium precipitated onto the activated carbon was observed in the loosening water. This argues strongly in favour of the assumption that the chromium was removed by anion exchange or adsorption rather than by catalytic reduction. Furthermore, while regeneration with caustic only enabled the hexavalent chromium to be eluted but did not restore chromium fixing capability to the GAC, acid regeneration offered neither of these facilities.

3 Reduction of Hexavalent Chromium

Two reducing agents, sodium bisulphite and iron sulphate, are used for industrial chromium removal. The effluent is doped with sodium bisulphite in the presence of sulphuric acid. The sulphite is released and reduces the chromates and bichromates. The reaction takes place at pH 2.5 - 3 and any excess of sulphuric acid releases the sulphite that is exhausted to the atmosphere. These two points make the application of the technique very delicate in the case of Meulan.

The iron sulphate also acts in a sulphuric medium:



The reduction of 1 g of hexavalent chromium requires 16 g of iron sulphate in the form of a pure crystallized product with seven molecules of water.

The hexavalent chromium content in the feedstock reached the very exceptional value of $400 \mu\text{g l}^{-1}$ as against the normal $200 \mu\text{g l}^{-1}$ on average. The water needs no treatment other than chromium removal and so it was decided to proceed directly with filtration of the precipitates formed in a special reactor. Tests were conducted on a big pilot unit on the site of the projected Meulan treatment plant.

The elements studied were: the stoichiometric factor; contact time; nature of filtering media; limit of filtration velocity; conditions for de-clogging and rinsing filters.

The quality of the water treated was ascertained by a series of analyses at two levels on site several times a day; in two reference laboratories on an average daily sample.

We report here the essential facts concerning the most meaningful results for the design of the treatment line.

Stoichiometric Dosing of Reagents

The curve in Fig. 2 shows that the hexavalent chromium content of $50 \mu\text{g l}^{-1}$ corresponding to the MCL in European standards, represents a stoichiometric factor 125% of the ideal value and $20 \mu\text{g l}^{-1}$ corresponds to 200%. The initial hexavalent chromium content is $220 \mu\text{g l}^{-1}$. In these conditions the non-precipitated iron content of $150 - 650 \mu\text{g l}^{-1}$ upstream of the filter is high. The MCL stipulated in the European standard for iron is $200 \mu\text{g l}^{-1}$. In fact the treatment replaces the pollution with an undesirable metal content.

As regards contact time, we have shown that when a traditional type of flocculator is used with hydrodynamic or mechanical stirring, it should not be less than 20 minutes including an initial 30 seconds flash mixing. On the other hand, in the case of a Raschig ring type reactor, the reduction efficiency is independent of contact time within the limits of 7 to 20 minutes.

Additional filtration must therefore take into account:

- the removal of microflocs of precipitates of iron hydroxide and trivalent chromium for which we have tested the effectiveness of a coagulating aid and a smaller grain-size sand;
- the removal of dissolved ferrous iron, i.e. oxidation prior to filtration.

Oxidation of Excess Ferrous Iron

Chlorine has turned out to be too powerful an oxidizing agent which makes the chromium soluble while having no effect on the iron (Table

1). The same applies to ozone. Cascade aeration upstream of the sand filter greatly improved the iron-removal efficiency without oxidizing the chromium, although this increased the total chromium content and turbidity owing to the adverse effect on chromium hydroxide precipitation (Table 2). Had the cascade system been adopted it would have required optimizing but the reduced granulometry of the sand proved sufficient to deal with the iron-removal problem.

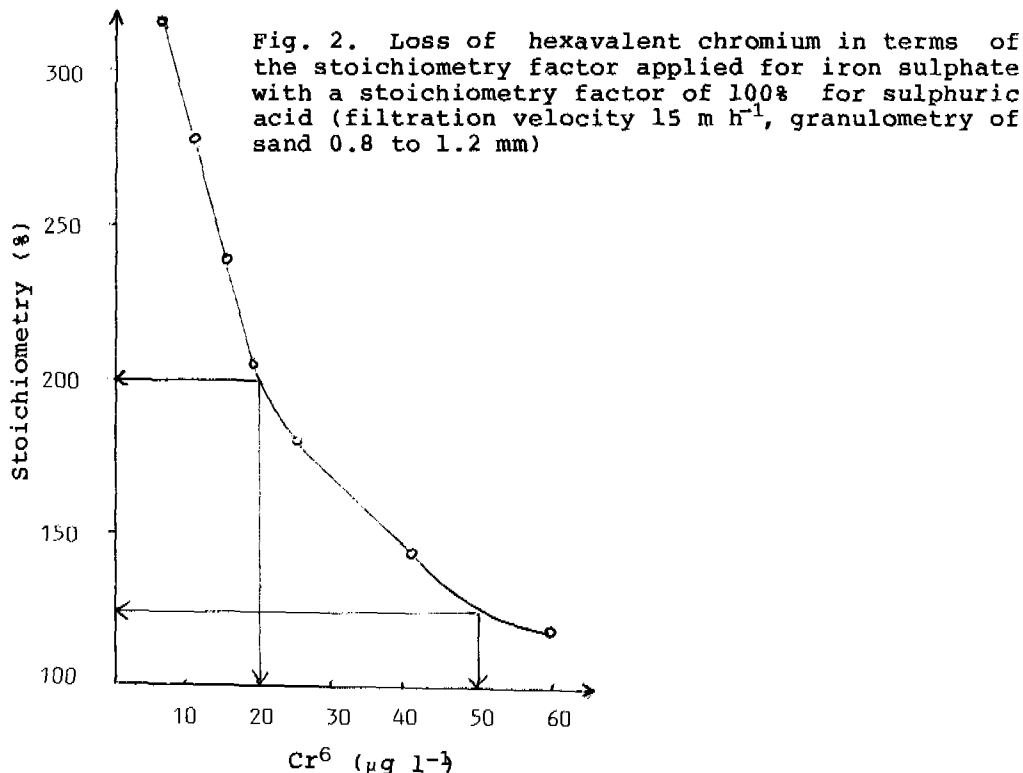


TABLE 1 Effect of Chlorination

| Activated chlorine g m^{-1} | Turbidity NTU | Iron $\mu\text{g l}^{-1}$ | Hexavalent chromium $\mu\text{g l}^{-1}$ | Total Cr $\mu\text{g l}^{-1}$ |
|---|------------------|------------------------------|---|----------------------------------|
| 0 | 0.48 | 375 | 0 | 60 |
| 0.80 | 0.5 | 350 | 30 | 105 |

Filtration velocity 15 m h^{-1}
Granulometry of sand TE 0.8 mm.
100% iron-sulphate stoichiometry.

TABLE 2 Effect of aeration

| Cascade aeration | Turbidity | Iron | Hexavalent chromium | Total Cr |
|---------------------|-----------|----------------------|------------------------|----------------------|
| | NTU | $\mu\text{g l}^{-1}$ | $\mu\text{g l}^{-1}$ | $\mu\text{g l}^{-1}$ |
| Yes | 0.45 | 120 | 12 | 45 |
| No | 0.35 | 190 | 16 | 35 |

Filtration velocity 15 m h^{-1}

Granulometry of sand TE 0.8 mm.

150% iron-sulphate stoichiometry.

Granulometry of sand

Two grain-sizes were tested: 0.80 mm and 0.40 mm. Several tests were carried out at two filtration velocities, all other pilot unit operating characteristics being identical. Significant results of these tests are presented in Table 3. The finer granulometry gave iron and chromium concentrations well below levels imposed by health regulations. We also found that it allowed an overdose of iron sulphate up to 200% of the stoichiometric rate, thus lowering the total chromium content in the filtered water and obviating the necessity of using a coagulant to fix the microfloc on the sand.

If fresh sand is used, the optimum filtration efficiency is obtained after 200 hours of operation, during which time the sand has become coated with iron hydroxide that catalyzes the ferrous iron precipitate: we noted no real surface clogging but rather a tendency to clog in depth. We also pointed out the presence of ferrous bacteria in the depth of the sand medium.

Table 3 also gives the filtration velocities. After a series of tests with coated sand it appears that a velocity of 20 m h^{-1} is possible, but that is the upper limit. We have chosen a velocity of 15 m h^{-1} for the design of the proposed plant.

TABLE 3 Effect of Filter Sand Granulometry

| | 15 m h^{-1} | | 20 m h^{-1} | |
|--------------|----------------------|--------------|----------------------|--------------|
| | Iron | Chromium (1) | Iron | Chromium (1) |
| Sand 0.80 mm | 305 | 75 | 325 | 82 |
| Sand 0.40 mm | 52 | 39 | 62 | 71 |

Concentrations are expressed in $\mu\text{g l}^{-1}$.

(1) Total chromium stoichiometry: 150%.

4 Mixed Treatment

We tested the effectiveness of a mixed filter consisting of the following.

- Reduction by iron sulphate with maximum 120% stoichiometry (beneath the optimum).

- Filtration on GAC. The layer of GAC plays a twofold part: it arrests the iron hydroxide and chromium precipitates and it absorbs the residual hexavalent chromium since the stoichiometry applied is limited. The filtration velocity was as indicated above. The GAC was declogged every 2 days and regenerated in the conditions defined above but the exhaustion time was extended (2 weeks). This treatment has the advantage of ensuring very safe operating conditions and makes allowances for any possible mistake in the dose rate. On the other hand, like GAC, it entails the problem of regeneration eluates containing hexavalent chromium.

CONCLUSION

The above study that lasted for a year enabled us to make a complete survey of the situation with regard to the removal of chromium from potable water. A full report will be published at a later date.

The treatment line adopted is based on the reduction of chromium by iron sulphate. The problems created by the overdose of iron sulphate in order to obtain the most thorough reduction of hexavalent chromium at a near neutral pH value have been solved by the use of very high-rate filtration on very fine sand. This arrests the fine precipitates and ensures a reduction of the residual ferrous iron content by catalysis and biological effect.

The treatment is rendered reliable in all circumstances by the continuous metering of the hexavalent chromium content and adapting the rate of treatment to the measurement obtained. The total chromium and iron in the treated water are also measured continuously. These measurements are obtained by differential pulse polarography.

REFERENCES

- Hamon, J.L., Lamblin, H. and Régnier, Y. (1979). Production d'eau potable: efficacité des filières actuelles de traitement pour l'élimination des métaux lourds. La Technique de l'Eau et de l'Ass., No. 386 02.
- Huang, C.P. (1975). Chromium removal by carbon adsorption. JWPCF, 47 (10).
- Morani, D. and Mezzana, M. (1981). Treatment of industrial effluents for heavy metal removal using the water soluble starch scanthate process. CEP. Consultants Ltd, Amsterdam.
- Rauzy, S.C. (1980). Contribution à l'amélioration de la qualité des eaux par l'utilisation d'argiles en cours de traitement de flocculation - décantation. Etude de l'élimination des métaux toxiques et des micropolluants organiques. Thèse, Paris V.

EFFECTS OF AGRICULTURE ON WATER QUALITY

THE CONTRIBUTION OF AGRICULTURAL LOADING TO EUTROPHICATION IN FINNISH LAKES

L. Kauppi

*Water Research Institute, National Board of Waters, P.O. Box 250,
SF-00101 Helsinki 10, Finland*

ABSTRACT

Agriculture accounts for 9 per cent of the total surface area of Finland and generates the greatest single nutrient input to Finnish watercourses. Since agricultural activity is scattered throughout the whole country its effects in lakes are less pronounced than those of domestic and industrial effluents. On the other hand, point source phosphorus loading of lakes and rivers decreased significantly during the nineteen-seventies.

Phosphorus is the nutrient which primarily limits production in most Finnish lakes. The availability of phosphorus in agricultural runoff waters is therefore a crucial question in the evaluation of the eutrophicating effects of agriculture. Our results indicated that in runoff waters available phosphorus can be 60-70 per cent of the total phosphorus. However, the concentrations of available P were so low that they could be achieved in Finnish lakes of low ionic concentration through simple chemical desorption without the assistance of the algal uptake. The utilization of the spring maximum of runoff phosphorus in lakes would thus not depend on the concurrence of the maxima of loading and algal growth.

KEYWORDS

Agricultural pollution; nonpoint source pollution; phosphorus; nitrogen; algal-available P; eutrophication.

INTRODUCTION

During the nineteen-seventies point source loading of lakes and rivers decreased in Finland due to the measures for pollution control. Particularly phosphorus and organic loading in domestic effluents went down (Fig. 1). As a result the recovery of polluted areas has started, eg. in Lake Vesijärvi (Keto, 1982). However, in some cases even the diversion of effluents to another recipient has not reversed the eutrophication trend. In these cases it has often been found

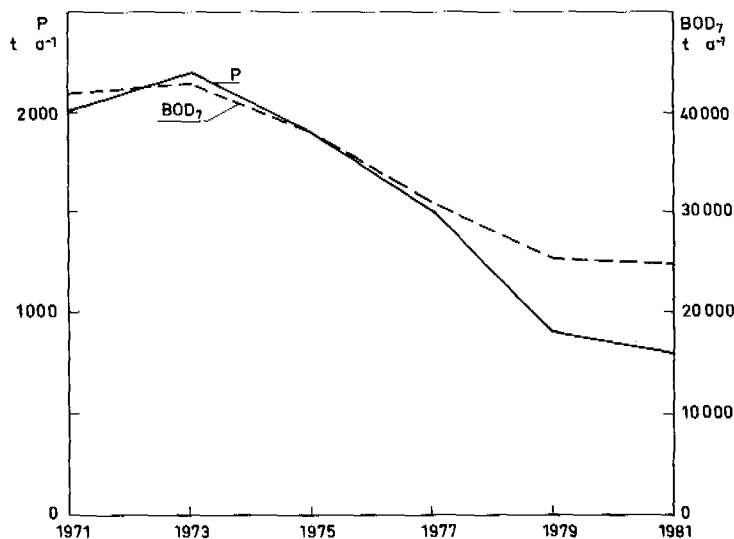


Fig. 1. Loads of phosphorus and organic matter from domestic effluents in Finland 1971-1981.

that nonpoint loading, together with loading from sediments, is sufficient to maintain high production levels. For example in Lake Tuusulanjärvi diffuse loading was almost as high as sewage loading during the period 1974-1977 (Ojanen, 1979). After the diversion of sewage no rapid recovery was observed. Ojanen (1979) calculated that even the diffuse load was greater than the critical loads given by Vollenweider (1970).

Agriculture accounts for 9 per cent of the total surface area of Finland. In the most intensively cultivated area in south-western Finland arable land totals 30 per cent of the surface area (Fig. 2). This is also the area in which the most severe water pollution problems due to agriculture occur. For example in the river Aura-joki agricultural loading has caused problems for water supply. Particularly during the melting period in spring, odour and taste problems have become a common phenomenon. The same is also true for some other neighbouring rivers in south-western Finland. Generally, however, slow eutrophication is typical for waters under agricultural influence.

It is to be expected that agricultural loading has increased during the last few decades. Fertilizer use has more than doubled from 1960 to 1980 (Fig. 3). Also structural changes in agriculture - especially the growth of the size of production units - have contributed to water pollution.

The primary objective of this study is to improve basis for assessing the significance of agricultural nutrient loading to the deterioration of fresh waters in Finland. First, methods for quantifying loads were developed and, second, the actual contribution of these loads to the alteration of watercourses was studied.

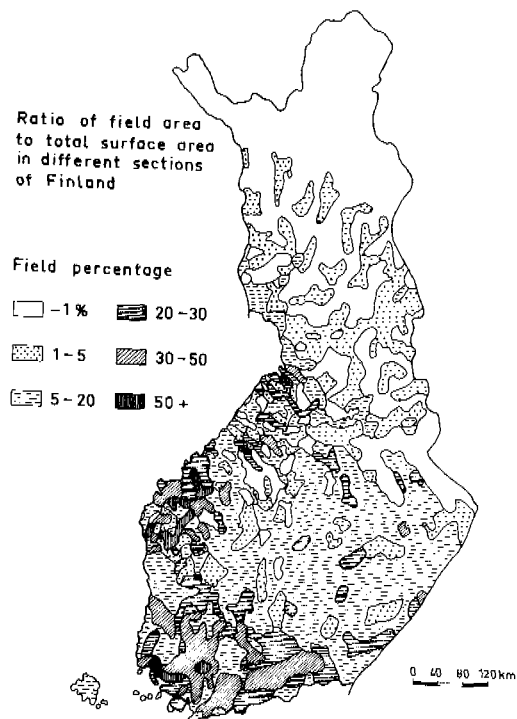


Fig. 2. Percentage of agricultural land of the total surface area in Finland.

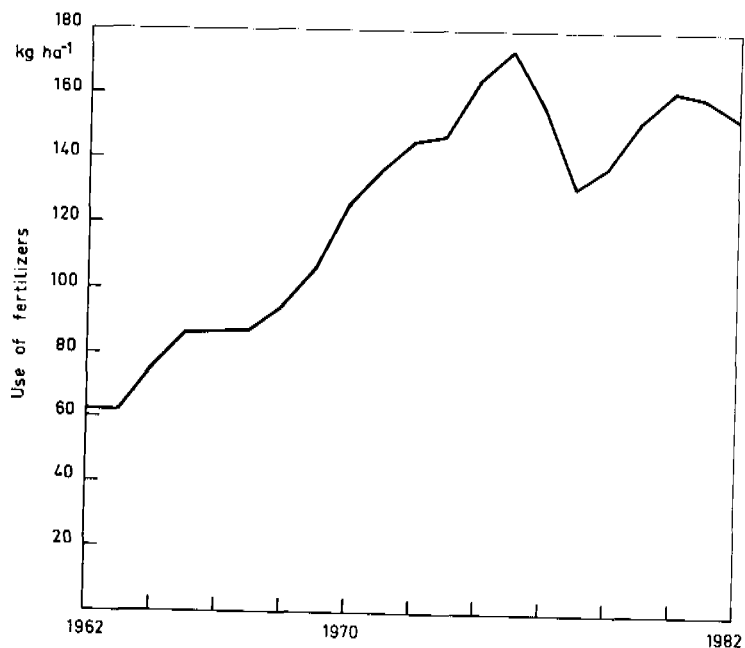


Fig. 3. Use of fertilizers in Finland 1962-1982.

LOADS OF NITROGEN AND PHOSPHORUS FROM AGRICULTURE

Estimates of nutrient losses from agricultural fields in Finland are mainly based on observations in small hydrological basins. The monitoring of runoff water quality in these basins started in 1962. From this data Kauppi (1978) calculated the dependence of phosphorus and nitrogen loads on the percentage of agricultural fields (FP, %) in the basin. For phosphorus the equation was of the form

$$P\text{-load } (\text{kg km}^{-2}\text{yr}^{-1}) = 15.1 \log_{10}(\text{FP} + 1) + 1.9 \quad (1)$$

and for nitrogen

$$N\text{-load } (\text{kg km}^{-2}\text{yr}^{-1}) = 9.8 \text{ FP} + 180 \quad (2)$$

On the basis of observations in six southern basins during the period 1965-1976, estimates were presented of specific nutrient loads per hectare of cultivated land (Kauppi, 1979). They were 0.57 kg ha⁻¹ for phosphorus and 12 kg ha⁻¹ for nitrogen and thus of the same order of magnitude as in other Nordic countries (Ah1, 1977; Holmen, 1977; Larsen, 1977). These losses were equivalent to 1 % and 13 %, respectively, of the amounts of P and N given in fertilizers. Using these specific loads agricultural nutrient loading is on an average 1 400 t yr⁻¹ phosphorus and 31 000 t yr⁻¹ nitrogen. This implies that agriculture comprises the most important single nutrient input to the watercourses (Table 1).

Table 1 Phosphorus and nitrogen loads from point and non-point sources in Finland in 1980 (Kauppi 1979; National Board of Waters, 1981, 1983)

| Source | Nutrient load (t yr ⁻¹) | |
|----------------------|-------------------------------------|----------|
| | Phosphorus | Nitrogen |
| Industrial effluents | 770 | 7 200 |
| Domestic effluents | 800 | 13 000 |
| Agriculture | 1 400 | 31 000 |

In addition to field percentage many other physiographic factors, such as slope steepness and soil particle size, have a strong influence on nutrient losses. The agricultural nutrient loads also depend strongly on hydrological factors and thus vary from year to year. In order to describe processes associated with nutrient losses in more detail several models have been proposed. Haith (1982) has reviewed the existing models. One of these was the CREAMS (Chemicals Runoff and Erosion from Agricultural Management Systems) model (Knisel, 1980), which was developed by the US Department of Agriculture. This model has been applied in many European countries in the context of the IIASA (International Institute for Applied Systems Analysis) research project on the environmental problems of agriculture (Svetlosanov and Knisel, 1982).

One of the case study areas was a small cultivated basin in southern

Finland (Kauppi, 1982). Simulation of monthly and annual runoff values was successful, whereas the soil and nutrient losses calculated by the model deviated considerably from the observed values. This may have been due to the rough approximation of the parameter values. In particular, the nutrient contents of the soil should be measured in the basin being investigated, because considerable variation may occur even between basins situated near to each other.

In principle, the CREAMS model seemed to be potentially suitable as a model for the estimation of agricultural pollution in Finnish conditions. However, its use is restricted to field scale. Furthermore, the number of parameters in the model is large and for many of them it is difficult to find a reliable value from the literature. It would therefore be necessary to carry out field measurements before applying the model. As long as the use of the model is restricted to field scale it seems that in most cases the information needed for water protection planning would be easier to obtain by other, simpler methods.

EFFECTS IN LAKES

Phosphorus is the primary limiting nutrient in Finnish lakes. The question of the availability of non-point phosphorus has therefore gained importance during recent years since non-point sources have received more attention. Phosphorus transported by particles is often the most important component of the non-point P loading of lakes, whereas algae mainly utilize P in a soluble form. This means that adsorbed P must become soluble before algae can use it.

The fraction of runoff P that could be taken up by algae was studied in the Finnish Water Research Institute by algal assays using Selenastrum capricornutum as test organism. Algal assays were performed with both filtered and nonfiltered runoff waters in order to study the influence of adsorbed P. Different proportions (0, 10, 50, 100 %) of nonfiltered runoff water were also mixed with oligotrophic lake water and the algal growth potentials (AGP) of the mixtures were measured.

The highest AGP values ($74\text{-}76 \text{ mg l}^{-1}$ f.w.) were measured in samples from the totally cultivated basin in the spring. In autumn the AGP was rather small in all the samples, possibly because plants had taken almost all the available P from the soil during the summer. Filtration of samples decreased the AGP by 5-82 %, indicating the significance of adsorbed P to the growth of algae.

Spring runoff waters flowing from cultivated areas clearly increased the AGP of lake water (Fig. 4a). The relative increase was strongest with the most dilute (10 %) additions, i.e. this was the most favourable mixture for P utilization. In these mixtures, 27-100 % of the added total P became available for algal growth, the mean value being 64 %. In autumn samples the percentage availability was even higher, but because the absolute values of the total P concentrations in runoff were low, only a slight effect on the lake AGP was recorded (Fig. 4b). In general the lower the total P concentration in the culture solution, the more efficient was the utilization of runoff P. This may reflect more favourable conditions for desorption and in any case implies that the availability of runoff in lakes might be

quite high, about 60-70 %, because runoff waters become diluted by lake waters.

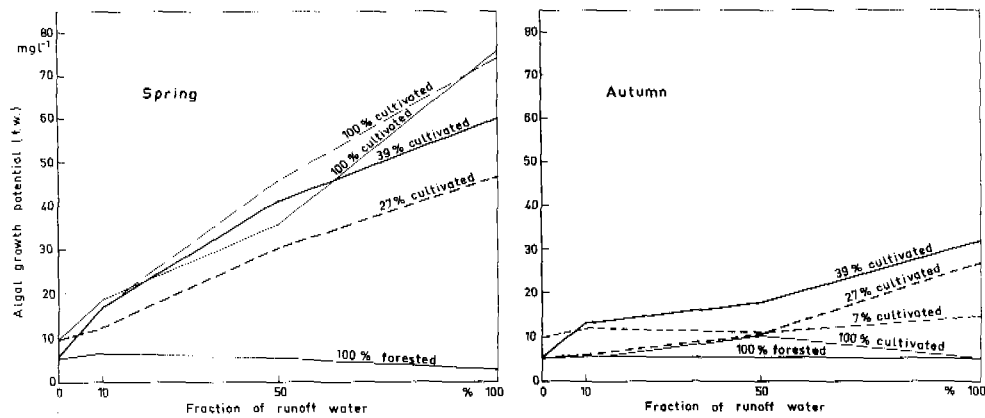


Fig. 4. Effect of different runoff waters on the AGP of the water of an oligotrophic lake; a) spring runoff waters, b) autumn runoff waters.

There are, however, other factors which may limit the utilization of runoff P in Finnish lakes. The most important of these is the time delay in spring from the maximum loading to the attainment of a water temperature optimal for algal growth, although the role of psychrophilic algae should not be neglected.

If desorption as a merely chemical process is capable of transforming P into a bioavailable form to the degree found in this study, then the time delay is not a problem. Most of the desorbed P simply remains in solution until algae take it up. If, however, it is assumed that algae are needed to enhance desorption by removing P from solution or that they utilize particulate P through direct contact with particles, then the time delay is a key factor. During the delay of one or one and a half months, particles have sufficient time to settle down to the bottom and thus remove the adsorbed P from the water. In this case non-point P would have almost no effect on the productivity of the lake.

The capability of chemical desorption to transform P into a soluble form was evaluated by comparing the concentrations of available P in our study with the equilibrium P concentrations obtained in desorption studies by Hartikainen (1979). On the basis of this comparison it appeared that desorption could account for the transformation of P into a bioavailable form at the concentration observed in this study. If that is the case, the availability estimates obtained in this study can be applied to spring loading despite the fact that the peaks of P loading and algal growth do not coincide. This conclusion should be verified by monitoring the spring development of soluble phosphate concentrations in lakes.

CONCLUSIONS

Agriculture generates the most important single nutrient input to Finnish watercourses, although it accounts for only 9 per cent of the total surface area of the country. However, agricultural activity is scattered throughout the country, whereas industrial and domestic effluents are mainly concentrated in certain watercourses. This difference results in different environmental effects.

In addition to the regular spatial distribution other factors may also decrease the eutrophication effect of agricultural nutrients. Most of the non-point phosphorus is transported adsorbed to soil particles and thus has to be desorbed before becoming available for algal growth. If algal uptake of phosphorus is needed to enhance desorption then the spring maximum of non-point loading can have only little effect on the eutrophication of lakes. There is at least one month's time delay between the maximum loading and the attainment of a water temperature optimal for algal growth. This means that phosphorus adsorbed to particles would be sedimented out of the active nutrient cycle before the onset of rapid algal growth.

However, the ionic concentration of Finnish lake waters is low. This indicates that simple chemical desorption may transform significant amounts of phosphorus into an algal-available form. It is possible that the concentrations of available phosphorus measured in this study by algal tests were obtained through desorption without algae. In this case the estimates of 60-70 % availability of total phosphorus to algae in agricultural runoff waters could be quite realistic despite the fact that the peaks of P loading and algal growth do not coincide.

REFERENCES

- Ahl, T. (1977). Diffusa föroreningar i relation till markanvändning. Diffuse vannföroreningar. Nordforsk, Miljövårdssekretariatet, Publ. 1977, 2, 483-490.
- Haith, D.A. (1982). Models for analyzing agricultural nonpoint-source pollution. International Institute for Applied Systems Analysis. RR-82-17. Laxenburg. 29 p.
- Hartikainen, H. (1979). Phosphorus and its reactions in terrestrial soils and lake sediments. J. Scient. Agric. Soc. Finl. 51, 537-624.
- Holmen, S.A. (1977). Er tilførslene av nitrogen og fosfor fra jordbruket undervurdert i Norge. Diffuse vannforurensninger. Nordforsk, Miljövårdssekretariatet, Publ. 1977, 2, 235-238.
- Kauppi, L. (1978). Effect of drainage basin characteristics on the diffuse load of phosphorus and nitrogen. Publications of the Water Research Institute, Finland, 30, 21-41.
- Kauppi, L. (1979). Phosphorus and nitrogen input from rural population, agriculture and forest fertilization to watercourses. Publications of the Water Research Institute, Finland, 34, 35-46.
- Kauppi, L. (1982). Testing the applicability of the CREAMS model to estimation of agricultural nutrient losses in Finland. Publications of the Water Research Institute, Finland, 49, 30-39.
- Keto, J. (1982). The recovery of L. Vesijärvi following sewage diversion. Hydrobiologia, 86, 195-199.
- Knisel, W.G. (ed., 1980). CREAMS: A field scale model for chemicals, runoff, and erosion from agricultural management systems. U.S.

- Department of Agriculture, Conservation Research Report 26. 640 p.
Larsen, V. (1977) Oversigt over diffus stoftilførsel till vandløb fra landbruget. Diffuse vannforurensninger. Nordforsk, Miljövårdssekretariatet, Publ. 1977, 2, 165-181.
- National Board of Waters (1981). Vesihuoltolaitokset 31.12.1980.
English summary: Water supply and sewer systems 31.12.1980.
- National Board of Waters, Finland, Report 214. Helsinki. 207 p.
- National Board of Waters (1983). Tecollisuuden vesitilasto 1979-1980.
English summary: Industrial water statistics in 1979-1980. National Board of Waters, Finland, Report 224. Helsinki. 71 p.
- Ojanen, T. (1979). Phosphorus and nitrogen balance of the eutrophic Lake Tuusulanjärvi. Publications of the Water Research Institute, Finland, 34: 74-87.
- Svetlosanov, V., and W.G. Knisel (eds., 1982). European and United States case studies in application of the CREAMS model. International Institute for Applied Systems Analysis. CP-82-S11. Laxenburg. 148 p.
- Vollenweider, R.A. (1970). Scientific fundamentals of the eutrophication of lakes and flowing waters, with particular reference to nitrogen and phosphorus as factors in eutrophication. OECD. Paris. 159 p.

MODELING WATER QUALITY AND THE EFFECTS OF AGRICULTURAL BEST MANAGEMENT PRACTICES IN THE IOWA RIVER BASIN

B. R. Bicknell,* Anthony S. Donigian, Jr.* and
T. A. Barnwell**

*Anderson Nicholas & Co., Resources Technology Division, Palo Alto,
California, U.S.A.

**U.S. Environmental Protection Agency, Athens, Georgia, U.S.A.

ABSTRACT

This paper describes a demonstration application of comprehensive hydrology and water quality modeling on a large river basin to evaluate the effects of agricultural nonpoint pollution and proposed best management practices (BMP). The model application combines detailed simulation of agricultural runoff and soil processes, including calculation of surface and subsurface pollutant transport to receiving water, with subsequent simulation of instream transport and transformation. The result is a comprehensive simulation of river basin water quality.

The investigation of the Iowa River Basin described in this paper was part of a large study which included application and evaluation of the Hydrological Simulation Program - FORTRAN (HSPF) to both the data-intensive Four Mile Creek watershed and the Iowa River above Coralville Reservoir. In this study, the methodology developed on Four Mile Creek was extrapolated to the Iowa River Basin to demonstrate its applicability and functionality on a large river basin. Many model parameter values from Four Mile Creek were applied directly to the study area without adjustment while other parameters were modified based on available information and calibration. This study allowed the exploration of problems associated with modeling hydrology, sediment, and chemical fate and transport in a large river basin with varying meteorologic conditions, soils, and agricultural practices.

KEYWORDS

Runoff; erosion; sediment transport; pesticides; nutrients; agricultural BMPs; basin-scale modeling; water quality modeling.

INTRODUCTION

Mathematical models are being used to analyze and predict the quantity and quality of runoff from agricultural lands. The ultimate goal is to use these models to develop a Best Management Practice (BMP) plan that will maintain agricultural productivity while minimizing adverse water quality impacts. However, runoff models by themselves are not sufficient to predict water

quality effects of BMPs since instream transport and transformations are not represented. These models must be linked with receiving water quality models to assess the quality in receiving waters resulting from BMPs applied to the watershed.

The investigation of the Iowa River Basin described in this paper was part of a large study which included application and evaluation of the Hydrological Simulation Program - FORTRAN (HSPF) (Johanson et al. 1981) to both the data-intensive Four Mile Creek watershed (Donigian et al. 1983a) and the Iowa River Basin above Coralville Reservoir (Donigian et al. 1983b). In this study, the methodology developed on Four Mile Creek was extrapolated to the Iowa River to demonstrate its applicability on a large river basin. Many model parameter values from Four Mile Creek were applied directly to the study area without adjustment while other parameters were modified based on available information and engineering judgement. This study allowed the investigation of HSPF capabilities to simulate hydrology, sediment, and chemical fate and transport in a large river basin with varying meteorologic conditions, soils, and agricultural practices.

BASIN DESCRIPTION

The portion of the Iowa River Basin modeled in this study encompasses an area of 7240 km² in Central Iowa, and terminates at the Coralville Reservoir near Marengo, Iowa (Fig. 1). The river later joins with the Cedar River before emptying into the Mississippi. There are three distinct topographical areas in the watershed. The upper portion is gently rolling to flat with poor drainage and is characterized by depressions which collect water and prevent rapid runoff. The central area is more hilly, and the southern portion is relatively level. Elevations range from 900 to 1200 feet. Most of the basin is covered with prairie soil formed from glacial drift; in the lower portions, loess covers the glacial drift. Soils in the basin are primarily loams and silty clay loams. The soil associations are Clarion and Webster in the upper areas, and Tama-Muscatine in the lower portion. The climate in the basin is humid with average temperatures of 47 degrees and mean annual precipitation of 32 inches. Land use is primarily agricultural with about 45% in corn cropland, 22% in soybeans, and 33% in other uses, primarily pasture.

DATA COLLECTION AND WATERSHED SEGMENTATION

Meteorologic, streamflow, and water quality data necessary to calibrate HSPF were selected and examined, along with soils characteristics, topography, and land use information, in order to segment the Iowa Basin. Variation in precipitation and air temperature over the basin indicated that the Iowa River Basin could be divided into three segments, in order to perform a reasonable hydrologic simulation for the purposes of this demonstration study. Tentative boundaries for the segments, based on long term isopleth information on rainfall and air temperature, were then adjusted slightly based on spatial distribution of soils. Three NOAA/NWS weather station records (Sheffield in the north, Iowa Falls in the central area, and Traer in the southeast) were selected as most representative of the precipitation on these segments based on comparison of long term averages. Similarly, the air temperature stations chosen were Iowa Falls, Marshalltown, and Cedar Rapids. Additional time series required for hydrologic calibration of HSPF are wind speed, potential evapotranspiration, and solar radiation. Single data sets were used to represent these quantities over the entire basin.

because of limited variation and/or availability of data. The segment boundaries and locations of meteorologic stations used for the simulation are shown in Fig. 1.

Final subdivision of the three segments into pervious land segments (PLSS) was based on land use. Between 65% and 85% of each county in the basin is cropland, and only grassland comprises more than 10% of the total usage. Most of the croplands are planted in either corn or soybeans. Given the differences in fertilizer and pesticide applications for the two crops, separate land uses were assumed. All lands not planted in corn or soybeans were considered as a third composite land use. Thus, a total of nine PLSSs were modeled - one to represent each of the three land use types in each of the three meteorologic/soil segments.

Streamflow data was available for nine U.S.G.S. gages in the basin; however, only three were located on the main branch. Daily sediment loadings collected by the U.S. Army Corps of Engineers at Marengo were used, along with limited (grab samples, etc.) water quality data obtained from the U.S. EPA.

The main channel of the Iowa River between the confluence of the east and west branches and the U.S.G.S. gage near Marengo was divided into 13 reaches for simulation. Of the 12 intermediate reach boundaries between the study limits, one was selected at the Iowa Falls Power Dam channel discontinuity, two were selected at U.S.G.S. streamflow gage sites (Rowan and Marshalltown), eight corresponded to sites of major tributary inflow, and one was chosen arbitrarily to subdivide a long section of the river. The 13 reaches and contributing area to each are illustrated in Fig. 2.

HYDROLOGIC/HYDRAULIC SIMULATION

A limited calibration effort was undertaken in this study in order to demonstrate sufficient agreement between model results and available data so that the model could be used for preliminary BMP analysis and evaluation. In general, an accurate hydrologic calibration is necessary since errors in the hydrology directly impact the chemical and sediment simulations.

Initial hydrologic simulations were performed on two test watersheds in order to provide preliminary adjustments to the parameter values developed for the Four Mile Creek watershed. Differences in the soils and topography between the upper and lower parts of the basin indicated that significant changes would be necessary. The watersheds were the East Branch of the Iowa River above Klemme in the northern extreme of the basin and Salt Creek above Elberon in the southern portion (near Four Mile Creek). Based on these initial simulations, a number of parameter adjustments were made prior to the first basin-wide simulation.

In addition, adjustments were necessary to the meteorologic data for the basin-wide simulation. Long-term meteorologic patterns in each segment group were compared with the mean characteristics at each of the stations used for the simulation. Based on this comparison, multipliers were developed and applied to the precipitation and temperature time series.

A limited hydrologic calibration effort (three simulation runs) was made to further adjust the parameter values until an acceptable basin-wide hydrology simulation was obtained. Table 1 provides comparisons of recorded and simulated runoff at the three U.S.G.S streamflow gages along the Iowa River

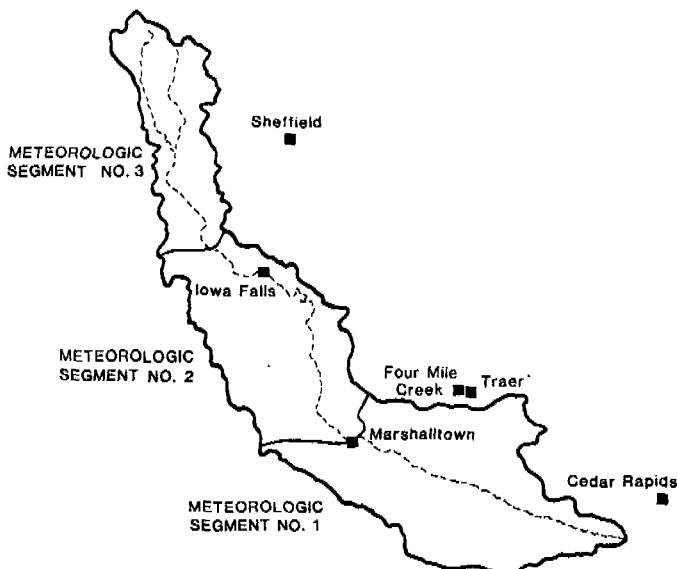


Figure 1. Segment Boundaries and Locations of Meteorological Stations in the Iowa River Basin.



Figure 2. Channel Reaches and Contributing Areas for the Iowa River Basin.

for the five year simulation period (1974-1978). Representative results for simulated mean daily flow are shown in Fig. 3. Simulated runoff volumes for the first four years of the study period were generally fair to good at the three gages. The final set of hydrologic parameter values resulted in a fairly consistent oversimulation of runoff at Rowan by approximately 15-20% prior to 1978. Simulated runoff at Marshalltown and Marengo was less than observed for this period. Undersimulation at Marshalltown was generally in the range of 20-25% of recorded annual totals, while Marengo was within 5% of recorded runoff for the years 1975-1977.

TABLE 1 Hydrology Simulation Results (expressed as runoff in mm)

| YEAR | ROWAN | | MARSHALLTOWN | | MARENGO | |
|-------|-------|------|--------------|------|---------|-------|
| | REC | SIM | REC | SIM | REC | SIM |
| 1974 | 154. | 183. | 313. | 232. | 391. | 321. |
| 1975 | 152. | 124. | 216. | 169. | 234. | 228. |
| 1976 | 59.* | 80. | 136. | 107. | 139. | 138. |
| 1977 | 9.* | 49. | 65. | 67. | 98. | 95. |
| 1978 | 102. | 300. | 169. | 297. | 227. | 348. |
| TOTAL | 477. | 734. | 899. | 874. | 1089. | 1129. |

REC - recorded

SIM - simulated

* - does not include 10/76-6/77 runoff; data not available

Runoff for the year 1978 was drastically oversimulated due to problems with the Sheffield precipitation record which was used to represent the upper segment group. Recorded rainfall totals for two storms in June and July of that year were 84 mm and 114 mm in 12 and 5 hours, respectively. It is unlikely that rainfall of comparable intensity occurred on the entire segment. Overall, simulated runoff for 1978 at Rowan was 190% greater than recorded, resulting in a 76% oversimulation downstream at Marshalltown and 53% at Marengo. Similarly, during an August 1974 storm, the rainfall recorded at Iowa Falls and Traer was not nearly enough to induce the large flow recorded at Marengo. These discrepancies indicate the problems associated with using a single rainfall record to represent a large segment of land.

Another major problem with the hydrologic simulation was the timing and volumes of snowmelt runoff. Modeling snow accumulation, melt, and resulting runoff is a traditional weakness in watershed modeling. For example, the occurrence and effects of frozen ground conditions are not well defined quantitatively, but they exert major impact on snowmelt runoff. We attempted to account for frozen ground effects by reducing infiltration during the winter months. Simulated runoff from snowmelt generally preceded recorded values in the Iowa Basin. In most years the snow pack melted in a short 2-3 week period producing a peak flow in about mid-March; the model generally produced a more gradual melting and lower peak flows. These problems are likely due to deficiencies in the model and input meteorologic data, primarily air temperature and solar radiation.

For the purposes of this demonstration study, comparison of recorded and

simulated flow frequency data provides an adequate indication of the acceptability of the simulation results. Fig. 4 shows the simulated and recorded flow frequency curves for the 1974-1978 period at Rowan, Marshalltown, and Marengo. This figure indicates that modeling results for the upstream gage at Rowan were not good; simulated mean flow was over 50% greater than recorded mean flow. However, since only 15% of the basin area is above the Rowan gage, simulation results for this gage are not as important as results at the downstream gages at Marshalltown and Marengo. At the lower gages simulated flows had a much better fit to recorded values; mean simulated flows at both gages differed from mean recorded flows by less than 5%. While these statistics verify that the simulated flows were acceptable for the purposes of this study, additional calibration is recommended if the information developed in this study is to be used for planning decisions in the study area.

SEDIMENT SIMULATION

Separate HSPF module sections were used to simulate detachment/removal of sediment from the land surface and instream sediment transport processes. In both cases, initial parameter values were taken directly from the Four Mile Creek study. Since recorded sediment erosion data were not available anywhere in the basin, adjustments to parameter values were made on an intuitive basis following an initial run in which erosion was obviously too low; three calibration runs were made. The final sediment erosion simulation showed a total washoff of 2.7 tonnes/ha for the five year simulation period. Totals for the nine segments were as follows:

| | SOYBEANS | CORN | PASTURE/OTHER |
|--------------|----------|------|---------------|
| UPPER BASIN | 5.4 | 5.4 | 0.8 |
| MIDDLE BASIN | 0.8 | 1.1 | 0.06 |
| LOWER BASIN | 5.2 | 5.6 | 0.7 |

The totals for the upper watershed were biased by the high 1978 erosion which was caused by the large oversimulation of runoff in this area. In a year with good fit between simulated and recorded runoff, such as 1974, approximately 80% of the total basin washoff emanates from the lower area, 17% from the middle area, and only 2% from the upper portion (as opposed to 49% in 1978). This distribution is more reasonable considering the topography, soils, and relative amounts of area in the three portions of the basin. The upper area is characterized by low overland flow slopes and depressions which retard runoff and trap eroded sediment. The hilly terrain of the middle portion enhances erosion. The effects of the gentler slopes of the lower basin area are overcome by larger quantities of rainfall and much more erodible soils than are found in the northern areas. Consequently, a large fraction of the sediment washoff emanates from the lower area.

Instream sediment transport is a complex problem, and effective calibration with HSPF requires data to characterize the depth and composition of the bed sediments as well as particle hydraulic characteristics and recorded storm suspended particle size distributions. For the Iowa River, the only available data were daily sediment loadings at Marengo.

Three instream sediment calibration runs were performed, using the sediment washoff as loading to the channel, and starting with parameter values developed in Four Mile Creek. Parameters were adjusted until a reasonable fit to recorded data for 1974 was achieved. The results are illustrated in Fig. 5, where the flow simulation is shown for comparison; loadings for the

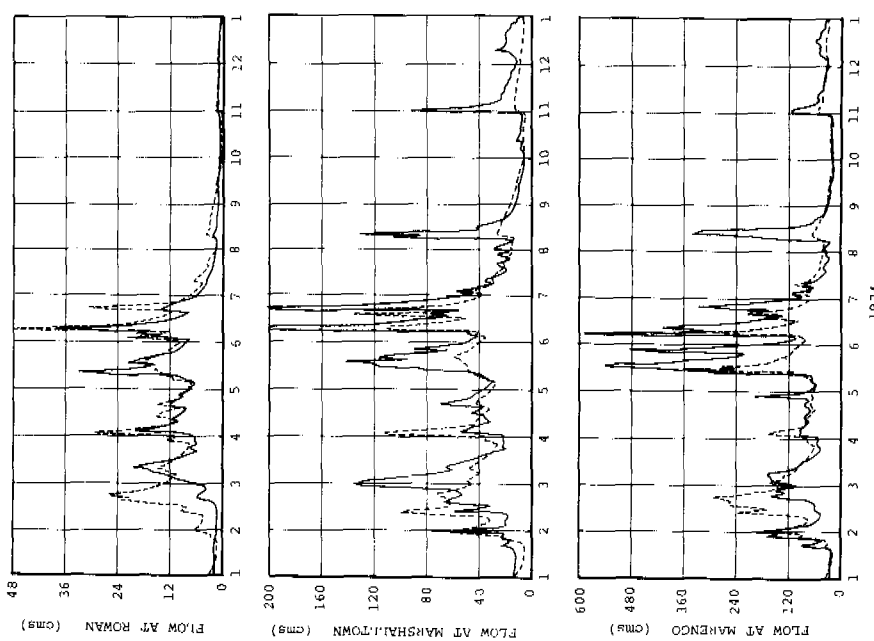


Figure 3 Comparison of Flow Simulation Results with Streamflow Records at Rowan, Marshalltown, and Marengo, Iowa

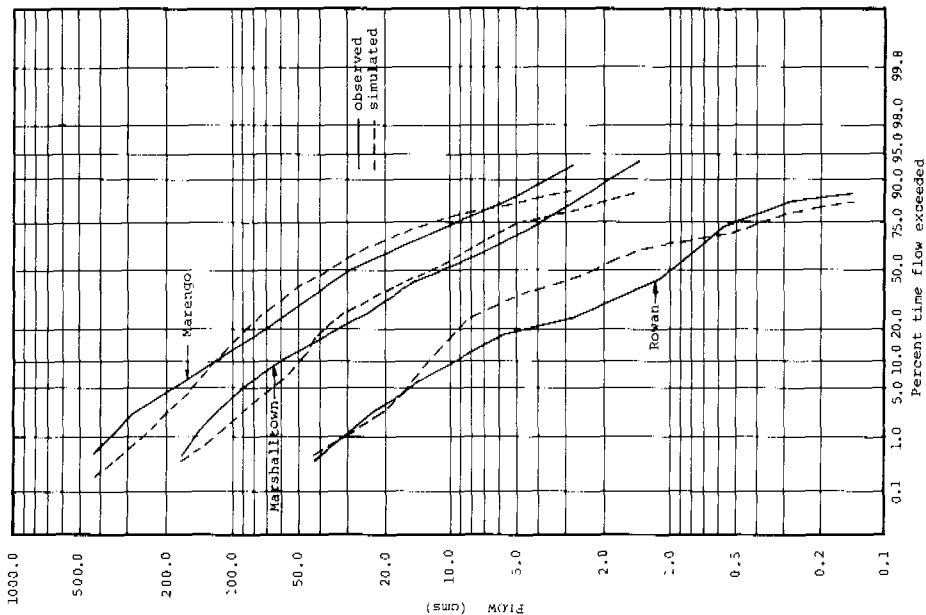


Figure 4 Comparison of Simulated and Observed Flow Frequency at Rowan, Marshalltown, and Marengo, Iowa (1974-1978)

entire simulation period are provided in Table 2. Generally the sediment calibration results were fair to good considering the lack of recorded erosion data and information for characterization of the sediment bed, and discrepancies between recorded and simulated streamflow. A major question of the simulation concerns the source of loadings at Marengo; simulated results showed 14% of the 1974 total resulted from surface washoff while the remaining loadings resulted from channel scour.

TABLE 2 Sediment Simulation Results at Marengo

| YEAR | SEDIMENT (kg/ha) | | |
|-----------|---------------------|-----------|-------------|
| | RECORDED | SIMULATED | SIMULATED * |
| 1974 | | | |
| January | 28. | 5. | 4. |
| February | 190. | 984. | 20. |
| March | 227. | 66. | 4. |
| April | 203. | 375. | 13. |
| May | 1432. | 509. | 140. |
| June | 1380. | 1952. | 354. |
| July | 247. | 11. | 8. |
| August | 245. | 2. | 1. |
| September | 7. | 0. | 0. |
| October | 6. | 0. | 1. |
| November | 69. | 1. | 0. |
| December | 13. | 0. | 0. |
| TOTAL | 4047. | 3905. | 545. |
| 1975 | 1501. | 875. | 207. |
| 1976 | 1233. | 559. | 74. |
| 1977 | 332. | 19. | 17. |
| 1978 | 1802. | 5690. | 1880. |

* Edge of stream loadings - included for comparison.

PESTICIDE SIMULATION

The herbicide alachlor was simulated in order to demonstrate HSPF capabilities for modeling chemical fate and transport in the Iowa Basin. Alachlor is used extensively on corn and soybean cropland in the basin, and it had been modeled previously in Four Mile Creek. However, the simulation was limited by lack of recorded alachlor concentration data in the basin.

Alachlor simulation with HSPF involved applications to corn and soybean cropland, adsorption to soil, degradation, dissolved and adsorbed transport to streams, and instream adsorption, decay, and transport. Land surface and instream pesticide parameters were used directly from the Four Mile Creek HSPF application; no calibration was performed due to lack of data. During the five year simulation period, significant alachlor runoff to the river system occurred only in May-July since the alachlor half-life of 6-15 days depleted the 2.8 kg/ha application amount to less than 0.25 kg/ha by mid July. Typical simulated instream alachlor concentrations during storms were in the range of 10-100 ppb during these months. No recorded data were

available in the study area; however, alachlor concentrations recorded downstream of Coralville Reservoir during 1975 and 1976 showed maximum values of 1.0 and 1.7 ppb (Schnoor et al. 1979) compared to simulated values upstream of 27. and 17. ppb. This range of concentrations is also consistent with data on other Iowa streams (Schnoor et al. 1982).

NUTRIENT SIMULATION

Edge-of-stream nitrogen nutrient loadings were calculated by the land portion of HSPF and used as input to the stream section for instream simulation in order to calculate the nutrient loadings and concentrations downstream at Marengo. The processes modeled were application of fertilizer and plant residue in chemical form to the land surface or incorporated into the soil, the complete soil nitrogen cycle as represented in HSPF, adsorption/desorption, nutrient movement with soil and water to the stream, instream transport, and ammonia volatilization and nitrification.

The nutrient simulation followed the same general procedure as the pesticide simulation. Parameters were adopted from Four Mile Creek and used in conjunction with the watershed hydrology and stream hydraulics to model nutrients in the basin for 1974-1978. Simulated nitrate and ammonia concentrations at Marengo and Marshalltown for 1978 are illustrated in Fig. 6. Limited observed data at nearby sampling sites are included for comparison. Since the simulated nutrient concentrations are generally in the same range as observed values, the results are good for a model application without calibration.

BMP EFFECTS ON WATER QUALITY

The effects of a proposed BMP scenario were simulated to analyze the resulting impacts on water quality. The effects of the chosen BMP (conservation tillage plus contouring) on model parameters were estimated (Donigian et al. 1983c) and the model was run with the adjusted parameters with subsequent comparison to the base conditions.

The primary components of the BMP scenario were (1) a shift from moldboard plowing to chisel plowing and field cultivation as primary tillage, (2) one summer cultivation for weed control instead of two, and (3) allowing crop residues to remain on the field following harvest. These components were modeled by increasing parameter values for soil moisture retention (UZSN), rainfall interception, surface roughness (Manning's n), and land cover; and decreasing the sediment fines produced by tillage. There were no changes in the infiltration parameter, chemical parameters, soil bulk density, soil temperature, or chemical application amounts, although fall fertilizer application was replaced by increasing the spring and summer applications.

Using these assumptions and associated changes in parameter values, the resulting comparison of this BMP scenario and the base conditions is shown in Tables 3 and 4 for 1974. Over the simulation period, annual runoff reductions from corn and soybean cropland ranged from 4% to 17%. Surface runoff decreased significantly with average reductions of 30% and 26% for corn and soybeans. Corresponding sediment losses, which come entirely from the surface were also reduced dramatically (52% and 47%). BMP effects on erosion were much more pronounced than the resulting loading since most of the simulated sediment loading at Marengo resulted from channel scour rather than land surface erosion.

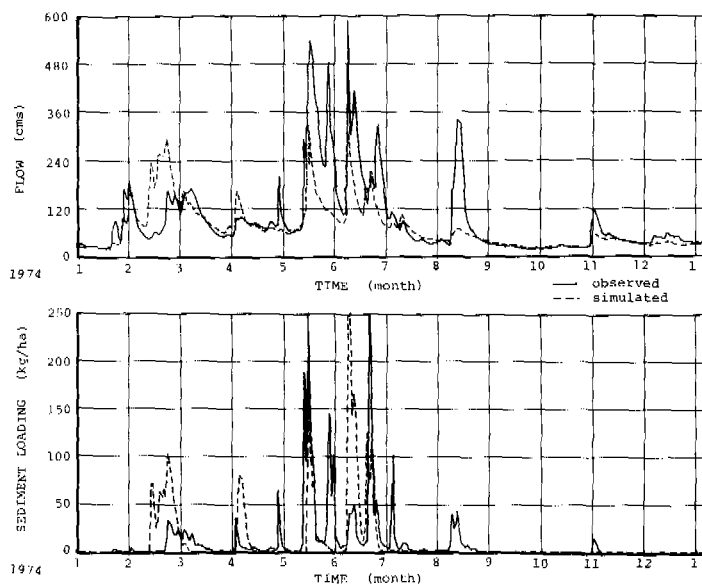


Figure 5 Comparison of Simulated and Recorded Flow and Sediment Load near Marengo

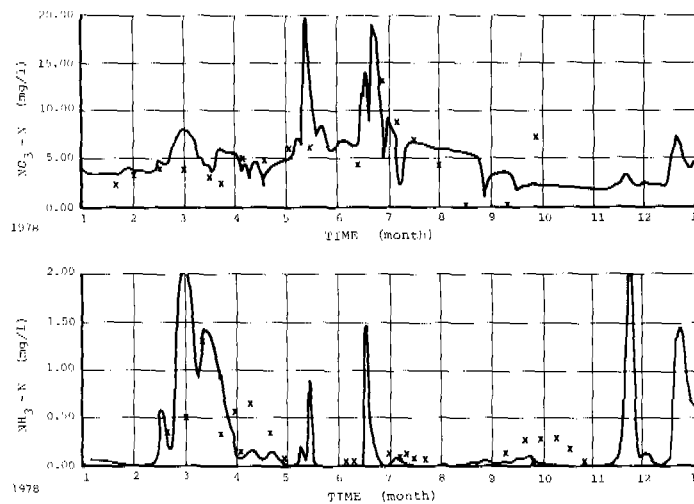


Figure 6 Comparison of Simulated and Recorded Nutrient Concentrations near Marengo

TABLE 3 Comparison of Edge-of-Stream Loadings for Base Condition and BMP Simulations in 1974

| SOYBEANS | | | CORN | | |
|-----------------------------|-------|----------|-------|-------|----------|
| BASE | BMP | % CHANGE | BASE | BMP | % CHANGE |
| RUNOFF (mm) | | | | | |
| Surf. | 32. | -23. | 42. | 31. | -25. |
| Intf. | 51. | -13. | 59. | 53. | -11. |
| Grndw. | 205. | -1.5 | 212. | 202. | -4.5 |
| Total | 288. | -6.5 | 312. | 296. | -8.3 |
| SEDIMENT 0.61 (tonne/ha) | 0.34 | -45. | 0.90 | 0.60 | -33. |
| ALACHLOR 0.091 (kg/ha) | 0.063 | -30. | 0.19 | 0.15 | -19. |
| NITRATE (kg/ha) | | | | | |
| Surf. | 0.036 | -30. | 0.120 | 0.073 | -39. |
| Intf. | 2.6 | -9. | 16.2 | 15.5 | -4. |
| Grndw. | 20.7 | -2. | 35.5 | 33.8 | -5. |
| Total | 23.3 | -3. | 51.8 | 49.4 | -5. |
| AMMONIA (kg/ha) | | | | | |
| Surf. | 0.16 | -25. | 0.77 | 0.56 | -26. |
| Intf. | 0.49 | -26. | 2.2 | 1.6 | -29. |
| Grndw. | 0.064 | -1.4 | 0.067 | 0.064 | -4.5 |
| Total | 0.72 | -23. | 3.1 | 2.2 | -28. |

Surf. - surface runoff

Intf. - interflow runoff

Grndw.- groundwater runoff

The resulting effects of the BMP scenario on water quality in the river measured at Marengo are shown in Table 4. Over the five-year simulation period, total flow reductions at Marengo averaged 7.5% while sediment reductions averaged 21%. Total instream ammonia reductions were considerably greater than nitrate because reduced sediment erosion prevents adsorbed ammonia from reaching the stream while erosion control has limited effect on the mobile nitrate species.

TABLE 4 Comparison of Loadings at Marengo for Base Condition and BMP Simulations in 1974

| | BASE | BMP | % CHANGE |
|---------------------|-------|-------|----------|
| Runoff (mm) | 183. | 170. | -7.1 |
| Sediment(tonnes/ha) | 3.9 | 2.6 | -33. |
| Alachlor (kg/ha) | 0.028 | 0.022 | -21. |
| Nitrate (kg/ha) | 31. | 30. | -3.9 |
| Ammonia (kg/ha) | 0.48 | 0.41 | -15. |

One of the possible uses of continuous simulation modeling of chemical fate and transport is to evaluate the risk or exposure of aquatic organisms to various magnitudes and durations of chemical concentrations. Using a methodology developed by Onishi et al. (1979) to assess the risk of chemical exposure to aquatic organisms, the simulated alachlor concentrations under both base conditions and the BMP scenario were analyzed to determine the percent of time acute, chronic, and sublethal conditions would exist. The results of this analysis are shown in Table 5; the table title indicates a hypothetical organism because all the values observed for alachlor concentrations were considerably below any of the MATC (maximum acceptable toxicant concentration) values for common species of fish found in the Iowa River.

TABLE 5 Lethality Analysis of BMP Scenario for Alachlor in
the Iowa River at Marengo, Iowa (Hypothetical Organism)

| | GLOBAL EXCEEDANCE (% of time) | | |
|----------------------------------|----------------------------------|--------------|----------|
| | BASE CONDITION | BMP SCENARIO | % CHANGE |
| ACUTE REGION | 0.49 | 0.49 | 0. |
| ABOVE MATC VALUE | 3.5 | 2.7 | -23. |
| SUBLETHAL REGION (below MATC) | 96.5 | 97.3 | -0.8 |

As shown in Table 5, the specific choice of MATC and lethality data chosen for this analysis resulted in no change in the percent of time when acute conditions existed; a 23% reduction in time of chronic conditions was seen. Although the values listed here are specific to the conditions under which this BMP scenario was simulated, the analysis indicates how the procedures described here can be used to evaluate the effects of BMP scenarios on resulting risk of exposure of organisms to chemicals.

SUMMARY

This demonstration application of HSPF to the Iowa River Basin has shown that HSPF can be used to model the flow, sediment, and water quality (specifically pesticides and nitrogen nutrients) from large agricultural river basins. Extrapolation of parameter values from nearby or representative calibrated watersheds can be performed with a reasonable degree of confidence. Determination of representative meteorologic time series data, primarily precipitation and air temperature, for different portions of the basin is a critical component in basin-scale modeling. Lacking representative data, comparison of frequency information is a better measure of overall simulation accuracy than comparison of storm event data.

With minimal calibration effort, simulation of flow frequencies on the main stem of the Iowa River was fair to good in this study, in spite of problems with deficient rainfall data and with modeling volume and timing of snowmelt runoff. Sediment simulation was poor due to insufficient calibration, lack of data, and model deficiencies. Simulated alachlor loadings and concentrations in the Iowa River were in the expected range. Simulated nitrate and ammonia concentrations were usually within the range of observed

grab sample data.

The simulation of the Iowa River Basin would be improved with additional calibration, refinement of the sediment simulation through additional calibration, and verification of both hydrology and sediment simulation. Recommended improvements in HSPF include accomodation of nutrient and chemical inputs with precipitation, simulation of both ionized and un-ionized forms of ammonia and sediment-ammonia interactions, and better definition of river bed water quality and sediment processes.

This study has demonstrated that HSPF provides a flexible and realistic means of approximating the impacts (quantity and quality) of candidate BMPs in large river basins. However, true verification of the ability to simulate the effects of BMPs must await the availability of post-BMP implementation data.

ACKNOWLEDGEMENT

This work was performed under Contract No. 68-03-2895 for the U.S. Environmental Protection Agency. Mr. Thomas Barnwell of the Environmental Research Laboratory, Athens, Georgia was Project Officer.

REFERENCES

- Donigian, A.S. Jr., J.C. Imhoff, and B.R. Bicknell (1983a). Modeling Water Quality and the Effects of Agricultural Best Management Practices in Four Mile Creek, Iowa. U.S. EPA Environmental Research Laboratory, Athens, GA.
- Donigian, A.S. Jr., J.C. Imhoff, and B.R. Bicknell (1983b). Preliminary Application of HSPF to the Iowa River Basin to Model Water Quality and the Effects of Agricultural Best Management Practices. U.S. EPA Environmental Research Laboratory, Athens, GA.
- Donigian, A.S. Jr., J.L. Baker, D.A. Haith, and M.F. Walter (1983c). HSPF Parameter Adjustments to Evaluate the Effects of Agricultural Best Management Practices. U.S. EPA Environmental Research Laboratory, Athens, GA.
- Johanson, R.C., J.C. Imhoff, H.H. Davis, J.L. Kittle, and A.S. Donigian, Jr. (1981). User's Manual for the Hydrological Simulation Program - FORTRAN (HSPF), Release 7.0. U.S. EPA Environmental Research Laboratory, Athens, GA.
- Onishi, Y., S.M. Brown, A.R. Olsen, M.A. Parkhurst, S.E. Wise, and W.H. Walters (1979). Methodology for Overland and Instream Migration and Risk Assessment of Pesticides. Battelle Pacific Northwest Laboratories, Richland, WA, U.S. EPA Environmental Research Laboratory, Athens, GA.
- Schnoor, J.L., D.C. McAvoy, C.E. Ruiz-Calzada, and M.R. Wiesner (1979). Verification of a Pesticide Transport and Bioaccumulation Model. U.S. EPA, Environmental Research Laboratory, Athens, GA.
- Schnoor, J.L., N.B. Rao, K.J. Cartwright, and R.M. Noll (1982). Fate and Transport Modeling for Toxic Substances. In: Modeling the Fate of Chemicals in the Aquatic Environment. A.W. Maki and J. Cairns, Editors, Ann Arbor Science, Ann Arbor, MI.

SURFACE WATER QUALITY IN RELATION TO SOIL TYPE, LAND USE AND DISCHARGE IN A RURAL CATCHMENT AREA

M. C. H. Witmer

*Environmental Research Group, State University of Utrecht, P.O.B. 80 007,
3508 TA Utrecht, The Netherlands*

ABSTRACT

Surface water quality and the factors that influence it were investigated in a rural area that lies between an ice-pushed ridge and river backlands. The influences of soil type, land use and household wastewater on the concentrations of nutrients were studied during base-flow as well as peak-flow periods. Samples were taken in ditches and canals, more frequently as discharge increased. Average values of the base-flow quality in ditches were calculated per soil type and land use and for all measure points in the canals. The fluctuations of water quality were plotted and analyzed in concentration-time and concentration-discharge diagrams. The relative importance for the quality of total discharge in the main canal of the loads coming from several parts of the drainage basin, was investigated with a stepwise multiple variable regression analysis. During base-flow situations sources of nutrients are the intensively cultivated sandy soils. In addition the concentration of orthophosphate is increased by household wastewater. During peak-flows, potassium and nitrate run off from all soil types with all types of land use, resulting in high concentrations in the surface water, in spite of dilution by rainwater. It is concluded that for proper management, intensity of manuring and fertilizing should decrease, especially on sandy soils. Wastewater should be drained outside the basin, to lower the concentration of orthophosphate.

KEYWORDS

Surface water; water quality; base-flow; run-off; nutrients; nonpoint source pollution.

INTRODUCTION

The properties of a drainage basin are reflected in the quantity and quality of its surface water output as a result of rainfall input. Type of soil, land use and vegetation influence surface water, either directly by surface run-off or indirectly by groundwater flow.

For a proper management of the water ecosystem, it is necessary to know what factors and processes control it.

Recently researchers have grown aware that more attention should be paid to pollution by nonpoint sources within the drainage area, for two main reasons:

1. nonpoint source pollution is difficult to fight as it is a cumulative effect of many spatially scattered activities. This obstructs the possibility of reducing the amount of pollutants at the source and makes it difficult to implement technical measures to combat it.
2. the processes involved in the diffusion of nonpoint source pollution are usually slow. When the effects on the surface water become obvious, the pollution may have been going on for a long time already, a large area may be contaminated and measures to deal with it may be costly.

BACKGROUND OF THE "LANGBROEK" PROJECT

The Langbroek drainage basin is a priority area for designation as a national landscape. This means that in the future no activities that affect the historical and natural values will be allowed. With this goal in mind, the soils, vegetation and land uses of the area were classified and mapped (Kromme Rijn Projekt, 1974). The results of these monodisciplinary investigations were combined to compose a map of "ecotopes", i.e. spatially basic units that are internally homogeneous in all ecologically important properties (Cerutti and van Oostenbruggen, 1981).

During the years in which the project took place, research was focused on the nutrient transport by flowing water, within and between ecotopes and from the land- towards the water ecosystems. Therefore samples were taken of groundwater and surface water draining different ecotopes and in upstream to downstream gradients.

In this paper, the part of the investigation that deals with surface water will be described. The results should be combined with those of the groundwater research, in order to derive a complete water and nutrient balance (Beltman and Bleuten, 1979).

DESCRIPTION OF THE AREA UNDER INVESTIGATION

The Langbroek area lies in the transition zone between an ice-pushed ridge and river backlands. Elevation above sealevel varies between fifty and two metres. A great natural variety, combined with a wealth of man-made elements that have been inherited from a long occupation history, provide for a differentiated, small-scale landscape.

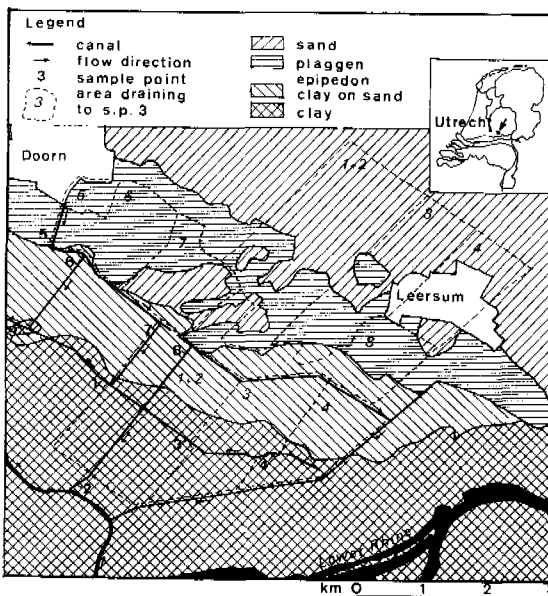
The basin, 2290 ha in dimension, consists of fluvial sands and gravels, that are partly deformed into the ice-pushed ridge and partly covered by fluvioglacial sands, aeolian sands, peat and river clay (fig. 1).

In the sandy deposits, spodosols have been formed. The aeolian sands are often covered by a plaggen epipedon. The river clays can be classified as inceptisols.

The fluvial and fluvioglacial sands are predominantly used for forestry, especially pine forest, the aeolian sands for pasture and

corn-fields, the river clays for pasture, hay and coppice.

Fig. 1. Location of the Langbroek drainage basin and sampling sites



Mean annual rainfall exceeds the evapotranspiration by approximately 300 mm/yr. The basin is drained by a man-made system of a main canal, lateral canals and ditches, that receive groundwater and surface run-off directly from the adjacent plots as well as seepage water from the ice-pushed ridge and the river Rhine. A characteristic flora and fauna have developed under these surface water conditions, particularly in the main canal (Cerutti et al., 1979). Direct sources of surface water pollution are small amounts of wastewater from scattered cottages and the intake of Rhine water during dry seasons.

METHODS

Sampling

The surface water research was carried out in the years 1979-1981. The sample programme was focused on three levels:

1. the ecotope level. Samples were taken from ditches, draining plots with one soil type and one soil use.
2. the transect level. Samples were taken from and discharges measured in canals, draining transects that consist of different soil types and land uses. In each transect one property, either soil type, land use or groundwater seepage, dominated (table 1).
3. the output level. Samples were taken from and discharge continuously measured at two exits of the drainage basin (sample points 1 + 2, fig. 1).

TABLE 1 Characteristics of the transects

| Transect, draining to sample point(s): | soil type: | Area (ha) | | | | | | | total: 2289 | |
|---|------------|-------------------------------|------------------|---------------------|------|----------------|---------------------------|---------------------------|-------------|--|
| | | soil use: | | grass | | | intensively cultivated | extensively cultivated | | |
| | | total | built-up area | orchard/ nursery | corn | forest/coppice | | | | |
| 1 + 2 | directly | clay on sand | 114 | - | - | 2 | 98 | 6 | 8 | |
| | | clay (inceptisols) | 293 | 17 | 19 | 4 | 150 | 25 | 78 | |
| | by seepage | sand (spodosols, entisols) | 151 | - | - | - | - | - | 151 | |
| | | sand (plaggen epipedon) | 118 | 10 | 15 | 34 | 35 | - | 24 | |
| | | total | 676 | 27 | 34 | 40 | 283 | 31 | 261 | |
| 3 | directly | clay on sand | 120 | - | - | - | 90 | 6 | 24 | |
| | | clay (incept.) | 143 | 8 | 6 | 3 | 46 | 6 | 74 | |
| | by seepage | sand (spod., ent.) | 246 | - | - | 13 | - | - | 233 | |
| | | sand (plaggen ep.) | 61 | 2 | - | 15 | 26 | - | 18 | |
| | | total | 570 | 10 | 6 | 31 | 162 | 12 | 349 | |
| 4 | directly | clay on sand | 103 | 1 | 5 | - | 87 | 8 | 2 | |
| | | clay (incept.) | 72 | 2 | 8 | - | 45 | 17 | - | |
| | by seepage | sand (spod., ent.) | 222 | - | - | - | - | - | 222 | |
| | | sand (plaggen ep.) | 13 | 2 | - | - | 11 | - | - | |
| | | total | 410 | 5 | 13 | - | 143 | 25 | 224 | |
| 6 | directly | clay on sand (incept.) | 3 | - | - | 2 | 1 | - | - | |
| | | sand (spod., ent.) | 6 | - | - | - | - | - | 6 | |
| | | sand (plaggen ep.) | 265 | 104 | - | 23 | 99 | 8 | 31 | |
| | | total | 274 | 104 | - | 25 | 100 | 8 | 37 | |
| | | | | | | | | | | |
| 7 | directly | clay on sand (incept.) | 22 | - | - | - | 20 | 2 | - | |
| | | sand (plaggen ep.) | 105 | - | 5 | 17 | 68 | 8 | 7 | |
| | | total | 127 | - | 5 | 17 | 88 | 10 | 7 | |
| 8 | directly | clay on sand (incept.) | 152 | 2 | 1 | 18 | 78 | 28 | 25 | |
| | | sand (plaggen ep.) | 80 | 4 | - | - | 61 | 11 | 4 | |
| | | total | 232 | 6 | 1 | 18 | 139 | 39 | 29 | |

Measurements were done in both base and peak-flow conditions. If rainfall was forecasted after a dry period, grab samples were taken of the base-flow at all measure points. During the following peak flow, the surface water output at one exit of the basin was sampled every four hours, all other measure points daily. Also, daily samples of rainwater were taken at two points within the basin. This high frequency sampling was continued until the base-flow situation had returned or the next peak-flow had arrived.

The samples were stored in polyethylene bottles in a refrigerator at 4°C. Analyses were done on the following: electroconductivity, pH and concentrations of chloride, bicarbonate, nitrate, orthophosphate, sodium and potassium.

Data evaluation

The study had a twofold aim: first to compare the spatial variety in surface water quality with differences in properties within the drainage basin; secondly to investigate the fluctuations in concentration of nutrients and the correlation between surface water discharge and quality.

Concentrations of nutrients in the base-flow samples that were taken in ditches were averaged per ecotope type. Values of the base-flow samples, taken in the canals were averaged per sample point to give a spatial view of the dissolved load contributions of different transects. Those of the base-flow samples taken in summer and winter at the exits of the basin were averaged separately.

Average values do not provide information on fluctuations in concentration, however. A direct view of the parameter behaviour gives a plot of the data as a function of time. This was done for samples, taken at all scale levels during peak-flow. These plots give an indication of possible patterns in the parameters examined and some insight into regularities in behaviour, but they do not provide information on the different factors that control the concentrations.

To visualize the influence of flow on concentration, discharge (Q) - concentration (c) diagrams were made, separately for samples taken in summer and in winter. By using this relationship for regression analysis the assumption is made that the independent variable (Q) exerts the main influence upon the dependent variable (c). However, other factors, e.g. the different contributing sources of surface water may cause considerable variation in concentration which can lead to difficulties in the interpretation of the relationship between Q and c (Davis and Keller, 1983). Therefore a stepwise multivariable regression analysis was applied to the data, with the concentration at the exit of the basin as dependent variable and discharge at the exit and netto dissolved load coming from the transects, as independent variables. As it is likely that some correlation between the independent variables exists, the results show either the main variables of a group with related behaviour, or those that have their own characteristic variation in influence. This must be taken into account when interpreting the results. If correlation coefficients are low, either the relation is nonlinear or influences other than contributing loads and discharge play a role.

The impact of several human activities on the surface water quality was examined when noticed in the field. These were e.g. manuring and the use of salt on the roads in winter.

RESULTS AND CONCLUSIONS

Average concentrations in base-flow samples, taken in ditches at the ecotope level show that nutrient contents increase with the intensity of cultivation in the case of sandy soils (fig. 2). On clay soils this relation is not apparent. An explanation may be found in either the higher adsorption capacity together with low drainage velocities in clay soils, or the greater amount of seepage water coming from the ice-pushed ridge, that dilutes the concentration.

A similar pattern is found in the samples from the canals (fig. 3). Transects in sandy soils are sources of nutrients that influence the concentrations in the main canal downstream. The high contents of orthophosphate in the main canal correlate with the high density of cottages along this stream.

Fig. 2. Average values of concentrations in base-flow samples, taken in ditches at the ecotope level

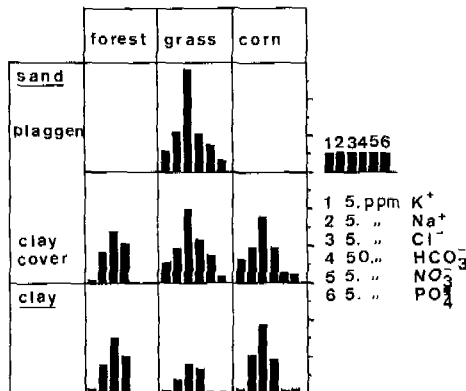
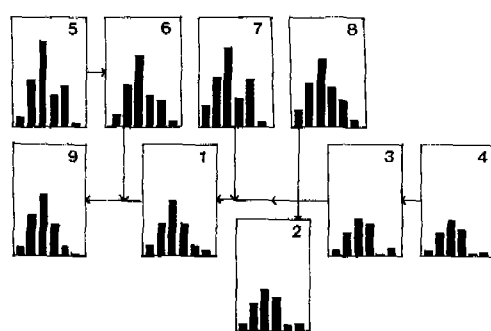


Fig. 3. Average values of concentrations in base-flow samples, taken at the sampling sites in the canals (see fig. 1)



The base-flow water quality in ditches varies considerably due to the impact of manuring. However the extremes of the values found for these water samples are not found again in the main canal because they are cancelled out by the mixing processes the water is subjected to before it reaches the main canal. Thus a fairly constant base-flow quality is found at the exit of the basin. Orthophosphate, that comes into the main canal directly by household wastewater, is an exception (table 2).

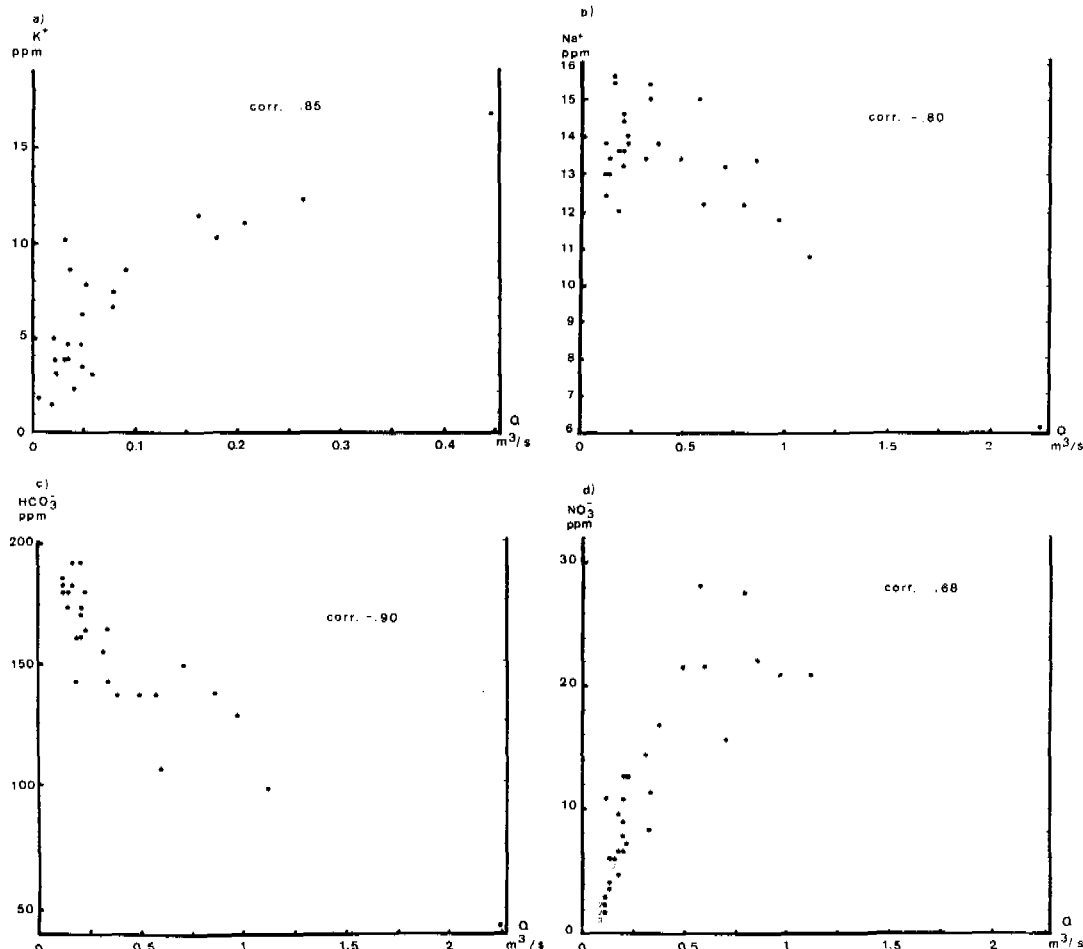
The higher concentrations in winter than in summer can be explained by two factors. Water rich in nutrients that drains from the sandy transects is withheld in summer for irrigation, and biological activity and nutrient uptake is higher during this season. These two influences exceed the effect of higher evaporation rates in summer.

The fluctuations in the concentrations of ions over time do not follow a constant pattern for all peak-flows. Also the discharge-concentration diagrams are scattered (fig. 4a-d).

TABLE 2 The quality of the base-flow at the sampling sites

| | | | Concentration (ppm): | | | | | |
|-----------------------|------------------|--|----------------------|-----------------|-----------------|-------------------------------|------------------------------|---------------------------------|
| | | | K ⁺ | Na ⁺ | Cl ⁻ | HCO ₃ ⁻ | NO ₃ ⁻ | o-PO ₄ ³⁻ |
| summer (May-Oct.) | weighted mean | | 3.5 | 13.2 | 21.7 | 186 | 1.2 | .9 |
| winter (Nov.-Apr.) | weighted mean | | 4.1 | 14.4 | 23. | 177 | 2.2 | 3.5 |
| total | weighted mean | | 3.7 | 13.6 | 22.3 | 180 | 1.7 | 1.8 |
| | min. | | 2.7 | 9.8 | 19.4 | 160 | .5 | .5 |
| | max. | | 5.4 | 16.8 | 25.7 | 191 | 6.3 | 9.2 |

Fig. 4. Discharge (Q) -concentration diagrams of samples, taken in winter at site 4 (a) and sites 1+2 (c-d)



Nevertheless they show that high concentrations of potassium and nitrate and in the contrary low concentrations of sodium and chloride correspond with high discharges. Bicarbonate is strongly negatively correlated with discharge, orthophosphate does not show any relation to discharge. Apparently the effect caused by the run-off of potassium and nitrate exceeds the effect of dilution by rainwater. This is not so for sodium and chloride. The strongly negative correlation between the concentration of bicarbonate and discharge is explained by its buffer capacity for acid rainwater.

The stepwise multivariable regression analysis shows that the variation in concentrations of potassium, bicarbonate and orthophosphate in the surface water at the exit of the drainage basin, is well accounted for by the contributing loads of the transects and discharge (table 3). The low correlation coefficients of sodium and chloride are explained by the influence of the intake of Rhine water, which was not included in the regression analysis. The explanation of the concentration of nitrate is complicated by the process of denitrification.

The concentration of potassium is mainly defined by a constant base-load and the loads coming from the transects in sandy soils.

TABLE 3 Results of the stepwise multivariable regression analysis. The dependent variable is the concentration at the sample points 1 + 2, the independent variables are the discharge at s.p. 1 + 2 (Q1 + 2) and the nett dissolved loads (NDL) coming from the transects that drain to s.p. 3, 4, 7 and 8

| ion | constant ppm | coefficients for: | | | | | correlation coefficient |
|-------------------------------|-----------------|------------------------------|------------------------------|------------------------------|------------------------------|------------------------------|----------------------------|
| | | Q1+2 litres/s | NDL3 mg/s | NDL4 mg/s | NDL7 mg/s | NDL8 mg/s | |
| K ⁺ | .001 3.36 | - - | - - | - - | .021 .33*10 ⁻² | .16 .38*10 ⁻² | .84 |
| Na ⁺ | .0 14.51 | .024 .19*10 ⁻¹ | .25 .8*10 ⁻³ | .069 .18*10 ⁻² | - - | .16 .27*10 ⁻² | .55 |
| Cl ⁻ | .0 24.19 | .068 .96*10 ⁻² | .046 .17*10 ⁻² | - - | - - | .34 .14*10 ⁻² | .32 |
| HCO ₃ ⁻ | .0 174.0 | .0 .19 | - - | .005 .16*10 ⁻² | - - | - - | .88 |
| NO ₃ ⁻ | .016 8.7 | .26 .17*10 ⁻¹ | .33 .32*10 ⁻² | - - | .37 .39*10 ⁻² | .12 .14*10 ⁻² | .69 |
| PO ₄ ³⁻ | .0 1.4 | .0 .41*10 ⁻² | .0 .11*10 ⁻¹ | .029 10 ⁻³ | - - | .005 .34*10 ⁻¹ | .99 |

.021
.33*10⁻²: coefficient = .33*10⁻², rejection significance = .021

.001

3.36 : constant = 3.36; rejection significance = .001

- : addition of this variable does not improve the correlation

Discharge does not itself contribute to the variation in potassium concentration, as it is already correlated with the loads. The bicarbonate concentration is mainly influenced by a constant base-load and discharge, orthophosphate by the loads coming from the transects that drain directly into the main canal. This, together with the negative correlation with discharge, confirms the theory that household wastewater is the main source of pollution with orthophosphate.

After the nutrient sources were located, additional fieldwork was done to test the theories about causes. Fig. 5 shows the influence of run-off after a high intensity rainstorm on the water quality in ditches. An example of the impact of manuring during the same period on surface water quality is given in table 4.

The sprinkling of salt on the roads in winter may cause a severe increase of salt content in adjacent ditches during thaws (fig. 6).

Fig. 5. The influence of run-off on the water quality in ditches

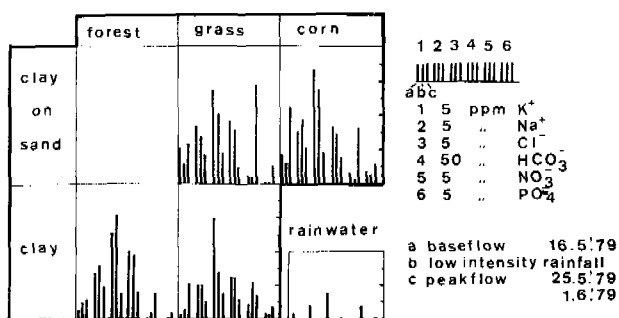


Fig. 6. The inflow of sprinkled salt from a road into a ditch during thaw in winter

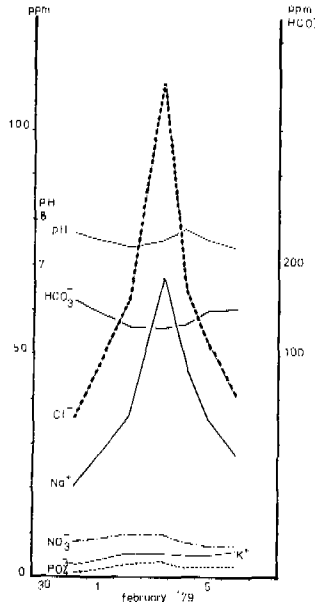


TABLE 4 The impact of run-off on the water quality in a ditch, draining a recently manured plot (intensively cultivated pasture, clay on sand)

| date | pH | K ⁺ | concentration (ppm) | | | | |
|----------|-----|----------------|---------------------|-----------------|-------------------------------|------------------------------|---------------------------------|
| | | | Na ⁺ | Cl ⁻ | HCO ₃ ⁻ | NO ₃ ⁻ | O-PO ₄ ³⁻ |
| 16-5-'79 | 7.3 | 4.02 | 14. | 22.6 | 273. | 4.1 | 4.1 |
| 25-5-'79 | 7.5 | 62. | 33. | 72. | 259. | 117. | 0.13 |

To summarize the following conclusions can be made from the results:

1. The method of investigation on the three scale levels with a sample frequency depending on discharge, provides good data material to give insight into the effects of basin properties and human activities on surface water quality, under different meteorological circumstances. Extreme situations must be taken into account, as most displacements of material occur then.
2. The concentration of nutrients in the base-flow is mainly determined by the use of manure and fertilizer on sandy soils. If eutrophication of the canals is to be arrested, the use of manure and fertilizer should be limited especially on sandy soils. In addition, household wastewater should be drained outside the basin to lower the orthophosphate content.
3. During high intensity rainstorms, run-off of nutrients from plots with sandy soils as well as clay soils into the ditches takes place. This occurs in the case of relatively natural vegetation as well as intensively cultivated land, though the amounts of run-off differ.
4. The effect of run-off of potassium and nitrate on surface water quality exceeds the dilution by rainwater. This is not so for sodium and chloride. The bicarbonate content is strongly influenced by rainwater input and negatively correlated with discharge.

REFERENCES

- Beltman, B. en Bleuten, W. (1979). Een modelstudie ter verbetering van de waterkwaliteit in Zuidoost Utrecht. H₂O(12), no. 13, 282-289.
- Cerutti, M.F.A., van Oostenbruggen, R., Ros, J.H.A. en Witmer, M.C.H. (1979). De gevolgen van inlaat van Rijnwater in een randgebied van de Utrechtse Heuvelrug. Werkgr. Landsch. Ek., Rijksuniversiteit Utrecht.
- Cerutti, M.F.A. en van Oostenbruggen, R. (1982). Hydro-ekologisch onderzoek naar het effekt van menselijke aktiviteiten op het ondiepe grondwater in het stroomgebied van de Langbroeker Wetering. Fys. Geogr. Landschapsk., Rijksuniversiteit Utrecht.
- Davis, J.S. and Keller, H.M. (1983). Dissolved loads in streams and rivers-discharge and seasonally related variations. In: Dissolved loads of rivers and surface water quantity/quality relationships, B.W. Webb (Ed.), IAHS Publication, no. 141, 79-89.
- Kromme Rijn Projekt (1974). Het Kromme Rijnlandschap, een ekologische visie. Stichting Natuur en Milieu, Amsterdam.
- Witmer, M.C.H. (1981). Van de regen in de drup. Een onderzoek naar de invloeden van oppervlakkige afspoeling, losing, bodem en bodemgebruik op de chemische kwaliteit van het oppervlaktewater in de Langbroeker Wetering ten oosten van Nederlangbroek. Werkgr. Landsch. Ek., Rijksuniversiteit Utrecht.

URBAN RUN-OFF

CHRONIC POLLUTION OF INTERCITY MOTORWAY RUNOFF WATERS

J. D. Balades,* M. Cathelain,* P. Marchandise,**
J. Peybernard ** and J. C. Pilloy*

**Laboratoires Regionaux des Ponts et Chaussées, 75732 Paris, Cedex 15,*
France

***Laboratoire Central des Ponts et Chaussées, BP 19, 44340 Bouguenais,*
France

ABSTRACT

From 1980 to 1982, two investigations of the chronic pollution of roadway runoff water were carried out in areas having different pluviometric characteristics. The runoff from two hundred pluviometric events was characterized using highly rigorous methodologies, with a view to estimating the annual pollution load.

The annual loads were determined ; they show that the official instructions hitherto followed were rather pessimistic. On the other hand, greater vigilance is required as regards the loads that may be contributed by an isolated event, but it is not possible to characterize the parameters that will give rise to such an event. A few rain events can introduce into the environment, in a short time, as much as 30% of the annual pollution load of motorway runoff waters.

KEYWORDS

Motorway; Water Pollution.

INTRODUCTION

The pollution of highway runoff waters has been a subject of study in France, as in other countries (Pope et al, 1978 - Unknown 1972), since 1975. Campaigns of measurements had shown that urban runoff water might carry pollution loads comparable to those of urban waste waters. By extension, highways have been regarded as a source of chronic, seasonal, and accidental pollution.

In the absence of objective data, the French Highway Department's provisional instruction of January 1978 (Unknown, 1978) recommended assuming from 15,000 to 20,000 kg of dust per kilometre per year, 3,250 kg of COD per kilometre per year, and 90 kg of lead per kilometre per year.

The essential objectives of the current study are to assess the mean pollution charges discharged into the environment over a relatively long period, e.g., a year, and to characterize pluviometric events likely to disturb the environment significantly. The research programme was complemented at one site by a study of winter pollution and a very thorough investigation of solid pollution, and at the other site by a study of the cumulative effects of chronic pollution on the environment.

PRESENTATION OF THE SITES AND PROGRAMMES OF INVESTIGATION

The equipment used, sampling devices, and ISCO flow meters are the same as were chosen for the study of the urban experimental basins (Hemain, 1981 - Hemain, 1983). The size of the catchment areas made it possible to use calibrated gauging sills.

A4 MOTORWAY

Description of the site.

The experimental station was set up on the A4 motorway (Paris-Strasbourg) 27 km east of Metz. Eastern Lorraine is in the northern foothills of the Vosges mountains. A definite semi-continental climate prevails.

The section chosen is straight, on an embankment, with a longitudinal slope of 2.1 %. The pavement width considered is 10.50 m. The size of the catchment area is 1,470 m². A fillet of bituminous mix along the edge directs the runoffs to two down-pipes that feed them to the measurement system. The pavement is covered with a 0/14-mm bituminous concrete laid down in 1973 that carries an average traffic of 5,500 vehicles a day. There is a galvanized safety fence along the edge of the pavement ; it drips onto the pavement when there is rain.

The waters collected on the pavement flow down through a series of three calibrated channels covering the range of flowrates from 0.09 to 53.5 l/s. The sampling device is controlled by the pneumatic flow meter. Two limnographs serve as a check on the flow meter. At the end of the flowrate measurement system, two 1.6-m³ tanks collect and clarify the liquid wastes before they are returned to the natural environment.

A recording rain gauge and a temperature recorder complete the equipment.

A4 MOTORWAY

Investigatory programme.

The station was operated from March 1980 to June 1982 by the Regional Laboratory at Nancy.

The flowrates and rainfall were continuously recorded. Twice-weekly maintenance led to only the rains that had been sampled being analyzed. The sampling device is limited to 28 bottles. The mean sample of each rain chosen for study was reconstituted and COD, SM, lead, zinc, and hydrocarbons determined by standardized methods. 112 Events were analyzed. Eight rains were studied sequentially, making it possible to plot pollutograms for them. The total sediments deposited in the tanks and measurement channels by 20 rain groups underwent analysis of particle size distribution and determinations of the lead, zinc, copper, and cadmium trapped. Finally, the results of measurements of seasonal pollution during the two winters have been reported elsewhere (Pilloy *et al.*, 1983).

A61 MOTORWAY

Description of the site.

The experimental station was set up on the A61 motorway 20 km southeast of Bordeaux. The climate is oceanic.

This catchment area, 600 m long, includes two travel lanes, from which water runs off into the concrete gutter of the central reserve. The width covered is 10.50 m. The breakdown lane drains towards the exterior of the right-of-way. The surface covering is cement concrete with transverse grooving.

From this catchment area, the waters flow into a ditch that discharges into a stream 20 km downstream from its source. Before discharge into the ditch and after tranquillization in a channel, the waste water flows through a gauging sill having a maximum allowable flowrate of 150 l/s. The measurement equipment - recording rain gauge, bubble-type flow meter, automatic sampling device controlled by the flow meter, and multi-channel recorder - is managed by a microcomputer that makes it possible to store all the data (instantaneous rain intensity, height of water, instantaneous flowrate, day, hour, and minute of the event, identification of the individual samples).

A61 MOTORWAY

Investigatory programme.

The station was operated from March 1980 to March 1982 by the Bordeaux Regional Laboratory, with twice-weekly maintenance.

From March 1980 to March 1981, 86 rains were sampled and their mean samples reconstituted, making it possible to determine the same parameters, by the same methods, as at the A4 site. The pollution fluxes were measured continuously at the inlet and outlet of the ditch and the sediments analyzed in the ditch and in the stream. From the hydrobiological viewpoint, the cumulative effects of pollution by metals were investigated using the rainbow trout and the digger carp. The impact on the natural environment of pollution by metals is dealt with in other papers.

STUDY OF CHRONIC POLLUTION. DETERMINATION OF ANNUAL LOADS

This examination of the data may be divided into two stages :

- a descriptive stage aimed at perfecting the validity of the data and studying inter-parameter relations ;
- an explanatory stage aimed at finding correlations between pollution loads and the parameters of rainfall, flowrate, and road traffic.

RESULTS OF THE INVESTIGATION.

For each parameter measured, the minimum and maximum values, the range, the mean value, the standard deviation, and the coefficient of variation were calculated.

This first step gives a good overall picture of the content of the investigation, without going into correlations among the parameters. The results of these calculations are given in tables I and II. To make the results easier to understand, the loads are given for 1 km of two-lane carriageway.

TABLE I Loads

| | | mean (g) | max.(g) | min.(g) | Standard deviation | CV (%) | Number of values |
|-----|-----|----------|---------|---------|--------------------|--------|------------------|
| A4 | COD | 4,714 | 30,764 | 21 | 6,500 | 138 | 110 |
| | SM | 6,550 | 120,714 | 13 | 17,200 | 263 | 110 |
| | Zn | 50.7 | 2,929 | 0.07 | 340 | 669 | 105 |
| | Pb | 5.93 | 114 | 0.02 | 15 | 253 | 102 |
| | HC | 68.6 | 1,300 | 0.33 | 159 | 239 | 105 |
| A61 | COD | 1,995 | 19,333 | 87 | 1,794 | 90 | 86 |
| | SM | 2,508 | 25,645 | 37 | 2,667 | 106 | 86 |
| | Zn | 17.83 | 120 | 1.72 | 13.15 | 74 | 45 |
| | Pb | 10.5 | 100 | 0.5 | 10.1 | 96 | 45 |
| | HC | 16.2 | 125 | 0.3 | 12.4 | 77 | 47 |

While of the same order of magnitude, the loads calculated for the A4 site are considerably higher than those calculated for the A61 site. The results obtained on the A4 seem to have been significantly affected, as will be explained later, by the winter samplings. The coefficients of variation, 138 to 669 % on the A4 and 74 to 106 % on the A61, agree with this finding. Only the load of lead was smaller on the A4 site than on the A61 site.

TABLE II Concentrations

| | | mean (mg/l) | max. (mg/l) | min. (mg/l) | Standard deviation | CV(%) | Number of values |
|-----|-----|----------------|----------------|----------------|-----------------------|-------|---------------------|
| A4 | COD | 208 | 2,913 | 7 | 356 | 171 | 110 |
| | SM | 182 | 1,125 | 8 | 240 | 132 | 110 |
| | Pb | 0.184 | 2.00 | 0.01 | 0.284 | 154 | 102 |
| | Zn | 0.848 | 25.50 | 0.04 | 2.942 | 347 | 105 |
| | HC | 2.175 | 10.35 | 0.1 | 1.874 | 86 | 105 |
| A61 | COD | 60 | 459 | 18 | 61 | 100 | 86 |
| | SM | 65 | 505 | 5 | 73 | 112 | 86 |
| | Zn | 0.39 | 1.60 | 0.13 | 0.33 | 85 | 45 |
| | Pb | 0.24 | 1.50 | 0.01 | 0.25 | 104 | 45 |
| | HC | 0.34 | 1.15 | 0.2 | 0.22 | 65 | 47 |

The same remarks apply to table II (concentrations) as to table I. These findings are completed by the matrices of correlation of the pollution parameters (table III).

TABLE III Correlation matrix

| | | COD | SM | Pb | Zn | HC |
|-----|-----|-------|-------|-------|---------|----|
| A4 | COD | 1 | | | | |
| | SM | 0.294 | 1 | | | |
| | Pb | 0.233 | 0.374 | 1 | | |
| | Zn | 0.046 | 0.433 | 0.418 | 1 | |
| | HC | 0.261 | 0.493 | 0.051 | - 0.114 | 1 |
| A61 | COD | 1 | | | | |
| | SM | 0.930 | 1 | | | |
| | Pb | 0.133 | 0.007 | 1 | | |
| | Zn | 0.809 | 0.863 | 0.305 | 1 | |
| | HC | 0.831 | 0.783 | 0.164 | 0.619 | 1 |

The correlations found at the A4 site are quite mediocre, while those calculated for the A61 site are of good quality, except for lead, but no satisfactory explanation can be offered for this behaviour.

To improve our knowledge of the content of the investigation and study the relations between the parameters and the behaviour of the events, we used main-component factor analysis (Lebart et al, 1973). This gives, in addition to the matrix of correlation coefficients among the parameters, representations in planes (principal planes) of all of the events and variables.

Examination of the graphs produced by the analysis makes it possible to observe resemblances between the events. Detailed analysis of these events, at first sight singular, helps both to correct possible acquisition errors and to identify particular events which can then be given closer attention.

Thirty variables were tested for the analysis into principal components ; only six were retained to characterize the events :

- duration of rain in thousandths of a day (DURATION) ;
- mean flowrate in litres per second (MFL) ;
- peak mean intensity in mm for 0.007 day (INT7) ;
- total height of rain in mm (THR) ;
- the interval of dry weather preceding the event, in thousandths of a day (DW) ;
- the total traffic during the period of dry weather, in number of vehicles (TOTT).

ANALYSIS OF THE RESULTS

One of the basic aims of the study was to find relationships making it possible to explain, and perhaps subsequently estimate, the pollution loads on the basis of the other parameters.

We assumed a priori that the correlations between the pollution loads and the other parameters were linear and multiparametric, but did not impose any restriction on the type or number of parameters chosen. The aim was therefore to find, for each parameter, the best subset of explanatory variables.

The calculations were made using the P9R program of the BMDP library (Unknown, 1983). The algorithm used in the program makes it possible to find (Furnival et al, 1974) the best subset of explanatory variables among all possible subsets. This is the subset for which the residual mean square is the smallest. In addition to the results usually delivered by multiple regression programs, the P9R program gives for each event a certain number of guides to interpretation and decision-making.

Theoretical studies (Prescott, 1975) show that the standardized residual follows a certain probability law. It is therefore possible to test, for a significance level, whether or not the standard residue exceeds a critical value given by the table (Lund, 1975). If the standard residue exceeds the critical value, the event may be regarded as an outlier and possibly removed from the sample.

The Mahalanobis distance, the distance of each event from the mean of the set, calculated in the space engendered by the explanatory variables chosen, provides information about the position of the event with respect to the set ; this indicator is used in conjunction with the foregoing in the search of outliers.

The Cook distance (Cook, 1977) "measures" the contribution of each event to the values of the regression coefficients. It is possible in this way to find out which events have contributed to the regression. If a very small number of points make a large contribution to the regression, there are grounds for wondering about the validity of the model, and also about the representativeness of the sample.

Table IV gives an example of the search for the best correlation with COD at the A61 site ; it may be noted that two events were discarded.

TABLE IV Example of search for best correlation with COD at the A61 site

| Stage | Variables chosen | Multiple Correlation coefficient | standard deviation of residues | Points eliminated aberrant residues | | |
|-----------------|------------------------|----------------------------------|--------------------------------|-------------------------------------|------------|------------------|
| 1 83 samples | THR MFL | R = 0.69 | S = 1,323 | 80 81 | 124 013 | 669 847 |
| 2 81 samples | DURATION THR MFL | R = 0.84 | S = 559 | year | day | 0.001 of the day |

The correlations found at the A4 site are given in table V.

TABLE V Correlations found for A4 site.

| Element | Coefficients of relation | Standard deviation of coefficients | Significant 5% | Estimate of total load (g) and standard deviations |
|---------|------------------------------|------------------------------------|----------------|--|
| COD | DURATION 1.468 | 0.182 | YES | 54887 S = 3808 |
| | MFL 214.725 | 41.624 | YES | |
| | DW 0.278 | 0.058 | YES | |
| | TOTT - 0.47 | 0.011 | YES | |
| | CSTE - 26.004 | 56.271 | NO | |
| SM | DURATION 0.780 | 0.236 | YES | 55978 S = 4623 |
| | INT7 283.634 | 40.834 | YES | |
| | DW 0.365 | 0.084 | YES | |
| | TOTT - 0.65 | 0.015 | YES | |
| | CSTE - 15.409 | 68.626 | NO | |
| Zn | DURATION 0.002 | $6.00 \cdot 10^{-4}$ | YES | 172 S = 9.5 |
| | THR 0.044 | 0.018 | YES | |
| | INT7 0.392 | 0.157 | YES | |
| | MFL 0.246 | 0.107 | YES | |
| | TOTT $1.971 \cdot 10^{-5}$ | $0.44 \cdot 10^{-5}$ | YES | |
| | CSTE - 0.54 | 0.158 | NO | |
| Pb | THR 0.032 | $4.33 \cdot 10^{-3}$ | YES | 60 S = 3.9 |
| | INT7 0.183 | 0.044 | YES | |
| | DW $6.535 \cdot 10^{-4}$ | $8.59 \cdot 10^{-5}$ | YES | |
| | TOTT - $1.098 \cdot 10^{-4}$ | $1.53 \cdot 10^{-5}$ | YES | |
| | CSTE - 0.031 | 0.054 | NO | |
| HC | DURATION 0.013 | $3.48 \cdot 10^{-3}$ | YES | 718 S = 43 |
| | THR 0.140 | 0.064 | YES | |
| | MFL 1.129 | 0.365 | YES | |
| | DW $5.502 \cdot 10^{-3}$ | $1.05 \cdot 10^{-3}$ | YES | |
| | TOTT - $9.243 \cdot 10^{-4}$ | $1.81 \cdot 10^{-4}$ | YES | |
| | CSTE 0.665 | 0.655 | NO | |

DISCUSSION OF THE RESULTS

To standardize and compare the results, the loads for 1 km of two-lane carriageway were calculated. These estimated annual loads are compared in table VI to the loads proposed in the conclusion of an earlier study (Cathelain *et al.*, 1981).

At the A1 site, the annual load estimates had been based on analyses of samples of 375 mm of rainfall out of the annual rainfall of 620 mm. The hydrological data for the A61 site are highly reliable and the estimate may be regarded as representative.

Because of the gaps in the series of hydrological parameters, determining the annual loads at the A4 site is, strictly speaking, difficult. We have therefore attempted to assess the representativeness of the series of 112 events dealt with

in the course of the 28 months of the investigation by comparing them to the set of all events in 1981.

TABLE VI Annual loads

| | A4 site | A61 site | Al site |
|----------|--------------------|------------|-------------|
| | Mean daily traffic | | |
| | 5,400 veh. | 7,000 veh. | 13,600 veh. |
| COD (kg) | 392 | 231 | 289 |
| SM (kg) | 399 | 199 | 764 |
| Zn (kg) | 1.23 | 1.48 | 2.3 |
| Pb (kg) | 0.43 | 0.86 | 1.2 |
| HC (kg) | 5.13 | 1.71 | / |

The pluviometric characteristics of the two series of events were compared. The total rainfall of the 112 events was 789 mm, that of 1981 801 mm. The extreme rain values (duration, THR, INT7) are of the same order, but the means for the sample of 112 rains are generally about 30 % higher than the means of the rain characteristics for 1981. The use of the sample of 112 rains to draw up an annual assessment is to be regarded as having a penalizing effect, while the discarding of discrepant points leads to lower estimates of pollution loads.

The orders of magnitude obtained in the three estimates are satisfactory. It should be noted that proportionality to traffic is found only in the case of zinc and lead. Other factors are involved : typology of the catchment area and climate.

ADDITIONAL STUDIES

A4 SITE

Study of events of which fractional samples were taken.

The analyses of the fractional samples show that 80% of COD, SM, and lead are eliminated by 52% of the initial runoff. On the other hand, it takes more than 60% of the runoff to discharge 80% of the load of zinc and more than 70% to eliminate 80% of the hydrocarbon load.

Study of individual events.

The characteristics of two individual events are given in table VII.

TABLE VII Pollution from two events

| | Duration (10^{-3} d) | TH (mm) | INT7 | DW (10^{-3} d) | % Annual load | |
|--------------------|----------------------------|------------|------|----------------------|---------------|-----|
| | | | | | COD | SM |
| Rain 65 5/12/80 | 485 | 6.8 | 0.63 | 1,375 | 5.8 | 4.1 |
| Rain 71 | 962 | 20 | 1.31 | 14,137 | 4.6 | 9.2 |

It will be noted that nothing marks these two winter events as exceptional events other than the duration of rain 71, one of which occurred following a short dry period and the other following a long dry period. Together, they account for 10.4% of the total annual COD load and 13.3% of the total annual SM load.

Examination of 7 of 112 events (6 % of the number of rains) shows that taken together, they evacuated 32.4% of the COD load and 31.4% of the SM load of the 112 events.

Analysis of matter in suspension.

In the course of 20 operations, all of the sediments deposited in the flowrate measurement system and in the two 1.6-m³ tanks were recovered. The particle size distribution of these sediments was analyzed and the metals trapped by these particles (lead, zinc, cadmium, and copper) were determined. In addition, for a few of these operations, the weight of the sediments was compared to the suspended matter as calculated from the determination on the mean sample of liquid waste. This calculated mean SM load should, strictly speaking, have been the same as the weight, after allowance for the distortions introduced by the sampling techniques. But it turns out that the calculated SM load is only a third or even a quarter of the sediment taken from the system and weighed.

One might be tempted to blame the sampling technique, even though the design of the system, the distance between the roadway and the sampling device, and the type of equipment used are such that the sample could be expected to be quite representative. It should be borne in mind that the ISCO sampling device was selected following an investigation of the performance of commercially available sampling devices (Cathelain, 1980).

The results of the 24 particle size distribution analyses are summarized in table VIII.

TABLE VIII Particle size distribution of sediments

| Dia. | < 12.5μm | 12.5μm < | < 2mm | < 2mm |
|--------------------|----------|----------|-------|-------|
| Mean | 49 | 37 | 14 | |
| Standard deviation | 17.8 | 16.8 | 12.6 | |

The determinations of such metals as lead, closely bonded to the SM, are affected by this same distortion of representativeness by a factor of 3 or even 4. The distortion is less in the case of zinc (a factor of 2), which is partially dissolved in the water sample.

The finding to be emphasized following these investigations is that the site conditions are primordial in the determination of pollution loads, and in particular of solid pollution. An assessment is possible, provided that it is systematically placed in its experimental context.

A61 SITE

Study of the drainage ditch

The effectiveness of the ditch as a retention basin for highway pollution was studied for eight months. It played this role perfectly for the whole of the dry season. More than 90 % of the rains are retained, the water infiltrates the underlying gravel-sand, and there is no outflow from the ditch.

From the autumn, when the rainfall becomes more abundant, the ditch functions normally, retaining a large share of the pollution during episodes of rain, which are not very heavy.

In winter, there is an almost permanent outflow, the concentrations in the incoming waste water are often equalled by the concentrations in the outgoing water ; but when the flowrate becomes very large, there is often a "salting out" of the pollution retained during the earlier periods.

CONCLUSIONS

The chronic annual pollution load carried by motorway runoff waters has been estimated on the basis of long-term measurements with a rigorous experimental design and execution. The two estimates obtained are of the same order of magnitude as those obtained earlier on the A1 motorway (Cathelain et al, 1981). It is clear that the characteristics and climate of the site may be more important than the mean daily traffic. The larger pollution fluxes and concentrations measured at the A4 motorway site are explained primarily by winter runoff. The supplemental tests carried out at this site give rise to a criticism of the sampling methodology used. If the best sampling device available was chosen, it can be estimated to sample only from a third to a half of the matter in suspension and associated metals, depending on the geometrical conditions of the site. No relation between traffic level and pollution can be put forth. Our proposed annual load range limits are summed up in table IX. They apply to motorway traffic ranging from 5,000 to 13,600 vehicles a day, a range of climates from semi-continent to oceanic, and a petrol containing 0.40 g of lead per litre.

They are compared to the values proposed by the provisional instruction of January 1978 (Unknown, 1978)

TABLE IX Annual loads, two-lane roadway

| | COD (kg/km) | SM (kg/km) | ZINC (kg/km) | LEAD (kg/km) |
|-------------------------|-------------|------------|--------------|--------------|
| Studies made | 230-400 | 200-1,200 | 1.5-2.5 | 0.9-1.3 |
| SETRA instruction 1978. | 3,250 | 15,000 | 35 | 90 |

The load of organic matter is small, comparable to the wastes of ten people, or 200 people if only the periods of actual runoff are taken into account.

The load of lead is the only parameter of concern calling for action.

Further studies, dealing both with the mobility and potential toxicity of the lead and with the relative importance of lead of highway origin in human accumulation, would seem to be necessary.

The manner in which these pollution loads are entrained and the form in which they reach the environment are very important. It was shown at the A4 motorway site that two rains could carry more than 10 % of the load contained in 112 events, and that 6% of events evacuated more than 30% of the COD and SM loads. At the A61 site, three rain episodes would be enough to attain 30% of the annual COD load. These data should be used to anticipate the immediate impact on the environment in the absence of treatment.

Table X gives the quantities of pollution entrained by an especially polluting singular event (10% of the annual load) compared to the values recommended in the DRCR study document (Unknown, 1980).

It was shown by the studies of sediments and of living organisms that cumulative effects of highway pollution exist, but are quite limited in the cases investigated.

From the series of results obtained at the A61 site, it will be possible to attempt to model the phenomena of deposition and entrainment of pollution, since the pluviometric data are complete and reliable.

TABLE X Maximum load from a single polluting event.

| | COD (kg/km) | SM (kg/km) | Pb (kg/km) | Zn (kg/km) |
|-------------------------------|----------------|---------------|---------------|---------------|
| Studies made | 40 | 120 | 0.25 | 0.13 |
| Proposed value, DRCR, 1980 | 60 | 540 | 1.0 | 0.4 |

REFERENCES

- Cathelain, M., J.P. Demiautte (1980). Etude bibliographique des préleveurs pour la mesure de la qualité des eaux de ruissellement. St-Quentin, LR, PV 80-692, 70p.
- Cathelain, M., G. Friant, J.L. Olié (1981). Les eaux de ruissellement de chaussées autoroutières : évaluation des charges de pollution. Paris, Bulletin de Liaison des Laboratoires des Ponts et Chaussées, 116, 9-24.
- Cook R.D. (1977) Detection of influential observation in linear regression. Technometrics, 19, 1, 15-18.
- Furnival G.M., R.W. Wilson (1974) Regressions by leaps and bounds. Technometrics, 16, 4, 499-511.
- Hemain J.C. (1981). Méthodologie de caractérisation du phénomène de pollution du ruissellement pluvial urbain. Montpellier, Laboratoire d'Hydrologie Mathématique, 70p.
- Hemain J.C. (1983). Mesure de la pollution du ruissellement pluvial urbain. Rapport n°1 suivi et bilan de la campagne expérimentale. Montpellier, Laboratoire d'Hydrologie Mathématique, 54p.
- Lebart L., J.P. Fenelon (1973). Statistique et informatique appliquées. Paris, Dunod, 457p.
- Lund R.E. (1975). Tables for an approximate test for outliers in linear models. Technometrics, 17, 14, 473-476.
- Pilloy J.C., S. Tchittarath (1983). Pollution des eaux de ruissellement par les fondants chimiques. Paris, Bulletin de Liaison des Laboratoires des Ponts et Chaussées, 124, 49-63.
- Pope W., R.J. Young, R. Perry (1978). Correlations of hydrological conditions with water quality in motorway runoff. Rapport du Symposium sur le drainage des routes Berne, Paris, OCDE, 384-400.
- Prescott P. (1975). An approximate test for outliers in linear models. Technometrics, 17, 1, 129-132.
- Unknown (1972). Water pollution aspects of street surface contaminants. Rapport. EPA R2. 72-081, 237 p.
- Unknown (1978). Etudes d'impact des projets routiers en milieu urbain. Directive provisoire. Bagneux, DRCR.
- Unknown (1983). Biomedical data serie P statistical software. University of California press, 733 p.
- Unknown (1980). Protection des eaux contre la pollution d'origine routière. Données générales. Document d'étude. Bagneux, SETRA, 82 p.

COLLECTION AND ANALYSIS OF URBAN RUNOFF DATA IN FINLAND

M. J. Melanen

*Technical Research Office, National Board of Waters, P.O. Box 250,
SF-00101 Helsinki 10, Finland*

ABSTRACT

An extensive three-year urban hydrology programme was carried out in Finland. Data were collected and analysed on the quantity and quality of precipitation and runoff water at seven urban test catchments. During rainfall events, on the average, the proportion of surfaces generating direct runoff was found to account for 50-80 per cent of the proportion of paved surfaces in the residential catchments, and for 80-90 per cent in the city centres. Under Finnish conditions, the pollutant loads discharged to recipients with untreated runoff waters are relatively minor in comparison to those of purified waste waters, regarding organic matter and nutrients. Further measures in the Finnish sewage works should thus be focused on other factors, such as increasing the effectiveness of the existing waste water treatment plants, and decreasing the amount of leakage inflows to sewer networks.

KEYWORDS

Urban hydrology; sewerage systems; precipitation; urban runoff; aerial particle deposition.

INTRODUCTION

A sparse population (4.8 million inhabitants) and an abundance of watercourses are typical features of Finland. (The capital - Helsinki - has a population of slightly less than half a million.) In the beginning of the 1980s the proportion of total population, served by public sewage works, was about 70 per cent. Three quarters of the waste waters are purified by biological-chemical processes. A separate sewer system is the dominant one. After the mid 1970s, the uncertainty of the actual role of urban runoff waters, as far as the Finnish water pollution problems were concerned, placed emphasis on the need to solve this question by data collected from Finland. For this purpose, an extensive three-year field research programme

- The Finnish Urban Storm Water Project - was started in 1977.

METHODOLOGY AND DATA

Experimental Catchments

The field experiments of the Project were carried out in 1977-1979 at seven different types of urban catchments in four cities (Table 1). All of the catchments had separate sewer systems with closed conduits, roughly 10-15 years old.

TABLE 1 Characteristics of the Experimental Catchments of the Finnish Urban Storm Water Project (Melanen, 1982)

| Catchment | | Area ha | Ratio of Imperviousness % | Slope % | Land Use |
|----------------|----------|------------|---------------------------------|------------|---|
| Name | City | | | | |
| Hämeenpuisto | Tampere | 13.2 | 67 | 2.2 | City centre - Commercial |
| Nekala | Tampere | 14.2 | 60 | 1.3 | Industrial (small and medium-size industry) |
| Herttoniemi | Helsinki | 14.7 | 35 | 1.3 | Traffic (motor way, underground railway) |
| Kajaani Centre | Kajaani | 18.5 | 64 | 1.6 | City centre - Commercial |
| Pakila | Helsinki | 20.2 | 29 | 3.0 | Suburban residential (low-rise houses) |
| Kontula | Helsinki | 22.9 | 40 | 1.8 | Suburban residential (high-rise houses) |
| Kaukovainio | Oulu | 40.5 | 30 | 1.0 | Suburban residential (high-rise houses) |

Quantity of Precipitation and Runoff, and Other Hydrological Data

During the vegetation period, rainfall was continually recorded by a pluviograph of the Hellmann type in each test site (Melanen and Laukkanen, 1981). The measured rainfall was estimated to be, on the average, 10 per cent less than the rainfall reaching the ground. A modification of the Palmer-Bowlus Venturi flume for pipes was used for continual runoff quantity recording (Melanen and Laukkanen, 1981). On the basis of field calibrations performed by small current meters, the accuracy of the flow measurement was estimated to be \pm 5 to \pm 15 per cent, on the average, and \pm 5 to \pm 10 per cent for the peak flows. The data of the daily and monthly air temperature, and the data of the monthly wind speed used in the analysis, were taken from the closest climatological stations (2 to 10 kilometres).

Emissions and Aerial Particle Deposition

An emission inventory (particulates, hydrocarbons, nitrogen oxides, oxides of sulphur, vanadium, cadmium, lead) was performed at the catchments, and in their immediate surroundings, called local backgrounds (Melanen and Tähtelä, 1981). At each test site, aerial particle deposition was sampled on a monthly basis by two deposition gauges of the NILU type, applying the Finnish standard of the measurement of particulate fallout (Melanen and Tähtelä, 1981). On a monthly basis, the accuracy of the measured deposition was estimated

to be on the order of ± 50 per cent, and to be sufficient to give the magnitude of the various component depositions and to distinguish the different levels.

Sampling of Runoff Water

Runoff was sampled in each test catchment at the runoff-measurement station by an automatic sampling device of the SAM 120 type (Melanen, 1981). The analysed samples were flow-proportional composite ones (one sample representing each rainfall-runoff event studied). The accuracy of the runoff-quality data was estimated to be on the order of ± 20 to ± 40 per cent.

Statistical Methods

In the statistical analysis, special attention was directed to the application of both parametric and non-parametric methods (Table 2).

TABLE 2 Statistical Procedures Used (Melanen, 1982)

| Method | Task |
|---|--|
| Kolmogorov-Smirnov test | Testing of distributions |
| Student's t test* | Testing of correlations and means (2 populations) |
| Welch's approximation* | Testing of means (2 populations) |
| Variance ratio test* | Testing of variances (2 populations) |
| Bartlett's test* | Testing of variances (> 2 populations) |
| One-way analysis of variance* | Testing of means (> 2 populations) |
| Kruskal-Wallis test*,** | Testing of population means and locations (> 2 populations) |
| Spearman's rank correlation coefficient** | Testing of association of populations (2 populations) |
| Wilcoxon's rank-sum test** | Testing of population locations (2 populations) |
| Stepwise multiple regression | Regression analysis |

* A test for normally distributed variables; ** A test for non-normally distributed variables

RESULTS AND DISCUSSION

Quantity of Runoff Water

The number of rainfall-runoff events studied ranged from 70 to 160 per catchment (Melanen and Laukkanen, 1981). During rainfall events, on the average, the proportion of surfaces generating direct runoff was found to account for 50-80 per cent of the proportion of paved surfaces in the residential catchments, and for 80-90 per cent in the city centres and industrial catchments. These results match with the findings of other investigations performed in similar hydro-meteorological and urban conditions (e.g. Arnell and Lyngfelt, 1975). A wide variance was characteristic of the runoff coefficients, both between and within different catchments (the standard deviations on the order of 50-75 per cent of the arithmetic means). Roughly one half of the variance of the runoff coefficients in individual catchments could be explained by variables characterizing the rainfall

events, and seasonal and antecedent conditions.

Aerial Particle Deposition

The average rates of deposition of the components studied are given in Table 3. The number of the monthly observations ranged from 13 to 29 per parameter and catchment. (The Nekala catchment is excluded because of unrepresentative observations.) Compared to the rates of deposition observed in non-urban regional background points (Järvinen and Haapala, 1980), the rates in the urban catchments are, for example, roughly 100 per cent higher in the case of total organic carbon, 50-100 per cent higher for total phosphorus, 50-200 per cent higher for sulphate, but of the same order of magnitude in the case of total nitrogen. By comparison to the measurements in Finnish cities a decade ago (e.g. Laamanen, 1969), some growth could be observed in the rate of deposition of sulphate in the 1970s, while the pH of precipitation had decreased.

TABLE 3 Average Rates of Aerial Deposition at the Experimental Catchments (Melanen and Tähtelä, 1981)*

| Parameter | Rate of Deposition (mg/m ² in 30 days) in Catchment | | | | | |
|---|--|--------------|----------------|--------|---------|--------------|
| | Hämeen-puisto | Hertto-niemi | Kajaani Centre | Pakila | Kontula | Kauko-vainio |
| Total deposition, D _{tot} | 2800 | 2900 | 2900 | 2100 | 2300 | 1200 |
| Volatile deposition, D _{vol} | 1200 | 1400 | 880 | 930 | 800 | 690 |
| Total organic carbon, D _{TOC} (C) | 150 | 270 | 140 | 210 | 200 | 96 |
| Total phosphorus, D _{totP} (P) | 2.6 | 2.3 | 2.6 | 3.0 | 2.4 | 2.1 |
| Total nitrogen, D _{totN} (N) | 63 | 56 | 38 | 62 | 69 | 47 |
| Chloride, D _{Cl} (Cl) | 35 | 45 | 18 | 45 | 43 | 12 |
| Sulphate, D _{SO4} (SO ₄) | 460 | 590 | 520 | 360 | 480 | 220 |
| Vanadium, D _V (V) | 0.96 | 0.43 | 0.51 | 0.21 | 0.27 | 0.19 |
| Zinc, D _{Zn} (Zn) | 2.3 | 4.2 | 1.9 | 1.1 | 1.7 | 1.1 |
| Copper, D _{Cu} (Cu) | 0.57 | 0.45 | 1.2 | 0.39 | 0.39 | 0.85 |
| Lead, D _{Pb} (Pb) | 4.5 | 2.1 | 1.9 | 1.0 | 1.4 | 0.79 |
| pH value, D _{pH} ** | 4.1 | 4.0 | 4.6 | 4.3 | 4.1 | 4.4 |
| Conductivity, D _{Y25} ** | 6.1 | 6.7 | 6.4 | 3.9 | 4.5 | 3.8 |

* Medians observed over the 1977-1979 period; ** pH and conductivity (mS/m) of precipitation

A wide variance was typical of the deposition too, both between and within different test catchments (standard deviations of the order of 50-100 per cent of the arithmetic means). Of the order of one third to one half of the total variance of the deposition rates of total nitrogen, chloride, sulphate, vanadium, copper and lead plus the variance of the conductivity of precipitation could be explained by the following: hydrometeorological factors, catchment category (suburban residential vs. other type of catchments), local emission levels and regional background deposition levels.

Quality of Runoff Water and Proportion of the Aerial Load

In the investigation, a total of 30 physical, chemical and biological parameters of the runoff water were measured. The number of observations (from flow-proportional composite samples) ranged from

5 to 60 per parameter and catchment. Table 4 gives statistics of some parameters of general interest for the six catchments (Nekala excluded) in regression analysis performed. The observed quality is in accordance with results reported from other countries with similar circumstances (e.g. Lindholm and Balmér, 1978; Malmqvist and Svensson, 1975).

TABLE 4 Properties of the Distributions of Storm Water Quality Parameters. Combined Observations from the Six Catchments in Regression Analysis (See Table 11) (Melanen, 1981)

| Parameter | Statistics* (in mg/l, except for n, pH and γ_{25}) | | | | |
|--|--|--------|-------------|-------|------|
| | n | min | \bar{x} | s | max |
| Total solids, TS | 115 | 57 | 330 | 290 | 1500 |
| Volatile solids, VS | 104 | 13 | 84 | 60 | 400 |
| Suspended solids, SS | 209 | 12 | 250 | 270 | 1500 |
| Total organic carbon, TOC | 27 | 4 | 18 | 28 | 150 |
| Biochemical oxygen demand, $BOD_7 (O_2)$ | 92 | <2 | 19 | 20 | 130 |
| Chemical oxygen demand, $COD_{Cr} (O_2)$ | 199 | 15 | 150 | 110 | 620 |
| Total phosphorus, tot P | 223 | 0.019 | 0.35 | 0.30 | 2.3 |
| Total nitrogen, tot N | 182 | 0.35 | 1.9 | 1.3 | 10 |
| Chloride, Cl | 112 | 0.40 | 4.8 | 5.2 | 30 |
| Sulphate, SO_4 | 117 | 2.4 | 12 | 7.0 | 37 |
| Vanadium, V | 115 | <0.005 | 0.019 | 0.020 | 0.15 |
| Zinc, Zn | 92 | 0.039 | 0.36 | 0.22 | 1.7 |
| Copper, Cu | 91 | 0.010 | 0.079 | 0.097 | 0.68 |
| Lead, Pb | 225 | 0.013 | 0.22 | 0.22 | 1.5 |
| pH value, pH | 184 | 5.9 | 6.8(median) | | 8.1 |
| Conductivity, γ_{25}^{**} | 142 | 2.1 | 9.1 | 6.6 | 50 |

* n = number of observations, min = minimum observed, \bar{x} = arithmetic mean, s = standard deviation, max = maximum observed; ** In mS/m

According to the results, the quality of the runoff water cannot be generalized with regard to any of the parameters studied, but it depends on local conditions (Table 5). Respectively, the rates of the aerial particle deposition cannot as a rule be generalized either, but they are affected by local activities, and weather and climatic conditions (Table 6). (For the deposition of total phosphorus and the pH value of precipitation, however, the hypothesis on equal averages could not be rejected between the six studied test sites.) A statistically significant difference exists in the quality of urban runoff water between the suburban residential catchments and the other type of catchments (city centre-commercial, traffic) (Table 7). Respectively, between these two categories, the difference in the rates of aerial deposition is statistically significant in the case of parameters essentially reflecting the overall level of atmospheric deposition, the corrosion phenomena and industrial activity, and the traffic volume and intensity (Tables 8 and 9).

The variance of the quality parameters was found to be wide (standard deviations of the order of 50-100 per cent of the arithmetic means). The following fraction of the total variance could be explained by variables characterizing the catchment category, emission and deposition rates, and hydrometeorological factors (Table 10) in the case of storm water quality parameters studied: over half for total organic carbon, vanadium and lead; roughly one half for total and volatile solids and chloride; one third to one half for suspended solids, bio-

TABLE 5 Test of the Hypothesis on Identical Locations of the Populations of Storm Water Quality Parameters in the Six Catchments Studied. Kruskal-Wallis Test at 95 % Significance Level. Values of Test Statistic Corrected for Ties (TOC not Studied, Kontula Catchment Excluded in the Test of Zn and Cu) (Melanen, 1981)

| | Quality Parameter* | | | | | | | | | | | | | | |
|---|--------------------|------|------|------------------|-------------------|------|------|------|-----------------|------|------|------|-------|-------|-----------------|
| | TS | VS | SS | BOD ₇ | COD _{Cr} | totP | totN | Cl | SO ₄ | V | Zn | Cu | Pb | pH | γ ₂₅ |
| Kruskal-Wallis Test Statistic** | 51.9 | 27.9 | 41.1 | 37.3 | 54.9 | 39.1 | 26.0 | 93.3 | 49.7 | 57.1 | 37.3 | 72.8 | 137.5 | 100.6 | 90.4 |
| Degrees of Freedom (df) | 5 | 5 | 5 | 5 | 5 | 5 | 5 | 5 | 5 | 5 | 4 | 4 | 5 | 5 | 5 |
| Hypothesis on Identical Locations is Rejected | Yes | Yes | Yes | Yes | Yes | Yes | Yes | Yes | Yes | Yes | Yes | Yes | Yes | Yes | Yes |

* For notations see Table 4; ** Critical values of the chi-square distribution: $\chi^2_{0.95}$ (df=5) = 11.1, $\chi^2_{0.95}$ (df=4) = 9.5

TABLE 6 Test of the Hypothesis on Identical Locations of the Populations of Deposition Parameters in the Six Catchments Studied. Kruskal-Wallis Test at 95 % Significance Level. Values of Test Statistic Corrected for Ties (Melanen, 1981)

| | Deposition Parameter* | | | | | | | | | | | |
|---|-----------------------|------------------|------------------|-------------------|-------------------|-----------------|----------------|-----------------|-----------------|-----------------|-----------------|-----------------------------|
| | D _{tot} | D _{vol} | D _{TOC} | D _{totP} | D _{totN} | D _{Cl} | D _V | D _{Zn} | D _{Cu} | D _{Pb} | D _{pH} | D _{γ₂₅} |
| Kruskal-Wallis Test Statistic** | 29.8 | 13.6 | 19.9 | 6.9 | 31.6 | 70.9 | 46.3 | 37.7 | 34.5 | 74.9 | 10.2 | 28.6 |
| Degrees of Freedom (df) | 5 | 5 | 5 | 5 | 5 | 5 | 5 | 5 | 5 | 5 | 5 | 5 |
| Hypothesis on Identical Locations is Rejected | Yes | Yes | Yes | No | Yes | Yes | Yes | Yes | Yes | Yes | No | Yes |

* For notations see Table 3; ** Critical value in Table 5

TABLE 7 Test of the Hypothesis on Identical Locations of the Populations of Storm Water Quality Parameters in the Categories of Suburban Residential Catchments (Pakila, Kontula, Kaukovainio) and Other Type of Catchments (Hämeenpuisto, Herttoniemi, Kajaani Centre). Two-sided Testing by the Wilcoxon's Rank-Sum Test (Melanen, 1981)*

| | Quality Parameter** | | | | | | | | | | | | | | |
|---|---------------------|----------------|----------------|------------------|-------------------|-------------|----------------|--------------|-----------------|------------|----------------|----------------|--------------|----------------|-----------------|
| | TS | VS | SS | BOD ₇ | COD _{Cr} | totP | totN | Cl | SO ₄ | V | Zn | Cu | Pb | pH | γ ₂₅ |
| Wilcoxon's Rank-Sum | 6870 | 4823 | 19704 | 4789 | 18189 | 20686 | 13588 | 6453 | 6113 | 6869 | 2801 | 2096 | 24661 | 12244 | 5935 |
| Test Statistic | (6928) | (4881) | (19887) | (4903) | (18432) | (20988) | (13997) | (6482) | (6253) | (6993) | (2869) | (2158) | (24871) | (13411) | (6032) |
| Significance Level (%) at which Hypothesis on Identical Locations is Rejected | 99.9 (99.9) | 99.9 (99.9) | 99.9 (99.9) | 99.9 (99.9) | 99.9 (99.9) | <95 (99) | 99.9 (99.9) | 99 (99.9) | 99.9 (99.9) | 99 (95) | 99.9 (99.9) | 99.9 (99.9) | <95 (<95) | 99.9 (99.9) | |

* Figures without brackets refer to test statistic with ties handled so that the value of the statistic is as small as possible, figures in brackets refer to test statistic with ties handled so that the value of the statistic is as large as possible, (TOC excluded); ** For notations see Table 4

TABLE 8 Test of the Hypothesis on Identical Locations of the Populations of Deposition Parameters in the Categories of Suburban Residential Catchments and Other Type of Catchments. Two-sided Testing by the Wilcoxon's Rank-Sum Test. Legend as in Table 7 (Melanen, 1981)

| | Deposition Parameter* | | | | | | | | | | |
|---|-----------------------|------------------|------------------|-------------------|-------------------|-----------------|-----------------|-----------------|-----------------|-----------------|------------------|
| | D _{tot} | D _{vol} | D _{TOC} | D _{totP} | D _{totN} | D _{Cl} | D _{Zn} | D _{Cu} | D _{Pb} | D _{pH} | D _{γ25} |
| Wilcoxon's Rank-Sum | 5221 | 3601 | 3339 | 4119 | 4773 | 3837 | 1386 | 1675 | 2658 | 4654 | 3431 |
| Test Statistic | (5225) | (3616) | (3349) | (4209) | (4816) | (3894) | (1392) | (1695) | (2670) | (4906) | (3470) |
| Significance Level (%) at which Hypothesis on Identical Locations is Rejected | 99.9 (99.9) | 95 (95) | <95 (<95) | <95 (<95) | <95 (<95) | <95 (<95) | 99.9 (99.9) | 95 (95) | 99.9 (99.9) | <95 (<95) | 99.9 (99.9) |

* For notations see Table 3

chemical and chemical oxygen demand, total phosphorus, total nitrogen, sulphate, zinc, copper and conductivity (Table 11).

TABLE 9 Test of the Hypothesis on Equal Means of the Normally Distributed Deposition Parameters in the Categories of Suburban Residential Catchments and Other Type of Catchments. Two-Sided Testing at 95 % Significance Level by t Test and Welch's Approximation Method (Melanen, 1981)*

| Parameter** | Values of Statistics*** | | | | | | Test Used | \bar{x}_1 and \bar{x}_2 Differ from Each Other | |
|-----------------------------|-------------------------|-------------|-------|-------|-------|-------|-----------|--|------------|
| | \bar{x}_1 | \bar{x}_2 | s_1 | s_2 | n_1 | n_2 | t | v | |
| D _{SO₄} | 550 | 370 | 250 | 210 | 65 | 65 | 4.36 | 128 | t Test Yes |
| D _V | 0.75 | 0.28 | 0.53 | 0.21 | 65 | 62 | 6.63 | 85 | Welch Yes |

* Percentiles of the Student's distribution: $t_{0.975}(80) = 1.99$, $t_{0.975}(120) = 1.98$; ** For notations see Table 3; *** \bar{x} = arithmetic mean, s = standard deviation, n = number of observations, t = test statistic, v = degrees of freedom of t distribution

TABLE 10 Properties of the Distributions of Hydrometeorological Variables Analysed in Connection with Storm Water Sampling. Combined Observations in the Regression Analysis (See Table 11). Number of Observations = 228 (Melanen, 1981)

| Variable | Unit | Statistics* | | | |
|--|------|-------------|-----------|-----|------|
| | | min | \bar{x} | s | max |
| Runoff volume, Q | mm | 0.1 | 1.3 | 1.4 | 9.4 |
| Rainfall volume, R | mm | 0.9 | 5.2 | 3.5 | 23 |
| Rainfall duration, t _R | min | 15 | 160 | 130 | 920 |
| Maximum rainfall intensity, i _{max} ** | mm/h | 1.2 | 11 | 9.2 | 54 |
| Preceding dry period, t _d | h | 1 | 47 | 80 | 760 |
| Volume of preceding rainfall event, R _p | mm | 0.3 | 3.7 | 3.9 | 27 |
| Maximum intensity of preceding rainfall event, i _{max,p} ** | mm/h | 0.6 | 7.0 | 7.6 | 56 |
| Mean daily temperature, T _m | °C | 1.1 | 12.2 | 4.0 | 19.0 |

* Notations as in Table 4; ** Over a 5-minute period

As for the sources of urban runoff water pollution, the aerial deposition was found to contribute a substantial basic pollutant load. The order of magnitude of this contribution is as follows for the various parameters: sulphate 1/2-3/4, total nitrogen 1/2-2/3, vanadium 1/4-1/2, volatile solids & TOC 1/4-1/3, copper 1/4-1/3, total phosphorus 1/4, lead 1/5-1/4, total solids 1/5, zinc 1/10-1/5, chloride 1/20-1/5 (Melanen, 1981 and 1982).

Washout of Pollutants with Urban Runoff Water

When a biological-chemical treatment (simultaneous-precipitation process) is applied to the waste water, the proportions of the total recipient loads of a separate sewer system, as caused by urban runoff water, are the ones shown in Table 12. Under Finnish conditions, a separate system yields a smaller pollutant load regarding organic matter, phosphorus and nitrogen. The annual recipient load contributed by a combined system is on the order of 10-20 per cent higher for BOD₇, 15-30 per cent higher for phosphorus, and 10-20 per cent higher for nitrogen in the case that overflows, and bypasses

TABLE 11 Regression Models of the Storm Water Quality Parameters (Notations: E_{HxCy} = rate of emission of hydrocarbons, E_{NO_x} = rate of emission of nitrogen oxides, others as in Tables 3, 4 and 10) (Melanen, 1981)*

| Explanatory Variables | Model of Parameter | | | | | | | | | | | | | |
|--------------------------------|--------------------|---------------------|--------|---------------------|---------------------|---------------------|--------------------|---------------------|---------------------|---------------------|---------------------|-------|---------------------|--------|
| | TS | VS | SS | TOC | BOD ₇ | COD _{Cr} | totP | totN | Cl | SO ₄ | V | Zn | Cu | Pb |
| R | | | | (-)X ^{0.5} | | | | | (-)X ^{0.5} | (-)lnX | | (-)X | (-)X | (-)lnX |
| t _R | | (-)lnX | (-)lnX | (-)lnX | | (-)lnX | (-)lnX | (-)X ^{0.5} | | | (-)lnX | | | |
| i _{max} | | | | (+)X ^{0.5} | | | | (+)lnX | | | | | (+)lnX | |
| t _d | (+)X | (+)X | (+)X | (+)X | (+)X ^{0.5} | (+)X | (+)X | (+)X | (+)X ^{0.5} | (+)X ^{0.5} | (+)X ^{0.5} | (+)X | (+)X | |
| R _p | | (-)X ^{0.5} | | | | (-)X ^{0.5} | | | | | (-)lnX | | (-)X ^{0.5} | |
| i _{max,p} | | | (-)lnX | | | | (-)lnX | | | | | | | |
| T _m | | | | | | | | | | | | | (-)X | |
| D _{tot} | (+)X | | | | | | | | | | | | | |
| D _V | | | | | | | | | | (+)X | | | | |
| D _{Pb} | | | | | | | | | | | | | (+)X | |
| E _{HxCy} | | (+)X _c | | (+)X _c | | (+)X _c | | | | | | | | |
| E _{NO_x} | | | | | | | (+)X _{lb} | | | | | | | |
| d ₁ ** | | | (+)X | | (+)X | | (+)X | | (+)X | (+)X | | (+)X | (+)X | |
| Number of Events | 115 | 104 | 209 | 27 | 92 | 199 | 223 | 182 | 112 | 117 | 115 | 92 | 91 | 225 |
| Fraction of Variance Explained | 0.504 | 0.532 | 0.409 | 0.710 | 0.424 | 0.391 | 0.398 | 0.272 | 0.474 | 0.315 | 0.416 | 0.328 | 0.351 | 0.610 |
| Significance Level (%) | 99.9 | 95 | 99 | 99 | 99 | 99.9 | 99 | 99 | 95 | 95 | 95 | 99.9 | 95 | 99 |

* X shows that a variable is included in the model in the original form, $X^{0.5}$ shows a square-root transformation and lnX a logarithmic transformation of an explanatory variable. (+) indicates increasing and (-) decreasing effect of a variable in the model. Significance level shows the level at which each or the weakest of regression coefficients of the explanatory variables in the model is significant in two-sided testing by t test. Footnote c refers to emission in catchment and lb to emission in local background; ** Catchment category (dichotomous variable)

occur rather often, and the sewage is purified by a biological-chemical process in the combined system, too (Melanen, 1982). The difference is reverse as to suspended solids and lead: the loads caused by a combined system are smaller than those of a separate system under Finnish conditions.

TABLE 12 Estimates for the Annual Washout of Pollutants with Untreated Urban Runoff Waters in the Finnish Separate Sewer Systems and the Proportion of the Total Recipient Loads Caused by Them (Melanen, 1981, 1982)

| Parameter | Range of Washout t/km ² .a | Approximate Proportion of Total Load as Caused by Runoff Water* |
|---|--|---|
| | | % |
| Suspended solids | 10 - 100 | 50 - 75 |
| Biochemical oxygen demand (BOD ₇) (O ₂) | 1.0 - 10 | 10 - 20 |
| Total phosphorus (P) | 0.020 - 0.20 | 5 - 10 |
| Total nitrogen (N) | 0.20 - 1.0 | < 5 |
| Lead (Pb) | 0.010 - 0.15 | > 90 |
| Zinc (Zn) | 0.020 - 0.15 | (no estimate) |
| Copper (Cu) | 0.0030 - 0.050 | " |
| Cadmium (Cd) | 0.00010 - 0.00050 | " |

* Waste water is supposed to be purified by a biological-chemical process

CONCLUDING REMARKS

Analysis with the gathered data of the quantity and quality of urban runoff waters proved that, under Finnish conditions, their loads of organic matter and nutrients are relatively minor in comparison to those of purified waste waters. Further measures in the Finnish sewage works should thus be focused on other factors, such as increasing the effectiveness of the existing waste water treatment plants, and decreasing the amount of leakage inflows to the sewer networks. Local management of storm water - in practice storm water infiltration - has, however, raised interest among municipal planning and construction agencies. Beyond this item, future research is needed regarding the effects of storm and snow-melt waters on the sewage treatment processes, and regarding the significance of the micro-pollutants of urban runoff water.

ACKNOWLEDGEMENT

The Finnish Urban Storm Water Project was financed by the Maj and Tor Nessling Foundation and the National Board of Waters, Finland.

REFERENCES

- Arnell, V. and Lyngfelt, S. (1975). Nederbörls-avrinningsmätningar i Bergsjön, Göteborg 1973-1974 (Rainfall-runoff measurements in Bergsjön, Gothenburg 1973-1974, in Swedish). Report of the Geo-hydrological Research Group No. 13. Chalmers University of Technology, Gothenburg.

- Järvinen, O. and Haapala, K. (1980). Sadeveden laatu Suomessa 1971-1977 (Summary: The quality of wet and dry deposition in Finland according to observations made from 1971 to 1977). Report No. 198. National Board of Waters, Finland, Helsinki.
- Laamanen, A. (1969). Particulates in the outdoor air of Finland. Work - Environment - Health, 6 (5-6), 23-30.
- Lindholm, O. and Balmér, P. (1978). Pollution in storm runoff and combined sewer overflows. In: Urban Storm Drainage, P.R. Hellierwell (Ed.). Pentech Press, London. pp. 575-585.
- Malmqvist, P-A. and Svensson, G. (1975). Dagvattnets sammansättning i Göteborg (Summary: Urban storm water quality - Interim report from a study in Gothenburg). Report of the Geohydrological Research Group No. 14. Chalmers University of Technology, Gothenburg.
- Melanen, M. (1981). Quality of runoff water in urban areas. Publications of the Water Research Institute, 42, 123-190.
- Melanen, M. (1982). Quantity, composition and aerial load of urban runoff water in Finland. Acta Polytechnica Scandinavica Ci No. 80. Helsinki.
- Melanen, M. and Laukkanen, R. (1981). Quantity of storm runoff water in urban areas. Publications of the Water Research Institute, 42, 3-39.
- Melanen, M. and Tähtelä, H. (1981). Particle deposition in urban areas. Publications of the Water Research Institute, 42, 40-122.

STANDARDS

MARINE QUALITY STANDARDS: THEIR DERIVATION AND APPLICATION IN THE UNITED KINGDOM

G. Mance and A. R. O'Donnell

*Water Research Centre, Stevenage Laboratory, Elder Way, Stevenage,
Hertfordshire, U.K.*

ABSTRACT

This paper discusses the derivation of environmental quality standards for coastal waters and the difficulties of using such standards for controlling industrial discharges. Attention is focused on the common List II substances, copper, chromium, lead, nickel, zinc and arsenic - and their effects on marine life. The adequacy of existing toxicity data is discussed and it is concluded that long exposure tests are required to provide information on sublethal effects. Such data are currently limited. It is also important that consideration be given to the effects that reducing salinities and increasing temperatures have in increasing the toxicity of these substances. The complexity of interpreting the results of laboratory toxicity data to coastal waters is discussed with reference to a study of the impact of an industrial discharge.

KEYWORDS

Marine standards; metals; derivation; salinity; Dangerous Substances Directive.

INTRODUCTION

The Council of European Communities (E.C.) Directive on the discharge of Dangerous Substances (1976) requires Member States to eliminate pollution by List I substances and to reduce pollution by List II substances. This Directive and its derivatives (E.C., 1982; 1983) are intended for the control of point source discharges. Limit values for List I substances, whether for effluents or for the aquatic environment, are agreed at the Community level. For the List II substances, individual Member States are required to specify limit values by the environmental quality objective (EQO) approach. In the United Kingdom, the Water Research Centre (WRC) was contracted by the Department of the Environment to review available information for ten List II substances and to recommend environmental quality standards (EQSs) for both fresh and salt waters (Mance and O'Donnell, 1983). This paper explains the approach adopted and, by reference to information contained in detailed reports on the EQS recommendations for six of these substances (Mance and colleagues, 1984a; 1984b; 1984c; 1984d; 1984e; 1984f), indicates difficulties currently experienced in developing EQSs for tidal waters.

WHAT IS THE EQO APPROACH?

The EQO approach has been discussed in detail elsewhere (Otter 1979; Mance and O'Donnell, 1983) and is summarised here in relation to tidal waters. In developing a management policy for a given area of estuarine or coastal water the controlling authority will identify the uses made of that particular body of water and its associated intertidal areas.

For each of these uses an EQS is identified for each substance of concern. Where more than one use is relevant to the same body of water, then the most stringent of the relevant EQSs for each substance will apply. The resulting matrix of EQS values is then used in calculating emission standards for individual waste discharges entering that water body. Inherent in this approach is the concept of a zone of mixing within which the EQS may be exceeded. The size of the mixing zone is determined by the controlling authority in relation to the other water uses in the vicinity of the discharge point.

Previously this approach has been applied to industrial discharges individually by regional authorities in the United Kingdom (Hammerton, Newton and Allcock, 1980). With the implementation of the Dangerous Substances Directive, however, EQS values for the most common uses of water have been identified nationally. Five uses may be prescribed for tidal waters; the support of fish life, the support of other aquatic life, industrial abstraction, recreational usage, and the harvesting of food for human consumption.

It is recognised that other locally specific uses of salt waters may occasionally arise and that these would be most effectively resolved by the relevant regional authority.

WHAT IS AN EQS?

Under the Dangerous Substances Directive (E.C., 1976) EQS values for individual dangerous substances are required for use in calculating licence conditions for individual waste discharges. The EQS is the maximum concentration that will safely protect a specific use of the environment, when continuously exposed to that concentration. This EQS applies close to the point of discharge, after some initial mixing and dilution of the effluent has occurred. Such EQSs are generally very low relative to acutely toxic concentrations and have therefore been expressed as annual average concentrations rather than some extreme percentile or maximum concentration. Furthermore, because these EQSs are for the control of discharges and apply after initial dilution of the effluent, they are higher than the concentrations which would prevail at greater distances from the point of discharge.

It is recognised that existing knowledge on the environmental effects of these substances is limited. Therefore standards will be reviewed after an initial period of use in controlling discharges. Such reviews will involve assessment of the adequacy of the existing EQS value in the light of practical experience in licensing discharges, knowledge of actual environmental impact and, where necessary, consideration of any additional toxicity information.

DERIVATION OF MARINE STANDARDS

The List II substances for which the recommended EQS values have so far been agreed are the metals copper, chromium, lead, nickel, zinc and arsenic (Mance and O'Donnell, 1983). It was concluded that these substances were unlikely to

cause problems for the major industrial use of salt water (for cooling purposes) and that national standards were not relevant. Similarly it was concluded that aesthetic problems would only arise as a result of local conditions primarily resulting from discolouration of the water and that national standards were not required.

Standards for the concentrations of these substances in foods produced in or harvested from, tidal waters have been recommended for copper and zinc (Food Additives Committee, 1982). In the case of lead and arsenic there are statutory limits (Great Britain Parliament, 1961; 1980) specifying acceptable levels for foods including fish and shellfish. No such guidance is available for chromium or nickel, or the other substances currently under consideration. However the Ministry of Agriculture, Fisheries and Food and the Department of Health and Social Services have indicated that there is little risk from these substances and that standards are considered inappropriate. This conclusion followed consideration of the estimated weekly intake of these metals by people with an extremely high consumption (the 90th percentile) of fish and shellfish. Furthermore it was assumed that the entire intake derived from the single species of fish and shellfish with the highest reported tissue concentrations of the particular metal in UK waters.

Most effort has therefore been applied to the derivation of EQSs for the protection of marine fish and other aquatic organisms. The approach adopted is shown schematically in Fig. 1. The initial stage is a comprehensive review of the literature on the toxicity of the substance to estuarine and marine organisms and on field studies of the observed environmental effects. The literature is vetted to ensure that the approaches adopted are scientifically sound and that the data reported support the conclusions as presented. The intention of the EQS is to provide protection for marine life continuously exposed to a substance and considerable effort has been directed to searching for information relating to chronic toxicity effects or long-term sublethal effects. The information reviewed is evaluated and then used to identify the lowest concentration reported to cause a significant adverse effect. This effect may be toxicity, physical damage, or preferably a measurable physiological effect such as reduction in growth or reproduction. To this lowest adverse effect concentration is applied a safety factor, the size of which reflects the severity of the adverse effect and the conditions to which the data relate. Wherever possible complicating factors such as the species and life stage tested and the chemical and physical conditions of the test are taken into account.

A tentative limit concentration results from the application of the safety factor to the data produced in laboratory experiments. This value is then compared with published information relating observed concentrations in marine and estuarine locations to the abundance, diversity and apparent health of the biota when such information is available (which is seldom the case). If this comparison indicates that problems may occur at lower environmental concentrations, then both the laboratory and field information are reviewed. Once a tentative EQS value is identified that is compatible with both sets of information, this value is circulated for comment to those authorities with responsibility for either monitoring or controlling discharges to the estuarine and marine environment. If there is no adverse comment the tentative value is confirmed as the standard. However, if the tentative value is criticised on the basis of monitoring data, such data are assessed in comparison with the published information. A revised EQS value is then circulated for comment a second time before the value is confirmed as the EQS. As indicated earlier the adequacy of these EQSs will be reviewed in the light of practical experience and, where necessary, the standard revised.

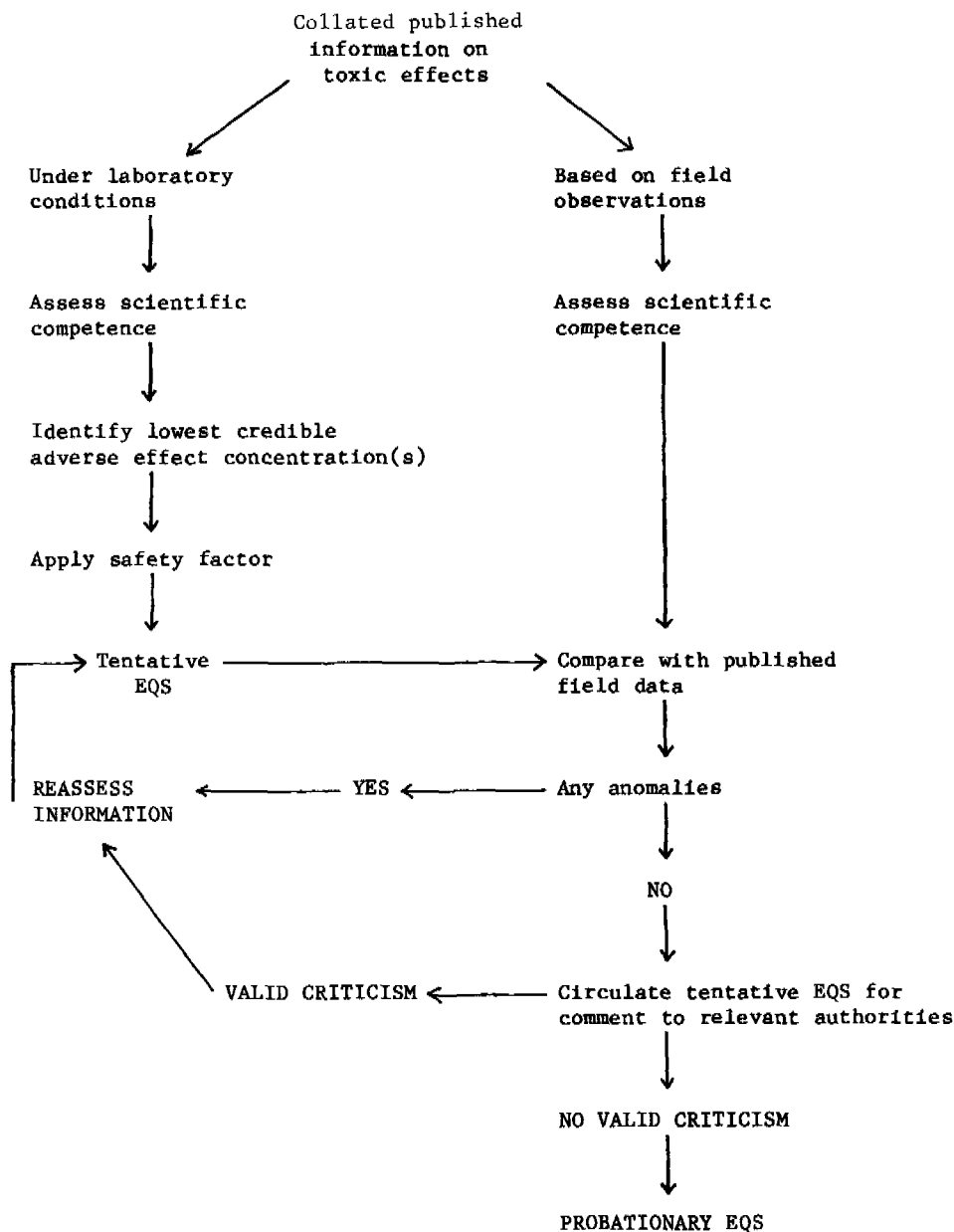


Fig. 1. Schematic flow chart for the derivation of environmental quality standards (EQS)

This general approach has been applied to the List II substances considered to date. However, the data available vary between substances, in quantity, quality and the attention given to the importance of complicating factors such as life stage and salinity. The limitation and complexities of the data available for these relatively common List II substances are considered in detail below.

DURATION OF EXPOSURE

Interest in the toxicity of pollutants to marine life is relatively recent and therefore the testing techniques are not as well developed or as uniformly applied as is the case for the testing of freshwater organisms. Furthermore the prolonged maintenance of marine organisms in laboratory conditions may require specialist food sources and the presence of specific substrates in the test chambers. As a consequence marine toxicity data are largely limited to tests of acute toxicity over short time periods. The main features of the toxicity data reviewed for a number of List II substances are summarised in Table 1. There are no data relating to the exposure of fish for periods in excess of 30 d and very few relating to invertebrates. Also the majority of the data relates to lethal effects primarily resulting from exposures of 4 days or less. Clearly the relevance of these data in determining acceptable levels for continuous exposure is limited. In general, however, the data suggest that longer exposure periods result in adverse effects resulting at lower concentrations.

Intraphyletic Variation

The results of 96 h median lethal concentration (LC50) tests for several phyla are summarised in Fig. 2 for the three metals for which reasonable data are available. This indicates the range of values for adult invertebrates, and both adult and larval fish, together with the number of species for which results are available. The median value is indicated for each phyla considered. The relative sensitivities of the phyla are similar for both zinc and copper but different for chromium to which the Annelida are more sensitive. It is also apparent that there is very wide range of response between species within a single phylum, thus making generalisation difficult.

Toxicity data for marine fish are limited and therefore the marine EQSs have been based on information for invertebrates. Additional acute toxicity tests were commissioned by WRC for two estuarine species Limanda limanda and Chelon labrosus (Hugman and Mance, 1983). The available information relating to marine fish indicates that they are less susceptible than marine invertebrates to the toxic effects of these metals.

Variation with life stage

Comparison of the information for larval and adult fish in Fig. 2 suggests that the larval forms are considerably more sensitive than the adults. However analysis of the data for invertebrates indicates that there is no clear trend in differential susceptibility. In contrast, information for the toxicity of metals to freshwater fish consistently indicates that the early life stages are more susceptible than are the adult fish (Alabaster and Lloyd, 1980). On the basis of the available data for marine organisms no such generalisation is possible and prediction of probable toxic effects to various life stages is therefore ill advised.

TABLE 1 A summary of the number of reported effect concentrations for List II substances according to severity of effect and duration of exposure
(* Inorganic forms only)

| EFFECT | Zn | Cu | Pb* | Cr | SUBSTANCE | | | | |
|-------------------------|----|----|-----|----|-----------|---|---|---|---|
| | Ni | As | V | B | Sn* | | | | |
| INVERTEBRATES | | | | | | | | | |
| LETHAL EFFECT | | | | | | | | | |
| Less than 4 d | 49 | 57 | 4 | 18 | 22 | 4 | - | 1 | 1 |
| 4-30 d | 16 | 16 | 6 | 6 | 1 | - | 3 | - | - |
| Longer than 30 d | - | 3 | 1 | 1 | - | - | - | - | - |
| SUBLETHAL EFFECT | | | | | | | | | |
| Less than 30 d | 10 | 7 | 10 | 2 | 6 | 2 | - | 1 | - |
| Longer than 30 d | - | 1 | 1 | 1 | - | - | - | - | - |
| FISH | | | | | | | | | |
| LETHAL EFFECT | | | | | | | | | |
| Less than 4 d | 24 | 14 | 1 | 12 | 3 | 4 | 4 | 3 | 3 |
| 4-30 d | 4 | 5 | - | - | - | - | - | 1 | - |
| SUBLETHAL EFFECT | | | | | | | | | |
| Less than 30 d | - | 2 | 1 | - | - | - | - | - | - |
| Longer than 30 d | - | - | - | - | - | - | - | - | - |

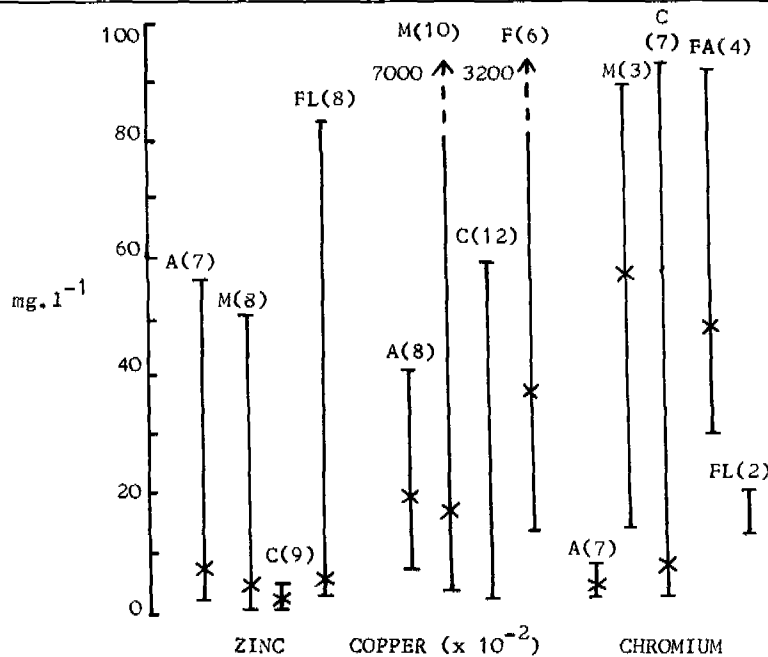


Fig. 2. A summary of the range of 96-h LC50 values reported for three List II substances for each of four phyla. The median value is indicated ('x') and the number of species studied is given in parentheses

A = Annelida, M = Mollusc, C = Crustacea,
FL = Larval Fish and FA = Adult Fish

Effects of Salinity and Temperature

Most published marine toxicity information for the List II substances refers to tests conducted in full-strength seawater. However two studies dealing with two species of marine isopods (Jones, 1975) and fish (Herbert and Wakeford, 1964) respectively demonstrate that the toxicity of zinc to these organisms increases with decreasing salinity. This relationship is supported by a study of the effect of salinity on the toxicity of chromium to three UK estuarine species, Macoma balthica, Corophium volutator and Nereis diversicolor (Bryant, McLuskey and Broddie, 1984). The data for Macoma balthica are shown in Fig. 3, which indicates the significance of not only salinity, but also temperature and the duration of the test exposure. All three species became more susceptible to chromium as the salinity of the test medium decreased over a period of 12 days with the same relationship observed for the whole period of exposure. It was also evident that the LC50 concentration decreased by as much as an order of magnitude with the increasing duration of exposure from 1 d to 12 d. This underlines the difficulties which arise in interpreting the bulk of the toxicity data which are currently available.

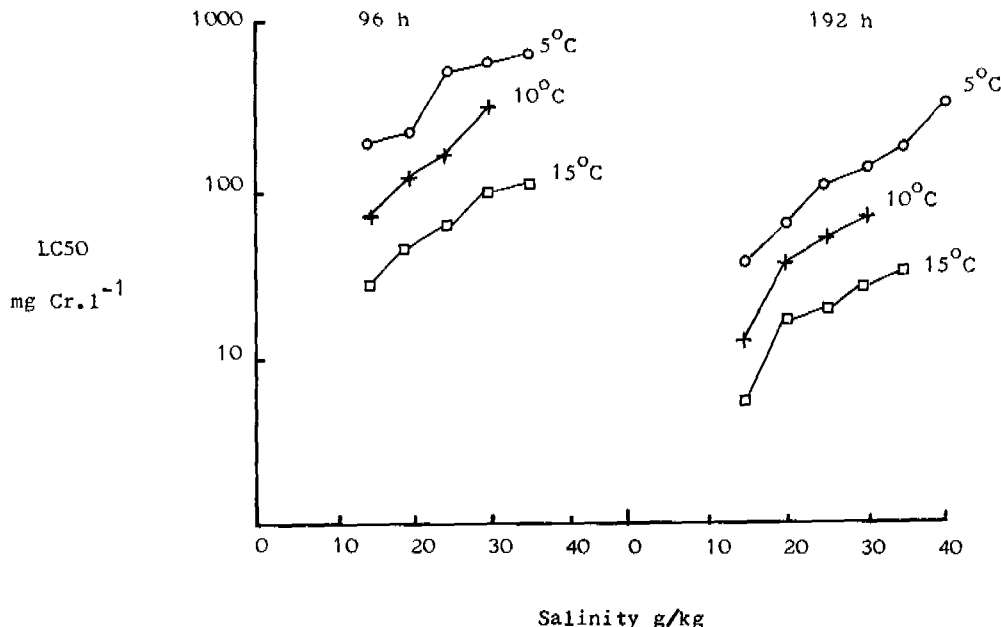


Fig. 3. The effect of temperature and salinity on the 96-h and 192-h median lethal concentration (LC50) of hexavalent chromium to Macoma balthica.

A further complicating factor is the effect of temperature on toxicity. The chromium study demonstrated that an increase in temperature increased toxicity (Fig. 3). In the case of Nereis a rise in temperature from 5°C to 15°C caused an order of magnitude decrease in the acutely toxic concentration. Furthermore the effect of temperature generally became more marked as the salinity approached that of seawater. The temperature range tested is not inappropriate to UK estuaries and coastal waters (MAFF, 1981), however considerably higher temperatures commonly occur in Mediterranean coastal waters of Europe (Aubert and colleagues, 1982). Consequently it is difficult to accept that the single

EQS values published by the EC for mercury (E.C., 1982) and cadmium (E.C., 1983) can be credible when their application to all EC coastal waters is considered. This doubt is accentuated by the EQS values for mercury and cadmium which are less stringent for estuaries than they are for coastal waters.

ACCLIMATION

It is possible that greater resistance to metal toxicity may result from prolonged exposure to elevated concentrations of a given heavy metal, whether resulting from industrial discharge or from areas naturally rich in mineral deposits. Any such acclimation may be due to either individual physiological or genetic adjustment within the exposed population. Such acclimation has been reported for freshwater organisms (Alabaster and Lloyd, 1980), but there is little direct evidence for marine organisms. One study (Bryan and Hummerstone, 1971) considered the relative toxicity of copper to Nereis diversicolor derived from sediments of differing copper content. Those taken from sediments with low copper content were three times more susceptible to copper in acute toxicity tests. The occurrence of acclimated populations poses problems in interpreting the significance of field studies relating water quality and biota and due consideration needs to be given to the longevity of exposure to any elevated environmental concentrations.

APPLICATION OF MARINE STANDARDS

Consideration is limited here to standards for the protection of fish and invertebrates rather than the full range of standards and the EQSs proposed in the UK are summarised in Table 2 (Mance and O'Donnell, 1983).

Generally the marine EQS values are of the same order of magnitude as those proposed for salmonid fish in freshwater. However, they are substantially lower than the EQS values for coarse fish in fresh waters with a high concentration of calcium carbonate. It should be noted that there is a very rapid change in the composition of the biota at the interface between fresh and saline water in estuaries with very few freshwater species inhabiting waters with a salinity greater than 5 g/kg. Thus for the controlling authority responsible for the quality of a lowland river supporting coarse fish and for the estuary to which that river discharges, there is the practical problem of licensing discharges when there is potentially a step change in the relevant EQS at the transition between fresh and salt water. This transition is probably most realistically identified by the observed composition of the biota. Consequently licensing of any discharge to the freshwater zone immediately landward of the transition will need to take due account of its potential impact on the estuarine biota.

Compared with riverine systems, assessment of the potential impact of individual discharges on the quality of tidal waters is considerably more difficult. In rivers, flow is unidirectional and under conditions of minimum river flow the available dilution is predictable and consistent. At open coastal locations the dispersion and dilution available will be influenced by many factors. The tidal currents are often disturbed by weather conditions and their strength and direction will vary throughout a single tidal cycle as well as through the lunar cycle of tides. Furthermore the actual position of the discharge will vary relative to the water's edge during the ebb and flood of the tide, as will the depth of water at the point of discharge. These complicating factors mean that there are few published studies which fully describe the water quality to which the biota are exposed in the locality of metal-bearing discharges. In contrast the freshwater EQSs in Table 2, with the exception of those for arsenic are

TABLE 2 UK guideline EQSs for fresh and salt water life

(A = Annual average; P = 95%-ile; M = MAC; D = Dissolved; T = Total)

| Use | LEAD | CHROMIUM | ZINC (all values as µg/l) | COPPER | NICKEL | ARSENIC |
|--|---------|----------|------------------------------|--------------|-------------|---------|
| Protection of freshwater fish | | | | | | |
| Salmonid fish | | | | | | |
| Total hardness (as mg/l CaCO ₃) | 0-50 | 4AD | 5AD | 10AT(30P) | 1AD(5P)* | 50AD |
| | 50-100 | 10AD | 10AD | 50AT(200P) | 6AD(22P)* | 100AD |
| | 100-150 | 10AD | 20AD | 75AT(330P) | 10AD(40P)* | 150AD |
| | 150-200 | 20AD | 20AD | 75AT(300P) | 10AD(40P)* | 150AD |
| | 200-250 | 20AD | 50AD | 75AT(300P) | 10AD(40P)* | 200AD |
| | 250+ | 20AD | 50AD | 125AT(500P) | 28AD(112P)* | 200AD |
| Coarse fish | | | | | | |
| Total hardness (mg/l as CaCO ₃) | 0-50 | 50AD | 150AD | 75AT(300P) | 1AD(5P)* | 50AD |
| | 50-100 | 125AD | 175AD | 175AT(700P) | 6AD(22P)* | 100AD |
| | 100-150 | 125AD | 200AD | 250AT(1000P) | 10AD(40P)* | 150AD |
| | 150-200 | 250AD | 200AD | 250AT(1000P) | 10AD(40P)* | 150AD |
| | 200-250 | 250AD | 250AD | 250AT(1000P) | 10AD(40P)* | 200AD |
| | 250+ | 250AD | 250AD | 500AT(2000P) | 28AD(112P)* | 200AD |
| Protection of other freshwater life | | | | | | |
| Total hardness (as mg/l CaCO ₃) | 0-50 | 5AD | 5AD | 100AD | 1AD | 8AD |
| | 50-100 | 60AD | 10AD | 100AD | 6AD | 20AD |
| | 100-150 | 60AD | 20AD | 100AD | 10AD | 50AD |
| | 150-200 | 60AD | 20AD | 100AD | 10AD | 50AD |
| | 200-250 | 60AD | 50AD | 100AD | 10AD | 100AD |
| | 250+ | 60AD | 50AD | 100AD | 28AD | 100AD |
| SALTWATER | | | | | | |
| Protection of saltwater fish and shellfish | 25AD | 15AD | 40AD | 5AD* | 30AD | 25AD |
| Protection of other saltwater life | 25AD | 15AD | 40AD | 5AD* | 30AD | 25AD |

* Higher values acceptable where acclimation expected or copper present in organic complexes

NB For zinc and copper the 95% ile concentrations apply to EC designated fisheries only.

Average values apply in all other rivers.

supported by considerable field exposure information. Furthermore the calculation of discharge licence conditions for freshwater systems is now based on an understanding of the percentile water quality distribution of the receiving water (Warn, 1982). This is not so for tidal waters.

A recent study by the Water Research Centre (O'Donnell and Mance, 1983) of the chemical and biological impact of an industrial discharge to an estuary has provided insight into the variability of the water quality around the discharge. Concentrations of arsenic at a fixed distance (2 km) seawards of the discharge are presented in Fig. 4 in relation to distance from the water's edge. The information provides a comparison between the water concentrations on the ebb and flood periods of a single spring tide. In addition information is included for the ebb period of a neap tide. Clearly the ebb tide carries the effluent seawards along the shore in a relatively narrow band with little lateral dispersion. The faster water movements on the spring tide provide for greater dilution and therefore the maximum concentrations are evident during the ebb phase of the neap tide. In contrast the flood phase of the tide brings water with concentrations that are much lower than those experienced during the ebb phase, and which are only marginally above background.

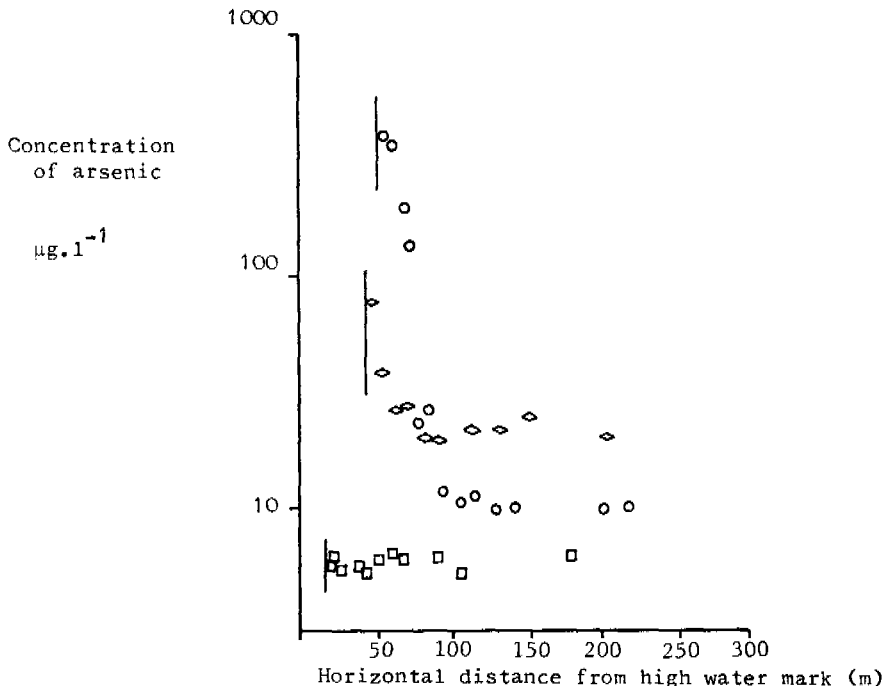


Fig. 4. Variation in the estuarine water concentration of arsenic with distance from the edge of the water (|) 2 km seawards of an industrial discharge. Data are presented for the ebb (○) and flood (□) phases of a spring tide and for the ebb phase (◇) of a neap tide

The implications of such concentration patterns for the benthic biota are considerable, as apart from the immediate vicinity of the discharge, the biota are only exposed to high concentrations for a small portion of the tidal cycle. Also within the flood or ebb phases the period of exposure of the benthos to the effluent components is further limited by the migration of water up and down the shore. On the spring tide the edge of the water moved some 50 m horizontally whilst the vertical tidal range was approximately 7 m at this particular point on the estuary. Translation of the toxicity data for continuous exposures to such field conditions is clearly problematical.

The difficulties in deriving EQS values for marine life have been considered in some detail. These problems should not be allowed to prevent the rational control of waste discharges by the EQO approach. As already indicated an integral part of this system of control is revision of EQSs in the light of the practical experience gained from the licensing of discharges in the real world. It must also be recognised that the success of the alternative method of control requiring the application of best technical means of treatment to all discharges can only be judged against an estimate of acceptable environmental concentrations (ie an EQS), if environmental protection is to be guaranteed.

CONCLUSION

Marine toxicity data are largely limited to relatively short exposure periods under conditions of constant temperature, salinity, and concentration of test substance. Insufficient attention has been directed to investigating the significance of such environmental factors as salinity and temperature on the toxicity of the List II heavy metals. Field studies of the environmental impact of heavy metal discharges to coastal waters are required that adequately describe the spatial and temporal variations in water quality as well as biota. The difficulties in deriving EQS values for marine life have been considered in some detail. These problems should not be allowed to prevent the rational control of waste discharges by the EQO approach.

In practice the available toxicity data enable an initial assessment of the EQS. Progressive extension of regulatory controls to all tidal discharges, with the phased implementation of Part II of the Control of Pollution Act (HMSO, 1974), means that these tentative EQSs will be judged against the real world by their use in licensing existing discharges. Implementation of these controls will undoubtedly increase the availability of field impact assessments enabling the EQSs to be reviewed and subsequently restated with increased confidence.

ACKNOWLEDGEMENT

The work on the derivation of EQSs for the List II substances was undertaken for, and funded by, the Department of the Environment, whose permission to publish has been given. The authors would like to thank the many people in government departments, water authorities, river purification boards and industry who have freely contributed ideas, advice and guidance.

REFERENCES

- Alabaster, J. S., and R. Lloyd (1980) (Ed). Water quality criteria for freshwater fish. Butterworths, London.
Aubert, M., P. Revillon., G. Flatau., and J. Aubert (1982). Metaux Lourds en Mediterranee. Revue Internationale d'Oceanographie Medicale. Tome LXV.

- Bryan, G. W. and L. G. Hummerstone (1971). Adaptation of the polychaete Nereis diversicolor to estuarine sediments containing high concentrations of heavy metals. 1. General observations and adaptation to copper. J. Mar. Biol. Assoc. U.K., 51, 845.
- Bryant, V., D. S. McLuskey, and K. Broddie (1984). Toxicity of chromium to three species of estuarine invertebrate. WRC Technical Report. (In press).
- Council of European Communities (1976). Directive on the discharge of dangerous substances. On pollution caused by certain dangerous substances discharged to the aquatic environment in the Community. 76/464/EEC, OJL 129.
- Council of European Communities (1982). Directive on limit values and quality objectives for mercury discharges by the chlor-alkali electrolysis industry. 82/176/EEC. OJL.
- Council of European Communities (1983). Directive on limit values for cadmium discharges. 83/513/EEC, OJL 291/1.
- Food Additives and Contaminants Committee (1981). Survey of copper and zinc in food. Food Surveillance Paper No. 5. HMSO.
- Great Britain - Parliament (1960). Arsenic in Food Regulations. Statutory Instrument No. 2261.
- Great Britain - Parliament (1974). Control of Pollution Act 1974. HMSO.
- Great Britain - Parliament (1979). Lead in Food Regulations. Statutory Instrument No. 1254.
- Hammerton, D., A. J. Newton, and R. Allcock (1980). Determination of marine consent conditions. Eff. Wat. Treat. J., 20, 261-269.
- Herbert, D. W. M., and A. C. Wakeford (1964). The susceptibility of a salmonid fish to poison under estuarine conditions. 1. Zinc sulphate. Intern. J. Wat. Pollut., 8, 251.
- Hugman, S. J., and G. Mance (1983). The acute toxicity of the priority List II substances to marine fish. WRC Report 616-M.
- Jones, M. B. (1975). Synergistic effects of salinity, temperature and heavy metals on mortality, and osmoregulation in marine and estuarine isopods (Crustacea). Marine Biol., 30, 13.
- Mance, G., V. M. Brown, J. Gardiner, and J. Yates. (1984a). Proposed Environmental Quality Standards for Inorganic Lead in Water and Associated Materials. WRC Technical Report (in Press).
- Mance, G., V. M. Brown, J. Gardiner, and J. Yates (1984b). Proposed Environmental Quality Standards for Chromium in Water and Associated Materials. WRC Technical Report (in Press).
- Mance, G., V. M. Brown, and J. Yates (1984c). Proposed Environmental Quality Standards for Copper in Water and Associated Materials. WRC Technical Report (in Press).
- Mance, G., C. C. Musselwhite, and V. M. Brown (1984d). Proposed Environmental Quality Standards for Arsenic in Water and Associated Materials. WRC Technical Report (in Press).
- Mance, G., and J. Yates (1984e). Proposed Environmental Quality Standards for Nickel in Water and Associated Materials. WRC Technical Report (in Press).
- Mance, G., and J. Yates (1984f). Proposed Environmental Quality Standards for Zinc in Water and Associated Materials. WRC Technical Report (in Press).
- Mance, G., and A. R. O'Donnell (1983). Application of the European Communities Directive on Dangerous Substances to List II Substances in the UK. Water Sci. Tech., 16, 159-169.
- Ministry of Agriculture, Fisheries and Food (1981). Atlas of the Seas around the British Isles. HMSO.
- O'Donnell, A. R., and G. Mance (1983). A study of the local impact of an industrial discharge on an estuary. 1. Field Studies. WRC Report 638-M.
- Otter, R. J. (1979). EEC 'Dangerous Substances Directive'. Chemistry and Industry, 5 May, 302-305.
- Warn, A. E. (1982). Calculations consent conditions to achieve River Quality Objectives. Effl. Wat. Treat. J., 22, 152-155.

THE EEC SHELLFISH DIRECTIVE IN WALES

S. N. Young and P. Wathern

*Dept. of Botany and Microbiology, University College of Wales,
Aberystwyth, Dyfed, SY23 3DA, U.K.*

ABSTRACT

This paper contains details of the procedures adopted by the UK Government in implementing the EEC shellfish directive and a review of the water quality monitoring programmes used by the Welsh Water Authority with respect to these provisions. Six shellfish beds have been surveyed in detail by the Authority, but only one has been designated. This is the only shellfishery which meets the standards. Raising the remainder to the required standards would involve considerable capital expenditure, mainly for sewage treatment. The UK Government has precluded such expenditure. It has claimed that any public health measures inherent in the directive are covered adequately by current UK practice. This stance is questioned in the light of a recent viral study. This paper highlights the potential problems when there is conflict between international and national water quality priorities.

KEYWORDS

EEC; international standards; shellfish directive; water quality monitoring; UK.

INTRODUCTION

Since 1973 the EEC, under the auspices of three consecutive environmental Action Programmes, has adopted over 70 legislative measures to protect or improve the environment. Most of these legislative measures are directives and many relate to water pollution and its control within Europe. Under Community law, each Member State is obliged either to specify which of its existing statutes are to be employed in enforcing each directive, or to adopt new statutes capable of enforcement. Thus, EEC directives are not themselves legally binding, but Member States must adopt their own legally binding statutes to ensure that agreed Community objectives are achieved. This has led to considerable variation between Member States, not only in the type of legislation used to enforce a directive but also in its efficacy. It is, therefore, difficult to ascertain whether any apparent success or failure of directives is attributable to the directives themselves or to the various implementation procedures adopted.

A detailed study of the directive on the quality required of shellfish waters

(Council of the European Communities, 1979) and the way in which it has been implemented in Wales is presented in this paper. This study highlights some of the problems encountered by both Member States and the European Commission when transforming the aspirations in Environmental Action Programmes into positive pollution control policy.

THE SHELLFISH DIRECTIVE

The objective of the shellfish directive is to protect and, where necessary, improve the quality of waters available for the growth of molluscan shellfish. The directive lays down certain water quality standards and minimum monitoring requirements for waters which have been designated by Member States as shellfisheries. Those fisheries which are not designated remain unaffected by the protective provisions of the directive. Legal compliance in Britain will be fully ensured on implementation of the appropriate sections of the Control of Pollution Act, 1974 (COPA). Water Authorities (WAs) are the agencies responsible for enforcing COPA in coastal waters, and have been elected the competent authorities for designating shellfish waters and implementing the directive in England and Wales.

The directive adopts a two tier structure for defining acceptable water quality standards with respect to specific parameters listed in an Annex. The 'G', or guideline, standard represents the recommended upper concentration of individual pollutants, whilst the 'I', or imperative, standard represents the maximum admissible concentration. Numerical values are attached to only a few of the parameters listed but provision is made for national governments to establish their own limit values for the remainder. In the case of organohalide and metal pollutants, the 'I' values which are adopted must not be exceeded in any sample. Acceptable percentage compliance figures for the remaining specified parameters are defined in the directive. The designation and subsequent monitoring of shellfish beds deemed to be in need of protection or improvement has been left to the discretion of individual Member States, with the proviso that any necessary improvements in water quality must be achieved within six years of designation.

The primary function of the directive is to protect shellfish health, although there has been controversy over the extent to which it also constitutes a public health measure. A recommended upper limit on the number of E. coli in shellfish flesh and intervalvular fluid, in addition to limits on those parameters which could adversely affect shellfish life, is included in the directive. This adds support to the view of both the EEC (Andreopoulos, 1981) and the Association of Sea Fisheries Committees (ASFC) (quoted in Lancashire and Western Sea Fisheries Joint Committee, 1982), that the directive has the dual role of protection of both human and shellfish health, an interpretation which is resolutely refuted by the Department of the Environment (DoE) (1980b).

The directive was originally welcomed by many environmentalists and shellfishermen in the UK as a measure to ensure that tidal and coastal water quality was adequately protected and where necessary improved. Sewage contamination represents the most widespread form of pollution over shellfish beds, and is a characteristic of many of the most productive beds in Britain. Therefore, while the inclusion of an E. coli limit value in the directive caused considerable debate, it also provided the opportunity to use the legislation to improve water quality in these areas. The DoE, in attempting to minimise the financial implications of implementing the directive, however, has limited its scope to such an extent that no real improvements in shellfish water are likely to accrue.

Although the DoE have insisted that the directive is not a public health measure, two separate E. coli 'I' values have been proposed. Current UK public health

legislation is used as the basis of these limit values. Under the terms of the Public Health (Shellfish) Regulations, 1934, local authorities have powers to issue closure orders prohibiting the distribution of molluscan shellfish for sale for human consumption from specified areas, if they are satisfied that a danger to public health exists from such distribution. Prohibition may be complete if the risk is severe, or may allow sale subject to conditions. Such conditions involve the satisfactory cleansing of shellfish to reduce the concentration of faecal coliforms in the flesh and intervalvular fluid to acceptable levels. Concentration in excess of 5000 E. coli/100 ml shellfish would usually be sufficient to warrant complete prohibition of the sale of molluscs, while lower concentrations are deemed satisfactory where cleansing is enforced. Where closing orders are in operation and shellfish cleansed, the DoE has proposed that the maximum permissible E. coli concentration of 5000/100 ml shellfish be adopted as the shellfish directive 'I' value. If shellfish are sold directly, with no cleansing before consumption, the EEC's 'G' value of 300 E. coli/100 ml shellfish will be used as an 'I' value.

These faecal coliform limit values effectively restrict possible designation of commercially significant beds in many parts of Britain to those which are covered by closure orders. Concomitantly, the establishment of the upper limit value of 5000 E. coli/100 ml shellfish essentially facilitates the designation of some of the most severely contaminated shellfisheries, with no obligation under the terms of the directive to improve sewage pollution control. This has caused considerable consternation amongst many of the interested parties. The ASFC has reacted particularly strongly to the DoE's interpretation of the directive, stating that "It is a tragedy for the shellfish industry in this country that the opportunity presented by this directive for significant improvements to be made to the quality of coastal waters, has been thrown away." (ASFC, 1982).

UK Interpretation of the Directive

Many competent authorities were originally reluctant to proceed with the designation of shellfish waters, because of confusion over both the objectives of the directive and the possible costs of achieving them. Consequently, the UK Government convened the Working Group on the EEC Shellfish Water Directive. This group was charged with the interpretation of the directive, ".... to see to it that it was implemented in the way Government Ministers had agreed....", and to produce advice on implementation for the relevant agencies (DoE, 1980a). Each of the competent authorities was represented in the Working Group, together with representatives of the DoE, Department of Health and Social Security, Ministry of Agriculture, Fisheries and Food (MAFF), ASFC, Department of Agriculture and Fisheries, Scotland and the Scottish Development Department. The Working Group was strongly led by DoE (Owens and Halcrow, 1981).

The most significant document, related to implementation of the directive in England and Wales (DoE, 1980b), concerns the effect of implementation on WA expenditure. Article 5 of the advice note states that " in the current economic circumstances the Government accepts that the implementation of the directive should not have undue effect on Water Authorities' capital expenditure plans. For this reason Water Authorities should aim, in the initial round, to designate only a small number of waters which either already meet the appropriate standards or which are capable of doing so by October 1987 after improvements which are already programmed." It is because of this restriction on capital expenditure that the quality of water over shellfish beds around the British coast is not expected to improve following implementation of the directive, and no active attempts to control pollution as a direct result of this legislation will be made. Any work undertaken in designating shellfish beds will be largely

administrative. The DoE advice note on implementation further stipulates that WAs must ".... ensure that the necessary resources are available" to satisfy the monitoring requirements associated with the designation of shellfish waters. Any additional monitoring effort which is expended during the designation process, therefore, will result in a redistribution of WA revenue budgets.

Establishment of 'G' and 'I' Limits for Welsh Shellfish Waters

Firm guidance to be followed for much of the designatory process was provided by DoE. Within these guidelines there were several aspects which were left to the discretion of the individual WAs. These included the establishment of 'G' and 'I' values for many of the parameters listed in the Annex to the directive. MAFF provided advice on suitable levels at which to set these limits (DoE, 1980b), although, provided the 'I' values stipulated in the directive were not exceeded, the WAs could depart from these suggestions.

MAFF recommendations are based on acute toxicity tests performed on oyster larvae, although these tests have been criticised for several reasons. The proposed limit values are those concentrations at which no incidence of abnormal development was detected in a sample of 100 embryos after 48 hours' exposure to the pollutant. This assumes that oyster larvae are the most sensitive indicators of the effects of pollution on molluscan shellfish. This is believed to have resulted in the setting of limit values which are too lax, particularly with respect to some metal and organohalide pollutants. Recent research (Strömgren, 1982) has indicated that shell length growth in 12-16 month old *Mytilus edulis*, used to ascertain threshold toxicity levels for this species, is significantly reduced in sea water containing concentrations of either 0.0003 mg Hg/l, 0.003 mg Cu/l or 0.01 mg Cd/l. These values are all considerably lower than those proposed by MAFF as acceptable for shellfish waters. *M. edulis* was shown to be less sensitive to lead and nickel pollution than the oyster larvae used by MAFF, while sensitivity to zinc was the same for both species. Experiments were performed over a period of 10-22 days, considerably longer than the duration of the MAFF tests, although not sufficient to evaluate long-term toxicity effects. This work illustrates that oyster larvae are not the most sensitive shellfish when metal pollution is present, and that the use of a single species to estimate acceptable pollution levels for all shellfish is not appropriate.

Welsh Water Authority (WWA) criticisms of the MAFF limits are based on the fact that the test takes no account of the effects of bioaccumulation, acclimation or of the way in which interaction between pollutants affects their toxicity (WWA, 1981). WWA accepted the MAFF guidelines for all but three parameters. These were arsenic, cadmium and zinc. Lower limit values were imposed by WWA for arsenic and cadmium, whilst a higher value was proposed for zinc. These changes reflect WWA conclusions on toxicity and bioaccumulation, based on toxicological studies. MAFF and WWA limit values are presented in Table 1.

Designation of Shellfish Waters in Wales

The WWA initially intended to designate as many waters as possible within the constraints imposed by expenditure limits. These constraints effectively restrict consideration of shellfish beds for designation to those which are of commercial significance. In accordance with DoE advice, the initial list of shellfish beds for designation is not definitive, and may be augmented in the future.

Initially, the quality of the water and shellfish flesh from six beds was intensively monitored to assess potential compliance. Potential designatory

TABLE 1 Imperative and Guide Values of Parameters Specified in the Directive

Where numerical 'I' values are not specified in the Directive these have been derived from DoE/MAFF recommendations, other EEC Directives and standards being considered for the Severn Estuary.

| <u>PARAMETER</u> | <u>'G'</u> VALUE | <u>'I'</u> VALUE | <u>MONITORING FREQUENCY</u> | <u>COMPLIANCE REQUIRED</u> | <u>SOURCE of 'I' VALUE</u> |
|----------------------------|-------------------|-----------------------------------|-----------------------------|----------------------------|----------------------------|
| pH | - | 7-9 | Quarterly | 75% | Directive |
| Temperature | 2°C above ambient | 2°C above ambient | Quarterly | 75% | DoE |
| Colour | - | 10 mg/l Pt above ambient | Quarterly | 75% | Directive |
| Suspended Solids | - | 30% above ambient | Quarterly | 75% | Directive |
| Salinity | 12-38% | 40% | Monthly | 95% | Directive |
| Dissolved Oxygen | 80% Sat. | 70% | Monthly | 95% | Directive |
| Hydrocarbons | - | None visible No harmful effect | Quarterly | 75% | Directive |
| Organohalogens | - | No harmful effect | 6 monthly | 100% | Directive |
| DDT | - | 33 µg/l | | | MAFF |
| Lindane | - | 100 µg/l | | | MAFF |
| Parathion | - | 100 µg/l | | | MAFF |
| Dieldrin | - | 100 µg/l | | | MAFF |
| Metals (Soluble) | - | No harmful effects | 6 monthly | 100% | Directive |
| Silver | - | 0.01 mg/l | | | MAFF |
| Arsenic | - | 0.05 mg/l | | | WWA |
| | | 3.00 mg/l | | | MAFF |
| Cadmium | - | 0.005 mg/l 0.33 mg/l | | | WWA MAFF |
| Chromium | - | 1.00 mg/l | | | MAFF |
| Copper | - | 0.01 mg/l | | | MAFF |
| Mercury | - | 0.001 mg/l | | | MAFF |
| Nickel | - | 0.10 mg/l | | | MAFF |
| Lead | - | 0.10 mg/l | | | MAFF |
| Zinc | - | 0.04 mg/l 0.01 mg/l | | | WWA MAFF |
| Faecal Coliforms* | 300/100 ml | 5000/100 ml | Quarterly | 75% | DoE/MAFF |
| Substances affecting taste | - | No taint | | | Directive |
| Saxitoxin | - | - | - | - | - |

* The 'G' value for faecal coliforms will apply when molluscs are directly consumed by man. Where cleansing or sterilisation is carried out then the 'I' value of 5000/100 ml will apply.

TABLE 2 Important Welsh Shellfish Beds Actively Considered for Designation

| SITE | REASON FOR NON-DESIGNATION & POTENTIAL DESIGNATORY PROBLEMS |
|---------------------------|---|
| Menai Straits | Mussel/oyster fishery. Only Welsh designated fishery. Some minor beds not designated due to severe faecal contamination. |
| Cardigan Bay | Scallop fishery. Data inadequate for water quality assessment. Expected to comply as no major polluting discharges in vicinity. |
| St Brides Bay | Queens fishery. Status - as Cardigan Bay. |
| Milford Haven | Oyster/mussel fishery. Gross bacterial pollution initially prevented designation. Bacterial counts $> 61\ 500/100\ ml$ in oysters. Closing order imposed 1982, allowing consideration for designation in 1983. |
| R. Taf, Tywi & Gwendraeth | Cockle fishery lacking closure order. Fails to comply with 300 <u>E. coli</u> /100 ml limit value. Further data collection required. |
| Burry Inlet | Cockle fishery. Most valuable Welsh shellfishery. No closure order and only 19% compliance with 300 <u>E. coli</u> /100 ml limit value. At present only 71% compliance with 5000 limit. Therefore, even with closure order, compliance would be marginal. |

problems are described in Table 2. Technical difficulties have restricted the number of samples collected from the Cardigan Bay, St. Brides Bay and 'Three Rivers' areas. The major difficulties likely to be encountered in designating some of the more minor shellfisheries are outlined in Table 3. The location of the six major shellfisheries is shown in Figure 1.

With the exception of a small area which fails the E. coli limit of 5000/100 ml shellfish flesh, the majority of the Menai Straits mussel and oyster beds have been found to comply with the defined standards and were designated in 1982. Further investigations of the Cardigan Bay and St. Brides Bay fisheries is expected to result in designation of these offshore beds in the future, as neither is likely to suffer from the effects of pollution. Compliance in the other commercially significant Welsh shellfisheries is expected to be more marginal.

TABLE 3 Shellfish Areas Not Considered for Designation

| SITE | REASONS FOR NON-CONSIDERATION FOR DESIGNATION |
|--------------|--|
| Porthmadog) | Very small fisheries, |
| Barmouth) | each with severe faecal contamination. |
| Aberdovey) | |
| Aberconwy | Gross faecal contamination - alleviation would involve £17M capital expenditure. Previously significant fishery, for unknown reasons declining. Planned road tunnel construction would require immediate derogation due to expected high suspended solids. Disused metal mines in R. Conwy catchment. Effects of metal-rich drainage waters on tidal water quality not fully understood. |
| Dee Estuary | Lack of accurate information on water quality. Previously, high Zn and NH ₃ -N levels prevented good shellfish development. Now abated. Area being promoted as mussel fishery and may be considered for designation. |

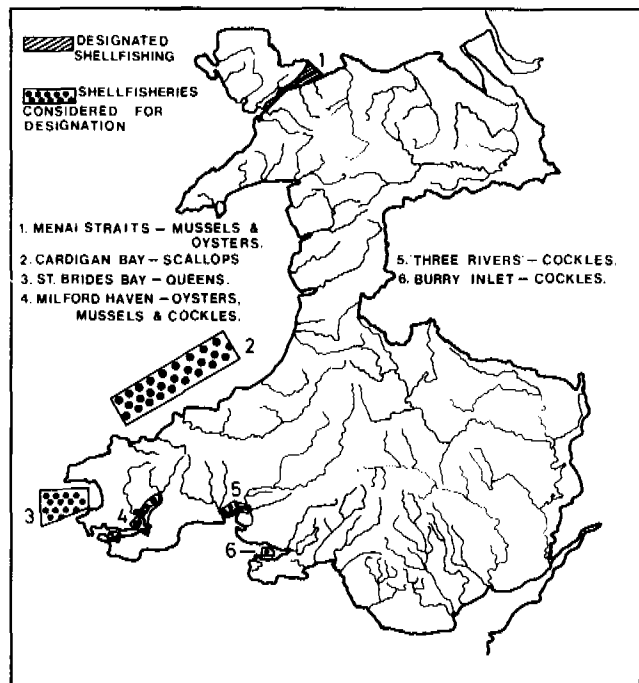


Fig. 1. Major shellfisheries in Wales

Thirteen sites were sampled in the pre-designation monitoring of the Menai Straits. Samples were taken at monthly intervals for six months, and compliance with the parameters included in the annex to the directive assessed. Following designation the number of sampling sites was reduced to four, and the sampling frequency reduced in accordance with Table 1.

The overall costs incurred by the WWA in implementing the directive is presented in Table 4. These estimates give no indication of the total costs which will

TABLE 4 Total Costs to Date of Implementing the Directive (at 1983 £ Prices)

| SITE AND SURVEY TYPE | TOTAL COSTS (ANALYTICAL) | MANPOWER COSTS | OVERALL COST |
|---|--------------------------|----------------|----------------|
| <u>Pre-designation Surveys</u> | | | |
| Menai Straits | 3220.4 | 1979.0 | 4122.7 |
| Burry Inlet | 1253.2 | 555.0 | 1808.2 |
| Milford Haven, 'Three Rivers' Cardigan Bay and St Brides Bay | 2379.7 | 1584.9 | 3964.6 |
| TOTAL COSTS | 6853.3 | 4118.9 | 10972.2 |
| <u>Post-designation Monitoring</u> | | | |
| Menai Straits | 455.7 | 566.7 | 1022.4 |

eventually be incurred by the Authority, as further detailed surveys are planned. The cost of sample collection is high, especially in offshore areas such as Cardigan Bay and St. Brides Bay. Completion of the pre-designatory surveys in these areas is expected to add considerably to WWA expenditure. The estimated costs of post-designatory monitoring are comparatively low, and although it is anticipated that additional areas will be designated, these costs can be readily accommodated. The costs of sampling and analysing individual parameters accounts for over 60% of the total pre-designatory expenditure, metal analysis being particularly expensive (Table 5).

TABLE 5 Sampling Intensity Used and Analytical Costs
Incurred to Date in Implementing the Directive (at 1983 £ Prices)

| SITE AND SURVEY TYPE | METALS | PESTICIDES | SS | <u>E.coli</u> | COLOUR |
|---|--------|------------|-------|---------------|--------|
| <u>Pre-designation surveys</u> | | | | | |
| Menai Straits: No.of samples | 125 | 24 | 126 | 55 | |
| Analytical Costs (£) | 2175 | 417.6 | 136.1 | 491.7 | |
| Burry Inlet: No.of samples | 41 | 13 | 42 | 30 | |
| Analytical Costs (£) | 713.4 | 226.2 | 45.4 | 268.2 | |
| Milford Haven, 'Three Rivers' Cardigan Bay & St Brides Bay: No.of samples | 98 | 14 | 101 | 36 | |
| Analytical Costs (£) | 1705.2 | 243.6 | 109.1 | 321.8 | |
| TOTAL COSTS | 4593.6 | 887.4 | 290.6 | 1081.7 | |
| <u>Post-designation Monitoring</u> | | | | | |
| Menai Straits: No.of samples | 8 | 8 | 16 | 16 | 16 |
| Annual Analytical Costs | 139.2 | 139.2 | 173 | 1430 | 17.0 |

Metals, suspended solids and E.coli analytical costs are probably underestimates.

None of the costs quoted represents resources which have been made available to the Authority specifically for implementation of the directive. The work has been achieved by redistribution of resources which had been set aside for other purposes. One consequence of this redistribution was that a programmed major water quality survey of the Menai Straits, which would have contributed to the formulation of a water quality model for the area, was suspended to free manpower to satisfy the monitoring requirement of the directive.

Prior to publication of the directive, the WWA had begun a preliminary study of contamination of shellfish and shellfish waters by enteroviruses in areas known to be contaminated by sewage discharges. This study showed that contamination of edible shellfish was widespread, and that current cleansing practice was not entirely successful in dealing with the problem.

In adopting a high faecal coliform limit value for shellfish, the UK Government has effectively facilitated the designation of some of the more severely sewage-contaminated shellfisheries under the aegis of Directive 79/923/EEC. The DoE has relied heavily upon the effectiveness of closing orders to ensure protection of the health of consumers of shellfish taken from such fisheries. While British cleansing practice may be reasonably efficient in purifying shellfish flesh of faecal contamination, the enterovirus study indicates that a health risk may

remain after cleansing. This is of significance where shellfish either are eaten raw or are inadequately cooked.

CONCLUSIONS

The extension of WA functions to the control of discharges to coastal waters is a recent development in the UK, even though they have been responsible for pollution control in the major estuaries of England and Wales for a number of years. Generally, data collection has been geared to the investigation of specific pollution incidents and the formulation of water quality models. Such models help determine future water pollution control requirements and priorities (Howells et al. 1978). This approach is a reflection not only of the technical difficulties involved in obtaining representative samples from tidal waters on a routine basis, but also of the relatively small numbers of WA staff directly engaged in tidal water quality management. One consequence of the extension of WA functions to the 3 mile offshore limit is that water quality surveillance is likely to be afforded reduced priority in the immediate future, as efforts are made to bring all discharges not previously consented under control. In contrast, the lack of comprehensive data on coastal and tidal water quality in Wales has necessitated intensive monitoring of potential shellfish sites to identify those which comply with the directive. The water quality monitoring requirements of the shellfish directive, therefore, represent a departure from current WWA practice.

An important conclusion to be drawn from this study is that considerable confusion and additional expenditure resulted from attempts to accommodate the ambiguous objectives of the directive. Had the objectives been restricted to defining water quality standards for shellfish growth and establishing measures to ensure that these standards are achieved in major shellfisheries, WWA could have designated the most economically important Welsh shellfisheries. The protective powers of the directive could then have been used to prevent any future degradation in the quality of these waters with respect to parameters of significance for shellfish health. The attempt to extend the objectives of the directive to public health protection, therefore, has restricted its potential utility in the UK. In addition, the use of E. coli as the sole measure of potential health risk can be criticised on the grounds that faecal coliform concentration alone does not provide an accurate guide to possible health hazards, as is illustrated by the WWA enterovirus study. This inadequacy is acknowledged by the EEC in two other directives. The drinking water directive (Council of the European Communities, 1980) and the bathing water directive (Council of the European Communities, 1976) include provisions for analysis for Salmonella and other pathogens, as well as faecal coliforms.

The shellfish directive, while entirely laudible in its intentions, has deflected consideration of more immediate coastal pollution problems in Wales. Nevertheless, the WWA and Sea Fisheries Committees generally are anxious to use the conditions laid down by the directive as an adjunct to coastal and tidal water pollution control policy. The directive could have been used as a factor in establishing new priorities for capital works, particularly the construction of long-sea sewage outfalls in certain areas. The inflexible financial constraints placed on WAs by the UK Government, however, have rendered this approach impossible. Consequently, most of the work undertaken to implement the directive has been administrative and cannot possibly result in direct improvements to shellfish water quality. There are only two potential practical benefits of implementation in the UK. First, the quality of water above those shellfish beds which are considered for designation will be better understood. Secondly, once designated, shellfish beds should be protected against future deterioration in water quality. The designation policy adopted by the UK Government in implementing the directive has guaranteed the

procedural compliance required by the EEC. However, this policy has also ensured that it will not be possible to use the directive to improve the quality of either British shellfish or the waters overlying British shellfish beds.

There is an interesting postscript to this paper. Shortly after the manuscript was prepared the Royal Commission on Environmental Pollution, in its 10th Report to Parliament (1984), criticised the implementation of the directive in the UK, saying: "Despite this directive's somewhat ambiguous nature, we see no advantage in the negative approach to its implementation which has been adopted in the UK". Further, the Commission has noted the fact that all 29 designated shellfish waters in the UK as a whole, appear to meet the water quality standards or will do so within the six year period following improvements already planned. The Commission concludes that implementation has had no effect on the quality of shellfish waters in the UK. In the light of these observations it has recommended that the competent authorities use the enhanced powers under COPA II and the shellfish directive to effect improvements in shellfish water quality, "... to the benefit of both the environment and human health".

ACKNOWLEDGEMENTS

The material upon which this paper is based derives from work undertaken by the authors in the course of a contract with the Commission to the European Communities, the objectives of which are to evaluate methods of assessing the environmental impact of Community policies in Wales. The authors acknowledge the invaluable assistance of the Welsh Water Authority (M Owens, W Halcrow and Dr J M Tyler), the Lancashire and Western Sea Fisheries Joint Committee (Dr C M G Vivian) and the Prince of Wales' Committee in undertaking this research. This paper reflects the views of the authors, and not necessarily those of either the Commission or those agencies which contributed to the research.

REFERENCES

- Andreopoulos, A. (1981). Letter to the Shellfish Association of Great Britain London.
- Association of Sea Fisheries Committees. (1982). Letter to the Water Quality Division of the Department of the Environment, 14 October 1982.
- Council of the European Communities. (1976). Concerning the quality of bathing water (76/160/EEC). Official Journal, L31 (5.2.76), 1-7.
- Council of the European Communities. (1979). On the quality required of shell-fish waters (79/923/EEC). Official Journal, L281 (10.11.79), 47-52.
- Council of the European Communities. (1980). Relating to the quality of water intended for human consumption (80/778/EEC). Official Journal, L229 (30.8.80), 11-29.
- Department of the Environment. (1980a). Minutes of a meeting of the Working Group on Implementation of the EEC Shellfish Water Directive in England and Wales, 7 July, 1980. DoE, Marsham St., London.
- Department of the Environment. (1980b). Advice on the implementation in England and Wales of the EEC Directive on the quality required of shellfish waters. DoE, Marsham St., London.
- Howells, R.W., Owens, M. and Stoner, J.H. (1978). Water quality aspects of Welsh estuarine and coastal waters. J. Inst. Wat. Engrs. & Sci., 32, 365-390.

- Lancashire and Western Sea Fisheries Joint Committee. (1982). Estuarial, coastal and marine pollution; Evidence presented to the Royal Commission on environmental pollution, July, 1982.
- Owens, M. and Halcrow, W. (1981). Report to Members of the Water Quality Committee, WWA, 14 April, 1981.
- Royal Commission on Environmental Pollution. (1984). Tenth Report: Tackling Pollution - Experience and Prospects. Cmnd. 9149, HMSO, London.
- Strömgren, T. (1982). Effect of heavy metals (Zn, Hg, Cu, Cd, Pb, Ni) on the length growth of Mytilus edulis. *Marine Biol.*, 72 (1), 69-72.
- Welsh Water Authority. (1981). Report to the Water Quality Committee, 8 September 1981.

TRANSPORT AND PROCESSES IN SEWERS

OPERATION AND EFFICIENCY OF AUTOMATICALLY OPERATING WEIR STRUCTURES — A CONTRIBUTION TO CLEANER WATERS

E. Macke

*Technische Universität Braunschweig, Leichtweiß-Institut, Beethovenstr.
51 A, D-3300 Braunschweig, F.R.G.*

ABSTRACT

The automatically operating weir structures presented are simple, largely maintenance-free structures which, when used as control elements in storm overflows, offer considerable advantages over the fixed weir sills. Irrespective of the intensity of rainfalls, these weirs do not discharge any surplus water into the receiving water, unless a maximum possible water level has been reached, which is then maintained at a virtually constant level until the floods subside. The maximum possible water level, the so-called impounding head, will be determined in such a way that, on the one hand, the sewer capacity will be fully utilized, and, on the other, any undesirable backwater in the sewer system can be precluded. The weirs are not only suited for installation in new structures, but may also be integrated in existing ones. Time and cost consuming constructional measures can be dispensed with, as the weirs can, owing to their configuration - they are composed of individual segments - be passed through the existing manholes. They allow considerable additional sewer capacities to be activated, in particular in low-head sewer systems, so that the installation of high-cost retaining basins, which normally require a high degree of maintenance, can either be limited or dispensed with altogether. As the receiving water will be affected only when a given impounding head has been reached, the amount of combined sewage discharged can be reduced to a minimum.

KEYWORDS

Storm overflows; stormwater retention; sewer capacities; weir structures; water protection.

INTRODUCTION

Faced with a growing public concern for the environment as well as with new effluent discharge acts, regional, municipal and communal authorities feel increasingly compelled to reduce the present degree

of pollution produced by waste waters. The required measures - new installations have to be provided or existing sewer systems modernized - will tie up a considerable amount of capital.

The present paper is to introduce two different types of automatically operating weirs which can help reduce the construction cost in connection with sewage disposal measures. This paper does, however, not only provide an operational description, but tries to demonstrate the efficiency of these novel structures with the aid of a concrete example.

Basic considerations

Storm-water drainage and combined-sewer systems are, mostly for economic reasons, provided with storm overflows. Arranged at certain intervals, these allow, in case of rainfalls of a specific intensity, the sewage to be discharged into the receiving water or retaining basin, thus avoiding sewer overloads.

In the past, fixed weir sills used to be installed subject to the state of the art, with their length and height calculated in such a way that the design flood can be discharged at a given impounding head, no backwater being produced.

The example in fig. 1 (left) shows this flow condition (Q_{\max}) at the weir head Δh and the relevant total depth of water t . The immediate problem with such fixed weir sills lies in the fact that according to the hydrograph large quantities of water are discharged into the receiving water not only before and after the impounding head has been reached, but that even minor rainfalls producing water depths in the sewer and resulting in low weir heads (e.g. Δh on the right in fig. 1) will also be discharged into the receiving water although the storage capacity up to the impounding head has not fully been utilized.

As soon as one succeeds in providing a system where sewage is discharged from the combined sewer only, and only then, when the impounding head has actually been reached, substantial sewer capacities can be activated, which implies that additional retaining basins or similar units can either entirely be dispensed with, or else that they can be much more limited in size.

The significance of the additional sewer capacity is demonstrated by figs. 2 and 3.

Fig. 2 shows a sewer of 2,000 mm inside width, its assumed permissible impounding head reaching the pipe crown in the area of the weir sill. The height of overfall at the fixed weir sill is dotted, the cross sectional area of the basic discharge to the sewage works is hatched. When installing automatically operating weir structures, the entire dotted cross section can be activated as additional storage capacity. The storage volume that can be utilized is subject to the originally planned weir sill overfall height as well as the sewer bottom gradient.

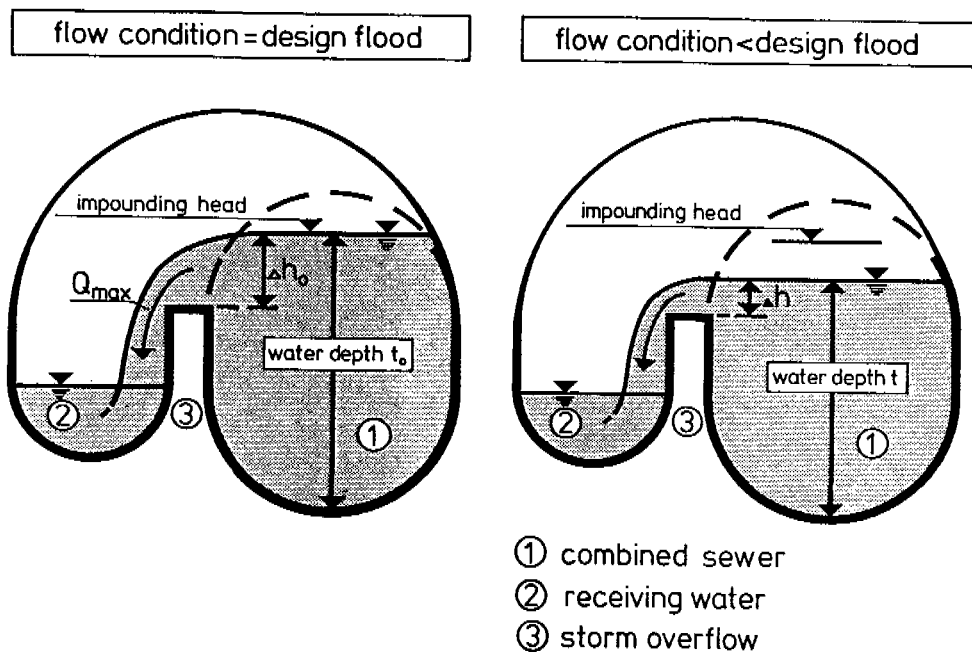


Fig. 1. Storm overflow with fixed weir sill under different flow conditions

Fig. 3 shows the storage capacity versus the bottom gradient for 0.4 m of overfall height. The bottom curve (broken line) represents the sewer capacity that can be utilized in connection with a fixed weir sill (RU). The continuous line represents the storage capacity when installing automatically operating weirs.

The graph illustrates in an impressive manner that substantial capacities can be activated in particular in sewers inclined at a small angle. The novel weir structures will increase the sewer capacity that can be utilized for waste-water storage by more than 60 % as compared to the capacity available in conventional systems with fixed weir sills in storm overflows.

Operation of automatically operating weirs

The next two paragraphs provide descriptions of two different weir structures which both allow a given sewer capacity to be utilized to the fullest possible extent.

Float-controlled shutter weir. The float-controlled shutter weir was tested and optimized in its functional behaviour at Technische Universität Braunschweig (Führbötter et al., 1978). Its operation is illustrated by the sectional views in fig. 4.

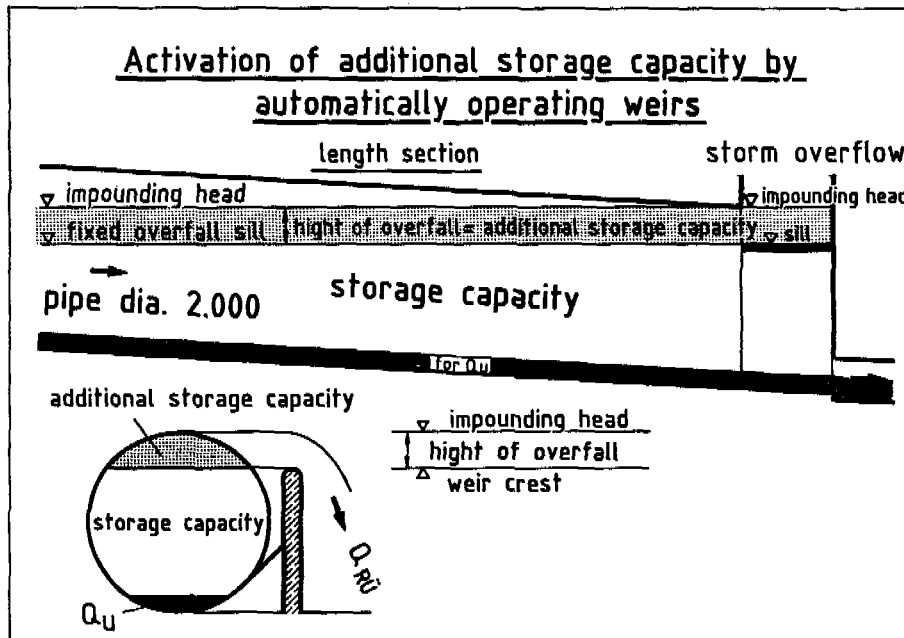


Fig. 2. Activation of additional storage capacity by automatically operating weirs

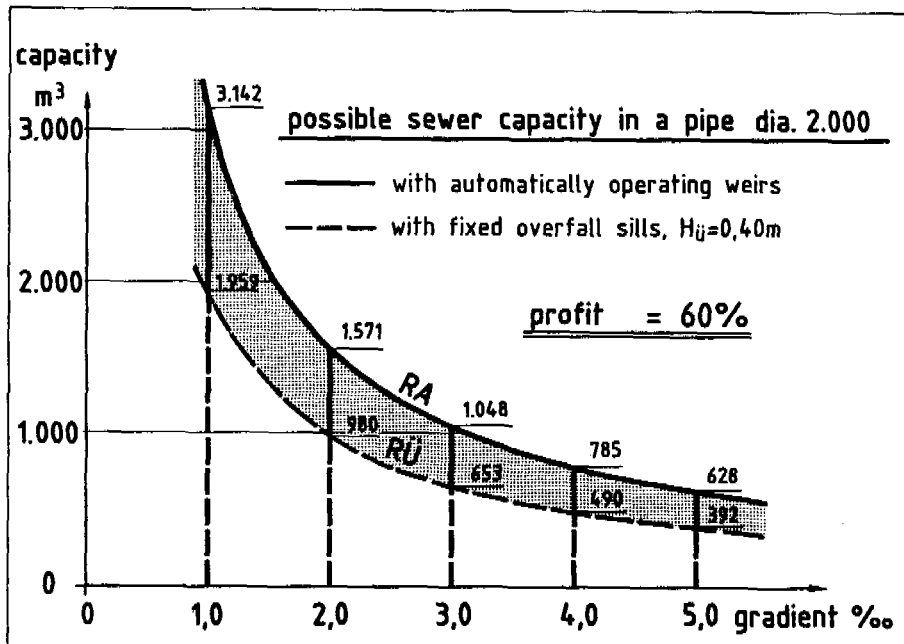


Fig. 3. Possible sewer capacity in a pipe
2,000 mm dia.

The sectional views show a stormwater discharge unit with the feeder 1 and the tail race 2 to the sewage works. The weir comprises a weir shutter 4, a float 5, and a common shaft 6. Both the weir shutter and the float are rigidly connected with this shaft which is rotatably fitted above the maximum headwater level, the impounding head. The weir shutter closes an outlet opening to the receiving water, the shutter bottom edge resting against a weir sill similar to that in a conventional storm overflow. A float chamber adjacent to the weir shutter is provided with a sill 8 separating it from the feeder. With the water level rising in the feeder or the discharge unit, the weir shutter will, irrespective of the level in the receiving water, not open unless the water level has risen up to the sill. As the water level rises further to the permissible impounding head, the float-chamber sill is flooded to a certain degree.

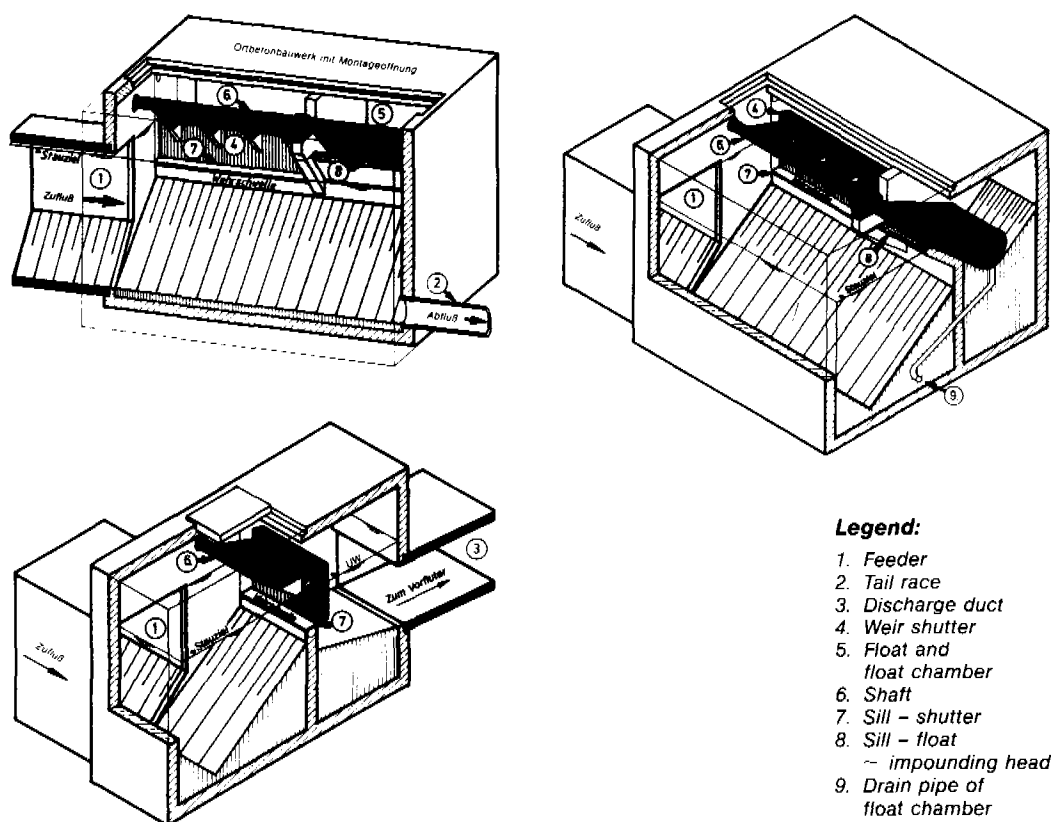


Fig. 4. Sectional views of a float-controlled shutter weir (schematics)

Water can now flow into the float chamber, leaving it however immediately through the drain pipe 9. The water level in the float chamber will rise as soon as more water enters this chamber than is discharged through the drain pipe. The float, rising with the water, opens the weir shutter through the common shaft. Subject to the amount of water supplied through the feeder, the weir shutter automatically opens to precisely the extent required to always dis-

charge the excess water and thus to maintain a virtually constant impounding head.

Should the weir shutter leave too large a flow cross section, and, consequently, allow too much water to be passed into the receiving water, the headwater level will fall producing also a falling level in the float chamber as the sill 8 will be flooded to a lesser degree. An increased water supply at too small a shutter opening will, inversely, produce a higher headwater level so that more water again enters the float chamber. The buoyancy force acting on the float increases, and the weir shutter is opened further.

Hence it follows that there is a quasi-steady discharge of any quantity of water between zero and the design flow, the headwater level - the impounding head - being maintained at a virtually constant level. Weir operation is controlled automatically, no external drive systems being required.

With the floods subsiding, the float chamber is entirely drained of any water, and the discharge opening to the receiving water can again be closed by the weir shutter. The waste water having been dammed up to the impounding head can now pass to the sewer works.

Air-regulated siphon. The second type of weir, which also permits discharge of any amount of water maintaining at the same time a given impounding head, is the air-regulated siphon. This unit, too, was model-tested and optimized at the Leichtweiß-Institut of Technische Universität Braunschweig (Führbötter et al., 1983), and, with the kind assistance of the Free Hanseatic City of Hamburg (Bielecki et al., 1983), subjected to prolonged tests in real systems.

Fig. 5 shows a conventional and an air-regulated siphon. Siphons of the known type (left) are primed when the inner siphon crest is

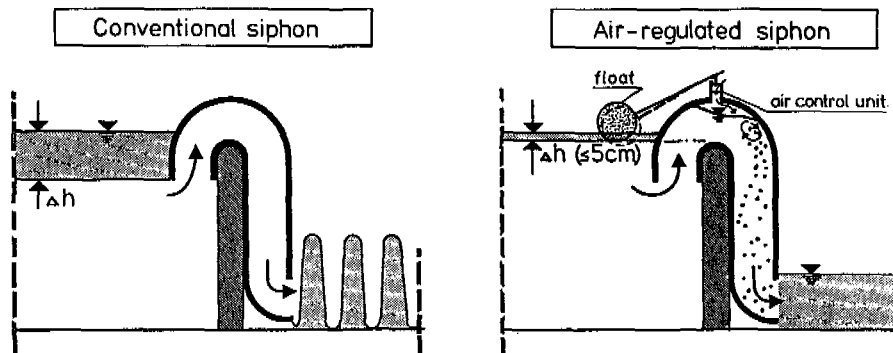


Fig. 5. Comparison of operation of a conventional and an air-regulated siphon

first flooded. The falling water evacuates the siphon which now runs at full bore discharging the water until the headwater level has fallen to such an extent (e.g. as a result of a reduced water supply) that air is taken in at the siphon inlet. The effect is that the siphon flow is interrupted. This cycle is repeated. The disadvantages are self-evident: major fluctuations in the headwater level, discontinuous discharge patterns.

The air-regulated siphon shown on the right does not entail these disadvantages as it is provided at its crown with the essential constructional feature of this type of weir - the float-operated air control unit. Such an arrangement of the control unit, by means of which the air inlet opening at the siphon crown can be varied, facilitates continuous discharge regulation for any amount of water $0 < Q \leq Q_{\max}$ with only minor fluctuations in the headwater level of

$$\Delta h \leq 5 \text{ cm}$$

and continuous tailwater flow.

Details of operation are shown in fig. 6

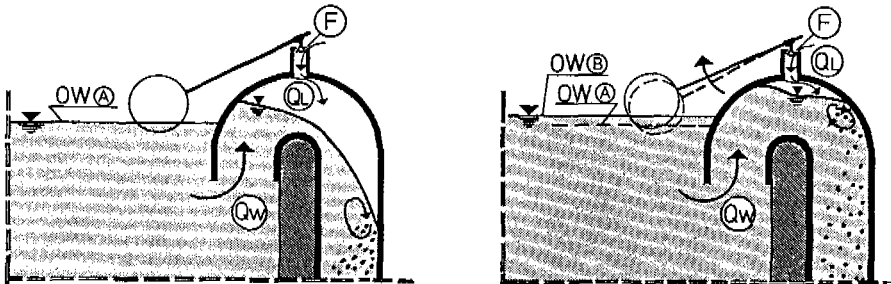


Fig. 6. Operation of the air-regulated siphon

Priming of the air-regulated siphon also proceeds by a free nappe. At this point, the siphon crest is flooded, i.e. the headwater level reaches the altitude A. Inside the siphon, the water entrains air as it plunges into the tailwater. A conventional siphon would now be evacuated and backwater flow be started. This cannot take place in an air-regulated siphon as, in case of a headwater level as shown, the float will adjust an air flap, to which it is connected by rods, leaving an air gap with the air inlet area F. An equilibrium is produced, which means that, at a constant air supply Q_L , there is a steady discharging of water of the quantity Q_w . In our example, this quantity remains significantly below the maximum discharge. The siphon is then said to be air partialized. Increasing amounts of water cannot be discharged under the conditions shown in fig. 6 (left). The headwater level inevitably rises to the altitude B. At the same time, the air inlet area is reduced through the float control mechanism thus throttling the air supply Q_L . The siphon can now pass the increased amount of water Q_w , for instance the amount shown in fig. 6 (right) approximating the maximum discharge. As soon as the headwater starts to rise beyond the altitude

B, the air intake opening is closed completely and the siphon operates at full bore with a discharge corresponding to the head between headwater and tailwater. With a reduced water supply at the upstream end, the headwater level will fall again, and the float

operates at full bore with a discharge corresponding to the head between headwater and tailwater. With a reduced water supply at the upstream end, the headwater level will fall again, and the float

with it. The consequence is a larger air inlet opening which in turn increases the air supply and reduces the discharge.

Application of the weir structures, efficiency

The automatically operating shutter weirs and siphons should be employed wherever it is not only a question of utilizing their hydrological advantage, but also an economical advantage in the form of reduced construction cost. Profitability considerations should be based on the following factors:

construction cost for conventional storm overflow or discharge systems with shutter weir or air-regulated siphon;
costs for flood discharge piping;
costs for the additionally activated sewer capacity.

The construction costs are calculated from the required cubic content as well as the required constructional components. For conventional storm overflows with fixed weir sills major overfall heights go along with short units and long discharge pipes when there is the danger of floods. Such a system implies, however, a serious loss of storage capacity. Minor overfall heights, on the other hand, go along with long and, consequently, high-cost structures.

With the weir structures presented in this paper, the unit lengths are determined directly by the prevailing conditions produced by the head between headwater and tailwater levels. The specific features of the weirs ensure that at any time only excess water is discharged into the receiving water, the water level at the upstream end corresponding to the permissible impounding head. This implies that the storage capacity available is always utilized to the fullest possible extent. Because of their configuration, these weirs also provide a flood protection as long as the level in the receiving water remains below the permissible water level in the sewer. As a consequence of this, the length of pipes designed to discharge floodwater may be much reduced.

The example of approx. 80 units (new installations) in Germany which are provided with the new weirs shows that by deciding against conventional systems with fixed weir sills approx. DM 10 million could be saved.

The installation of these new weirs should also be considered when modernizing existing, and sometimes fairly old, sewer systems. It is a known fact that considerable costs are involved when, in particular in congested areas, additional capacities are to be made available by providing retention basins.

Substantial additional storage area can be produced, as demonstrated by Pecher et al. (1982) just by utilizing existing sewer capacities. Measures, e.g. retaining basins, designed to reduce to a minimum receiving water loads, can thus either be limited or dispensed with altogether. For a selected urban combined-sewer system having a catchment area of approx. 100 ha, Barthauer (1980) found, in cooperation with the competent authorities of the city of Braunschweig, that the amount of water hitherto passed over the existing fixed weir sills may be reduced to approx. 62 % when utilizing the avail-

able sewer capacity. Measurements and calculations made in the city of Hamburg for part of a combined-sewer system having the reduced catchment area of approx. 140 ha (Schönfeld et al., 1981) also revealed that approx. 1,200 m³ of storage capacity can additionally be activated by fully utilizing the existing sewer capacities. Receiving water loads could thus be reduced by approx. 33 %.

Owing to its simple design - it is composed of standardized units - subsequent installation of the siphon in existing sewer systems does not require any conversion measures; it can be fitted through the sewer manholes. Utilization of existing sewer capacities can thus be achieved at much lower costs than would be involved if new facilities were provided (retaining basins).

When it comes to choosing between the two types of weirs, it should be considered that in principle the shutter weir is designed for heads between headwater and tailwater of less than 300 mm. With siphons, these heads may, as a result of protracted priming processes, lead to significant fluctuations in the impounding head. Where headwater/tailwater heads are more marked or where rehabilitation projects are involved, the siphon should be given preference over the shutter weir.

The annexes furnished provide examples for the design of these weir structures.

SUMMARY

The automatically operating weir structures represent simple, largely maintenance-free units which, when used as control elements in storm overflows, offer considerable advantages over fixed weir sills.

Their advantages can be summed up as follows:

Activation of sewer capacities. The activation of otherwise unused sewer capacities is an economical and low-cost way - as compared with stormwater retention basins - of reducing the quantities of sewage discharged into the receiving water.

Economical installation in new or existing structures. Economical installation is substantiated by a cost comparison with conventional systems. In particular rehabilitation measures are facilitated as the segmented siphon does not involve any time and cost consuming constructional requirements (open pits) and can easily and within a minimum of time be fitted to existing weir sills of any length.

Automatic control. An overdimensioned unit will not result in an increase of the amount of water discharged. The automatically operating control systems ensure that, subject to the given impounding head, only excess quantities of water are discharged. This means at the same time that an exact calculation of excess storm water can be dispensed with.

Minimum of maintenance requirements, high reliability. Due to their simple construction from corrosion-resistant materials, the weirs require hardly any maintenance.

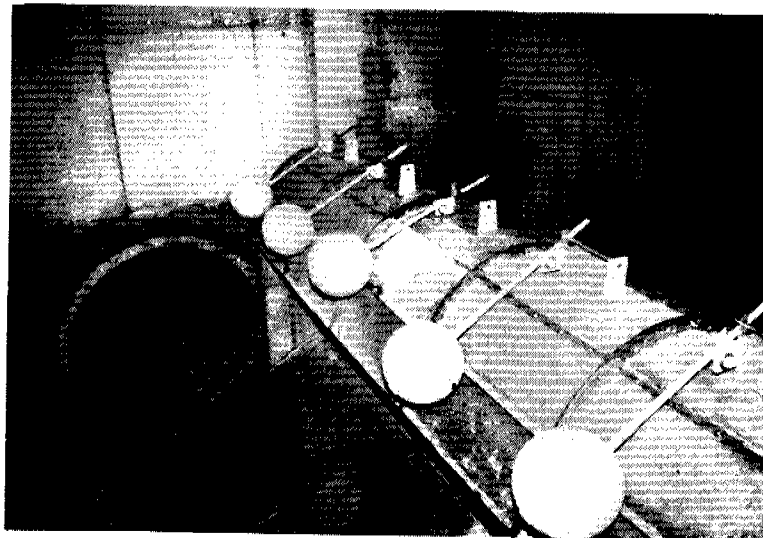
High efficiency resulting in short overall lengths. The high efficiency of these weirs results from the fact that the head between upstream and downstream water is fully utilized. This can lead to shorter weir lengths - as compared with other types of weirs, e.g. overfall weirs - for discharging the same amount of water.

No contaminations with oil, grease and solids. The relatively long suction branch of the siphon and the configuration of the shutter weir as an underflow weir ensure that the water is never taken from the top so that impurities at the surface, such as oil, grease, floating sludge etc., do not get into the receiving or, respectively, the downstream water.

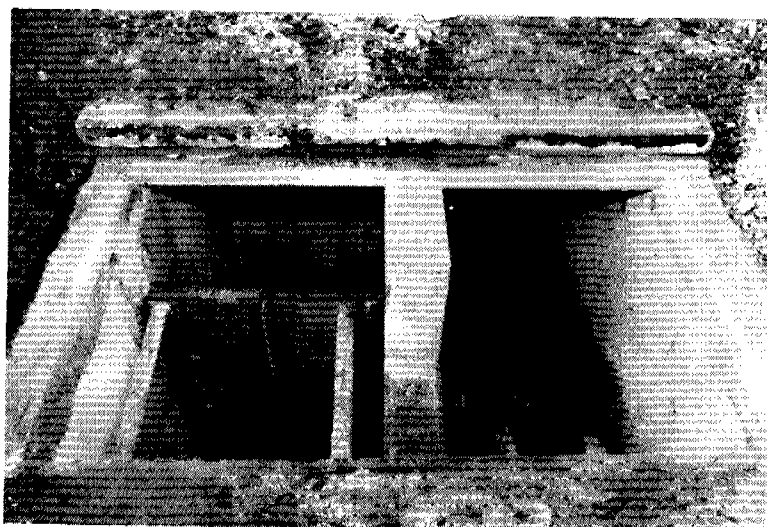
REFERENCES

- Barthauer, J. (1980). Zur Bestimmung der Abschlagsmengen aus einem Mischwasserkanalnetz und über Möglichkeiten zu deren Verhinderung durch den Einbau beweglicher Wehre. Diploma thesis at Leichtweiß-Institut.
- Bielecki, R., Macke, E., Hoppe, F., Stahn, R. (1983). Reduzierung von Überlaufwassermengen in Mischwasserkanälen mit einem luftgesteuerten Heberwehr - Ein Beitrag zur Dämpfung der Kosten nach dem Abwasserabgabengesetz - Korrespondenz Abwasser, Heft 2, pages 80-85.
- Führböter, A., Mittelstädt, M., Macke, E. (1978). Untersuchungen an Regenabschlagsbauwerken mit beweglicher Wehrklappe. Leichtweiß-Institut, Expert opinion, not published.
- Führböter, A., Mittelstädt, M., Fröhlich, G. (1983). Luftgesteuertes Heberwehr zur Abflußregulierung an Entlastungsbauwerken. Leichtweiß-Institut, Report No. 554.
- Pecher, R., Rieger, K.-H. (1982). Aus Regenaufzeichnungen ermittelte Überlaufdaten von Regenentlastungsanlagen. Korrespondenz Abwasser, Heft 11, pages 754-758.
- Schönfeld, I., Macke, E. (1981). Selbsttätig wirkendes Wehr in Regenauslaßbauwerken. Technische Mitteilungen des Hauses der Technik Essen, Heft 6, 74. Jahrgang.

ANNEX



View of a storm overflow with air-regulated siphons



View of a storm overflow with float-controlled shutter weir

SEDIMENTATION, MINERALIZATION AND RESUSPENSION OF SLUDGE IN A SEWERAGE SYSTEM: A CASE STUDY

A. S. Hogendoorn-Roozemond

*Witteveen+Bos Consulting Engineers, P.O. Box. 233, 7400 AE Deventer,
The Netherlands*

ABSTRACT

Quantitative information was obtained on the processes of sedimentation, mineralization and resuspension of organic matter in a combined sewerage system by means of statistical analysis of dry and wet weather data on sewage flows.

The effects of temperature and length of intermittent dry weather periods on daily pollutant loads were also evaluated.

For the sewerage system investigated it was found that in summer 5-26% of the BOD produced is mineralized in the system before reaching the sewage treatment plant. Due to sedimentation under dry weather conditions up to 12% of the daily organic load produced may be present in the sewers as resuspendable deposits; in winter this percentage may even amount to 20-30% because of slow mineralization.

KEYWORDS

Sewage sedimentation; sewage mineralization; resuspension of sewage sludge; combined sewer overflows; overflow pollution load; first flush.

INTRODUCTION

The design of combined sewerage systems allows a certain frequency of overflows. To date it has not been possible to quantify the pollution load from these sewer overflows adequately. Consequently the benefits of the various control measures are difficult to predict. Cost-effective optimization of sewerage system designs is therefore impossible.

The reasons for this gap in our knowledge reside in the complexity of all factors which determine the pollution load of every overflow event, such as:

- rainfall (intensity and spatial distribution, etc)
- sewerage system design (dimensions, flow characteristics, storage capacity, pumping rate)
- sewage water quality (organic content, settleable solids, etc)
- sewage quantity (diurnal, weekly and seasonal variations).

It is known that sedimentation and mineralization occur in a sewerage system together with resuspension of organic matter, which often becomes evident in first flush phenomena. Also, the occurrence of overflows is both incidental and unpredictable. It is, therefore, not easy to study the response of the pollution load to all these individual factors in the field.

Obtaining representative overflow samples is difficult and requires long term automated monitoring in order to give statistically valid results.

In this paper a different approach to the problem is presented in order to gain relevant information on the processes which determine the pollution load of an overflow event. To this end data on sewage water entering a large pumping station have been analyzed statistically. It was thus possible to quantify the effects of rain, the preceding dry weather period, temperature and other factors on the processes of sedimentation, mineralization and resuspension of sludge in the connected sewerage system.

METHOD OF DATA ANALYSIS

Data recorded

The site of the study was the 'Emerweg' main pumping station which serves the combined sewerage system of the city of Breda in the Netherlands. Here samples were collected on a continuous basis, proportional to the volume of waste water entering the pumping station.

The data recorded consisted of:

- daily pumping period (3 pumps with a fixed pumping rate of $3000 \text{ m}^3/\text{h}$ each),
- daily pollution loads entering the pumping station (expressed as BOD, COD and total nitrogen, N)
- daily rainfall from two weather stations.

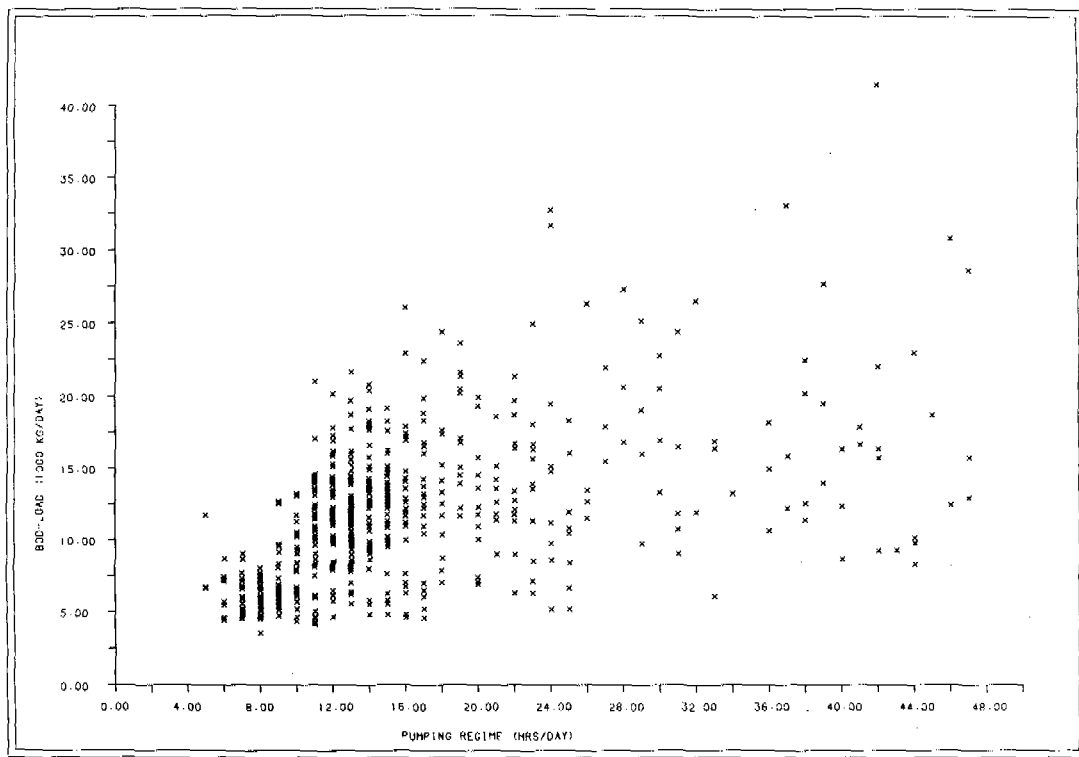


Fig. 1. Plot of BOD-load against volume of waste water

Procedure

A plot of the daily pollution load (BOD, COD or N) against the volume of waste water arriving per day gives a scatter diagram as is shown in Figure 1. The relation between pollution load and volume is diffuse and hardly discernible. This dispersion of data is due to:

- sedimentation of organics on dry days, the load arriving at the pumping station then being less than the average load produced in the system,
- resuspension of deposited organics and inflow of urban runoff pollutants during rain, the arriving load then being more than the average load produced,
- variations in waste water concentration,
- variations in the degree of mineralization (temperature effect),
- overflows.

The net result of sedimentation, mineralization and resuspension can be derived from the extra pollutant loads arriving on rainy days. These additional loads can in turn be evaluated for possible dependency on the length of the previous dry weather periods.

The effect of temperature on mineralization of organics in sewers can be obtained by analyzing the dry weather data during summer versus winter conditions.

Computer program

The statistical analysis was carried out using the computer model GLIM (Generalized Linear Interactive Modelling) (Baker and Nelder, 1978). This computer program allows multiple curve fitting, whereby the variable can be described as a function of any number of linear or linearized covariables, as affected by various factors or combination of factors. Covariance analysis forms the basis of this computational method.

The 'goodness of the fit' of the derived model is judged by the value of the scaled deviance. Whether or not effects or combination of effects investigated are statistically significant for the model is determined via the Student-t-Test.

Alternatively the fit can be checked by plotting the residuals of the predicted and measured values of the variables against the related covariables.

Definition of factors and variables

The data were grouped into several mutually exclusive subsets to fit different models to each subset. This grouping was done by defining and giving values to the following 'factors' or 'levels':

- Rainy days and dry days. A rainy day was defined as a day with 2 mm of rainfall or more, since below this precipitation level there will be hardly any runoff. In addition, every day following such a rainy day was also regarded as a rainy day, because of the extended transportation times in a sewerage system (it may take 10 to 25 hours before all the waste water in a full system reaches the pumping station). By definition, dry days relate to days with less than 2 mm of rainfall and not following a rainy day.
- Summer and winter. This factor is of special importance for the quantification of mineralization
- Weekend and weekday conditions to take into account industrial waste water supply.

The variables analyzed were:

- daily waste water volume, expressed as pumping period in hours per day (covariable)
- length of the previous dry weather period in days (covariable)
- daily pollution load arriving at the pumping station (Y-variable, BOD, COD and N, kg/d)

Dry days

The Y-variable for the dry days was described as a function of the volume of waste water arriving. The model was fitted through the origin since the pumps will not function if no waste water is supplied. The function was found in the form of a polynomial. The minimum number of terms in the polynomial was determined by the curve-fitting process. The separate and combined effects of the factors, weekend/weekday and summer/winter, were found in the values of the regression coefficients obtained. Whenever effects were not significant statistically, the factor was eliminated from the model.

Rainy days

A similar model was set up for the rainy day data, with the difference that the previous dry weather period was included as a second covariate. Hence this function contains three covariates: pumping time, dry weather period and, in order to investigate a combined effect, pumping time multiplied by dry weather period.

RESULTS AND DISCUSSION

Dry days

Waste water volume

A significantly smaller volume of waste water is produced during weekends than on weekdays (average pumping time 9.6 and 15.5 hours respectively). The summer/winter factor was not significant on dry days. This means that the average daily volume of waste water produced in summer can be considered equal to that produced in winter.

Pollution loads

Figures 2, 3 and 4 show the dry day models for the daily pollution load as a function of pumping time (for BOD, COD and N, respectively). The formulae of the functions derived are presented in Table 1. These functions accounted for 63-66% of the total variance. So the correlation coefficients ranged between 0.79 and 0.81.

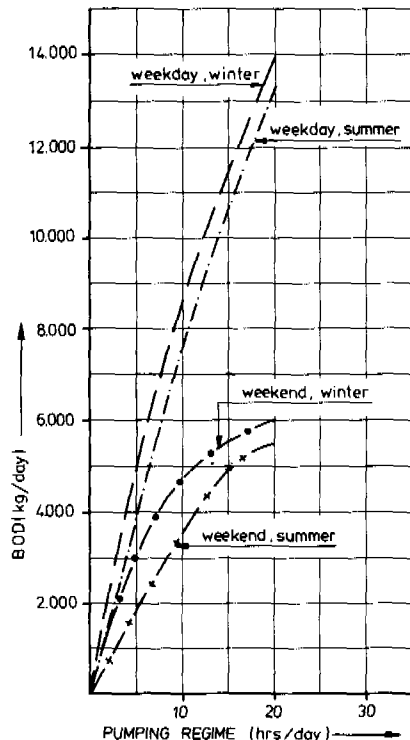


Fig. 2. Fitted curves for the dry day BOD-load as a function of the waste water volume.

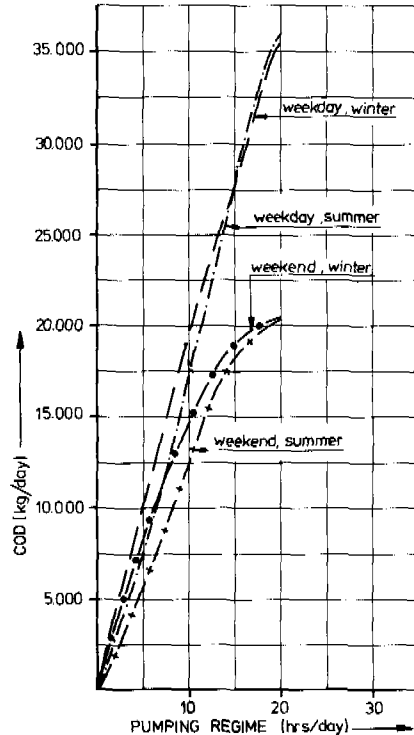


Fig. 3. Fitted curves for the dry day COD-load as a function of the waste water volume.

Analysis of the dry day data shows strongly significant differences between weekend and weekday loading, reflecting the industrial waste water supply.

Quite apparent was also the consistent effect of summer and winter in the BOD and COD-loading on dry days. In winter a significantly larger load of BOD and COD arrived at the pumping station than in summer. This indicates that organic matter is mineralized in the system.

Under average flow conditions the mineralization in summer (difference between winter and summer load) amounted to about 600 kg BOD for the weekday and 1200 kg for the weekend situation. It was thus estimated that up to 26% of the BOD produced in summer weekends is mineralized within the sewers. On weekdays the mineralization amounted to 5%. This marked difference in mineralization can be explained by the lower flow conditions during weekends.

The combined effects of the weekend/weekday and summer/winter factors were not significant.

Concerning nitrogen, a larger load arrived in winter than in summer, but the differences were limited. The effect of weekend/weekday were also less distinct, indicating that the waste water produced by the particular industries contained proportionally little nitrogen.

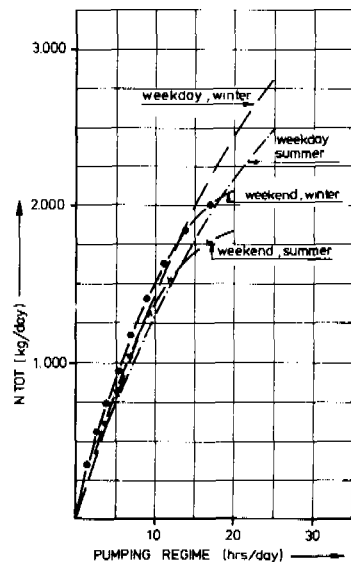


Fig. 4. Fitted curves for the dry day nitrogen load as a function of the waste water volume.

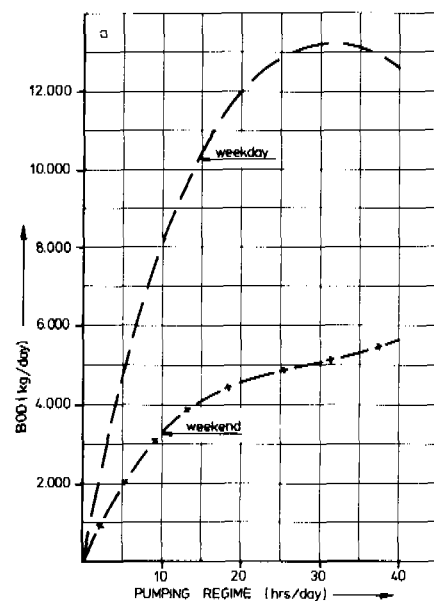
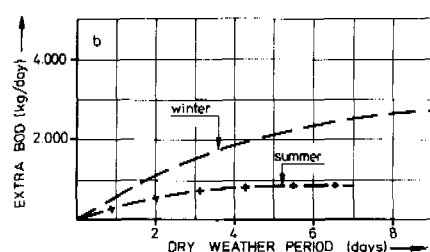


Fig. 5. a) Model describing the BOD-load as a function of waste water volume on rainy days with no preceeding dry weather period.
Fig. 5. b) Model describing the extra BOD-load arriving at the pumping station due to the previous dry weather period.



Rainy days

Waste water volume

The average volume of waste water during rainy days showed a significant change with the season and with the weekend/weekday factor.

The average daily pumping period is as follows:

- 14.2 hours in the summer weekend
- 16.8 hours in the winter weekend
- 18.9 hours on summer weekdays
- 21.5 hours on winter weekdays.

Pollution loads

For the rainy days not preceded by a dry weather period the fitted curves for BOD and COD are drawn in the Figures 5a and 6a.

Both curves tend to level off at pumping times exceeding 20 hours, indicating that the additional inflowing water mainly has a diluting effect. In this specific functional relationship no significant summer/winter effects were detected. There is, however, a strongly significant difference between weekdays and the weekend.

The function for the nitrogen load is given in Figure 7a. In this case four curves were required to fit the data, as both weekend/weekday and summer/winter effects were significantly different, both separately and combined.

It appeared that, on winter weekdays, a smaller nitrogen load arrived than was to be expected on the basis of the individual weekend/weekday and summer/winter effects.

Table 1. Summary of the model describing the pollutant load as a function of the waste water volume on dry days (loads in BOD, COD and N, kg per day; volume P in pumping hours/day) (var = variance accounted for; r = correlation coefficient).

| BOD model (var = 65.5%; r = 0.81) | | | |
|--------------------------------------|--------|---------------------------------|--|
| Weekend | summer | $333 P + 8.47 P^2 - 0.569 P^3$ | |
| | winter | $785 P - 37.1 P^2 + 0.652 P^3$ | |
| Weekday | summer | $725 P + 8.47 P^2 - 0.569 P^3$ | |
| | winter | $1177 P - 37.1 P^2 + 0.652 P^3$ | |
| COD model (var = 65.1%; r = 0.81) | | | |
| Weekend | summer | $820 P + 73.2 P^2 - 3.14 P^3$ | |
| | winter | $1844 P - 31.7 P^2 - 0.468 P^3$ | |
| Weekday | summer | $1237 P + 73.2 P^2 - 2.25 P^3$ | |
| | winter | $2261 P - 31.7 P^2 - 0.420 P^3$ | |
| N-model (var = 62.9%; r = 0.79) | | | |
| Weekend | summer | $183 P - 4.54 P^2$ | |
| | winter | $196 P - 4.54 P^2$ | |
| Weekday | summer | $151 P - 2.03 P^2$ | |
| | winter | $164 P - 2.03 P^2$ | |

Table 2. Summary of the models describing the pollutant load on rainy days as a function of the waste water volume and preceding dry weather period (loads in BOD, COD and N, kg/day; volume P in pumping hours/day and dry weather period D in days) (var = variance accounted for; r = correlation coefficient).

| BOD model (var = 56.5%; r = 0.75) | | | |
|--------------------------------------|--------|---|--|
| Weekend | summer | $466 P - 15.4 P^2 + 0.185 P^3 + 371 D - 37.2 D^2$ | |
| | winter | $466 P - 15.4 P^2 + 0.185 P^3 + 642 D - 37.2 D^2$ | |
| Weekday | summer | $1045 P - 25.6 P^2 + 0.185 P^3 + 371 D - 37.2 D^2$ | |
| | winter | $1045 P - 25.6 P^2 + 0.185 P^3 + 642 D - 37.2 D^2$ | |
| COD model (var = 52.8%; r = 0.73) | | | |
| Weekend | summer | $1125 P - 13.6 P^2 + 989 D - 83.3 D^2$ | |
| | winter | $1125 P - 13.6 P^2 + 1705 D - 83.3 D^2$ | |
| Weekday | summer | $2153 P - 32.6 P^2 + 989 D - 83.3 D^2$ | |
| | winter | $2153 P - 32.6 P^2 + 1705 D - 83.3 D^2$ | |
| N-model (var = 59.2%; r = 0.77) | | | |
| Weekend | summer | $162 P - 5.36 P^2 + 0.0573 P^3 + 43.9 D - 3.23 D^2$ | |
| | winter | $176 P - 5.36 P^2 + 0.0573 P^3 + 72.3 D - 3.23 D^2$ | |
| Weekday | summer | $183 P - 5.36 P^2 + 0.0573 P^3 + 43.9 D - 3.23 D^2$ | |
| | winter | $182 P - 5.36 P^2 + 0.0573 P^3 + 72.3 D - 3.23 D^2$ | |

When a rainy day is preceded by a dry weather period longer than 24 hours the pollutant load increased significantly. Resuspension of sewage sludge and inflow of accumulated street refuse is the most likely cause. During the two years under investigation the periods of dry weather varied from 0-19 days, but more than 90% lasted less than 8 days.

Quite remarkably, the extra load due to the previous dry weather period was significantly influenced by the summer/winter factor, while no weekend/weekday effect was apparent. Combined effects were absent as well. Independently of each other, this appeared to be the case for all three pollution load parameters. In addition, the best fit for the effect of preceding dry weather period is unanimously found in a quadratic function. The curves and formulae for this partial relationship are presented in the Figures 5b, 6b and 7b and in Table 2.

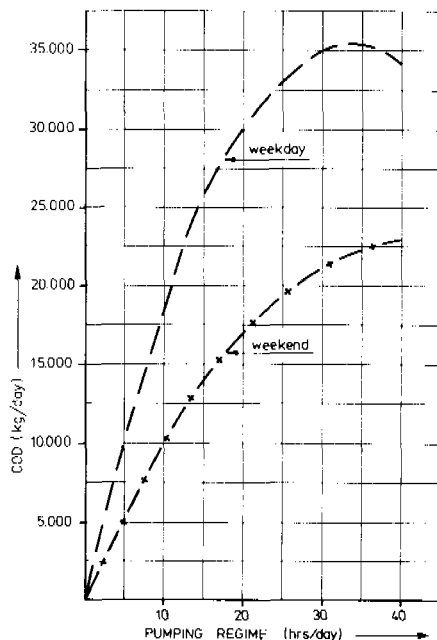


Fig. 6. a) Model describing the COD-load as a function of waste water volume on rainy days with no preceding dry weather period.

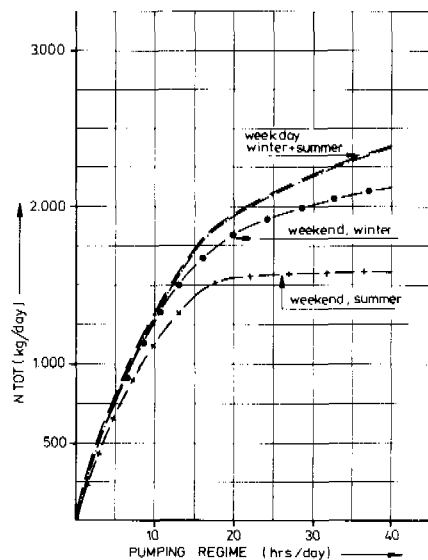


Fig. 7. a) Model describing the nitrogen load as a function of waste water volume on rainy days with no preceding dry weather period.

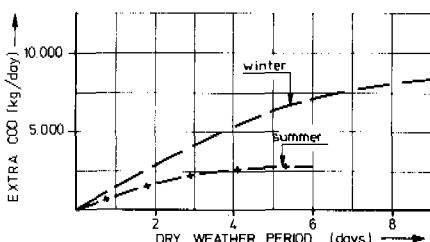


Fig. 6. b) Model describing the extra COD-load arriving at the pumping station due to the previous dry weather period.

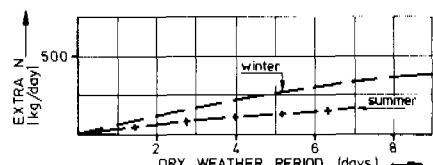


Fig. 7. b) Model describing the extra nitrogen load arriving at the pumping station due to the previous dry weather period.

Apparently, with increasing length of the preceding dry weather period the net quantity of resuspendable sludge builds up at an increasingly slower rate, until a stage of equilibrium is attained. At this stage the indications are that the same amount of sludge is mineralized as is supplied by (resuspendable) deposits and inflow of runoff refuse.

The mathematical 'maximum' for the pollution load deposited in the sewers occurs when the length of the dry weather period ranges from 5 to 7 days in summer and between 7 and 11 days in winter. Since only a limited amount of dry weather periods exceeded 8 days, the effect of longer periods of dry weather remains somewhat obscure.

The maximum expected resuspendable loads in the sewerage system are summarized in Table 3. The relative quantity of these loads (expressed as percentage of the total expected weekday load) is also given.

For the rainy day model correlation coefficients ranged between 0.73 and 0.77.

Table 3. Estimated 'maximum' resuspendable deposits in the sewers expressed as loads (kg BOD, COD and N) and as percentage of the average load on weekdays.

| | 'Maximum' deposits in summer | | 'Maximum' deposits in winter | |
|-----|---------------------------------|----|---------------------------------|----|
| | kg | % | kg | % |
| BOD | 900 | 10 | 2800 | 24 |
| COD | 2900 | 10 | 8700 | 30 |
| N | 150 | 12 | 400 | 20 |

Residual variance

In general the fitted models accounted for the greater part of the total variance (53-66%). The remaining residual variance is to be attributed to a number of effects and factors not included in the curve-fitting process, such as:

- retardation phenomena (lag between inflow and arrival)
- overflows; these events, however, are only incidental (averaging about 7 times per year) due to the considerable in-storage capacity of this particular sewerage system,
- variations in summer and winter temperatures, rainfall, rainfall intensities and the resulting flow velocities,
- fluctuations in waste water concentration on dry days,
- accuracy of measurements.

CONCLUSIONS

Statistical evaluation of sewage data can offer relevant information on such elusive processes as sedimentation, mineralization and resuspension in a sewerage system.

Sedimentation and mineralization of organics within the sewers is considerable. On rainy days deposited material is distinctly resuspended.

The preceding dry weather period is an essential variable in the prediction of sludge deposits in sewers.

In the area investigated the waste water volume supplied on weekdays exceeded the supply during weekends, due to the waste water contribution of industries. The industrial waste water appeared to contain little nitrogen.

Because of mineralization in the sewers a great deal of the BOD produced (26% on weekends and 5% on weekdays in the summer) did not reach the pumping station.

Deposition and mineralization of organic matter take place simultaneously. The models predicted that a steady state situation was attained after 5-7 days in the summer and after 7-11 days in winter.

It was predicted that in summer, the net 'maximum' pollutant load deposited in the sewers amounts to approximately 10-12% of the daily load supplied on weekdays. In winter this would even rise to 20-30%, due to a slower mineralization rate.

FINAL REMARKS

It is evident that the above conclusions only are valid for the sewerage system studied. As there are many site-specific factors which have a strong effect on the relevant processes, the results can by no means be generalized. It is therefore recommended that similar statistical investigations are carried out on data from different sewerage systems. This will give quantitative information and further insight into the individual combined sewer overflow pollution loads.

Optimization of sewerage system designs would then be possible, enabling a cost effective municipal water pollution abatement strategy.

ACKNOWLEDGEMENTS

I would like to acknowledge gratefully the Water Authority of West-Brabant for supplying the necessary set of data, in particular special thanks are due to ir. R.E.M. van Oers.

REFERENCES

Baker, R.J. and Nelder, J.A. (1978). GLIM Manual. Numerical Algorithms Group, Oxford.

| | | | |
|--|------|---|------|
| Ozone Enhanced Biological Activated Carbon Filtration and its Effect on Organic Matter Removal, and in Particular on AOC Reduction J. G. JANSSENS, J. MEHEUS and J. DIRICKX | 1055 | Modeling Water Quality and the Effects of Agricultural Best Management Practices in the Iowa River Basin B. R. BICKNELL, A. S. DONIGIAN, JR and T. A. BARNWELL | 1141 |
| Ozonation of Non-ionic Surfactants in Aqueous Solutions N. NARKIS, B. BEN-DAVID and M. SCHNEIDER ROTEL | 1069 | Surface Water Quality in Relation to Soil Type, Land Use and Discharge in a Rural Catchment Area M. C. H. WITMER | 1155 |
| Influence of Bubble Sizes on Ozone Solubility Utilization and Disinfection M. AHMAD and S. FAROOQ | 1081 | Urban Run-off | |
| The Role of Rapid Mixing Time on a Flocculation Process R. J. FRANÇOIS and A. A. VAN HAUTE | 1091 | Chronic Pollution of Intercity Motorway Runoff Waters J. D. BALADES, M. CATHELAIN, P. MARCHANDISE, J. PEYBERNARD and J. C. PILLOY | 1165 |
| Management of Urban Waste Water Physico-chemical Treatment Stations: Servocontrol of Reagent Additions at the Quiberon Sewage Treatment Plant, France P. MARCHANDISE, J. P. LEGENDRE, D. DELACROIX and J. L. RIVOAL | 1103 | Collection and Analysis of Urban Runoff Data in Finland M. J. MELANEN | 1175 |
| Modelling of the Coagulation-Adsorption Process in Treatment Systems A. M. DZIUBEK and A. L. KOWAL | 1113 | Standards | |
| Hexavalent Chromium Removal from Drinking Water J. M. PHILIPOT, F. CHAFFANGE and J. SIBONY | 1121 | Marine Quality Standards: Their Derivation and Application in the United Kingdom G. MANCE and A. R. O'DONNELL | 1187 |
| Effects of Agriculture on Water Quality | | Transport and Processes in Sewers | |
| The Contribution of Agricultural Loading to Eutrophication in Finnish Lakes L. KAUPPI | 1133 | Operation and Efficiency of Automatically Operating Weir Structures—A Contribution to Cleaner Waters E. MACKE | 1211 |
| | | Sedimentation, Mineralization and Resuspension of Sludge in a Sewerage System: A Case Study A. S. HOGENDOORN-ROOZEMOND | 1223 |